Catalytic Role of Amino Acids in Organic Reactions
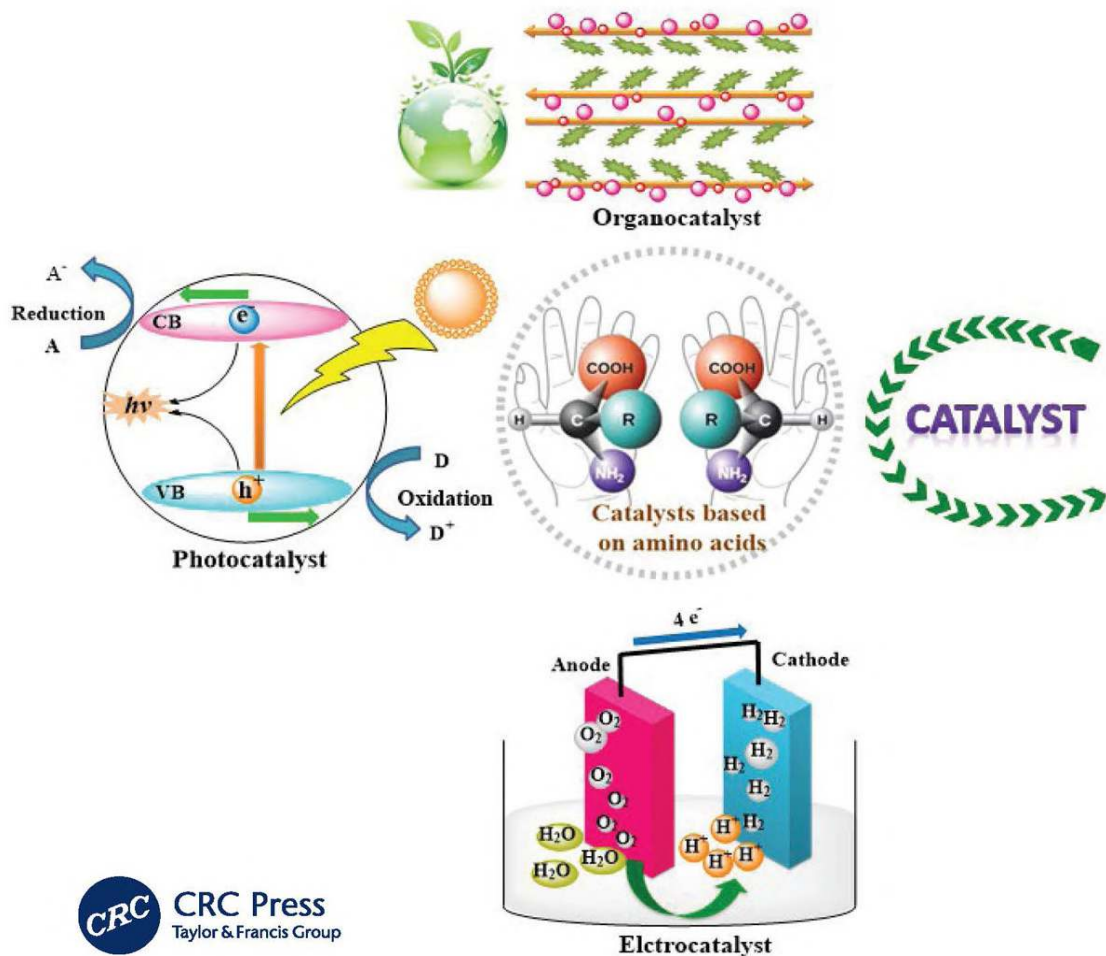
Zahra Taherinia, Arash Ghorbani-Choghamarani,
Zahra Moradi, Zahra Heidarnezhad,
Farhad Khanmohammadi-Sarabib,
and Mohammad Zolfigol

Organocatalyst

Photocatalyst

Catalysts based on amino acids

CATALYST

Elctrocatalyst

Catalytic Role of Amino Acids in Organic Reactions

Asymmetric organometallic and organocatalytic processes have attracted great interest. Asymmetric synthesis using both natural and unnatural amino acids has been tremendously important from synthetic as well as industrial viewpoints, and numerous new methodologies have been developed in the last decades. Herein we provide an overview of old and very recent advances and applications in the area of heterogeneous catalysis, homogeneous catalysis, electrocatalysis, photocatalysis, organocatalysis, thermal catalysis using amino acids (proline, glycine, alanine, valine, serine, threonine, cysteine, methionine, asparagine, glutamine, lysine, arginine, histidine, aspartate, glutamate, phenylalanine, and tryptophan) (supported or unsupported), an amino acid containing materials or amino acids derivatives as an essential component of catalysts; this book highlights the most important and recent developments to immobilize or support amino acids on various support materials. This book is suitable as supplementary reading for courses targeting the design, synthesis, and application of chiral catalysts, asymmetric catalysis, and sustainable production.

New Directions in Organic and Biological Chemistry

Series Editor:

Philip Page

Emeritus Professor, School of Chemistry, University of East Anglia

Catalytic Role of Amino Acids in Organic Reactions
Zahra Taherinia, Arash Ghorbani-Choghamarani, Zahra Moradi, Zahra Heidarnezhad, Fahrad Khanmohammadi-Sarabi, and Mohammad Ali Zolfigol

Chiral Ligands: Evolution of Ligand Libraries for Asymmetric Catalysis
Montserrat Diéguez

Biocontrol of Plant Diseases by Bacillus subtilis
Makoto Shoda

Advances in Microwave Chemistry
Bimal Krishna Banik and Debasish Bandyopadhyay

Carbocation Chemistry: Applications in Organic Synthesis
Jie Jack Li

Modern NMR Techniques for Synthetic Chemistry
Julie Fisher

Concerted Organic and Bio-organic Mechanisms
Andrew Williams

Capillary Electrophoresis: Theory and Practice
Patrick Camilleri

Chiral Sulfur Reagents
M. Mikolajczyk, J. Drabowicz, and P. Kielbasiń ski

Chemical Approaches to the Synthesis of Peptides and Proteins
Paul Lloyd-Williams, Fernando Albericio, and Ernest Giralt

Organozinc Reagents in Organic Synthesis
Ender Erdik

Chirality and the Biological Activity of Drugs
Roger J. Crossley

C-Glycoside Synthesis
Maarten Postema

The Anomeric Effect
Eusebio Juaristi and Gabriel Cuevas

Mannich Bases Chemistry and Uses
Maurilio Tramontini and Luigi Angiolini

Dianion Chemistry in Organic Synthesis
Charles M. Thompson

For more information about this series, please visit: https://www.crcpress.com/New-Directions-in-Organic--Biological-Chemistry/book-series/CRCNDOBCHE

Catalytic Role of Amino Acids in Organic Reactions

Zahra Taherinia, Arash Ghorbani-Choghamarani,
Zahra Moradi, Zahra Heidarnezhad,
Farhad Khanmohammadi-Sarabi,
and Mohammad Ali Zolfigol

Contents

Preface

Green chemistry focuses on designing products and processes that minimize the generation or use of hazardous substances. It is widely acknowledged that there is a growing need for more environmentally acceptable processes in the chemical engineering industry. Catalysts offer numerous green chemistry benefits, including lower energy requirements, catalytic versus stoichiometric amounts of materials, increased selectivity, decreased use of processing and separation agents, and allow for the use of less toxic materials. Chiral and highly functionalized natural amino acids are readily available by renewable methods in high quantities and are identified as green catalysts. Amino acids are the building blocks of proteins. More than 300 amino acids have been described, but only 20 amino acids take part in protein synthesis. Furthermore, natural amino acids have proved to be an outstanding class of ligands that are studied in the enantiomeric and organocatalysis processes (as Brønsted acid or base), ionic liquids, and organometallic catalysis.

In this book, special attention has been given to the materials used to support amino acids because the interactions between the amino acids and support provide advantages in terms of the shape and/or size of catalysts, selectivity, and recoverability of organic reactions. This book provides an overview of the reported different synthetic approaches to immobilize or support amino acids on various support materials (such as SiO_2, mesoporous, magnetic materials, etc.), along with their catalytic applications in organic functional group transformations and synthesis. The synthesis part discusses numerous appropriate protocols for amino acid–based nanoparticles, whereas the application sections describe their utility as heterogeneous catalysis, homogeneous catalysis, electrocatalysis, photocatalysis, organocatalysis, and thermal catalysis using amino acids for diverse reactions. We believe this critical appraisal will provide the necessary background information to further advance the applications in the area of heterogeneous and homogeneous catalysis.

This book aims to be comprehensive, authoritative, critical, and accessible of general interest to the chemistry community, which includes an overview of old and very recent advances and applications in the area of heterogeneous catalysis, homogeneous catalysis, electrocatalysis, photocatalysis, organocatalysis, thermal catalysis using amino acids (proline, glycine, alanine, valine, serine, threonine, cysteine, methionine, asparagine, glutamine, lysine, arginine, histidine, aspartate, glutamate, phenylalanine, and tryptophan), (supported or unsupported), an amino acid–containing materials or amino acids derivatives as an essential component of catalysts. This book targets organic chemists working in industry and academia and deserves a place in every laboratory.

About the Authors

Zahra Taherinia completed her BS studies in pure chemistry at Ilam University, Iran (2012). She received her MSc in organic chemistry (2014), and subsequently began her PhD studies in organic chemistry at the same university. She finished her PhD program at Ilam University in 2019. She conducted postdoctoral studies at Ilam University in the laboratory of Prof. Arash Ghorbani-Choghamarani.

Arash Ghorbani-Choghamarani completed his BS studies in applied chemistry at Bu-Ali Sina University, Hamadan, Iran (2001), received his MSc in organic chemistry (2003), and subsequently began his PhD studies in organic chemistry at the same university. During his PhD program, he completed a sabbatical fellowship at the University of Western Ontario, London, Ontario, Canada (from September 2005 to September 2006). He obtained his PhD degree in 2007. He then joined the Department of Chemistry at Ilam University, Ilam, Iran, as a faculty member from September 10, 2007, until September 2020. He was a Visiting Professor at the University of Western Ontario, London, Canada, from March 2018 until October 2018. He has been a faculty member at Bu-Ali Sina University since September 2020. He is currently Professor of Organic Chemistry.

Zahra Moradi completed her BS studies in pure chemistry at Ilam University, Iran (2016) and received her M.Sc. degree in organic chemistry (2018), and subsequently began her PhD studies in organic chemistry at the same university. She completed her PhD program at Ilam University in 2022.

Zahra Heidarnezhad completed her BS studies in pure chemistry at Ilam University, Iran (2017) received her M.Sc. in organic chemistry (2019), and subsequently began her PhD studies in organic chemistry at the same university. She finished her PhD program at Ilam University in 2023.

Farhad Khanmohammadi-Sarabi completed his BS studies in applied chemistry at Razi University, Kermanshah, Iran (2019) and received his M.Sc. in organic chemistry (2021) at Bu-Ali Sina University, Hamedan, Iran and subsequently began his PhD studies in organic chemistry at the same university.

Mohammad Ali Zolfigol completed his BSc at Arak University, Iran, MSc at the Isfahan University of Technology, Iran, under the supervision of Prof. Shadpour Mallakpour, and his PhD from Shiraz University, Iran, with Prof. Nasser Iranpoor and Prof. Habib Frouzabadi as supervisor and advisor, respectively. Zolfigol has been a Bu-Ali Sina University faculty member since 1997 and was promoted to Professor Degree in 2005.

1 Introduction to Amino Acids

1.1. INTRODUCTION

Peptides made from a long chain of amino acids (AAs) that linked to their neighbors via covalent bonding form a peptide bond. More than 300 amino acids exist in nature, but only make up the proteins found in the human body. Amino acids received considerable attention due to their biological significance. They contain two important functional groups: —NH$_2$ and —COOH, and an interesting side chain on the carbon that connected the amino group to the carboxyl group. Amino acids are traditionally classified as nutritionally essential and nonessential for animals and humans (Scheme 1.1). Of the 20 amino acids, 9 are termed essential because the body cannot ably synthesize and they must be supplied through food sources. Essential amino acids include phenylalanine, valine, threonine, tryptophan, methionine, leucine, isoleucine, lysine, and histidine.

Nonessential amino acids (11 amino acids) can be produced in sufficient amounts in the body as substrates to meet maximal growth and health requirements. Nonessential amino acids are mainly synthesized using glucose. These include alanine, arginine, asparagine, aspartic acid (aspartate), cysteine, glutamine, glutamic acid (glutamate), glycine, proline, serine, and tyrosine.

The amino acid molecules are optically active and exist as L- or D-enantiomers, except for glycine which does not have a chiral center [1]. L-amino acids are mostly available and produced by fermentation from inexpensive and renewable natural sources [1]. This classification method corresponds to the solubility characteristics (i.e., ionization and polarity) of the side chains (*R*-groups).

They can be classified into different classes based on their *R*-groups and differ in size, shape, and other properties.

The *R*-groups fall into four classes:

1. Nonpolar (hydrophobic)
2. Polar negatively charged (acidic)
3. Polar positively charged (basic)
4. Polar neutral (unionized)

The two functional groups of amino acids containing a carboxylic and an amine group enabled them to act as both an acid and a base [2]. Adding acid to a solution containing zwitterion leads to the transfer of a positive charge on the carboxylate group and the formation of positively charged amino acids. On the other hand,
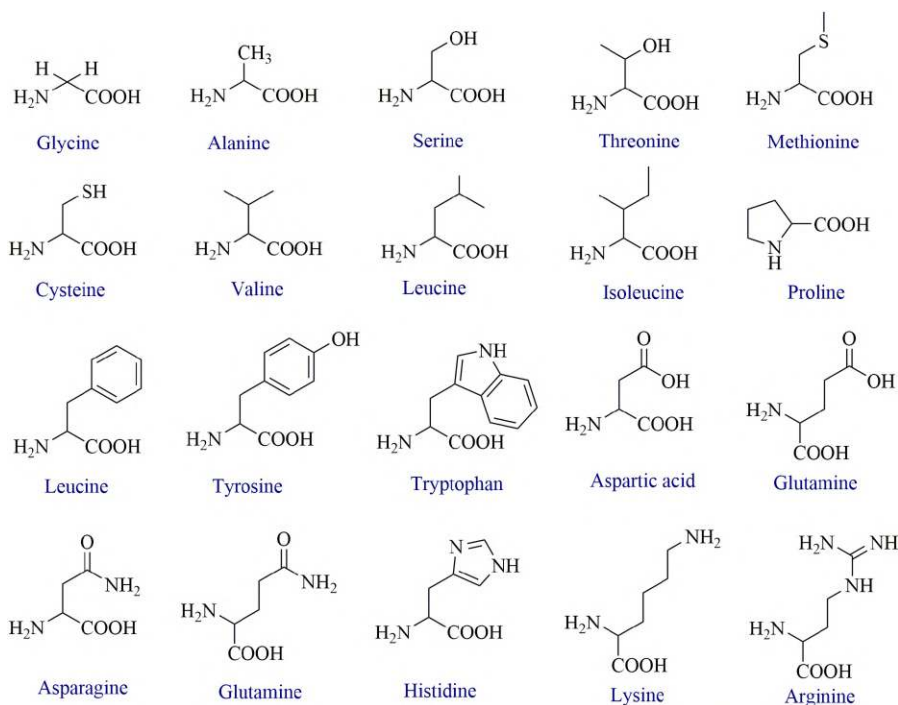
SCHEME 1.1. Essential and nonessential amino acids.

adding base to a solution containing zwitterion leads to the transfer of positive charge from the amino group and the formation of a negatively charged amino acid (Scheme 1.2) [2]. The amino acids exist as zwitterions in neutral conditions that contain both positively and negatively charged groups [2]. Moreover, the isoelectric point of any amino acid is the pH at which it bears a net charge of zero. These properties have exerted an important influence on the interactions of amino acid residues in polypeptides and proteins and significantly affect the 3D structure and properties of protein [2].

1.2. PROPERTIES OF POLAR AMINO ACIDS

Amino acids that are classified as hydrophobic include alanine, valine, isoleucine, leucine, methionine, phenylalanine, tryptophan, and tyrosine. The hydrophobic properties are usually accompanied by repulsion from water, so this affects the position of these amino acids in the protein tertiary structure. The polar, hydrophilic amino acids can be divided into three major classes: the polar uncharged, the acidic, and the basic. Polar amino acid residues usually appear on the proteins exterior after polymerization due to their hydrophilic side chains. Four amino acids are classed as polar without any charge (asparagine, glutamine, serine, and threonine).
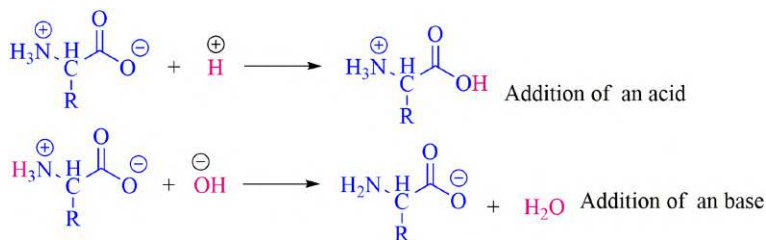
SCHEME 1.2. The behavior of amino acids using both base and acid.

1.3. PROPERTIES OF AROMATIC AMINO ACIDS

Of the 20 amino acids found in protein structures, 4 of them are aromatic. These are phenylalanine, tyrosine, tryptophan, and histidine, and they are of significant interest in both health science and biotechnology. Amino acids absorb UV wavelengths less than 200 nm and only the aromatic amino acids phenylalanine, tyrosine, and tryptophan are slightly redshifted absorption bands around 280 nm [3].

1.4. SYNTHESIS OF AMINO ACIDS

Various methods have been utilized to synthesize amino acids, including α-halo acids' alkylation, nucleophilic substitution of α-halo carboxylic acids, Gabriel synthesis, and Strecker synthesis.

1.4.1. THE ALKYLATION OF α-HALO ACIDS

Alkylation has been successfully utilized for the synthesis of such amino acids as serine, leucine, ornithine, phenylalanine, and tryptophan. The procedure is based on the alkylation of acetamido malonate followed by amide and ester hydrolysis and finally decarboxylation (Scheme 1.3).

1.4.2. NUCLEOPHILIC SUBSTITUTION OF α-HALO CARBOXYLIC ACIDS

Nucleophilic substitution is the most general method involving the displacement reaction of halogen of halo acids with amines (Scheme 1.4).

1.4.3. STRECKER SYNTHESIS

This procedure involves the combination of an aldehyde and ammonia using potassium cyanide to afford an α-aminonitrile, which is hydrolyzed to afford the desired amino acid (Scheme 1.5). By varying the *R*-group on the imine, a wide range of amino acids may be produced in this way. It should be noted that using ammonium salts leads to the production of unsubstituted amino acids. Alternatively, the use of primary and secondary amines also gives substituted amino acids.
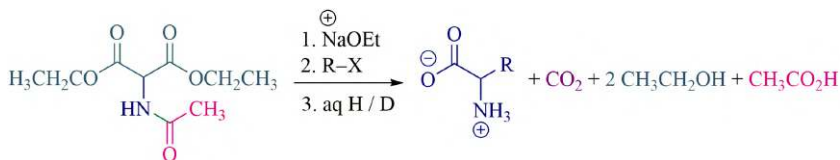
SCHEME 1.3. The alkylation of α -halo carboxylic acids for the preparation of some amino acids.
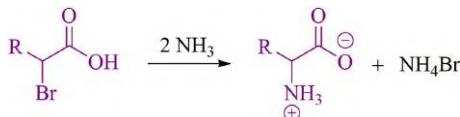
SCHEME 1.4. Nucleophilic substitution of α-halo carboxylic acids.
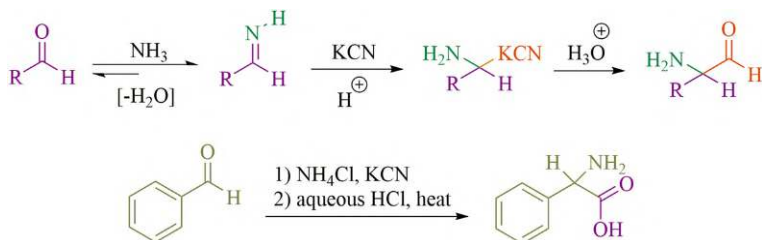
SCHEME 1.5. Strecker synthesis for the preparation of amino acid.

1.4.4. GABRIEL SYNTHESIS

Gabriel synthesis is recognized as a way to produce α-amino acids through *N*-phthalimido malonic ester and an alkyl halide followed by hydrolysis (Scheme 1.6).

1.5. APPLICATION OF AMINO ACIDS

Researchers and scientists have long known the importance of selecting appropriate amino acids for developing processes for chemicals and related products to consider both environmental and economic metrics [4]. According to all of the 12 principles of green chemistry, biocatalysis has attracted tremendous attention owing to potential applications for green and sustainable technology [4]. Amino acids are widely used in protein biosynthesis to increase their enantioselectivity, activity, and stability [4]. Amino acids are usually considered as important scaffolds for peptides and proteins and act as versatile organocatalysts in a wide range of asymmetric transformations. In the following, we have overviewed several fields of amino acid applications.
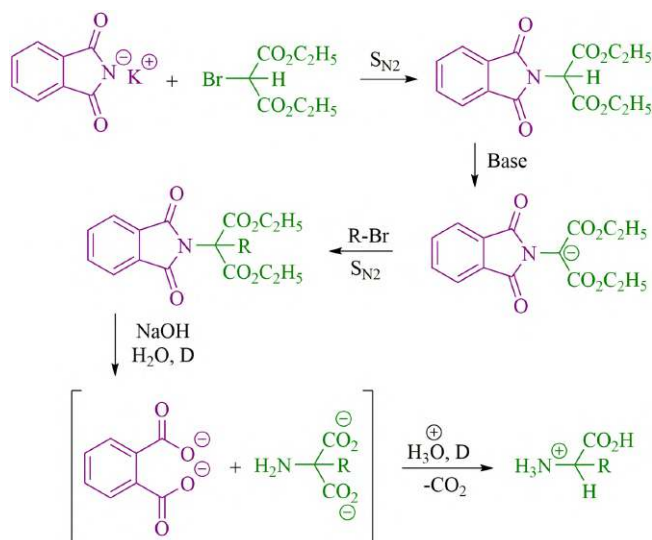
SCHEME 1.6. Gabriel synthesis to produce α-amino acids.

1.5.1. DRUGS

Natural products have been employed as a major source of drugs for many centuries; however, the application of natural products is related to poor solubility and low activity [4]. One of the drawbacks of the drug is its low solubility in water [4]. Drugs that have poor aqueous solubility have slower drug absorption [4]. There is an urgent need to develop novel approaches for improving these shortcomings. In this sense, amino acids overcome these issues. These features have made amino acids potential candidates in drug synthesis and modification strategies. Experimental data indicate that mixing a compound with an amino acid leads to an increase in the pharmacological activity and water solubility of the compound [4].

1.5.2. IONIC LIQUID

Amino acids and their derivatives are used for the production of ammonium cations in ionic liquids (ILs) [5]. Recently, ionic liquids have been proclaimed green alternatives to volatile organic solvents owing to their unique properties such as their low vapor pressure. Thus, the development of new "green" ionic liquids with low cost and easy preparation continues to attract great attention of researchers [5]. Various cations and anions are used in the production of ionic liquids. In this method, functionalized ionic liquids with both acidity and chirality are prepared and used as catalysts in reactions, such as the Diels–Alder cyclization, as substitutes for volatile organic solvents to make the system greener [5]. In the last decade, amino acid ionic liquids were intensively studied due to their features such as being nontoxic and biodegradable, and are employed as green solvents, catalysts, and adsorbents containing

multifunctional groups [6–8]. Ionic liquids were recognized as carbon precursors for high-performance supercapacitors. The preparation of heteroatoms-doped carbon materials could lead to improved material performance and specific capacitance. Amino acid protic ionic liquids (AA-PILs)-rich heteroatom elements are considered promising materials for use as electrodes for high-rate supercapacitors [9]. In this sense, Zhou et al. demonstrated the production of N/S-doped micro-mesoporous carbon materials, and it is used as supercapacitors. In this study, the authors prepared N/S-doped micro-mesoporous carbon materials using AA-PILs as abundant, inexpensive, nontoxic amino acids (Figure 1.1) [9].

Ionic liquids have emerged as an attractive alternative for CO_2 capturing because they have negligible volatility, nonflammability, high thermal stability, and virtually unlimited chemical tenability [10]. In this context, Latini et al. designed the production of choline/amino acid–based ionic liquids via ionic metathesis, their activity was examined for CO_2 absorption performances and were studied by employing different experimental studies (Scheme 1.7) [11].

Chen et al. designed the immobilized task-specific ILs via the ionic pair coupling of imidazolium cations of the modified polystyrene with amino acid anion (Scheme 1.8). The prepared ILs displayed considerable ability for metal scavenging (e.g., CuI, $Pd(OAc)_2$, Pd^0, and $IrCl_3$) [12].

A phase-transfer catalyst (PTC) is a tool for transforming reactants from one phase into another phase. Ionic reactants are insoluble in an organic phase [13]. PTC revealed great potential for the improvement of various aspects: mild aqueous reaction conditions, easier operation, higher production yield, and the ability to eliminate expensive solvents [14]. PTC has been widely applied in different areas, including
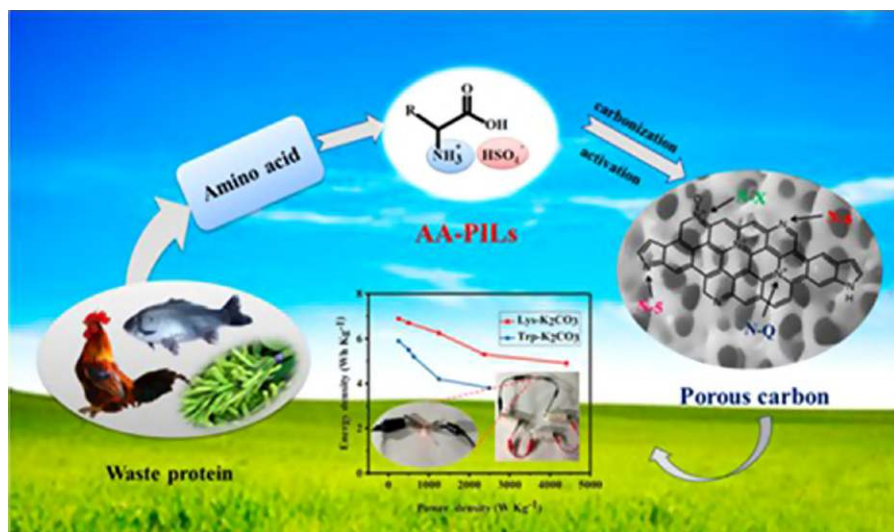
FIGURE 1.1.   Schematic illustration of the synthesis of porous carbon materials. *Source: Reproduced with permission from Ref. [9]. Copyright 2019, American Chemical Society.*
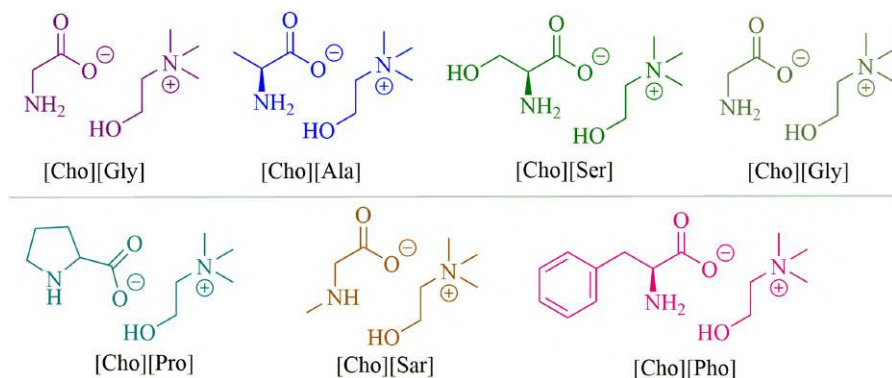
SCHEME 1.7. Molecular structures of the synthesized [Cho][AA] ILs.
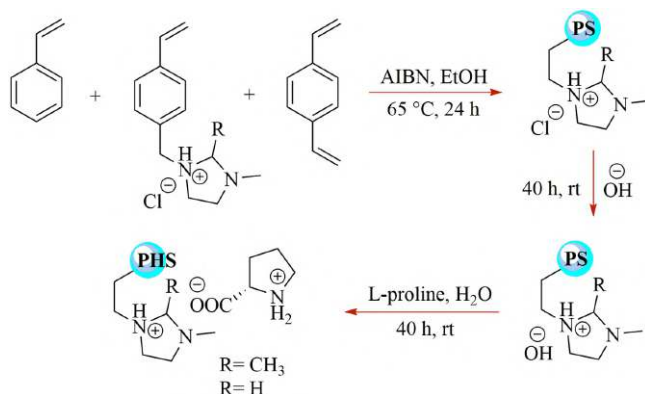
SCHEME 1.8. Production of the polymer-supported task-specific ILs PS[DMVBIM][Pro] and PS[MVBIM][Pro].

organic preparation, heterocyclic compound synthesis, polymer chemistry, agrochemical, organometallic chemistry, and so forth [14]. Asymmetric phase-transfer catalysis emerged as an alternative greener media for organic synthesis in both the industry and academia and has evolved into one of the most practical methods in challenging enantioselective synthesis [14]. Despite this, several asymmetric phase-transfer catalysts are still limited. Amino acids are recognized as an inexpensive and accessible chiral source [14]. Moreover, using amino acid derivatives as chiral skeletons and hydrogen bonding donors provides a kind of structurally variable chiral quaternary ammonium salts that may be a kind of effective phase-transfer catalyst [14].

1.5.3. Deep Eutectic Solvents

Deep eutectic solvents (DESs) are prepared by combining hydrogen bond donor (HBD) and hydrogen bond acceptor (HBA) molecules that consist of natural plant

metabolites, amino acids, and ionic molecules. Deep eutectic solvents as alternative extraction solvents have been the object of much interest due to their benefits of having good electrical conductivity and stability, being environment-friendly, and its easy preparation with a wide range of applications [15]. In context, Shavandi et al. introduced the combination of lactic acid and L-cysteine as a new green deep eutectic solvent for the isolation of keratin [16].

1.5.4. SURFACTANTS

Surfactants are amphiphilic molecules that have hydrophobic and hydrophilic parts. Natural amino acids have been investigated as surfactant source materials with chiral properties that can be designed and tailored for specific biological applications. Amino acid–based surfactants (AAS) are synthesized by reacting an amino acid with a fatty acid or its derivatives. The nature of the amino acid residue, the chirality, and the ability for hydrogen bond formation strongly relate to the surface-active properties and self-assembly behavior of AAS [17].

1.5.5. PROTECTING GROUPS

The tremendous interest in synthetic peptides has led to the development of viable methods for sustainable production. Peptide coupling reactions are essential for the chemical synthesis of polypeptides and proteins. Protecting reactive amino acids minimizes unwanted side reactions that interfere with producing a specifically ordered sequence of amino acids. An ideal protecting group should be quantitatively introduced and removed under relatively mild conditions. In context, Matsuda and coworkers introduced a highly convergent approach for the efficient solution-phase synthesis of peptides containing *N*-methyl amino acids (Scheme 1.9) [18].

1.5.6. CATALYST

Organometallic and organocatalytic bases on amino acids have attracted the considerable attention of both the academic and industrial chemistry communities. Amino acids are widely a versatile ligand class in enantiomeric organocatalysis (as Brønsted acid or base) [18–22], ionic liquids [23], and organometallic catalysis [24]. Despite the strong applications of amino acids in various fields (e.g., catalyst, organocatalyst, phase-transfer catalyst, protecting groups, ionic liquid, surfactants, etc.), the use of these compounds in the industry is restricted due to their difficult recycling process [25–29]. Currently, the immobilization of a chiral organocatalyst on inorganic or organic supports, such as mesoporous materials [30–32], metals [33–36], layered compounds [37–39], polymers [40–47], peptides [48–54], and dendrimers [55], has been widely investigated; the immobilization of the amino acids and support offer a lot of advantages such as their use in industrial processes, which overcome unavoidable drawbacks of homogeneous catalytic processes. However, the immobilization of homogeneous chiral catalysts is accompanied by a loss in enantioselectivities or

SCHEME 1.9. Coupling of N-protected amino acids and N-, C-terminal unprotected amino acids with ISTA-X and silylating agents.
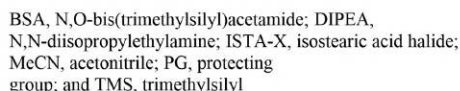
efficiencies and several applied cycles. Therefore, new types of heterogeneous catalytic systems need to be developed that offer enhanced selectivities and activities.

1.5.7. Switchable Aqueous Catalytic Systems for Organic Transformations

Catalytic systems based on the use of stimuli-responsive materials could be effectively switched "on" (stable) and "off" (unstable) by several external stimuli [56]. Switchable activity catalytic in aqueous environments offers new opportunities for developing intelligent materials for biomedicine and chemical biology. In a related example, Zhang et al. designed a pH-switchable artificial hydrolase using a catalytic histidine residue at the terminus of a pH-responsive peptide, VK2H (Scheme 1.10) [57]. The performances of the catalyst were studied for hydrolysis of *p*-nitrophenyl acetate (*p*NPA) at different pH values. The experimental result exhibited that catalytic activity can be influenced by pH-induced assembly/disassembly of the fibrils into random coils. By changing pH from acidic (pH 6.0) to basic (pH 9.0), the peptide showed a conformational change from random coil to β-sheet. Moreover, the phase behavior can be changed from gel to fluid, where the catalytically inactive state is observed for disassembled random coils.

1.5.8. Amino Acid–Based Self-Assembled Nanostructures

Amino acids are the simplest biomolecules that can self-assemble into different types of nanostructures such as fibers, vesicles, nanorods, nanoflakes, and nanotubes via several noncovalent interactions, including hydrogen bonding, electrostatic attraction, van der Waals forces, and aromatic stacking, thereby forming thermodynamically stable, ordered, hierarchical nanostructures (Figure 1.2) [58].
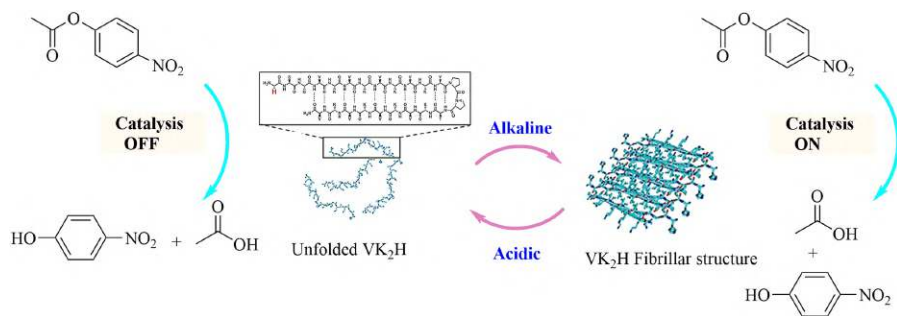
SCHEME 1.10. Schematic illustration of the pH-switchable VK$_2$H peptide as an artificial hydrolase.
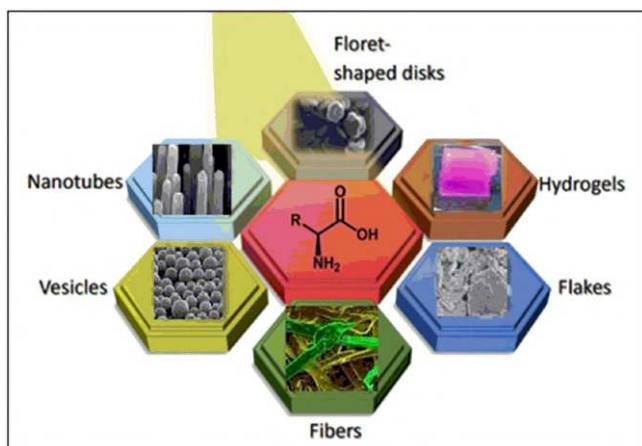
FIGURE 1.2. Production nanostructures via amino acid–assisted self-assembly. *Source:* Reproduced with permission from Ref. [58]. Copyright 2018, Wiley-VCH Verlag GmbH & Co. KGaA, Weinheim.

Silica is the most widely recognized among minerals and has received great attention due to its usefulness in industrial fields such as optical filters, pharmaceutical binders, photographic emulsions, chromatographic agents, sensing elements, catalysts, chemical and mechanical polishing materials, stabilizers, and coating layers [59]. Stöber method is an effective sol–gel strategy for the production of colloidal silica spheres by hydrolysis and condensation of silicon in alcoholic solvents in the presence of water and a base catalyst (e.g., NH$_3$). Recently, silica nanospheres (SNSs) were synthesized to undergo *hydrolysis and polycondensation reactions* of TEOS in the emulsion system containing TEOS, water, and basic amino acids such as lysine and arginine under weakly basic conditions (pH 9–10) [60].

1.6.   CONCLUSION

According to previous studies, amino acids are recognized as useful synthetic precursors for the synthesis of biologically active drugs, in synthetic organic chemistry as organocatalysts and ligands to tune reactivity and control selectivity. The preparation and designing of catalysts using amino acids as a building block led to the introduction of novel catalysts with outstanding properties in organic reactions. Replacement of metal complexes by organocatalysts caused longer reaction times, increased catalyst amounts and costs, and difficulties in recovery. To overcome these problems, the immobilization of amino acids on the supported materials has received considerably increasing interest in recent years and used in a variety of fields. Also, the functionalization of natural products and the application of amino acids can develop many properties. Therefore, amino acids have displayed potential medical applications due to their broad spectrum. This chapter provides a summary of the available literature survey and, based on this, we strongly believe that asymmetric organocatalysis will be increasingly employed by medicinal chemists to obtain enantiopure molecules from a green chemistry perspective.

REFERENCES

1. Zhang, D; Jing, X., Zhang, W., Nie, Y., Xu, Y. Highly selective synthesis of D-amino acids from readily available L-amino acids by a one-pot biocatalytic stereoinversion cascade. *RSC Adv.*, 2019, 9, 29927–29935. https://doi.org/10.1039/C9RA06301C.
2. Killian, J. A., von Heijne, G. How proteins adapt to a membrane-water interface. *Trends Biochem. Sci.*, 2000, *25*(9), 429–434. https://doi.org/10.1016/S0968-0004(00)01626-1.
3. Antosiewicz, J. M., Shugar, D. UV–Vis spectroscopy of tyrosine side-groups in studies of protein structure. Part 2: Selected applications. *Biophys. Rev.*, 2016, *8*, 163–177. https://doi.org/10.1007/s12551-016-0197-7.
4. Xu, Q., Deng, H., Li, X., Quan, Z. S. Application of amino acids in the structural modification of natural products: A review. *Front. Chem*., 2021, *9*, 650569. https://doi.org/10.3389/fchem.2021.650569.
5. Tao, G. H., He, L., Liu, W. S., Xu, L., Xiong, W., Wang, T., Kou, Y. Preparation, characterization and application of amino acid-based green ionic liquids. *Green Chem.*, 2006, *8*, 639. https://doi.org/10.1039/B600813E.
6. Balsamo, M., Erto, A., Lancia, A., Totarella, G., Montagnaro, F., Turco, R. Post-combustion CO_2 capture: on the potentiality of amino acid ionic liquid as a modifying agent of mesoporous solids. *Fuel.*, 2018, 218, 155–161.
7. Greaves, T. L., Drummond, C. J. Protic ionic liquids: Evolving structure-property relationships and expanding applications. *Chem. Rev.*, 2015, *115*(20), 11379–11448. (b) Yang, Q., Wang, Z., Bao, Z., Zhang, Z., Yang, Y., Ren, Q., Xing, H., Dai, S. New insights into CO_2 absorption mechanisms with amino-acid ionic liquids. *ChemSusChem.*, 2016, *9*(8), 806–812.
8. Tao, G.-H., He, L., Liu, W.-S., Xu, L., Xiong, W., Wang, T., Kou, Y. Preparation, characterization and application of amino acid-based green ionic liquids. *Green Chem.*, 2006, *8*(7), 639.

9. Zhou, H., Zhou, Y., Li, L., Li, Y., Liu, X., Zhao, P., Gao, B. Amino acid protic ionic liquids: multifunctional carbon precursor for N/S codoped hierarchically porous carbon materials toward super capacitive energy storage. *ACS Sustain. Chem. Eng.*, 2019, *7*(10), 9281–9290. https://doi.org/10.1021/acssuschemeng.9b00279.

10. Wang, X., Akhmedov, N. G., Duan, Y., Luebke, D., Hopkinson, D., Li, B. Amino acid-functionalized ionic liquid solid sorbents for post-combustion carbon capture. *ACS Appl. Mater. Interfaces.*, 2013, *5*(17), 8670–8677. https://doi.org/10.1021/am402306s.

11. Latini, G., Signorile, M., Rosso, F., Fin, A., d'Amora, M., Giordani, S., Bocchini, S. Efficient and reversible CO_2 capture in bio-based ionic liquids solutions. *J. CO_2 Util.*, 2022, *55*, 101815. https://doi.org/10.1016/j.jcou.2021.101815.

12. Chen, W., Zhang, Y., Zhu, L., Lan, J., Xie, R., & You, J. A concept of supported amino acid ionic liquids and their application in metal scavenging and heterogeneous catalysis. *J. Am. Chem. Soc.*, 2007, *129*(45), 13879–13886. https://doi.org/10.1021/ja073633n.

13. J. Tan and N. Yasuda, Contemporary asymmetric phase transfer catalysis: Large-scale industrial applications. *Org. Process Res. Dev.*, 2015, *19*, 1731–1746. https://doi.org/10.1021/acs.oprd.5b00304.

14. Liu, Y., Wei, Z., Liu, Y., Cao, J., Liang, D., Lin, Y., Duan, H. Novel α-amino acid-derived phase-transfer catalyst application to a highly enantio-and diastereoselective nitro-Mannich reaction. *Org. Biomol. Chem.*, 2017, *15*, 9234–9242. https://doi.org/10.1039/C7OB02501G.

15. Chen, Y., Mu, T. Revisiting greenness of ionic liquids and deep eutectic solvents. *GreenChE.*, 2021, *2*(2), 174–186. https://doi.org/10.1016/j.gce.2021.01.004.

16. Shavandi, A., Jafari, H., Zago, E., Hobbi, P., Nie, L., De Laet, N. A sustainable solvent based on lactic acid and l-cysteine for the regeneration of keratin from waste wool. *Green Chem.*, 2021, *23*(3), 1171–1174. https://doi.org/10.1039/D0GC04314A.

17. Pinheiro, L., Faustino, C. Amino acid-based surfactants for biomedical applications. *App. Char. Surf.*, 2017, *6*, 111–133. https://doi.org/10.5772/67977.

18. Nagaya, A., Murase, S., Mimori, Y., Wakui, K., Yoshino, M., Matsuda, A., Nishizawa, N. extended solution-phase peptide synthesis strategy using isostearyl-mixed anhydride coupling and a new C-terminal silyl ester-protecting group for N-methylated cyclic peptide production. *Org. Process Res. Dev.*, 2021, *25*(9), 2029–2038. https://doi.org/10.1021/acs.oprd.1c00078.

19. Fitznar, H. P., Lobbes, J. M., Kattner, G. Determination of enantiomeric amino acids with high-performance liquid chromatography and pre-column derivatisation with o-phthaldialdehyde and N-isobutyrylcysteine in seawater and fossil samples (Mollusks). *J. Chromatogr. A* 1999, *832*(1–2), 123–132.

20. Sibi, M. P., Itoh, K. Organocatalysis in conjugate amine additions. Synthesis of β-amino acid derivatives. *J. Am. Chem. Soc.* 2007, *129*(26), 8064–8065.

21. Rueping, M., Sugiono, E., Azap, C. A highly enantioselective Brønsted acid catalyst for the Strecker reaction. *Angew. Chemie Int. Ed.* 2006, *45*(16), 2617–2619.

22. Häussinger, D., Lames, W. H., Moorman, A. F. M. Hepatocyte heterogeneity in the metabolism of amino acids and ammonia. *Enzyme*, 1992, *46*, 72–93.

23. Ohno, H., Fukumoto, K. Amino acid ionic liquids. *Acc. Chem. Res.*, 2007, *40*(11), 1122–1129.

24. Severin, K., Bergs, R., Beck, W. Bioorganometallic chemistry-transition metal complexes with A -amino acids and peptides. *Angew. Chemie Int. Ed.*, 1998, *37*(12), 1634–1654.

25. Jarvo, E. R., Miller, S. J. Amino acids and peptides as asymmetric organocatalysts. *Tetrahedron*, 2002, *58*(13), 2481–2495.

26. Corey, E. J., Noe, M. C., Xu, F. Highly enantioselective synthesis of cyclic and functionalized α-amino acids using a chiral phase transfer catalyst. *Tetrahedron Lett.*, 1998, *39*(30), 5347–5350.

27. Isidro-Llobet, A., Alvarez, M., Albericio, F. Amino acid-protecting groups. *Chem. Rev.*, 2009, *109*(6), 2455–2504.

28. Morán, M. C., Pinazo, A., Pérez, L., Clapés, P., Angelet, M., García, M. T., Vinardell, M. P., Infante, M. R. "Green" amino acid-based surfactants. *Green Chem.*, 2004, *6*(5), 233–240.

29. White, R. J., Luque, R., Budarin, V. L., Clark, J. H., Macquarrie, D. J. Supported metal nanoparticles on porous materials. Methods and applications. *Chem. Soc. Rev.*, 2009, *38*(2), 481–494.

30. Reddy, E. P., Davydov, L., Smirniotis, P. TiO_2-loaded zeolites and mesoporous materials in the sonophotocatalytic decomposition of aqueous organic pollutants: The role of the support. *Appl. Catal. B Environ.*, 2003, *42*(1), 1–11. https://doi.org/10.1016/S0926-3373(02)00192-3.

31. Walcarius, A. Mesoporous materials-based electrochemical sensors. *Electroanalysis*, 2015, *27*(6), 1303–1340.

32. Taguchi, A., Schüth, F. Ordered mesoporous materials in catalysis. *Microporous Mesoporous Mater.*, 2005, *77*(1), 1–45. https://doi.org/10.1016/j.micromeso.2004.06.030.

33. Haller, G. L., Resasco, D. E. Metal–support interaction: Group VIII metals and reducible oxides. *Adv. Catal.*, 1989, *36*(C), 173–235. https://doi.org/10.1016/S0360-0564(08)60018-8.

34. Kubička, D., Kumar, N., Venäläinen, T., Karhu, H., Kubičková, I., Österholm, H., Murzin, D. Y. Metal-support interactions in zeolite-supported noble metals: Influence of metal crystallites on the support acidity. *J. Phys. Chem. B*, 2006, *110*(10), 4937–4946. https://doi.org/10.1021/jp055754k.

35. Regmi, Y. N., Waetzig, G. R., Duffee, K. D., Schmuecker, S. M., Thode, J. M., Leonard, B. M. Carbides of group IVA, VA and VIA transition metals as alternative HER and ORR catalysts and support materials. *J. Mater. Chem.*, 2015, *3*(18), 10085–10091. https://doi.org/10.1039/c5ta01296a.

36. Mohammadi, M., Khodamorady, M., Tahmasbi, B., Bahrami, K., Ghorbani-Choghamarani, A. Boehmite nanoparticles as versatile support for organic–inorganic hybrid materials: Synthesis, functionalization, and applications in eco-friendly catalysis. *J. Ind. Eng. Chem.*, 2021, *97*, 1–78. https://doi.org/10.1016/j.jiec.2021.02.001.

37. Nyabadza, A., Shan, C., Murphy, R., Vazquez, M., Brabazon, D. Laser-synthesised magnesium nanoparticles for amino acid and enzyme immobilisation. *OpenNano*, 2023, *11*, 100133. https://doi.org/10.1016/j.onano.2023.100133.

38. Lazarin, A. M., Airoldi, C. Layered crystalline barium phenylphosphonate as host support for N-alkylmonoamine intercalation. *J. Incl. Phenom.*, 2005, *51*(1), 33–40. https://doi.org/10.1007/s10847-004-5391-8.

39. Yue, X., Zhang, T., Yang, D., Qiu, F., Li, Z., Zhu, Y., Yu, H. Oil removal from oily water by a low-cost and durable flexible membrane made of layered double hydroxide nanosheet on cellulose support. *J. Clean. Prod.*, 2018, *180*, 307–315. https://doi.org/10.1016/j.jclepro.2018.01.160.

40. Zhang, W., Zhang, Y., Wang, R., Zhang, P., Zhang, Y., Randell, E., Jia, Q. A review: Development and application of surface molecularly imprinted polymers toward amino acids, peptides, and proteins. *Analytica Chimica Acta*, 2022, 340319. https://doi.org/10.1016/j.aca.2022.340319.

41. Leiske, M. N., Mazrad, Z. A., Zelcak, A., Wahi, K., Davis, T. P., McCarroll, J. A., Kempe, K. Zwitterionic amino acid-derived polyacrylates as smart materials exhibiting cellular specificity and therapeutic activity. *Biomacromolecules*, 2022, *23*, 2374–2387. https://doi.org/10.1021/acs.biomac.2c00143.

42. Kavya, K. V., Vargheese, S., Shukla, S., Khan, I., Dey, D. K., Bajpai, V. K., Haldorai, Y. A cationic amino acid polymer nanocarrier synthesized in supercritical CO_2 for co-delivery of drug and gene to cervical cancer cells. *Colloids Surf. B*, 2022, *216*, 112584. https://doi.org/10.1016/j.colsurfb.2022.112584.

43. Li, C., You, X., Xu, X., Wu, B., Liu, Y., Tong, T., Zhao, M. A metabolic reprogramming amino acid polymer as an immunosurveillance activator and leukemia targeting drug carrier for T-cell acute lymphoblastic leukemia. *Adv. Sci.*, 2022, *9*(9), 2104134. https://doi.org/10.1002/advs.202104134.

44. Wu, Y., Chen, K., Wang, J., Chen, M., Chen, Y., She, Y., Liu, R. Host defense peptide mimicking antimicrobial amino acid polymers and beyond: design, synthesis and biomedical applications. *Prog. Polym. Sci.*, 2023, 101679. https://doi.org/10.1016/j.progpolymsci.2023.101679.

45. Sawamoto, A., Nishimura, S. N., Higashi, N., Koga, T. Synthesis of amino acid-derived vinyl polymers with precisely controlled hydropathy and their thermoresponsive behavior in water. *Polym. Chem.*, 2023. https://doi.org/10.1039/D3PY00353A.

46. Bera, A., Ghosh, P., Goswami, K., De, P. Amino acid-based polymer-coated silver nanoparticles as insulin fibril inhibitors. *ACS Appl. Nano Mater.*, 2023. https://doi.org/10.1021/acsanm.3c01078.

47. Aslani, R., Namazi, H. Fabrication of a new photoluminescent and pH-responsive nanocomposite based on a hyperbranched polymer prepared from amino acid for targeted drug delivery applications. *Int. J. Pharm.*, 2023, *636*, 122804. https://doi.org/10.1016/j.ijpharm.2023.122804.

48. Grasso, P., Leinung, M. C., Ingher, S. P., Lee, D. W. In vivo effects of leptin-related synthetic peptides on body weight and food intake in female ob/ob mice: Localization of leptin activity to domains between amino acid residues 106–140. *Endocrinology*, 1997, *138*(4), 1413–1418. https://doi.org/10.1210/endo.138.4.5087.

49. Navab, M., Anantharamaiah, G. M., Hama, S., Garber, D. W., Chaddha, M., Hough, G., Fogelman, A. M. Oral administration of an Apo AI mimetic Peptide synthesized from D-amino acids dramatically reduces atherosclerosis in mice independent of plasma cholesterol. *Circulation*, 2002, *105*(3), 290–292. https://doi.org/10.1161/hc0302.103711.

50. Wang, X., Li, J., Hayashi, Y. Highly sterically hindered peptide bond formation between α, α-disubstituted α-amino acids and N-alkyl cysteines using α, α-disubstituted α-amidonitrile. *J. Am. Chem. Soc.*, 2022, *144*(23), 10145–10150. https://doi.org/10.1021/jacs.2c02993.

51. Yang, Y., Hansen, L., Baldi, A. Suppression of simultaneous Fmoc-His (Trt)-OH racemization and N α-DIC-endcapping in solid-phase peptide synthesis through design of experiments and its implication for an amino acid activation strategy in peptide synthesis. *Org. Process Res. Dev.*, 2022, *26*(8), 2464–2474. https://doi.org/10.1021/acs.oprd.2c00144.

52. Parfenova, L. V., Galimshina, Z. R., Gil'fanova, G. U., Alibaeva, E. I., Danilko, K. V., Aubakirova, V. R., Valiev, R. Z. Modeling of biological activity of PEO-coated titanium implants with conjugates of cyclic RGD peptide with amino acid bisphosphonates. *Materials*, 2022, *15*(22), 8120. https://doi.org/10.3390/ma15228120.

53. Zhang, Y., Hu, Z., Li, X., Ding, Y., Zhang, Z., Zhang, X., Yang, Z. Amino acid sequence determines the adjuvant potency of AD-tetra-peptide hydrogel. *Biomater. Sci.*, 2022, *10*(12), 3092–3098. https://doi.org/10.1039/D2BM00263A.

54. Ghorbani-Choghamarani, A., Taherinia, Z., Heidarnezhad, Z., Moradi, Z. Application of nanofibers based on natural materials as catalyst in organic reactions. *J. Ind. Eng. Chem.*, 2021, *94*, 1–61. https://doi.org/10.1016/j.jiec.2020.10.028.

55. Sheveleva, N. N., Tarasenko, I. I., Vovk, M. A., Mikhailova, M. E., Neelov, I. M., Markelov, D. A. NMR Studies of two lysine based dendrimers with insertion of similar histidine-arginine and arginine-histidine spacers having different properties for application in drug delivery. *Int. J. Mol. Sci.*, 2023, *24*(2), 949. https://doi.org/10.3390/ijms24020949.

56. Ghorbani-Choghamarani, A., Taherinia, Z. Recent advances utilized in artificial switchable catalysis. *RSC Adv.*, 2022, *36*, 23595–23617. https://doi.org/10.1039/D2RA03842K.

57. Zhang, C., Shafi, R., Lampel, A., MacPherson, D., Pappas, C. G., Narang, V., Ulijn, R. V. Switchable hydrolase based on reversible formation of supramolecular catalytic site using a self-assembling peptide. *Angew. Chem. Int. Ed.*, 2017, *56*(46), 14511–14515. https://doi.org/10.1002/anie.201708036.

58. Chakraborty, P., Gazit, E. Amino acid based self-assembled nanostructures: Complex structures from remarkably simple building blocks. *ChemNanoMat*, 2018, *4*(8), 730–740. https://doi.org/10.1002/cnma.201800147.

59. Choi, K. M., Kuroda, K. Double function of tris (hydroxymethyl) aminomethane (THAM) for the preparation of colloidal silica nanospheres and the conversion to ordered mesoporous carbon. *ChemComm.*, 2011, *47*(39), 10933–10935. https://doi.org/10.1039/C1CC14743A.

60. Yokoi, T., Wakabayashi, J., Otsuka, Y., Fan, W., Iwama, M., Watanabe, R., Okubo, T. Mechanism of formation of uniform-sized silica nanospheres catalyzed by basic amino acids. *Chem. Mater.*, 2009, *21*(15), 3719–3729. https://doi.org/10.1021/cm900993b.

2 The Catalytic Role of L-Arginine in Organic Reactions

2.1. INTRODUCTION

The performance of amino acids and their derivatives as organocatalysts has led to the development of green and sustainable heterogeneous catalytic systems, such as organocatalyst-immobilized solid inorganic supports, for efficient and selective synthesis of optically pure compounds in various organic reactions. Herein, we provide a recent overview of reactions where amino acids are used as catalysts and organocatalysts in organic reactions.

2.2. CATALYTIC APPLICATION OF L-ARGININE-CONTAINING SOLID SUPPORTS IN THE MULTICOMPONENT REACTIONS

L-Arginine-based supported and unsupported catalysis has been applied in various organic functional group transformations [1]. In 2022, Khabnadideh et al. described the performance of L-arginine-immobilized graphene oxide (GO-Arg) for the one-pot preparation of benzo[*b*]pyran and pyrano[3,2-*c*] chromene derivatives in ethanol/water as a green and eco-friendly solvent with desirable yields [2]. The experimental results showed that aldehydes with electron-poor aryl halides produced desired products at higher rates within a short reaction time (Scheme 2.1).

A three-component reaction between malononitrile, benzaldehyde derivatives, and β-nitrostyrene derivatives using $CoFe_2O_4@SiO_2@$L-arginine magnetic nanoparticles (MNPs) was reported [3]. This method offers several advantages such as easy separation, recyclability of catalyst, short reaction time, and high yields (Scheme 2.2).

In 2020, Amirnejat et al. reported $Fe_3O_4@Alg@CPTMS@Arg$-catalyzed multicomponent reaction involving a domino reaction of ammonium acetate, aldehyde derivatives, and benzil under reflux in ethanol. Nanocatalyst was achieved by direct insertion of magnetic and alginate. Thereafter, the solid product was modified with tetraethylorthosilicate (TEOS) as the silica source and arginine to afford $Fe_3O_4@Alg@CPTMS@Arg$ (Scheme 2.3) [4]. The multicomponent reactions were found to give better yields with electron-rich groups than with electron-poor groups on aryl bromides (Scheme 2.4).

Zarnegar et al. reported the decoration of starch nanoparticles with arginine amino acid (Scheme 2.5) [5]. Thereafter, the activity of the catalyst for a three-component

reaction between methylcarbonyls, thiourea, and iodine in DMSO has been considered by the authors (Schemes 2.6).

The proposed mechanism for the synthesis of diheteroaryl thioethers is described in Scheme 2.7.

One-pot synthesis of pyrazole derivatives, via cyclocondensation reaction of various aldehydes, malononitrile, and phenylhydrazine catalyzed by Fe_3O_4@Alg@ CPTMS@Arg in EtOH as solvent has been presented in Scheme 2.8 [6].

The mentioned nanocatalyst was prepared via the layer-by-layer techniques by immobilizing alginate (Alg) and ferric salts to produce Fe_3O_4@Alg that reacted with 3-chloropropyltrimethoxysilane (CPTMS) in the next step. Finally, connection with L-Arginine produces desired magnetic nanocatalyst (Scheme 2.9) [6].

In a related example, the performance of Fe_3O_4@L-arginine was studied for the preparation of 1,3-diphenyl-2-azaphenalene and n-acyl-1,3-diaryl 2-N-azaphenylene derivatives by a combination of 2,7-naphthalenediol, aromatic aldehydes, and ammonium salts (ammonium acetate or ammonium hydrogen phosphate) in a mixture of EtOH and H_2O (Scheme 2.10) [7]. Only poor yield was obtained in the absence of
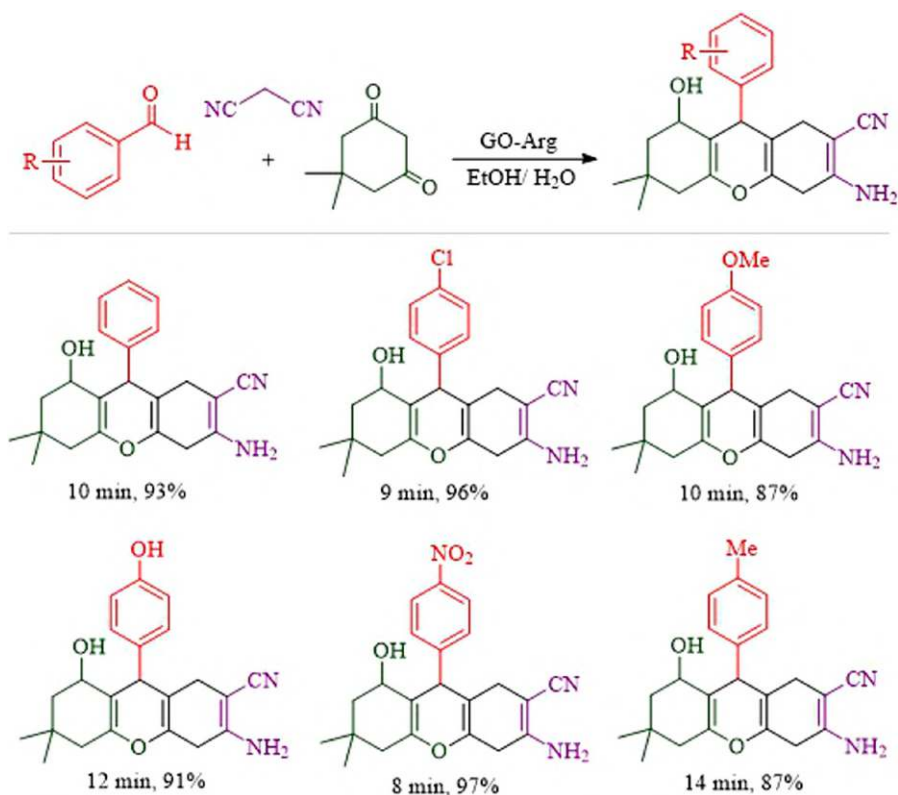
SCHEME 2.1. GO-Arg catalyzed the preparation of benzo[b]pyrans and pyrano[3,2-c] chromenes.
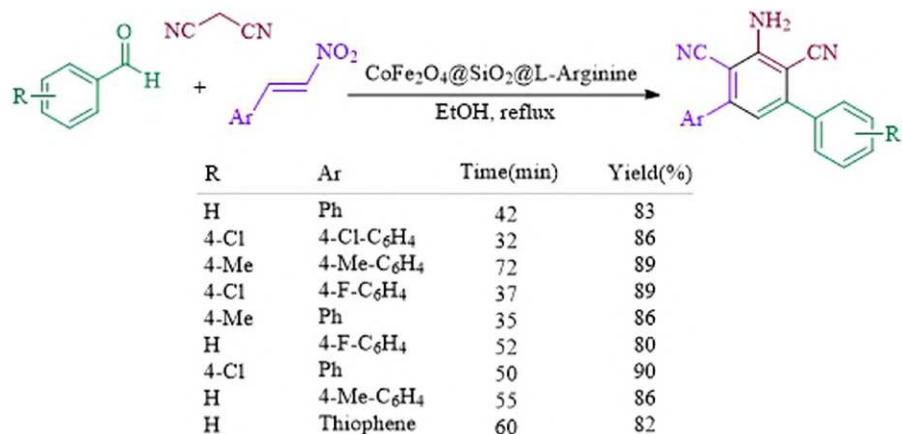
SCHEME 2.2.   CoFe$_2$O$_4$@SiO$_2$@L-arginine catalyzed multicomponent reaction.
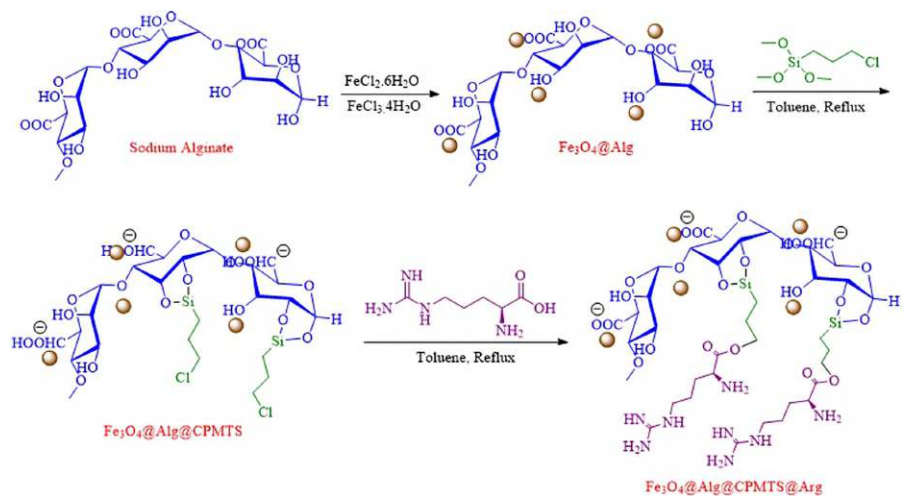
SCHEME 2.3.   Synthesis of Fe$_3$O$_4$@Alg@CPTMS@Arg magnetic nanocomposite.

the catalyst. This system is effective for a variety of aldehydes that result in products with excellent yields.

Ghasemzadeh et al. demonstrated the synthesis of spiropyranopyrazoles using Fe$_3$O$_4$@L-arginine under solvent-free conditions via the combination of hydrazines, β-keto esters, isatins, and malononitrile or ethyl cyanoacetate (Scheme 2.11) [8]. The system is compatible with isatins including either electron-poor groups or electron-rich groups under solvent-free conditions. In addition, the reaction failed without a catalyst.
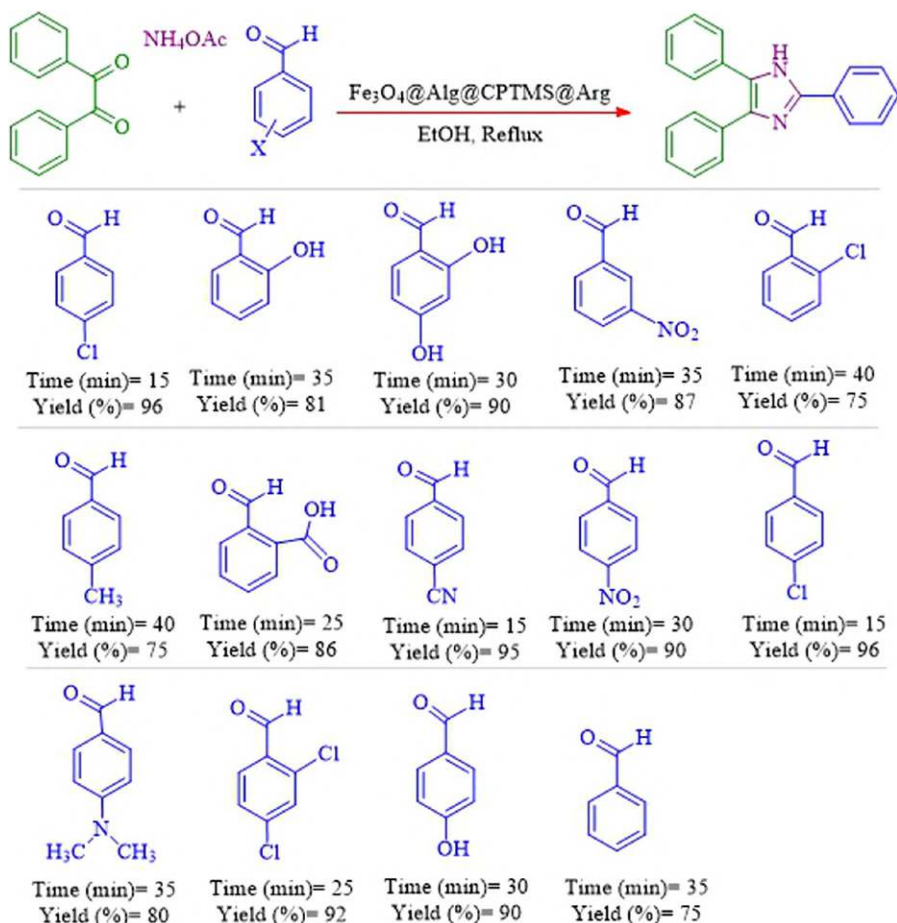
SCHEME 2.4. The preparation of 2,4,5-triaryl-1H-imidazoles using magnetic nanocatalyst.

Moreover, the authors reported the proposed mechanism for the synthesis of spiro[indolline-3,4-pyrano[2,3-C] pyrazole], as outlined in Scheme 2.12.

The synthesis of thiazolo[3,2- a]pyrimidine in EtOH via a four-component reaction between 4-dihydropyrimidine-2(1H)-thiones, various aromatic aldehydes and chloroacetyl chloride was accomplished using Fe_3O_4@L-arginine, as reported by Afradi et al. [9]. Experimental results showed the reaction of this system was compatible with various aldehydes in the one-pot multicomponent reaction to yield the corresponding product in excellent yields (Schemes 2.13 and 2.14).

In another research, Fe_3O_4 modified with L-arginine (Fe_3O_4@L-arginine NPs) investigated for multicomponent reactions leading to the synthesis of chromene derivatives via cyclocondensation of α- or β-naphthol, malononitrile, and aromatic aldehydes under ultrasound irradiation [10]. The experimental result showed all reactions progressed and led to the final products in good yield (Scheme 2.15).
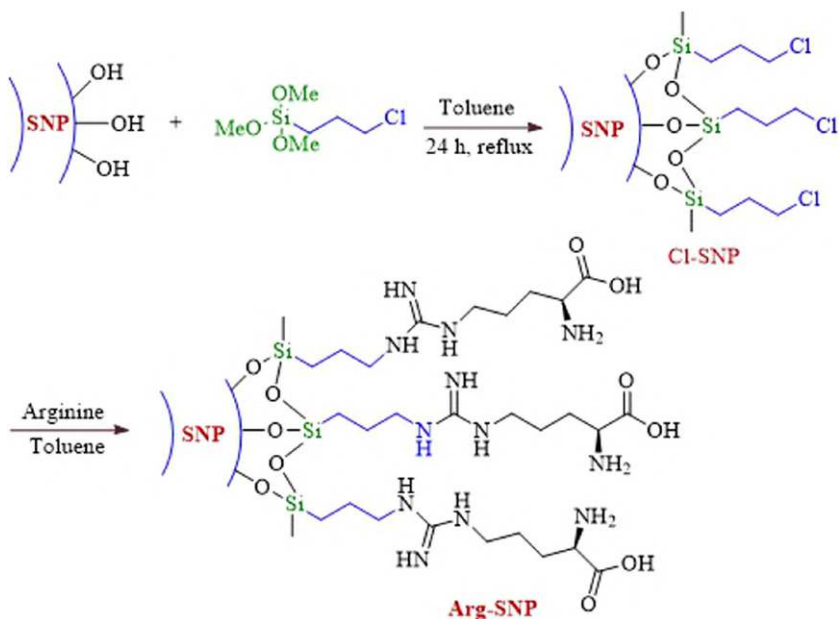
SCHEME 2.5.   The preparation of Arg-SNPs.
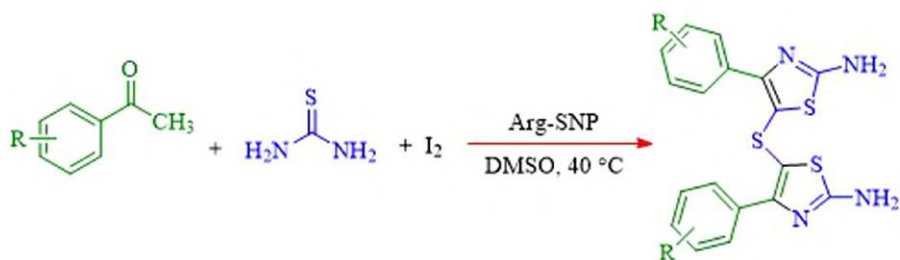
R: H, 4-OH, 2-OH, 4-Br, 4-Cl, 4-Me, 3-Me, 4-OMe, 4-NO₂, 4-Morpholin
Yield (%): 96, 72, 70, 79, 76, 97, 91, 98, 90, 99

SCHEME 2.6.   Arg-SNP catalyzed preparation of diheteroaryl thioether.

2.3.   APPLICATION OF METAL COMPLEXES OF L-ARGININE-CONTAINING SUPPORTED MATERIAL AS A CATALYST IN THE MULTICOMPONENT REACTION

Our group has recently reported a sustainable protocol for the preparation of 5-substituted 1*H*-tetrazole derivatives under green conditions (Scheme 2.16) [11]. In this system, Pd-Arg@boehmite was applied as a heterogeneous catalyst. The catalyst was prepared in several steps: initially, Boehmite was prepared by the precipitation
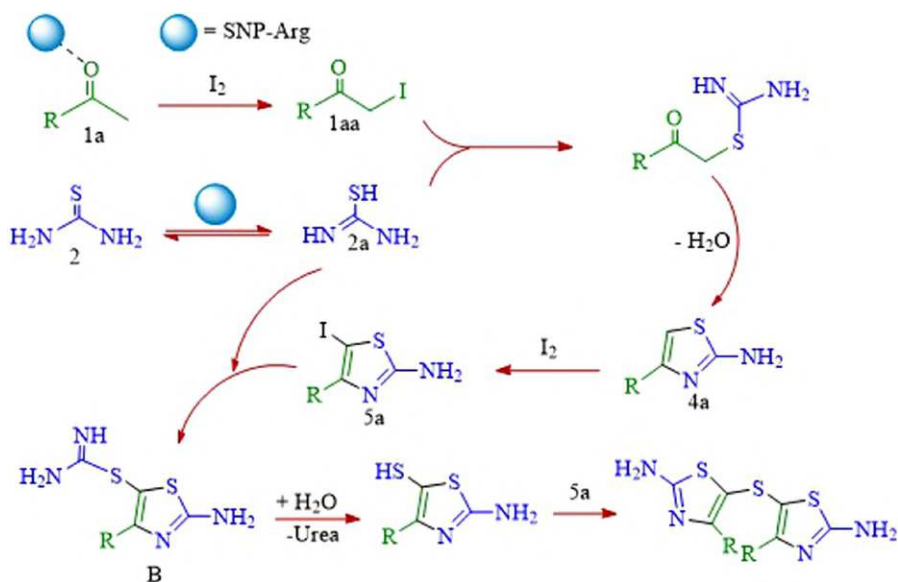
SCHEME 2.7. A plausible mechanism for the synthesis of diheteroaryl thioethers.
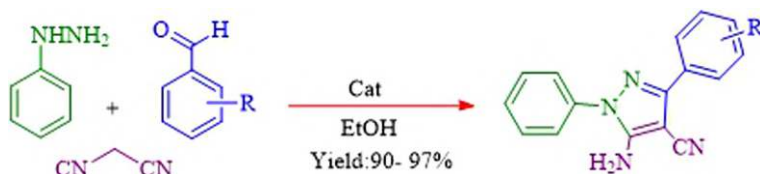
SCHEME 2.8. Fe_3O_4@Alg@CPTMS@Arg catalyzed the preparation of pyrazoles.

method, followed by modification with arginine, coordination of palladium, and reduction of palladium (II) into palladium (0) with $NaBH_4$ (Scheme 2.17). The resulting nanoparticles were quite homogeneous with obtained diameters in the range of 20–25 nm. The leaching study of palladium, performed using a hot filtration test and ICP-OES analysis, showed that the amount of palladium decreased slightly from the first to the sixth run (from 1.35 mmol g^{-1} to 1.26 mmol g^{-1}).

Ghadari et al. described a green protocol for the synthesis of 2-phenyl benzimidazole derivatives using $Cu_{0.5}Co_{0.5}Fe_2O_4$@Arg-GO and $Ni_{0.5}Co_{0.5}Fe_2O_4$@Arg-GO as the separable and reusable heterogeneous catalysts (Schemes 2.18–2.20) [12, 13]. The material was synthesized in several steps. Initially, graphene oxide (GO) support was modified with L-arginine. Subsequently, Arg-GO was treated with $FeCl_3 \cdot 6H_2O$, $CoCl_2 \cdot 6H_2O$, and $CuCl_2 \cdot 2H_2O$ or $NiCl_2 \cdot 6H_2O$ at room temperature and sonicated for 1 h; thereafter, the temperature was raised to 80 °C for 30 min. Finally, the addition of NaOH solution (0.1 M) to the reaction mixture (to obtain pH 10) afforded $Cu_{0.5}Co_{0.5}Fe_2O_4$@Arg-GO and/or $Ni_{0.5}Co_{0.5}Fe_2O_4$@Arg-GO nanocatalysts.
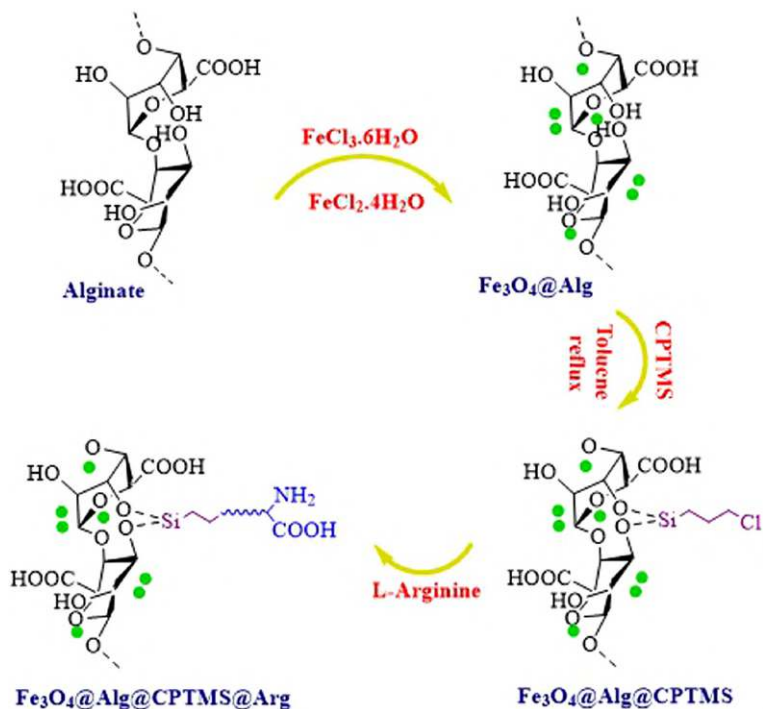
SCHEME 2.9.   Preparation of Fe$_3$O$_4$@Alg@CPTMS@Arg.
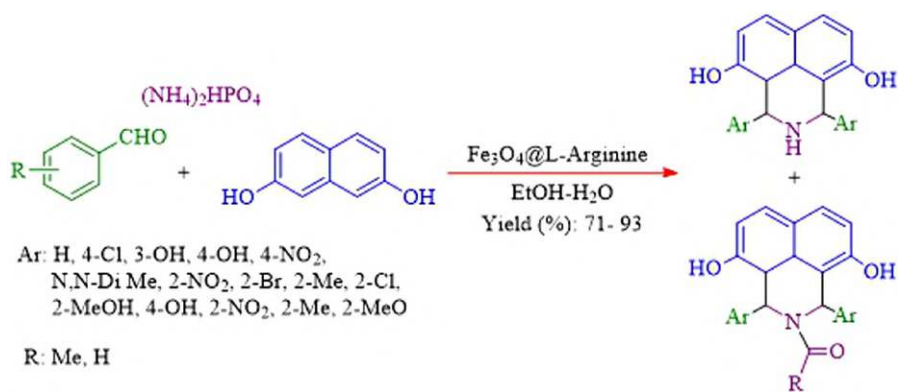
SCHEME 2.10.   Multicomponent one-pot reaction catalyzed using Fe$_3$O$_4$@L-arginine.

R_1= H, Ph R_3= H, Br, Cl, CH_3 Yield (%): 85-97
R_2= Ph, CH_3 R_4= CN, $CO_2C_2H_5$
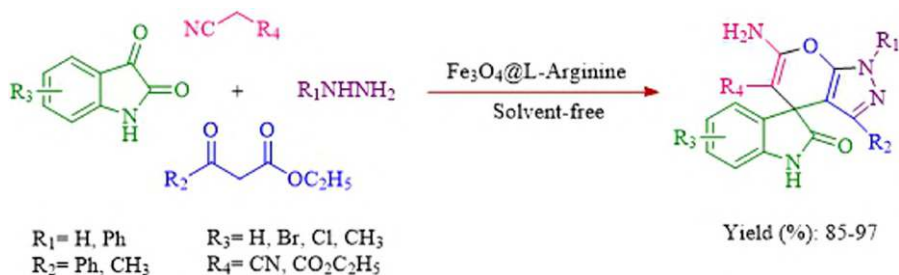
SCHEME 2.11. Fe$_3$O$_4$@L-arginine catalyzed synthesis of multicomponent reaction.
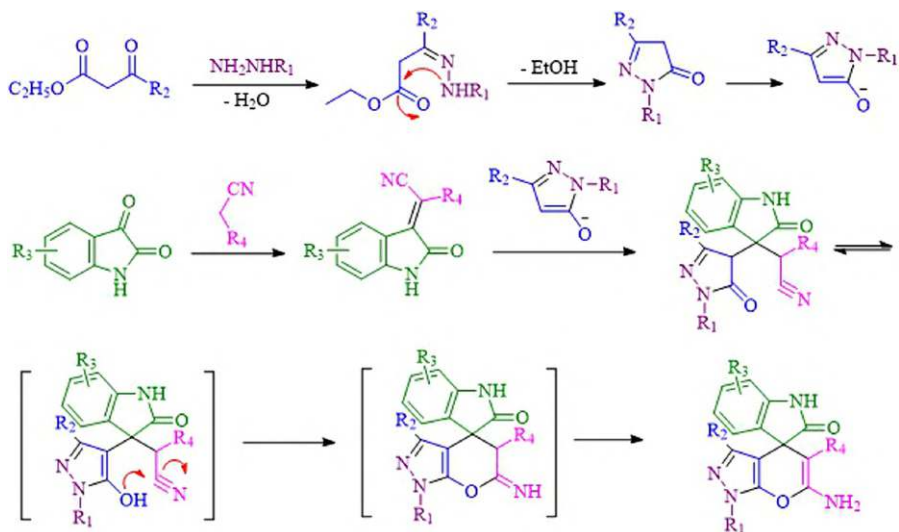
SCHEME 2.12. The proposed mechanism for the synthesis of spiro[indolline-3,4-pyrano[2,3-C] pyrazole.

Our laboratory has recently reported the use of a Cu(II) modified on Fe$_3$O$_4$@ SiO$_2$@L-Arginine for the preparation of 5-substituted-1H-tetrazoles under mild reaction conditions in polyethylene glycol (PEG), (Schemes 2.21 and 2.22) [14]. Only a trace amount of the product was obtained in the absence of the catalyst. The reaction's scope was studied with nitriles bearing diverse substituents, including halogens, nitro, hydroxyl, acetyl, isopropyl, and MeO, to yield desired products in excellent yields (60–98%). The magnetic nanocatalyst could be removed with an external magnet and reused for at least four consequence runs without a significant decrease in the catalyst activity.
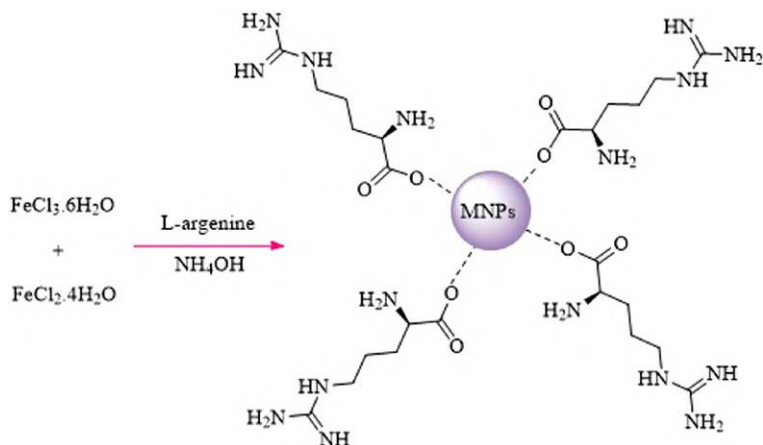
SCHEME 2.13.   Preparation of Fe_3O_4@L-arginine.

R: H, 2-Cl, 4-Cl, 2-OH
4-OH, 2-CH₃, 4-CH₃
3-NO₂, 2-NO₂, 4-OCH₃

R₁: 4-OCH₃, 3-NO₂, 4-CH₃
3-NO₂, 4-OH, 4-Cl, 4-CH₃
4-Cl, 2-NO₂, 3-NO₂

Yield (%): 67- 71
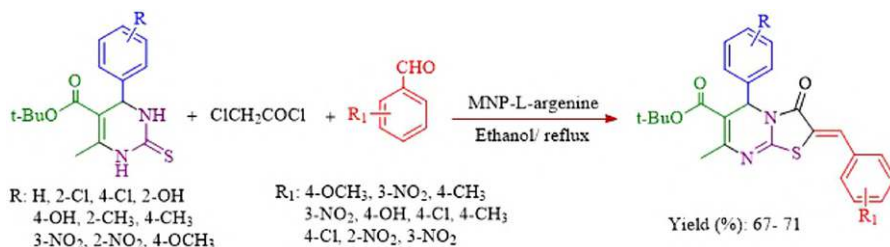
SCHEME 2.14.   Application of Fe_3O_4@L-arginine for thiazolo[3,2- *a*]pyrimidine derivatives.

2.4.   APPLICATION OF L-ARGININE AS AN ORGANOCATALYST IN KNOEVENAGEL CONDENSATION

Knoevenagel condensations were achieved by L-arginine as an organocatalyst, and the versatility was demonstrated using aromatic, heteroaromatic, or α,β-unsaturated aldehydes with malononitrile and/or acetylacetone to afford α,β-unsaturated nitriles and ketones in 1-ethyl-3-methylimidazolium ethyl sulfate (Scheme 2.23) [15]. Experimental results showed that the product was produced in good yield (45–100%). In addition, L-arginine/ionic liquid was easily removed (water removed through vacuum distillation from the reaction mixture) and recycled five times, without any loss of catalytic performance.

2.5.   APPLICATION OF L-ARGININE DERIVATIVE AS AN ORGANOCATALYST IN A CONDENSATION REACTION

One way to activate amino acids is the protonation of basic α-amino acids with Brønsted acids. In this context, Lombardo et al. have demonstrated a symmetric
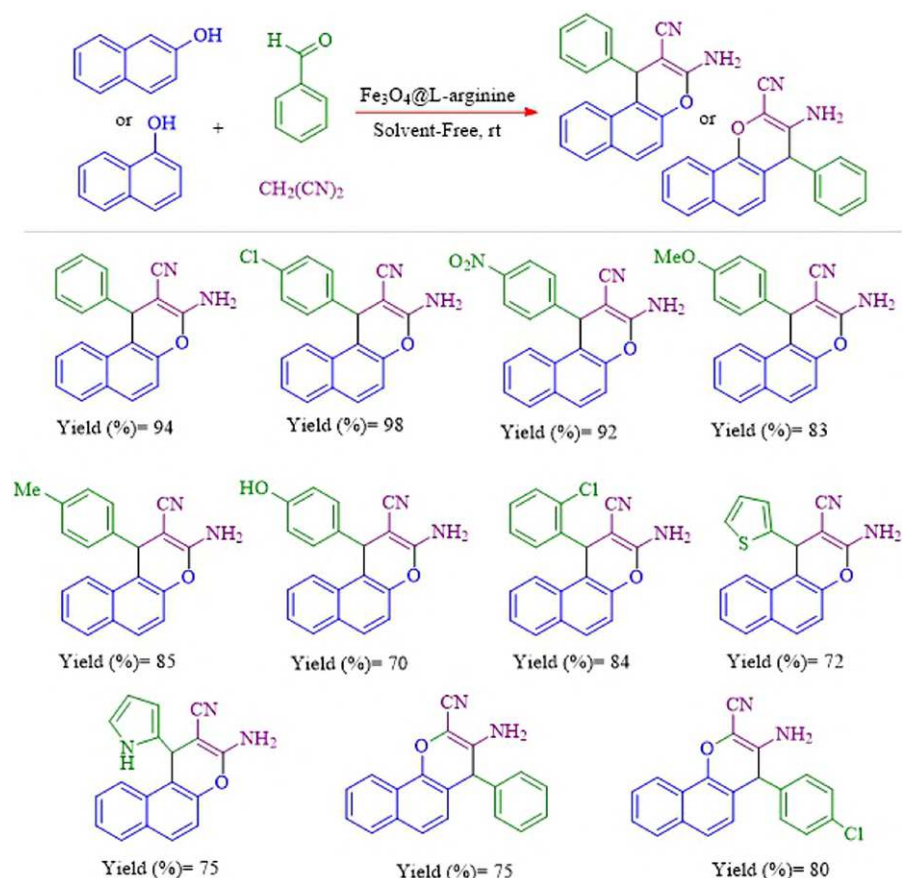
SCHEME 2.15. Application of Fe$_3$O$_4$@L-arginine for preparation of multicomponent reaction.

cross-aldol reaction of cyclic ketones with aromatic aldehydes in ionic liquids and DMSO. Experimental studies show the lowest reaction rate was obtained in *N*-butyl-*N*-methyl pyrrolidinium bis(trifluoromethane)sulfonamide[bmpy][Tf$_2$N] and the best *anti/syn* diastereomeric ratio (dr) was achieved in [bmim][N(CN)$_2$]. Control experiments showed that reasonable yields could be obtained with ee's in DMSO solvent. Thereafter, the reaction's scope was remarkably broad using various ketones and aromatic aldehydes. Under these conditions, a variety of ketones and aromatic aldehydes were examined and final products were synthesized in good to excellent yields (Scheme 2.24) [16]. The catalysts could be removed using a liquid/liquid phase separation without any loss of activity.

In 2008, the reactivity of arginine was reported to catalyze direct aldol reactions. The arginine exhibited high activity for the reactions of the electron-deficient benzaldehydes with ketones in pure water, efficiently promoting the consideration to provide the desired product (Scheme 2.25) [17].
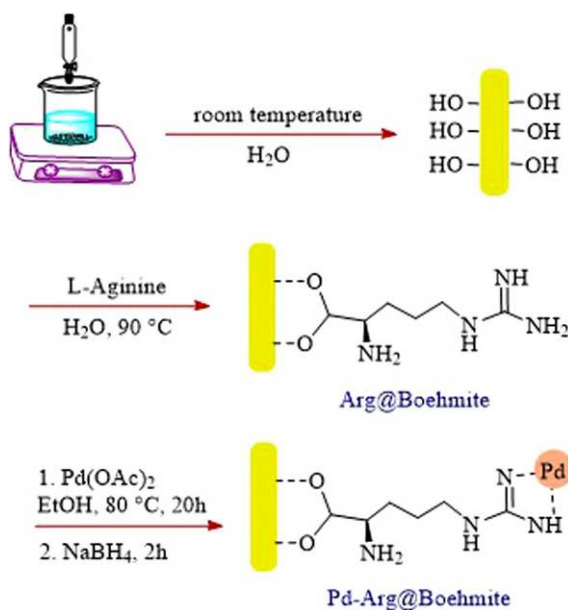
SCHEME 2.16. Preparation of Pd-Arg@boehmite.
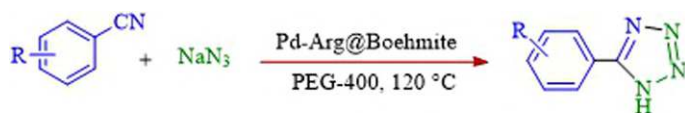
Nitrile	Time (h)	Yield(%)
Benzonitrile	7	97
4-Nitobenzonitile	3	96
4-Acetylbenzonitrile	24	90
3-Chlorobenzonitrile	8	91
2-Chlorobenzonitrile	3	91
2-Hydroxybenzonitrile	7	90
Terephthalonitrile	6	85
3-Nitrobenzonitrile	8	89
4-Hydroxybenzonitrile	4	95
4-Chlorobenzonitrile	5	90
2-Benzylidenemalononitrile	24	73
2-(4-Nitrobenzylidene)malononitrile	22	75
2-Phenylacetonitrile	24	74
Malononitrile	3	91
[1,1-Biphenyl]-4-carbonitrile	24	69
4-Methoxybenzonitrile	26	78

SCHEME 2.17. Application of Pd-Arg@boehmite in the synthesis of 5-substituted 1*H*-tetrazoles.
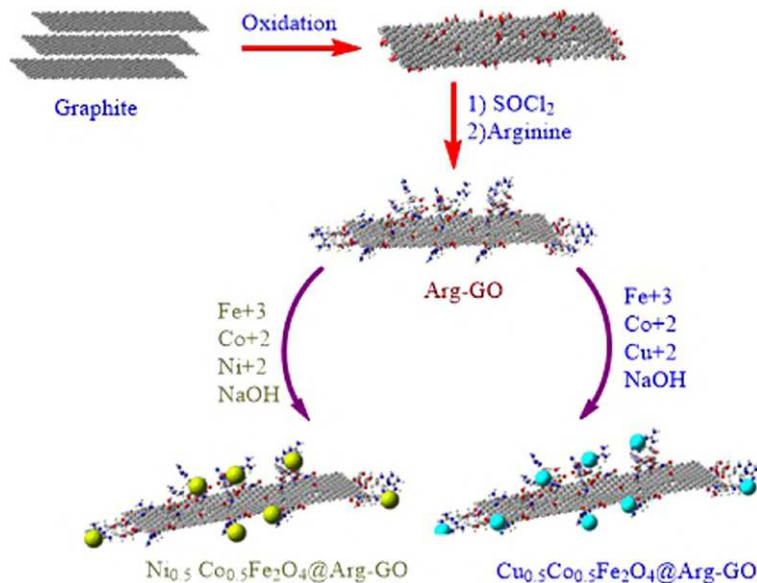
SCHEME 2.18. Synthesis of $Cu_{0.5}Co_{0.5}Fe_2O_4$@Arg-GO, and $Ni_{0.5}Co_{0.5}Fe_2O_4$@Arg-GO nanocatalysts.

Damine	Alcohol	Yield(%)
O-Phenylenediamine	Benzyl alcohol	79
O-Phenylenediamine	2-Methylbenzyl alcohol	81
O-Phenylenediamine	2-Methylbenzyl alcohol	89
O-Phenylenediamine	4-Bromobenzyl alcohol	90
O-Phenylenediamine	2-Methoxybenzyl alcohol	88
O-Phenylenediamine	4-Methoxybenzyl alcohol	91
O-Phenylenediamine	4-Chlorobenzyl alcohol	87
O-Phenylenediamine	2-Nitrobenzyl alcohol	90
O-Phenylenediamine	4-Nitrobenzyl alcohol	93
4-Methyl-O-Phenylenediamine	Benzyl alcohol	85
4-Methyl-O-Phenylenediamine	2-Chlorobenzyl alcohol	81

SCHEME 2.19. Application of Ni0.5Co0.5Fe$_2$O$_4$@Arg-GO nanocomposite for the oxidative synthesis of 2-phenyl benzimidazole derivatives.

Damine	Alcohol	Yield (%)
O-Phenylenediamine	Benzyl alcohol	82
O-Phenylenediamine	2-Methylbenzyl alcohol	85
O-Phenylenediamine	2-Methoxybenzyl alcohol	91
O-Phenylenediamine	2-Nitrobenzyl alcohol	92
O-Phenylenediamine	3-Methylbenzyl alcohol	78
O-Phenylenediamine	3-Bromobenzyl alcohol	84
O-Phenylenediamine	4-Methylbenzyl alcohol	92
O-Phenylenediamine	4-Bromobenzyl alcohol	88
O-Phenylenediamine	4-Methoxybenzyl alcohol	90
O-Phenylenediamine	4-Chlorobenzyl alcohol	90
O-Phenylenediamine	4-Nitrobenzyl alcohol	94
O-Phenylenediamine	3,4-Dimethoxybenzyl alcohol	95
4-Methyl-O-Phenylenediamine	Benzyl alcohol	82
4-Methyl-O-Phenylenediamine	2-Chlorobenzyl alcohol	86

SCHEME 2.20. $Cu_{0.5}Co_{0.5}Fe_2O_4$@Arg-GO nanocomposite catalyzed oxidative synthesis of 2-phenyl benzimidazole derivatives.
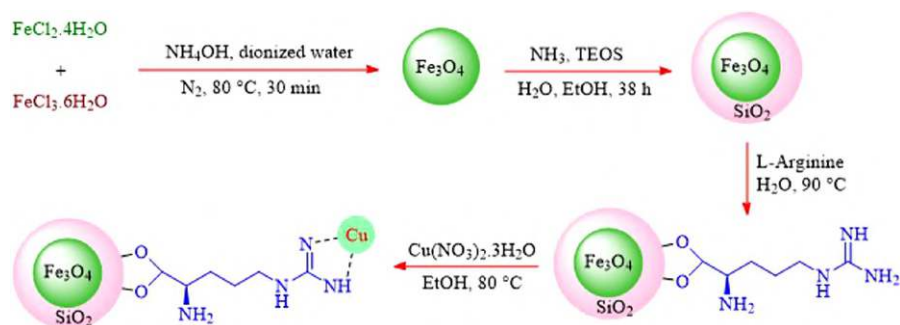
SCHEME 2.21. The preparation of Cu(II) on Fe_3O_4@SiO_2@L-arginine.

The catalytic system of arginine was investigated for the aldolization of methyl vinyl ketone in water. Under the standard conditions, different aldehydes were examined and it was shown to accommodate structurally and electronically diverse aldehydes as well as isatins (Scheme 2.26) [18].

2.6. APPLICATION OF L-ARGININE-CONTAINING IONIC LIQUID IN THE MULTICOMPONENT REACTION

In 2019, the activity of Fe_3O_4@PS-Arg[HSO_4] MNPs is used for the one-pot reaction of α-naphthyl amine, aromatic aldehydes, and malononitrile (or dimedone) to afford

R$_1$= 3-Cl, 2-OH, 4-NO$_2$, 3-NO$_2$, 4-Cl,
4-Br, CN, H, Isopropyl, Acetyl, MeO

Yield (%): 60- 95
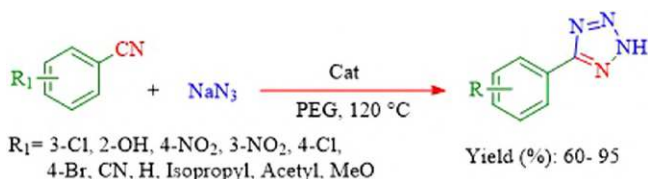
SCHEME 2.22.   Application of Cu(II)@Fe$_3$O$_4$@SiO$_2$@L-arginine in the synthesis of different structurally 5-substituted-1H-tetrazoles.

R= OMe, Me, Cl, H, CN

Time: 4 min- 96 h
Yield (%): 45- 100

IL: 1-ethyl-3-methylimidazolium ethylsulfate
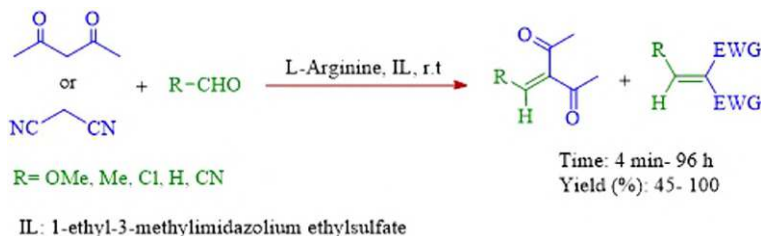
SCHEME 2.23.   Application of L-arginine/IL for Knoevenagel condensations.

2-amino-4-arylbenzo[h]quinoline-3-carbonitrile and 10,10-dimethyl-7-aryl-9,10,11, 12-tetrahydrobenzo[c]acridin-8(7H)-one derivative (Scheme 2.27) [19].

Fe$_3$O$_4$@PS-Arg[HSO$_4$] MNPs are prepared by modification of Fe$_3$O$_4$ n-propylsilan and arginine, respectively, followed by treatment with H$_2$SO$_4$ to generate Fe$_3$O$_4$@ PS-Arg[HSO$_4$] MNPs NPs (Scheme 2.28) [19]. Moreover, it could be recycled up to five times without any noteworthy loss of conversion.

In another study, the application of Fe$_3$O$_4$@PS-Arg MNPs was used for the synthesis of chromene derivatives by the reaction of β -naphthol, malononitrile, and different aldehydes (Scheme 2.29) [20]. It was found that the high yields of products were achieved in short reaction times.

Fe$_3$O$_4$@PS-Arg MNPs were prepared via modification of Fe$_3$O$_4$ with chloropropylsilane and L-arginine (at pH = 12), respectively (Scheme 2.30).

2.7.   APPLICATION OF L-ARGININE-CONTAINING MATERIALS IN TRANSFER HYDROGENATION

Tao et al. reported immobilizing Pd nanoparticles on Mg-Al hydrotalcite with the aid of L-arginine and applied for transfer hydrogenations of ketones (Scheme 2.31) [21]. The highest conversion (100%) was obtained with NaOH in 2-propanol (0.5 mol/L) at 85°C.

R= 4-Cl-C$_6$H$_4$,
4-Br-C$_6$H$_4$,
4-CN-C$_6$H$_4$,
C$_5$H$_4$N,
3-Me-Ar,
C$_6$F$_5$CHO,
2-NO$_2$-C$_6$H$_4$,
C$_6$H$_5$NO,
4-NO$_2$-C$_6$H$_4$
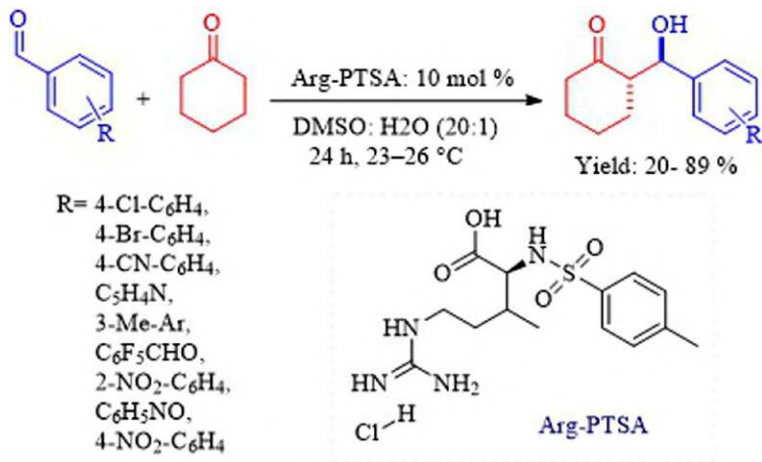
SCHEME 2.24. Application of Arg-PTSA for Aldol reaction.

R	Yield of 1(%)	Yield of 1(%)
p-NO$_2$	83	-
m-NO$_2$	71	-
o-NO$_2$	74	-
p-CF$_3$	76	6
o-Cl	73	9
2,3-di-Cl	82	2
2,4-di-Cl	69	20
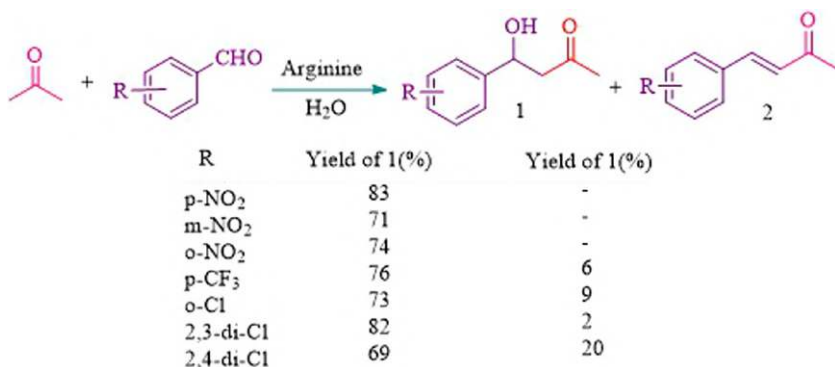
SCHEME 2.25. Aldol reactions of acetone with various benzaldehydes in water using arginine.

2.8. APPLICATION OF L-ARGININE-CONTAINING MATERIALS IN THE OXIDATION

The oxidation of sulfides and oxidative coupling of thiols was investigated to study the catalytic activity of the as-synthesized Cu@Fe$_3$O$_4$@SiO$_2$@L-Arginine; conversions of 85% or more were achieved (Schemes 2.32–34) [22].

Oxidation of primary alcohols and benzyl halides to the carboxylic acids using *t*-butyl hydrogen peroxide under neat conditions proceeded well with Fe$_3$O$_4$@L-arginine-CD-Cu(II) (Schemes 2.35 and 2.36) [23]. The electronic influence of the substituents on the oxidation reaction was investigated by the authors. They observed that the oxidation reactions successfully occurred and products were produced in

R: o-NO$_2$, m-NO$_2$, p-CN,
4-Cl-3-NO$_2$, p-CF$_3$, p-Cl
m-Cl, o-Cl, p-Br, p-F,
4-Cl-3-NO$_2$, o-CHO

Time (h): 5- 48
Yield (%): 30- 70

R$_1$: Me, PhCH$_2$
R$_2$: H, Br
R$_3$: H, Cl, Br, NO$_2$

Time (min): 15- 180
Yield (%): 59- 94

R$_1$: H, Me, PhCH$_2$
R$_2$: H, Br
R$_3$: Me, Ph

Time (min): 10- 120
Yield (%): 89- 96
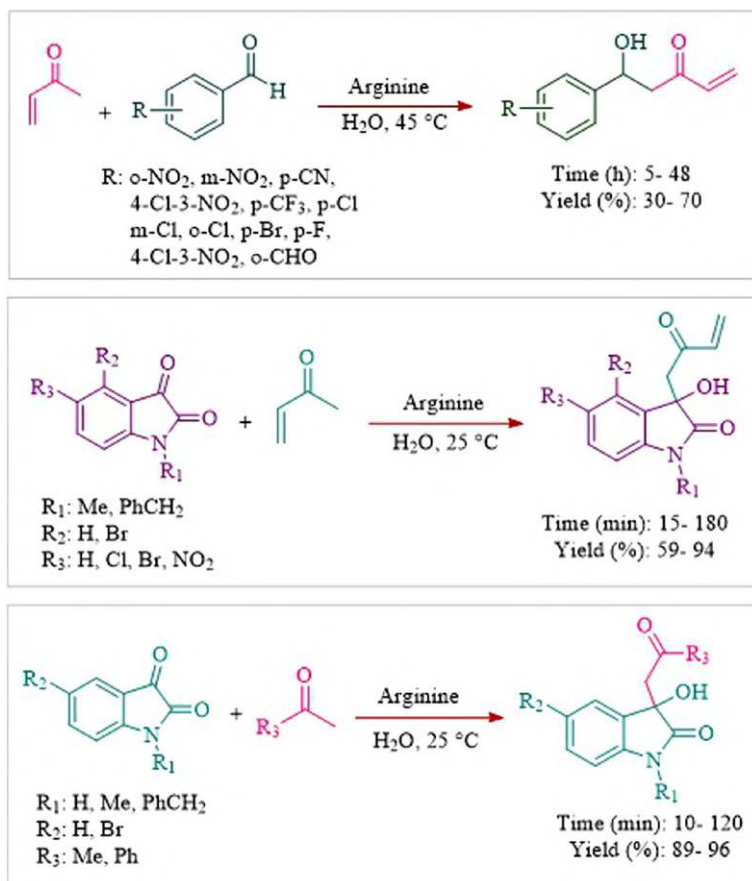
SCHEME 2.26. Aldolization of methyl vinyl ketone.

SCHEME 2.27. Fe$_3$O$_4$@PS-Arg[HSO$_4$] MNPs catalyzed the preparation of multicomponent reaction.
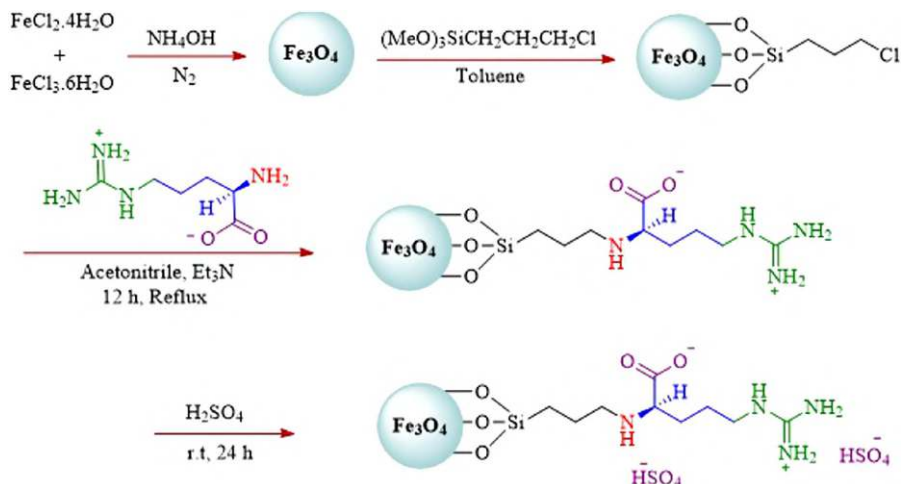
SCHEME 2.28. The preparation of Fe$_3$O$_4$@PS-Arg [HSO$_4$] MNPs.

R: H, 4-Br, 4-Cl, 3-Cl, 2-Cl, 4-F,
4-NO$_2$, 4-Me, 4-OMe, 2,4-diCl

Time (min): 5- 10
Yield (%): 88- 96
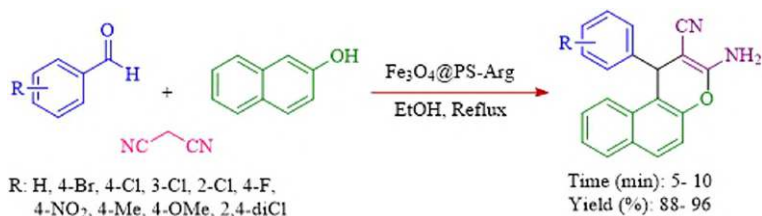
SCHEME 2.29. Fe$_3$O$_4$@PS-Arg MNPs catalyzed multicomponent reaction.

high to excellent yields. In addition, the magnetic catalyst can be recycled at least five times with little loss in its activity.

Moreover, the authors have suggested a proposed mechanism for the oxidation of mentioned organic compounds in the presence of Fe$_3$O$_4$@L-arginine-CD-Cu(II) as a catalyst (Scheme 2.37).

2.9. APPLICATION OF SUPPORTED METAL COMPLEXES OF L-ARGININE AS A CATALYST IN THE MULTICOMPONENT REACTION

In 2022, our group demonstrated the immobilization of the Ni complex of L-arginine on hercynite magnetic nanoparticles [24]. The [Hercynite@SiO$_2$-L-Arginine-Ni] nanocomposite showed reliable heat stability according to thermogravimetric (TG) analyses. X-Ray mapping and XRD were used to characterize the homogeneous dispersion of nickel species on the surface of the L-arginine-modified hercynite. Additionally, this magnetic nanocatalyst was easily removed from the reaction mixture by using an external magnet. The catalytic performance of catalyst NPs was
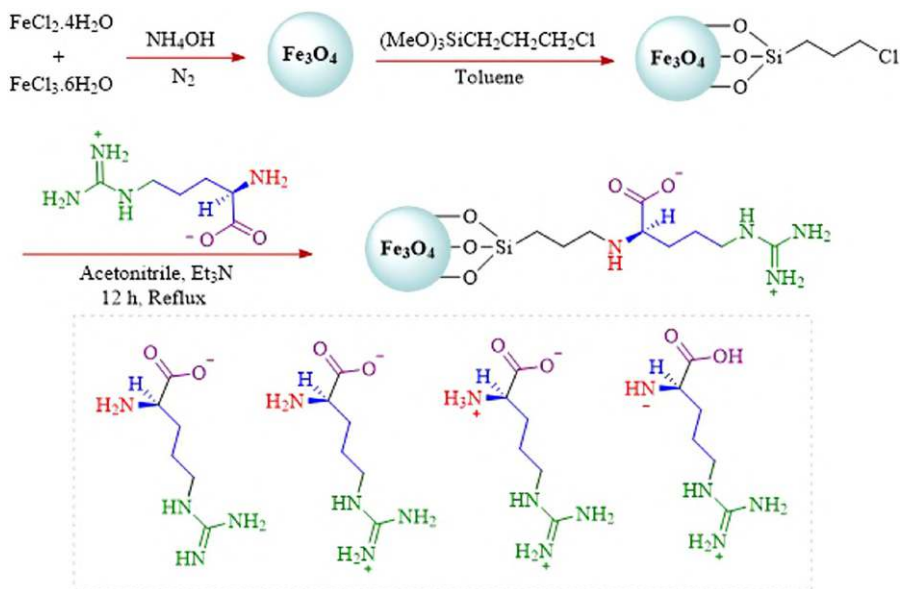
SCHEME 2.30. Preparation of Fe₃O₄@PS-Arg magnetic nanoparticles.

R	Time (h)	Con(%)
4-OCH₃	6	83.3
4-Cl	3	99
4-Br	3	98.6
4-tertbutyl	3	93.9
4-Me	3	90.2
4-H	2	99
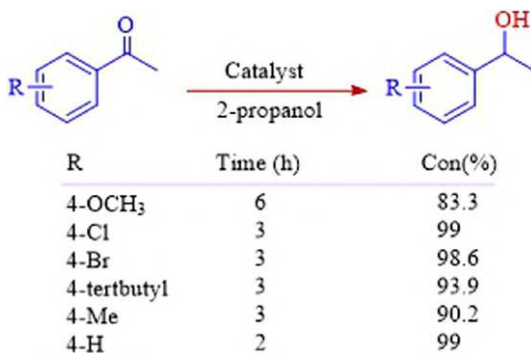
SCHEME 2.31. Application of HT-Arg-Pd for transfer hydrogenation of aromatic ketones.

comparable in the synthesis of polyhydroquinolines and 2,3-dihydroquinazolin-4(1H)-ones (Scheme 2.38).

In 2022, our group reported the synthesis of $ZnFe_2O_4$@L-arginine-Ni and its performance as an efficient nanocatalyst for the synthesis of 1H-tetrazole derivatives and the chemoselective oxidation of sulfides to the sulfoxide [25]. The heterogeneous nature of this magnetic nanocatalyst was studied in our lab through a hot filtration test. Various aldehydes substituents on benzonitrile were studied, giving moderate to good yields of the desired products (Scheme 2.39). A small decline in the recycled nanocatalyst's activity was observed throughout the course of at least five cycles of investigation.
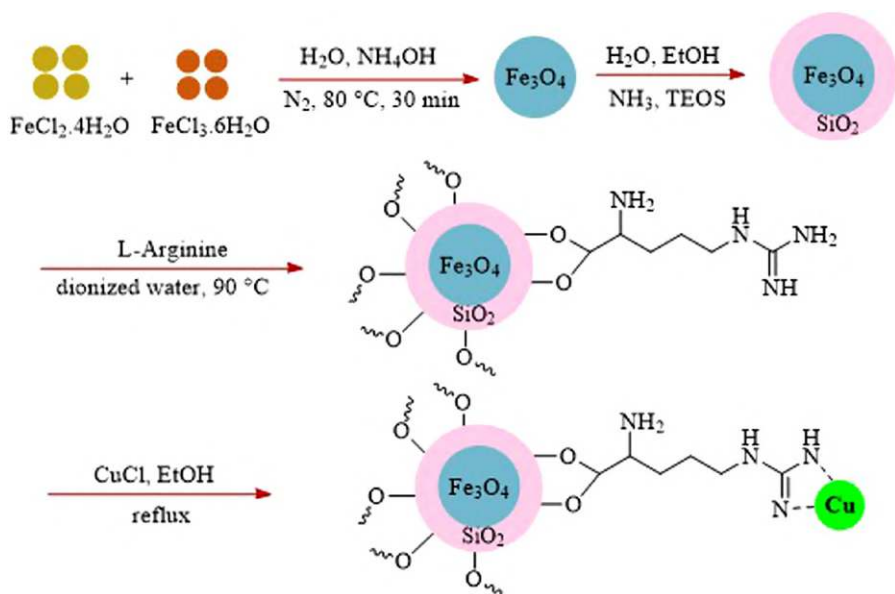
SCHEME 2.32 Preparation of Cu on $Fe_3O_4@SiO_2@$L-arinine.
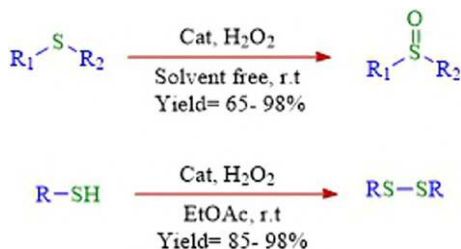
SCHEME 2.33. Application of magnetic catalyst in oxidation and coupling reaction.
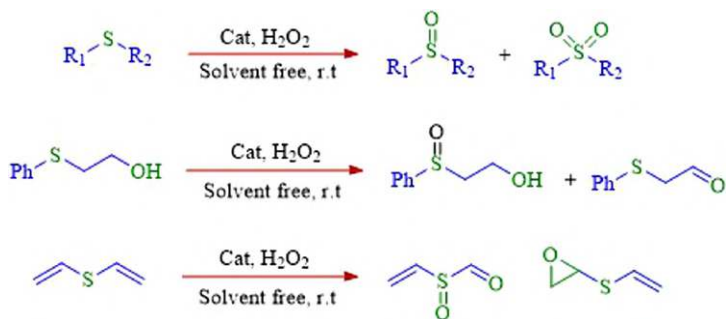
SCHEME 2.34. Chemoselective sulfoxidation of sulfides in the presence of a magnetic catalyst.
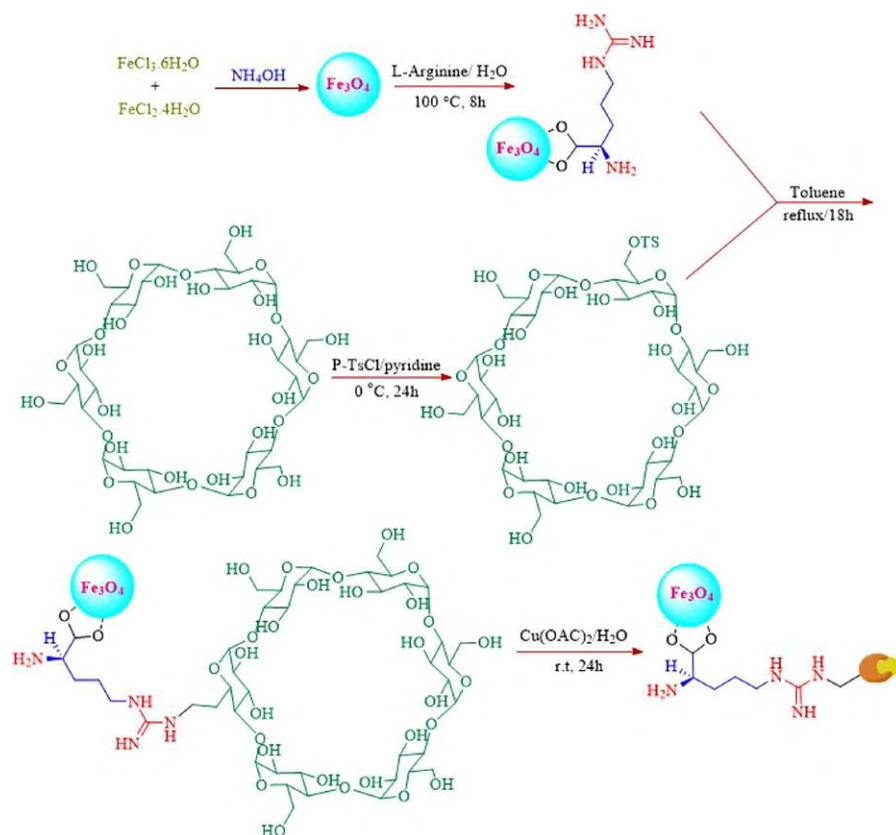
SCHEME 2.35. Synthesis of Fe$_3$O$_4$@L-arginine-CD-Cu(II).
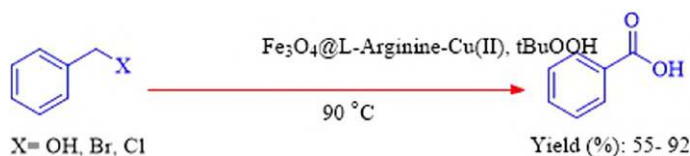
SCHEME 2.36. Application of Fe$_3$O$_4$@L-arginine-CD-Cu(II) for the oxidation reaction.

2.10. APPLICATION OF SUPPORTED METAL COMPLEXES OF L-ARGININE AS A CATALYST IN THE COUPLING REACTION

Bentonite is layered silicate-based material that is employed as a solid support for expensive reagents, organometallic complexes, and nanoparticles. Our laboratory has recently described the preparation of bentonite@ L-arginine-WO$_3$ by immobilization of bentonite nanoclay with L-arginine makes it a good heterogeneous ligand for the decoration of sodium tungstate (Scheme 2.40) [26]. The activity
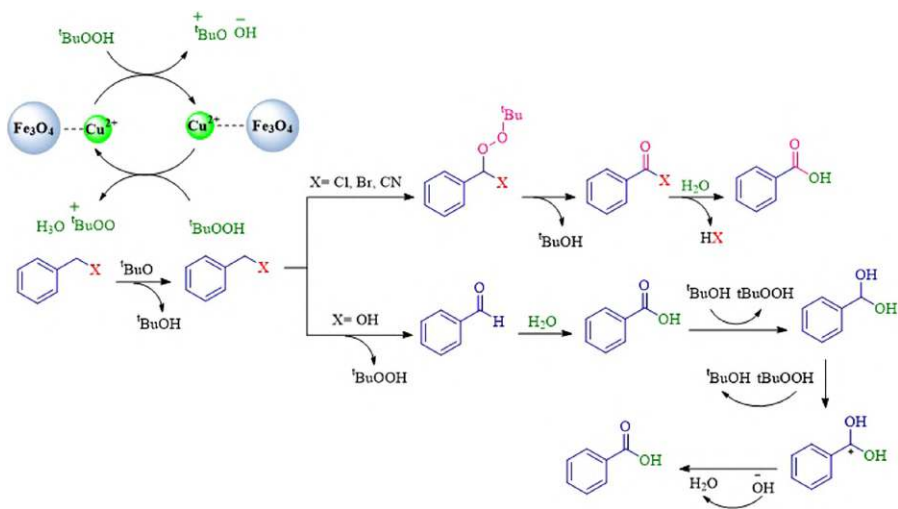
SCHEME 2.37. Proposed mechanism for the oxidation in the presence of magnetic nanocatalyst.

of the catalyst was examined for C—C coupling via a combination of triphenyltin chloride and phenylboronic acid with aryl halides. The protocol was efficient for different aryl halides, to yield the corresponding desired product in excellent yields (Scheme 2.41).

Our group described the application of Pd(0)-Arg-boehmite NPs for C—C coupling reactions through the combination of phenylboronic acid, 3,4-difluoro phenylboronic acid, sodium tetraphenylborate, butyl acrylate, methyl acrylate, acrylonitrile, and styrene with different aryl halides [27]. The catalyst was synthesized by immobilization of boehmite with L-arginine, followed by the addition of palladium acetate and its reduction into Pd NPs with $NaBH_4$ (Scheme 2.42). The morphology and particle size of the palladium nanoparticles were studied by TEM analysis which indicates that particle sizes are formed on the surface, from 5 nm to 7 nm. The leaching tests of palladium species, carried out using the hot-filtration step followed by ICP-OES technical, determined that the amount of palladium species decreased on going from the first to the sixth cycle (from 1.35 mmol/g to 1.28 mmol/g). The coupling proceeded with good to excellent yields for different aryl halides (Scheme 2.43).

Our group prepared Fe_3O_4@SiO_2@L-arginine@Pd(0) by immobilization of Fe_3O_4@SiO_2@ with L-arginine and palladium. Thereafter, it is used for C—C coupling reactions of aryl halides with $NaBPh_4$ and phenylboronic acid at 100°C in PEG (Schemes 2.44 and 2.45) [28]. SEM analysis confirmed the formation of spherical nanoparticles of about 8 nm, and the existence of Pd in the synthesized nanocatalyst was revealed by the EDS analysis. The heterogeneous catalyst can be separated and reused five times, which shows a slight decrease in its activity.

Ar: C₆H₅, 4-ClC₆H₄, 4-CH₃C₆H₄, 4-OCH₃C₆H₄, 4-NO₂C₆H₄, 3-OHC₆H₄,   Time (min): 75-195
4-OHC₆H₄, 4-BrC₆H₄, 3-BrC₆H₄, 4-FC₆H₄, pyridine, thiophene   Yield (%):86-96

Ar: C₆H₅, 4-CHOC₆H₄, 4-ClC₆H₄, 4-CH₃C₆H₄, 4-OCH₃C₆H₄,   Time (min): 35- 250
3,4-OCH₃C₆H₃, 4-NO₂C₆H₄, 4-OHC₆H₄, 4-BrC₆H₄, 3-BrC₆H₄,   Yield (%):84- 95
4-FC₆H₄, pyridine, thiophene

[Hercynite@SiO₂-L-Arginine-Ni]
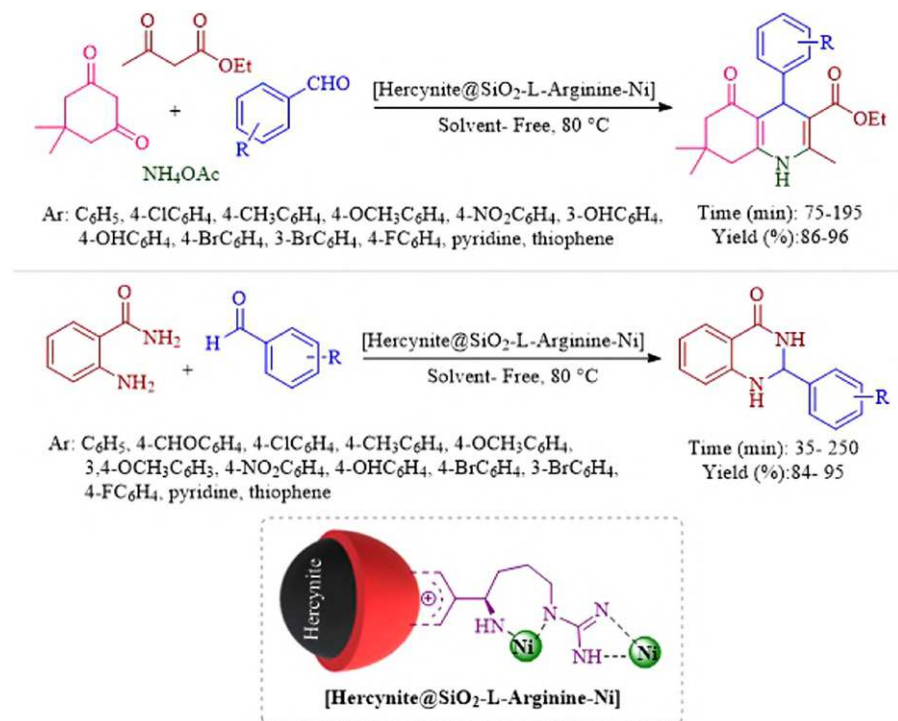
SCHEME 2.38. Application of [Hercynite@SiO₂-L-arginine-Ni] in organic reaction.

Peptides are composed of natural L-amino acids with the ability to produce nano-fibers via the self-assembling method or other procedures. Recently, research projects in our group have focused on the synthesis of peptide nanofibers using amino acids by self-assembly method. Peptide nanofibers are an effective template for the coordination of a variety of metals (such as ZrO, Pd, Ni, and Cu) with catalytic ability in a wide range of organic reactions such as cross-coupling reactions and multicomponent domino reactions [29–34]. This protocol is employed for various substrates, giving good to excellent yields. An extensive review by our group in 2020 focused on the application of nanofibers with variable structures as catalysts in organic reactions, which are briefly shown in Schemes 2.46–2.48 [35].

2.11. APPLICATION OF METAL COMPLEXES OF L-ARGININE-CONTAINING SUPPORTED MATERIAL AS A CATALYST IN HENRY REACTION

The Henry reaction of α-keto amide with nitromethane in the presence of arginine in water at room temperature has been investigated. The Henry reaction proceeded with the products with good functional group tolerance (Scheme 2.49) [36].

Ar: C_6H_5, 3-$NO_2C_6H_4$, 4-$NO_2C_6H_4$, 2-ClC_6H_4,   Time (min): 90- 160
2-OHC_6H_4, 4-OHC_6H_4, 4-CNC_6H_4,   Yield (%): 88- 96
4-ClC_6H_4, 4-BrC_6H_4

R_1: C_6H_5, $CH_2C_6H_5$, $C_{12}H_{25}$, C_4H_9 Time (min): 30- 20
R_2: CH_3, $CH_2C_6H_5$, C_2H_5O, $C_{12}H_{25}$, C_4H_9, C_6H_5 Yield (%):70- 96

$ZnFe_2O_4$@L-arginine-Ni
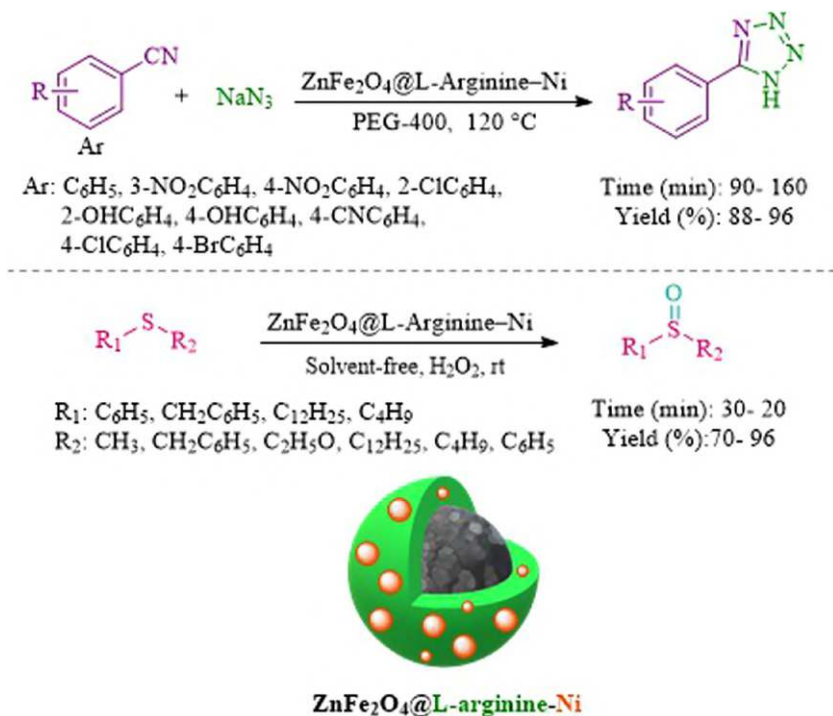
SCHEME 2.39. Application of $ZnFe_2O_4$@L-arginine-Ni in organic reaction.

SCHEME 2.40. The preparation of bentonite@ L-arginine-WO_3.

2.12. CONCLUSION

In this chapter, we found that arginine amino acid has received great attention due to its versatility and applicability in green chemistry and the field of catalytic application. This chapter highlighted the potential utility of L-arginine as an organocatalyst and catalyst in organic reactions. This chapter also provides guidance and procedures used for the immobilization of L-arginine on various inorganic supported materials

X= I, Br, Cl

Bentonite@ L-Arginine-WO₃

B(OH)₂

R—

+

+ Ph₃SnCl

R= H, Me, OMe, Cl, NO₂

Time (h): 1- 18
Yield (%): 55- 92

R= H, Me, OMe, Cl, NO₂

Time (h): 1- 15
Yield (%): 50- 90
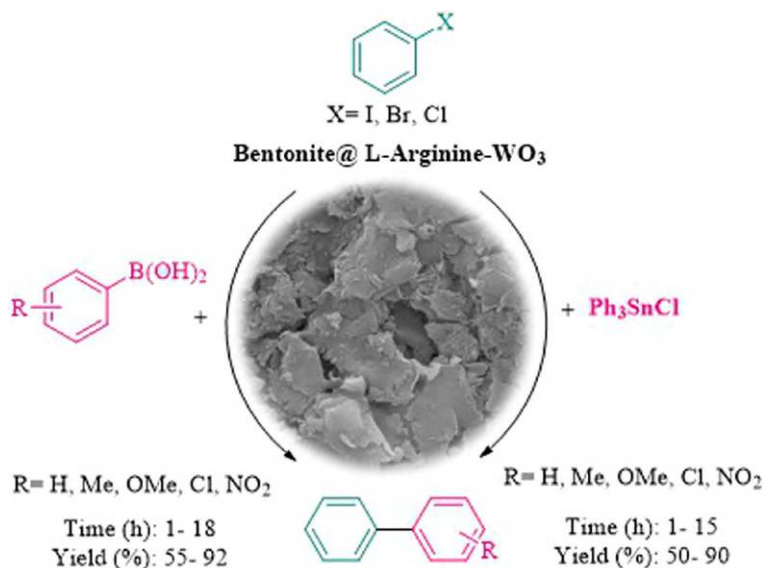
SCHEME 2.41. Application of bentonite@ L-arginine-WO₃ in C— C coupling reaction.

Pd-Arg-boehmite

1. Pd(OAc)₂,
EtOH, 80 °C, 20 h

2. NaBH₄, 2 h

Boehemite NPS

L-Arginine
H₂O. 90 °C
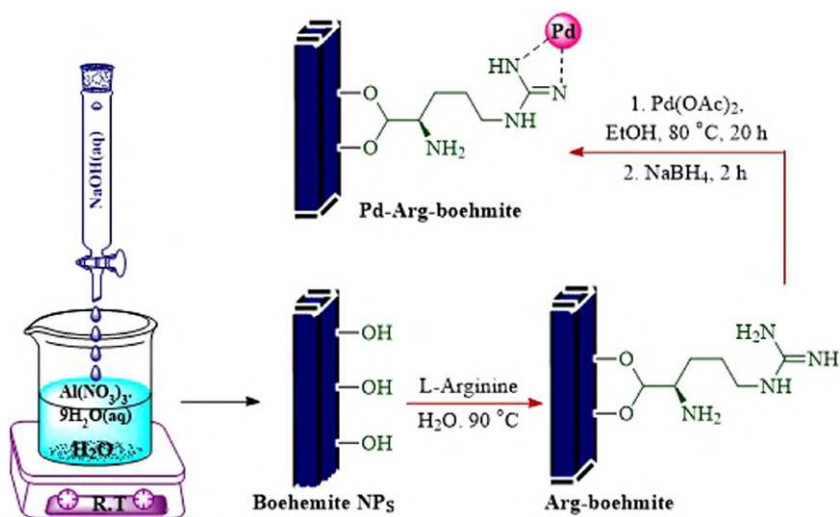
Arg-boehmite

SCHEME 2.42. Preparation of Pd(0)-Arg-boehmite.
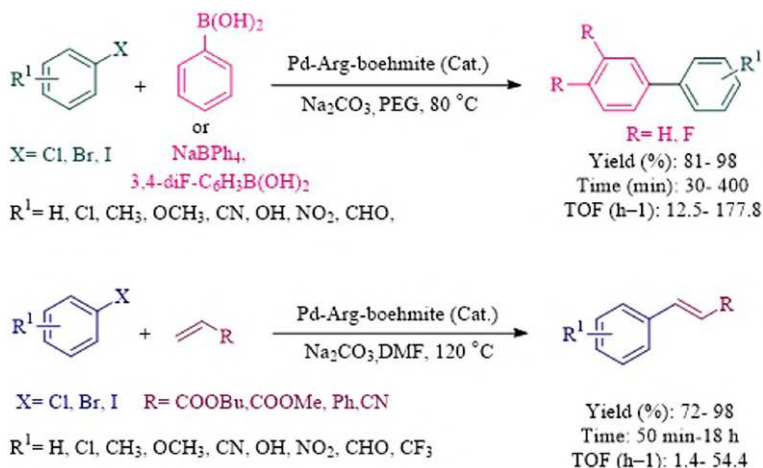
SCHEME 2.43. Application of Pd(0)-Arg-boehmite in C— C coupling reaction.
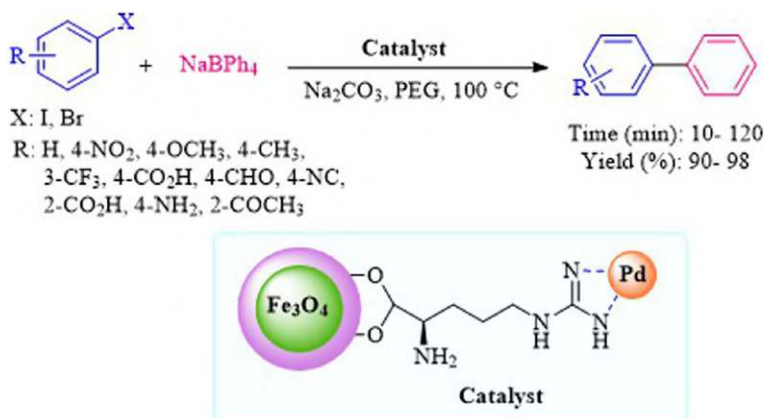
SCHEME 2.44. Application of Fe$_3$O$_4$@SiO$_2$@L-arginine@Pd(0) in C— C coupling reaction.
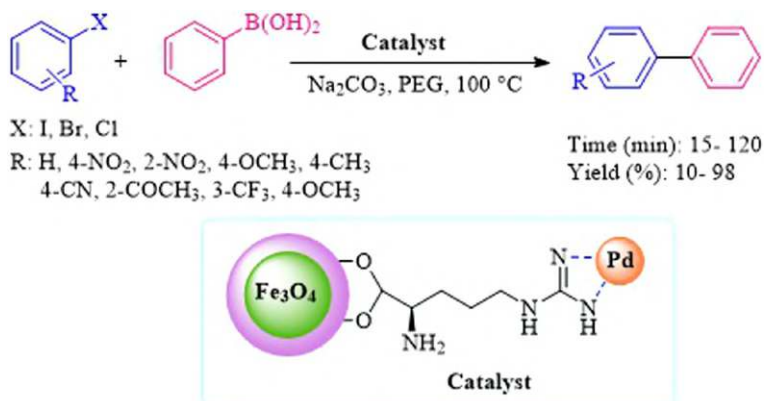
SCHEME 2.45. Application of $Fe_3O_4@SiO_2@$L-arginine@Pd(0) in C— C coupling reaction.

M= Pd, Cu, Ni, ZrO
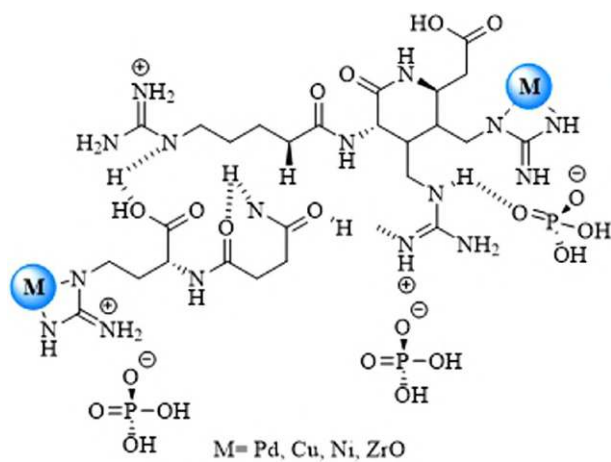
SCHEME 2.46. Immobilization of peptide nanofiber with nanoparticles.
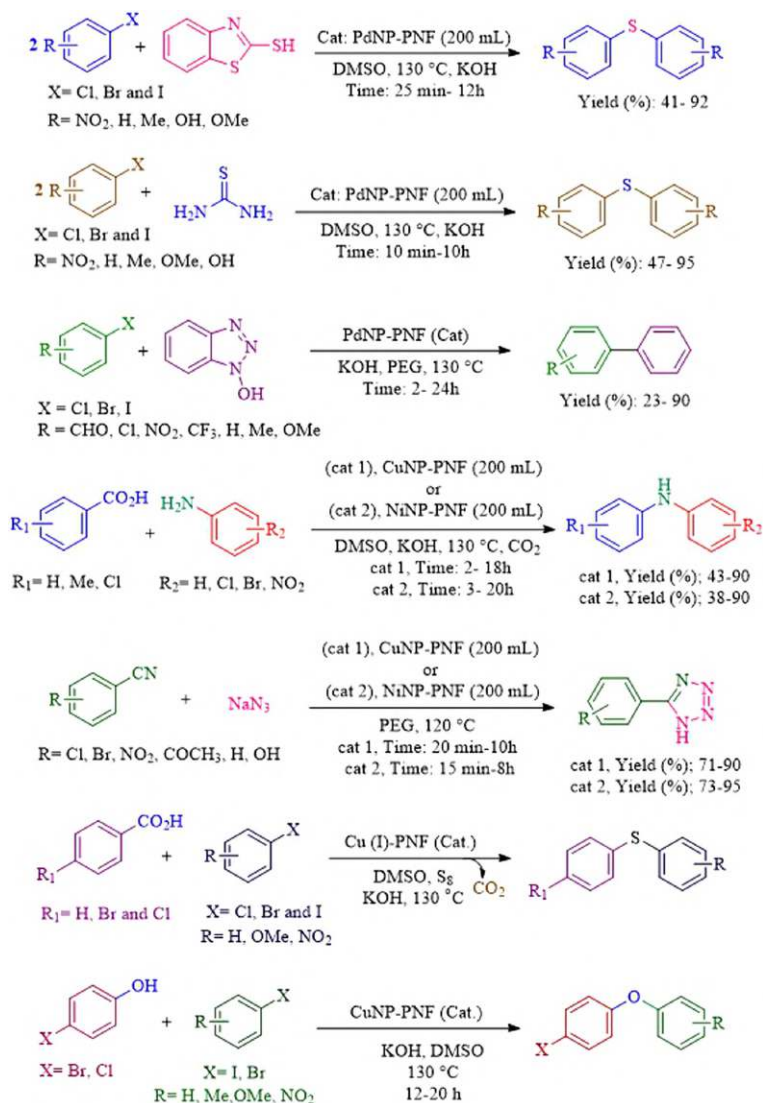
SCHEME 2.47. Application of peptide nanofibers in the coupling reaction.
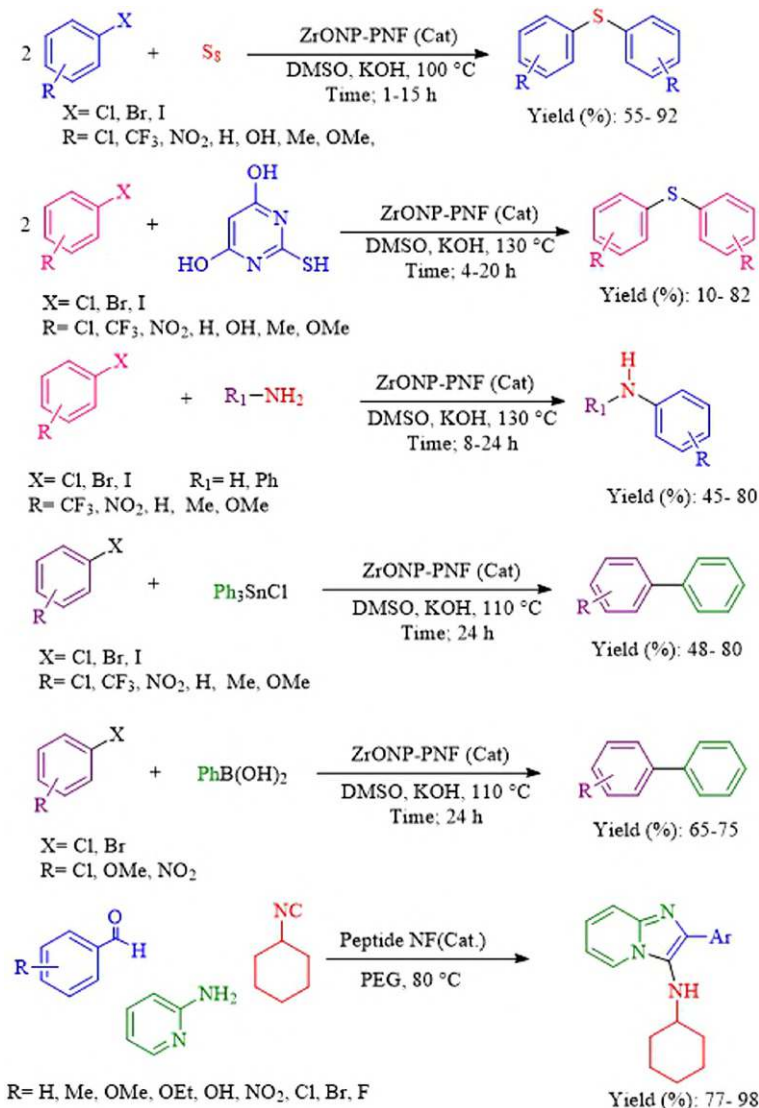
SCHEME 2.48. Application of peptide nanofibers in organic reactions.
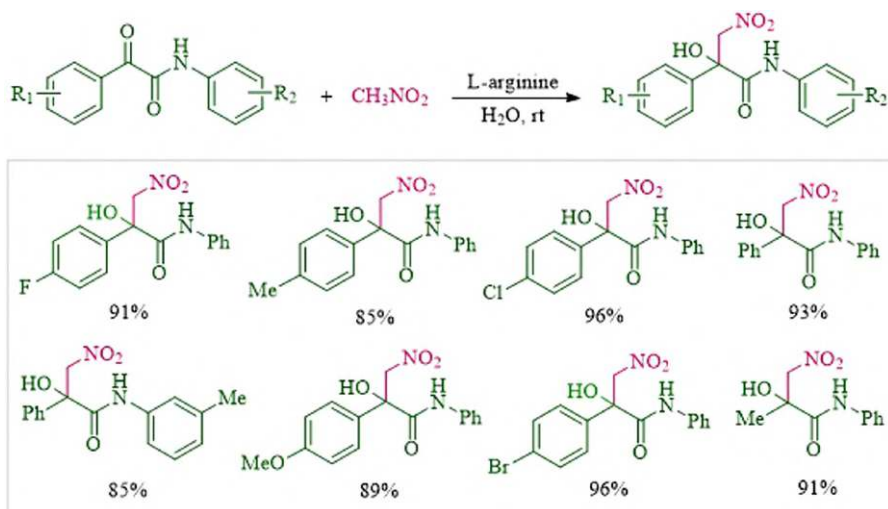
SCHEME 2.49. Scope of α-keto amide with nitromethane.

to achieve advantages like cost-efficiency, higher stability, and several recycling in different reactions to make greener the industrial processes.

REFERENCES

1. Wojaczyńskaa, E., Zielińska-Błajetb, M. Graphene-based materials for asymmetric catalysis. *Arkivoc*, *2023*, (part v), 0-0.
2. Khabnadideh, S., Mirzaei, E., Amiri-Zirtol, L. L-arginine modified graphene oxide: A novel heterogeneous catalyst for the synthesis of benzo [b] pyrans and pyrano [3, 2-c] chromenes. *J. Mol. Struct*., 2022, *1261*, 132934. https://doi.org/10.1016/j.molstruc.2022 .132934.
3. Yari, M., Shiri, L., Rostami, H. One-pot Synthesis of 3, 5-disubstituted-2, 6-dicyano-aniline Derivatives using $CoFe_2O_4@ SiO_2@$ L-arginine as a magnetically nanocatalyst. *ChemistrySelect*., 2022, *7*(19), e202200230. https://doi.org/10.1002/slct.202200230.
4. Amirnejat, S., Nosrati, A., Javanshir, S., Naimi-Jamal, M. R. Superparamagnetic algi-nate-based nanocomposite modified by L-arginine: An eco-friendly bifunctional cata-lysts and an efficient antibacterial agent. *Int. J. Biol. Macromol*., 2020, *152*, 834–845. https://doi.org/10.1016/j.ijbiomac.2020.02.212.
5. Zarnegar, Z., Monjezi, H. R., Safari, J. Arginine-based surface modification of nanostarch, a catalytic carbohydrates in synthesis of heteroaryl sulfides. *J. Mol. Struct*., 2019, *1193*, 14–23. https://doi.org/10.1016/j.molstruc.2019.05.017.
6. Amirnejat, S., Nosrati, A., Javanshir, S. Synthesis of functionalized thiopyrano [2,3-b] Quinolines via cascade reactions catalyzed by magnetic arginine/alginate biocompos-ite. In *Chemistry Proceedings*; Multidisciplinary Digital Publishing Institute, 2020; Vol. 3, p. 129. https://doi.org/10.3390/ecsoc-24-08413.

7. Eftekhari, A., Foroughifar, N., Hekmati, M., Khobi, M. Fe3O4@L-arginine magnetic nanoparticles: A novel and magnetically retrievable catalyst for the synthesis of 1′3-Diaryl-2N-azaphenalene. *J. Chinese Chem. Soc.*, 2019, *66*(7), 761–768. https://doi.org/10.1002/jccs.201800274.

8. Ghasemzadeh, M. A., Mirhosseini-Eshkevari, B., Abdollahi-Basir, M. H. Green synthesis of Spiro[Indoline-3,4′-Pyrano[2,3-c]Pyrazoles] Using Fe3O4@L-Arginine as a robust and reusable catalyst. *BMC Chem.*, 2019, *13*(1), 1–11. https://doi.org/10.1186/s13065-019-0636-1.

9. Afradi, M., Foroughifar, N., Pasdar, H., Moghanian, H., Foroughifar, N. Facile green one-pot synthesis of novel thiazolo[3,2-a]pyrimidine derivatives using Fe3O4@l-arginine and their biological investigation as potent antimicrobial agents. *Appl. Organomet. Chem.*, 2017, *31*(9), e3683. https://doi.org/10.1002/aoc.3683.

10. Azizi, K., Karimi, M., Shaterian, H. R., Heydari, A. Ultrasound irradiation for the green synthesis of chromenes using L-arginine-functionalized magnetic nanoparticles as a recyclable organocatalyst. *RSC Adv.*, 2014, *4*(79), 42220–42225. https://doi.org/10.1039/c4ra06198e.

11. Tahmasbi, B., Ghorbani-Choghamarani, A. First report of the direct supporting of palladium–arginine complex on boehmite nanoparticles and application in the synthesis of 5-substituted tetrazoles. *Appl. Organomet. Chem.*, 2017, *31*(7), e3644. https://doi.org/10.1002/aoc.3644.

12. Ghadari, R., Namazi, H., Aghazadeh, M. Synthesis of graphene oxide supported copper–cobalt ferrite material functionalized by arginine amino acid as a new high–performance catalyst. *Appl. Organomet. Chem.*, 2018, *32*(1), e3965. https://doi.org/10.1002/aoc.3965.

13. Ghadari, R., Namazi, H., Aghazadeh, M. Nickel-substituted cobalt ferrite nanoparticles supported on arginine-modified graphene oxide nanosheets: Synthesis and catalytic activity. *Appl. Organomet. Chem.*, 2017, *31*(12), e3859. https://doi.org/10.1002/aoc.3859.

14. Ghorbani-Choghamarani, A., Shiri, L., Azadi, G. The first report on the eco-friendly synthesis of 5-substituted 1: H-Tetrazoles in PEG catalyzed by Cu(Ii) immobilized on Fe3O4@SiO2@l-arginine as a novel, recyclable and non-corrosive catalyst. *RSC Adv.*, 2016, *6*(39), 32653–32660. https://doi.org/10.1039/c6ra03023h.

15. Hu, Y., Guan, Z., He, Y. H., Louwagie, N., Yao, M. J. L-arginine as a cost-effective and recyclable catalyst for the synthesis of α,β-unsaturated nitriles and ketones in an ionic liquid. *J. Chem. Res.*, 2010, *34*(1), 22–24. https://doi.org/10.3184/030823409X12615671424822.

16. Lombardo, M., Easwar, S., Pasi, F., Trombini, C., Dhavale, D. D. Protonated arginine and lysine as catalysts for the direct asymmetric aldol reaction in ionic liquids. *Tetrahedron*, 2008, *64*(39), 9203–9207. https://doi.org/10.1016/j.tet.2008.07.061.

17. Peng, Y. Y., Wang, Q., He, J. Q., & Cheng, J. P. (2008). Arginine catalyzed direct aldol reactions in pure water: An environmentally friendly reaction system. *Chin. J. Chem.*, 2008, *26*(8), 1454–1460. https://doi.org/10.1002/cjoc.200890264.

18. Inani, H., Jha, A. K., Easwar, S. An arginine-mediated protocol for the aldol addition of methyl vinyl ketone in water. *ChemistrySelect*, 2017, *2*(35), 11666–11672. https://doi.org/10.1002/slct.201702502.

19. Karkhah, M. K., Kefayati, H., Shariati, S. Synthesis of Benzo[h]Quinolone and Benzo[c]Acridinone derivatives by Fe3O4@PS-Arginine[HSO4] as an efficient magnetic nanocatalyst. *J. Heterocycl. Chem.*, 2020, *57*(12), 4181–4191. https://doi.org/10.1002/jhet.4125.

20. Kargar Karkhah, M., Kefayati, H., Shariati, S. Enantioselective synthesis of 3-Ami no-1-Aryl-1H-Benzo[f]Chromene-2-carbonitrile derivatives by Fe3O4@PS-arginine as an efficient chiral magnetic nanocatalyst. *Appl. Organomet. Chem.*, 2019, *33*(10), e5139. https://doi.org/10.1002/aoc.5139.

21. Tao, R., Xie, Y., An, G., Ding, K., Zhang, H., Sun, Z., Liu, Z. Arginine-mediated synthesis of highly efficient catalysts for transfer hydrogenations of ketones. *J. Colloid Interface Sci.*, 2010, *351*(2), 501–506. https://doi.org/10.1016/j.jcis.2009.12.025.

22. Nikoorazm, M., Moradi, P., Noori, N., Azadi, G. L-arginine complex of copper on modified core–shell magnetic nanoparticles as reusable and organic–inorganic hybrid nanocatalyst for the chemoselective oxidation of organosulfur compounds. *J. Iran. Chem. Soc.*, 2021, *18*(2), 467–478. https://doi.org/10.1007/s13738-020-02040-8.

23. Nejad, M. J., Salamatmanesh, A., Heydari, A. Copper (II) immobilized on magnetically separable L-arginine-β-cyclodextrin ligand system as a robust and green catalyst for direct oxidation of primary alcohols and benzyl halides to acids in neat conditions. *J. Organomet. Chem.*, 2020, *911*, 121128. https://doi.org/10.1016/j.jorganchem.2020.121128.

24. Taherinia, Z., Ghorbani-Choghamarani, A. Immobilized Na2WO4. 2H2O on arginine modified bentonite (Bentonite@ L-Arginine-WO3): An efficient and sustainable catalyst for the C− C bond formation. *ChemistrySelect*, 2021, *6*(40), 11054–11059.

25. Mohammadi, M., Ghorbani-Choghamarani, A. Complexation of guanidino containing l-arginine with nickel on silica-modified Hercynite MNPs: A novel catalyst for the Hantzsch synthesis of polyhydroquinolines and 2, 3-Dihydroquinazolin-4 (1H)-ones. *Res. Chem. Intermed.*, 2022, *48*(6), 2641–2663. https://doi.org/10.1007/s11164-022-04706-9.

26. Aghavandi, H., Ghorbani-Choghamarani, A. ZnFe$_2$O$_4$@ L-arginine-Ni: A novel, green, recyclable, and highly versatile catalyst for the synthesis of 1H-tetrazoles and oxidation of sulfides to the sulfoxides. *J. Phys. Chem. Solids.*, 2022, *170*, 110952. https://doi.org/10.1016/j.jpcs.2022.110952.

27. Tahmasbi, B., Ghorbani-Choghamarani, A. Pd(0)-Arg-Boehmite: As reusable and efficient nanocatalyst in suzuki and heck reactions. *Catal. Letters*, 2017, *147*(3), 649–662. https://doi.org/10.1007/s10562-016-1927-y.

28. Ghorbani-Choghamarani, A., Azadi, G. Fe$_3$O$_4$@SiO$_2$@ l-Arginine@Pd(0): A new magnetically retrievable heterogeneous nanocatalyst with high efficiency for C-C bond formation. *Appl. Organomet. Chem.*, 2016, *30*(4), 247–252. https://doi.org/10.1002/aoc.3424.

29. Ghorbani-Choghamarani, A., Taherinia, Z. Synthesis of peptide nanofibers decorated with palladium nanoparticles and its application as an efficient catalyst for the synthesis of sulfides: Via reaction of aryl halides with thiourea or 2-mercaptobenzothiazole. *RSC Adv.*, 2016, *6*(64), 59410–59421. https://doi.org/10.1039/c6ra02264b.

30. Ghorbani-Choghamarani, A., Taherinia, Z. Synthesis of biaryls using palladium nanoparticles immobilized on peptide nanofibers as catalyst and hydroxybenzotriazole as novel phenylating reagent. *Cuihua Xuebao/Chinese J. Catal.*, 2017, *38*(3), 469–474. https://doi.org/10.1016/S1872-2067(17)62586-X.

31. Ghorbani-Choghamarani, A., Taherinia, Z. High catalytic activity of peptide nanofibres decorated with Ni and Cu nanoparticles for the synthesis of 5-substituted 1H-tetrazoles and N-arylation of amines. *Aust. J. Chem.*, 2017, *70*(10), 1127–1137. https://doi.org/10.1071/CH17176.

32. Taherinia, Z., Ghorbani-Choghamarani, A. Cu (I)–PNF, an organic-based nanocatalyst, catalyzed C–O and C–S cross-coupling reactions. *Can. J. Chem.*, 2019, *97*(1), 46–52.

33. Ghorbani-Choghamarani, A., Taherinia, Z. The first report on the preparation of peptide nanofibers decorated with zirconium oxide nanoparticles applied as versatile catalyst for the amination of aryl halides and synthesis of biaryl and symmetrical sulfides. *New J. Chem.*, 2017, *41*(17), 9414–9423. https://doi.org/10.1039/c7nj00628d.

34. Ghorbani-Choghamarani, A., Taherinia, Z. Eco-friendly synthesis of 3-aminoimidazo [1, 2-a] pyridines via a one-pot three-component reaction in PEG catalyzed by peptide nanofibers: As hydrogen-bonding organocatalyst. *J. Iran. Chem. Soc.*, 2020, *17*(1), 59–65. https://doi.org/10.1007/s13738-019-01744-w.

35. Ghorbani-Choghamarani, A., Taherinia, Z., Heidarnezhad, Z., Moradi, Z. Application of nanofibers based on natural materials as catalyst in organic reactions. *J. Ind. Eng. Chem.*, 2021, *94*, 1–61. https://doi.org/10.1016/j.jiec.2020.10.028.

36. Wu, C., Hu, B., Liu, H., Jiang, J., Kim, J. Arginine-catalyzed henry reaction of α -keto amides with nitromethane on water. *ChemistrySelect*, 2022, *7*(7), e202104433. https://doi.org/10.1002/slct.202200230.

3 The Catalytic Role of L-Cysteine in Organic Reactions

3.1. INTRODUCTION

L-cysteine is a versatile amino acid for selective chemical modification of proteins with both chemical and biological innovations, which plays a key role in different organic reactions. L-cysteine is employed as a novel sulfur source in the synthesis of symmetrical diaryl sulfides from a variety of aryl iodides in moderate to excellent yields. Herein, we focused on the activity of L-cysteine as a catalyst in organic reactions.

3.2. APPLICATION OF L-CYSTEINE AND L-CYSTEINE DERIVATIVES-SUPPORTED MATERIAL AS AN ORGANOCATALYST IN MULTICOMPONENT REACTIONS

Amino acids attract considerable research interest due to their unique properties and are a promising class of green material for applications in various functional parts as chiral starting materials, auxiliaries, and catalysts in modern organic synthesis [1–3]. In 2022, Safaei-Ghomi et al. reported the synthesis of nano-Fe_3O_4-L-cysteine. The activity of the catalyst was investigated for the preparation of indeno[1,2-c]pyrazol4(1H)-ones through a three-component reaction of phenylhydrazine, aromatic aldehydes, and indan-1,2,3-trione at room temperature in acetonitrile as solvent [4]. Various substituents on the aromatic aldehydes were studied. Interestingly, it proceeds smoothly at room temperature in acetonitrile and is performed for a wide variety of functional groups, including OMe, Me, Cl, Br, and NO_2. Experimental data showed that the existence of electron-poor groups on the aromatic aldehydes provided yields better than the existence of electron-rich groups (Scheme 3.1).

Nikoorazm et al. have demonstrated the preparation of the 5-substituted H-tetrazoles from a combination of a variety of nitriles with sodium azide in PEG-400 (as solvent) using a catalytic amount of L-cysteine-Pd@MCM-41 [5]. The catalysts were produced through the immobilization of L-cysteine onto MCM-41 channels, followed by the insertion of Pd(OAc)$_2$ into this modified mesoporous material (Scheme 3.2).

The resulting nanoparticles are found to be spherical around 30 nm, and according to the ICP analysis, the Pd content in the MCM-41 was found to be 1.47×10^{-3}

R: H, 4-OMe, 4-Me, 4-Cl, 4-Br,
4-NO$_2$, 3-NO$_2$, 4-OH

Timre (min): 25- 50
Yield (%): 80- 94
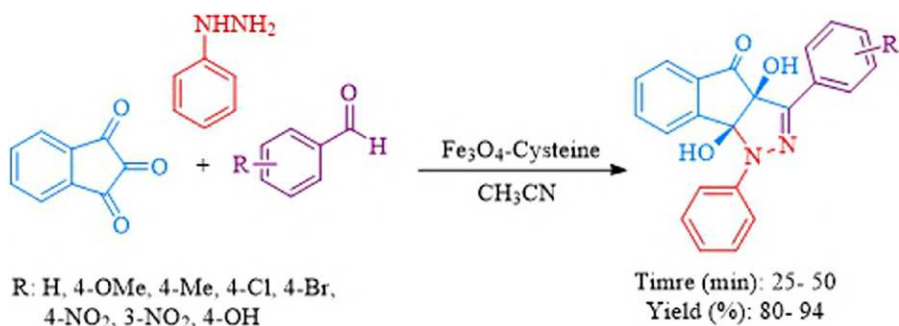
SCHEME 3.1. Synthesis of indenopyrazolones using nano-Fe$_3$O$_4$-cysteine.
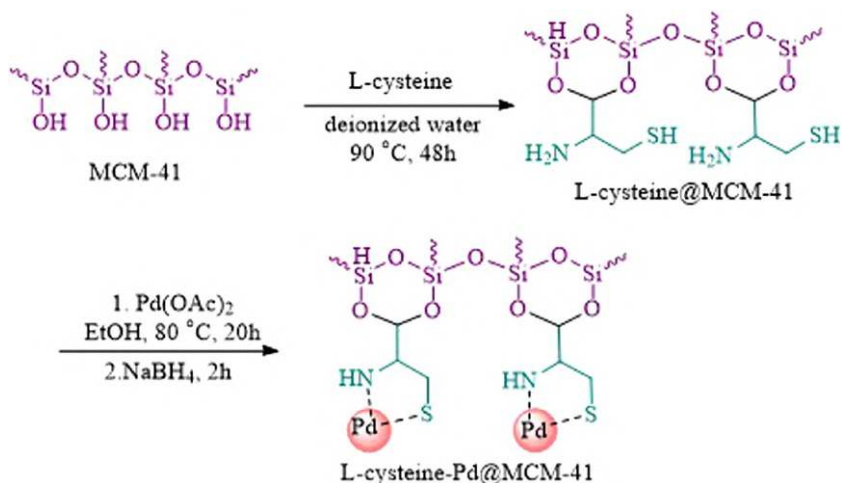
SCHEME 3.2. The preparation of MCM-41 (L-cysteine-Pd@MCM-41).

mmol/g. These NPs demonstrated high performance in the cycloaddition of azides and nitriles in PEG at 100°C, efficiently promoting the cycloaddition of azides and nitriles to provide an array of 5-substituted-1H-tetrazoles in high yields (Scheme 3.3).

In 2016, Khalafinejad's group designed LCMNP (L-cysteine-modified magnetic nanoparticles) as a new catalyst. To synthesize the catalyst, Fe$_3$O$_4$@SiO$_2$ magnetic nanoparticles were first treated with trimethoxy(vinyl)silane to afford vinyl magnetic nanoparticles (VMNP). Then a combination of azobisisobutyronitrile (AIBN), L-cysteine, and VMNP afforded LCMNP (Scheme 3.4).

This research group studied the performances of catalyst for the synthesis of 9-(1H)-indol-3-yl) xanthen-4-(9h)-one through the reaction of 2-hydroxybenzalde-hyde, daimedone, and indole (Scheme 3.5) [6]. The corresponding products were
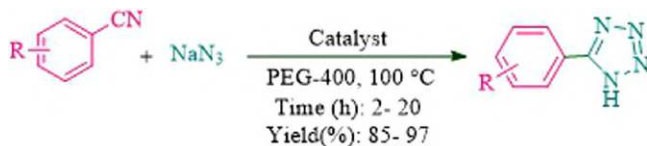
Nitrile: benzonitrile, 4-nitrobenzonitrile
4-acetylbenzonitrile, 4-Bromobenzonitrile
3-Chlorobenzonitrile, 4-Chlorobenzonitrile
terephthalnitrile, 3-nitrobenzonitrile, Malononitrile
4-methoxybenzonitrile, 4-isopropylbenzonitrile

SCHEME 3.3. L-cysteine-Pd@MCM-41 catalyzed the production of 5-substituted-1*H*-tetrazoles.
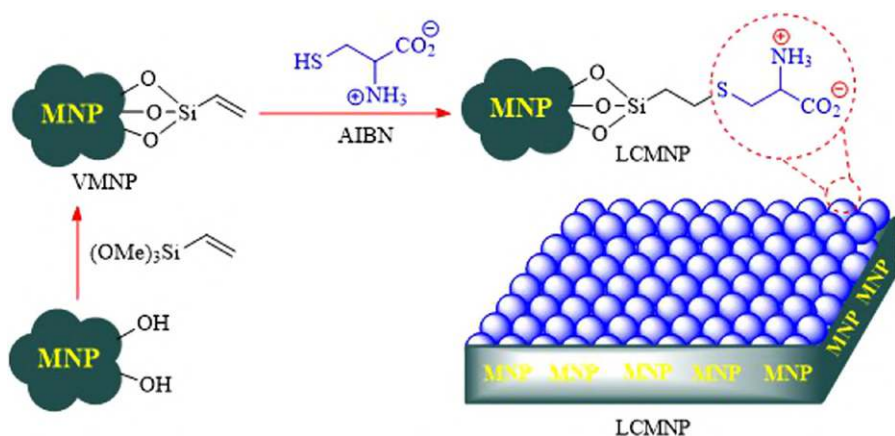
SCHEME 3.4. Production steps of LCMNP as a magnetic catalyst.

synthesized with high efficiency and short reaction times under very green condi-
tions. In addition, this solid catalyst demonstrated a modest loss of activity after
being reused six times. The mechanism of this reaction is identified in Scheme 3.6.

Bahrami et al. have demonstrated a multicomponent reaction catalyzed by
L-cysteine-functionalized magnetic nanoparticles. In this research work, two-step
processes were carried out for the synthesis of magnetic catalysts, including soni-
cating magnetic nanoparticles with (3-choloropropyl)triethoxysilane (CPTES), fol-
lowed by immobilizing L-cysteine [7]. This research group employed the resulting
nanoparticles as catalysts for the preparation of α-amino phosphonates using the
reaction of synthetic aldehydes-containing nucleobases, amines, and diethyl phos-
phonate under mild and clean conditions. The experimental results showed both
electron-poor and electron-rich substituents on the amines to yield the corresponding
products in excellent yield (Scheme 3.7).
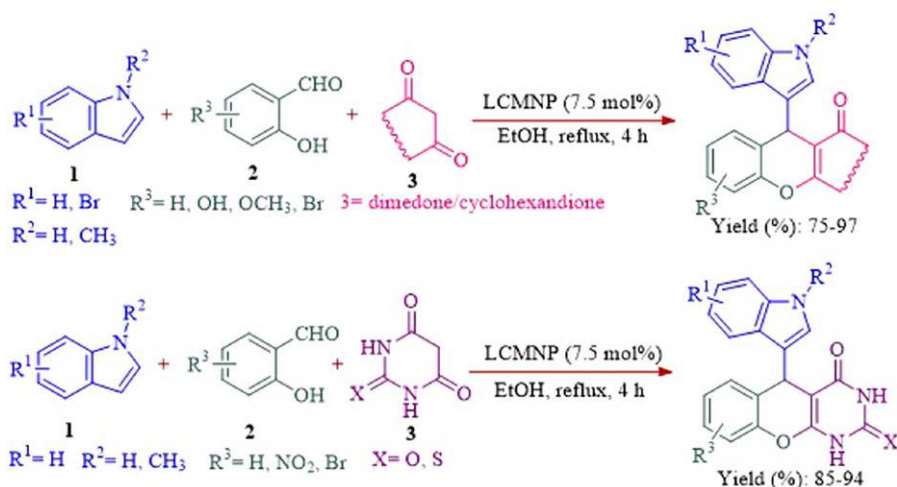
SCHEME 3.5.   Synthesis of 9-(1*H*)-indol-3-yl)xanthen-4-(9*H*)-one catalyzed by LCMNP.

Khalafi-Nezhad et al. have introduced the synthesis of magnetic nanoparticles (LCMNP) by treating $Fe_3O_4@SiO_2$ with trimethoxy(vinyl)silane to produce vinyl-functionalized magnetic nanoparticles followed by a combination of the solid product with L-cysteine to produce L-cysteine-modified magnetic nanoparticles (LCMNP) (Scheme 3.8).

The material efficiently catalyzed the one-pot synthesis of 2-amino-4*H*-chromene-3-carbonitrile derivatives (Scheme 3.9) [8]. The supported catalyst demonstrated reasonable yield in these reactions in H_2O at 80°C. The experimental result shows this magnetic organocatalyst system was reusable seven times in the designed protocol with a slight reduction in catalytic activity.

Rafiee et al. investigated the performance of CuI/II@Cys-MGO, prepared via immobilization of the Cu^I and Cu^{II} catalytic species on the magnetic cysteine-modified graphene oxide to perform the azidonation reaction of aryl boronic acids and one-pot synthesis of 1,4-diaryl-1,2,3-triazoles [9]. Under the optimized reaction conditions, the broad substrate scope using CuI/II@Cys-MGO magnetic NPs was explored, and it was shown to accommodate structurally and electronically diverse aryl boronic acids under aqueous solutions (Schemes 3.10 and 3.11). This procedure offers advantages over conventional methods such as short reaction times, mild reaction conditions, and reusability of the catalyst for up to eight times.

Heydari and coworkers designed and synthesized $Fe_3O_4@LDH@cystine-Cu(I)$ as a nanostructural composite (Scheme 3.12) [10]. To study the catalytic properties, $Fe_3O_4@LDH@cystine-Cu(I)$ was used to catalyze triazole's synthesis using different organic halides, different alkynes, and choline azide as reagent (Scheme 3.13). A variety of halides and alkyne provided the desired product in excellent yields. Catalyst recovery and reuse studies showed that after five runs, the catalytic activity did not change too much.
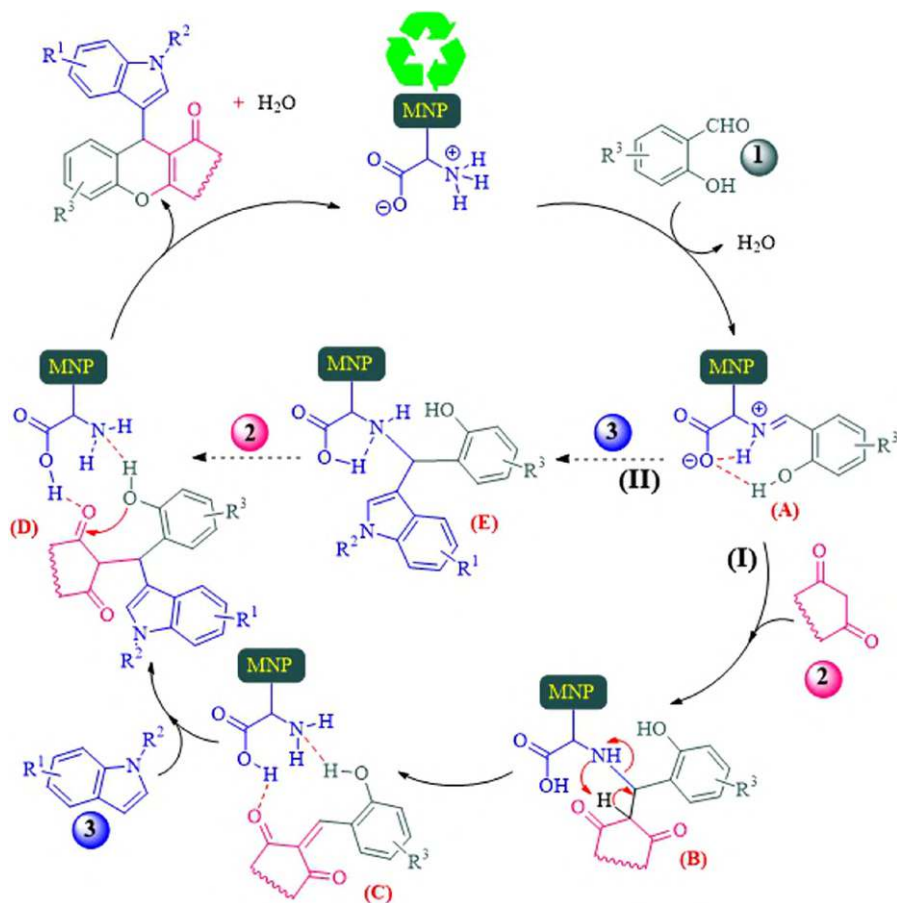
SCHEME 3.6.   The multicomponent reaction mechanism in the presence of LCMNP.

Bankar et al. were able to synthesize catalyst nano-Fe_3O_4@L-cysteine using mixing $FeCl_3 \cdot 6H_2O$ and urea in water at 80–90°C for 2 h and a brown solution was obtained, followed by the addition of $FeSO_4 \cdot 7H_2O$ and sodium hydroxide to a mixture reaction until the pH turned into 10. The material was sonicated and concentrated to afford a black (Fe_3O_4). The resulting nanoparticles were then treated with cysteine to produce nano-Fe_3O_4@L-cysteine (Scheme 3.14) [11].

Authors characterized nano-Fe_3O_4@L-cysteine by several analyses, including FT-IR, TEM, and FEG-SEM-EDS. Fe_3O_4@L-cysteine was used as a catalyst for bis(indolyl)methanes synthesis, which was carried out under solvent-free and microwave irradiation conditions (Scheme 3.15). Fe_3O_4@L-cysteine, as a recyclable and reusable catalyst, showed no significant reduction in activity after ten runs.
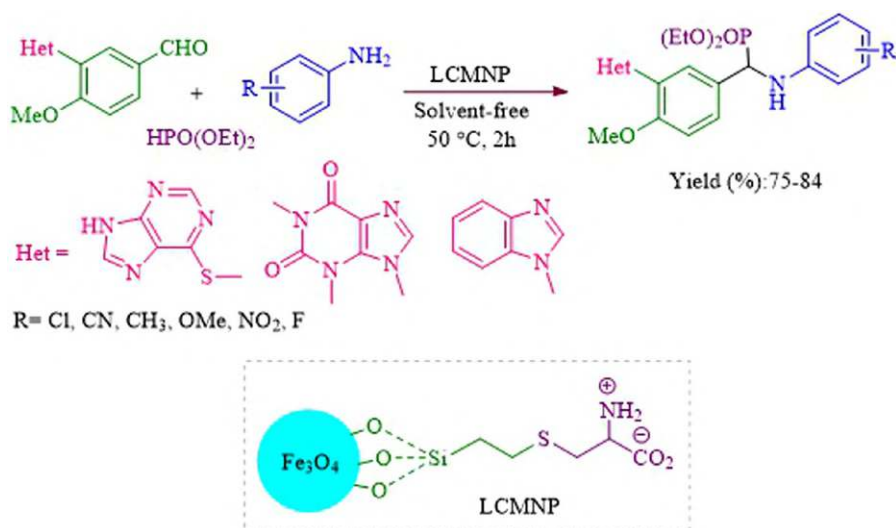
SCHEME 3.7.   Preparation of new α-aminophosphonate derivatives.
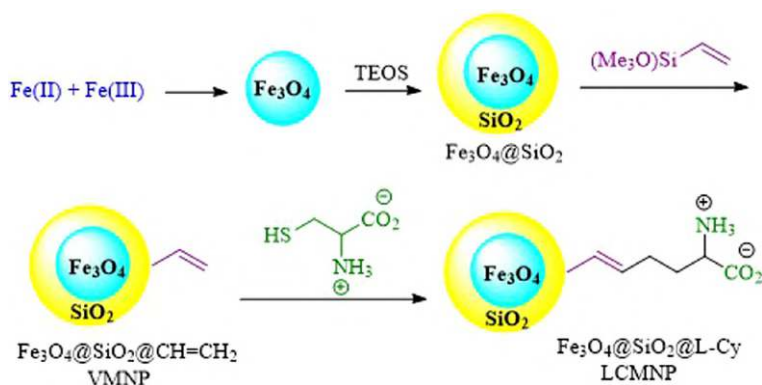
SCHEME 3.8.   The synthetic strategy for the synthesis of LCMNP material.

3.3. CATALYTIC APPLICATION OF METAL COMPLEXES OF L-CYSTEINE IN THE CROSS-COUPLING REACTION

Microspheres recognized are defined as spherical particles and have a particle size of 1–1,000 μm. There are two classifications of microencapsulation-based encapsulation of active drug moieties: microcapsule (loosely defined as [spherical] particles in the size range between 50 nm and 2 mm) and micromatrices. In recent years, significant efforts have been made to explore new utilization of microspheres. For example, biomedicines, catalysis, paints, and various technical methods developed for hydrogen storage and CO_2 adsorption capacity have been developed due to their unique
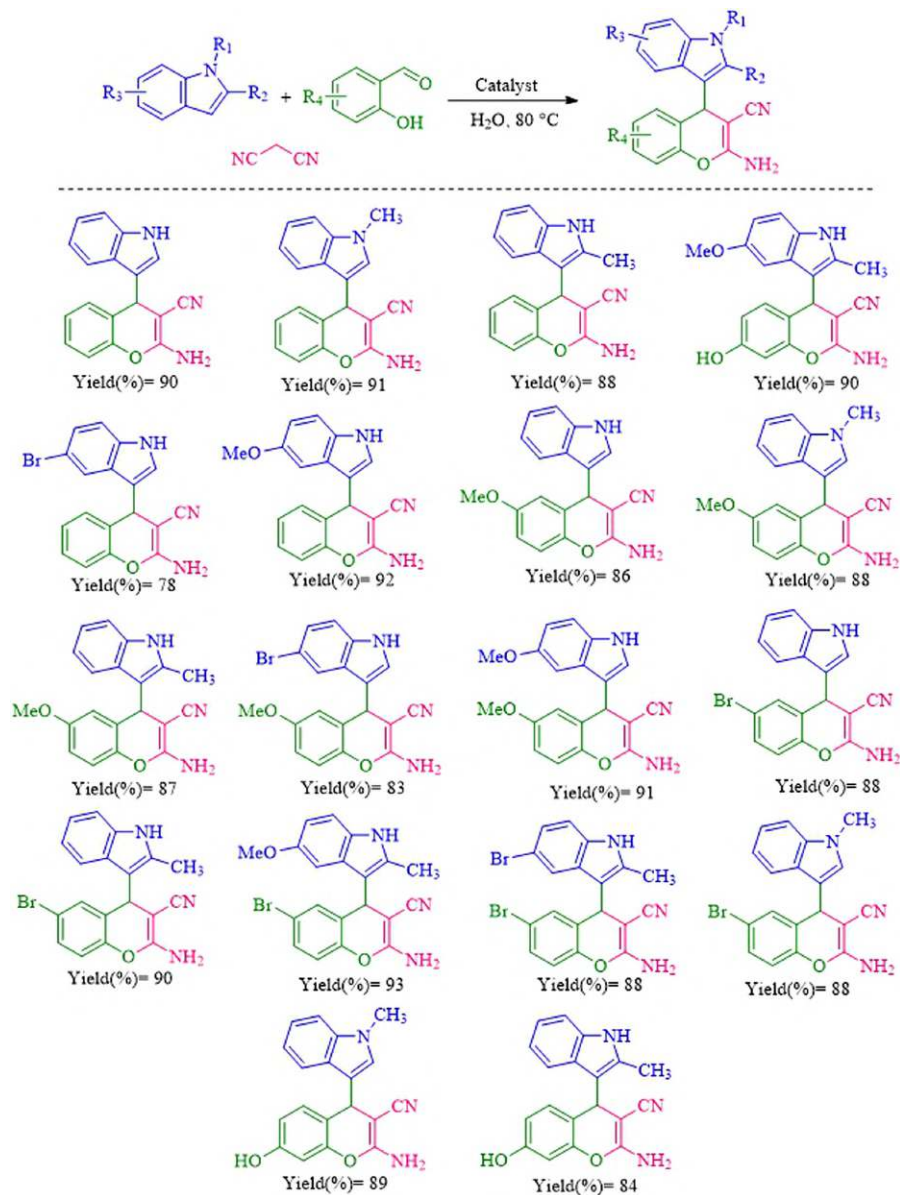
SCHEME 3.9. LCMNP nanoparticles catalyzed the synthesis of multicomponent reaction.

ArB(OH)₂	Time(min)	Yield(%)
2-OMe-phenyl B(OH)₂	20	95
phenyl B(OH)₂	150	90
4-MeO-phenyl B(OH)₂	70	85
4-Me-phenyl B(OH)₂	120	85
trifluoro-phenyl B(OH)₂	90	90
1,4-phenylene bis-B(OH)₂	150	75
Cl-phenyl B(OH)₂	90	95
thiophene B(OH)₂	90	90
naphthyl B(OH)₂	50	95
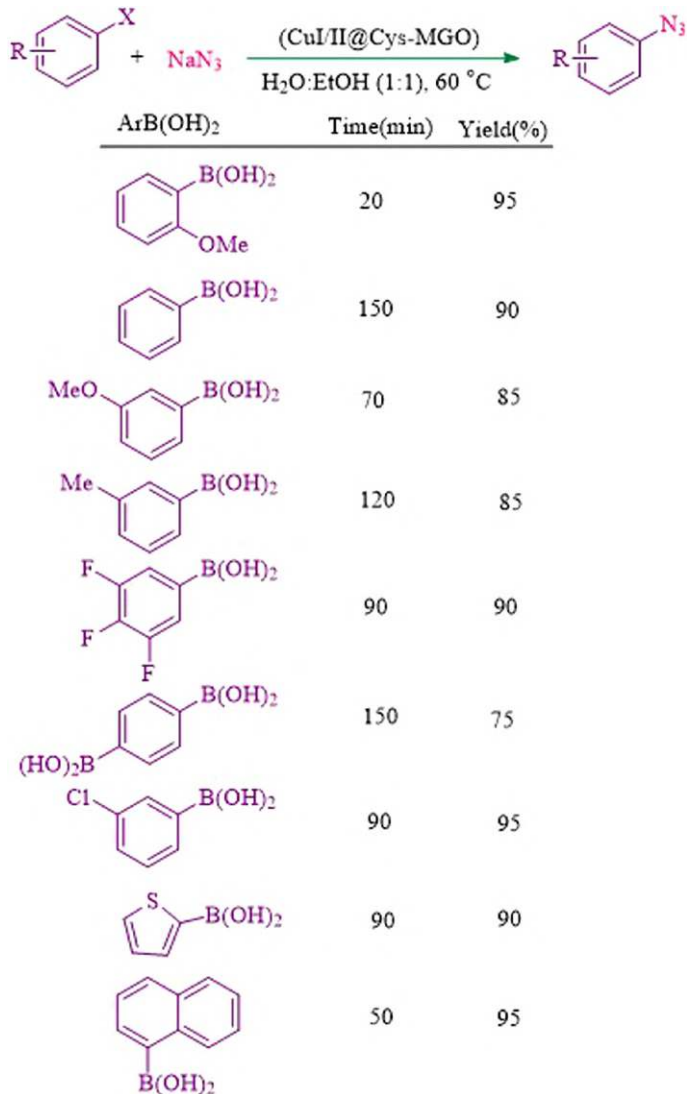
SCHEME 3.10. CuI/II@Cys-MGO nanocomposite catalyzed coupling reaction of aryl boronic acids with NaN₃.

properties. Our research group synthesized the preparation of Bi_2S_3 microspheres using L-cysteine employed as both the sulfur source and directing molecule for the formation of Bi_2S_3 (Scheme 3.16). Thereafter, it is employed as a heterogeneous cat-alyst in the Suzuki–Miyaura cross-coupling reactions and nucleophilic opening of epoxides (Schemes 3.17 and 3.18) [12]. This strategy provides several advantages such as the doing reaction under solvent-free conditions, using H_2O as a green solvent,
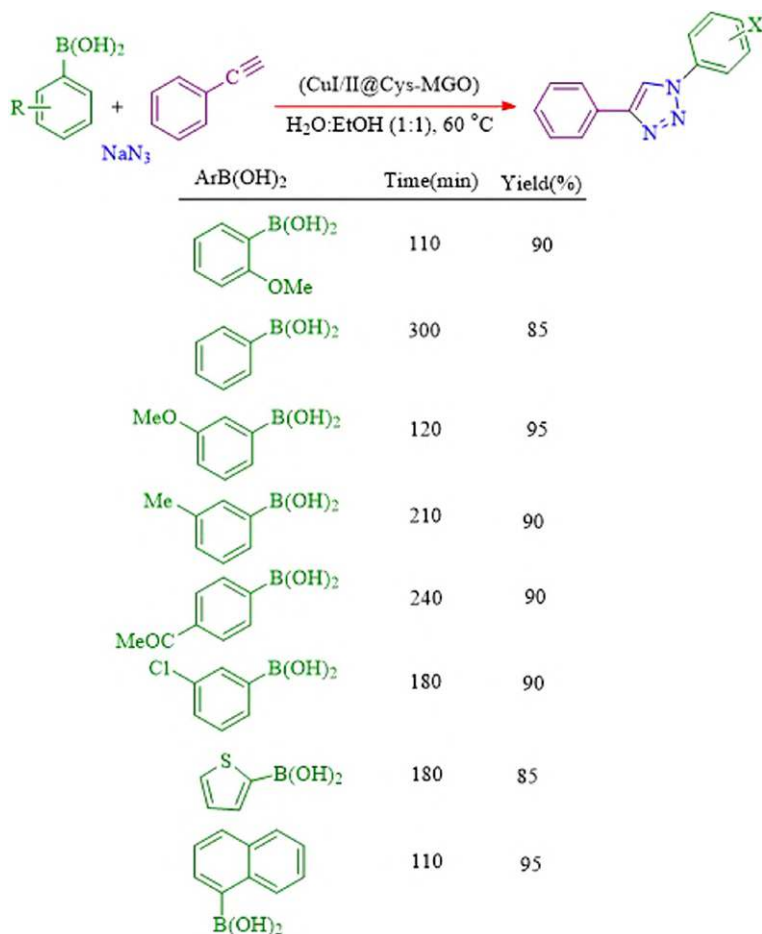
SCHEME 3.11. CuI/II@Cys-MGO nanoparticle catalyzed the synthesis of multicomponent reaction.

short reaction time, high turnover frequency at room temperature, and high regio- and chemoselectivity. The catalyst was recovered and reused without significant loss of catalytic activity. For the C—C coupling reaction, excellent catalysts were obtained with electron-rich substituents than with the electron-poor substituents.

The C—N and C—O cross-coupling reactions were achieved by MNPs@Cys-Pd (Pd treated with the surface of cysteine-functionalized magnetic) as a nanocatalyst (Scheme 3.19) [13]. Employing KOH as the base resulted in the formation of the desired product. EtOH was suitable to be the best solvent for this reaction. The substrate scope of the reaction MNPs@Cys-Pd was studied with a range of aryl halides and secondary amines and ethers resulting in a good yield of the desired product (Scheme 3.20).

Recently, we performed homocoupling reactions of various aryl halides using L-cysteine via a homolytic aromatic substitution mechanism (through the replacement
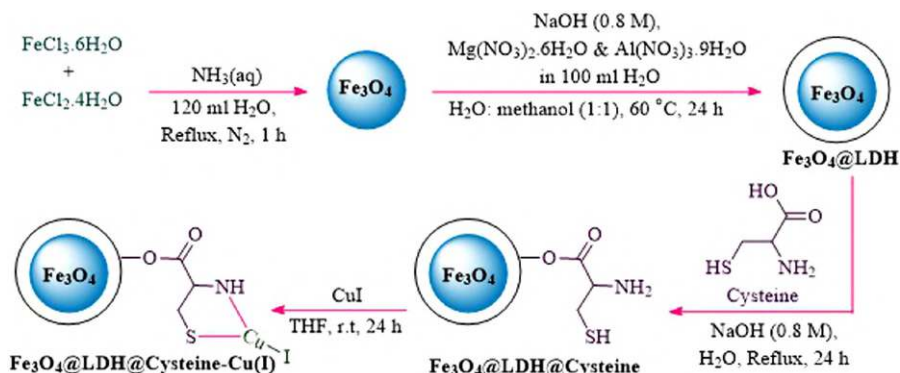
SCHEME 3.12. Fe_3O_4@LDH@cystine-Cu(I) nanocatalyst preparation method.

Yield (%) = 80-97
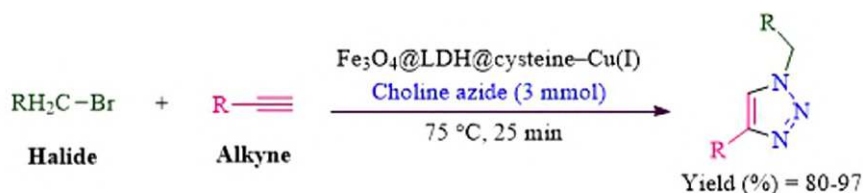
Alkyne = ethynylbenzene, 1-ethynylcyclohexan-1-ol, 1-ethynyl-4-methylbenzene, propiolic acid, prop-2-yn-1-ol

Halide = (bromomethyl)benzene, 1-(bromomethyl)-4-fluorobenzene, 3-bromoprop-1-ene 1-(bromomethyl)-4-nitrobenzene,1-bromo-4-(bromomethyl)benzene, 1-(bromomethyl)-4-methoxybenzene, 1-(bromomethyl)-2,4-dichlorobenzene, 1-(chloromethyl)-3-methylbenzene, 2-bromo-1-(4-chlorophenyl)ethan-1-one, 2-bromo-1-phenylethan-1-one, 2-bromo-1-(4-nitrophenyl)ethan-1-one, (chloromethyl)benzene,

SCHEME 3.13.   Triazole synthesis catalyzed by Fe_3O_4@LDH@cystine-Cu(I).

of a leaving group (X) on the aromatic ring by an attacking radical species) (Scheme 3.21).

It is known that L-cysteine can be oxidized by dimethyl sulfoxide; this process leads to the release of two electrons. Experimental results show that there are two reaction paths: (1) the oxidation of the L-cysteine was observed under pH (8) and (2) β-elimination is carried out under pH 10.6 (Scheme 3.23). Therefore, the optimal focusing of biaryls was observed using KOH as the base and DMSO as a solvent to yield the corresponding desired products in yields (45–88%)(Scheme 3.22). We then examined the scope of the substrate for this transformation coupling reaction using various aryl halides bearing diverse substituents, including electron-poor and electron-rich substituents (Scheme 3.23). Under optimal reaction conditions, symmetrical biphenyls were synthesized from different aryl halides, and high yields were obtained [14].
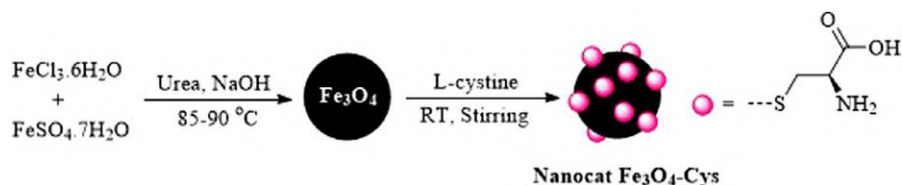
SCHEME 3.14.   Preparation of Fe$_3$O$_4$-Cys MNPs.

R$_1$= Aryl, Alkyl
R$_2$= H, Alkyl
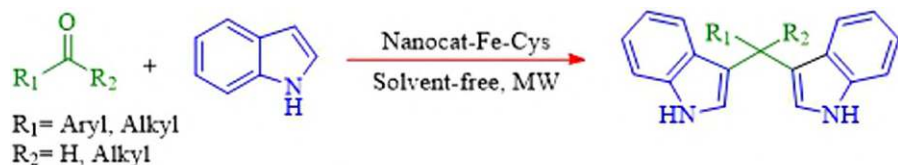
Reactants		Yield (%)
Indole	Benzaldehyde	92
Indole	4-Chlorobenzaldehyde	89
Indole	4-Nitrobenzaldehyde	93
Indole	3-Nitrobenzaldehyde	90
Indole	Acetone	83
Indole	4-Formylbenzonitrile	90
Indole	4-Methylbenzaldehyde	84
Indole	Cyclohexanone	89

SCHEME 3.15.   Synthesis of bis(indolyl)methanes catalyzed by Nano-Fe$_3$O$_4$-Cys.

3.4.   CATALYTIC APPLICATION OF METAL COMPLEXES OF L-CYSTEINE IN THE OXIDATION REACTION

In 2016, Nikorzem et al. designed an amino acid–based mesoporous catalyst through immobilization of MCM-41 with L-cysteine followed by coordination with VO(acac)$_2$ (Scheme 3.24).

They applied this mesoporous material as a versatile catalyst for the oxidation reaction of sulfides and the synthesis of disulfides in green conditions using hydrogen peroxide (Scheme 3.25) [15]. In both of the reactions, corresponding products were obtained in a short time, with excellent efficiency and high purity.

3.5.   CATALYTIC APPLICATION OF METAL COMPLEXES OF L-CYSTEINE-SUPPORTED MATERIAL IN THE OXIDATION REACTION

In 2022, Zamani et al. described the synthesis of copper (II)-cysteine/SiO$_2$-Al$_2$O$_3$ by a simple adsorption method [16]. The performance of the catalyst is used for the selective oxidation of different aromatic alcohols to the desired product in high
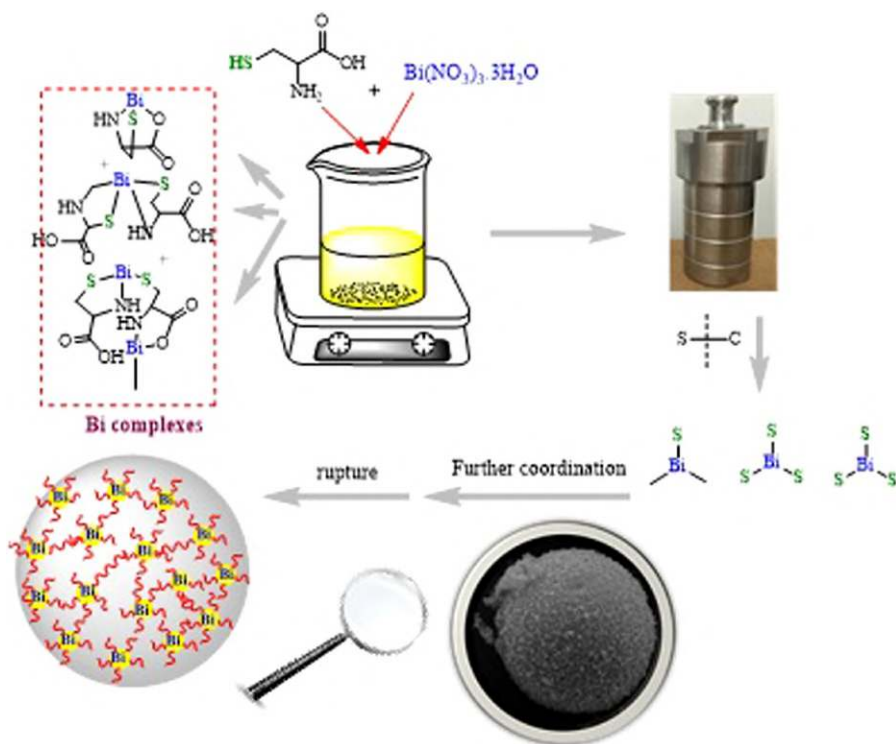
SCHEME 3.16. Schematic synthesis of Bi$_2$S$_3$ microspheres. *Source:* Reproduced with permission from Ref. [12]. Copyright 2020, Elsevier B.V.
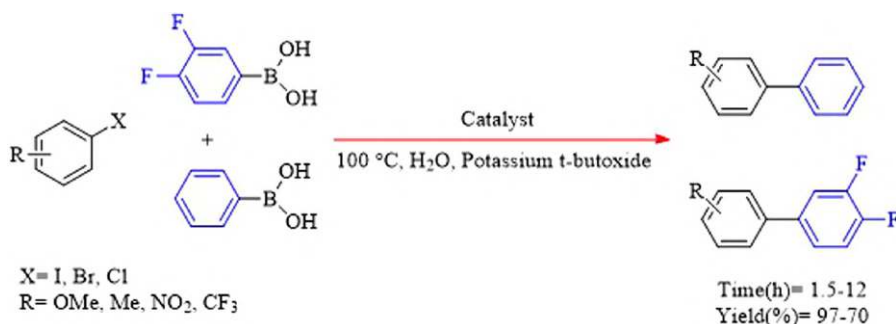
SCHEME 3.17. Bi$_2$S$_3$ microspheres catalyzed the synthesis of biaryl.

yields with hydrogen peroxide as a green oxidant at room temperature under solvent-free conditions (Scheme 3.26).

In 2018, Maurya et al. prepared oxovanadium (IV) complexes by a combination of salicylaldehyde and L-cysteine (H$_2$sal-cys) and employed it as catalyst for the

Ph−X

$\triangle$ + X = NH$_2$, SH, and OH

Ph

Ph⌒OH

R−CH$_2$OH

Catalyst
⟶
Solvent-free

HO
Ph　　XPh
+
PhX
Ph　　OH

Time (h): 10 min- 4.5 h
Yield (%): 50-95
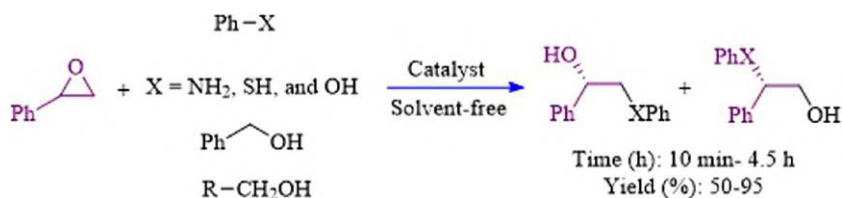
SCHEME 3.18. Ring-opening reactions.

MNPs --O-Si⌒⌒Cl
---O

NaI
⟶
Acetone, reflux

MNPs --O-Si⌒⌒I
---O

Cysteine
⟶
Acetonitrile

MNPs --O-Si⌒⌒⌒S⌒C(O)OH
---O　　　NH$_2$

Pd(OAc)$_2$
⟶
EtOH

MNPs --O-Si⌒⌒⌒S⌒C(O)O
---O　　　NH$_2$ ˙Pd
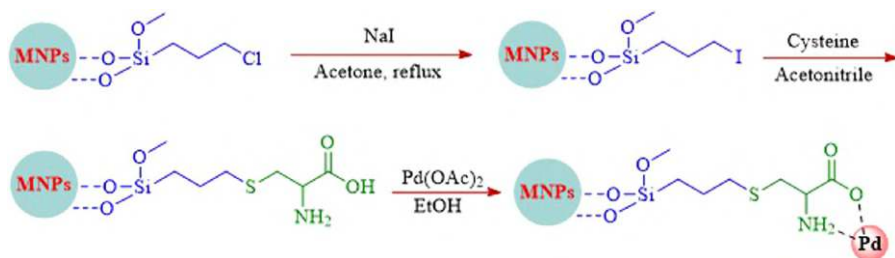
SCHEME 3.19. Synthetic route for the production of nanocatalysts.

R⌬−X + Alcohol
MNPs@CYs-Pd
⟶
EtOH, KOH, 60 °C
Ether

R	X	Alcohol	Yield(%)
H	I	phenol	98
H	I	2,3,6-trimethylphenol	72
H	I	(4-chlorophenyl)methanol	95
H	I	2-chloro-6-nitrophenol	88
H	I	phenol	97
H	I	5-bromo-2-hydroxybenzaldehyde	86
H	I	3,5-dinitrophenol	100
H	I	resorcinol	73
4-Me	I	2,6-dimethylphenol	71
H	Br	4-hydroxybenzaldehyde	92
H	Br	naphthalen-1-ol	76
4-NO$_2$	Br	(4-chlorophenyl)methanol	90
H	Cl	(4-chlorophenyl)methanol	93

SCHEME 3.20. *O*-arylation of aryl halides and different alcohols.

oxidative amination of styrene with various amines, including diethylamine, imidazole, and benzimidazole. This procedure offers yielding a product using oxygen and triethylamine (Scheme 3.27) [17]. The reaction of sterically hindered secondary amine under these conditions gave anti-Markovnikov products.

R	X	Amine	Yield(%)
H	I	morpholine	93
H	Br	morpholine	94
4-NO$_2$	Br	diphenylamine	81
4-NO$_2$	Cl	diphenylamine	79
2,4-di-NH$_2$	Cl	morpholine	72
4-OMe	Br	morpholine	87
H	Br	propan-1-amine	trace
2-NO$_2$	Br	morpholine	81
H	Br	N-methylbenzenamine	93
4-NO$_2$	Br	N-methylbenzenamine	98
4-Br	Br	morpholine	92
4-NO$_2$	Cl	morpholine	87
H	Cl	morpholine	80
9-bromophenanthrene	Br	morpholine	86
3-COCH$_3$	Br	morpholine	trace

SCHEME 3.21. *N*-arylation of aryl halides and different amines.
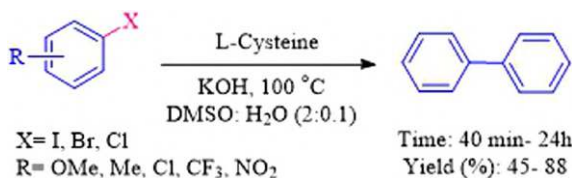
SCHEME 3.22. Metal-free homocoupling of aryl halides.

3.6. APPLICATION OF L-CYSTEINE DERIVATIVES AS ORGANOCATALYSTS FOR THE ADDITION OF DIETHYLZINC TO ALDEHYDES

Braga et al. designed and synthesized several new cysteine-derived chiral sulfides and disulfides and investigated their performances in the reaction of various alde-hydes with diethyl zinc (Scheme 3.28).

Among the prepared catalysts, catalyst 1 offers the best performance and yields the final product with high enantioselectivity in *S* configuration (Scheme 3.29) [18].

Serra et al. synthesized several thiazolidine ligands derived from the combina-tion of D-penicillamine and L-cysteine and then investigated their catalytic proper-ties in the alkylation reaction of benzaldehyde with diethyl zinc (Scheme 3.30) [19]. The formation of *R* and *S* isomers was observed in the presence of these catalysts and excellent results were obtained, although D-penicillamine-derived thiazolidine ligands showed better activity. Finally, the alkylation reaction of different aldehydes
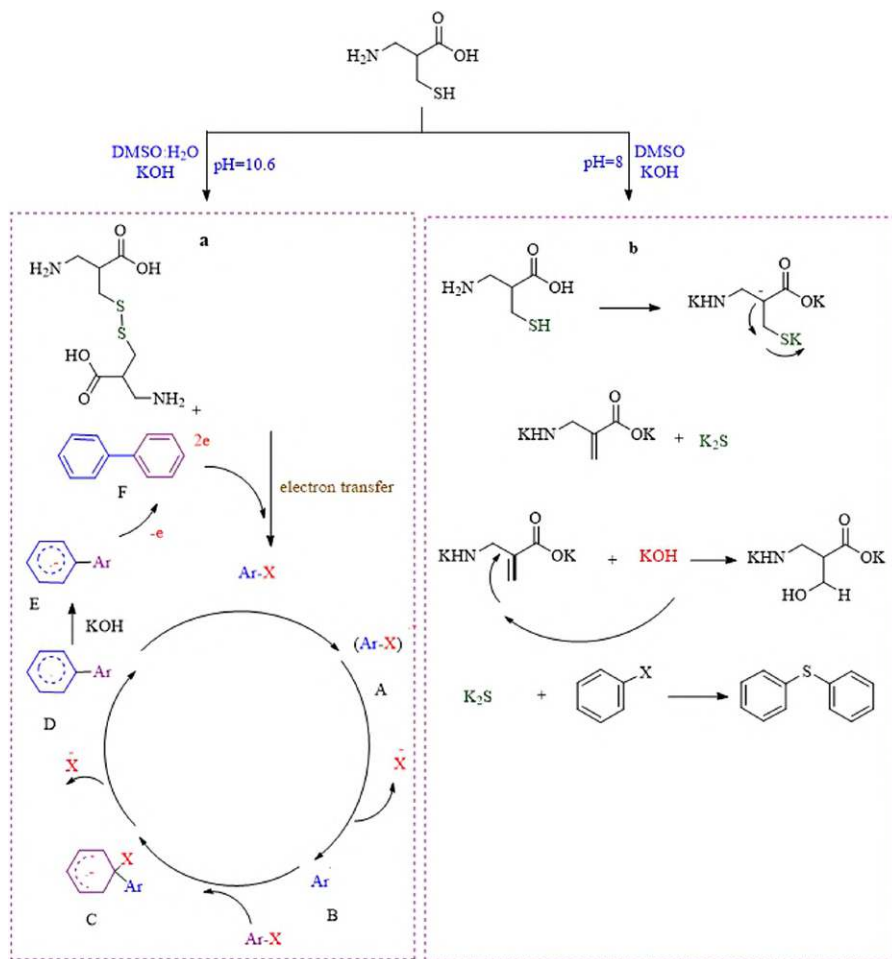
SCHEME 3.23. Suggested route for the synthesis of C—C coupling (a) and symmetrical aryl sulfides (b). *Source:* Reproduced with permission from Ref. [14]. Copyright 2018, Royal Society of Chemistry.

with diethyl zinc was performed in the presence of catalyst **2a** (thiazolidine ligand derived from D-penicillamine), and products with high enantiomeric excesses and *R* configuration were obtained.

   Braga et al. synthesized several chiral sulfides and disulfides in short steps from L-cysteine (Scheme 3.31). Cysteine was first reacted with an aldehyde to form the thiazolidine 1 ring; thiazolidine 1 was then reduced in the presence of $NaBH_4/I_2$ to produce the amino alcohol disulfide 2. Disulfide 2 reacted with paraformaldehyde to give thiazolidine 3. Finally, sulfides 2 and 3 were reduced with $NaBH_4$ and then alkylated with MeI to give methyl thioethers 4 and 5.

SCHEME 3.24. Step synthesis of VO@MCM-41-Cys.

$R^1 = $ Ph, Benzyl, -(CH$_2$)$_4$-, Me, p-ClC$_6$H$_4$, C$_{12}$H$_{25}$, Et, p-MeC$_6$H$_4$
$R^2 = $ Me, -(CH$_2$CH$_2$OH), Ph, Benzyl, Et, C$_{12}$H$_{25}$

R= benzo[d]oxazole-2-thiol, phenylmethanethiol, propane-1-thiol,
4,6-dimethylpyrimidine-2-thiol, 2-aminobenzenethiol,
2-mercaptobenzoic acid, pyridine-2-thiol, benzo[d]thiazole-2-thiol,
naphthalene-2-thiol, 4-methylbenzenethiol, 4-bromobenzenethiol
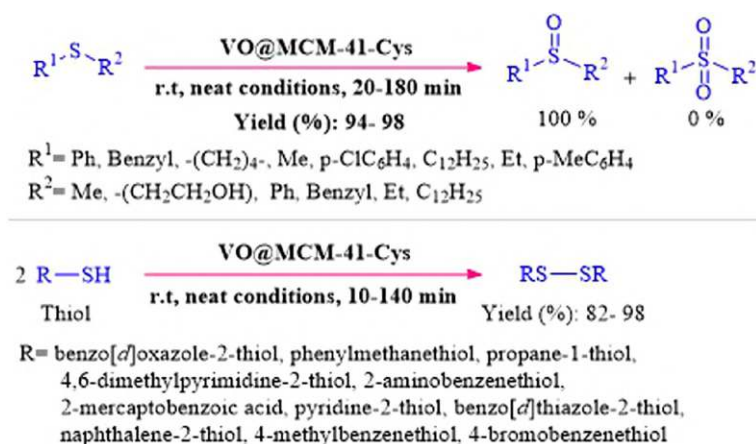
SCHEME 3.25. Oxidation of sulfides and oxidative coupling of thiols catalyzed by VO@ MCM-41-Cys.

These cysteine-derived materials were used as catalysts to perform the diethylzinc addition to aromatic and aliphatic aldehydes to produce alcohols with high ee%, of which the (R,R)-bis[(3-benzyloxazolan-4-yl)-methane]disulfide catalyst exhibited the best activity and enantioselectivity (Scheme 3.32) [20].

3.7. CATALYTIC APPLICATION OF L-CYSTEINE-BASED IONIC LIQUID IN ADDITIVE-FREE OXIDATIVE COUPLING OF ALCOHOLS AND AMINES

Leng et al. prepared Au$_a$/DVB-[MimLcy]$_3$ using free radical copolymerization between divinyl benzene (DVB) and imidazolium ionic liquid (IL) and then replaced

—CH$_2$OH	—CHO 60 min, 95%
Br—CH$_2$OH	Br—CHO 45 min, 95%
Cl—CH$_2$OH	Cl—CHO 45 min, 75%
O$_2$N—CH$_2$OH	O$_2$N—CHO 50 min, 90%
—CH$_2$OH (CH$_3$)	—CHO (CH$_3$) 45 min, 98%
OH (Cl-benzhydrol)	O (Cl-benzophenone) 80 min, 80%
OH (benzhydrol)	O (benzophenone) 70 min, 85%
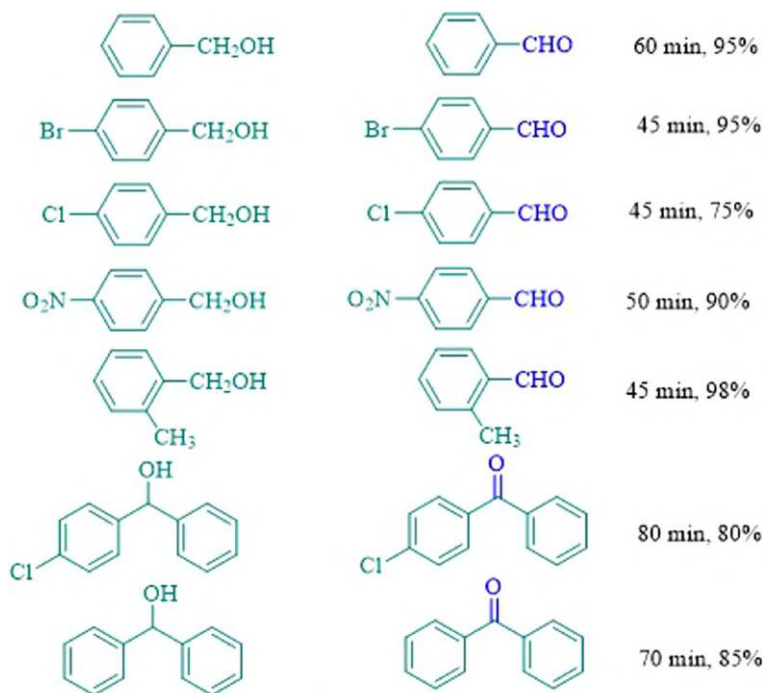
Reaction conditions: alcohol (1 mmol), H$_2$O$_2$ (4 mmol),
Cu(II)–cysteine/SiO$_2$-Al$_2$O$_3$), solvent-free, room temperature

SCHEME 3.26. Cu(II)-cysteine/SiO$_2$-Al$_2$O$_3$-catalyzed oxidation of various aromatic alcohols.
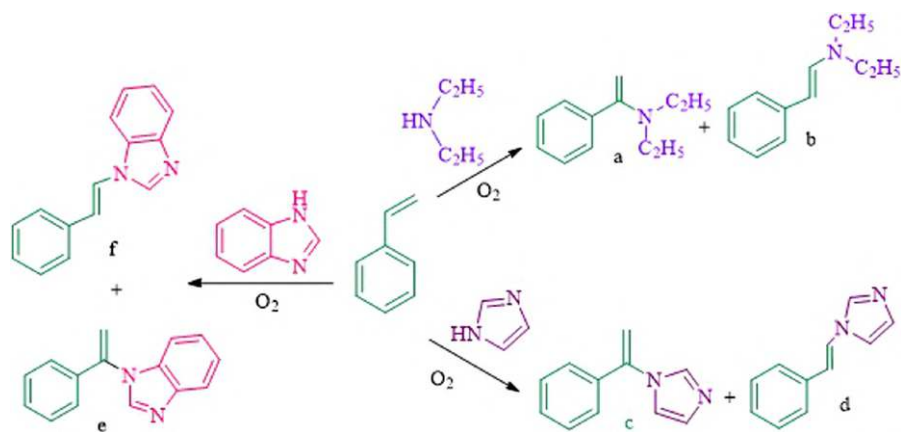
SCHEME 3.27. (a) *N,N*-diethyl-1-phenylethylamine. (b) *N,N*-diethyl-1,2-phenylethylamine. (c) 1-(1-phenyl vinyl)-1*H*-imidazole. (d) 1-styryl-1*H*-imidazole. (e) 1-(1-phenyl vinyl)-1*H*-benzimidazole. (f) 1-styryl-1*H*-benzimidazole.
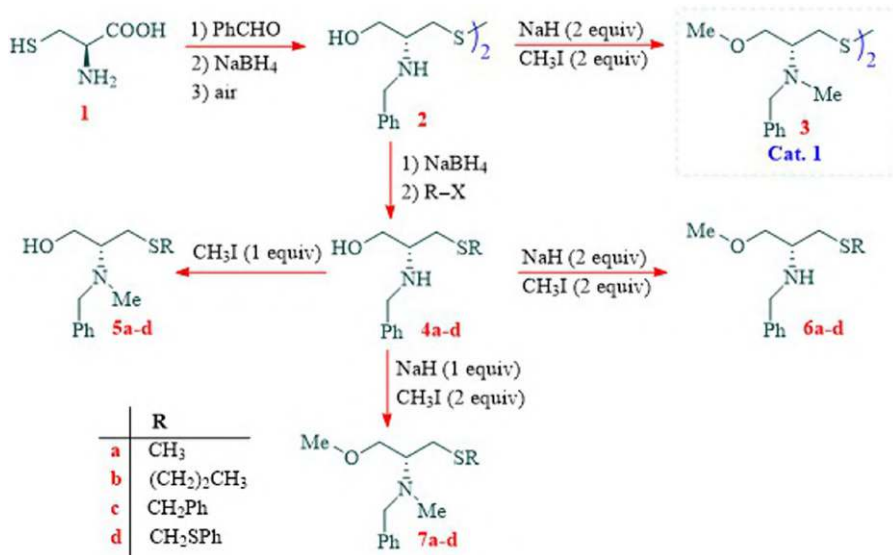
SCHEME 3.28.   Synthesis of sulfide and disulfide ligands.
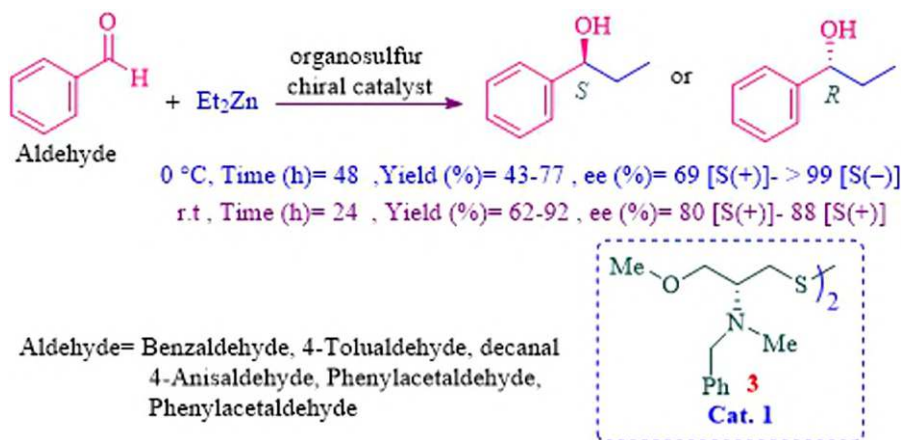
SCHEME 3.29.   The reaction of various aldehydes with diethyl zinc in the presence of catalyst 1.

the anion with L-cysteine; they then synthesized DVB-[MimLcy]$_n$, which was a good stabilizer for metal nanoparticles due to its $-NH_2$, $-SH$, and $-COO^-$ groups, as well as its porous framework. They finally decorated DVB-[MimLcy]$_3$ with Au metallic ions (Scheme 3.33) [21].

In the Au$_a$/DVB-[MimLcy]$_3$ preparation process, various tools such as CHNS elemental analysis, FT-IR, TG, SEM, TEM, ICP-AES, powder XRD, XPS, isothermal N_2 absorption–desorption analysis, and EDS elemental mapping were used to identify
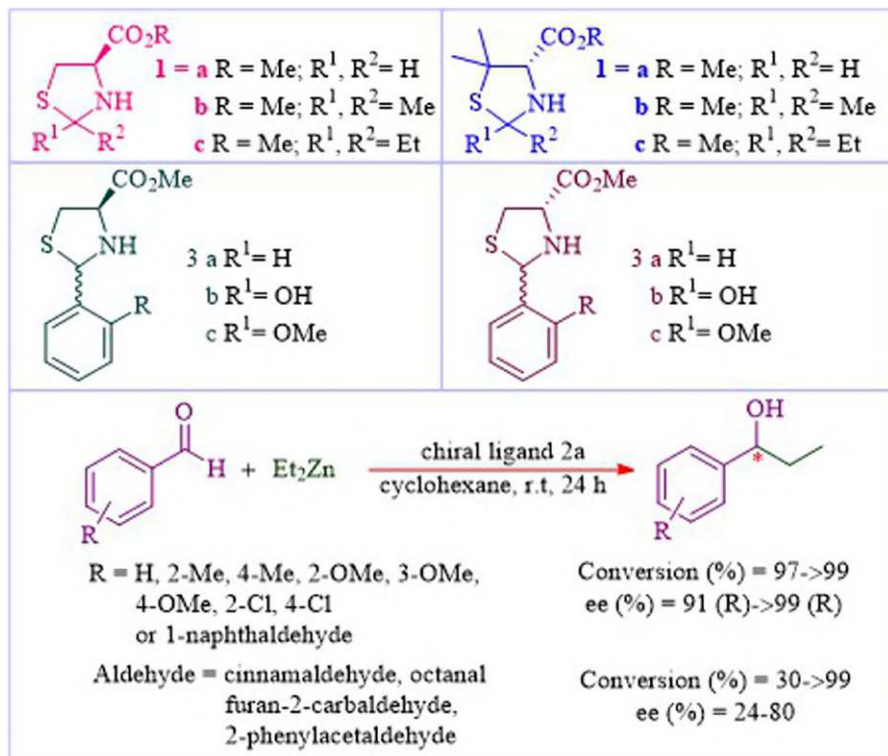
SCHEME 3.30. Alkylation reaction catalyzed by thiazolidine ligands derived from D-penicillamine and L-cysteine.

its characteristics. The authors examined the performance of Au_a/DVB[MimLcy]$_3$ as an active catalyst to the oxidative coupling of alcohols and amines without the use of any additives (Scheme 3.34).

3.8.   APPLICATION OF METAL COMPLEXES OF L-CYSTEINE DERIVATIVE AS A CATALYST FOR REGIOSELECTIVE HYDROCARBOXYLATION CATALYST FOR 2-PHENYLPROPANOIC ACID

Real et al. designed and synthesized a palladium (II) complex containing L-cysteine and investigated its catalytic properties in the hydrocarboxylation reaction of styrene under two different times in variable temperature conditions, the results of which are shown in Scheme 3.35 [22].
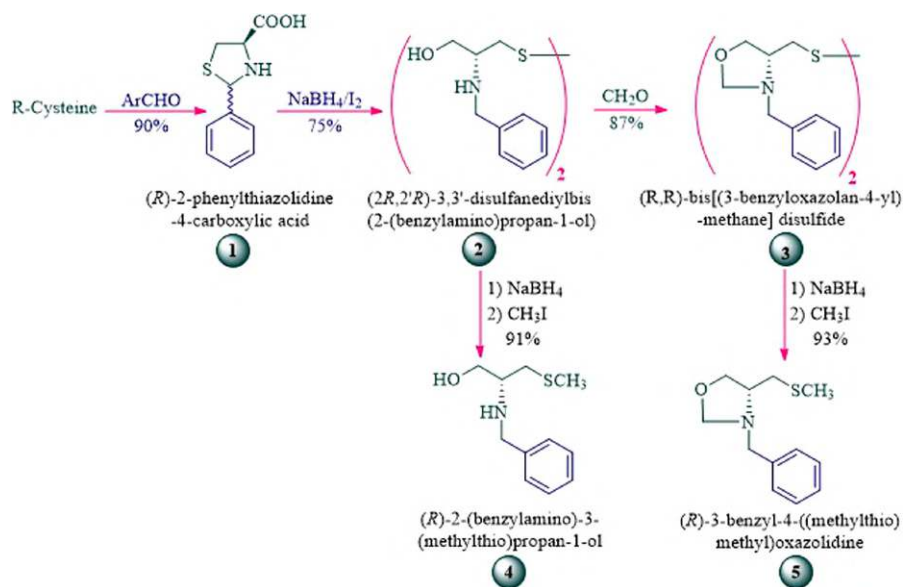
SCHEME 3.31. Synthesis of cysteine-derived chiral sulfide and disulfide ligands.

Entry	Aldehyde	Yield (%)	ee (%) [config]
1	Benzaldehyde	81	>99 [S(-)]
2	4-Tolualdehyde	71	86 [S(-)]
3	4-Anisaldehyde	65	70 [S(-)]
4	Phenylacetaldehyde	38	92 [S(+)]
5	Hexanal	58	>99 [S(+)]
6	Decanal	50	40[S(+)]
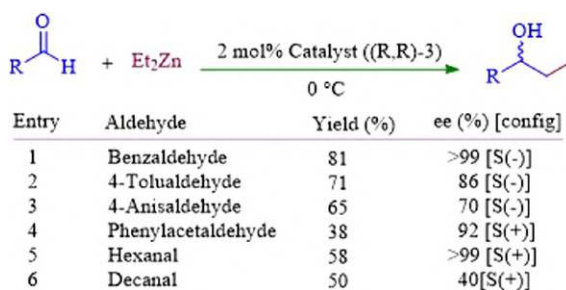
SCHEME 3.32. (R,R)-3 catalyzed the addition of diethylzinc to different aldehydes.

3.9. APPLICATION OF L-CYSTEINE AS AN EFFICIENT AND REUSABLE PHOTOCATALYST FOR HYDROGEN PRODUCTION

Nanocluster-modified semiconductor-based photocatalysts have received increasing research attention in recent years and exhibited potential for wide application in hydrogen evolution from water [23]. However, the available ligand protection strategy for the synthesis of nanoclusters is limited to a few metals: Au, Ag, Cu, and their alloys. In this sense, Wang et al. explore the solution-phase synthesis of Ru nanoparticles and it is utilized as cocatalysts for assisting photocatalytic H_2 generation [24]. Moreover, the experimental result showed that the combination of hybrid CdS photocatalyst with Ru nanoclusters provides an increase in the photocatalytic

SCHEME 3.33. Ionic copolymers DVB-[MimLcy]$_n$ preparation pathway.

catalytic activity: (benzylamine conversion%, benzyl alcohol conversion%) selectivity%
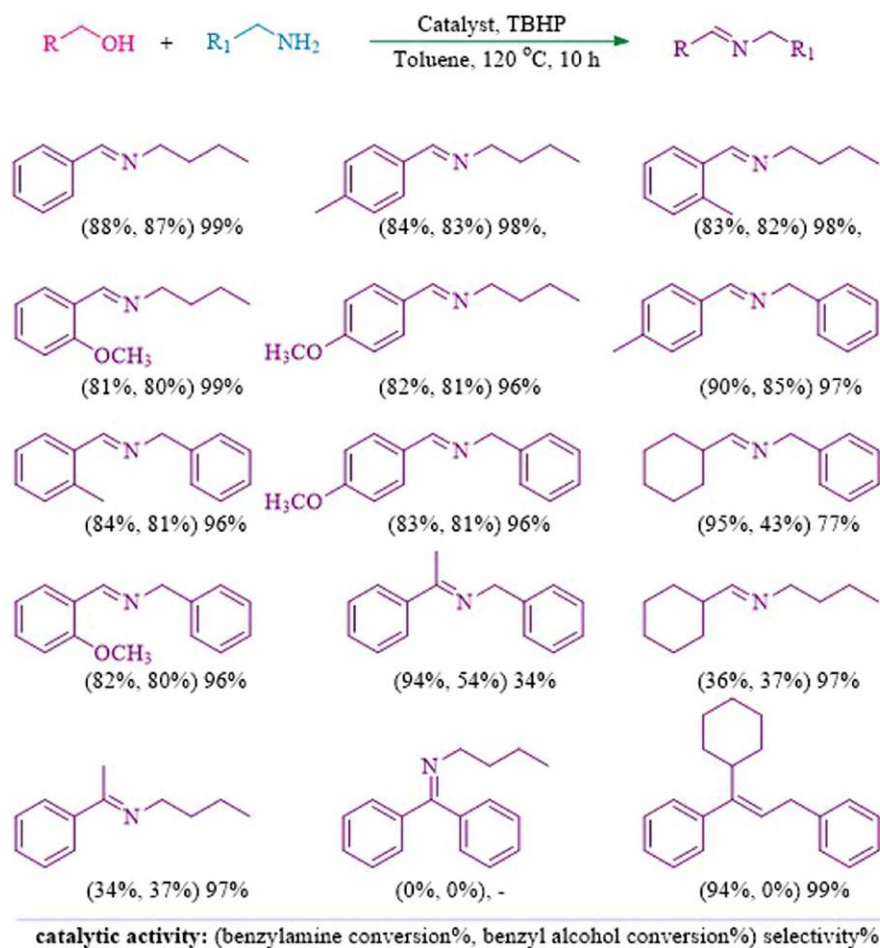
SCHEME 3.34. Catalysis of the oxidative coupling of different alcohols and amines by Aua/DVB-[MimLcy]$_3$.
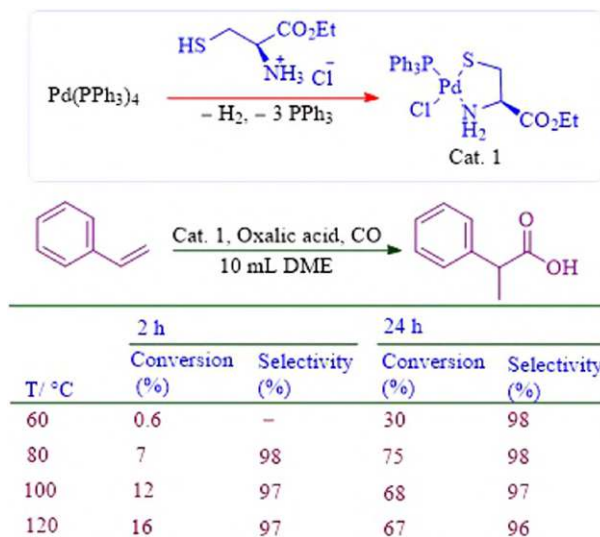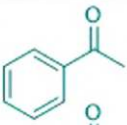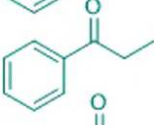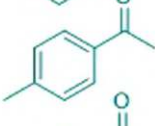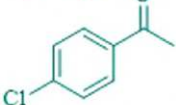
SCHEME 3.35. Hydrocarboxylation of styrene with Cat.1.

H_2 generation of the nanocomposite photocatalysts under visible light irradiation. In another study, the application of L-cysteine-capped $CoNiS_x$ (L-CNS_x) nano-plates generate Mn-Cd-S solid solution (MCS) nanomaterials in situ for the efficient construction and it is employed for photocatalytic hydrogen evolution reaction (HER) [25]. In this context, Zhang et al. introduced a highly effective and robust L-Mo2C/Zn0.67Cd0.33S heterojunction through intimate Mo-S covalent bonds. In this study, L-cysteine-capped Mo_2C and Zn0.67Cd0.33S were used to construct L-Mo_2C/Zn0.67Cd0.33S heterojunction. Experimental results showed L-Mo_2C/Zn0.67Cd0.33S-5 heterojunction enables efficient and stable H_2-releasing photocatalysis [26].

3.10. APPLICATION OF COMPLEXES OF L-CYSTEINE FOR ASYMMETRIC ELECTRON REDUCTION OF AROMATIC KETONES

In 2021, Yue et al. described the synthesis of L-cysteine-CuPt using the combination of L-cysteine and CuPt and it is used for the electroreduction of aromatic ketones to the final products, giving aromatic alcohol compounds in good yields [27]. (R)-α-(trifluoromethyl)benzyl alcohol with 73% yield and 43% ee was obtained on the L-cysteine-CuPt cathode under the optimized electrolytic reaction conditions. The protocol carries out for different aromatic ketones besides the model substrate 2,2,2-trifluoro acetophenone (Scheme 3.36).

Ketones	Yield(%)	R-ee(%)
	69	30
	46	31
	59	30
	22	17

Anode: Mg, cathode: L-cysteine-CuPt-5,
20 mL co solvent (MeCN/n-amyl alcohol=1/1),
0.1 M ketone, sup porting electrolyte: 0.1 M TEAI,
current density: 3 mAcm-2, charge: 2 F mol-1, temperature: 25 °C

SCHEME 3.36.   Asymmetric electroreduction of aromatic ketones using L-cysteine-CuPt-5.

3.11.   APPLICATION OF COMPLEXES OF L-CYSTEINE FOR THE CYCLOADDITION OF CO_2 WITH 2-(PHENOXYMETHYL)OXIRANE)

Metal sulfide is recognized as a semiconductor material, where sulfur is an anion associated with a metal cation; and the metal ions may be in mono-, bi-, or multi-form. Recent progress in exploring layered transition metal sulfide (LTMS) including layered transition metal dichalcogenides (LTMDs) has received increasing attention from the scientific and technology community. In this context, our group described the synthesis of mesoporous vanadium sulfides, including VS_2 (flower-like), VS_4 (urchin-like), VS_4 (microsphere), and VS_2 (nanosheet assemblies), through adjusting the molar ratios of ligand and metal under solvothermal method [28]. Thereafter, the activity of the catalyst was examined for the cycloaddition of CO_2 with epoxide and oxidation reactions (Scheme 3.37-3.38). The ascribed mechanism for this reaction is shown in Schemes 3.39.

3.12.   CONCLUSIONS

This chapter has highlighted the catalytic activity of supported and unsupported chiral L-cysteine as organocatalysts and catalysts in organic reactions. Decoration

Morphologies	Cat. (mol%)	Yield(%)
VS_2(Flower-like)	0.5	75
VS_4(Urchin-like)	0.5	70
VS_4(Microsphere)	0.5	80
VS_2(Nanosheet assemblies)	0.5	88

Reaction conditions: 2-(phenoxymethyl)oxirane (17 mmol), catalyst, Pressure=1.2 MPa of CO_2, DMF(2 mL); reaction time: 6h
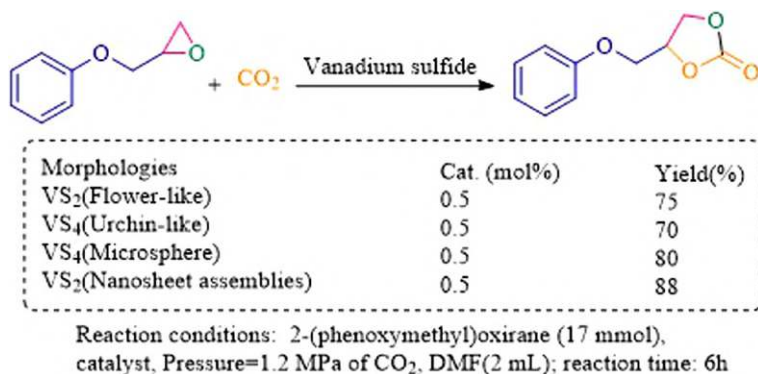
SCHEME 3.37. The reaction of CO_2 and epoxide using vanadium sulfides.
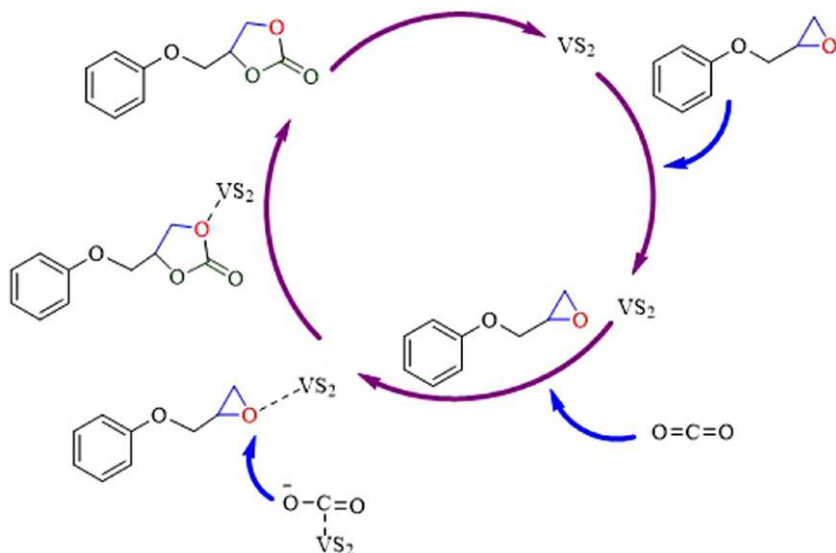
SCHEME 3.38. Suggested route for the CO_2 cycloaddition with epoxide.

of amino acids on supported material has attracted promising results on catalysts' reactivity, selectivity, and recyclability. There is no doubt that it has been developed rapidly in recent years and has become a practical technology to provide green chemistry.
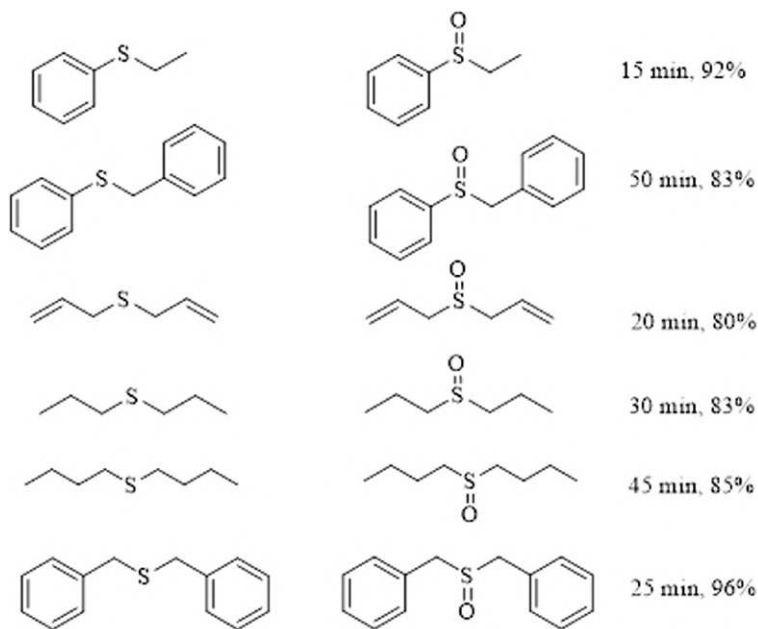
Reaction condition: sulfide (1 mmol), H_2O_2 30% (0.3 mL), ethyl acetate, r.t.
Catalyst= VS_2(Nanosheet assemblies)

SCHEME 3.39. VS_2-catalyzed selective oxidation of sulfides to sulfoxides using H_2O_2 at room temperature.

REFERENCES

1. Sameem, B., Khan, F., Niaz, K. L-Cysteine. In *Nonvitamin and Nonmineral Nutritional Supplements*; Elsevier, 2019, 53–58. https://doi.org/10.1016/B978-0-12-812491-8.00007 -2.
2. Loibl, S. F., Harpaz, Z., Seitz, O. A type of auxiliary for native chemical peptide ligation beyond cysteine and glycine junctions. *Angew. Chem., Int. Ed.*, 2015, *54*(50), 15055–15059. https://doi.org/10.1002/anie.201505274.
3. Hasija, V., Singh, P., Thakur, S., Nguyen, V. H., Van Le, Q., Ahamad, T. Wu, K. C. W. O and S co-doping induced N-vacancy in graphitic carbon nitride towards photocatalytic peroxymonosulfate activation for sulfamethoxazole degradation. *Chemosphere*, 2023, *320*, 138015. https://doi.org/10.1016/j.chemosphere.2023.138015.
4. Safaei-Ghomi, J., Ebrahimi, S. M. Nano-Fe₃O₄-Cysteine as a Superior catalyst for the synthesis of indeno [1, 2-c] pyrazol-4 (1H)-ones. *Polycyclic. Aromat. Compd.*, 2022, *42*(5), 2693–2703. https://doi.org/10.1080/10406638.2020.1852276.
5. Nikoorazm, M., Moradi, P., Noori, N. L-cysteine complex of palladium onto mesoporous channels of MCM-41 as reusable, homoselective and organic–inorganic hybrid nanocatalyst for the synthesis of tetrazoles. *J. Porous Mater.*, 2020, *27*(4), 1159–1169. https://doi.org/10.1007/s10934-020-00894-0.

6. Nourisefat, M., Panahi, F., Nabipour, M., Heidari, S., Khalafi-Nezhad, A. L-cysteine-functionalized magnetic nanoparticles (LCMNP): As a magnetic reusable organocatalyst for one-pot synthesis of 9-(1H-Indol-3-Yl) Xanthen-4-(9H)-Ones. *J. Iran. Chem. Soc.*, 2016, *13*(10), 1853–1865. https://doi.org/10.1007/s13738-016-0902-2.

7. Bahrami, F., Panahi, F., Daneshgar, F., Yousefi, R., Shahsavani, M. B., Khalafi-Nezhad, A. synthesis of new α-aminophosphonate derivatives incorporating benzimidazole, theophylline and adenine nucleobases using l-cysteine functionalized magnetic nanoparticles (LCMNP) as magnetic reusable catalyst: Evaluation of their anticancer properties. *RSC Adv.*, 2016, *6*(7), 5915–5924. https://doi.org/10.1039/c5ra21419j.

8. Khalafi-Nezhad, A., Nourisefat, M., Panahi, F. L-cysteine functionalized magnetic nanoparticles (LCMNP): A novel magnetically separable organocatalyst for one-pot synthesis of 2-amino-4H-chromene-3-carbonitriles in water. *Org. Biomol. Chem.*, 2015, *13*(28), 7772–7779. https://doi.org/10.1039/c5ob01030f.

9. Rafiee, F., Khavari, P. Preparation of aryl azides of aryl boronic acids and one-pot synthesis of 1,4-Diaryl-1,2,3-triazoles by a magnetic cysteine functionalized GO–CuI/II nanocomposite. *Appl. Organomet. Chem.*, 2020, *34*(9), e5789. https://doi.org/10.1002/aoc.5789.

10. Pazoki, F., Salamatmanesh, A., Bagheri, S., Heydari, A. Synthesis and characterization of copper (I)-cysteine complex supported on magnetic layered double hydroxide as an efficient and recyclable catalyst system for click chemistry using choline azide as reagent and reaction medium. *Catal. Letters*, 2020, *150*(4), 1186–1195.

11. Bankar, S. R. Nano-Fe$_3$O$_4$ @ L-cysteine as an efficient recyclable organocatalyst for the green synthesis of bis (Indolyl) methanes under microwave irradiation. *Curr. Organocatalysis*, 2018, *5*(1), 42–50. https://doi.org/10.2174/2213337205666180611112941.

12. Ghorbani-Choghamarani, A., Taherinia, Z. Synthesis, characterization and catalytic application of Bi$_2$S$_3$ microspheres for Suzuki-Miyaura cross-coupling reaction and chemoselective ring opening of epoxides. *Mol. Catal.*, 2021, *499*(September), 111283. https://doi.org/10.1016/j.mcat.2020.111283.

13. Hajipour, A. R., Khorsandi, Z., Fatemeh Mohammadi Metkazini, S. Palladium Nanoparticles Supported on cysteine-functionalized MNPs as robust recyclable catalysts for fast O- and N-arylation reactions in green media. *J. Organomet. Chem.*, 2019, *899*, 120793. https://doi.org/10.1016/j.jorganchem.2019.05.011.

14. Ghorbani-Choghamarani, A., Taherinia, Z. The first report on the transition metal-free homocoupling of aryl halides in the presence of l-cysteine. *New J. Chem.*, 2018, *42*(13), 10989–10992. https://doi.org/10.1039/c8nj01518j.

15. Noori, N., Nikoorazm, M., Ghorbani-Choghamarani, A. Oxo-vanadium immobilized on L-cysteine-modified MCM-41 as catalyst for the oxidation of sulfides and oxidative coupling of thiols. *Microporous Mesoporous Mater.*, 2016, *234*, 166–175. https://doi.org/10.1016/j.micromeso.2016.06.036.

16. Zamani, F., Izadi, E. Synthesis and characterization of copper (II)–cysteine/SiO$_2$–Al$_2$O$_3$ as an efficient and reusable heterogeneous catalyst for the oxidation of aromatic alcohols. *J. Inorg. Organomet. Polym. Mater.*, 2013, *23*, 1501–1510.

17. Maurya, M. R., Kumar, U., Correia, I., Adão, P., Costa Pessoa, J. A polymer-bound oxidovanadium (IV) complex prepared from an l-cysteine-derived ligand for the oxidative amination of styrene. 2008.

18. Braga, A. L., Alves, E. F., Silveira, C. C., Zeni, G., Appelt, H. R., Wessjohann, L. A. A new cysteine-derived ligand as catalyst for the addition of diethylzinc to aldehydes: The importance of a "free" sulfide site for enantioselectivity. *Synthesis (Stuttg).*, 2005, *2005*(4), 588–594. https://doi.org/10.1055/s-2005-861801.

19. Serra, M. E. S., Costa, D., Murtinho, D., Tavares, N. C. T., Pinho e Melo, T. M. V. D. D-penicillamine and L-cysteine derived thiazolidine catalysts: An efficient approach to both enantiomers of secondary alcohols. *Tetrahedron*, 2016, *72*(39), 5923–5927. https://doi.org/10.1016/j.tet.2016.08.036.

20. Braga, A. L., Appelt, H. R., Schneider, P. H., Silveira, C. C., Wessjohann, L. A. A new functionalized, chiral disulfide derived from L-cysteine: (R,R)-Bis[(3-Benzyloxazolan-4-Yl)-Methane] disulfide as a catalyst in the diethylzinc addition to aldehydes. *Tetrahedron Asymmetry*, 1999, *10*(9), 1733–1738. https://doi.org/10.1016/S0957-4166(99)00145-7.

21. Du, S., Zhang, C., Jiang, Y., Jiang, P., Leng, Y. Au nanoparticle-immobilized L-cysteine-paired porous ionic copolymer as an efficient catalyst for additive-free oxidative coupling of alcohols and amines. *Catal. Commun.*, 2019, *129*, 105746. https://doi.org/10.1016/j.catcom.2019.105746.

22. Real, J., Pagès, M., Polo, A., Piniella, J. F., Álvarez-Larena, Á. Low symmetry metal complexes: Chloro cysteine ethyl ester-N,S triphenylphosphine palladium(II), a new regioselective hydrocarboxylation catalyst for 2-phenylpropanoic acid, and its crystal structure. *Chem. Commun.*, 1999, *3*, 277–278. https://doi.org/10.1039/A809130G.

23. Opoku, F., Govender, K. K., van Sittert, C. G. C. E., Govender, P. P. Recent progress in the development of semiconductor-based photocatalyst materials for applications in photocatalytic water splitting and degradation of pollutants. *Adv. Sustain. Syst.*, 2017, *1*(7), 1700006.

24. Wang, X., Yu, B., Wang, Q., Cao, J., Wang, M., Yao, W. L-cysteine-protected ruthenium nanoclusters on CdS as efficient and reusable photocatalysts for hydrogen production. *Int. J. Hydrog. Energy.*, 2023. https://doi.org/10.1016/j.ijhydene.2023.04.199.

25. Zhou, Y., Feng, S., Ma, C., Wu, W., Ye, Z., Dai, X., Fan, L. L-cysteine capped CoNiSx combined with Mn-Cd-S solid solution form S-scheme heterojunction for efficient and stable H_2-releasing photocatalysis. *J. Environ. Chem. Eng.*, 2023, *11*(1), 109133.

26. Zhang, X., Tian, F., Gao, M., Yang, W., & Yu, Y. L-Cysteine capped Mo_2C/Zn0.67Cd0.33S heterojunction with intimate covalent bonds enables efficient and stable H_2-Releasing photocatalysis. *J. Chem. Eng.*, 2022, *428*, 13262.

27. Yue, Y. N., Wang, Z. L., Yang, L. R., Zhao, Y. J., Wang, H., Lu, J. X. L-cysteine-functionalized CuPt: A chiral electrode for the asymmetric electro reduction of aromatic ketones. *Electrochimica Acta*, 2021, *375*, 137926.

28. Ghorbani-Choghamarani, A., Taherinia, Z. Synthesis and characterization of mesoporous vanadium sulfides as environmental catalysts for the cycloaddition of CO2 with 2-(phenoxymethyl) oxirane) and oxidation reactions. *Mol. Catal.*, 2023, 535, 112829. https://doi.org/10.1016/j.mcat.2022.112829.

4 The Catalytic Role of L-Glycine in Organic Reactions

4.1. INTRODUCTION

L-glycine is one of the amino acids essential to the body's synthesis of the antioxidant glutathione, and it is the only achiral proteinogenic amino acid with a hydrogen atom as its side chain. L-glycine can serve as an environmentally benign and biocompatible organocatalyst in various reactions. This chapter focuses on the catalysis of L-glycine in different organic reactions.

4.2. APPLICATION OF L-GLYCINE AS AN ORGANOCATALYST IN MULTICOMPONENT REACTION

Amino acids are potentially utilized for various applications as both pharmaceutical and material [1, 2]. In 2022, Banerjee et al. reported an easy and effective method for the production of 2-amino pyran-annulated heterocyclic derivatives using glycine (Scheme 4.1) [3]. This protocol highlighted advantages such as excellent yields, reduced reaction time, and metal-free conditions.

In another study, the activity of glycine was used in the synthesis of a multicomponent based on the reaction of amines, acetylenedicarboxylate, and formaldehyde [4]. Under solvent-free conditions, experimental results show that the reaction proceeded well giving the final products in high to excellent yields in MeOH (Scheme 4.2). Cu/MCM-41 NPs were employed in synthesizing propargylamines via a combination of amines, acetylenedicarboxylate, and aldehydes. Under solvent-free conditions, the corresponding products were produced in excellent yields with high atom economy (Scheme 4.2).

Authors suggested the mechanistic pathway for the production of polyfunctionalized dihydro-2-oxypyrroles using glycine, as shown in Scheme 4.3.

Synthesis of 1,4-dihydropyridines through the combination of aldehyde, alkyl acetoacetate, and anhydrous ammonium carbonate has been reported in the presence of glycine-HCl buffer as solvent (this mixture also plays a catalytic role in this multicomponent reaction) (Scheme 4.4) [5]. Good yields of the desired products were separated using glycine-HCl buffer.

Chaudhry et al. have demonstrated the use of glycine for the catalysis of pyrazole acryloyl analogs in DMSO at room temperature within 3–15 h (Scheme 4.5) [6]. The

Ar	R	Time(min)	Yield(%)
4-NO$_2$C$_6$H$_4$	CN	15	98
2,4-diCl-C$_6$H$_3$	CN	25	96
3,4,5-triOMeC$_6$H$_2$	CN	30	96
4-OH-3-OMeC$_6$H$_3$	CN	45	98
4-NO$_2$C$_6$H$_4$	COOEt	60	93
4-NO$_2$C$_6$H$_4$	CN	25	99
2,4-diCl-C$_6$H$_3$	CN	30	99
3,4,5-tri OMeC$_6$H$_2$	CN	40	97
Chromone-3-yl	CN	45	96
2,4-diClC$_6$H$_3$	COOEt	65	75
4-OMeC$_6$H$_4$	COOEt	55	85
	CN	25	99
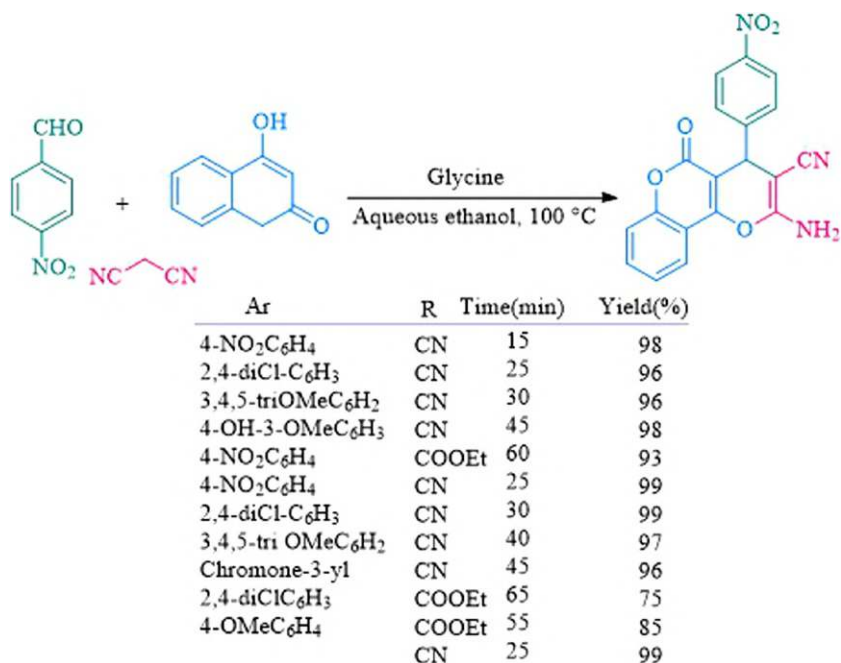
SCHEME 4.1. Glycine-catalyzed multicomponent reaction.

R$_1$= n-C$_4$H$_9$, PhCH$_2$, C$_6$H$_5$, 4-Cl-C$_6$H$_4$, 4-Br-C$_6$H$_4$,
    4-Me-C$_6$H$_4$, 4-Et-C$_6$H$_4$, 4-OMe-C$_6$H$_4$, 4-F-C$_6$H$_4$,
R$_2$= CH$_3$, C$_2$H$_5$.
Ar= 4-Br-C$_6$H$_4$, 4-F-C$_6$H$_4$, 3,4-Cl$_2$-C$_6$H$_3$, C$_6$H$_5$,
    4-Cl-C$_6$H$_4$, 4-Et-C$_6$H$_4$, 4-OMe-C$_6$H$_4$, 4-Me-C$_6$H$_4$
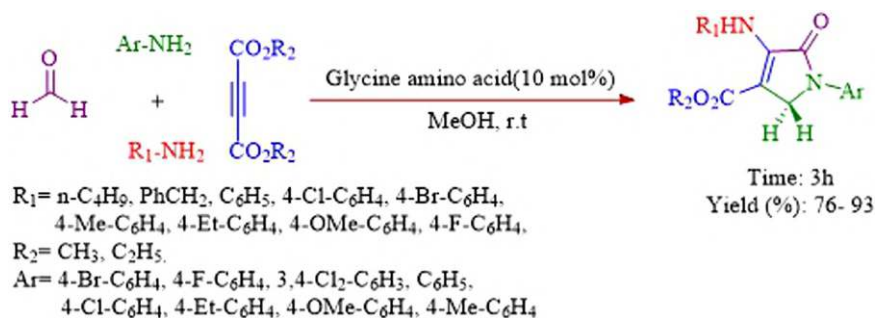
SCHEME 4.2. Production of multicomponent reaction using glycine.

reaction worked well by Knoevenagel condensation of pyrazole-4-carbaldehydes with active methylenes and pyrazolone.

4.3. APPLICATION OF L-GLYCINE-BASED IONIC LIQUID AS AN ORGANOCATALYST IN MULTICOMPONENT REACTION

Sharma et al. designated an efficient catalytic system for the multicomponent synthesis of 3,4-dihydropyrimidin-2(1H)-ones via the reaction of diverse series of aldehydes,
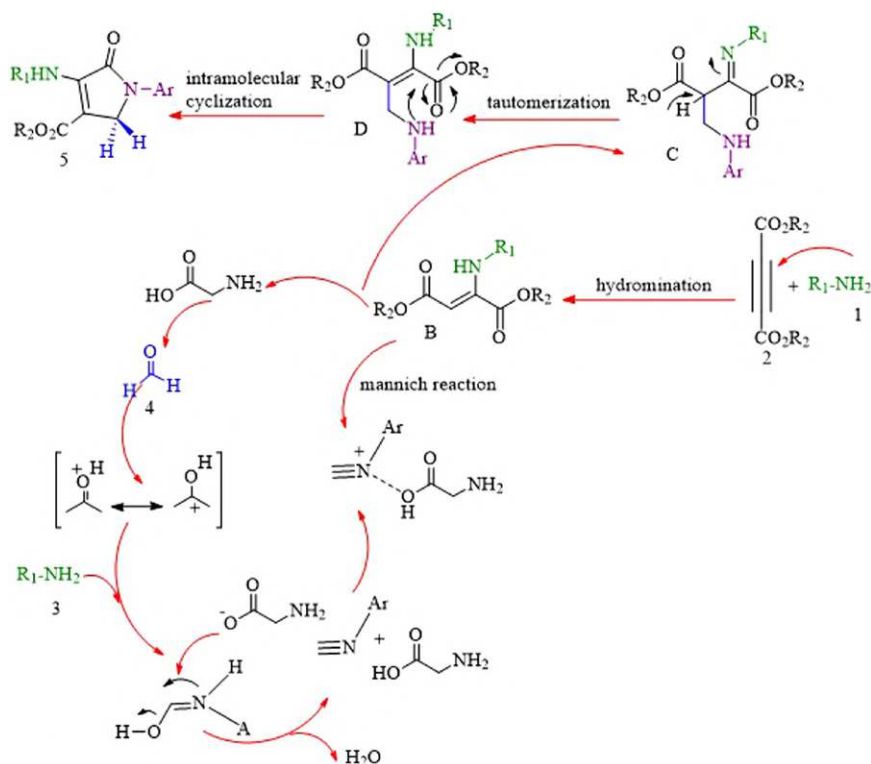
SCHEME 4.3.   Mechanistic pathway for multicomponent reaction.

R_1–CHO   + NH_4OAc

HCl-Glycine Buffer, pH= 2.2

Heat at 50-65 °C

R_1= H, 4-Me, 4-MeO, 4-Cl, 4-NO_2

R_2= OEt, OMe

Yield (%): 75- 97
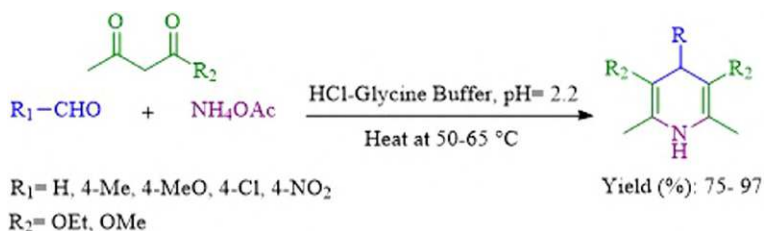
SCHEME 4.4.   Glycine-HCl buffer catalyzed the synthesis of 1,4-dihydropyridines.

ethyl acetoacetate, and urea or thiourea in excellent yields and short reaction time (Scheme 4.6) [7]. They utilized a glycine nitrate (GlyNO$_3$) ionic liquid catalytic system in ethanol under microwave irradiation to promote this multicomponent reaction. Glycine nitrate (GlyNO$_3$) ionic liquid can be reused for more than ten consecutive runs.

In a related example, glycine nitrate (GlyNO$_3$) ionic liquid has been employed for the preparation of symmetrical and unsymmetrical 1,4-dihydropyridines, which the multicomponent condensation performed in ethanol (Scheme 4.7) [8].

R_1= Ar, CH_3
R_2= H, CH_3
R_3= CH_3, C_2H_5

Glycine, DMSO, Room temperature
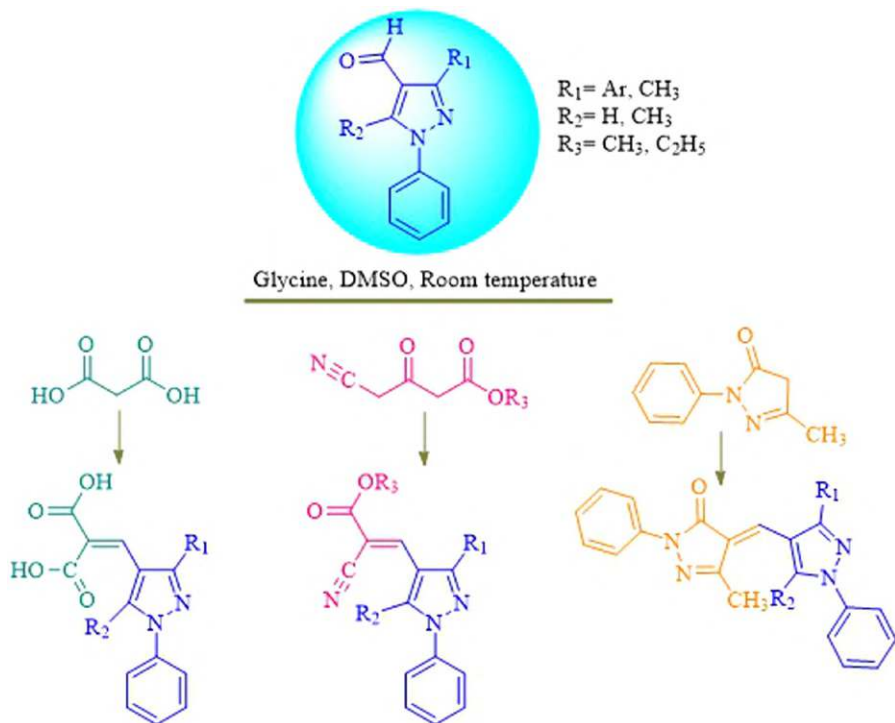
SCHEME 4.5. The glycine-catalyzed synthesis of pyrazole acryloyl analogs.

R_1: H, 4-OMe, 2,4,5-(OMe), 3,4(OCH$_2$O),
4-OH, 3-OMe, 4-oh, 3-oh, 4-Cl, 3-Br,
4-Cl, 4-NO$_2$, C$_{10}$H$_7$, 4-N,N(CH$_3$)$_2$,
4-Me, 4-OH, 3-OMe, 3-OH

R_2: Et, CH_3, t-Bu

GlyNO$_3$

EtOH, MW

X= O, S

Yield (%): 74- 92
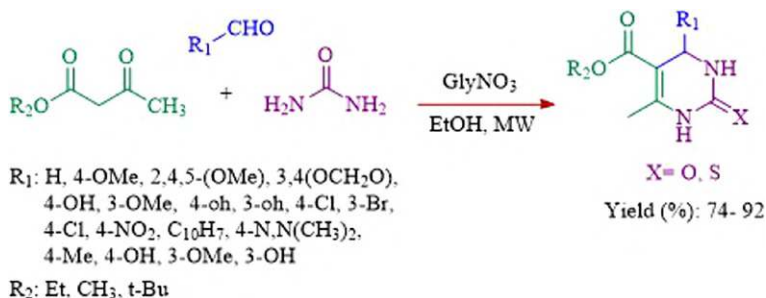
SCHEME 4.6. Biginelli reaction in the presence of GlyNO$_3$.

Li(Glycine)(CF$_3$SO$_3$) has been utilized to be an active catalyst for the production of 3,4-dihydropyrimidine-2-(1H)-ones by the one-pot condensation of an aldehyde, ethyl acetoacetate, and urea (Scheme 4.8) [9]. The generality and usefulness of the protocol are reflected in its compatibility with many different functional groups. Li(Glycine)(CF$_3$SO$_3$) could be easily recovered and reused for at least up to five consecutive cycles.
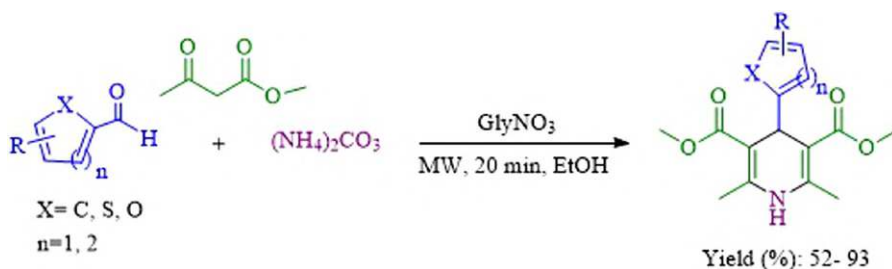
SCHEME 4.7. GlyNO$_3$-catalyzed synthesis of multicomponent reaction.

R: C$_6$H$_5$, 2-(Cl)-C$_6$H$_4$, 3-(Cl)-C$_6$H$_4$, 4-(Cl)-C$_6$H$_4$
    3-(Br)-C$_6$H$_4$, 2,4-(Cl)$_2$-C$_6$H$_3$, 3,4-(Cl)$_2$-C$_6$H$_3$, 4-(F)-C$_6$H$_4$
    2-(NO$_2$)-C$_6$H$_4$, 3-(NO$_2$)-C$_6$H$_4$, 4-(NO$_2$)-C$_6$H$_4$, 2-(OCH$_3$)-C$_6$H$_4$
    3-(OCH$_3$)-C$_6$H$_4$, 4-(OCH$_3$)-C$_6$H$_4$, 3,4-(OCH$_3$)$_2$-, 3-(CH$_3$O)-4-(OH),
    4-(CF$_3$)-C$_6$H$_4$, 2-(OH)-C$_6$H$_4$, 4-(OH)-C$_6$H$_4$, 4-(CH$_3$)-C$_6$H$_4$, C$_6$H$_5$-CH=CH, 2-Furyl

Time (min): 30- 40
Yield (%): 83- 98
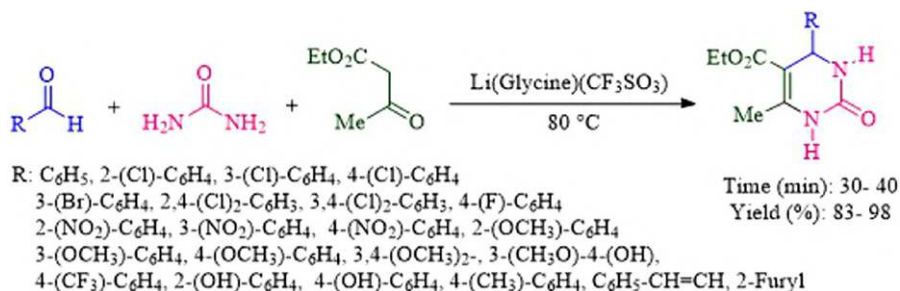
SCHEME 4.8. The Li(glycine) (CF$_3$SO$_3$)-catalyzed three-component Biginelli condensation.

4.4. APPLICATION OF METAL COMPLEXES OF GLYCINE AS A CATALYST MULTICOMPONENT REACTION

Benzimidazoles and benzothiazoles are a *significant class* of organic compounds that received a lot of interest in various fields related to biological activities [10] and clinical applications [11] such as anti-inflammatory [12, 13] as well as analgesic activity [14] and as antifungal and antibacterial [15], antiviral [16], anthelmintic [17], anti-proliferative [18], and anti-hypertensive [19]. Co(MCG)(H$_2$O)$_3$ have been employed as catalysts for the synthesis of benzimidazoles [20]. The catalysts were prepared in a three-step procedure. In the first stage, the reaction was carried out between resorcinol (1) and methyl acetoacetate for the synthesis of 7-hydroxy-4-methyl coumarin [HMC] (3) using Al$_2$O$_3$/MeSO$_3$H (AMA) at room temperature, followed by reaction of HMC (3) with glycine and formaldehyde in EtOH-afforded [7-hydroxy-4-methyl-8-coumarinyl]glycine [MCGH$_2$] (4). Finally, [Co(MCG)(H$_2$O)$_3$] was synthesized by treating cobalt chloride under reflux (Scheme 4.9). This protocol presented the success of the two steps for the synthesis of Mannich bases and benzimidazole/benzothiazole derivatives (Scheme 4.10).
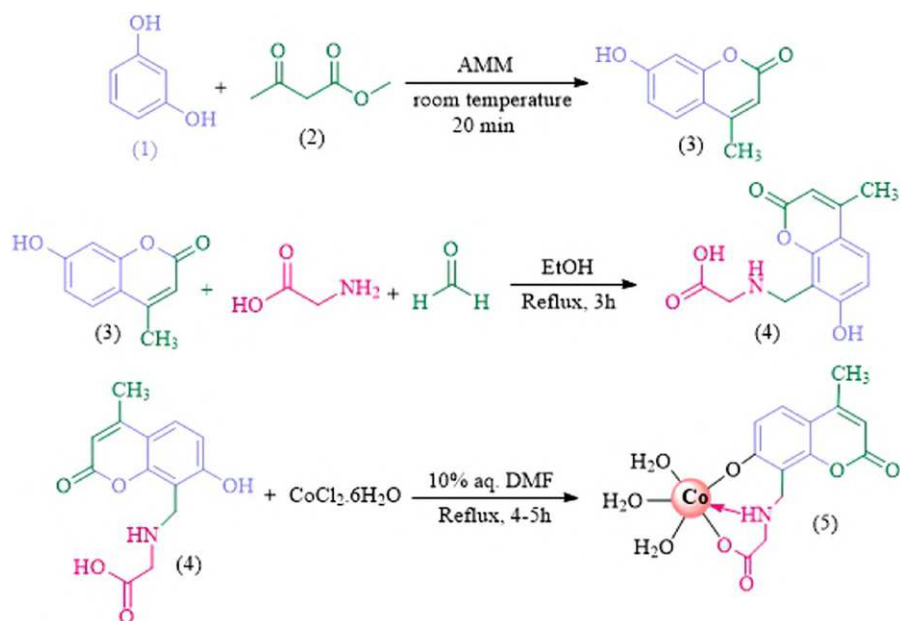
SCHEME 4.9.   The preparation of [Co(MCG)(H$_2$O)$_3$].
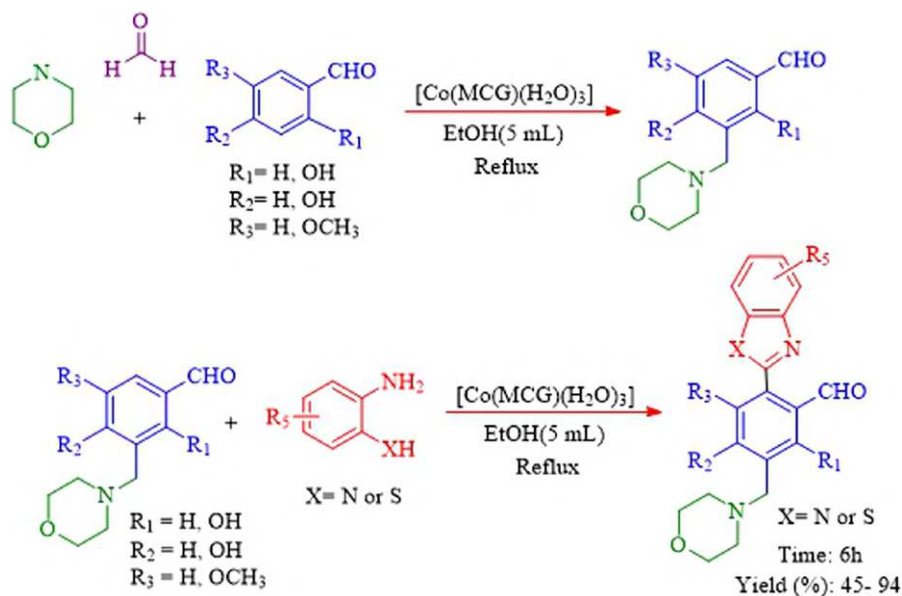
SCHEME 4.10.   [Co(MCG)(H$_2$O)$_3$] catalyzed the synthesis of benzimidazoles and benzothiazoles.

4.5.   APPLICATION OF METAL COMPLEXES OF GLYCINE-SUPPORTED MATERIAL AS A CATALYST IN THE MULTICOMPONENT REACTION

Tamoradi et al. have reported that Ni and Cu embedded in SBA-15 that functional-ized with glycine are effective for the one-pot preparation of 5-substituted tetrazole and polyhydroquinoline derivatives (Schemes 4.10–4.13) [21]. SBA-15@glycine-Cu were found to be better catalysts than SBA-15@glycine-Ni.

The Brunauer–Emmett–Teller (BET) results of the synthesized porous material are presented in Table 4.1. Specific surface area (SBET) was calculated for SBA-15, SBA15@glycine-Ni, and SBA-15@glycine-Cu. These results show that the immobi-lized SBA-15 has a decrease in its BET surface area and pore volume than SBA-15; this could be due to occupying of pores with Ni and Cu complexes with the surface of SBA-15.

Boehmite has been recognized as an ideal supporting material for different appli-cations, including catalysis studies. Recently, our group has designed isatine-boehm-ite nanoparticles in the first step and next the coordination of this solid support with
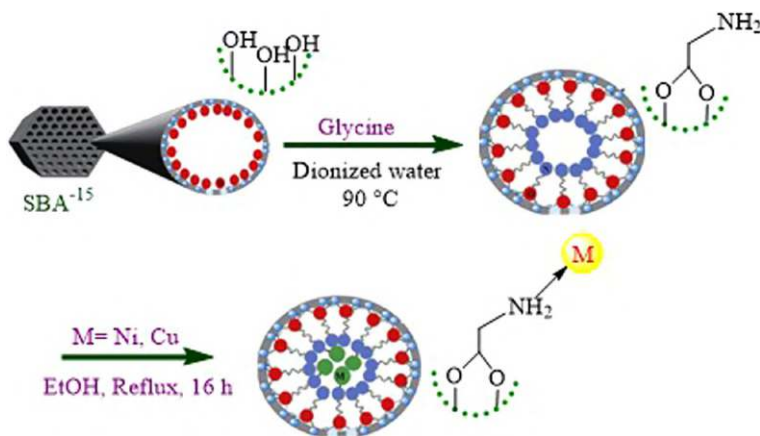
SCHEME 4.11.   Immobilization of glycine and metal on supported SBA-15.

SCHEME 4.12.   Application of Ni and Cu embedded on SBA-15 decorated with glycine for the synthesis of polyhydroquinolines.

R= Cl, Br, OH, NO$_2$, iso-propyl

Yield (Ni): 83-98%
Yield (Cu): 89- 98%
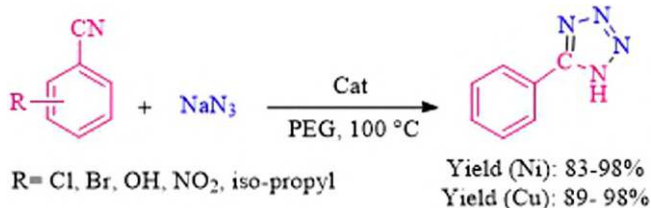
SCHEME 4.13. Application of Ni and Cu embedded on SBA-15 decorated with glycine for the synthesis of 5-substituted 1H-tetrazoles.

TABLE 4.1.
The BET result of the synthesized porous material

Sample	BET(m²/g)	Pore diameter by BJH method (nm)	Pore volume (cm³/g)
SBA-15	643	3.65	0.711
SBA-15@glycine-Ni	293	2.18	0.41
SBA-15@glycine-Cu	320	2.71	0.45

Cu and Ni ions to afford Ni(II) or Cu(I)@isatine-boehmite nanoparticles (Scheme 4.14) [22, 23].

In the first step of the catalyst's synthesis pathway, boehmite (AlOOH) is produced by the precipitation method through a mixture of aluminum nitrate and sodium hydroxide, followed by functionalization with glycine, which subsequently condensed with isatin and finally the corresponding nanoparticles decorated with Cu(I) or Ni(II) ions (Scheme 4.15). The catalytic activity of Ni or Cu(I)@isatine-boehmite nanoparticles was employed for the selective oxidation and one-pot domino multicomponent (Scheme 4.15).

Our group reported that CoFe$_2$O$_4$@glycine-M (M = Pr, Tb, and Yb) can serve as active catalysts for the synthesis of tetrazoles and oxidation of sulfides in green conditions [24]. The catalyst was synthesized from a basic solution containing iron chloride and cobalt chloride and refluxed for 1 h with stirring. After a simple filtration, the resulting material was washed with water and ethanol. Next, CoFe$_2$O$_4$ was immobilized with glycine, followed by addition of Pr(NO$_3$)$_3$·5H$_2$O, TbCl$_3$, and Yb(NO$_3$)$_3$·5H$_2$O (Scheme 4.16). Also, ICP atomic emission spectroscopy technique showed that the exact amount of Pr, Tb, and Yb loaded on the surface of modified CoFe$_2$O$_4$ are found to be 0.53, 0.43, and 0.31 mmol/g. The authors carried out this reaction with different sulfides and nitriles and the results are summarized in Scheme 4.17.
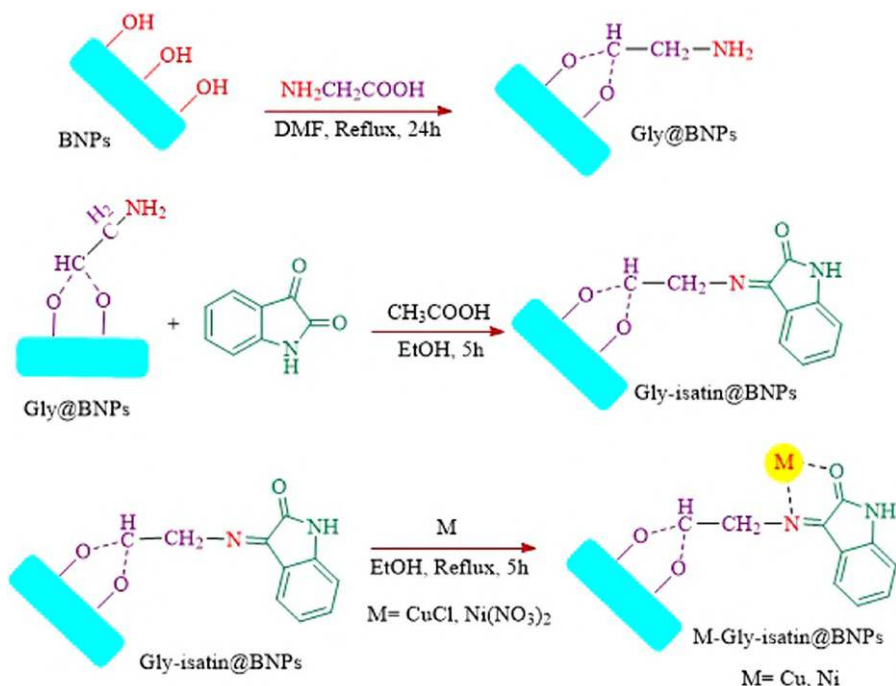
SCHEME 4.14. Synthesis of Ni or Cu-Gly-isatin@boehmite.

4.6.   APPLICATION OF GLYCINE AS A CATALYST
FOR THE OXIDATION REACTION

Glycine was used as a source of N and C and dopant in the manufacture of the cathodic part of PEMFCs because the ratio of C and N in glycine is high and this natural amino acid is nontoxic and inexpensive. The preferential oxidation of CO is one of the efficient ways for the removal of CO. Due to the importance of the method, noble material catalysts, including Pt, Ru, Rh, Pd, and Au employed, gave activities and good stabilities in CO-PrO$_x$. Yan et al. reported the application of Co/CeO$_2$ nanoparticles for or preferential oxidation of CO in excess H$_2$ could be catalyzed by Co/CeO$_2$ nanoparticles, which are produced by treating glycine with an aqueous solution and then heated to obtain nanoparticles (Figure 4.1) [25]. In their procedure, optimization studies showed that the Co/Ce ratio plays a critical role in the synthesis catalyst. Interestingly, the activity of the catalyst decreased as the cobalt loading increased; this may be attributed to the aggregation of active species. SEM was used to evolve the morphology and detailed structures of nanoparticles; it was discovered that particles of 1–20 nm and 100–200 nm in pore diameter are seen on the surface of the catalyst structure.

   Chen et al. have reported that the partial oxidation of methane to generate syngas can be carried out by nickel/alumina catalyst promoted by Li$_2$O and La$_2$O$_3$, which
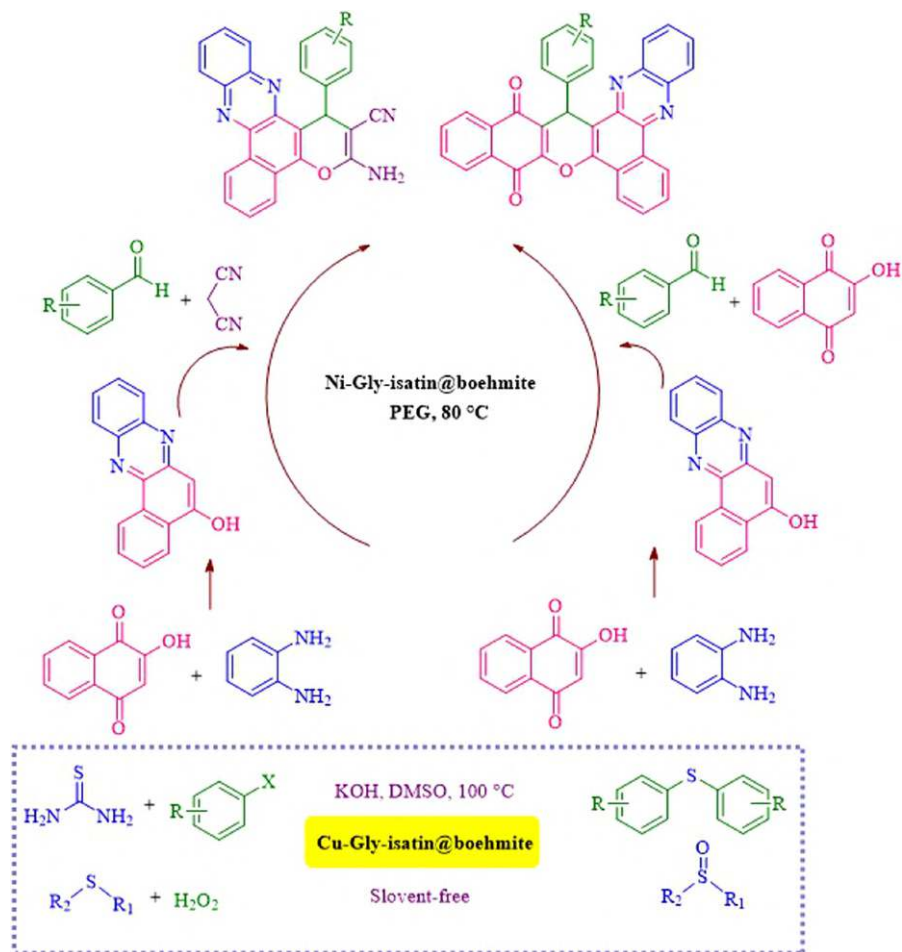
SCHEME 4.15. Application of Ni-Gly-isatin@boehmite and Cu-Gly-isatin@boehmite for multicomponent reaction, oxidation, and coupling reaction.

was prepared via the glycine nitrate process (GNP) [26]. Alumina existed mainly in a γ form, while the spinel phase of nickel aluminate also occurred. The morphology of fresh catalyst (A) and used catalyst (B) was studied by SEM analysis. As seen in SEM images, the catalyst seems to be porous and foam-like structures (Figure 4.2). The results demonstrated an interaction between the NiO and Al_2O_3 phase in the produced nanocomposite via GNP, which led to superior catalytic activity for partial oxidation of methane to the carbon monoxide with over 95% conversion and 99% selectivity at 85°C.
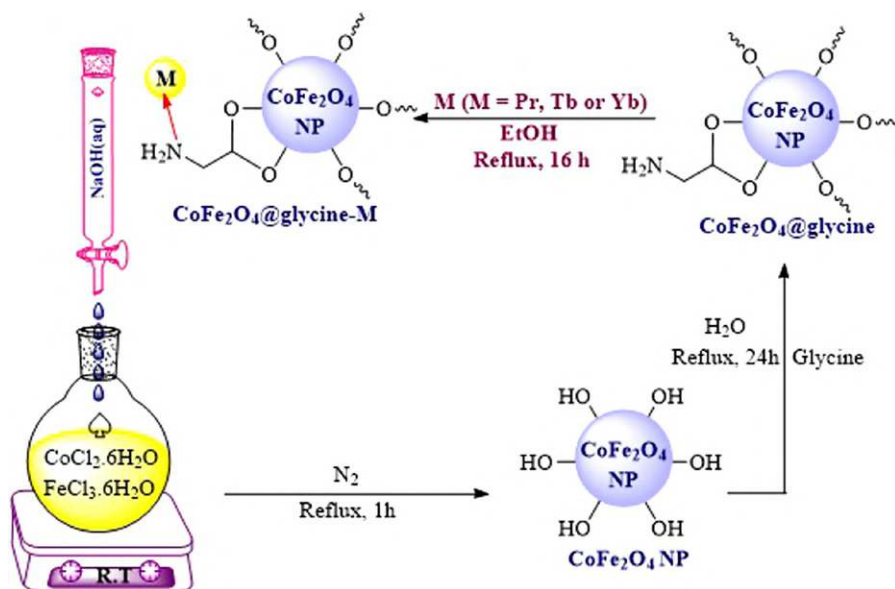
SCHEME 4.16.   Synthesis of CoFe$_2$O$_4$@glycine-M (M = Pr, Tb, and Yb).

4.7.   APPLICATION OF METAL COMPLEXES OF GLYCINE-SUPPORTED MATERIAL AS A CATALYST IN THE OXIDATION REACTION

Fe$_3$O$_4$@VO (salen) complex was employed for the selective oxidation of sulfides to sulfoxides via H$_2$O$_2$ in the room. All reactions progressed smoothly to completion at low temperatures and in short times in good to excellent yields and with high selectivity (Scheme 4.18) [27].

The nanocatalyst was prepared by adding VO(acac)$_2$ to Fe$_3$O$_4$@Schiff base NPs, which were synthesized by hydrothermal route (Scheme 4.19). The morphology of the Fe$_3$O$_4$@VO (salen) complex was determined by TEM analysis. The images clearly showed the formation of spherical NPs of 10–32 nm in size. This system was successfully applied for the oxidation of a wide range of sulfides with different functional groups (Scheme 4.20). It should be noted that only a trace amount of the product was obtained without a catalyst.

4.8.   APPLICATION OF GLYCINE FOR THE TRANSFORMATION OF CO$_2$ WITH AMINES

Xie et al. demonstrated that glycine betaine catalyzed the formation of C—N bonds through the combination of CO$_2$, amines, and PhSiH$_3$ as the reductant (Scheme 4.21) [28]. In the absence of glycine, the reaction failed to give the desired products. The author's studies showed that Et$_3$SiH, PMHS, Ph$_3$SiH, or Ph$_2$SiH$_2$ were not effective

$$R_1 \diagdown S \diagdown R_2 \xrightarrow[\text{Solvent-Free, } H_2O_2, \text{ rt}]{\textbf{CoFe}_2\textbf{O}_4\textbf{@glycine-M (Pr, Tb and Yb)}} R_1 \diagdown \overset{\overset{O}{\|}}{S} \diagdown R_2$$

Substrate	Time (min)			Yield (%)		
	Pr	Tb	Yb	Pr	Tb	Yb
methyl(phenyl)sulfane	55	50	40	92	94	98
dipropylsulfane	40	40	35	91	94	93
2-((methylthio)methyl)furan	45	40	45	95	92	96
benzyl(phenyl)sulfane	70	70	60	92	93	94
tetrahydrothiophene	10	5	5	91	90	95
2,2'-thiodiacetic acid	55	45	40	88	91	92
diphenylsulfane	105	100	90	92	90	96
3,3'-thiodipropionic acid	65	50	40	82	95	94
diethylsulfane	90	85	50	73	90	92
2-(phenylthio)ethan-1-ol	80	65	65	92	94	93
dodecyl(methyl)sulfane	50	55	40	93	91	96
dimethylsulfane	65	60	55	94	95	98
dibenzylsulfane	40	45	45	91	95	97

Substrate	Time (min)			Yield (%)		
	Pr	Tb	Yb	Pr	Tb	Yb
4-chlorobenzonitrile	160	150	140	93	94	93
2-chlorobenzonitrile	170	150	150	91	92	95
2-hydroxybenzonitrile	175	160	155	90	91	96
4-nitrobenzonitrile	145	140	140	94	96	96
benzonitrile	170	165	150	95	94	95
3-nitrobenzonitrile	145	150	130	92	91	94
4-hydroxybenzonitrile	180	160	150	94	96	95
2-bromobenzonitrile	160	155	145	88	92	95
4-isopropylbenzonitrile	130	150	150	92	92	93
4-bromobenzonitrile	145	145	130	91	93	92

SCHEME 4.17. Synthesis of oxidation of sulfides to the sulfoxides and 5-substituted 1*H*-tetrazole derivatives in the presence of CoFe$_2$O$_4$@glycine-M (M = Pr, Tb, and Yb).
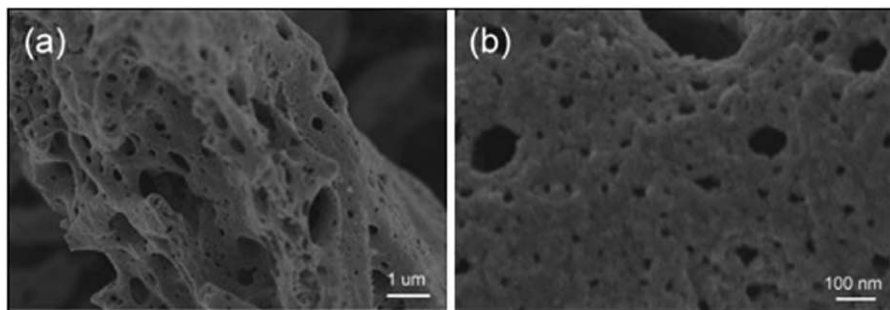
FIGURE 4.1. SEM micrographs of Co/CeO$_2$. *Source:* Reprinted with permission from Ref. [25]. Copyright 2007, Elsevier B.V. All rights reserved.
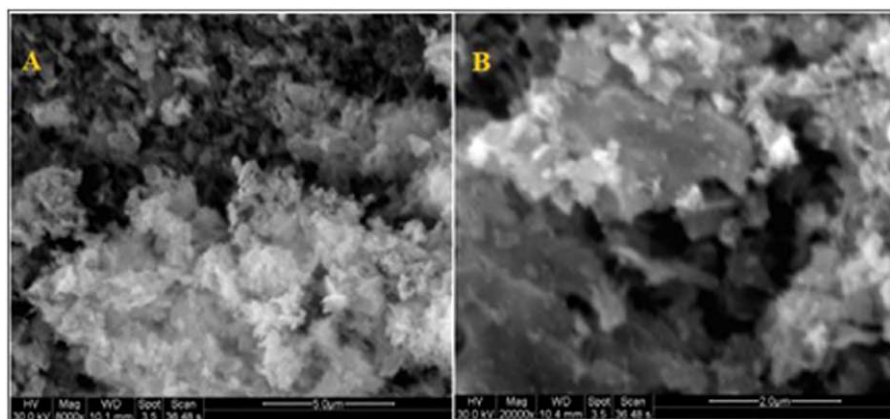
FIGURE 4.2. Scanning electronic micrograph of fresh catalyst (a) and used catalyst (b). *Source:* Reprinted with permission from Ref. [26]. Copyright 2007, Elsevier B.V. All rights reserved.

R$_1$, R$_2$= Aryl, Heterocyclic, and Alkyl   Yield (%): 90- 99
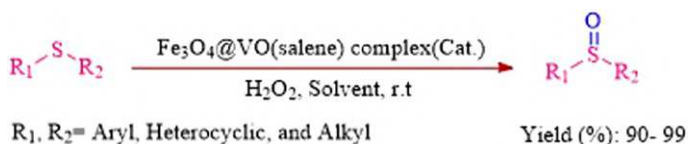
SCHEME 4.18. Fe$_3$O$_4$@VO (salen) complex–catalyzed oxidation of sulfide to sulfoxide.
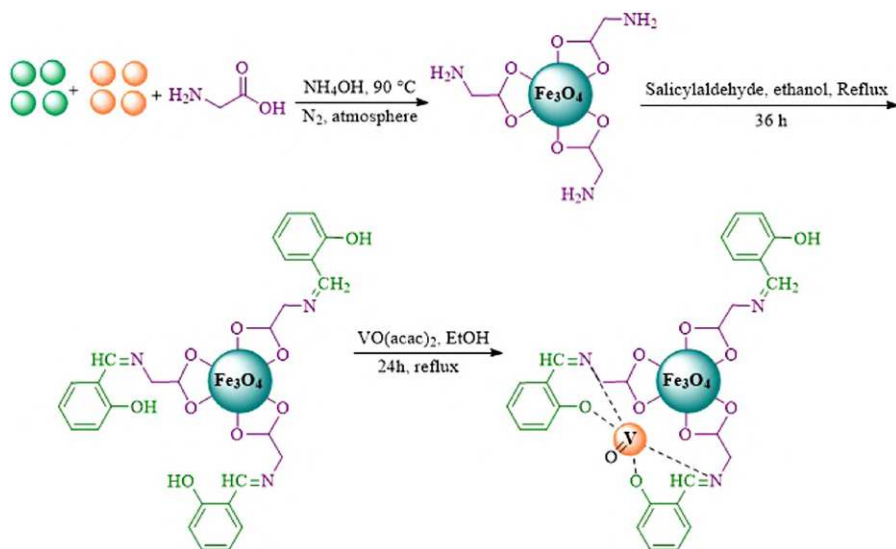
SCHEME 4.19.   The general route for the synthesis of Fe$_3$O$_4$@VO (salen) complex.

R$_1$, R$_2$ = Aryl, Heterocyclic, and Alkyl

Time (min): 25- 220
Yield (%): 90- 99
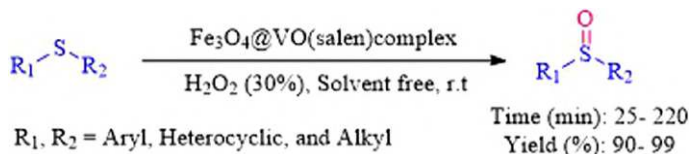
SCHEME 4.20.   Fe$_3$O$_4$@VO (salen) complex–catalyzed selective oxidation of sulfides to sulfoxides using H$_2$O$_2$ at room temperature.

reductants for described reactions. The system is compatible with secondary amines and primary amines produce the desired products (formamides) in good yields. The selective formation of different *N*-substituted compounds was found to be greatly affected by the molar ratio of reactants (i.e., CO$_2$, amines, and PhSiH$_3$) and the reaction temperature, which caused the carbon oxidation state of CO$_2$ to +2, 0, and -2, respectively; therefore, the preparation of formamides, aminals, and methylamines might occur.

A suggested route for the C—N bond formation catalyzed by glycine betaine through hydrosilylation of CO$_2$ in the presence of amine to produce formamides, aminals, and methylamines was proposed by the mentioned authors (Scheme 4.22).
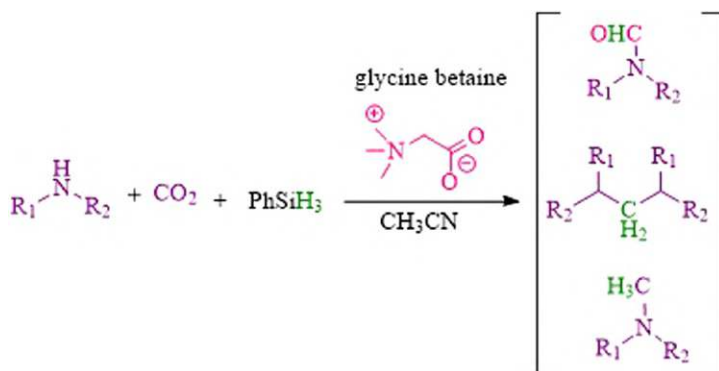
SCHEME 4.21.   Transformation of CO_2 with amines.

4.9.   APPLICATION OF METAL COMPLEXES OF GLYCINE AS A CATALYST FOR CYANOSILYLATION REACTION

Paul has reported the cyanosilylation reaction which has been catalyzed by glycine-templated cadmium sulfate open-framework material (Schemes 4.23 and 4.24) [29].

4.10.   APPLICATION OF GLYCINE SUPPORTED AS AN ORGANOCATALYST IN HYDROLYSIS AND ESTERIFICATION REACTIONS

Bolina et al. have designed an ion-exchange support via immobilization of silica-based materials with (3-glycidyloxypropyl)trimethoxysilane (GPTMS) to obtain epoxy groups (Epx-SiO$_2$); this solid material is modified by glycine to produce Gly-Epx-SiO$_2$. Finally, lipase (from *Thermomyces lanuginosus* [TLL]) immobilizes on
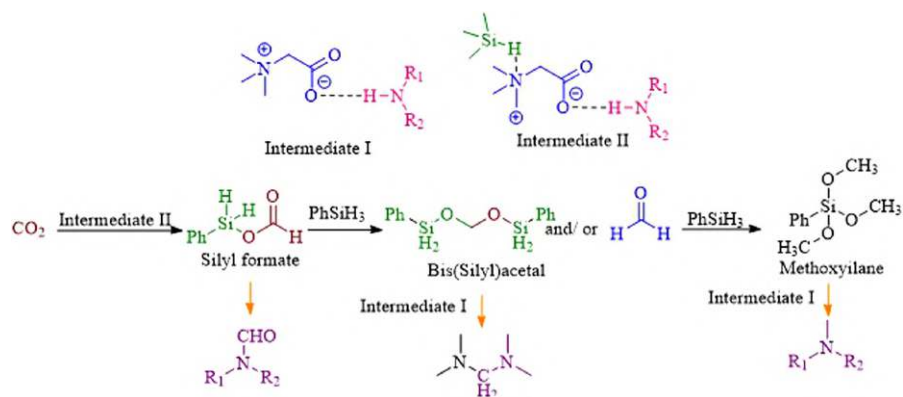
SCHEME 4.22.   The possible reaction mechanism for the transformation of CO_2 with amines.

$$3CdSO_4.8H_2O + 3NH_2CH_2COOH + 3 \ C_3H_4N_2 + 285 \ CH_3CN+1164 \ H_2O + 153 \ EtOH$$

$$\downarrow \quad \begin{array}{l} 125 \ °C, 6 \ days \\ pH= 6.5 \end{array}$$

$$Cd(NH_3CH_2COO)(SO_4)]$$
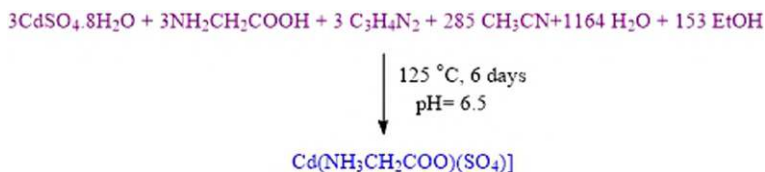
SCHEME 4.23. Synthesis of glycine-templated cadmium sulfate open-framework material.
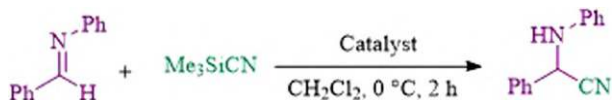
SCHEME 4.24. Cyanosilylation reaction catalyzed by glycine-templated cadmium sulfate open framework.

Gly-Epx-SiO$_2$ (Scheme 4.25) [30]. The immobilized TLL was successfully employed for the hydrolysis of olive oil emulsion and esterification synthesis of butyl stearate. In this study, the influence of pH ranging from 3 to 7 was examined on the immobilization parameters. The authors reported that TLL adsorption capacity was found in the range of 3.0–5.0 for commercial silica (Immobead S60S) and 3.0–4.0 for rice husk silica (RHS), respectively, and a rapid decrease in the adsorption process with an increase in pH.

4.11. APPLICATION OF GLYCINE IN THE SYNTHESIS OF CATALYST FOR HYDROGEN PRODUCTION

Using fossil led to severe environmental issues. Rapid development to establish alternative carbon-free energy has been considered as an effective strategy to reduce severe environmental issues. In this sense, H$_2$ is recognized as a source of green energy, which is found in some industrial applications to reduce the net greenhouse. In this sense, CuFeO$_2$-CeO$_2$ with different ratios of copper and cerium oxide is produced by the self-combustion glycine nitrate process (GNP) and used for hydrogen production from methanol steam reforming (SRM) [31]. The effect of the surface area on the catalytic activity was studied by the BET method (Table 4.2). Moreover, BET surface area studies showed that the high specific surface area of the 70CuFeO$_2$-30CeO$_2$ was found to be quite effective for hydrogen production.

4.12. APPLICATION OF GLYCINE IN THE SYNTHESIS OF CATALYST FOR THE SYNTHESIS OF METHANOL

Guo et al. prepared CuO-ZnO-ZrO$_2$ (CZZ) via the glycine–nitrate combustion method (the mixing of the metal nitrate/glycine/water solution and thermal evaporation of the water) (Scheme 4.26) and its structure examined by XRD, BET, N$_2$O chemisorption (applied for the metallic copper surface area (S$_{Cu}$)), SEM, and TPR
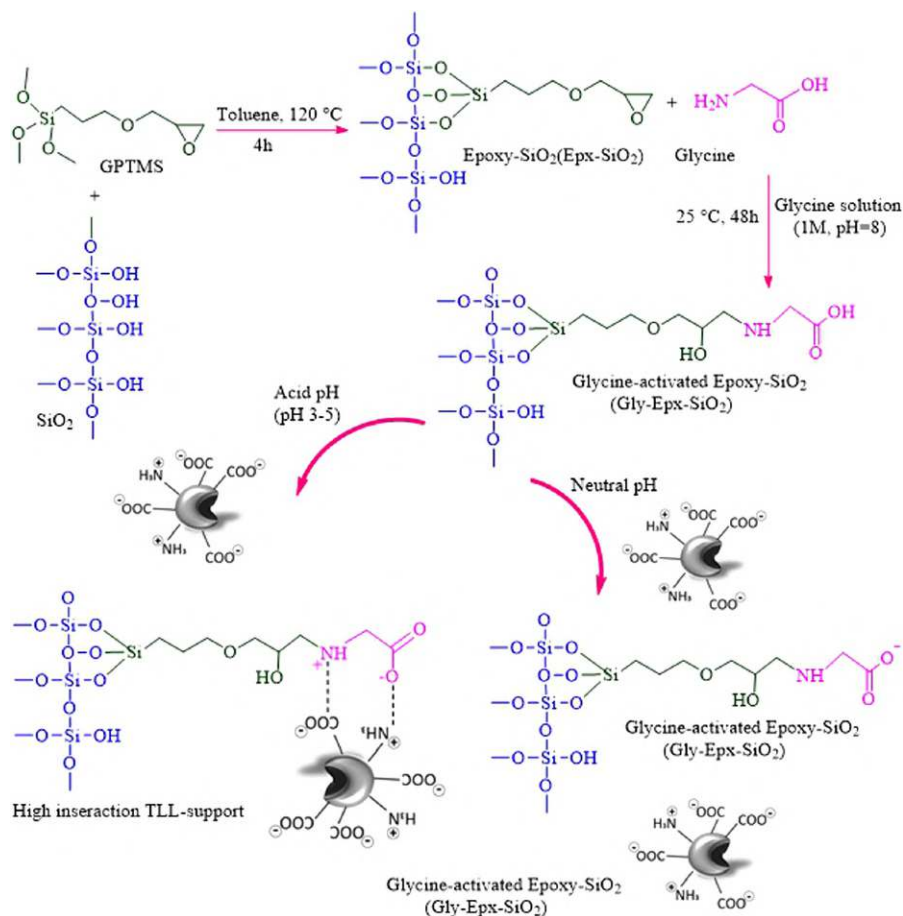
SCHEME 4.25. Production of Gly-Epx-SiO$_2$ and effect of pH of incubation on the physical adsorption of TLL via ionic interactions. *Source:* Reprinted with permission from Ref. [30]. Copyright 2020, Hydrogen Energy Publications LLC. Published by Elsevier Ltd. All rights reserved.

TABLE 4.2.

The BET surface areas of CuFeO$_2$-CeO$_2$ nanopowders

Composition	Specific surface area (m^2/g)
CuFeO$_2$	5.6248
90 CuFeO$_2$-10CeO$_2$	9.2436
80 CuFeO$_2$-20CeO$_2$	8.0609
70 CuFeO$_2$-30CeO$_2$	8.6265

$$CO_2 \; + \; 3H_2O \; \xrightarrow[\substack{CuO-ZnO-ZrO_2 \; (CZZ) \\ catalyst}]{Catalyst} \; CH_3OH \; + \; H_2O$$
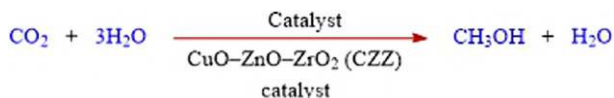
SCHEME 4.26. $CuO\text{-}ZnO\text{-}ZrO_2$ catalysts for the preparation of methanol from CO_2 hydrogenation.

techniques [32]. The described authors studied the catalytic activity of CuO-ZnO-ZrO_2 in the methanol synthesis process (CO_2 hydrogenation). To evaluate the effect of various glycine amounts on the activity of CuO-ZnO-ZrO_2, glycine addition was set from 50% to 150% of the stoichiometric amount. The obtained CZZ powder was termed 50-CZZ, 75-CZZ, 100-CZZ, 125- CZZ, and 150-CZZ. They observed that low molar ratio of glycine gave better results and a performance activity sequence of 50-CZZ > 150-CZZ > 100-CZZ was obtained.

4.13. APPLICATION OF GLYCINE IN THE SYNTHESIS OF CATALYST FOR THE OXYGEN REDUCTION REACTION

Great interest is being conducted in replacing Pt-based catalysts for oxygen reduction reactions (ORRs) in polymer electrolyte membrane fuel cells with cheaper and greener systems. Polymer electrolyte membrane fuel cells (PEMFCs) are recognized as promising and environment-friendly clean sources of energy due to their high power density, lightweight, and high energy density. However, the sluggish kinetics of the oxygen reduction reaction at the cathode allows its utilization for the oxygen reduction reaction. In recent years, reports to replace Pt-based catalysts for oxygen reduction reactions have gradually increased. In this sense, Choi's group reported the synthesis of bi-modal porous iron and nitrogen-doped carbon nanostructures as nonprecious metal catalysts using $FeCl_2 \cdot 4H_2O$ as a metal source and glycine as a nitrogen and carbon source with 500 nm and 20 nm silica beads as templates (Scheme 4.27) [33]. The material exhibits efficient catalytic properties in the oxygen reduction reaction in both acidic and alkaline media. It should be noted that the authors reported FeG500/20 improved catalytic activity in both acidic and alkaline media in comparison with commercial Pt catalyst; this could be due to the porous nanostructure with a high specific surface area of the mentioned catalyst.

4.14. APPLICATION OF METAL COMPLEXES OF GLYCINE AS A PHOTOCATALYST

Glycine-incorporated TiO_2 nanostructures (G-TiO_2) have been employed for the decomposition of naphthol Blue Black. The glycine-functionalized TiO_2 nanostructures (G-TiO_2) were prepared by a simple glycine-assisted hydrothermal posttreatment of titanate nanotubes [34]. TEM images revealed the formation of nanotube-like titanates with an outer diameter of 5–10 nm and lengths ranging from several hundreds
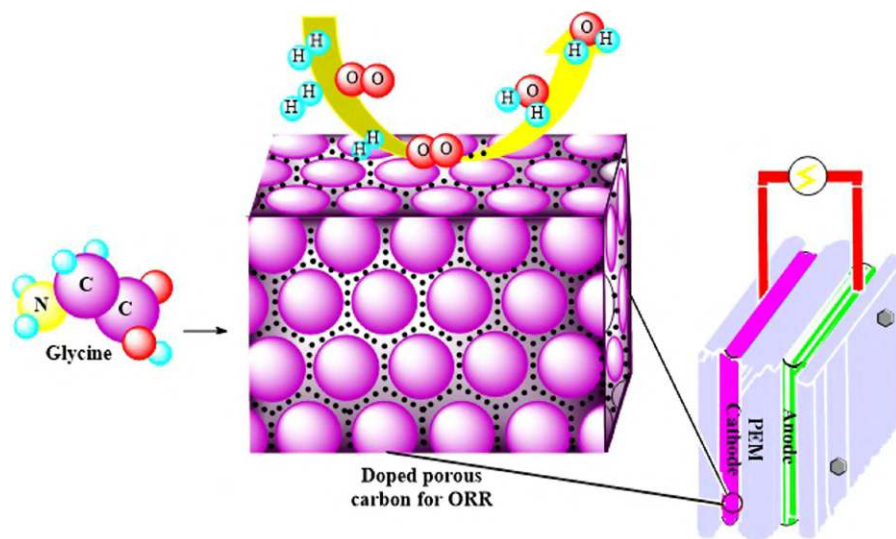
SCHEME 4.27. Application of doped porous carbon nanostructures for the oxygen reduction reaction. *Source:* Reprinted with permission from Ref. [33]. Copyright 2017, Elsevier B.V. All rights reserved.

of nanometers; also, a big pore size was identified by nitrogen adsorption–desorption analysis for this nanomaterial.

4.15. CONCLUSION

Green chemistry has been a significant focus in designing chemicals to use in place of those that have been proven to be problematic. According to previous studies, amino acids are widely used in industrial chemistry and are well-known to be suitable for green chemistry. Amino acids are very expensive and difficult to obtain and organocatalysts are difficult to recycle; therefore, to overcome these problems, new supports have also been synthesized. This chapter focuses on the application of glycine (or in its modified form) as a catalyst and organocatalyst in organic reactions.

REFERENCES

1. Razak, M. A., Begum, P. S., Viswanath, B., Rajagopal, S. Multifarious beneficial effect of nonessential amino acid, glycine: A review. *Oxid. Med. Cell. Longev.*, 2017, *2017*. https://doi.org/10.1155/2017/1716701.
2. Yadav, A., Kumar, R., Sahoo, B. Graphene oxide coatings on amino acid modified Fe surfaces for corrosion inhibition. *ACS Appl. Nano Mater.*, 2020, *3*(4), 3540–3557. https://doi.org/10.1021/acsanm.0c00243.

3. Banerjee, B., Kaur, M., Sharma, A., Singh, A., Priya, A., Gupta, V. K., Jaitak, V. Glycine catalyzed one-pot three-component synthesis of structurally diverse 2-amino substituted pyran annulated heterocycles in aqueous ethanol under refluxed conditions. *Curr. Green Chem.*, 2022, *9*, 162–173.

4. Mohamadpour, F. Imin-based synthesis of polyfunctionalized dihydro-2-oxypyrroles catalyzed by glycine amino acid via tandem Michael-Mannich cyclocondensation reaction under ambient temperature. *Res. Chem. Intermed.*, 2020, *46*(3), 1931–1940. https://doi.org/10.1007/s11164-019-04072-z.

5. Ebrahimlo, A. R. M., Hanaforoush, M., Attari, R. An efficient and eco-friendly synthesis of 1,4-dihydropyridines via Hantzsch reaction in glycine-HCl buffer as solvent and bio-catalyst. *Org. Commun.*, 2019, *12*(2), 109–114. https://doi.org/10.25135/acg.oc.58.19.05.1273.

6. Chaudhry, F., Asif, N., Shafqat, S. S., Khan, A. A., Munawar, M. A., Khan, M. A. Efficient ecofriendly synthesis of pyrazole acryloyl analogs by amino acid catalysis. *Synth. Commun.*, 2016, *46*(8), 701–709. https://doi.org/10.1080/00397911.2016.1164863.

7. Sharma, N., Kumar Sharma, U., Kumar, R., Richa; Kumar Sinha, A. Green and recyclable glycine nitrate (GlyNO3) ionic liquid triggered multicomponent Biginelli reaction for the efficient synthesis of dihydropyrimidinones. *RSC Adv.*, 2012, *2*(28), 10648–10651. https://doi.org/10.1039/c2ra22037g.

8. Kumar, R., Andhare, N. H., Shard, A., Richa; Sinha, A. K. Multicomponent diversity-oriented synthesis of symmetrical and unsymmetrical 1,4-dihydropyridines in recyclable glycine nitrate (GlyNO₃) ionic liquid: A mechanistic insight using Q-TOF, ESI-MS/MS. *RSC Adv.*, 2014, *4*(37), 19111–19121. https://doi.org/10.1039/c4ra02169j.

9. Abbaspour-Gilandeh, E., Azimi, S. C., Mohammadi-Barkchai, A. Li(Glycine)(CF3SO3) as an effective and recoverable catalyst for the preparation of 3,4-dihydropyrimidine-2-(1H)-one under solvent-free conditions. *RSC Adv.*, 2014, *4*(97), 54854–54863. https://doi.org/10.1039/c4ra07334g.

10. Akhtar, W., Khan, M. F., Verma, G., Shaquiquzzaman, M., Rizvi, M. A., Mehdi, S. H., Akhter, M., Alam, M. M. Therapeutic evolution of benzimidazole derivatives in the last quinquennial period. *Eur. J. Med. Chem.*, 2017, *126*, 705–753. https://doi.org/10.1016/j.ejmech.2016.12.010.

11. Digwal, C. S., Yadav, U., Sakla, A. P., Sri Ramya, P. V., Aaghaz, S., Kamal, A. VOSO4catalyzed highly efficient synthesis of benzimidazoles, benzothiazoles, and quinoxalines. *Tetrahedron Lett.* 2016, *57*(36), 4012–4016. https://doi.org/10.1016/j.tetlet.2016.06.074.

12. Gaba, M., Gaba, P., Uppal, D., Dhingra, N., Bahia, M. S., Silakari, O., Mohan, C. Benzimidazole derivatives: Search for GI-friendly anti-inflammatory analgesic agents. *Acta Pharm. Sin. B*, 2015, *5*(4), 337–342. https://doi.org/10.1016/j.apsb.2015.05.003.

13. El-Feky, S. A. H., Abd El-Samii, Z. K., Osman, N. A., Lashine, J., Kamel, M. A., Thabet, H. K. Synthesis, molecular docking and anti-inflammatory screening of novel quinoline incorporated pyrazole derivatives using the Pfitzinger reaction II. *Bioorg. Chem.*, 2015, *58*, 104–116. https://doi.org/10.1016/j.bioorg.2014.12.003.

14. Abdel-Alim, M., Anber F. Mohammed, Samia G. Abdel-Moty, Mostafa A. Hussein & Abdel-Alim. *Arch. Pharm. Res.*, 2013, *36*, 1465–1479.

15. Sakıyan, I., Loğoğlu, E., Arslan, S., Sari, N., Şakiyan, N. Antimicrobial Activities of N-(2-Hydroxy-1-Naphthalidene)-Amino Acid(Glycine, Alanine, Phenylalanine, Histidine, Tryptophane) Schiff bases and their manganese(III) complexes. *BioMetals*, 2004, *17*(2), 115–120. https://doi.org/10.1023/B:BIOM.0000018380.34793.df.

16. Evans, C. W., Atkins, C., Pathak, A., Gilbert, B. E., Noah, J. W. Benzimidazole analogs inhibit respiratory syncytial virus G protein function. *Antiviral Res.*, 2015, *121*, 31–38. https://doi.org/10.1016/j.antiviral.2015.06.016.

17. Mavrova, A. T., Wesselinova, D., Vassilev, N., Tsenov, J. A. Design, Synthesis and anti-proliferative properties of some new 5-substituted-2-iminobenzimidazole derivatives. *Eur. J. Med. Chem.*, 2013, *63*, 696–701. https://doi.org/10.1016/j.ejmech.2013.03.010.

18. Hranjec, M., Pavlović, G., Karminski-Zamola, G. Synthesis, crystal structure determination and antiproliferative activity of novel 2-Amino-4-Aryl-4,10-Dihydro[1,3,5]Triazino[1,2-a]Benzimidazoles. *J. Mol. Struct.*, 2012, *1007*, 242–251. https://doi.org/10.1016/j.molstruc.2011.10.054.

19. Sharma, M. C., Sharma, S., Sahu, N. K., Kohli, D. V. 3D QSAR KNN-MFA studies on 6-substituted benzimidazoles derivatives as nonpeptide angiotensin II receptor antagonists: A rational approach to antihypertensive agents. *J. Saudi Chem. Soc.*, 2013, *17*(2), 167–176. https://doi.org/10.1016/j.jscs.2011.03.005.

20. Sharghi, H., Razavi, S. F., Aberi, M., Tavakoli, F., Shekouhy, M. The Co2+ Complex of [7-Hydroxy-4-Methyl-8-Coumarinyl]glycine as a nanocatalyst for the synthesis and biological evaluation of new Mannich bases of benzimidazoles and benzothiazoles. *ChemistrySelect.*, 2020, *5*(9), 2662–2671. https://doi.org/10.1002/slct.201904700.

21. Tamoradi, T., Ghorbani-Choghamarani, A., Ghadermazi, M., Veisi, H. SBA-15@Glycine-M (M= Ni and Cu): Two green, novel and efficient catalysts for the one-pot synthesis of 5-substituted tetrazole and polyhydroquinoline derivatives. *Solid State Sci.*, 2019, *91*, 96–107. https://doi.org/10.1016/j.solidstatesciences.2019.03.020.

22. Ghorbani-Choghamarani, A., Sahraei, R., Taherinia, Z. Ni(II) immobilized on modified boehmite nanostructures: A novel, inexpensive, and highly efficient heterogeneous nanocatalyst for multicomponent domino reactions. *Res. Chem. Intermed.*, 2019, *45*(5), 3199–3214. https://doi.org/10.1007/s11164-019-03787-3.

23. Ghorbani-Choghamarani, A., Sahraei, R., Taherinia, Z., Mohammadi, M. Cu(I)@Isatin-glycine-boehmite nanoparticles: As novel heterogeneous catalyst for the synthesis and selective oxidation of sulfides. *J. Iran. Chem. Soc.*, 2021, *18*(4), 827–838. https://doi.org/10.1007/s13738-020-02072-0.

24. Tamoradi, T., Ghorbani-Choghamarani, A., Ghadermazi, M. CoFe$_2$O$_4$ @glycine-M (M= Pr, Tb and Yb): Three green, novel, efficient and magnetically-recoverable nanocatalysts for synthesis of 5-substituted 1H–tetrazoles and oxidation of sulfides in green condition. *Solid State Sci.*, 2019, *88*, 81–94. https://doi.org/10.1016/j.solidstatesciences.2018.10.011.

25. Yan, C. F., Chen, H., Hu, R. R., Huang, S., Luo, W., Guo, C., Li, M., Li, W. Synthesis of Mesoporous Co-Ce oxides catalysts by glycine-nitrate combustion approach for CO preferential oxidation reaction in excess H$_2$. *Int. J. Hydrogen Energy*, 2014, *39*(32), 18695–18701. https://doi.org/10.1016/j.ijhydene.2014.01.024.

26. Chen, Y., Zhou, W., Shao, Z., Xu, N. Nickel catalyst prepared via glycine nitrate process for partial oxidation of methane to syngas. *Catal. Commun.*, 2008, *9*(6), 1418–1425. https://doi.org/10.1016/j.catcom.2007.12.009.

27. Ghorbani-Choghamarani, A., Shiri, L., Azadi, G. Preparation and characterization of oxovanadium(IV)-glycine imine immobilized on magnetic nanoparticles and its catalytic application for selective oxidation of sulfides to sulfoxides. *Res. Chem. Intermed.*, 2016, *42*(6), 6049–6060. https://doi.org/10.1007/s11164-016-2444-8.

28. Xie, C., Song, J., Wu, H., Zhou, B., Wu, C., Han, B. Natural product glycine betaine as an efficient catalyst for transformation of CO2 with amines to synthesize N-substituted compounds. *ACS Sustain. Chem. Eng.*, 2017, *5*(8), 7086–7092. https://doi.org/10.1021/acssuschemeng.7b01287.

29. Paul, A. K. Synthesis, structure and topological analysis of glycine templated highly stable cadmium sulfate framework: A new Lewis acid catalyst. *J. Mol. Struct.*, 2018, *1157*, 672–678. https://doi.org/10.1016/j.molstruc.2017.12.102.

30. Bolina, I. C. A., Salviano, A. B., Tardioli, P. W., Cren, É. C., Mendes, A. A. Preparation of ion-exchange supports via activation of epoxy-SiO^2 with glycine to immobilize microbial lipase – use of biocatalysts in hydrolysis and esterification reactions. *Int. J. Biol. Macromol.*, 2018, *120*, 2354–2365. https://doi.org/10.1016/j.ijbiomac.2018.08.190.

31. Yu, C. L., Sakthinathan, S., Hwang, B. Y., Lin, S. Y., Chiu, T. W., Yu, B. S., Fan, Y. J., Chuang, C. CuFeO2–CeO2 nanopowder catalyst prepared by self-combustion glycine nitrate process and applied for hydrogen production from methanol steam reforming. *Int. J. Hydrogen Energy*, 2020, *45*(32), 15752–15762. https://doi.org/10.1016/j.ijhydene.2020.04.077.

32. Guo, X., Mao, D., Lu, G., Wang, S., Wu, G. Glycine-nitrate combustion synthesis of CuO-ZnO-ZrO2 catalysts for methanol synthesis from CO2 hydrogenation. *J. Catal.*, 2010, *271*(2), 178–185. https://doi.org/10.1016/j.jcat.2010.01.009.

33. Choi, I. A., Kwak, D. H., Han, S. B., Park, J. Y., Park, H. S., Ma, K. B., Kim, D. H., Won, J. E., Park, K. W. Doped porous carbon nanostructures as non-precious metal catalysts prepared by amino acid glycine for oxygen reduction reaction. *Appl. Catal. B Environ.*, 2017, *211*, 235–244. https://doi.org/10.1016/j.apcatb.2017.04.039.

34. Chang, Y., Liu, X., Cai, A., Xing, S., Ma, Z. Glycine-assisted synthesis of mesoporous TiO2 nanostructures with improved photocatalytic activity. *Ceram. Int.*, 2014, *40*(9 PART B), 14765–14768. https://doi.org/10.1016/j.ceramint.2014.06.066.

5 The Catalytic Role of L-Proline in Organic Reactions

5.1. INTRODUCTION

L-proline organocatalyst has received extensive study attention from synthetic organic chemists because it has been explored as an effective and ecologically friendly catalyst for the synthesis of organic molecules. Many notable developments in this field, including unique chiral catalyst design, new compound synthesis, applications for different reagents, and versatile reaction discovery, have been noted. This chapter primarily focuses on the supported and unsupported catalytic synthesis of compounds of relevance to medicinal chemistry using proline as a starting point.

5.2. APPLICATION OF L-PROLINE AS AN ORGANOCATALYST IN THE MULTICOMPONENT REACTION

Due to their advantageous characteristics like quick reaction durations, low cost, high yield, and simple purification procedures, multicomponent reactions (MCRs) are acknowledged as effective techniques in organic synthesis and medicinal chemistry. Neamani et al. have reported the synthesis of 1,4-dihydropyridines and spiro oxindole dihydropyridine derivatives, which play an essential role in chemical and biological systems, via treatment by L-proline as a green catalyst [1]. L-proline catalyzed the synthesis of two different categories of 1,4-DHP compounds from anilolactone, which was prepared via a reaction of tetronic acid and anilines. In a solution of water and EtOH (1:1) at 90°C, anilolactone and malononitrile are combined with benzaldehydes or isatin to yield two types of dihydropyridine derivatives. The substrate scope for the synthesis of 1,4-dihydropyridine and spiro oxindole dihydropyridine derivatives was explored using various substituted anilines and benzaldehydes (Scheme 5.1). The usage of anilines with electron-donor substituents effectively produced the desired compounds.

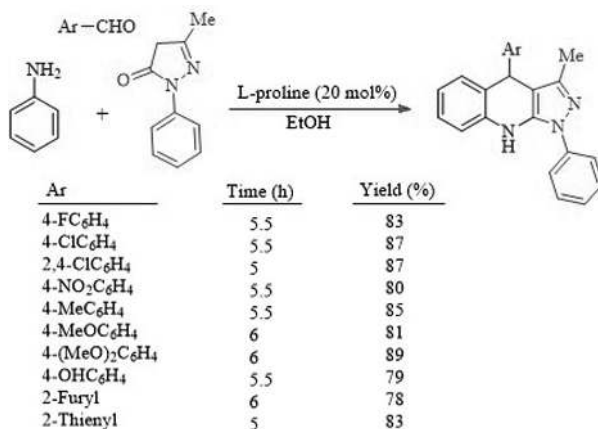In the presence of L-proline as the catalyst, the required products were produced in excellent quantities in a one-pot multicomponent reaction involving aniline, aromatic aldehydes, and 5-methyl-2-phenyl-2,4-dihydro-3*H*-pyrazol-3-one (Scheme 5.2) [2]. In the absence of L-proline, the reaction failed. The catalytic role of L-proline in the synthesis of 1*H*-pyrazolo[3,4-*b*]quinolones was proposed, as shown in Scheme 5.3.

In another study, Yazdani-Elah-Abadi et al. reported using L-proline as an effective, reusable, and bifunctional organocatalyst for the condensation reaction of 1,4-dihydrobenzo[a]pyrido[2,3-c]phenazines under conventional heating in a solvent-free condition (Scheme 5.4) [3]. The aromatic aldehyde worked well with electron-withdrawing and electron-donating substituents, producing the final products in moderate to good yields. Compared with conventional heating methods, this method has several advantages, including a nontoxic catalyst, faster reaction time without any by-products, avoidance of hazardous organic solvents, and a simple operation.

Quinoline and quinazoline are a class of biologically active compounds with anti-inflammatory, anticancer, antidiabetic, etc. properties. It should be mentioned that studies for the synthesis of quinazoline compounds utilizing quinoline scaffolding are attractive. In this context, Dixit created a quinoline scaffold of quinazoline compounds in 2015 utilizing L-proline as a catalyst (Scheme 5.5) [4].
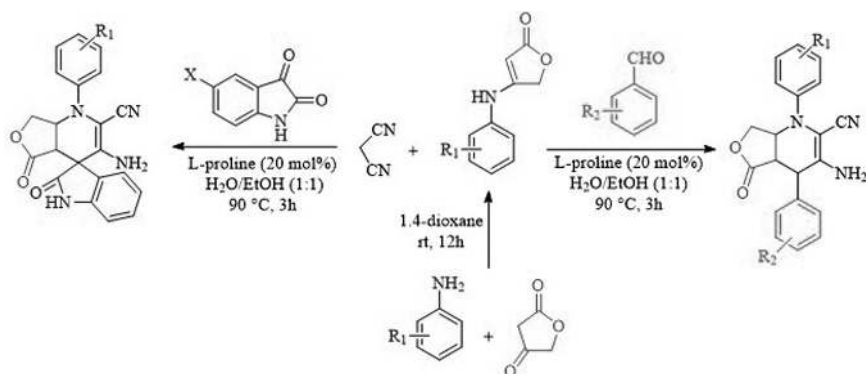
SCHEME 5.1.   Synthesis of two types of 1,4-DHPs with the catalytic treatment of L-proline.

Ar	Time (h)	Yield (%)
4-FC$_6$H$_4$	5.5	83
4-ClC$_6$H$_4$	5.5	87
2,4-ClC$_6$H$_4$	5	87
4-NO$_2$C$_6$H$_4$	5.5	80
4-MeC$_6$H$_4$	5.5	85
4-MeOC$_6$H$_4$	6	81
4-(MeO)$_2$C$_6$H$_4$	6	89
4-OHC$_6$H$_4$	5.5	79
2-Furyl	6	78
2-Thienyl	5	83

SCHEME 5.2.   Utilizing L-proline for the synthesis of 1H-pyrazolo[3,4-b]quinolones.
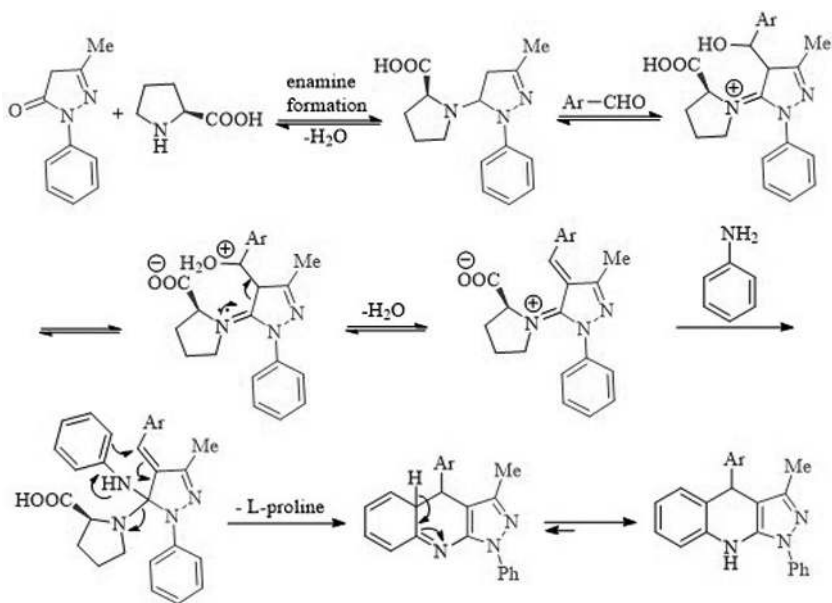
SCHEME 5.3. Proposed mechanism for the one-pot synthesis of 1*H*-pyrazolo[3,4-*b*]quino-lones utilizing L-proline as a catalyst.

R_1: H, Cl, Me

R_2: 4-Cl, 4-NO$_2$, 4-CN, 2-Cl, 3-NO$_2$, 4-Me,
4-OMe, 4-Cl, 4-Me, 4-Cl, 4-NO$_2$

CHO

OEt

R_2

NH$_4$OAc

L-Proline, Solvent-free
80 °C

Time (min): 20- 30
Yield (%): 76- 87
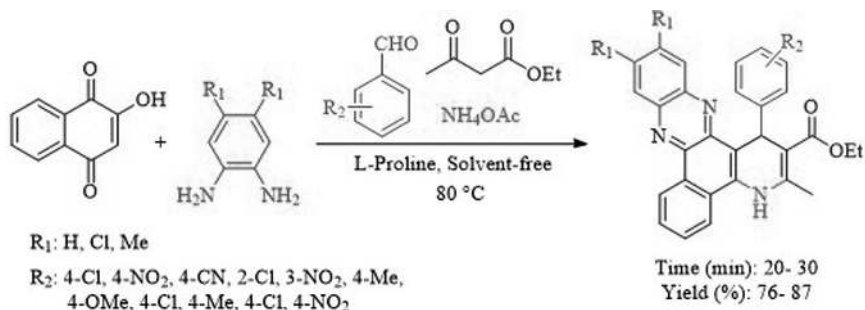
SCHEME 5.4. Synthesis of 1,4 dihydrobenzo[*a*]pyrido[2,3-*c*]phenazine derivatives using a domino one-pot, five-component method.

In addition, the authors offer potential routes for the synthesis of quinazoline using catalytic quantities of L-proline (Scheme 5.6).

A class of heterocyclic chemicals known as coumarins has significant biological effects, including anticancer, antifungal, anti-HIV, antibacterial, and antioxidant characteristics. Using salicylaldehyde and ethyl acetoacetate in the presence of L-proline as a catalyst in triethanolamine solvent was produced (Scheme 5.7). In this context, Srikrishna et al. reported the production of a 3-acetyl coumarin derivative
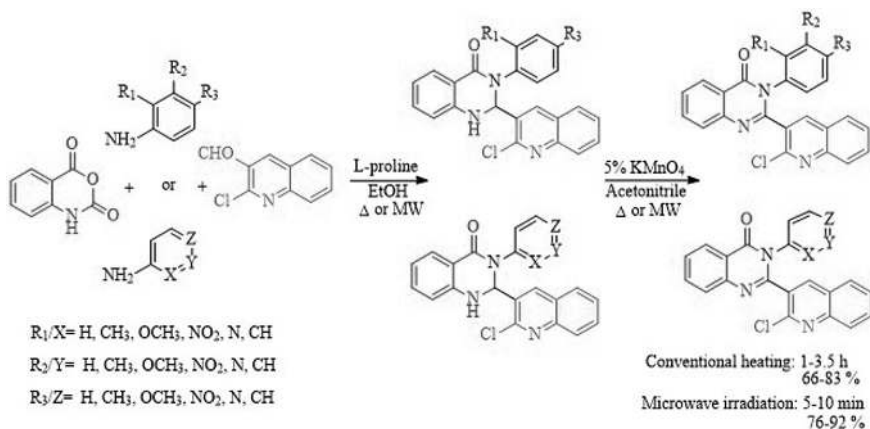
SCHEME 5.5.   The synthesized quinazoline compounds with quinoline scaffold.
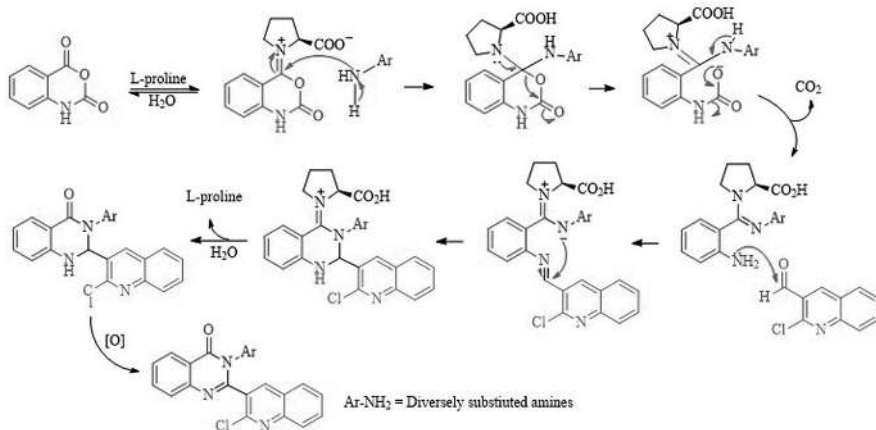
SCHEME 5.6.   Proposed mechanism for the synthesized quinazoline by L-proline.
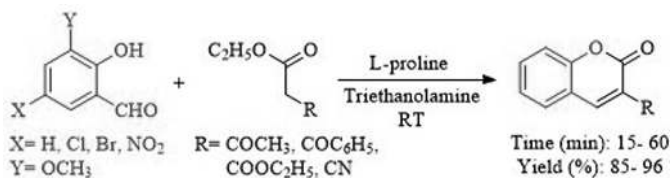
SCHEME 5.7.   3-Acetyl coumarin synthesis using L-proline as a catalyst.

in 2014, the experimental result shows that desired product was obtained in high yield [5].

In a related example, L-proline was used to produce the corresponding dihydro-1*H*-indeno[1,2-*b*]pyridines in very good yields from the corresponding aldehydes, ethyl acetoacetate, 1,3-indanedione, and ammonium acetate in water under conditions reflux (Scheme 5.8) [6]. In comparison to conventional heating methods, this method has a number of benefits, such as simplicity, high product yield, avoidance of column chromatography, commercial viability, safe handling, lack of toxicity, and the capacity to recycle the catalyst.
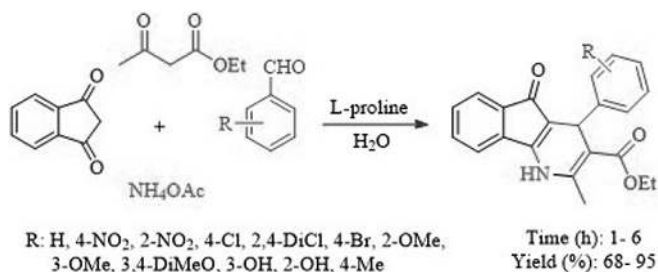
In a related example, L-proline employed a catalyst in the one-pot condensation of 2-hydroxy-1,4-naphthoquinone with aromatic 1,2-diamines to produce the corresponding quinoxalines, and then cyclocondensation with alkyl malonate and a cyclic carbonyl compound produces novel spiro[benzo[*c*]pyrano[3,2-*a*]phenazine] derivatives (Scheme 5.9) [7]. High yields, economic effectiveness, and ease of use are just a few benefits of this approach. In comparison to previous malono derivatives, the authors claimed that utilizing malononitrile resulted in a higher yield and quicker reaction time.
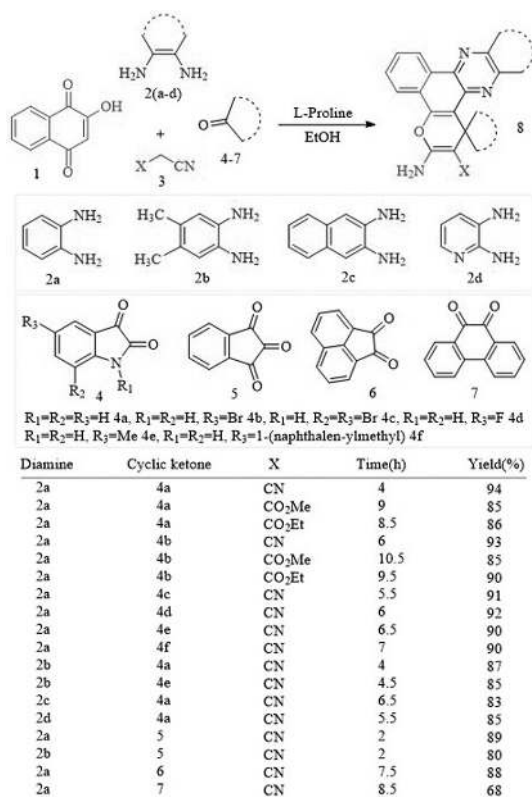
β-Acetamido ketones are a group of important mediators in biologically or pharmaceutically active compounds that can be readily converted to 1,3-amino alcohols and used to synthesize antibiotics. Roshani et al. (2012) created β-acetamide molecules in an appropriate and friendly environment utilizing L-proline as a catalyst (Scheme 5.10) [8].

Pyran is a nonaromatic six-membered ring with two double bonds that have two isomer forms, 2*H*-pyran and 4*H*-pyran, depending on where the double bonds are located. Pyran is composed of five carbon and one oxygen atom. L-proline was used as a natural catalyst by Elnagdi and Al-Hokbany in 2012 as an organocatalyst for the synthesis of pyran compounds that were successful in doing so (Scheme 5.11) [9].

An important class of substances in both chemistry and materials research is polysubstituted benzenes. Researchers suggest several approaches to their synthesis based on their features and applications. In 2012, Keshwal and Rajguru created a collection of polysubstituted benzene derivatives utilizing 1-butyl-3-methylimidazolium hexafluorophosphate as the solvent and L-proline as the catalyst (Scheme 5.12) [10].

R: H, 4-NO$_2$, 2-NO$_2$, 4-Cl, 2,4-DiCl, 4-Br, 2-OMe,   Time (h): 1- 6
3-OMe, 3,4-DiMeO, 3-OH, 2-OH, 4-Me   Yield (%): 68- 95

SCHEME 5.8.   Dihydro-1*H* [1,2-*b*]pyridine synthesis via L-proline catalysis.

R₁=R₂=R₃=H 4a, R₁=R₂=H, R₃=Br 4b, R₁=H, R₂=R₃=Br 4c, R₁=R₂=H, R₃=F 4d
R₁=R₂=H, R₃=Me 4e, R₁=R₂=H, R₃=1-(naphthalen-ylmethyl) 4f

Diamine	Cyclic ketone	X	Time(h)	Yield(%)
2a	4a	CN	4	94
2a	4a	CO₂Me	9	85
2a	4a	CO₂Et	8.5	86
2a	4b	CN	6	93
2a	4b	CO₂Me	10.5	85
2a	4b	CO₂Et	9.5	90
2a	4c	CN	5.5	91
2a	4d	CN	6	92
2a	4e	CN	6.5	90
2a	4f	CN	7	90
2b	4a	CN	4	87
2b	4e	CN	4.5	85
2c	4a	CN	6.5	83
2d	4a	CN	5.5	85
2a	5	CN	2	89
2b	5	CN	2	80
2a	6	CN	7.5	88
2a	7	CN	8.5	68

SCHEME 5.9. One-pot, four-component synthesis of 3-aminospirobenzo[c]pyrano[3,2-a] phenazine derivatives by L-proline.

X= H, 2-Cl, 4-Cl, 3-Br, 4-Br, 2-NO₂,
3-NO₂, 4-NO₂, 4-Me, 4-OMe, 4-Cl
Y= H, 4-Cl, 4-NO₂
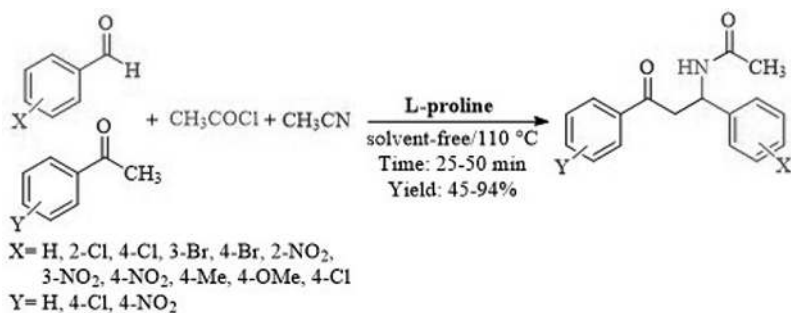
SCHEME 5.10. Catalyzed synthesis of β-acetamido ketones by L-proline.

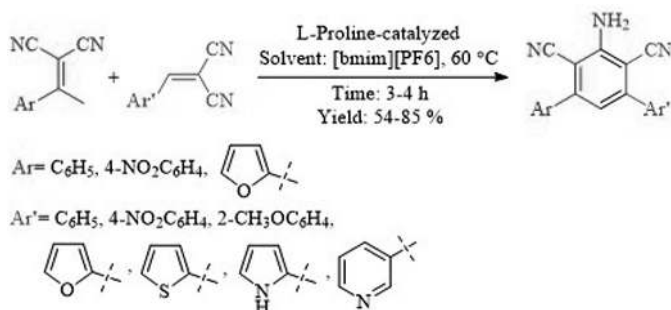| Compound	X	R₁	R₂	Yield (%)
a	O	CH₃	COOEt	72
b	O	CH₃	COCH₃	60
c	S	NH₂	CN	92
d	O			90
e	O	Ph	COOEt	87
f	O	CH₃	COCH₂Ph	65
g	O	Ph	CN	83
h	O			78
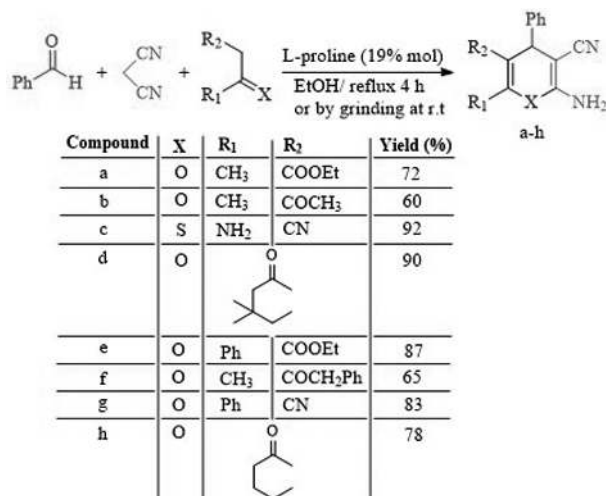
SCHEME 5.11. L-proline-catalyzed pyran derivative synthesis.

Ar= C₆H₅, 4-NO₂C₆H₄,

Ar'= C₆H₅, 4-NO₂C₆H₄, 2-CH₃OC₆H₄,

SCHEME 5.12. Synthesis of polysubstituted benzenes derivatives by L-proline catalyst.

Many pharmacological agents and natural alkaloids include spiro oxindoles as their fundamental structural component. Therefore, scientists are trying to figure out how to successfully synthesize these substances. In 2011, the Bazgir group used L-proline as a catalyst to create spiro oxindole compounds from the reaction of isatin, 1,3-indandione, and 3-aminocrotononitrile (Scheme 5.13) [11].
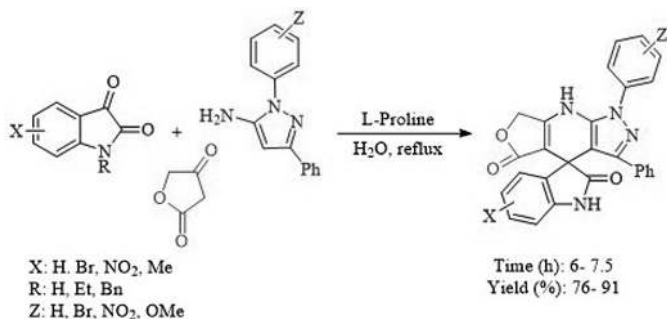
In a different instance, Dabiri et al. reported a three-component ecologically friendly procedure for the production of spiro compounds by a three-component reaction of isatins (1*H*-indole-2,3-diones) or acenaphthylene-1,2-dione, 1,3-diphenyl-1*H*-pyrazoles-5-amines, and tetronic acid (furan-2,4-(3*H*,5*H*)-dione or 2-hydroxy-1,4-naphthoquinone in the presence of a catalytic amount of l-proline in aqueous media (Schemes 5.14 and 5.15) [12]. Spiro compounds were synthesized from various isatins and 1*H*-pyrazol-5-amines, and they proceeded well with both electron-donating and electron-withdrawing substituents. The advantages of the current

procedure include good yields, an easy experimental process, simple purification, and other special benefits.
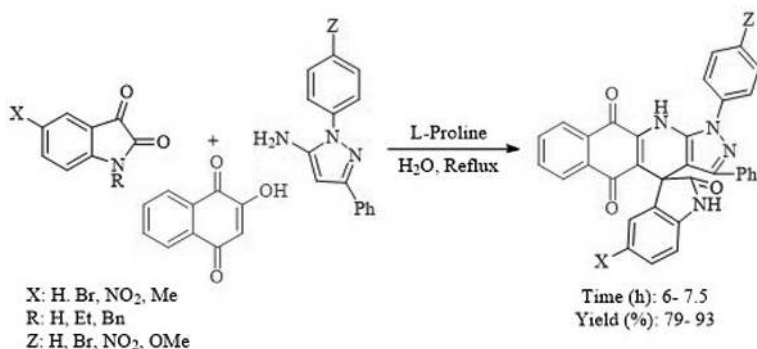
Isoxazole and its derivatives have prospective use in a number of medical and pharmaceutical industries. Therefore, it is highly helpful and significant to develop new and simpler processes for synthesizing this molecule and its derivatives. In 2011, Rajanarendar et al. used the L-proline as a natural catalyst for the synthesis

R= H, Me, Et
X= H, Br, NO₂
R'= CN, COOMe, COOEt

Yield (%): 78-87
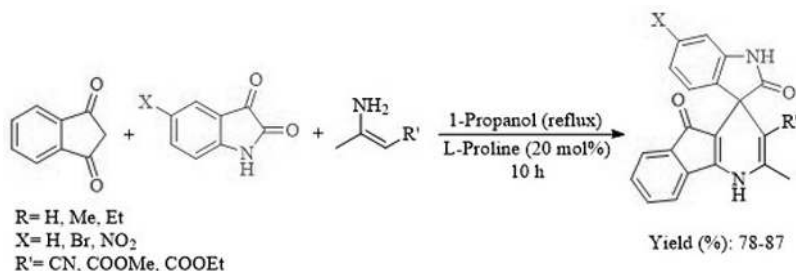
SCHEME 5.13. Synthesis of spiro oxindoles catalyzed by L-proline.

X: H, Br, NO₂, Me
R: H, Et, Bn
Z: H, Br, NO₂, OMe

Time (h): 6- 7.5
Yield (%): 76- 91

SCHEME 5.14. Synthesis of spiro oxindoles.

X: H, Br, NO₂, Me
R: H, Et, Bn
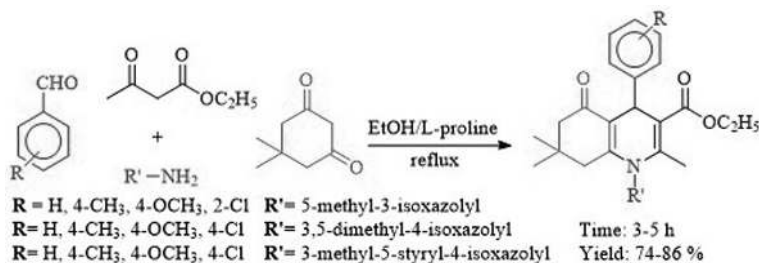Z: H, Br, NO₂, OMe

Time (h): 6- 7.5
Yield (%): 79- 93

SCHEME 5.15. Synthesis of spiro oxindoles.

of isoxazolyl polyhydroquinoline compounds through a reaction between different aldehydes, amines, daimedone, and ethyl acetate (Scheme 5.16) [13].
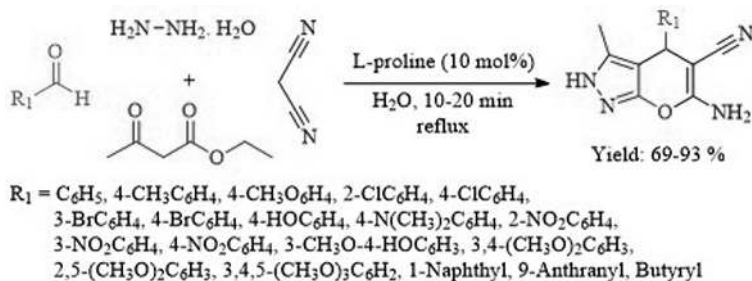
A class of heterocycles having a 4-pyran unit known as pyrano[2,3-*c*] pyrazoles have been used for its analgesic, antitumor, anticancer, and anti-inflammatory characteristics. Therefore, scientists concentrate on creating new processes for synthesizing these molecules. In 2011, the research team of Myrboh reacted different aldehydes with malononitrile, ethyl acetoacetate, and hydrazine hydrate to produce numerous derivatives of 6-amino-4-aryl-3-methyl-2,4-dihydropyrano[2,3-*c*] pyrazole 5-carbonitrile (Scheme 5.17) [14].

Spiro oxindoles are an example of a chemical that has oxygen atoms inside rings attached to the indole ring, such as chromene. Chromenes are particularly significant in chemistry because of their antiviral, antihypertensive, antidepressant, and anticancer effects. Singhs' research group demonstrated one instance of the production of spiro oxindoles at room temperature utilizing L-proline as a catalyst (Scheme 5.18) [15].

Coumarins are two-ring heterocyclic compounds with an oxygen heteroatom that belong to the benzopyrones family and are utilized in the manufacture of various medications, including the anticoagulant known as warfarin. Therefore, Shang's group synthesized coumarin derivatives using the reaction of ethyl acetate and 2-hydroxybenzaldehyde derivatives in the presence of L-proline in [emim]BF4 (Scheme 5.19) [16].


R = H, 4-CH$_3$, 4-OCH$_3$, 2-Cl   R'= 5-methyl-3-isoxazolyl
R= H, 4-CH$_3$, 4-OCH$_3$, 4-Cl   R'= 3,5-dimethyl-4-isoxazolyl   Time: 3-5 h
R= H, 4-CH$_3$, 4-OCH$_3$, 4-Cl   R'= 3-methyl-5-styryl-4-isoxazolyl   Yield: 74-86 %

SCHEME 5.16.   Synthesis of isoxazolyl polyhydroquinolines catalyzed by L-proline.

R$_1$ = C$_6$H$_5$, 4-CH$_3$C$_6$H$_4$, 4-CH$_3$O$_6$H$_4$, 2-ClC$_6$H$_4$, 4-ClC$_6$H$_4$,
        3-BrC$_6$H$_4$, 4-BrC$_6$H$_4$, 4-HOC$_6$H$_4$, 4-N(CH$_3$)$_2$C$_6$H$_4$, 2-NO$_2$C$_6$H$_4$,
        3-NO$_2$C$_6$H$_4$, 4-NO$_2$C$_6$H$_4$, 3-CH$_3$O-4-HOC$_6$H$_3$, 3,4-(CH$_3$O)$_2$C$_6$H$_3$,
        2,5-(CH$_3$O)$_2$C$_6$H$_3$, 3,4,5-(CH$_3$O)$_3$C$_6$H$_2$, 1-Naphthyl, 9-Anthranyl, Butyryl

SCHEME 5.17.   Synthesis of 6-amino-4-alkyl/aryl-3-methyl-2,4-dihydropyrano[2,3-*c*] pyrazole-5-carbonitriles catalyzed by L-proline.

R= H, Br
R$_1$= H, CH$_3$, COCH$_3$ X= CH$_2$, NH, NCH$_3$
R$_2$= CN, CO$_2$CH$_2$CH$_3$ Y= C(CH$_3$)$_2$, CO

85-96 %
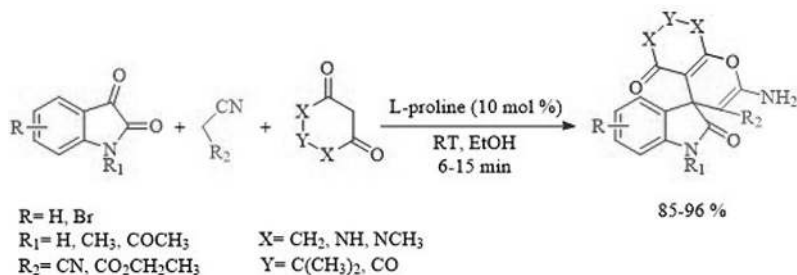
SCHEME 5.18.   L-proline-catalyzed synthesis of spiro oxindole derivatives.

R$_1$: H, CH$_3$
R$_2$: H, OCH$_3$, Cl, Br, NO$_2$, OH
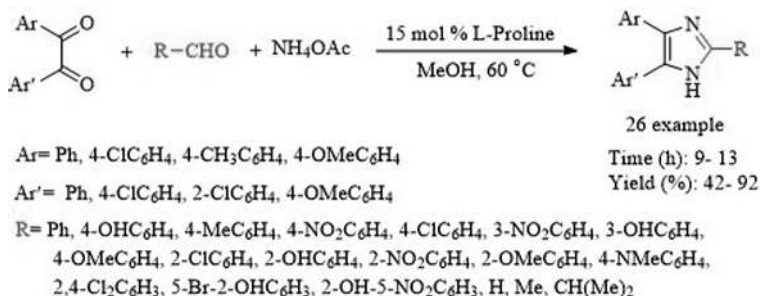
Time (h): 4- 24
Yield (%): 81- 95
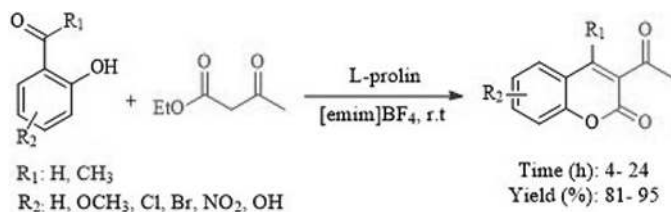
SCHEME 5.19.   L-proline is a useful and effective stimulator of coumarin production in ionic liquid.

Imidazole-based compounds are used as ionic liquids (ILs) as well as for the synthesis of many compounds widely used as drugs with antitumor and antibacterial properties. Singh and collaborators presented two techniques for producing imid-azoles at 60°C while employing an L-proline catalyst in a methanol solvent. The obtained results by this research group are summarized in Schemes 5.20 and 5.21 [17].
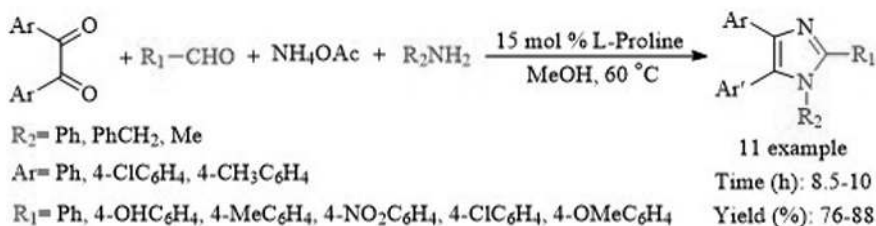
Utilizing aldehydes, 1,2-diketones, and ammonium acetate, the 2,4,5-trisubsti-tuted imidazoles product was created utilizing the first technique. Another technique involved combining 1,2-diketone, 1,2,4,5-tetrasubstituted imidazoles with amine, aldehyde, and ammonium acetate to get the desired reaction. Scheme 5.22 is an illus-tration of several mechanistic routes that authors have suggested for the synthesis of substituted imidazole.

In a different work, the L-proline was utilized as a catalyst by Shingare's team to quickly and effectively synthesize 2,4,5-triaryl substituted imidazoles in ethanol under reflux conditions (Scheme 5.23) [18].

Important substances known as 1,4-dihydropyridines provide a number of thera-peutic benefits, including antitumor, antidiabetic, antihypertensive, and vasodilator effects. Condensation of aldehyde, ethyl acetoacetate, dimedone, and ammonium acetate in the presence of L-proline as a flexible catalyst was employed for the syn-thesis of 1,4-dihydropyridines (Scheme 5.24) [19].

Ar= Ph, 4-ClC$_6$H$_4$, 4-CH$_3$C$_6$H$_4$, 4-OMeC$_6$H$_4$

Ar'= Ph, 4-ClC$_6$H$_4$, 2-ClC$_6$H$_4$, 4-OMeC$_6$H$_4$

R= Ph, 4-OHC$_6$H$_4$, 4-MeC$_6$H$_4$, 4-NO$_2$C$_6$H$_4$, 4-ClC$_6$H$_4$, 3-NO$_2$C$_6$H$_4$, 3-OHC$_6$H$_4$,
    4-OMeC$_6$H$_4$, 2-ClC$_6$H$_4$, 2-OHC$_6$H$_4$, 2-NO$_2$C$_6$H$_4$, 2-OMeC$_6$H$_4$, 4-NMeC$_6$H$_4$,
    2,4-Cl$_2$C$_6$H$_3$, 5-Br-2-OHC$_6$H$_3$, 2-OH-5-NO$_2$C$_6$H$_3$, H, Me, CH(Me)$_2$

26 example
Time (h): 9- 13
Yield (%): 42- 92

SCHEME 5.20. Synthesis of 2,4,5-trisubstituted imidazoles catalyzed by L-proline.

R$_2$= Ph, PhCH$_2$, Me

Ar= Ph, 4-ClC$_6$H$_4$, 4-CH$_3$C$_6$H$_4$

R$_1$= Ph, 4-OHC$_6$H$_4$, 4-MeC$_6$H$_4$, 4-NO$_2$C$_6$H$_4$, 4-ClC$_6$H$_4$, 4-OMeC$_6$H$_4$

11 example
Time (h): 8.5-10
Yield (%): 76-88

SCHEME 5.21. Synthesis of 1,2,4,5-tetrasubstituted imidazoles catalyzed by L-proline
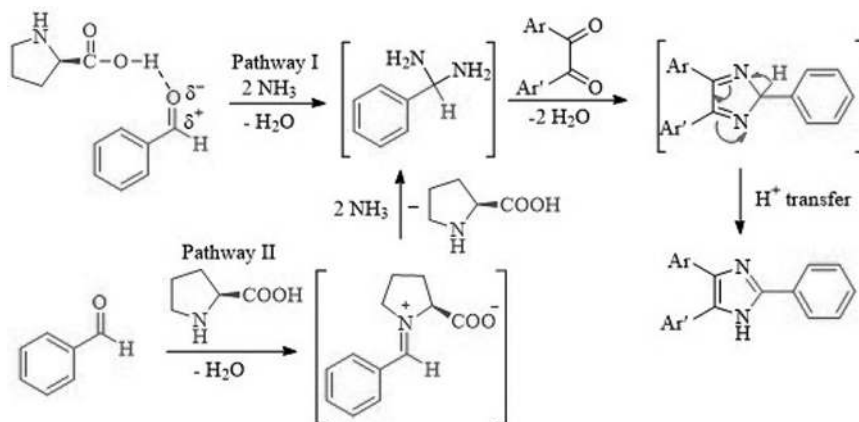

SCHEME 5.22. Imidazole synthesis mechanism with L-proline as a catalyst.

5.3. APPLICATION OF L-PROLINE DERIVATIVE AS AN ORGANOCATALYST IN THE MULTICOMPONENT REACTION

Basumatary et al. have reported the performance of 2-(3-phenylthioureido)ethyl prolinamide for the multicomponent synthesis of coumarin-based unsymmetrical trisubstituted methanes. 2-(3-Phenylthioureido)ethyl prolinamide was produced via a two-step reaction, as shown in Schemes 5.25 and 5.26 [20]. High catalytic activity
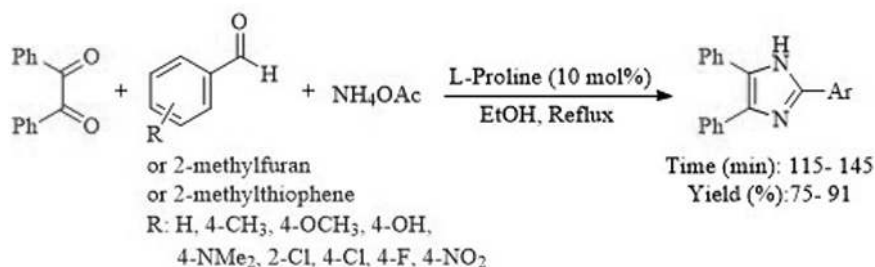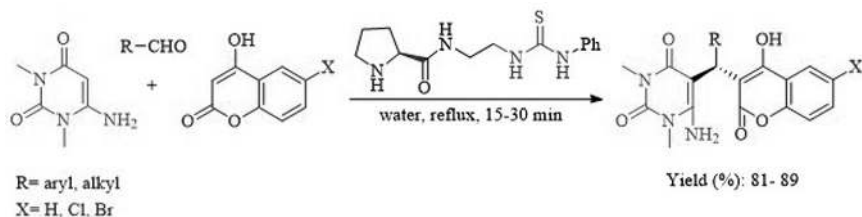
SCHEME 5.23.   Proline is an efficient catalyst for the production of 2,4,5-triaryl-1H-imidazoles.
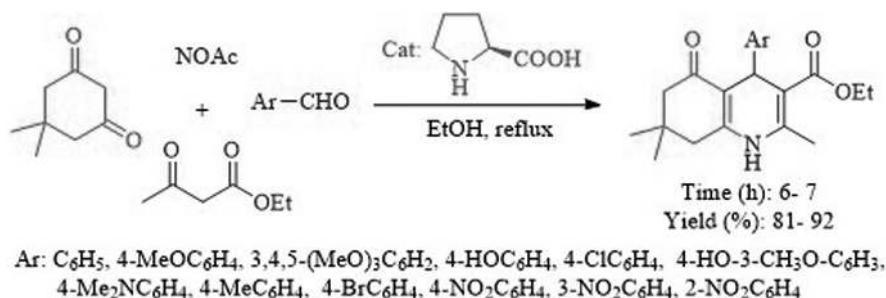
SCHEME 5.24.   L-proline is an efficient organocatalyst in the multicomponent Hantzsch reaction to produce 1,4-dihydropyridines.
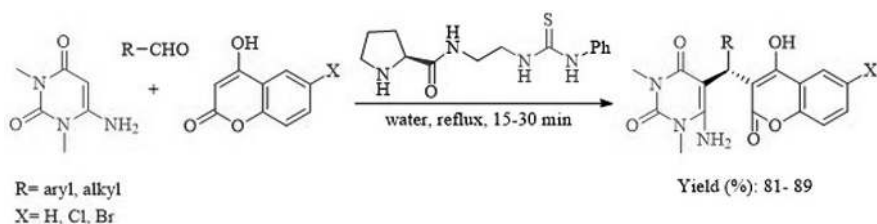
**SCHEME 5.25.**   Synthesis of amino thiourea generated from L-proline.

SCHEME 5.26.   Trisubstituted methane synthesis catalyzed by amino thiourea derived from L-proline.

was found for multicomponent due to 2-(3-phenylthioureido)ethyl prolinamide acting as a base and nucleophile. This process offers several advantages compared to traditional heating methods such as using water as the reaction medium, the product could be isolated by straightforward filtration, avoiding the need for toxic organic solvents in chromatographic separation.
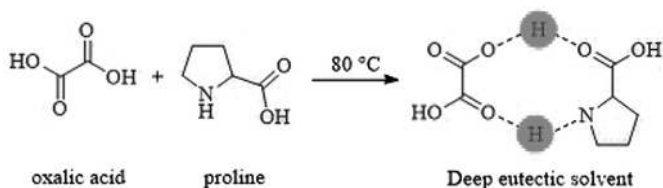
The intense search for more effective techniques for the synthesis of 4-aryl-substituted dihydropyrimidines (DHPMs) has been driven by an interest in biological, medical, and pharmacological properties. An effective catalytic method for the synthesis of 4-aryl-substituted dihydropyrimidines was described by Titova et al. (Scheme 5.27). They used chiral catalysts generated from L-proline in conjunction with nanosized SiO_2-ZrO_2 as a new catalytic medium [21]. By using the sol–gel technique, the single oxides SiO_2 and ZrO_2 were created. The respective sols were mixed in a preset ratio to create the mixed SiO_2-ZrO_2 nanomaterials, which were then dried at 100–120°C. Amorphous nanoparticles were the end product. The Brunauer–Emmett–Teller (BET) surface area of the synthesized nanoparticles was found to be 59 m²/g for SiO_2-ZrO_2 (1:1), 123 m²/g for SiO_2-ZrO_2 (2:1), 288 m²/g for SiO_2-ZrO_2 (4:1), 222 m²/g for SiO_2, and 33 m²/g for ZrO_2. In this study, the effect of mixed oxides, that is, SiO_2-ZrO_2 with various ratios (1:1, 2:1, and 4:1), as well as single oxides SiO_2 and ZrO_2 as heterogeneous promoters in combination with L-proline-derived chiral catalyst on the progress of a reaction was investigated. The results demonstrate that the presence of the Si-O-Zr bonds significantly increases the concentration and strength of Brønsted and Lewis acidic sites on the surface of mixed oxides SiO_2-ZrO_2, as well as the yield of the desired products and the content of its (R)-enantiomer.

A new class of solvents known as low melting mixes (LMMs) [25], low transition temperature mixtures (LTTMs) [22], or deep eutectic solvents (DESs) [23, 24]
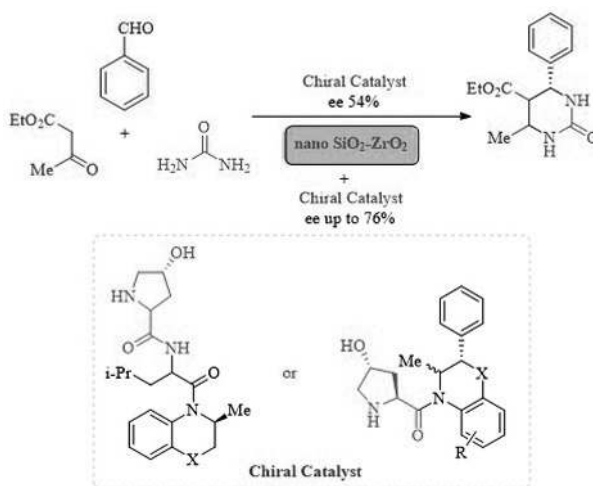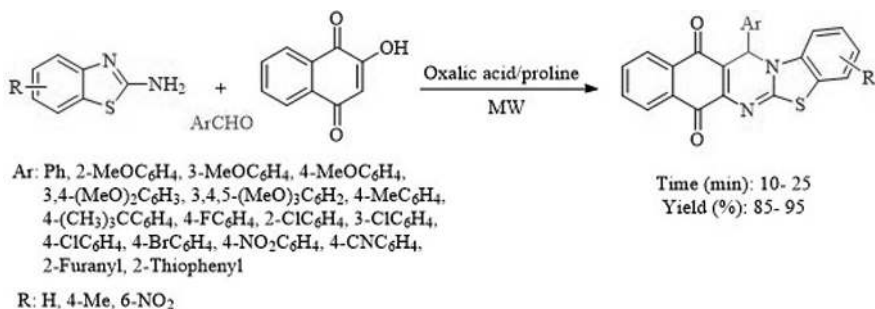

SCHEME 5.27. Schematic illustration for the synthesis of 4-aryl-substituted dihydropyrimidines (DHPMs) catalyzed by L-proline-derived chiral catalysts.

has recently come into the spotlight as a potential sustainable solvent. Ionic liquids and DESs share many of the same physical and chemical characteristics, including nonflammability, low volatility, low toxicity, recyclability, superior biodegradability, attractive low costs, and ease of synthesis. The majority of DESs remain liquid at room temperature and are mixes of two or more components with melting points (mp) lower than any of the separate components. A suitable hydrogen bond acceptor (HBA) like choline chloride (ChCl) and hydrogen bond donors (HBD) such as acids, alcohols, amines, or carbohydrates are combined and gently warmed to create them. Electrochemical synthesis has drawn a lot of interest in the production of nano-materials because of its low cost, low-temperature operation, high product purity, simplicity, and environmental friendliness. Due to their distinct properties, DESs can replace ILs and volatile organic solvents in a variety of physical and chemical processes, particularly those involving extraction and separation [25], polymeriza-tion and material science [26, 27], biomass processing [28], and organic synthesis [29, 30]. In a three-component reaction, including aromatic aldehydes, 2-amino ben-zothiazole, and 2-hydroxy-1,4-naphthoquinone, as well as oxalic acid and a deep eutectic solvent (DES) based on L-proline (as an efficient catalyst) under microwave irradiation, 13-aryl-13H-benzo[g]benzothiazolo[2,3-b]quinazoline-5,14-diones were produced (Schemes 5.28 and 5.29) [31]. Significant benefits of this technol-ogy include an environmentally friendly process, quick reaction times, great yields, chromatography-free purification, and the ability to reuse and recycle the DES.

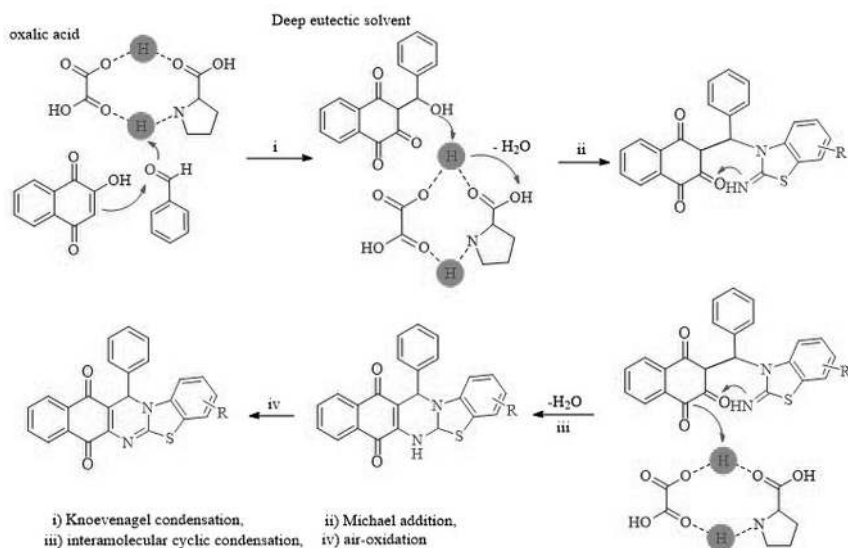**SCHEME 5.28.**   Oxalic acid and proline-based DES preparation.

Ar: Ph, 2-MeOC$_6$H$_4$, 3-MeOC$_6$H$_4$, 4-MeOC$_6$H$_4$,
    3,4-(MeO)$_2$C$_6$H$_3$, 3,4,5-(MeO)$_3$C$_6$H$_2$, 4-MeC$_6$H$_4$,
    4-(CH$_3$)$_3$CC$_6$H$_4$, 4-FC$_6$H$_4$, 2-ClC$_6$H$_4$, 3-ClC$_6$H$_4$,
    4-ClC$_6$H$_4$, 4-BrC$_6$H$_4$, 4-NO$_2$C$_6$H$_4$, 4-CNC$_6$H$_4$,
    2-Furanyl, 2-Thiophenyl

R: H, 4-Me, 6-NO$_2$

Time (min): 10- 25
Yield (%): 85- 95

SCHEME 5.29.   Oxalic acid/proline mixture-based 13-aryl-13H-benzo[g]benzolo [2,3-b] quinazoline-5,14-diones synthesis.

A plausible mechanism for the one-pot multicomponent condensation of 13-aryl-13*H*-benzo[*g*]benzothiazolo [2,3-*b*]quinazoline-5,14-diones has also been reported by the authors (Scheme 5.30).
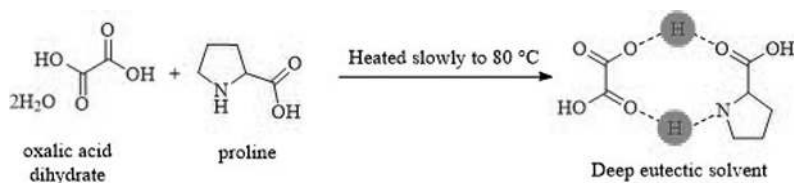
LTTMs are regarded as designer solvents due to unique qualities such as chemical and thermal stability, biodegradability, nonflammability, cost-effectiveness, and biodegradability that increase their usefulness in many organic transformations as a catalyst or solvents. They can be produced by a combination of natural high-melting-point starting materials, which give a liquid by hydrogen-bond interactions.

In a similar vein, proline LTTM with the dual role (solvent and catalyst) was described by Chandam et al. in a similar vein as a unique environmentally friendly synthetic strategy for the synthesis of spiro xanthene and dibarbiturate derivatives in the presence of oxalic acid dihydrate (Scheme 5.31) [32].
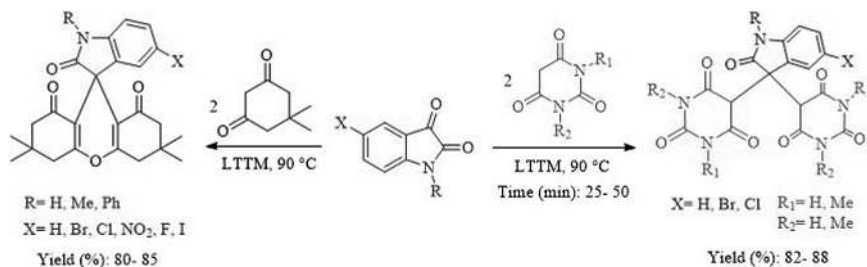
Utilizing LTTM, the efficient synthesis of spiro xanthene and dibarbiturate derivatives was accomplished, and high to excellent yields of the finished products were produced for both electron-donating and electron-withdrawing substituents (Scheme 5.32).

i) Knoevenagel condensation,   ii) Michael addition,
iii) interamolecular cyclic condensation,   iv) air-oxidation

SCHEME 5.30. A plausible method of producing 13-phenyl-12*H*-benzo[*g*]benzo[4,5] thiazolo[2,3-*b*].

SCHEME 5.31. Preparation of oxalic acid dehydrate/proline LTTM.

R= H, Me, Ph

X= H, Br, Cl, NO₂, F, I

Yield (%): 80- 85

X= H, Br, Cl   R₁= H, Me

R₂= H, Me

Yield (%): 82- 88

SCHEME 5.32. Oxalic acid dehydrate/proline-assisted synthesis of spiro[indoline-3,9′-xanthene]trione and dibarbiturate derivatives.
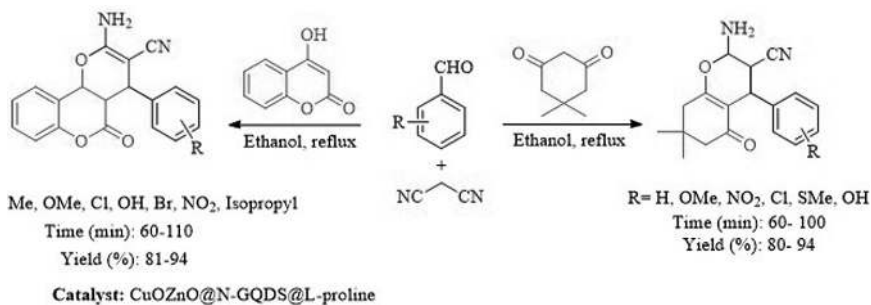
5.4. APPLICATION OF L-PROLINE DERIVATIVE-SUPPORTED MATERIAL AND ITS DERIVATIVES AS AN ORGANOCATALYST IN THE MULTICOMPONENT REACTION

A novel class of carbon nanomaterials includes graphene quantum dots (GQDs), which are graphene fragments with sizes in the multiple nanometer range [33, 34]. The important carbon nanomaterial nitrogen-doped graphene quantum dots (N-GQDs) can be used to create diverse metal-organocatalysts. In terms of catalytic activity, recyclability, thermal stability, and other factors, N-GQD modification is crucial. A three-component reaction involving malononitrile, dimedone, and aromatic aldehydes for the manufacture of 2-amino-4*H*-chromene using L-proline-assisted CuO/ZnO@N-GQDs nanocomposites was reported by Safaei-Ghomi and coworkers [35]. Ultrapure ethylenediamine and citric acid were combined to form the catalyst, and then calcined CuO/ZnO nanocomposites were added. The mixture was thoroughly mixed before being placed in a 150 ml Teflon-lined stainless steel autoclave for the hydrothermal reaction, which was carried out for 9 h at 180°C (Scheme 5.33). Then the resulting nanocomposite of CuO/ZnO@N-GQDs was reacted with L-proline. A wide variety of compounds containing aromatic aldehydes were studied for the reaction (Scheme 5.34), and the combination of ethanol and 10 mg of catalyst combined with MW irradiation produced the greatest yield.

Akhavan and Bekhradnia reported the synthesis of MnCoCuFe₂O₄@L-proline (MCCFe₂O₄@L-proline) magnetic nanorods and its use as an efficient nanocatalyst for the stereoselective synthesis of a new class of spiro heterocycle. The catalyst was created by mechanically combining 150 ml of distilled water with FeCl₃6H₂O, MnCl₂·2H₂O, CuCl₂·2H₂O, and CoCl₂·6H₂O. This mixture was then combined with NH₄OH to produce MCCFe₂O₄. Thereafter, MCCFe₂O was immobilized with L-proline to obtain MCCFe₂O₄@L-proline (Scheme 5.35) [36]. The nanoparticles exhibited a rod morphology and measured 30–60 nm in width and 150–300 nm in length, as seen by the SEM image, It can be said that MCCFe₂O₄@L-proline resembles nanorods. The corresponding *endo*-isomers of spirocyclic pyrrolidine/ pyrrolizidine/pyrrolothiazolidine derivatives were produced by a multicomponent reaction
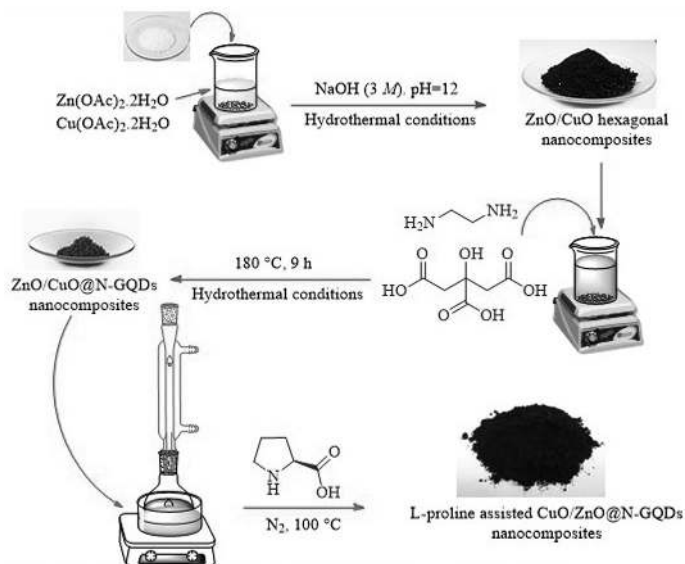
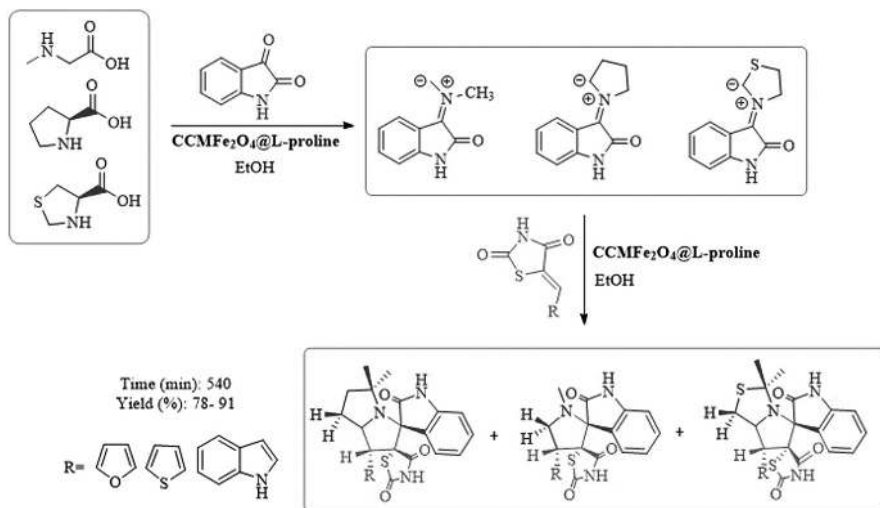**SCHEME 5.33.** An illustration of the creation of a CuO/ZnO@NGQDs nanocomposite helped by L-proline.

Me, OMe, Cl, OH, Br, NO$_2$, Isopropyl
Time (min): 60-110
Yield (%): 81-94

Catalyst: CuOZnO@N-GQDS@L-proline

R= H, OMe, NO$_2$, Cl, SMe, OH
Time (min): 60- 100
Yield (%): 80- 94

SCHEME 5.34. Synthesis of chromenes using L-proline-assisted CuO/ZnO@N-GQDs nanocomposite.
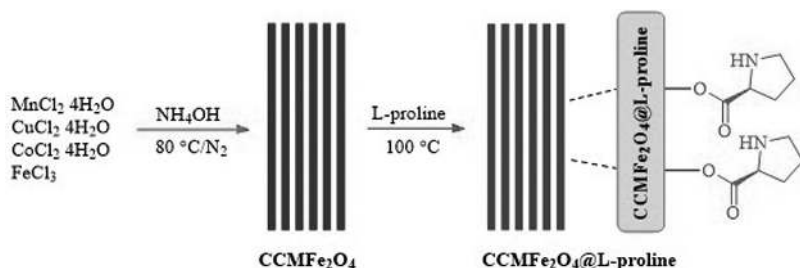
SCHEME 5.35. Preparation of CoCuMnFe$_2$O$_4$@L-proline MNRs.

in EtOH, including 5-arylidene thiazolidine-2,4-diones, isatin, and secondary amino acids (Scheme 5.36).

Safaei-Ghomi and Samadi published an ecologically friendly one-pot multicomponent synthesis of pyrimidine by using $Fe_3O_4@SiO_2$-L-proline NPs as catalysts and ethanol as the solvent [37]. To make $Fe_3O_4@SiO_2$-L-proline NPs, nano-$Fe_3O_4@SiO_2$ was dispersed in dry ethanol using an ultrasonic bath; it was then mixed with L-proline and H_2SO_4 and heated under reflux (Scheme 5.37).

SCHEME 5.36.   One-pot, three-component asymmetric 1,3-dipolar cycloaddition catalyzed by the CCMFe$_2$O$_4$@L-proline MNRs.
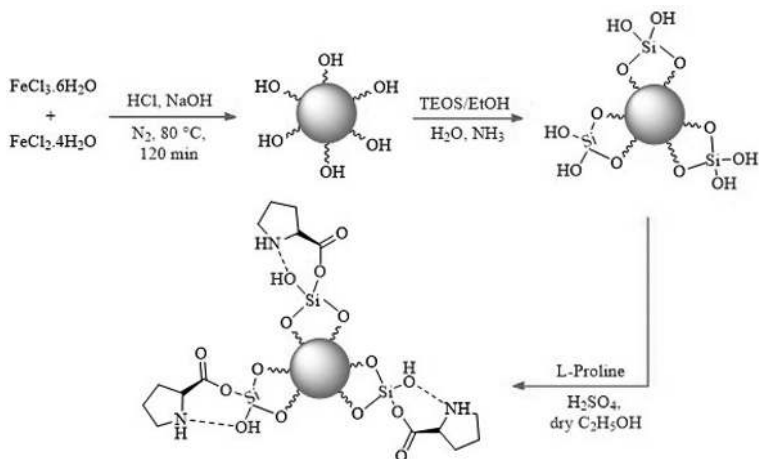
SCHEME 5.37.   Schematic illustration of the preparation of $Fe_3O_4@SiO_2$-L-proline nanoparticles.

The produced nanocatalysts were successfully used in the three-component reaction of 1,3-diethyl barbituric acid with aldehyde and arylamine to synthesize pyrimidine (Scheme 5.38). The sensible conversions for both electron-donating and electron-withdrawing groups further illustrated the catalytic media's adaptability.

In another study, the performance of $Fe_3O_4@SiO_2$-propyl@L-proline was investigated for the synthesis of pyridazinones, phthalazinones (from arenes, cyclic anhydrides, and phenylhydrazine), and amides (from arenes, cyclic anhydrides, and 2-amino benzimidazole) (Schemes 5.39 and 5.40) [38]. This catalytic procedure worked well with a variety of substrates and provided high product yields in each instance.

Fekri et al. studied the catalytic activity of $Fe_3O_4@SiO_2@$L-proline nanoparticles for the synthesis of benzoimidazo[1,2-a]pyrimidines and tetrahydro benzo[4,5] imidazo-[1,2-d]quinazolin-1(2H)-ones in water (Scheme 5.41) [39]. The catalyst was also easily recycled at least four times without seeing any noticeable loss of activity.

Keshavarz et al. designed a new nanomagnetic material (graphene oxide/Fe_3O_4/L-proline) By immobilizing L-proline on graphene oxide/Fe_3O_4 nanocomposite (Scheme 5.42) [40].

The authors investigated the synthesis of bis-pyrazole derivatives by catalytic promotion of superparamagnetic graphene oxide/Fe_3O_4/L-proline in ethanol (Scheme 5.43). It should be emphasized that at the same weight ratios, graphene oxide/


R_1= 4-CH_3, 4-OCH_3

R= 2-NO_2, 4-SCH_3, 4-Cl, 3-NO_2, 2,4-di-Cl, 4F, 4CH_3

Time (min):120- 150

Yield (%): 82- 93
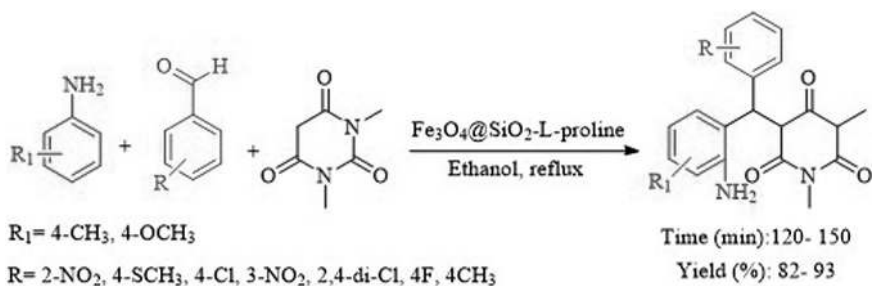
SCHEME 5.38. Synthesis of pyrimidines using $Fe_3O_4@SiO_2$-L-poline nanoparticles.

R= CH_3, OCH_3, Cl

Yield: 96- 98%

Yield: 92-96%
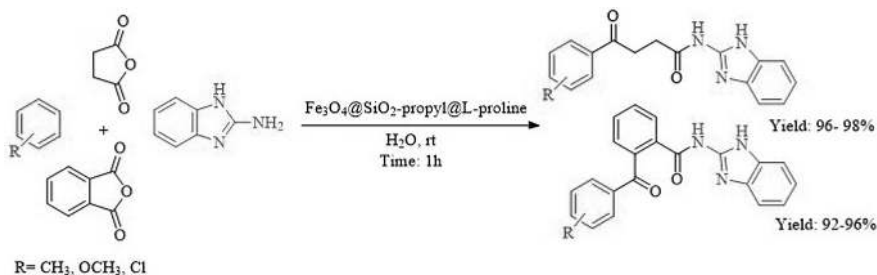
**SCHEME 5.39.** Schematic display of multicomponent synthesis of amides catalyzed by $Fe_3O_4@SiO_2$-propyl@L-proline.
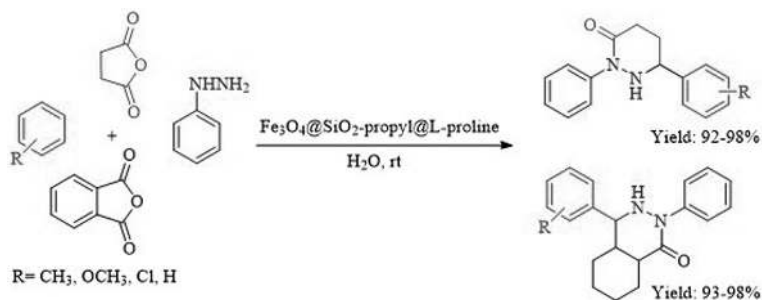
SCHEME 5.40. Schematic display of multicomponent synthesis of amides and pyridazi-nones catalyzed by Fe$_3$O$_4$@SiO$_2$-propyl@L-proline.
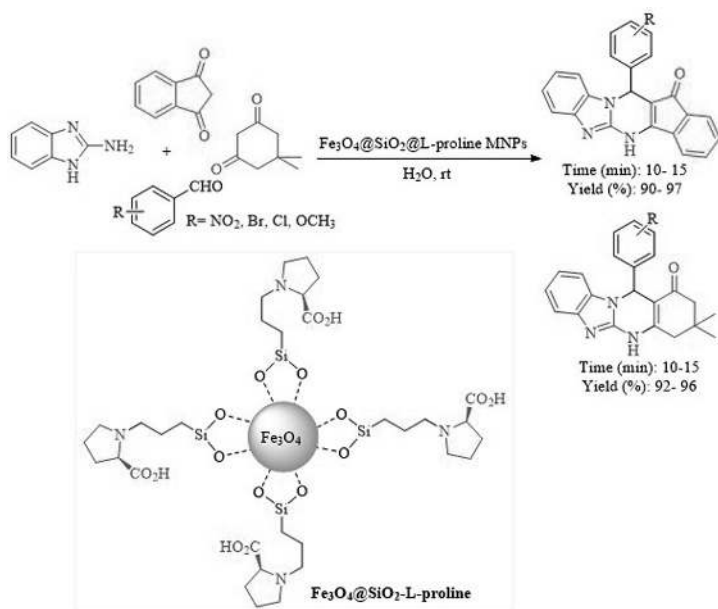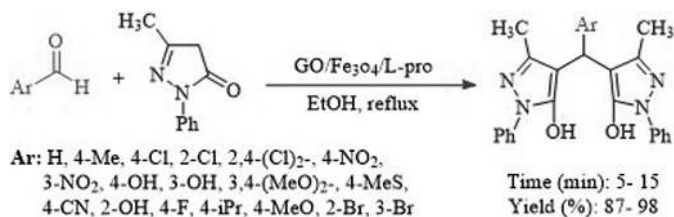

SCHEME 5.41. Multicomponent synthesis of benzimidazo[1,2-a]pyrimidinone and tetra-hydrobenzo[4,5]imidazo-[1,2-d]quinazolin-1(2H)-one catalyzed by Fe$_3$O$_4$@SiO$_2$@L-proline MNPs.

Fe$_3$O$_4$/L-proline showed better catalytic activity than virgin L-proline. By using an external magnet, the catalyst was successfully recycled and reused eight more times.
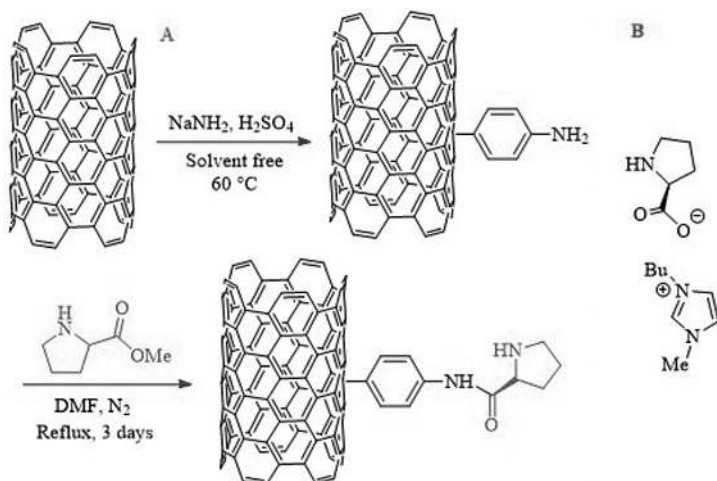
Hajipour and Khorsandi prepared the synthesis of two different catalysts in structures: [BMIm][Pro] and Pro/MWCNTs (L-proline supported on multiwalled carbon nanotube) [41]. Pro/MWCNTs were prepared using a modification of L-proline on MWCNTs via direct grafting amination (Scheme 5.44). The [BMIm][Pro] was prepared by the 1-butyl-3-methylimidazolium bromide, followed by an anion-exchange
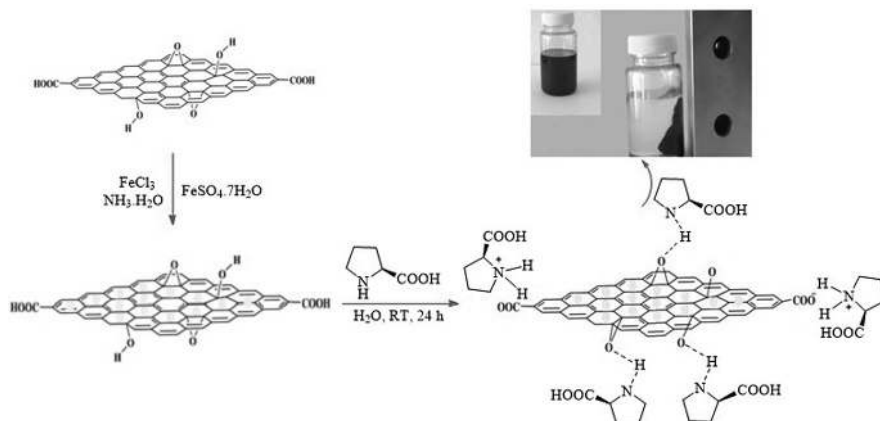
SCHEME 5.42. Graphene oxide (GO)/Fe$_3$O$_4$/L-proline nanohybrid preparation process.

Ar: H, 4-Me, 4-Cl, 2-Cl, 2,4-(Cl)$_2$-, 4-NO$_2$,
3-NO$_2$, 4-OH, 3-OH, 3,4-(MeO)$_2$-, 4-MeS,
4-CN, 2-OH, 4-F, 4-iPr, 4-MeO, 2-Br, 3-Br

Time (min): 5- 15
Yield (%): 87- 98

SCHEME 5.43. Bis-pyrazole derivative synthesis by GO/Fe$_3$O$_4$/L-proline.

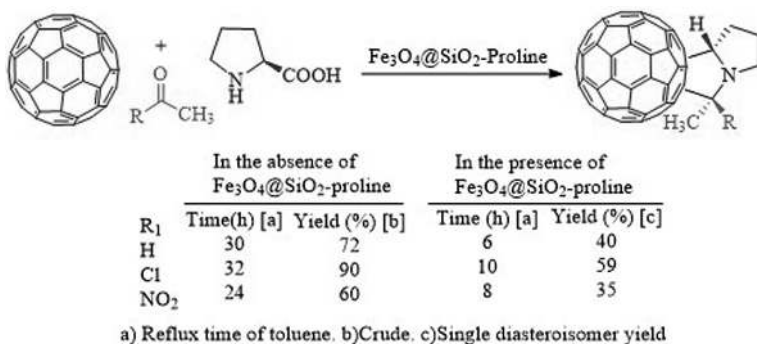**SCHEME 5.44.** Pro/MWCNTs nanocatalyst (a) and [BMIm][Pro] (b) preparation.

reaction with 201 × 7 styrene-DVB converted to 1-butyl-3- methylimidazolium hydroxide as a very facile route. Lastly, proline was used to neutralize 1-butyl-3-methylimidazolium hydroxide with the desired product [BMIm][Pro] in 85% yield.

Mentioned authors examined the catalytic properties of [BMIm][Pro] and Pro/MWCNTs in the synthesis of multi-substituted 2-amino-3-cyano-4*H*-pyrans by reaction of malononitrile and α-substituted-free chalcones. The findings demonstrated that Pro/ MWCNTs outperformed [BMIm][Pro] in terms of quicker reaction times and higher product yields (Scheme 5.45). Also, the Pro/MWCNTs catalyst exhibited good recyclability than [BMIm][Pro].

Fe_3O_4@SiO_2-L-proline has been used in the one-pot diastereoselective synthesis of fulleropyrrolidines from C_{60}, L-proline, and acetophenone in toluene under reflux and nitrogen ambient conditions (Scheme 5.46) [42]. It should be noted that when the reaction is conducted with a catalyst present, the reaction time is decreased in comparison to the conventional method.
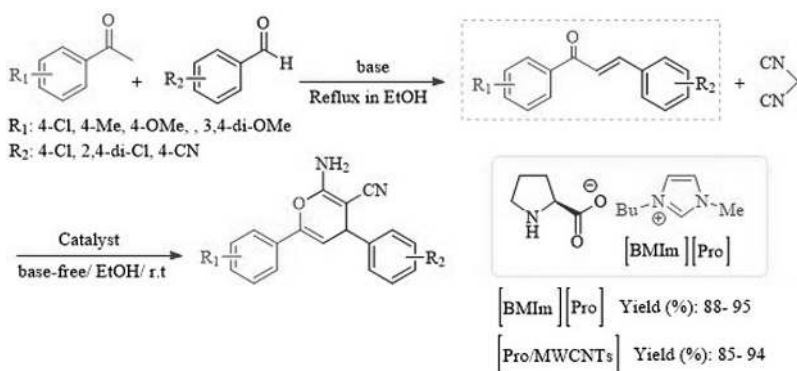
**SCHEME 5.45.** Synthesis of 2-amino-3-cyano-4*H*-pyrans catalyzed by [BMIm][Pro] or Pro/MWCNTs.

	In the absence of Fe_3O_4@SiO_2-proline		In the presence of Fe_3O_4@SiO_2-proline	
R_1	Time(h) [a]	Yield (%) [b]	Time (h) [a]	Yield (%) [c]
H	30	72	6	40
Cl	32	90	10	59
NO_2	24	60	8	35

a) Reflux time of toluene. b)Crude. c)Single diasteroisomer yield

SCHEME 5.46. Diastereoselective synthesis of fulleropyrolidines via the cycloaddition of L-proline and acetophenone derivatives with $C_{60.}$

It has been reported that a one-pot three-component condensation reaction involving thiourea, aromatic aldehydes, and *t*-butyl acetoacetate and catalyzed by MNP-L-proline-SO$_3$H results in high yields of the desired 3,4-dihydropyrimidine2-(1*H*)-thiones (Scheme 5.47) [43]. It should be noted, that without the catalyst, the reaction failed.

This novel nanocatalyst was obtained via the initial coprecipitation method through a combination of Fe(II), Fe(III), NH$_4$OH, and L-proline under an N$_2$ atmosphere; the obtained magnetic material is then treated with chlorosulfonic acid (ClSO$_3$H) which afforded MNP-L-proline-SO$_3$H with particle sizes of 8–20 nm (Scheme 5.48).

In 2014, Khalafi-Nezhad et al. produced L-proline-modified magnetic nanoparticles (LPMNP) and it is used in the synthesis of bis(indol-3-yl)methanes. In this method, a sol–gel process was used to obtain the original shell MNPs (Fe$_3$O$_4$@SiO$_2$)

R: H, Cl, OMe, 3-NO$_2$, 2-Cl, 2-OH, 4-Me, 2-Me, 2-NO$_2$, 4-OH

Yield (%): 87- 91
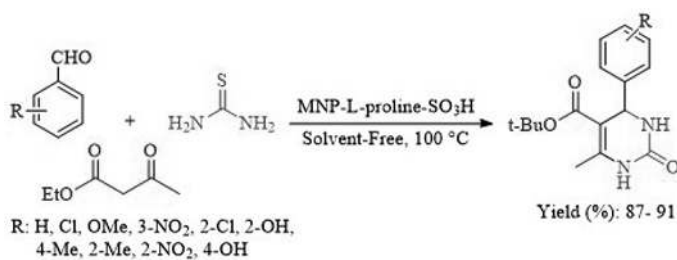
SCHEME 5.47. Preparation of 3,4-dihydropyrimidine-2-(1*H*)-thiones catalyzed by MNP-L-proline-SO$_3$H.
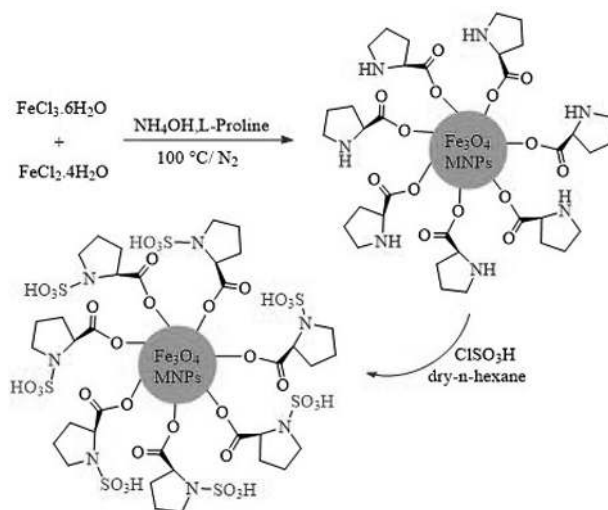

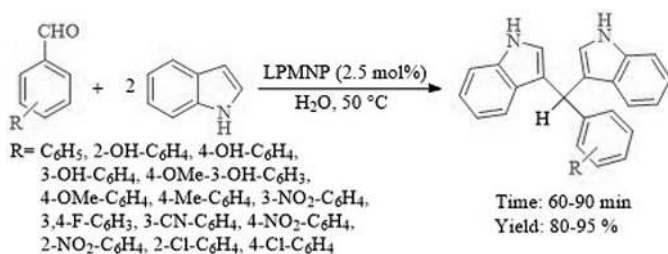**SCHEME 5.48.** Preparation of MNP-L-proline-SO$_3$H.

followed by modification with tri-methoxy (vinyl) silane to afford vinyl MNP substrate (VMNP). Next, MNP-oxirane (MNPO) is produced by oxidizing the VMNP substrate with H_2O_2. Finally, MNPO decorated with L-proline is used for the synthesis of L-proline-modified magnetic nanoparticles (LPMNP) (Scheme 5.49) [44]. The catalyst created is utilized to create heterocyclic compounds, such as indole-3-yl derivatives of methane (Scheme 5.50) [44].

Cyclohexenone and its derivatives serve as the structural basis in several natural compounds, like faurinone, β-cadinene, and dihydrojunenol, which have numerous uses in medications, pesticides, and photographic film materials [45]. The Si-LP (silica gel-supported) catalyst was used by the Gu group in 2014 to create cyclohexanone compounds with a variety of aldehydes under ideal circumstances (chromatographic column and ethanol for rinse) (Scheme 5.51) [46].
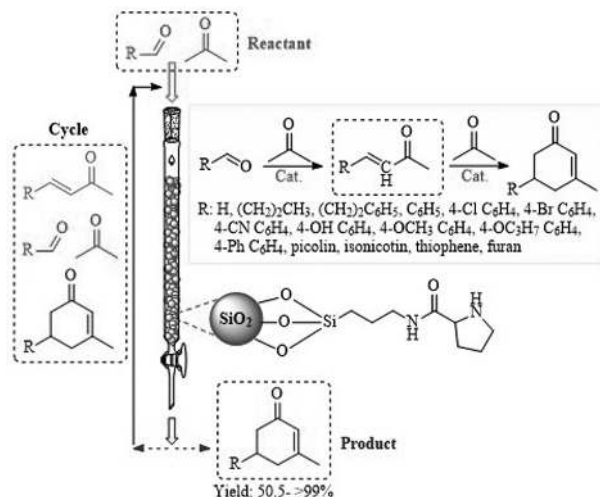
The use of a silica organocatalyst containing L-proline for the high-efficiency synthesis of spiro indole compounds was described by Khalafi-Nezhad et al. in 2013 (Scheme 5.52) [47]. By using spectroscopic techniques such as FT-IR, BET, TGA, and Raman spectroscopy, the proposed catalyst in this study was identified.
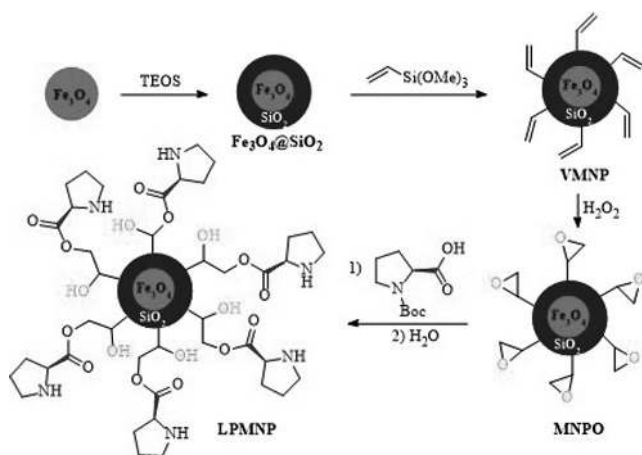

SCHEME 5.49. Synthesis of L-proline-modified magnetic nanoparticles (LPMNP) catalyst with magnetic nanoparticles Fe_3O_4.

R= C_6H_5, 2-OH-C_6H_4, 4-OH-C_6H_4,
3-OH-C_6H_4, 4-OMe-3-OH-C_6H_3,
4-OMe-C_6H_4, 4-Me-C_6H_4, 3-NO_2-C_6H_4,
3,4-F-C_6H_3, 3-CN-C_6H_4, 4-NO_2-C_6H_4,
2-NO_2-C_6H_4, 2-Cl-C_6H_4, 4-Cl-C_6H_4

Time: 60-90 min
Yield: 80-95 %

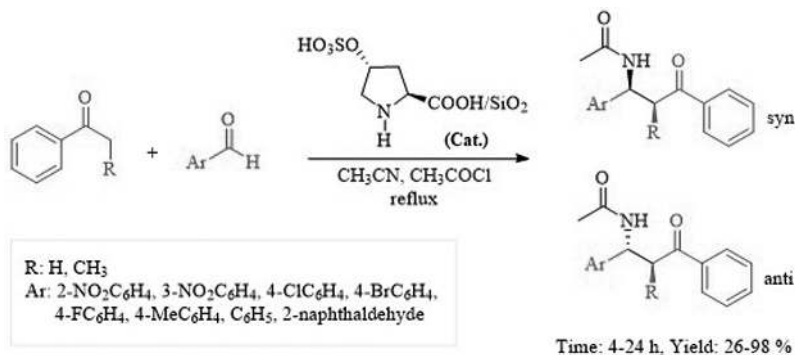**SCHEME 5.50.** Synthesis of bis(indol-3-yl) methanes catalyzed by LPMNP.

SCHEME 5.51. The aldol condensation reaction was catalyzed by Si-LP in a silica-packed chromatographic column.
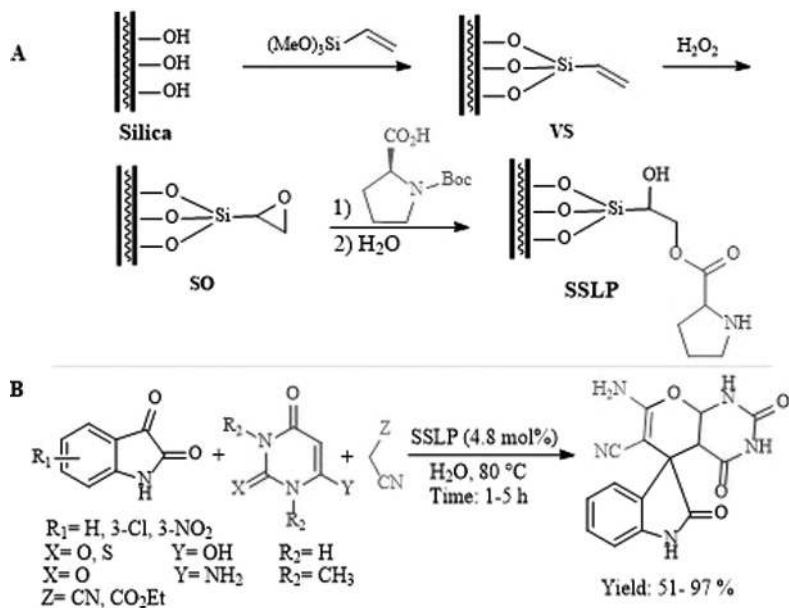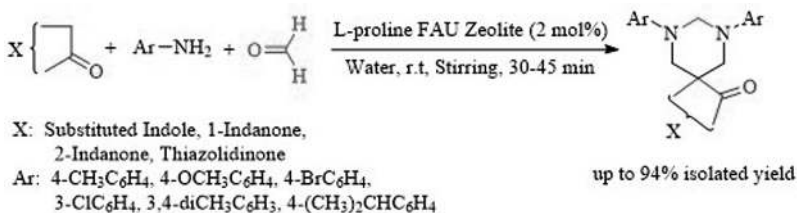

SCHEME 5.52. (a) Preparation route of SSLP catalyst. (b) Synthesis of spiro indole compounds catalyzed by SSLP.

A one-pot multicomponent reaction between aldehydes and enolizable ketones is one of the processes for making β-acetamido ketones. Therefore, it is crucial to create straightforward and gentle circumstances for making these chemicals. In 2014, in a research project, the application of L-pyrrolidine-2-carboxylic acid-4-hydrogen sulfate (supported on silica gel) as a catalyst in the presence of acetonitrile and acetyl chloride for the preparation of β-acetamido ketones has been reported (Scheme 5.53) [48]. *syn-* and *anti-*Isomers were produced as a result of this reaction.

The confinement of L-proline in faujasite zeolite (faujasite is a mineral group in the zeolite family of silicate minerals) has led to the development of a unique L-proline-contained FAU zeolite catalyst system. The trio of faujasites—Na, Mg, and Ca—make up the group. They all share the same basic formula $3.5[Al_7Si1_7O_{48}]\cdot32$ by varying the amounts of sodium, magnesium, and calcium; in this study, the L-proline-confined zeolite catalyst was synthesized by adding proline to an aluminosilicate gel containing $NaOH$, $NaAlO_2$, SiO_2, and H_2O, followed by crystallization at 100°C for 24 h. The resulting powder was centrifuged out of the solution, and any physically absorbed species on the surface of the zeolite were fully rinsed off with deionized water. The L-proline-confined FAU zeolite catalyst was used to design spiro heterocyclic compounds [49]. The reaction was performed between indole with aromatic amine and formaldehyde, which produced a high percentage of spiro derivatives (Scheme 5.54).


R: H, CH₃
Ar: 2-NO₂C₆H₄, 3-NO₂C₆H₄, 4-ClC₆H₄, 4-BrC₆H₄, 4-FC₆H₄, 4-MeC₆H₄, C₆H₅, 2-naphthaldehyde

Time: 4-24 h, Yield: 26-98 %

SCHEME 5.53.   Synthesis of β-acetamido ketones catalyzed by L-pyrrolidine-2-carboxylic acid-4-hydrogen sulfate.

X: Substituted Indole, 1-Indanone, 2-Indanone, Thiazolidinone
Ar: 4-CH₃C₆H₄, 4-OCH₃C₆H₄, 4-BrC₆H₄, 3-ClC₆H₄, 3,4-diCH₃C₆H₃, 4-(CH₃)₂CHC₆H₄

up to 94% isolated yield

SCHEME 5.54.   Procurement of spiro heterocycles via the Mannich reaction.

5.5.   CATALYTIC APPLICATION OF METAL COMPLEXES OF L-PROLINE IN THE MULTICOMPONENT REACTION

By easily coordinating zinc with L-proline (Scheme 5.72a), Tahmassebi et al. in 2019 created a zinc complex of L-proline (Zn(L-proline)$_2$), and it was utilized for the production of 2 amino-3 cyano-4H pyrans and pyran-annulated heterocyclic compounds (Scheme 5.55b and c) [50]. An ideal yield of the intended product was provided by an aromatic aldehyde that contained both electron-donating and electron-withdrawing groups. The use of the most prominent and modern homogeneous asymmetric organocatalysis cases for the synthesis of molecules of relevance to medicinal chemistry has been reported. The utilization of various organocatalysts that operate through noncovalent and covalent interactions is evaluated critically, and it is also discussed if some of these reactions may be carried out on a large or industrial scale.
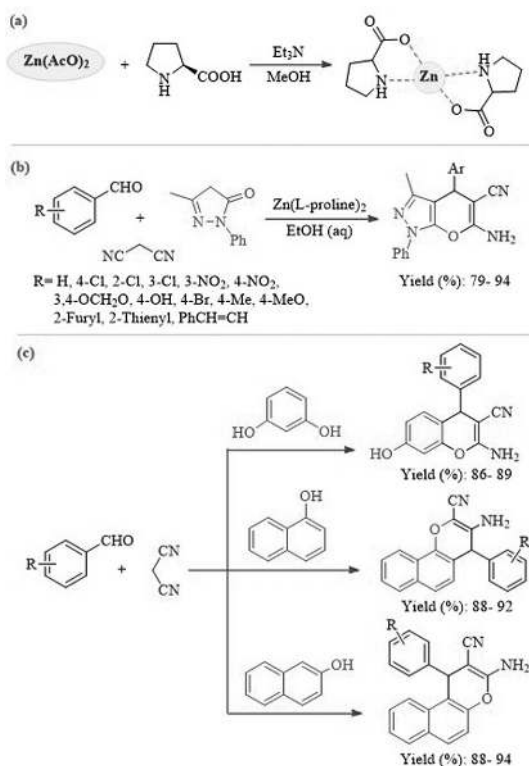
SCHEME 5.55.   (a) Synthesis of Zn(L-proline)$_2$ from zinc (II) acetate and L-proline. (b) Three-component reaction of benzaldehyde, malononitrile, and 6-methyl-1-phenyl-2-pyrazoline-5-one catalyzed by Zn(L-proline)$_2$. (c) Three-component reaction of aromatic aldehydes, malononitrile, and resorcinol, or 1-naphthol or 2-naphthol in the presence of Zn(L-proline)$_2$ catalyst.
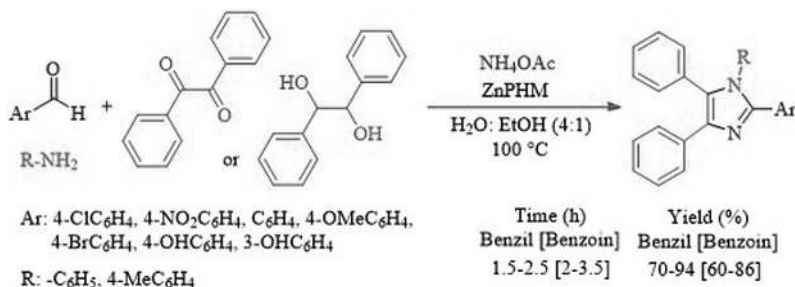
The same group reported using zinc-L-proline hybrid material (ZnPHM) in a mixture of water and ethanol (4:1) to produce triaryl-imidazoles and tetra-aryl imidazoles from the reaction of benzyl or benzoin, different aldehydes, aromatic amines, and ammonium acetate, respectively (Schemes 5.56 and 5.57) [51]. A low yield of the intended products was produced when zinc-L-proline hybrid material was absent; they also demonstrated the synthesis of 1,2,4,5-tetraarylimidazoles derivatives using various aromatic amines and aldehydes. The amines that included the electron-donating groups needed a shorter reaction time to achieve a respectable yield of the corresponding product. It was found that aldehydes containing electron-withdrawing groups provided the reaction at a fast rate with better yields of the desired product. Aldehydes with electron-withdrawing groups were found to have a high reaction rate and higher yields of the desired product.

Kaboudin et al. described the synthesis of 3-substituted 1,2,4-oxadiazoles from amidoximes and triethyl orthoformate using iron (III) chloride/L-proline as a catalyst (Scheme 5.58) [52].

After 24 h, just a very small amount of the desired product was seen without a catalyst. In this study, the scientists examined the impact of several salts on the outcome of the reaction; when $ZnCl_2$ was used as the catalyst, no product was found; however, when $HgCl_2$ or $FeCl_3$ was used, only a low yield of the desired product

R: 4-ClC₆H₄, C₆H₄, 4-NO₂C₆H₄, 4-OMeC₆H₄, 3-BrC₆H₄, 4-BrC₆H₄, 2-furfuryl, 1-napththy, 3,4 piperonyl, 2-thienyl, 3-thieny, 3-Br-C₆H₄ 2-OH C₆H₄, 3-OHC₆H₄, 4-OHC₆H₄

	Time (h)	Yield (%)
	Benzil [Benzoin]	Benzil [Benzoin]
	1-3 [1.5-3.5]	71-94 [62-87]
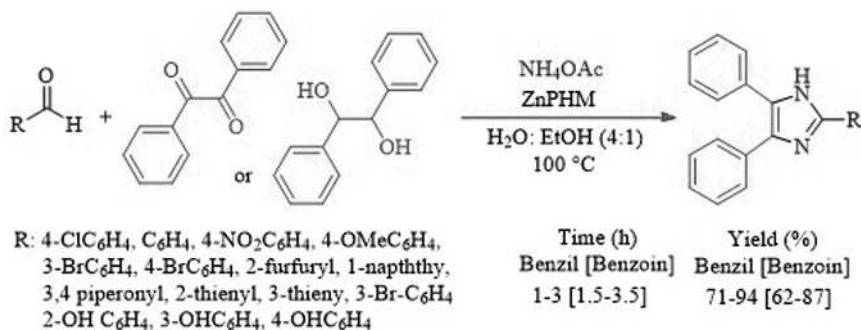
SCHEME 5.56. ZnPHM-catalyzed synthesis of 2,4,5-triaryl imidazoles.

Ar: 4-ClC₆H₄, 4-NO₂C₆H₄, C₆H₄, 4-OMeC₆H₄, 4-BrC₆H₄, 4-OHC₆H₄, 3-OHC₆H₄

R: -C₆H₅, 4-MeC₆H₄

|	Time (h)	Yield (%)
	Benzil [Benzoin]	Benzil [Benzoin]
	1.5-2.5 [2-3.5]	70-94 [60-86]

**SCHEME 5.57.** ZnPHM-catalyzed synthesis of 1,2,4,5-tetraarylimidazoles.

(35% and 51%, respectively) was obtained. The intended product was produced by this method with a 70% yield using FeCl$_3$/phenanthroline and FeCl$_3$/L-proline. The nontoxic nature of L-proline and its ease of availability led to its selection. Due to their significant characteristics, including their anticancer, antimalarial, anti-inflammatory, and pesticide activities, benzo[g]chromosomes have received a lot of interest. In another study, Maleki et al. used Zn(L-proline)$_2$ as a catalyst in 2015 to create compounds containing chromium 2-amino-4H-benzo (Scheme 5.59) [53].

The authors demonstrated how Zn(L-proline)$_2$ could be recycled in three consequent runs and used to carry out reactions up to these three runs without losing its catalytic efficiency. Additionally, a mechanism for this reaction is presented in Scheme 5.60.

L-proline's chiral nature, which enables its use in the creation of chiral compounds, is one of its standout characteristics. By creating a chiral catalytic system with L-proline, Jia et al. were able to synthesize the chiral polymer HSSP of DoDHPA from the achiral monomer DoDHPA (phenylacetylene, possessing two hydroxyl groups and a dodecyl group) in 2015 (Scheme 5.61) [54]. In this procedure, [Rh(nbd)Cl]$_2$ was made using RhCl$_3$ and the nbd compound, and then a proline and NaOH solution in 5 ml of water was added to a yellow suspension of [Rh(nbd)Cl]$_2$ in 2 ml methanol. After that, the lucid yellow solution was stirred at room temperature for an hour. The solvent was removed in a vacuum to yield Rh(nbd)(L-proline), and
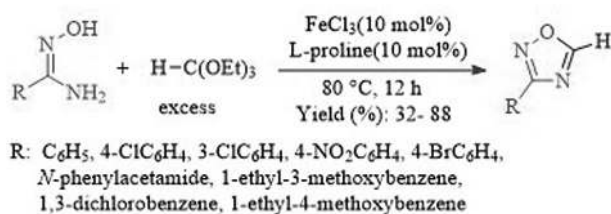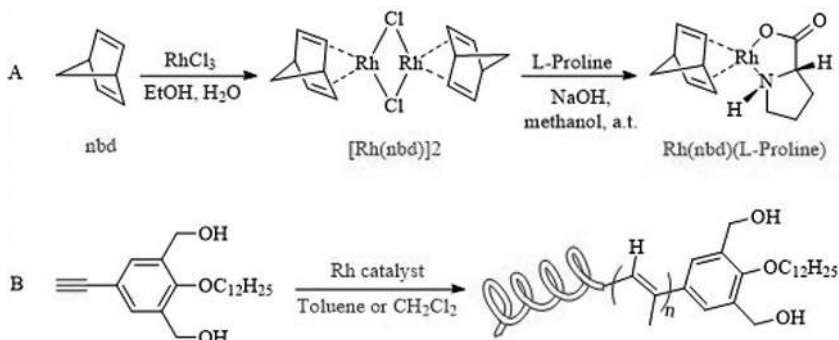

SCHEME 5.58. Reactions of amidoximes with triethyl orthoformate in the presence of FeCl$_3$/L-proline.
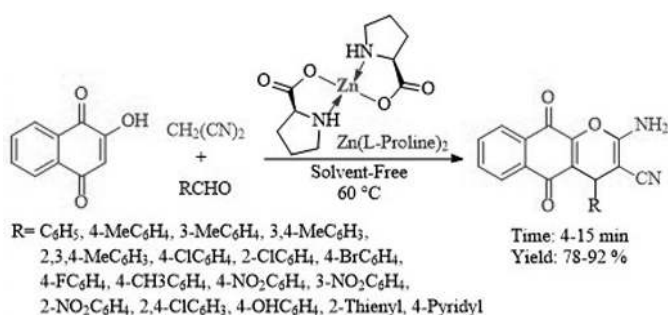
SCHEME 5.59. Chromic 2-amino-4H-benzo synthesis catalyzed by Zn(L-proline)$_2$.
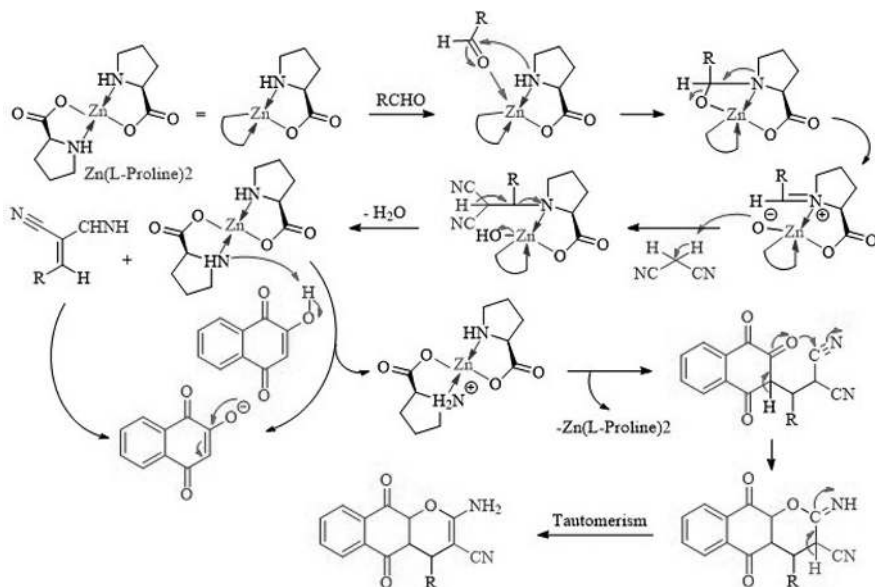
SCHEME 5.60. The proposed mechanism for chromium 2-amino-4*H*-benzo synthesis catalyzed by zinc (L-proline)$_2$.

SCHEME 5.61. (a) Create Rh(nbd)(L-proline). (b) Create chiral polymers catalyzed by Rh(nbd) (L-proline).

the product was then dissolved in dichloromethane. The precipitate was separated by centrifugation once it had formed.
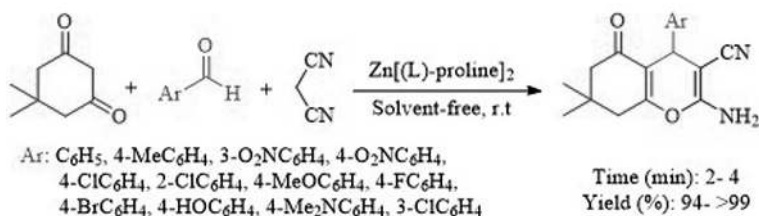
The performance of Rh(nbd)(L-proline) was utilized for the production of tetrahydrobenzo[*b*]pyrans by a combination of various aldehydes with malononitrile and dimedone in room temperature under solvent-free conditions (Scheme 5.62) [54].

One of the most significant drugs that lower vitamin K stores is dicoumarol. This important substance can be produced by reacting 4-hydroxycoumarin with different

aldehydes. In 2011, Siddiqui and Farooq employed Zn(L-proline)$_2$ as a catalyst to efficiently and quickly synthesize dicoumarol derivatives (Scheme 5.63) [55].

Pyrano[2,3-*d*]pyrimidine derivatives are a class of multicomponent reactions with therapeutic and antifungal effects. Some of these compounds also show analgesic, antihypertensive, antiviral, and antimalarial activity. Using Zn[(L)proline]$_2$ as a natural catalyst, Heravi et al. produced these compounds in ethanol as a solvent with good efficiency and appropriate reaction durations (Scheme 5.64) [56].

The reaction was tested with other aldehydes, and it was discovered that aliphatic aldehydes prevented the reaction from occurring. Additionally, no reaction occurred in the presence of 3,4-dimethoxybenzaldehyde and 4-*N*,*N*-dimethylaminobenzaldehyde

Ar: C$_6$H$_5$, 4-MeC$_6$H$_4$, 3-O$_2$NC$_6$H$_4$, 4-O$_2$NC$_6$H$_4$,
4-ClC$_6$H$_4$, 2-ClC$_6$H$_4$, 4-MeOC$_6$H$_4$, 4-FC$_6$H$_4$,
4-BrC$_6$H$_4$, 4-HOC$_6$H$_4$, 4-Me$_2$NC$_6$H$_4$, 3-ClC$_6$H$_4$

Time (min): 2- 4
Yield (%): 94- >99

SCHEME 5.62.   Tetrahydrobenzo[*b*]pyran synthesis mediated by Zn[(L)-proline]$_2$.

R: H, 4-OH, 2-OH,
4-Cl, 2-Cl, 3-NO$_2$,
3-OCH$_3$-2-OH

Catalyst: Zn(Proline)$_2$

Time (min): 5-8
Yield (%): 91-96
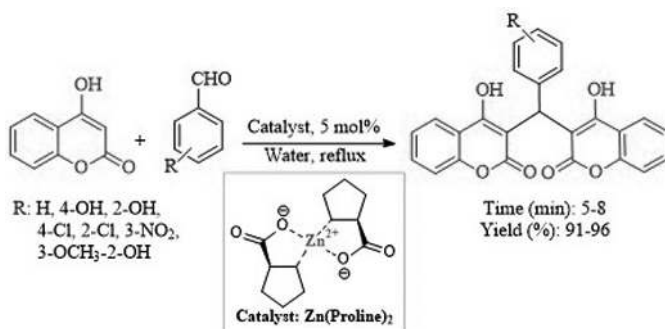
SCHEME 5.63.   Dicoumarol derivative synthesis mediated by Zn(L-proline)$_2$.

X= H, 4-Me, 2-Me, 4-MeO, 4-Cl,
2-MeO, 3-NO$_2$, 4-NO$_2$, 4-CF$_3$

Time (min): 30- 85
Yield (%): 82- 92
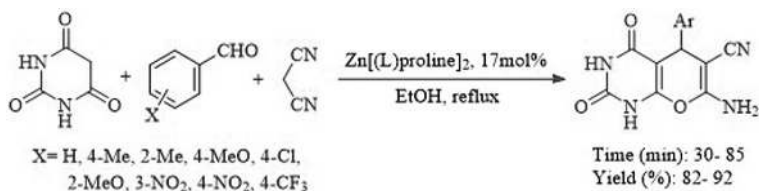
SCHEME 5.64.   Synthesis of pyrano[2,3-*d*] pyrimidine derivatives accelerated by Zn(L-proline)$_2$.

because of the potent electron donor groups' ability to inactivate the carbonyl group. This group provided the following mechanism for the synthesis of pyrano[2,3-*d*] pyrimidine derivatives (Scheme 5.65).

Quinoxalines and their derivatives are used in pharmacy and dyes and have a variety of biological actions, including antidepressants, antimycobacterial, and anticancer characteristics. Aryl 1,2-diamine reacts with 1,2-dicarbonyl molecules to create these chemicals, as well. In the presence of Zn[(L)proline] as a catalyst at room temperature with acetic acid as the solvent, Heravi et al. successfully synthesized quinoxalines in extremely brief reaction durations with good efficiency (Scheme 5.66) [57].

A class of chemical compounds known as 1,4-dihydropyridine compounds are widely used in pharmacy because of their heterocyclic rings' antidiabetic, antitumor, and vasodilator effects. Sivamurugan et al. successfully produced 1,4-dihydropyridine derivatives without the need for any solvents while employing different
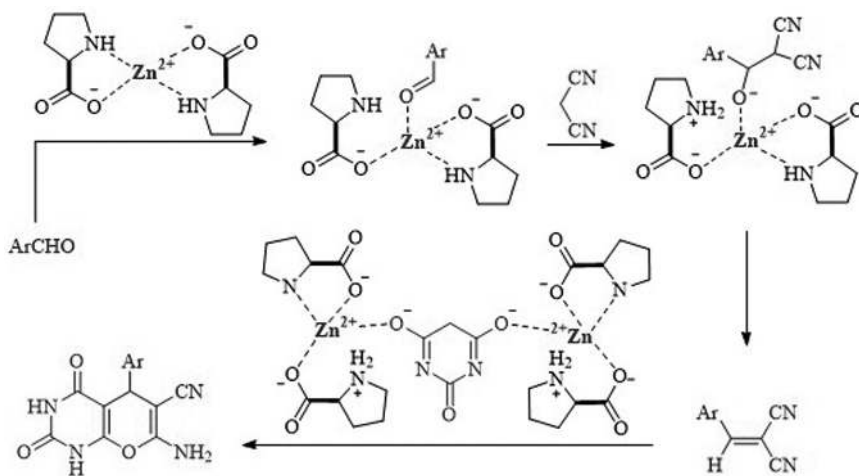
SCHEME 5.65. Mechanism of Zn(L-proline)$_2$-catalyzed pyrano[2,3-*d*]pyrimidine derivatives.
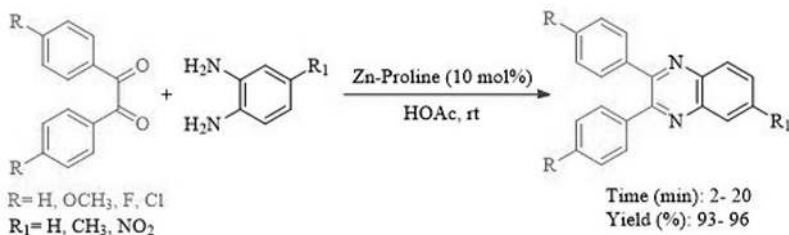

SCHEME 5.66. Quinocaline derivative synthesis by Zn(L-proline)$_2$.

aldehydes and a Zn[(L)proline]₂ complexes as a Lewis acid catalyst in thermal and microwave conditions (Scheme 5.67) [58].

Tomer and Soni used the high reactivity of the Fe₃O₄@L-proline/Pd nanocomposite for the one-pot production of the anticoagulant medication (±)-warfarin (Scheme 5.68) [59].

Palladium was decorated on Fe₃O₄@L-proline NPs produced by the hydrothermal technique to create Fe₃O₄@L-proline/Pd. Magnetic nanoparticles' size and shape have been studied by TEM examination, which revealed that they form as spherical particles of 10–15 nm in size. In addition to their predicted BET surface area and pore volume, the nitrogen adsorption–desorption isotherms for the produced Fe₃O₄@L-proline NPs and Fe₃O₄@L-proline/Pd NCs are shown in Table 5.1. The outcomes of the BET surface study demonstrated that Pd loading significantly affects the surface area and results in an increase in the surface.
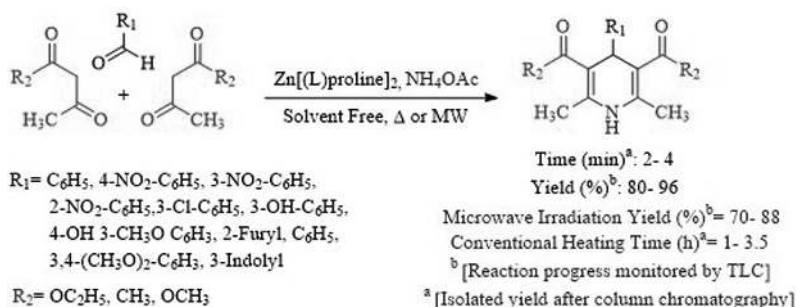
SCHEME 5.67. Synthesis of Hantzsch 1,4-dihydropyridines using Zn [(L) proline]₂ as Lewis acid catalyst.
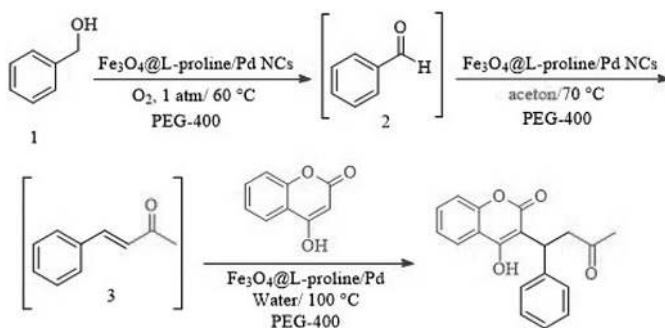
**SCHEME 5.68.** Synthesis of (±)-warfarin via three-way catalysis with Fe₃O₄@L-proline/Pd.

TABLE 5.1.

BET surface characterization of as-fabricated NPs and NCs

Parameters	Fe$_3$O$_4$@L-proline NPs	Fe$_3$O$_4$@L-proline NPs/Pd2 NCs
SBET (m^2/g)	59.39	65.23
Average pore diameter (Å)	114.99	111.67
Adsorption average pore width (4 VA$^{°-1}$ by BET) (A$^°$)	127.94	111.20
Pore volume in pores (cm^3/g)	0.19	0.18
Total volume pores (cm^3/g)	0.17 by DFT	0.16 (by DFT)
Total area in pores (m^2/g)	36.75 (by DFT)	34.68 (by DFT)

5.6. APPLICATION OF L-PROLINE-BASED IONIC LIQUID AS AN ORGANOCATALYST IN THE MULTICOMPONENT REACTION

Bifunctional C$_2$-symmetric ionic liquid–supported (S)-proline organocatalyst [BHEDIMP][CF$_3$CO$_2$], was prepared by Davanagere and Maiti. The synthesis process is shown in Scheme 5.69. After the performance of racemic β-amino ketones, derivatives were produced under neat conditions by the activity of an organocatalyst in one-pot Mannich reactions with substituted acetophenones, arylamines, and aryl aldehydes [60]. This method has several benefits, including a low catalyst loading percentage, solvent-free synthesis, quick reaction times, readily accessible substrates, and no chromatography purification. According to the findings, the organocatalyst was reused six times after being regenerated by the addition of ether, with no discernible loss of catalytic activity. Acetophenones, aryl aldehydes, and arylamines were found to work reasonably well with both electron-withdrawing and electron-donating substituents, producing moderate to good yields of the final products (Scheme 5.70).
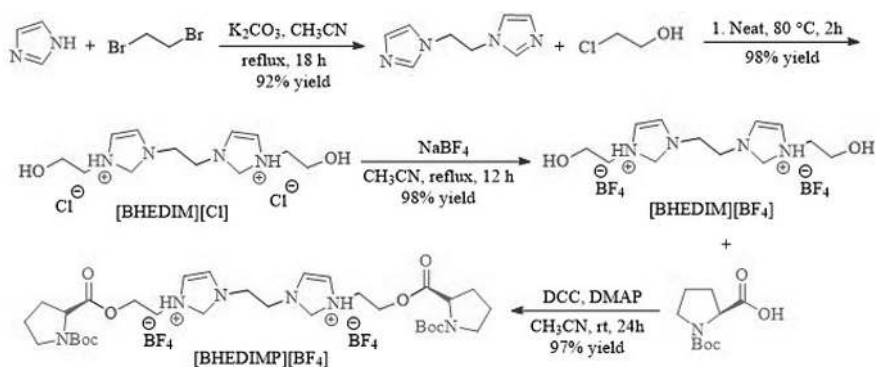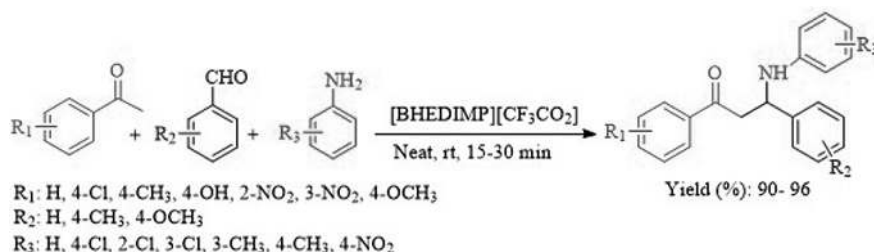

SCHEME 5.69. Synthesis of new bis-alcohol bifunctionalized di-imidazolium ionic [BHEDIM][BF$_4$].

L-proline and nitric acid were combined under a typical ultrasonic bath at room temperature to produce L-proline nitrate ionic liquid (Scheme 5.71) [61].
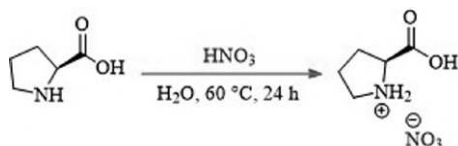
Under ultrasonic irradiation in water, it was demonstrated that L-proline nitrate ionic liquid has effective catalytic activity for the production of 5-benzylidene-1,3-di methylpyrimidine-2,4,6(1H,3H,5H)-trione and pyrano[2,3-d] pyrimidine diones (Schemes 5.72 and 5.73(. The method works with a wide variety of different arenas, including aromatic, fused aromatic, and heteroaromatic derivatives.

Additionally, a gram-scale reaction was carried out, and 86% of the yield resulted in the intended product (Scheme 5.74). Recycling tests revealed that the isolated yield progressively decreased, from 96% for the first run to 75% after five runs.

Chandak and coworkers reported the synthesis of a pseudo-five-component MCR using 10 mol% of L-proline nitrate ionic liquid as a completely green catalyst in


R$_1$: H, 4-Cl, 4-CH$_3$, 4-OH, 2-NO$_2$, 3-NO$_2$, 4-OCH$_3$
R$_2$: H, 4-CH$_3$, 4-OCH$_3$
R$_3$: H, 4-Cl, 2-Cl, 3-Cl, 3-CH$_3$, 4-CH$_3$, 4-NO$_2$

SCHEME 5.70. The range of substrates for β-amino carbonyl compounds.

SCHEME 5.71. Preparation of L-proline nitrate ionic liquid.

R: H, Me, OMe, Ph, Cl, Br, NO$_2$, 2-OH,
4-OH, hiophene, naphthalene

Method A= Conventional method
Method B= Ultra sonication

Method A: Time (min): 10- 15
Yield (%): 78- 94

Method B: Time (min): 1- 12
Yield (%): 80- 96
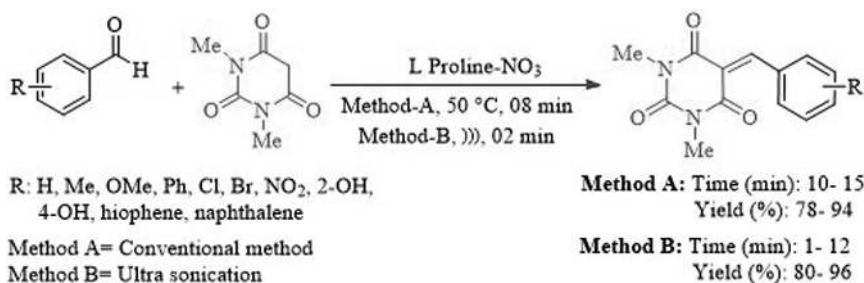
SCHEME 5.72. Synthesis of 5-benzylidene-1,3-dimethylpyrimidine-2,4,6(1H,3H,5H)-trione derivatives catalyzed by L-proline nitrate.
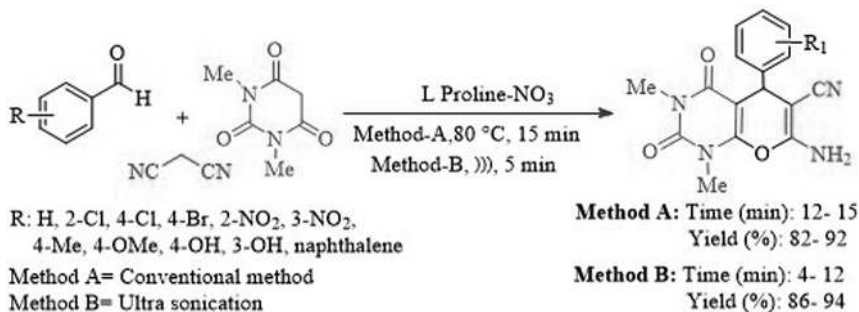
SCHEME 5.73. Synthesis of pyrano[2,3-*d*] pyrimidine dione derivatives with L-proline nitrate.
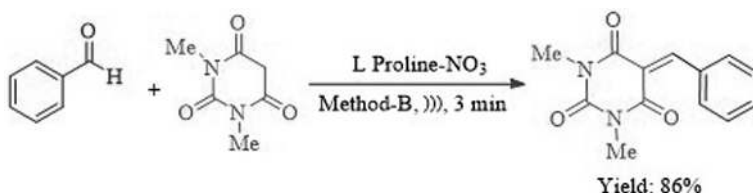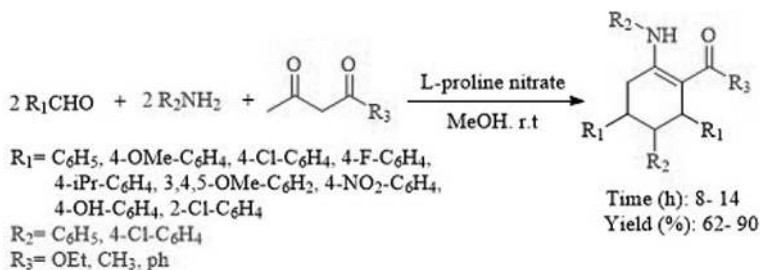

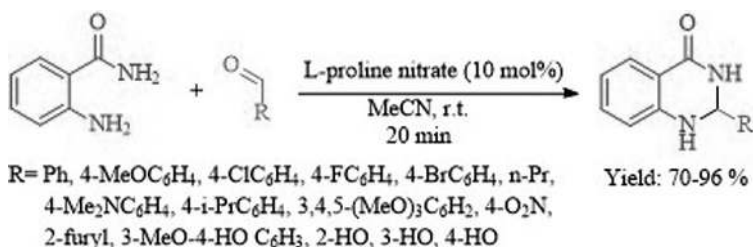**SCHEME 5.74.** A gram-scale reaction.

methanol at room temperature. This reaction went well and produced high to excellent yields of the intended products (Scheme 5.75) [62].

The notable features of quinazoline derivatives include antihistaminic, antihypertensive, antianxiety, tranquilizing, anticancer, antidepressant, vasodilating, and analgesic effects. Derivatives of quinolines are also employed as bactericides, insecticides, and fungicides. In 2015, 2,3-dihydro quinazoline-4 (1*H*)-one derivatives were produced at room temperature in acetonitrile and L-proline nitrate acting as a catalyst (Scheme 5.76) [63].

Imidazoles, pentagonal rings with two nitrogen atoms, are the building blocks of numerous antifungal medications, including the sedative midazolam. Su and

SCHEME 5.75. Synthesis of piperidine derivatives with L-proline nitrate.

R= Ph, 4-MeOC$_6$H$_4$, 4-ClC$_6$H$_4$, 4-FC$_6$H$_4$, 4-BrC$_6$H$_4$, n-Pr,   Yield: 70-96 %
4-Me$_2$NC$_6$H$_4$, 4-i-PrC$_6$H$_4$, 3,4,5-(MeO)$_3$C$_6$H$_2$, 4-O$_2$N,
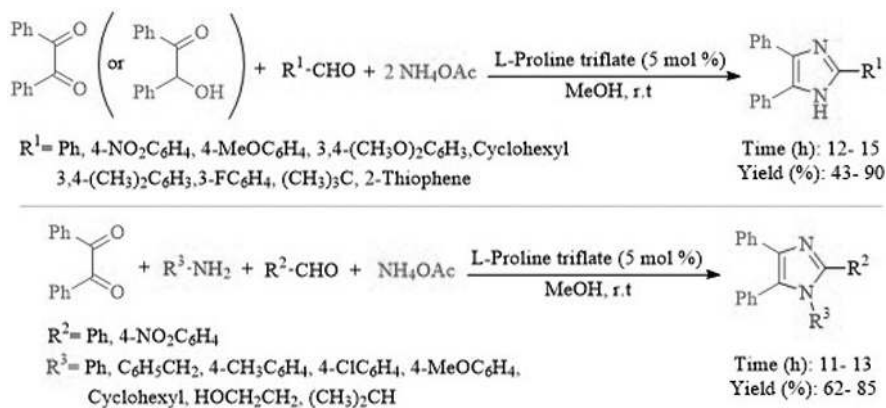2-furyl, 3-MeO-4-HO C$_6$H$_3$, 2-HO, 3-HO, 4-HO

SCHEME 5.76. One-pot production of 2,3-dihydro quinazoline-4 (1*H*)-ones by L-proline nitrate.

coworkers demonstrated a green method for synthesizing tri- and tetra-substituted imidazoles in ethanol as the solvent at room temperature using an L-proline triflate catalyst (Scheme 5.77) [64].

The authors have suggested an alternative mechanism that could follow both Paths I and II to get to the required imidazole molecule (Scheme 5.78).

5.7. APPLICATION OF L-PROLINE AS AN ORGANOCATALYST IN THE ALDOL REACTION

The aldol reaction, classically performed with a base or an acid as a catalyst, is one of the most powerful methods for the formation of carbon–carbon bond formation. According to a recent study, enzymes, amino acids, or tiny peptide organocatalysts all can be used to catalyze the aldol reaction. It is reported that an effective and environmentally friendly method for the manufacture of the stereoselective asymmetric aldol reaction uses (*S*)-proline in conjunction with SIL G3NTf (tri-glyme-trifluoro methane sulfonamide), lithium bis(trifluoromethane sulfonimide) (LiNTf2),

R^1= Ph, 4-NO$_2$C$_6$H$_4$, 4-MeOC$_6$H$_4$, 3,4-(CH$_3$O)$_2$C$_6$H$_3$,Cyclohexyl   Time (h): 12- 15
3,4-(CH$_3$)$_2$C$_6$H$_3$,3-FC$_6$H$_4$, (CH$_3$)$_3$C, 2-Thiophene   Yield (%): 43- 90

R^2= Ph, 4-NO$_2$C$_6$H$_4$
R^3= Ph, C$_6$H$_5$CH$_2$, 4-CH$_3$C$_6$H$_4$, 4-ClC$_6$H$_4$, 4-MeOC$_6$H$_4$,   Time (h): 11- 13
Cyclohexyl, HOCH$_2$CH$_2$, (CH$_3$)$_2$CH   Yield (%): 62- 85

SCHEME 5.77. One-pot synthesis of 2,4,5-trisubstituted and 1,2,4,5-tetrasubstituted imidazoles with L-proline triflate as catalyst.
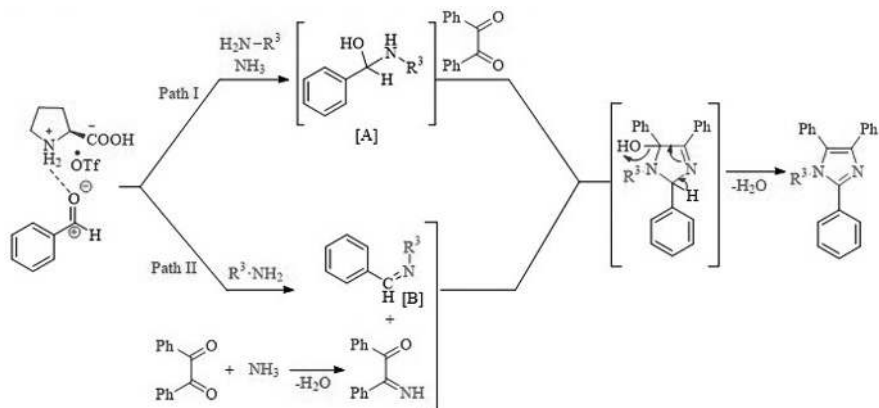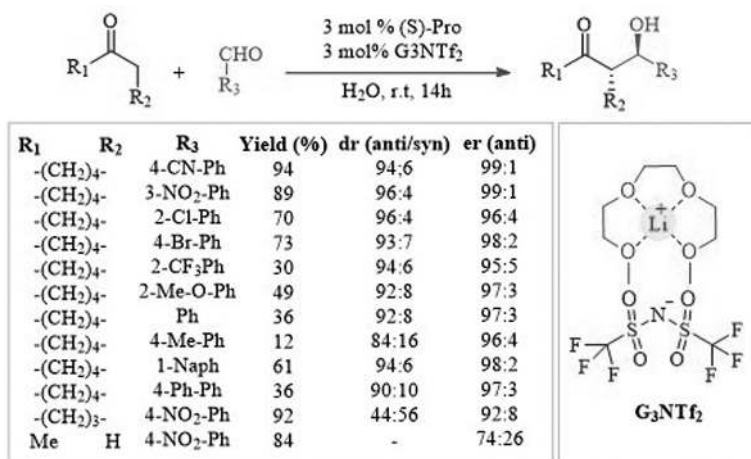
SCHEME 5.78.   The proposed mechanism for synthesizing 1,2,4,5-tetrasubstituted imidazoles catalyzed by L-proline-based ILs.
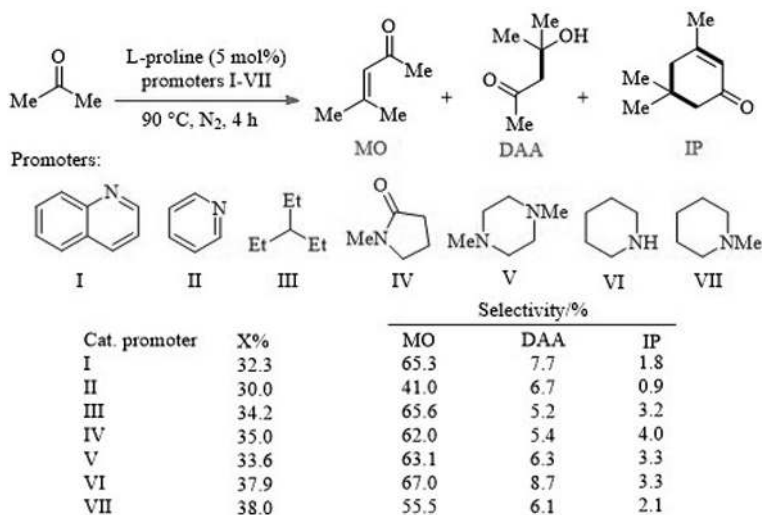
tri-glyme (G3), and water as the additive (Scheme 5.79) [65]. In the absence of ionic liquids (SILs), only subpar yields were obtained.

Mesityl oxide is an industrially useful product derived from acetone and employed in the production of natural and synthetic compounds in organic chemistry, pharmaceuticals, agriculture, and other fields. In 2015, Yu et al. produced isophorone (IP) and diacetone alcohol (DAA) as by-products of the synthesis of mesityl oxide (MO) from acetone utilizing L-proline as a catalyst and I–VII promoters (Scheme 5.80) [66].

In 2012, Cui and colleagues created several asymmetric organocatalyst ionic liquids and used them together with L-proline to catalyze asymmetric aldol reactions

R₁	R₂	R₃	Yield (%)	dr (anti/syn)	er (anti)
-(CH₂)₄-		4-CN-Ph	94	94:6	99:1
-(CH₂)₄-		3-NO₂-Ph	89	96:4	99:1
-(CH₂)₄-		2-Cl-Ph	70	96:4	96:4
-(CH₂)₄-		4-Br-Ph	73	93:7	98:2
-(CH₂)₄-		2-CF₃Ph	30	94:6	95:5
-(CH₂)₄-		2-Me-O-Ph	49	92:8	97:3
-(CH₂)₄-		Ph	36	92:8	97:3
-(CH₂)₄-		4-Me-Ph	12	84:16	96:4
-(CH₂)₄-		1-Naph	61	94:6	98:2
-(CH₂)₄-		4-Ph-Ph	36	90:10	97:3
-(CH₂)₃-		4-NO₂-Ph	92	44:56	92:8
Me	H	4-NO₂-Ph	84	-	74:26

SCHEME 5.79.   Asymmetric aldol condensation catalyzed by S-proline and G₃NTF₂.

SCHEME 5.80.   Making mesityl oxide (MO) from acetone using L-proline as a catalyst.

(Schemes 5.81 and 5.82) [67]. Catalyst **b** was discovered to be more effective for the asymmetric aldol reaction than the other catalysts used in this reaction.

A type of beta-unsaturated ketone called chalcones is widely present in edible plants. Moreover, important heterocycles such as flavones, 1,4-diketones, and pyrazoline benzothiazepines can be formed using these chalcones. In 2012, Bhupathi et al. demonstrated the use of L-proline as a catalyst in the reaction of various aldehydes with 3-acetyl-4-hydroxy-2-quinolone at room temperature to produce chalcone, and products were produced quickly and with good efficiency (Scheme 5.83) [68].

Qian et al. reported the use of 1-ethyl-3-methylimidazolium trifluoroacetate ([EMIm][CF$_3$COO]) ionic liquid as an effective additive for proline-catalyzed asymmetric aldol reactions between cyclic ketones and aromatic aldehydes in 1-butyl-3-methylimidazolium-tetrafluoroborate (BMIM BF$_4$) at room temperature. This reaction went smoothly and produced the intended products with excellent enantiomeric excesses (up to 98%). It was possible to reuse the catalyst, additive, and solvent ([BMIm]BF$_4$) for up to five runs with just a small loss in their activity (Scheme 5.84) [69].

The Merrifield resin was combined with 1-methyl-1*H*-imidazole in toluene at 100°C to create Merrifield resin-supported ionic liquids, according to Zhang and colleagues. For the asymmetric aldol reaction, they used Merrifield resin-supported ionic liquids/L-proline as effective and recyclable catalytic systems, which produced relevant products in good to excellent yields and with high ee values. Additionally, this assisted catalytic system can be recycled by straightforward filtering and reused five times without noticeably losing its effectiveness (Scheme 5.85) [70].

Reddy et al. described the asymmetric aldol reaction of heteroaromatic aldehydes and acetone with L-proline acting as a catalyst in bmim[BF$_4$] (Scheme 5.86) [71].
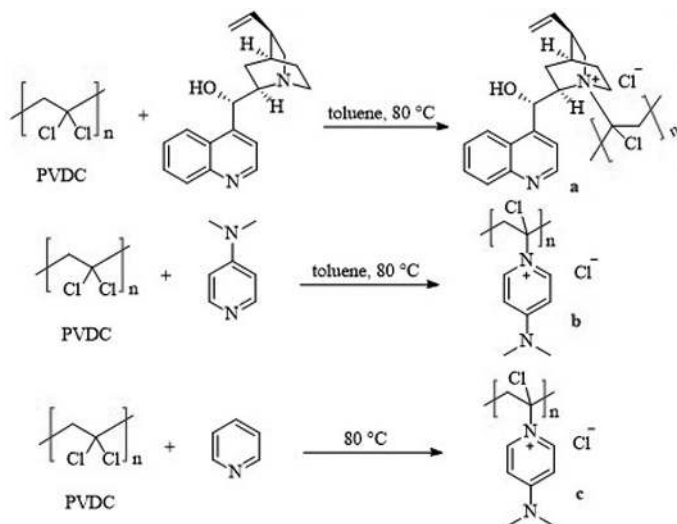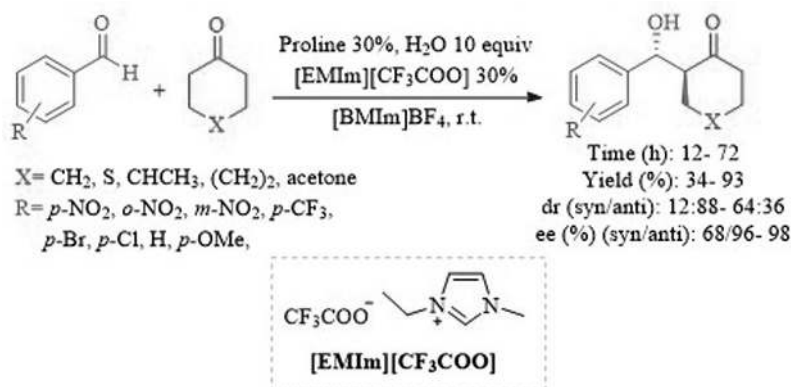
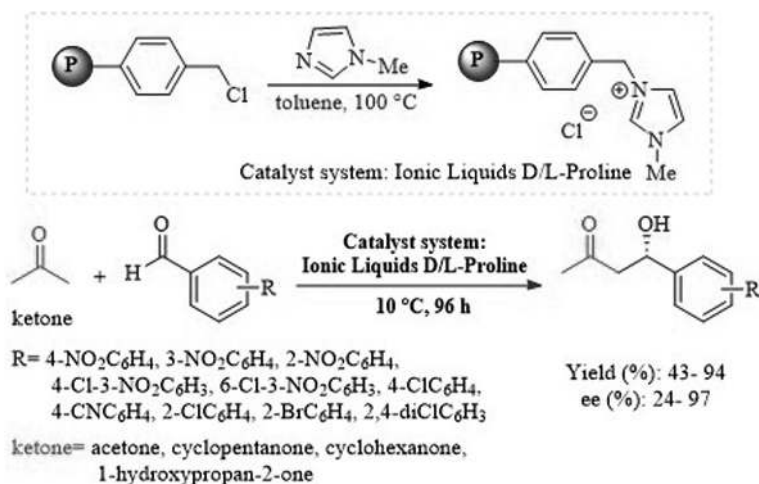**SCHEME 5.81.**   Synthesis of asymmetric ionic liquid organocatalysts.

Aldehyde: 4-NO$_2$, 2,4-Dinitro, 4-CN, 4-F, 4-Cl,
4-Br, 4-CH$_3$O, 2-NO$_2$, 3- NO$_2$
Ketone: Cyclohexanone, Acetone, Butanone-2

Yield (%): trace- 99
dr (anti/syn): 42:58- 6:94
ee (%): 67- 98
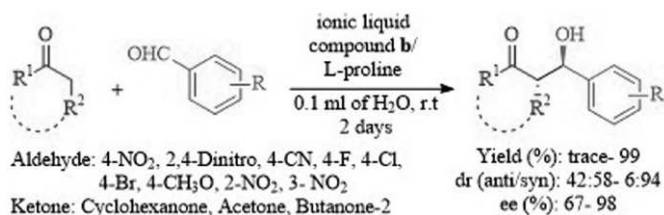
SCHEME 5.82.   Asymmetric aldol reactions catalyzed by ionic liquid **b**/L-proline.

Yield: 80- 92%

Aldehyde:
R$_1$= H,	R$_2$= H
R$_1$= OCH$_3$,	R$_2$= H
R$_1$= Cl,	R$_2$= H
R$_1$= F	R$_2$= H
R$_1$= NO$_2$,	R$_2$= H
R$_1$= OH,	R$_2$= H
R$_1$= H,	R$_2$= OH
R$_1$= N(CH$_3$)$_2$,	R$_2$= H
R$_1$= OCH$_3$,	R$_2$= OH
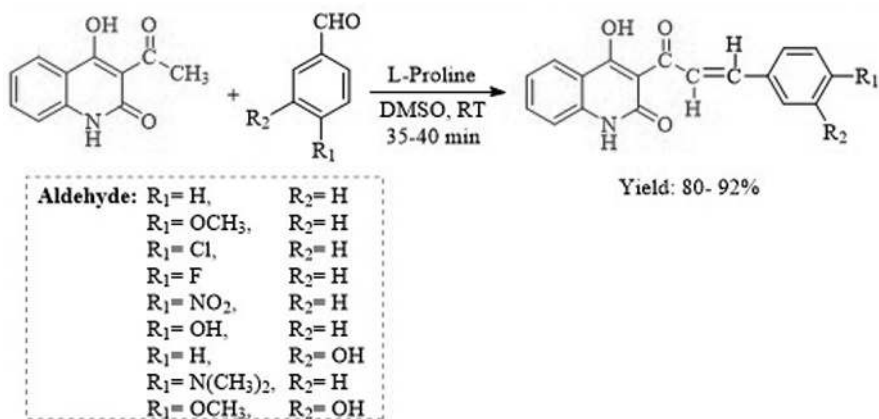
SCHEME 5.83.   Synthesis of chalcone derivatives catalyzed by L-proline.

X= CH₂, S, CHCH₃, (CH₂)₂, acetone
R= p-NO₂, o-NO₂, m-NO₂, p-CF₃,
  p-Br, p-Cl, H, p-OMe,

Time (h): 12- 72
Yield (%): 34- 93
dr (syn/anti): 12:88- 64:36
ee (%) (syn/anti): 68/96- 98

SCHEME 5.84. Direct asymmetric aldol reactions involving aromatic aldehydes and cyclic ketones.

R= 4-NO₂C₆H₄, 3-NO₂C₆H₄, 2-NO₂C₆H₄,
  4-Cl-3-NO₂C₆H₃, 6-Cl-3-NO₂C₆H₃, 4-ClC₆H₄,
  4-CNC₆H₄, 2-ClC₆H₄, 2-BrC₆H₄, 2,4-diClC₆H₃

Yield (%): 43- 94
ee (%): 24- 97

ketone= acetone, cyclopentanone, cyclohexanone,
  1-hydroxypropan-2-one

SCHEME 5.85. Asymmetric aldol reaction catalyzed by ionic liquids D/L-proline.

A= 2-pyridyl, 3-pyridyl, 4-pyridyl

Yieldb (%): 50- 98
ee (%): 56- 70
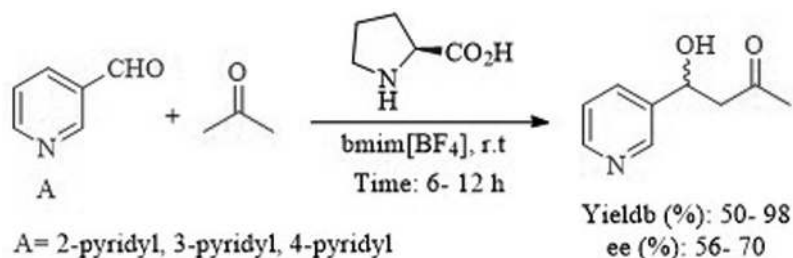
SCHEME 5.86. Proline-catalyzed asymmetric direct aldol reaction of heteroaromatic aldehydes and acetone.

L-proline in an ionic liquid can be recycled with comparable yields and enantioselec-tivities, according to further research on the topic of catalyst recycling.

In a different investigation, Liu et al. used an ionic liquid called (bmim)PF$_6$ and (4S)-phenoxy-(S)-proline as the organocatalyst to perform an asymmetric aldol reac-tion (Scheme 5.87) [72].

Toma and coworkers displayed the performance of L-proline for asymmetric direct aldol in an ionic liquid reaction (1-n-butyl3-methylimidazolium hexafluoro-phosphate [bmim]PF$_6$), and it produces the desired product in good yields of aldol-ization products with reasonable enantioselectivities (Scheme 5.88) [73].

In 2002, L-proline in imidazolium-based ionic liquids as green reaction media was successfully used as an efficient and reusable catalyst for direct asymmetric aldol reactions. This reaction proceeds in good yields with moderate to excellent ee values (Scheme 5.89) [74]. Further study regarding the recycling of the catalyst has demonstrated that L-proline in an ionic liquid can be reused at least four times with comparable yields and ee values.

X= H, 2-NO$_2$, 3-NO$_2$, 4-NO$_2$,   Yield %: 56.2- 93.2
2-Cl, 3-Cl, 4-Cl, 4-Br, 4-CH$_3$ ee (%): 46.5- 85.7

Cat. A: (4S)-phenoxy-(S)-proline
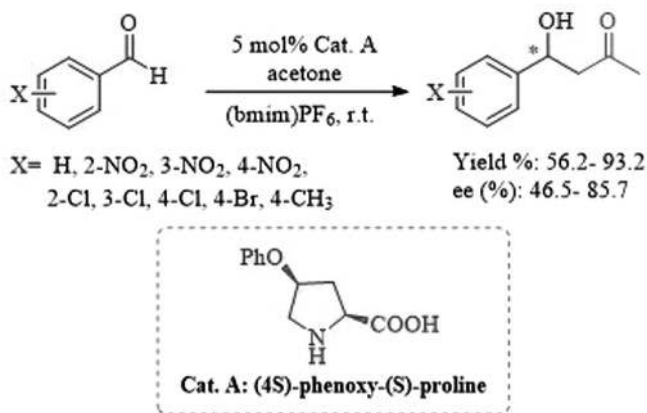
SCHEME 5.87. (4S)-Phenoxy-(S)-proline catalyzed direct asymmetric aldol reaction in ionic liquid (bmim) PF$_6$.

X: H, 2-Br, 4-CF$_3$, 4-CN, 4-OMe,   Yield (%): 55- 94
4-F, 2-OMe, 4-NO$_2$, 2-NO$_2$, 3-NO$_2$ ee (%): 48- 82
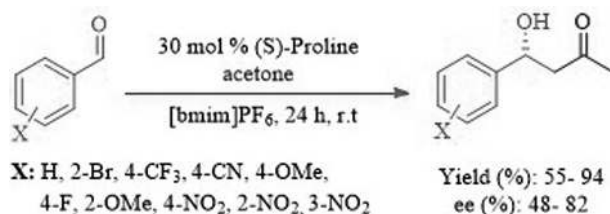
SCHEME 5.88. Asymmetric direct aldol reaction catalyzed by L-proline in [bmim]PF$_6$.

Entry	R—	Isolated Yield (%)	ee (%)
1		58	71
2		60	69
3	Br—	72	67
4		65	89
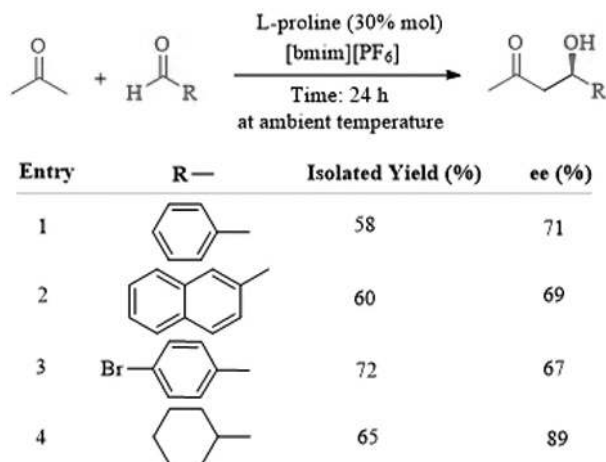
SCHEME 5.89. Asymmetric direct aldol reaction between acetone and various aldehyde catalyzed by L-proline.

5.8. APPLICATION OF L-PROLINE DERIVATIVES AS AN ORGANOCATALYST IN THE ALDOL REACTION

The performances of three bipyridine chiral catalysts (Z_1, Z_2, and Z_3) were studied for asymmetric aldol reaction of cyclohexanone with aldehyde (Scheme 5.90) [75]. Interestingly, modifying the chiral configurations of the bipyridine-proline and the polarity of the solvents utilized has a substantial influence on the performance of catalysis. According to optimization studies, the asymmetric aldol reaction mediated by Z_2 in the DMSO system showed high efficiency (yield 96%), good diastereoselectivity (dr up to 78:22), and moderate enantioselectivity (ee up to 41%). Most of these bigger molecules are structurally nonplanar as a result of the structural distinctions used in catalysis [Z_1 (phenyl-methyl groups), Z_2 (naphthyl groups), and Z_3 (bulkier benzyl groups)], which is easily what causes the steric hindrance effects.

Bhati et al. reported the performance of *cis* urea-tagged proline, in the direct asymmetric aldol reaction in the presence of water [76]. The stages of *cis* urea-tagged proline synthesis are shown in Scheme 5.91. Initially, *trans*-4-hydroxy-L-proline was transformed into the primary amine A, including NH_2 and COOH *cis* groups. The combination of amine B with phenyl isocyanate in CH_2Cl_2 at room temperature offered the catalyst precursor 4 with the appropriate urea substituent at the 4-position of proline. Finally, hydrogenolysis of B under the standard conditions revealed the amino acid and delivered the *cis* urea-tagged proline C.

The asymmetric aldol processes were effectively catalyzed by this chiral molecule (Scheme 5.92) [76]. The intended products were effectively produced with 2 mol% loading in the presence of water in high yields and with outstanding enantio- and diastereoselectivities. The authors also noted that proline with urea tag exhibited good recoverable characteristics.

Catalyst	Solvent	Yield (%)	dr (%, anti/ syn)	ee (%, anti)
Z_1	DMSO	99	78:22	35
Z_2	DMSO	96	78:22	41
Z_3	DMSO	27	59:41	29
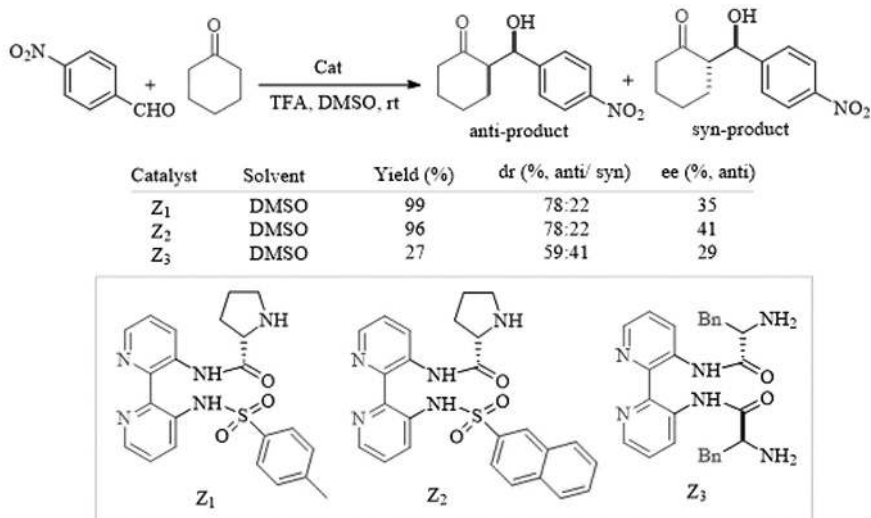
SCHEME 5.90. Aldol reaction of *p*-nitrobenzaldehyde and cyclohexanone in the presence of Z_1, Z_2, and Z_3.

Reagents and condition:
(i) PhNCO, CH$_2$Cl$_2$ (84%),
(ii) H$_2$, Pd/C (10%), MeOH,
    room temperature, 4h (90%)
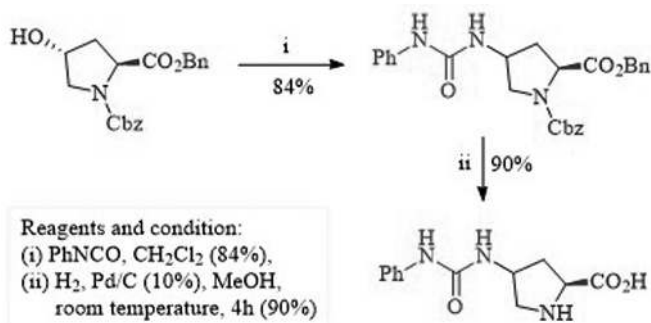
SCHEME 5.91. Synthesis of the *cis* urea-tagged proline catalyst **C**.

Yolacan and coworkers reported the preparation of new proline diamide organocatalysts with Pro-Phe peptide bond by simple amidation reactions of L-proline. More detailed and as outlined in Scheme 5.93, the protection of L-proline is followed by amidation with L-phenylalanine methyl ester, hydrolysis of the ester group, second amidation with different amines, and deprotection of Boc group (Scheme 5.93).

Proline-based tripeptide has been employed as a versatile organocatalyst in the aldol reaction of aliphatic ketones and aromatic aldehydes in water and using *p*-nitrobenzoic as a cocatalyst (Scheme 5.94) [77]. Due to the hydrogen bonding action of two amide NH groups, the scientists theorized that diamide structures were found to be more efficient than monoamide ones. The stereoselectivity is enhanced by the
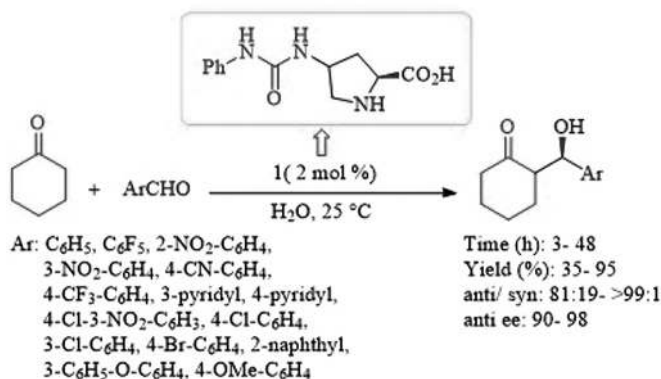
SCHEME 5.92. Asymmetric aldol reactions of cyclohexanone with various aldehydes catalyzed by **1b**.
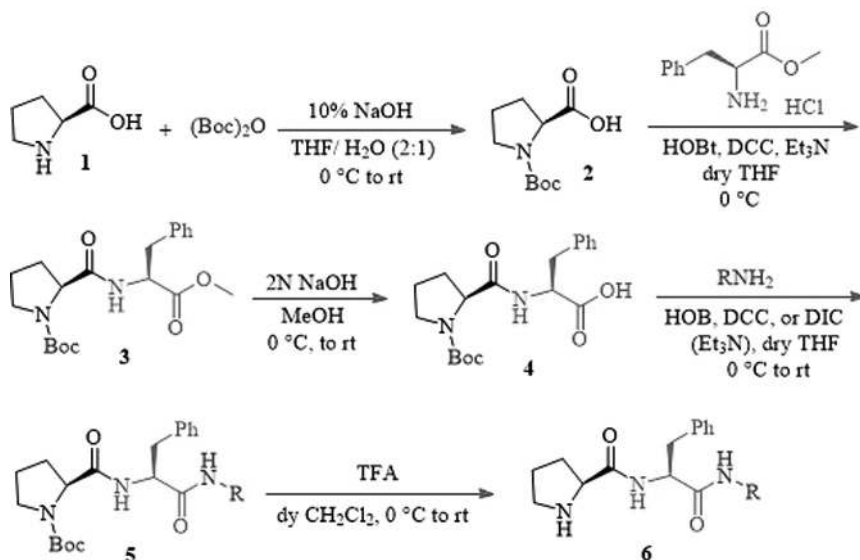
SCHEME 5.93. The synthetic route of proline-based tripeptide.

interaction of bulky groups with amide. With enantioselectivity up to 95% ee and diastereoselectivity(up to 97:3 and the high to excellent yield, this reaction delivers the desired result.

Four different types of catalysts, 1a, 1b, 1c, and 1d, were prepared by Wu and coworkers in 2012 using L-proline. After checking the catalytic performance, it was discovered that catalyst 1c serves as the main catalyst for the aldol reaction (Scheme 5.95). According to the results of the experiment, the proline-based organocatalyst 1c is a reliable and efficient catalyst for highly enantioselective stoichiometric
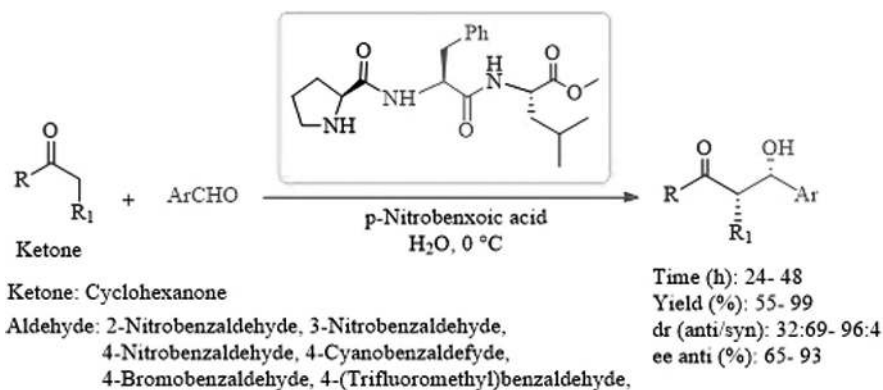
SCHEME 5.94. Screening of organocatalysts for the aldol reaction with benzoic acid cocatalyst.
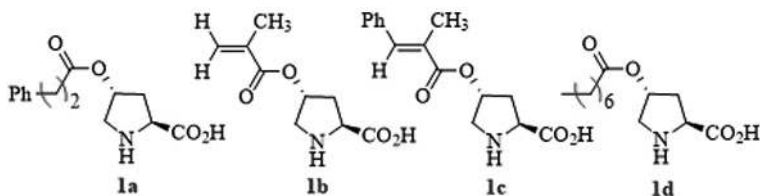
SCHEME 5.95. L-proline-derived organocatalysts.

aldol reactions of a variety of aromatic aldehydes with cyclic ketones in an aqueous medium (Scheme 5.96) [78]. Moreover, proline-based organocatalyst 1c can be easily recovered and reused for seven cycles, and enantioselectivities only slightly decreased. It should be emphasized that the proline-based organocatalyst 1c can be effectively used in large-scale reactions while maintaining the same level of enantioselectivities, demonstrating potential industrial use.

Chen et al. designed and synthesized several L-proline-based dipeptides. Proline was first mixed at 0°C with benzyl chloroformate and NaHCO$_3$, producing product b. Then, 2 mmol of ethyl chloroformate was added dropwise over 3 min at 0°C after it had been dissolved in 2 ml of triethylamine and 4 ml of dry THF. After 3 h of stirring, 2 mmol of an amino acid solution (glycine, D-valine, L-valine, D-phenylalanine, or L-phenylalanine) was dropped into 4 ml of NaHCO$_3$ at 0°C, and the mixture was agitated for 18 h at room temperature. Mixture C (1–5) was extracted with ethyl acetate after being acidified with diluted aqueous hydrochloric acid solution. Next, 10% Pd/C (20 mg) was added to each of the C (1–5) solutions in 2 ml of ethanol and agitated under nitrogen for 3 h before the mixture was filtered and washed with methanol (Scheme 5.97).

These proline-derived dipeptides' catalytic abilities in the asymmetric aldol reaction were investigated (Scheme 5.98) [79]. When acetone and *para*-nitrobenzaldehyde

R= p-NO$_2$-C$_6$H4, o-NO$_2$-C$_6$H$_4$, m-NO$_2$-C$_6$H$_4$,
p-CN-C$_6$H$_4$, p-CF$_3$-C$_6$H$_4$, m-MeO-C$_6$H$_4$,
p-Br-C$_6$H$_4$, p-Cl-C$_6$H$_4$, o-Cl-C$_6$H$_4$, p-F-C$_6$H$_4$,
2-naphthyl, 1-naphthyl, C$_6$H$_5$

Time/ h: 24- 30
Yield (%): 85- 99

Ketone: cyclopentanone,
4-methylcyclohexan-1-one

Yield (%): 98- 99

Time /h: 24- 36
Yield (%): 98- 99
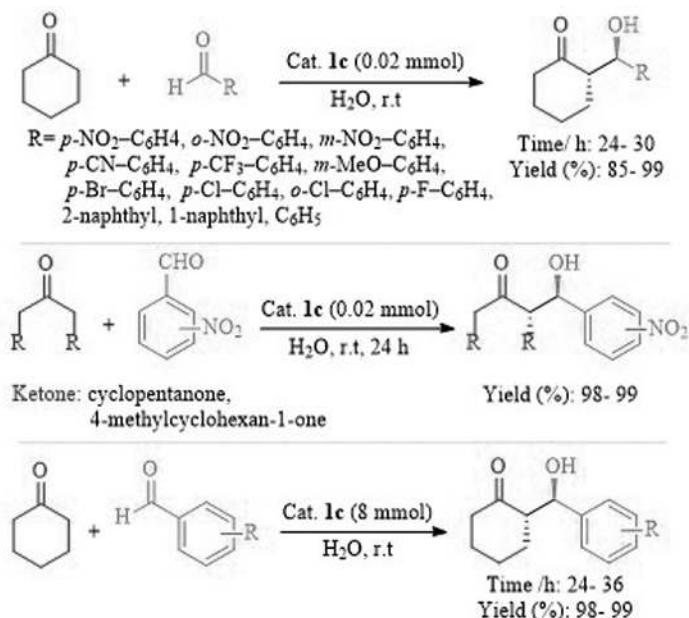
SCHEME 5.96. The reaction of catalyzed aldol with selected catalyst **1c.**

1 - L-Pro-Gly : R^1 = H, R^2 = H
2 - L-Pro-D-Val : R^1 = i-Pr, R^2 = H
3 - L-Pro-L-Val : R^1 = H, R^2 = i-Pr
4 - L-Pro-D-Phe : R^1 = Bn, R^2 = H
5 - L-Pro-L-Phe : R^1 = H, R^2 = Bn
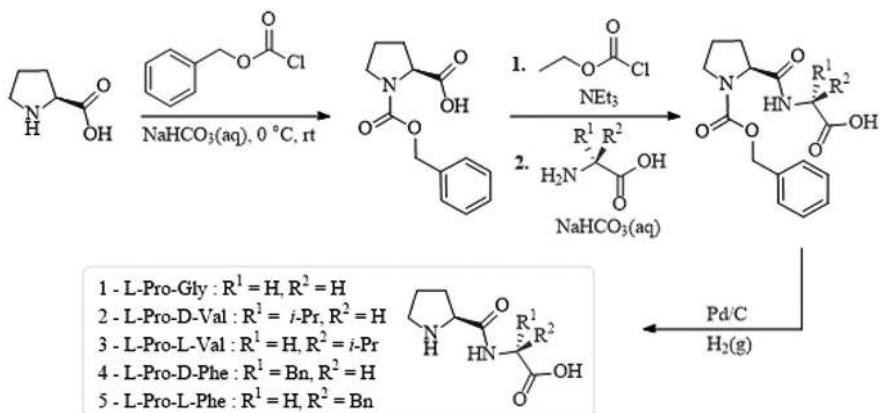
SCHEME 5.97. Synthesis of proline-derived dipeptides.

were combined with DMSO at 0°C, the dipeptide L-Pro-L-Phe produced the best results in terms of reaction yields and desired enantiomeric excess.

Tao and coworkers reported the production of both amphiphilic catalysts, M and N, using isosteviol-proline compounds, and their catalytic abilities were examined in the aldol reaction. In Scheme 5.99, the processes in the synthesis of the catalysts M and N are depicted [80].
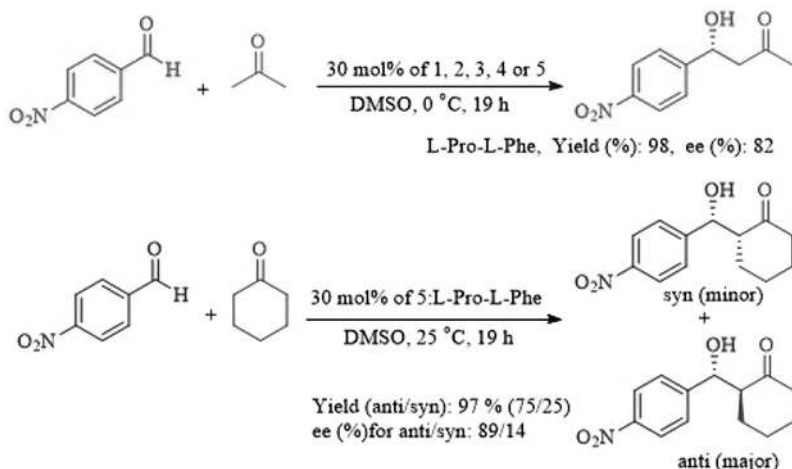
SCHEME 5.98.   Application of proline-derived dipeptides in the aldol reaction.
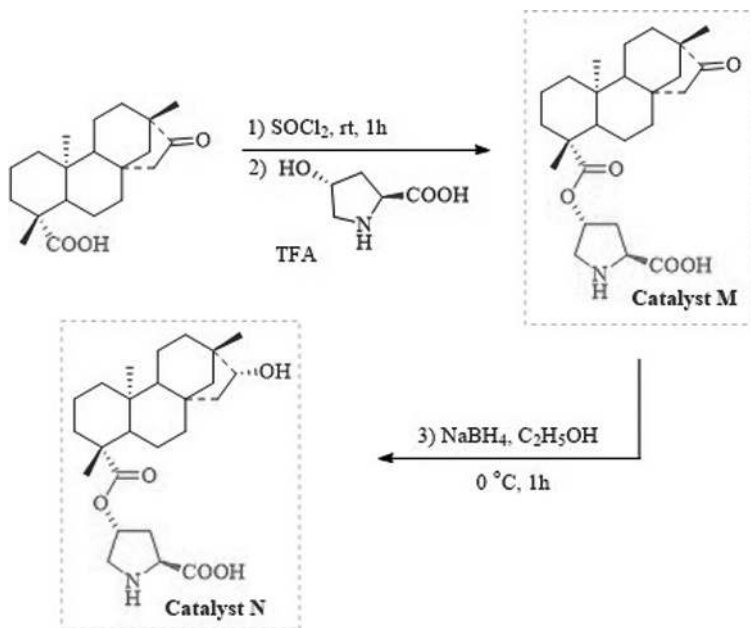
SCHEME 5.99.   Synthesis steps of catalysts M and N.

The authors reported that catalyst M showed the best results in water as the solvent at room temperature along with excellent activity (up to >99% yield) and stereoselectivity for the direct aldol reaction of cyclohexanone and substituted benz-aldehydes, as illustrated in Scheme 5.100. These findings show that the catalysts with

a chiral concave and hydrophobic substituent in the 4-position of L-proline furnished high activity and stereoselectivity for the reaction.

L-proline was employed in the production of the organocatalysts P1 and P2 from silica compounds with both organic and inorganic characteristics (Scheme 5.101). The production of materials with different organic loadings, pore sizes, and surface areas was made possible by selecting the Px/TEOS ratio (ranging from 1:10 to 1:40) and porogen (dodecyl amine, or none). Various materials are designated as Px/y-G, where Px is the molecular precursor, y is the TEOS/Px molar ratio, and G is D in the case of dodecyl amine porogen [81]. The catalytic activity of this produced organocatalyst was assessed using the aldol reaction between 4-nitrobenzaldehyde and acetone (Scheme 5.102). The authors' findings demonstrate that catalyst P_1 performs better than catalyst P_2 in terms of efficiency.

The usage of a-branched aldehydes is one technique for generating α-hydroxy carbonyl compounds. In 2006, Gong et al. used a catalyst made of L-proline to produce products of the hydroxy carbonyl reaction between a-branched aldehydes and 4-nitro benzene with a yield of more than 64% (Scheme 5.103) [82].
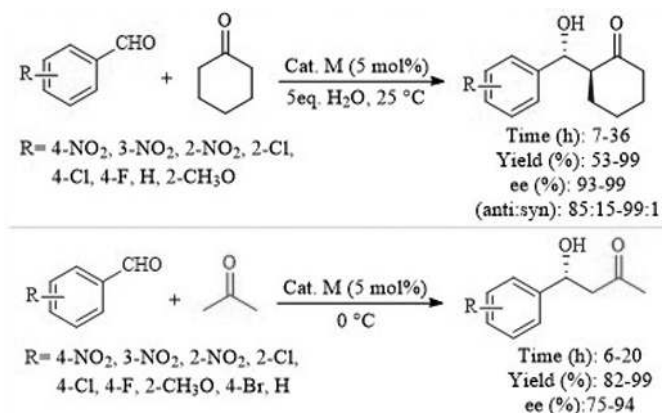
SCHEME 5.100.   Aldol reaction in the presence of catalyst M.
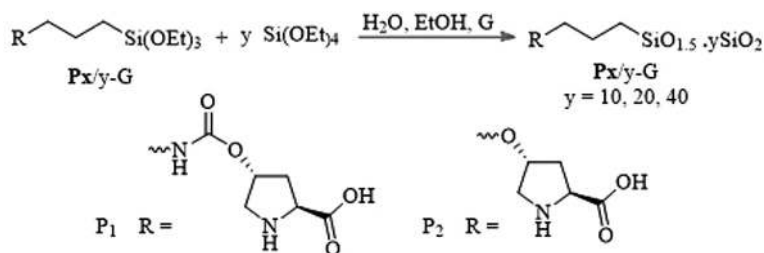
SCHEME 5.101.   Preparation of the hybrid silica via the sol–gel process using P1 or P2.
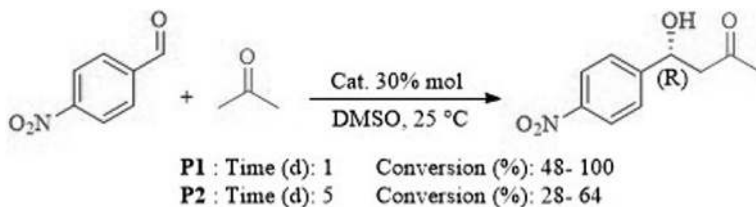
SCHEME 5.102.   The aldol reaction between 4-nitrobenzaldehyde and acetone was cata-
lyzed by P1 and P2.
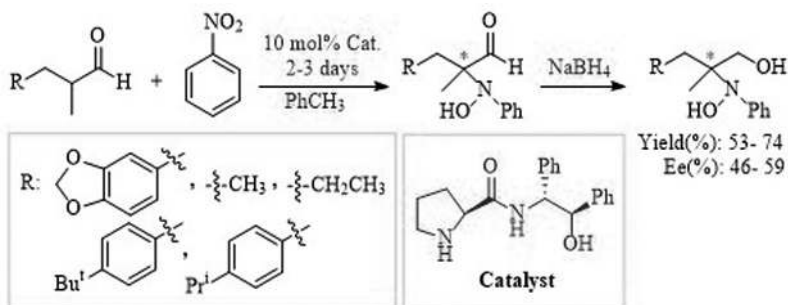
SCHEME 5.103.   *N*-nitro aldol reaction between α-branched aldehydes and 4-nitro benzene
by L-proline amide.

Sun and colleagues showed that L-proline can act as an effective catalyst for the
asymmetric aldol reaction. The aldol reaction of acetone and a variety of aromatic
aldehydes were used to create products with high enantioselectivity (Scheme 5.104)
[83].

5.9.   APPLICATION OF L-PROLINE AND L-PROLINE
DERIVATIVE-SUPPORTED MATERIAL AS AN
ORGANOCATALYST IN THE ALDOL REACTION

Generally, organocatalysts are small, organic molecules made of inexpensive and
nontoxic compounds. These characteristics make them employed in pharmaceutical
synthesis. Frequently, the amino acid L-proline has been used as an organocatalyst
for a wide range of organic transformations (aldol reactions, Robinson annulations,
Michael reactions, oxidations, and Diels–Alder reactions). Mutiah et al. described
the production of zirconium-sulfonated metal–organic framework (MOF)-supported
L-proline and its use for the asymmetric aldol reaction. This catalyst is prepared
by a combination of $ZrCl_4$ with benzene-1,4-dicarboxylic acid (H_2bdc) and sodium
4-carboxy-2-sulfobenzoate ($H_2bdc-SO_3Na$) in the presence of L-proline under the
solvothermal reaction (Scheme 5.105) [84]. The reaction between acetone and two
different aldehydes was studied and the catalyst demonstrated good activity and
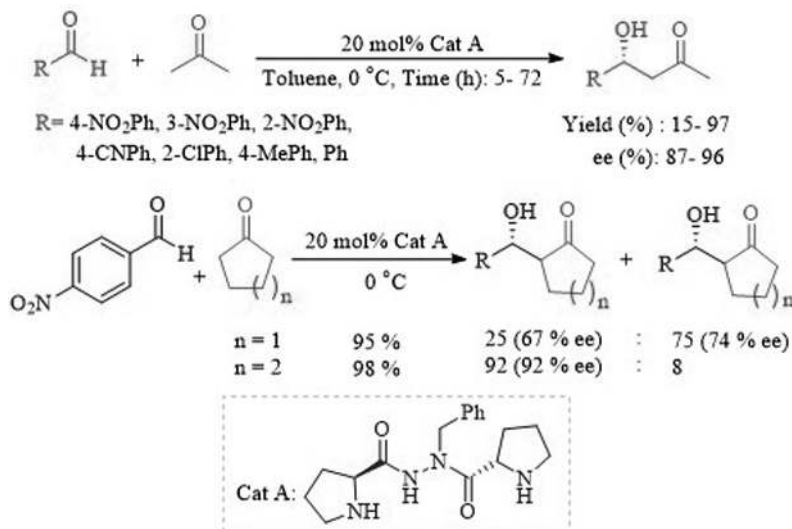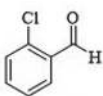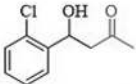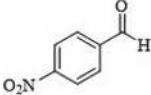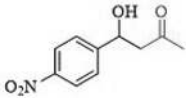
SCHEME 5.104. Protonated N'-benzyl-N'-prolyl proline hydrazide as a highly enantiose-lective catalyst for the direct asymmetric aldol reaction.
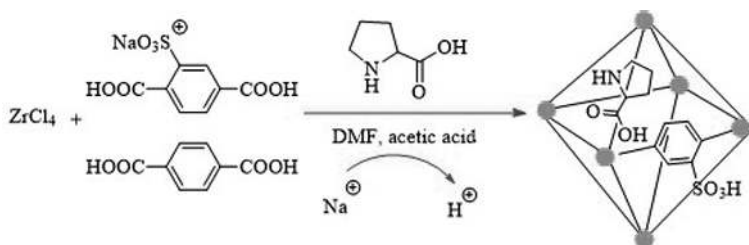
SCHEME 5.105. Proline immobilization by direct solvothermal method.

enantioselectivity, especially in the reaction with 4-nitrobenzaldehyde (83% enantiomeric excess and 85% conversion), (Scheme 5.106). The experimental result showed the catalytic activity of UiO-66-S30Pr was slightly lower than that of neat L-proline; it displayed excellent performance as a heterogeneous catalyst since it can be recycled for three-run reactions without significant decreases in stereoselectivity (ee) and reaction conversion.

In another study, Hu et al. reported the production of CuS@mSiO$_2$@L-proline, and it is used for the hydroxyl aldol condensation reaction of p-nitrobenzaldehyde and acetone. CuS@mSiO$_2$@L-proline with a combination of copper (II) chloride dihydrate (CuCl$_2$·2H$_2$O), cetyltrimethylammonium bromide (CTAB), and triamcinolone acetonide acetate (TAA) produced CuS nanosheets. Followed by the addition of tetraethyl orthosilicate (TEOS), the reaction mixture was placed in the oil bath at 60°C for 3 h [85]. Then the filtrate was refluxed three times for 12 h in 120 ml of

Aldehyde	Product	Catalyst	ee (%)	Conversionf (%)
		Proline	64 a	80
		UiO-66-S30-Pr	60 b	59
		Proline	83 c	85
		UiO-66-S30-Pr	80 d	73

Reaction for 4 h. b Reaction for 96 h. c Reaction for 2 h. d Reaction for 24 h.
e Determined by HPLC. f Determined by GC.

SCHEME 5.106. Enantioselectivity of 4-hydroxy-4-(2-chlorophenyl)-butane-2-one and 4-hydroxy-4-(4-nitrophenyl)-butane-2-one formed from the aldol reaction of 2-CBA and 4-NBA with acetone catalyzed by UiO-66-S30Pr and L-proline.

ethanol using fresh ethanol for each reflux to remove excess CTAB, and the intermediate product, CuS@mSiO$_2$, was dried in an oven at 60°C for 12 h. In the next step, CuS@mSiO$_2$ was treated with the silane-coupling agent kh560 that afforded CuS@SiO$_2$-kh560. Finally, CuS@mSiO$_2$@L-proline (CSPro) catalyst was synthesized using CuS@mSiO$_2$-kh560 with N-Boc-trans-4-hydroxy-L-proline methyl (Scheme 5.107). Hydroxyl aldol condensation reaction of p-nitrobenzaldehyde and acetone was placed in 96.1% yields and with 90.6% enantiomeric excess (ee) values under 808 nm laser assistance (Scheme 5.108). Furthermore, the catalytic activity did not decrease significantly after seven use cycles.

    In another example, Aghahosseini et al. have designed OAc-HPro@Fe$_3$O$_4$ artificial enzyme by immobilizing the O-acryloyl-trans-4-hydroxy-L-proline hydrochloride on amine-functionalized magnetite nanoparticles (NH$_2$-SiO$_2$-MNPs). The activity of the catalyst has been employed as efficient heterogeneous catalysts for efficient synthesis of 2,4,5-trisubstituted and 1,2,4,5-tetrasubstituted imidazoles in

CTAB: Cetyltrimethylammonium bromide
TAA: Triamcinolone Acetonide Acetate
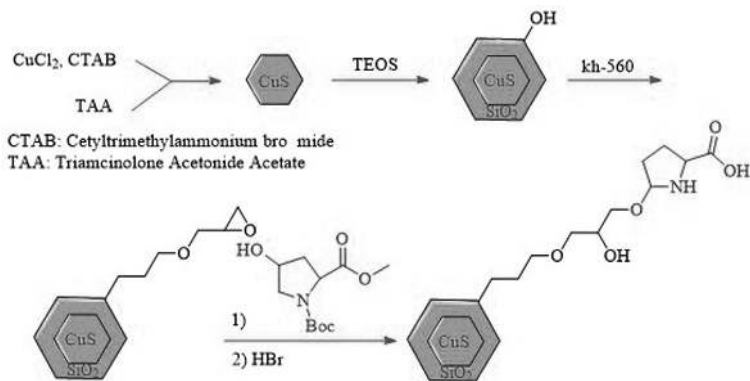
SCHEME 5.107. Flowchart of CuS@mSiO$_2$@L-proline catalyst preparation.

70–99% and 60–90% yields, respectively [86]. Under these conditions, a variety of imidazole derivatives were synthesized in good to excellent yields from benzil, aldehyde derivatives, primary amines, and ammonium acetate (Scheme 5.109). This catalyst can be reused five times without significant loss of activity.

Saberikia et al. introduced the production of a copper complex of proline-based mono (phenol) amine (HLPro) immobilized in SBA-15 and its use as an efficient nanocatalyst for the catalytic aerobic oxidation of primary alcohols to afford the final products using TEMPO as cocatalyst [87]. This catalyst was prepared by anchoring the copper complex proline-based phenolate amine ligand onto functionalized SBA-15 (Scheme 5.110). The resulting nanoparticles were ordered two-dimensional hexagonal with pores diameter and the wall thickness of pores are about 6.2 and 3.1 nm, respectively, and the content of copper was found to be 0.45 mmol/g by inductively coupled plasma atomic emission spectroscopy (ICP-AES). Experimental results show the desired products were obtained efficiently using various substituents (Scheme 5.111).

A recent report described the asymmetric aldol reaction using helical poly(phenyl isocyanide) bearing Boc-protected l-proline pendants (poly-1m) as organocatalysts (Scheme 5.112) [88]. The protecting Boc groups on the l-proline pendants could be adjusted by changing the formation of helical polymer poly-2m. Helical poly-2m successfully catalyzed asymmetric aldol reaction compared to small-molecule l-proline.

R: C_6H_5, 4-ClC_6H_4, 4-$NO_2C_6H_4$,
4-isopropylC_6H_4, furan, -CH(CH$_3$)$_2$

Yield (%): 39.8- 96.1
ee (%): 81.7- 96.5
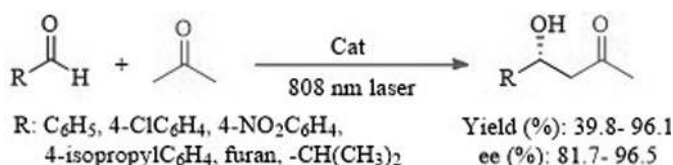
SCHEME 5.108.   808 nm laser-assisted catalytic hydroxy aldol condensation of acetone and a series of aromatic aldehydes.

Ar: Ph, 2-Naphthyl, 2-Thienyl
4-ClC_6H_4, 4-$NO_2C_6H_4$, 4-OMeC_6H_4,
4-MeC_6H_4, 4-OHC$_6H_4$, 2-Furanyl

Yield (%): 70- 99

Catalyst:

OAc-HPro@Fe$_3$O$_4$
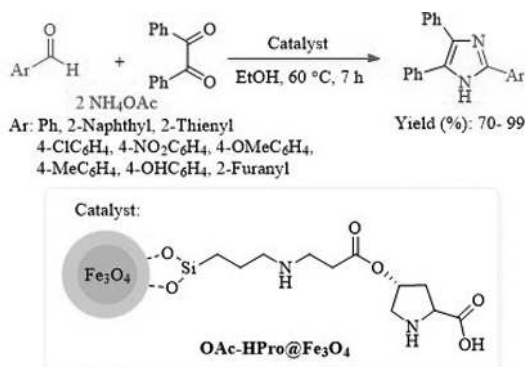
SCHEME 5.109.   Synthesis of 2,4,5-trisubstituted imidazoles.
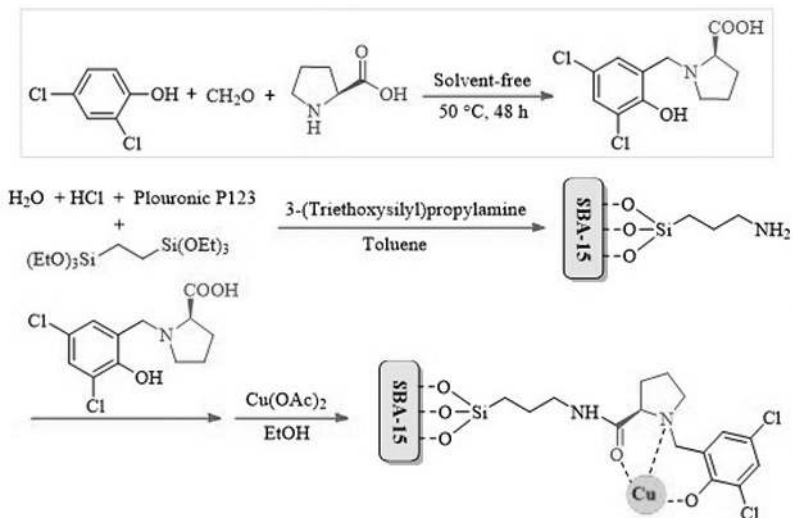
SCHEME 5.110. Schematically anchoring the copper complex of proline-based aminophenol ligand onto functionalized SAB-15.

Substrate: phenylmethanol, p-tolylmethanol, 1-phenylethan-1-ol,
(E)-3-phenylprop-2-en-1-ol, (4-methoxyphenyl)methanol,
pyridin-3-ylmethanol, (4-(methylthio)phenyl)methanol,
(4-isopropylphenyl)methanol, (4-chlorophenyl)methanol,
(2-chlorophenyl)methanol, 3-phenylpropan-1-ol, octan-1-ol,
(3-chlorophenyl)methanol, (2,4-dichlorophenyl)methanol
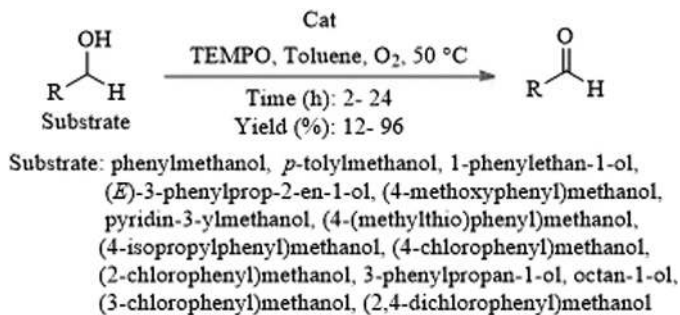
SCHEME 5.111. The chemoselective oxidation of benzyl alcohol in the presence of 1-phenyl ethanol.

The highest ee and dr values of the aldol reaction were obtained, respectively, up to 90% and >20/1 (Scheme 5.113). Furthermore, these catalysts could be recovered easily and the recycled catalysts were shown to maintain their efficiency in subsequent reactions.

Ishihara et al. prepared a recyclable fluorous proline catalyst from (2S, 4R)-trans-4-hydroxyproline via a radical addition reaction to introduce the perfluorooctyl group to the molecule (Scheme 5.114) [89]. The resulting fluorous proline was a viable catalyst for asymmetric aldol reactions (Scheme 5.115). It is worth noting that the catalyst was readily separated from the reaction mixture by adsorption onto
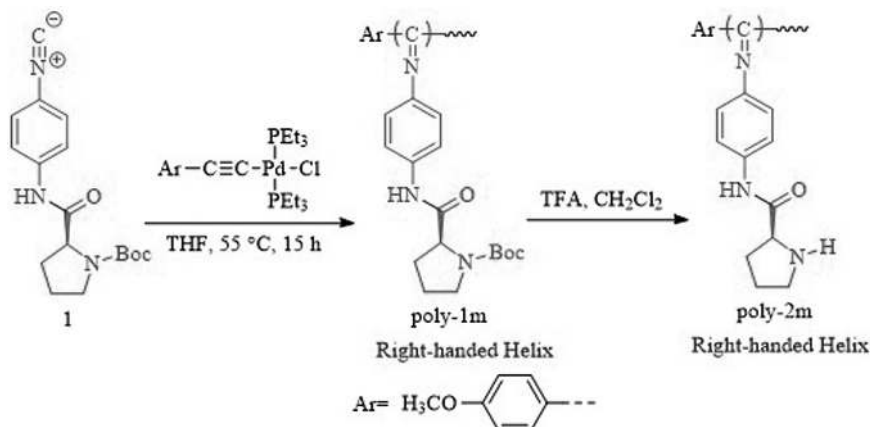
SCHEME 5.112. Synthesis of helical poly-2m.

R: 4-NO$_2$, 3-NO$_2$, 4-CN,
4-CF$_3$, 3-CF$_3$, 4-CH$_3$

Yield (%): 56- 70
anti/ syn: >20/1- 81/19
ee (%): 72- 90
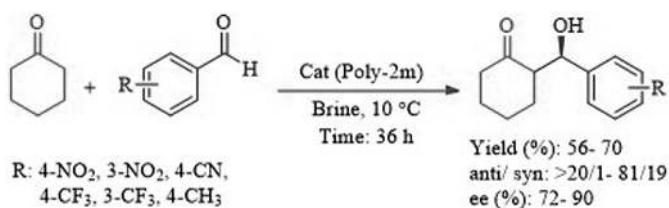
SCHEME 5.113. Enantioselective aldol reaction catalyzed by poly-2m.

Reagents and conditions:
(i) Cl(CO)OCH$_2$Ph, NaHCO$_3$;
(ii) NaH, DMF, BrCH$_2$CH=CH$_2$;
(iii) NaOH, H$_2$O; (iv) C$_8$F$_{17}$I, CuCl, NH$_2$CH$_2$CH$_2$OH;
(v) H$_2$, Pd/C.(vi) 3,5-bis(trifluoromethyl)benzene sulphonamide
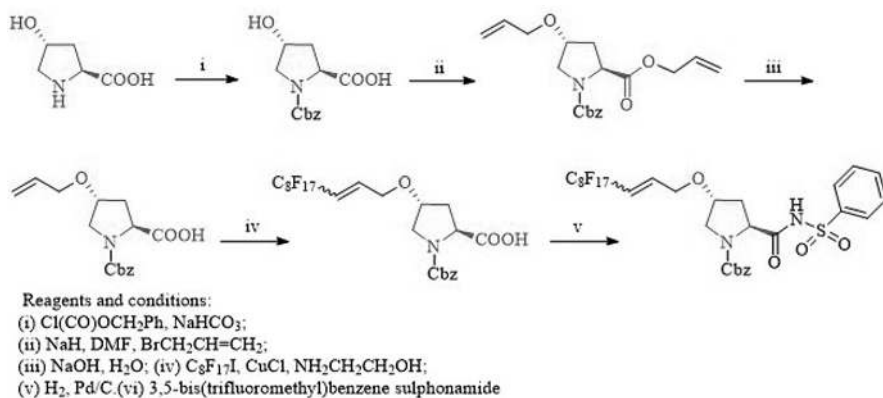
SCHEME 5.114. A synthetic route of fluorous proline catalyst.
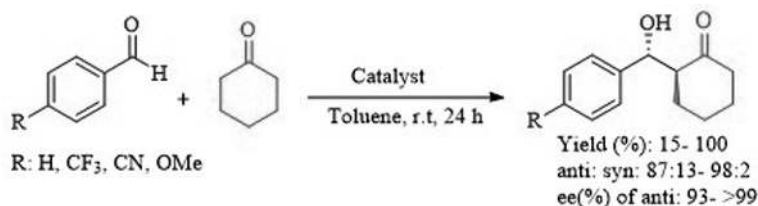
SCHEME 5.115.   Asymmetric aldol reaction of benzaldehydes and cyclohexanone.

FluoroFlash and could be reused a maximum of five times while maintaining a high stereoselectivity (Scheme 5.116) (Figure 5.1).

   L-proline-functionalized pH-responsive copolymers were used as an efficient organocatalyst for asymmetric aldol reactions in water [90]. This organocatalyst was synthesized using incorporated L-proline to a series of pH-responsive mPEG-PDL prepared by RAFT polymerization (Scheme 5.117). The effect of pH (4, 7, and 9) was investigated. However, it was observed that the yield and stereoselectivity of PDL
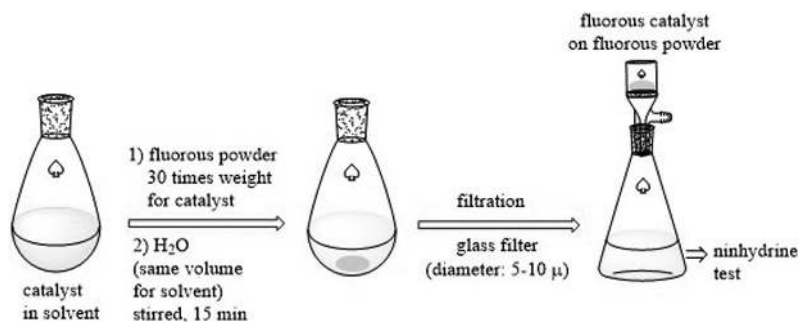
SCHEME 5.116.   Separation procedure employing medium fluorous strategy. *Source: Reprinted with permission from Ref. [89]. Copyright 2020, Elsevier Ltd. All rights reserved.*
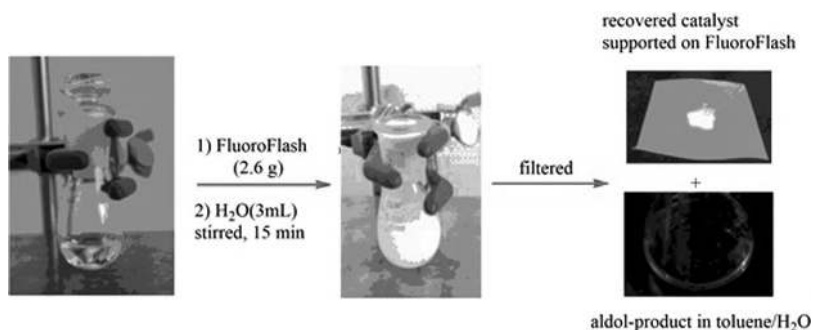
FIGURE 5.1.   The state of separation procedure of 1a in the first cycle. *Source: Reprinted with permission from Ref. [89]. Copyright 2020, Elsevier Ltd. All rights reserved.*

and mPEG-PDL-1 were obtained at pH 7 (Scheme 5.118). Transmission electron microscopy was applied to evaluate the effect of pH 7 and displayed that the assemblies are almost near-sphere and their average size is nearly 90 nm. The reusability of the aqueous catalyst solution was studied subsequently, and experimental results indicated that L-proline-functionalized pH-responsive copolymers could be recovered for four cycles with slight decrease in the yield of desired product due to small amounts of copolymers lost during extraction.

Feng et al. investigated the performance of three Zr-MOFs, including UiO-66, Zr-NDC, and UiO67, for diastereoselective aldol addition reactions (Schemes 5.119 and 5.120) [91]. The chirality is introduced into the catalytic system by attaching L-proline modulation to the metal-Zr node. The influence of different reaction temperatures (70°C, 12°C, and 150°C) on the preparation of L-proline-functionalized Zr-MOFs was investigated and it was the desired product that was generated in high
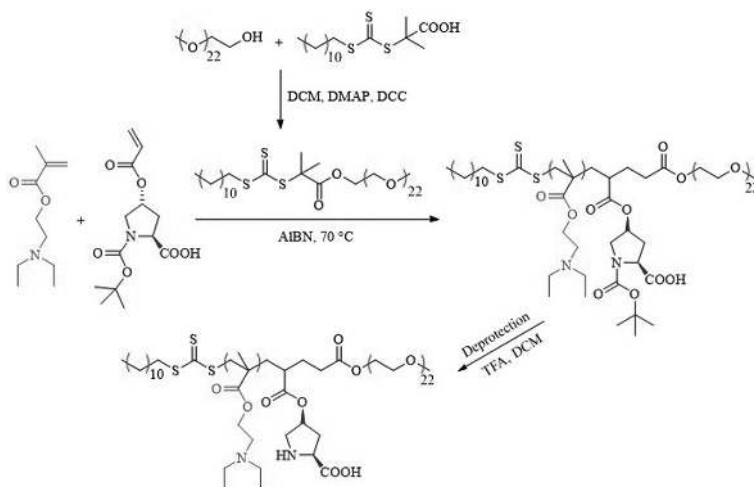
SCHEME 5.117. Synthesis of mPEG-DDMAT and mPEG-PDL.
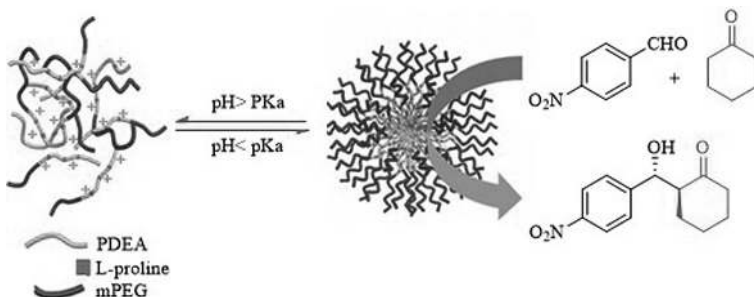
SCHEME 5.118. Assembly behavior and aldol reaction catalysis process of mPEG-PDL in aqueous solution.
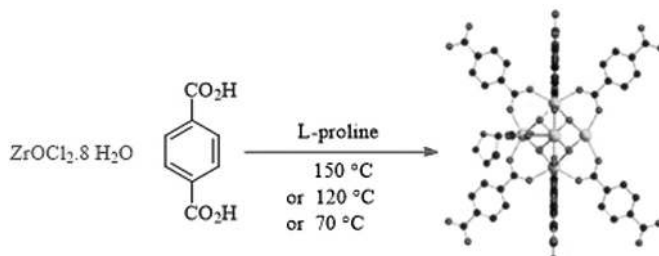
SCHEME 5.119. Preparation of UiO-66 using L-proline as a modulator.
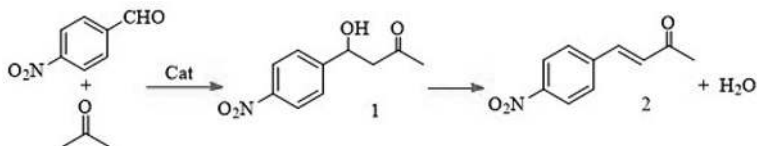
Catalyst	T (°C)	t (h)	Conversion (%)	Selectivitya (%)
L-proline	20	24	99	87
UiO-66-LP-150	20	24	60	96
UiO-66-LP-120	20	24	62	96
UiO-66-LP-70	20	24	4	75
Zr-NDC-LP-150	20	24	8	89
Zr-NDC-LP-120	20	24	3	70
Zr-NDC-LP-70	20	24	2	70
UiO-67-LP-150	20	24	6	83
UiO-67-LP-120	20	24	3	85
UiO-67-LP-70	20	24	3	79

Reaction conditions:
20 °C, 0.3 mmol of 4-nitrobenzaldehyde, 10 mL acetone, 20 mol % catalyst
(related to the proline amount in the material). a Towards aldol product 1.

SCHEME 5.120. Catalytic studies for the aldol addition.

yield and with good diastereoselectivity in presence of UiO-66 material synthesized at 120°C in DMSO. The nitrogen adsorption analysis shows the temperature effect on the density of defects in the resulting framework (Table 5.2).

The high reactivity of several silica-supported proline sulfonamide organocatalysts was exploited by Ferré et al. to catalyze the asymmetric direct aldol reaction in water and room temperature, with no acid additive (Scheme 5.121 and 5.122) [92]. Supported proline sulfonamide organocatalysts were easily prepared by sol–gel and grafting procedures. The authors reported that among various silica-supported proline sulfonamide organocatalysts screened (e.g., M_1, M_2, M_3, M_4, and M_6), M_3, M_4, and M_6 gave better conversions than M_1 and M_2. The porosity of silica-supported proline sulfonamide organocatalysts was investigated with N_2 adsorption–desorption isotherms. It showed a type IV isotherm for M_1 and M_3 with high specific surface areas, whereas M_4 was nonporous (Figure 5.2).

TABLE 5.2.
Structural properties of the three Zr-MOFs and the obtained number of defects at various synthesis temperatures

Zr-MOFs	150°C			120°C			70°C		
	$S_{Langmaier}$ (m²/g)	Mod/L	Number of missing linkers (per Zr_6)	$S_{Langmaier}$ (m²/g)	Mod/L	Number of missing linkers (per Zr_6)	$SL_{angmaier}$ (m²/g)	Mod/L	Number of missing linkers (per Zr_6)
UiO-66-LP	1572	0.77	2	1576	0.77	2	1850	0.85	2.7
Zr-NDC-LP	1625	0.51	1.5	1050	0.51	1.5	900	0.94	3
UiO-67-LP	1607	0.51	0.8	1806	0.51	0.8	2800	0	0
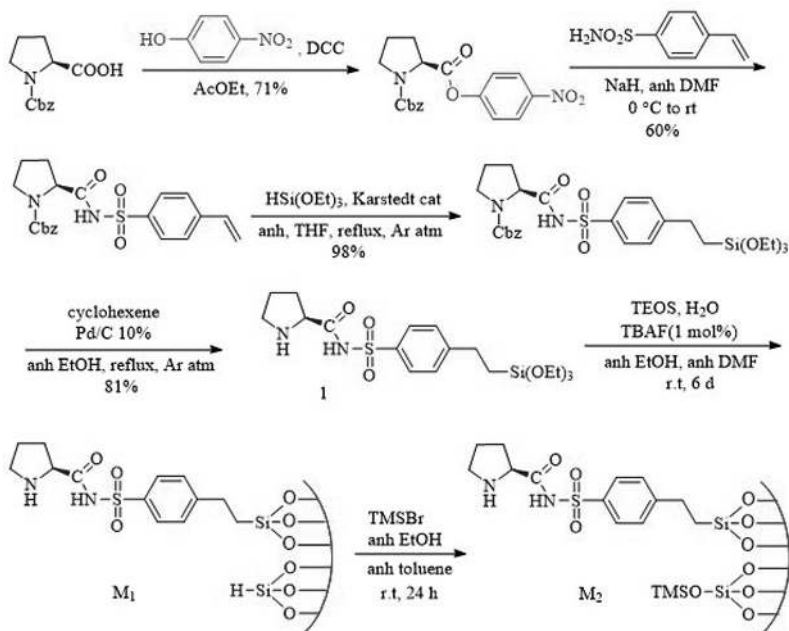
SCHEME 5.121. Synthesis of the silylated precursor 1 and structure of the organocatalyst M_1 and M_2.

The same group reported the production of L-proline-immobilized polymers by general solution of homopolymerization by azobisisobutyronitrile (AIBN) Cat.1 or copolymerization of L-proline-functionalized styrene monomer Cat.2 using 1,4-divinylbenzene as the cross-linking agent (Schemes 5.123 and 5.124) [93]. This heterogeneous catalyst has been employed in the direct aldol reaction of ketones with different aromatic aldehydes in good yields (up to 96%) and with high diastereose-lectivities (up to 8:92 dr) and excellent enantiomeric excess (up to 96% ee) (Scheme 5.125). The heterogeneous catalysts were separated and reused in the mixed solvent system with petroleum ether/water. Although Cat. II shows better recyclability than Cat. I.

Asymmetric reactions in aqueous solutions have attracted much attraction due to water is safe, nontoxic, environmentally friendly, and cheap. Several water-soluble chiral catalysts have been developed and offer many benefits from a green chemistry point of view. In some cases, the catalyst was functionalized to be more hydrophobic, such as forming a concentrated organic phase, which causes acceleration of reaction rates. Amphiphilic block copolymers have been widely used in catalytic systems, and they can also create a protected hydrophobic environment in water. Amphiphilic copolymers-supported catalysts can catalyze asymmetric reactions in water effec-tively and can be reused. But the catalyst isolated by precipitation in the organic solvent leads to environmental pollution. Using the phase-switchable behavior of
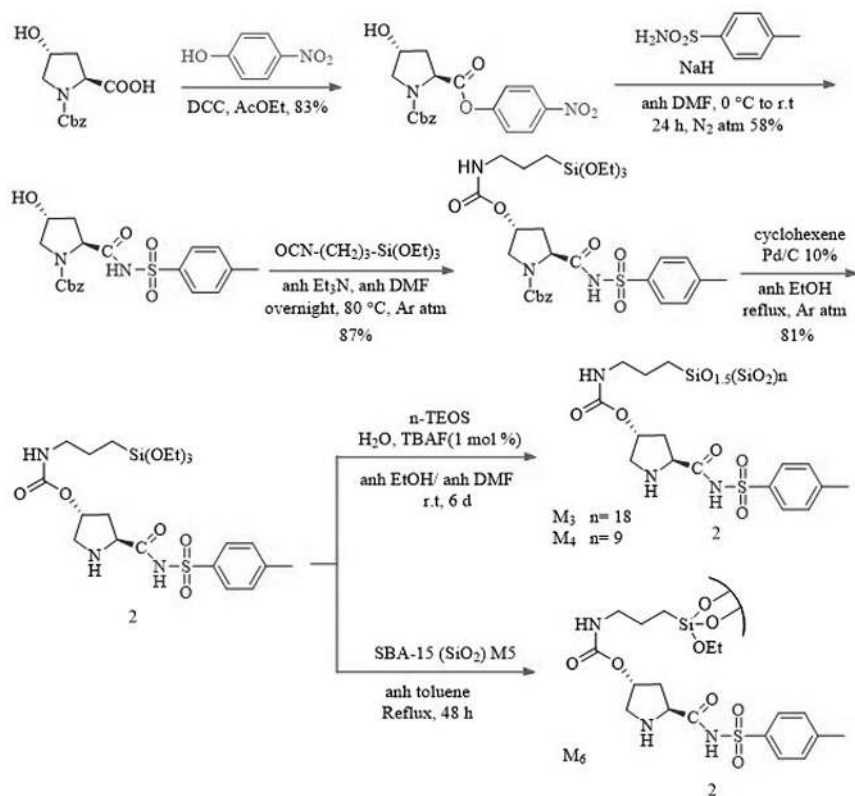
SCHEME 5.122. Synthesis of the silylated precursor.

Materials	BET specific surface area $(m^2 g^{-1})$	Por volume $(cm^3 g^{-1})$	Most probable pore diameter (nm)
M_1	450	0.43	3.5
M_3	353	0.60	4
M_4	<5	-	-
M_6	328	0.55	6

FIGURE 5.2. BET surface, pore volume, and most probable pore diameter for M_1 (black, squares), M_3 (red, triangles), and M_6 (blue, circles).

amphiphilic copolymer, the copolymer will collapse and precipitate for facile recovery. Li et al. have prepared three kinds of hairy particles-supported proline by RAFT precipitation polymerization combined with surface-initiated RAFT copolymerization. Hairy particle (1) contained hydrophobic styrene, N-iso-N-isopropyl acrylamide, and chiral polymer chain; while hairy particle (2) contained chiral polymer chain and NIPAM, without styrene; and hairy particle (3) contained chiral polymer
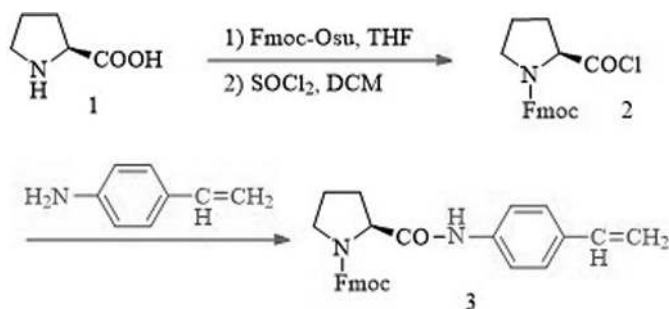
SCHEME 5.123. The preparation of L-proline functionalized styrene monomer 3.
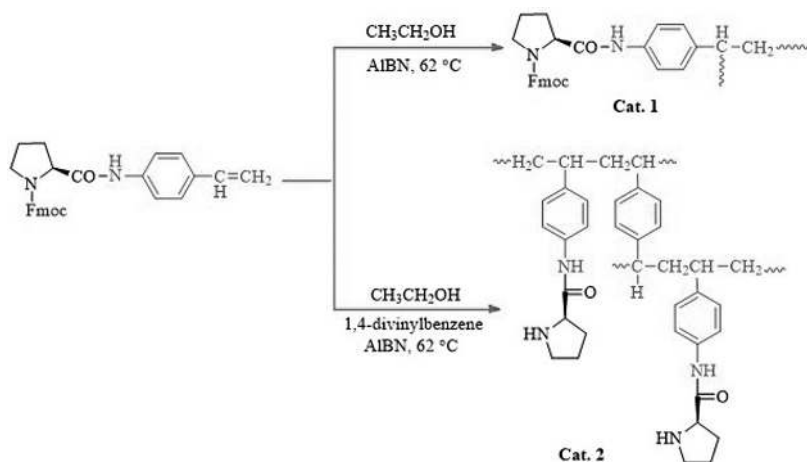
SCHEME 5.124. The polymerization of functionalized monomer 3 to afford Cat. 1 and Cat. 2.

chain and styrene, without NIPAM (Scheme 5.126) [94]. The authors reported that hairy particle (1) grafted with amphiphilic copolymer chains displayed a good conversion rate and outstanding enantioselectivity in pure water (Scheme 5.127).

Organometallic frameworks have a variety of applications due to their valuable properties such as high surface area, adjustable pore size, and high chemical and thermal stability, and their most important use is as a catalyst. Brunner and coworkers provided an aldol addition reaction from the reaction between cyclohexanone and 4-nitrobenzaldehyde using an asymmetric MOF-proline catalyst (Schemes 5.128 and 5.129) [95].

Several investigations have been reported in the preparation of supported amino acid and their derivatives. Among these polymeric supports, dendrimers have attracted vast and persistent interest because of their unique three-dimensional symmetrical structures, thus mimicking the globular structures of natural enzymes.
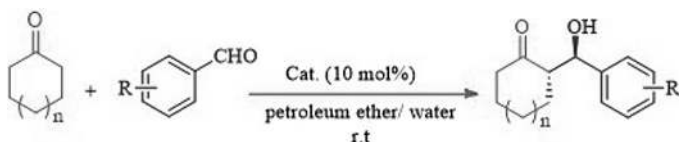
R	Catalyst	Time (h)	Yield(%)	dr (syn/anti)	ee (%; anti)
2,4-Dinitro	Cat.1	48	89	8:92	86
2,4-Dinitro	Cat.2	48	79	12:88	80
4-NO$_2$	Cat.1	48	92	15:85	94
4-NO$_2$	Cat.2	48	90	27:73	92
3-NO$_2$	Cat.1	48	85	11:89	80
3-NO$_2$	Cat.2	48	87	14:86	79
2-NO$_2$	Cat.1	48	73	10:90	84
4-CN	Cat.1	72	52	25:75	69
4-F	Cat.1	72	63	24:76	64
4-H	Cat.1	72	69	17:83	76
4-CH$_3$	Cat.1	72	58	32:68	83
4-OCH$_3$	Cat.1	72	45	43:57	84
4-NO$_2$	Cat.1	48	72	39:61	69
2-NO$_2$	Cat.1	48	76	31:69	88
4-NO$_2$	Cat.1	60	41	-	67
3-NO$_2$	Cat.1	60	52	-	65

SCHEME 5.125. Asymmetric aldol reactions catalyzed by polymer-supported catalysts.
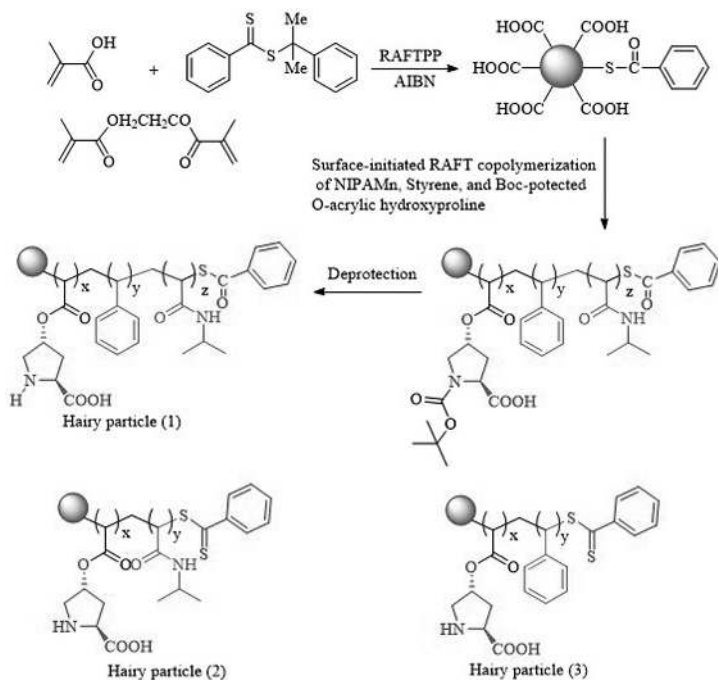
SCHEME 5.126. The synthesized method of hairy particles and the structure diagram of hairy particles.
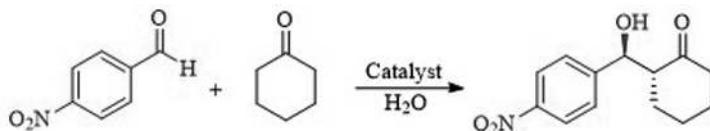
Catalysts	Temp. (°C)	% Conversion	syn/anti	% ee (anti)
Hairy particles (1)	0	84	9/91	>99
Hairy particles (1)	25	90	10/90	95
Hairy particles (1)	35	97	11/89	97
Hairy particles (1)	50	97	22/78	93
Hairy particles (2)	0	5	20/80	87
Hairy particles (2)	25	32	27/73	53
Hairy particles (2)	35	16	20/80	77
Hairy particles (2)	50	17	28/72	42
Hairy particles (3)	0	10	21/79	88
Hairy particles (3)	25	67	12/88	95

SCHEME 5.127.   Aldol reaction catalyzed by hairy particles.
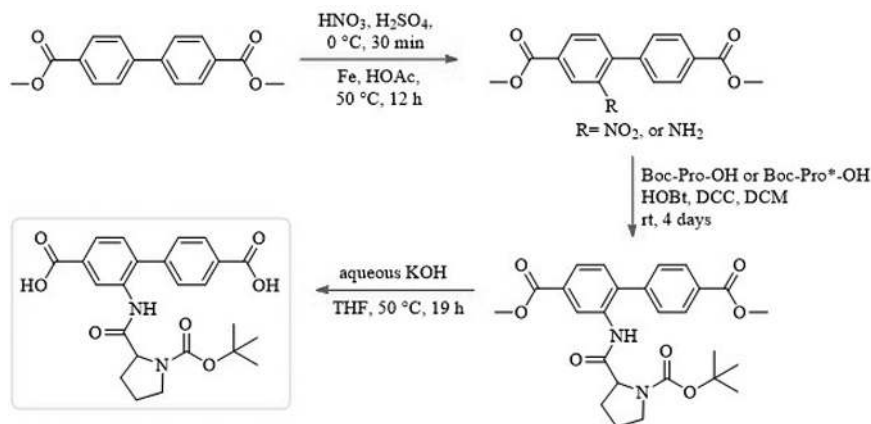
SCHEME 5.128.   Linker synthesis method for DUT-32-NHProBoc catalyst preparation.

   L-proline supported on hyperbranched polyethylene used a bottom-up copolymerization strategy, as reported by Wang et al. Initially, an acrylic comonomer bearing protected proline functionality was synthesized and copolymerized with ethylene via a chain walking mechanism catalyzed by Pd-diimine catalysts, followed by deprotection of the proline groups. Well-defined hyperbranched polyethylene (HBPE) containing pendant L-proline functionalities via Pd-catalyzed chain walking copolymerization of ethylene and protected proline-comonomer (4) was followed by de-protection of the proline groups. The activity of the catalyst was used for asymmetric reactions of aldol of p-nitrobenzaldehyde (p-NBA) and cyclohexanone, with p-NBA conversions up to 98%, *anti/syn* = 98/2, and ee >99%. Steric effect and
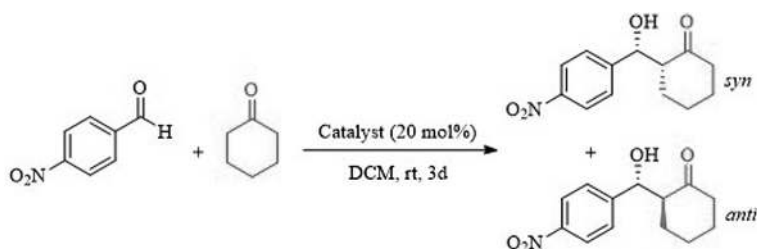
SCHEME 5.129. Aldol addition reaction between cyclohexanone and 4-nitrobenzaldehyde using MOF-proline.

diffusion limitation imposed by the hydrophobic HBPE scaffolds on the reactants leads to the high selectivity of the catalyst (Schemes 5.130 and 5.131) [96].

Gurka and coworkers reported the application of organic–inorganic hybrid catalyst Pro/c-Al$_2$O$_3$ for the aldol reactions between aldehydes of three different types (aromatic, aliphatic, and cycloaliphatic) and acetone/cycloalkanones as reaction partners (Scheme 5.132) [97]. Experimental studies show the aldol reaction between cycloaliphatic aldehydes and acetone/cycloalkanones in the presence of c-Al$_2$O$_3$ was 40% and of that without Al$_2$O$_3$ was 90%.

Organic–metal frameworks as an important category of porous materials due to their valuable attributes such as high surface area, adjustable pores size, and high chemical and thermal stability have various applications in gas storage and separation, ion-exchange, superconductivity, and catalysis. In recent years, these compounds have shown tremendous catalytic power due to their unique structure and properties. In 2014, Xin and coworkers used metal–organic frameworks made with
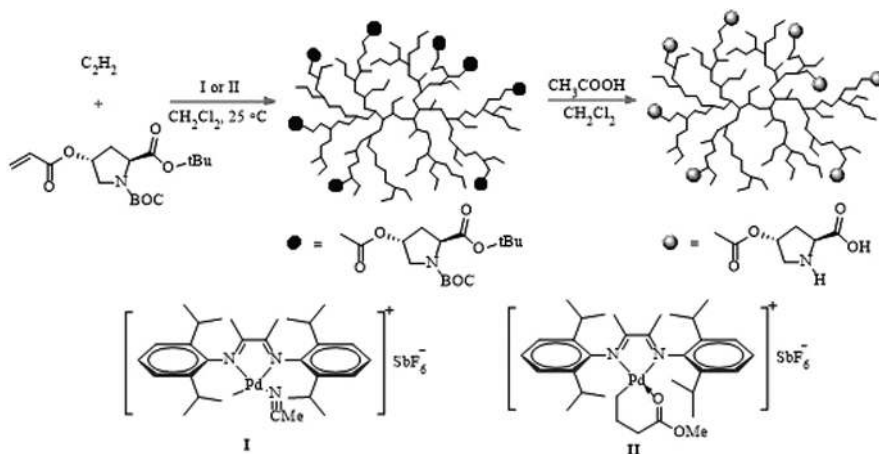
SCHEME 5.130. Create an organocatalyst of L-proline supported by supersaturated polyethylene.

R= Cl, Br, H, CF$_3$
R-ph= 2-naphthaldehyde

Yield (%)	anti/syn	ee (%)
94	91:9	88
75	96:4	95
92	90:10	89
33	91:9	86
88	99:1	93

SCHEME 5.131. Asymmetric reactions of aldol by organocatalyst of L-proline.

Aldol reaction between aldehydes and acetone

L-Pro or D-Pro
r.t, stirring
Time: 1-22 h
Yield: 51-94%

R: 2-NO$_2$C$_6$H$_4$	R: 2-NO$_2$C$_6$H$_4$	(R)	(S)
R: (CH$_3$)$_2$CH	R: (CH$_3$)$_2$CH	(R)	(S)
R: C$_6$H$_{11}$	R: C$_6$H$_{11}$	(R)	(S)

Aldol reaction between aldehyde and cyclohexanone or cyclopentanone

L-Pro or D-Pro
r.t, stirring
Time: 22- 44 h
Yield: 28- 99%

R: (CH$_3$)$_2$CH	n=1 ;	R: (CH$_3$)$_2$CH,	n=1	(S)	(R)
R: CH$_3$CH$_2$CH$_2$	n=0 ;	R: (CH$_3$)$_2$CH,	n=0	(S)	(R)
R: C$_6$H$_{11}$		R: CH$_3$CH$_2$CH$_2$,	n=1	(S)	(R)
		C$_6$H$_{11}$,	n=1	(S)	(R)

SCHEME 5.132. Aldol addition reaction between aldehydes and ketones L-proline/D-proline as a catalyst and γ-Al$_2$O$_3$.

L-proline for the aldol reaction and three-component coupling (Schemes 5.133 and 5.134) [98].

In 2014, He and coworkers synthesized L-proline-grafted mesoporous silica catalysts with a novel strategy that contains hydrophobic and hydrophilic blocks (Scheme 5.135) [99]. Due to its hydrophilic nature, silica catalyst has high catalytic activity and excitability in the reaction, resulting in faster development of aldol and

SCHEME 5.133. Perform aldol reaction with the metal–organic framework of proline.
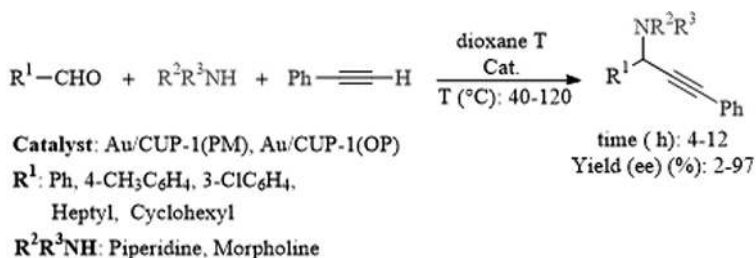
SCHEME 5.134. Coupling reaction by Au@CUP-1 catalysts.
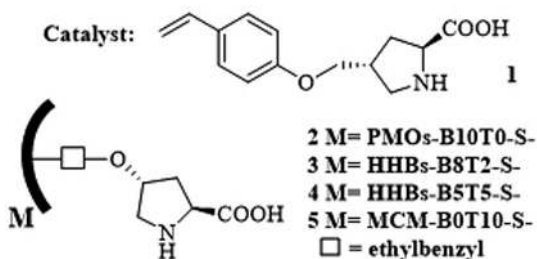
SCHEME 5.135. Outline of catalysts synthesized with L-proline.

Knoevenagel–Michael reaction. Cyclohexanone and acetone were used in the aldol reaction and acetone, malononitrile, and isatin were used for the Knoevenagel–Michael reaction (Scheme 5.136).

Bartók and coworkers reported application of L-proline-introduced H-Pro-MBHA (1); H-Pro-Pro-MBHA (2); H-Pro-Glu(OH)-MBHA (3); H-Pro-Pro-Pro-MBHA (4); H-Pro-Pro-Glu(OH)-MBHA (5) catalysts for aldol addition between aldehydes (2-methyl propanol, 2-nitrobenzaldehyde) with ketones (acetone, cyclohexanone) (Schemes 5.137–5.140) [100].

Aldol Reaction

R= p-nitrobenz-, -nitrobenz-
o-nitrobenz-, -CO$_2$Et

catalyst, 25 °C, 24 h
neat or medium

Cat.: 1-5   time (h): 8-72
yield (%): <3- >99

Knoevenagel-Michael Cascade Reaction

catalyst 2%
Toluene/Standard NaCl, rt

Cat.: 1-5   time (h): 10
yield (%): 26- 90
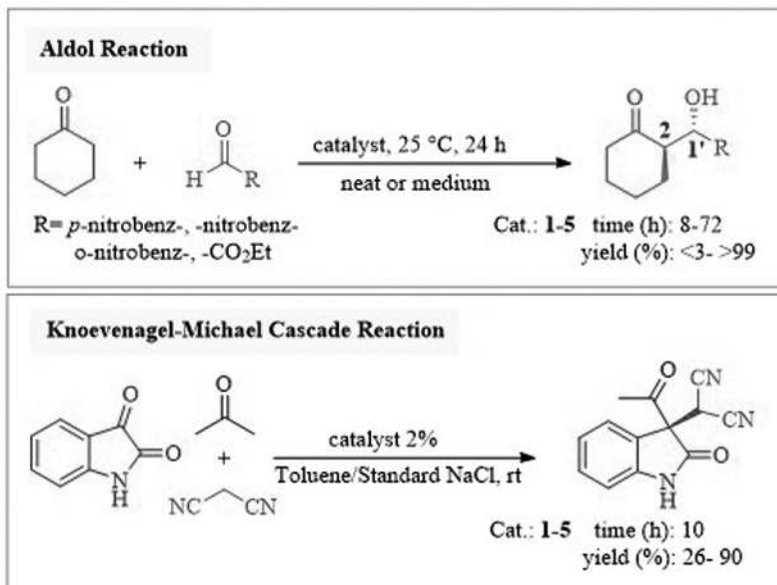
SCHEME 5.136. Aldol and Knoevenagel–Michael reactions by L-proline mesoporous silica.

H-Pro-Glu(OH)-MBHA   H-Pro-Pro-Glu(OH)-MBHA
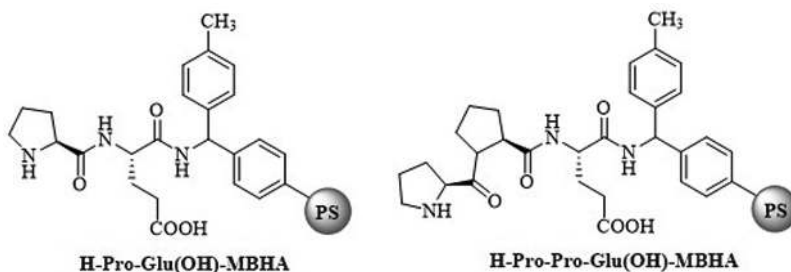
SCHEME 5.137. Scheme of catalysts synthesized with L-proline.

In 2014, Ma and coworkers designed a new and efficient catalyst for asymmetric aldol reaction by immobilizing L-proline on mesoporous SBA-16, which was able to complete the aldol reaction with good performance (Schemes 5.141 and 5.142) [101].

Duan and coworkers designed a new method for the preparation of the Co-Pro1 homochiral triangle as a homogeneous selective size catalyst by combining an L-proline moiety in a metal helical triangle prepared by metal ion assembly and two triple N$_2$O units containing amide groups at a benzene ring center at *meta* sites. The catalyst was employed for the aldol reaction (Schemes 5.143 and 5.144) [102].

Catalyst	Imidazole	Conversion (%)	Selectivity(%)	ee(%)	Config.
1	-	21	89	24	(R)
1	+	40	80	24	(R)
2	-	80	94	29	(R)
2	+	86	88	24	(R)
4	-	60	94	34	(R)
4	+	82	89	29	(R)
3	-	35	60	50	(R)
3	+	55	85	52	(R)
3	+	47	84	49	(R)
3	+	45	80	32	(R)
5	-	51	69	37	(S)
5	+	77	72	39	(S)
5	+	61	77	31	(S)
5	+	55	84	18	(S)

SCHEME 5.138. The reaction between 2-nitrobenzaldehyde and acetone with catalysts 1–5.

Catalyst	Conversion (%)	Selectivity(%)	ee(%)	Config.
1	31	99	76	(R)
3	28	98	94	(R)
5	31	97	50	(S)
5	31	98	51	(S)
5	33	98	51	(S)

SCHEME 5.139. The reaction between isobutyraldehyde and acetone with catalysts 1–5.

Catalys	Conversion (%)	Selectivity(%)	anti/syn	ee(%)	Config.
1	69	69	94/6	38	(S,S)
3	22	93	98/2	95	(S,S)
3	28	91	98/2	93	(S,S)
3	35	83	97/3	81	(S,S)
5	24	93	84/16	34	(R,R)
5	30	92	86/14	41	(R,R)
5	52	87	83/17	27	(R,R)

SCHEME 5.140. The reaction between cyclohexanone and acetone with catalysts 1–5.
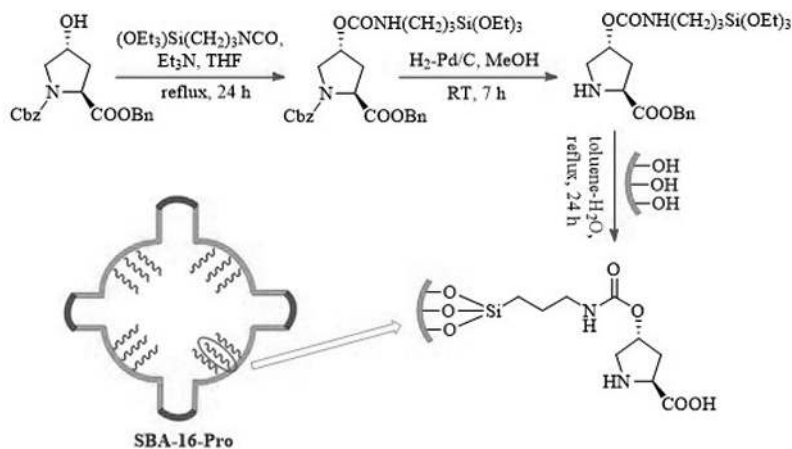
SCHEME 5.141.   Synthesis of mesoporous SBA-16 with L-proline.

R_1= 2-$O_2NC_6H_4$-, 3-$O_2NC_6H_4$-, 4-NCC_6H_4-, 4-ClC_6H_4-,
    C_6H_5-, 2-Furanyl-, 4-$MeOC_6H_4$-, 4-MeC_6H_4-

R_2= -$(CH2)4$-, -$(CH_2)_3$-, -$(CH_2)_5$-,
    CH_3,C_6H_5-, 4-$O_2NC_6H_4$-

R_3= H
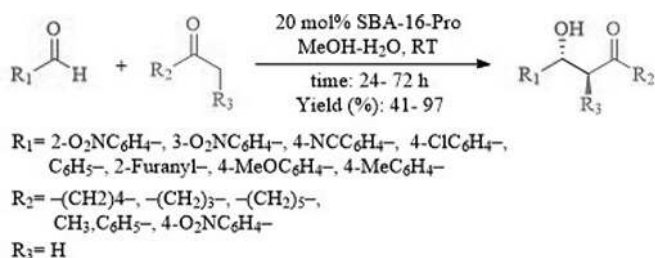
SCHEME 5.142.   Multicomponent-catalyzed mesoporous SBA-16-Pro.
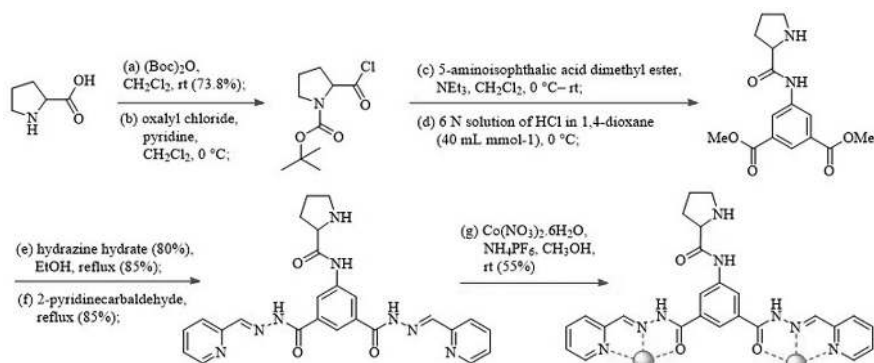
SCHEME 5.143.   Synthetic process for Co–**Pro1.**

In another study, polymer-immobilized L-proline derivatives were fabricated by Cui and coworkers, and their performance of catalyst employed in the aldol reaction (Scheme 5.145) [103].

The reaction was carried out in the presence of catalysts A(PTP), B(PEP), and C(PDP), and the best performances were found with catalyst A(PTP), which has the largest side chain. Experimental results show that 4-hydroxyproline and L-proline were not effective catalysts for this reaction. Under the standard reaction conditions, the desired products were isolated using a PTP catalyst in water solvent and synthesized (Scheme 5.146).

In one study, two proline-based polystyrene catalysts were synthesized by Liu et al. (Scheme 5.147) and then the aldol reaction between cyclohexanone and different aldehydes was performed by using 5 mol% of catalysts 1 and catalysts 2 in different mixtures of two solvents (water/dimethylformamide) and (water/ketone) (Scheme 5.148) [104]. In both cases, products with high *anti*-diastereoselectivity and enantiomeric excess

Aldehyde	Con. (%)	Anti:Syn	ee (%)
4-Nitrobenzaldehyde	42	6 : 1	73
3-Nitrobenzaldehyde	38	6 : 1	70
2-Nitrobenzaldehyde	24	10 : 1	62
3-Formyl-1-phenylene-(3,5-di-tert-butylbenzoate)	Trace	—	—
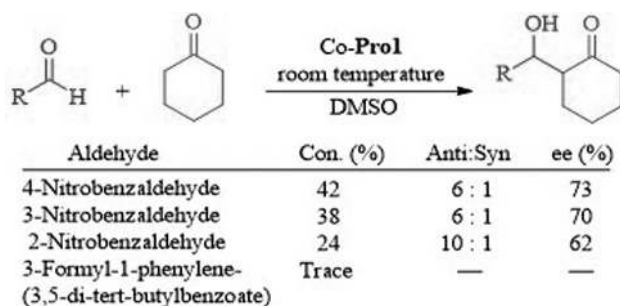
SCHEME 5.144.   Aldol reactions by Co–**Pro1.**
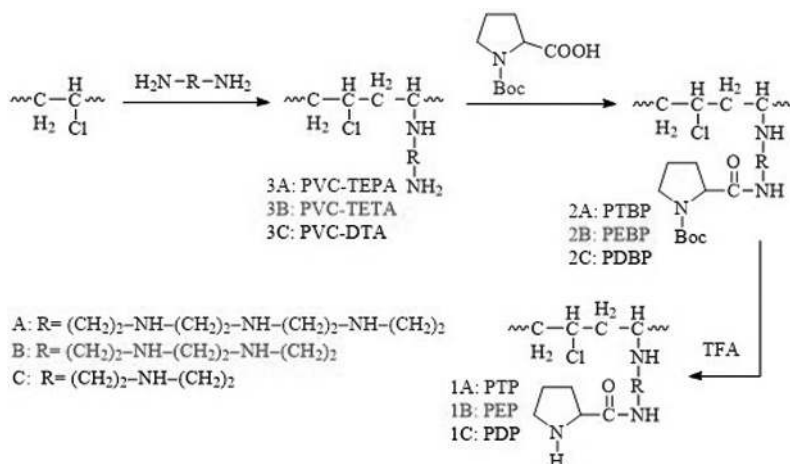
SCHEME 5.145.   Synthesis of PVC-TEPA-supported proline derivative.

R^1, R^2	R	Time (h)	Yield^a (%)	TOF (h^{-1})	dr anti : syn	ee anti (%)
-(CH₂)₄-	Pyridin-4-yl	20	89	0.44	76:24	52
-(CH₂)₄-	4-Nitrophenyl	72	69	0.09	91:9	94
-(CH₂)₄-	3-Nitrophenyl	24	52	0.22	83:17	72
-(CH₂)₄-	2-Nitrophenyl	24	60	0.25	>99:1	86
-(CH₂)₄-	4-Cyanophenyl	192	64	0.03	75:25	68
-(CH₂)₄-	4-Methyloxyphenyl	192	28	0.02	92:8	68
-(CH₂)₄-	2-Chlorophenyl	190	39	0.02	99:1	79
-(CH₂)₄-	5-Nitrofuran	20	93	0.47	76:24	71
-(CH₂)₄-	Styryl	190	44	0.23	95:5	77
-(CH₂)₄-	2,4-dinitrophenyl	72	66	0.92	92:8	84
H, CH₃	4-Nitrophenyl	24	72	0.3	-	16
-(CH₂)₃-	4-Nitrophenyl	40	56	0.14	39:61	32

SCHEME 5.146. Catalytic behavior of PVC-TEPA-supported proline derivative in the direct asymmetric aldol reaction.
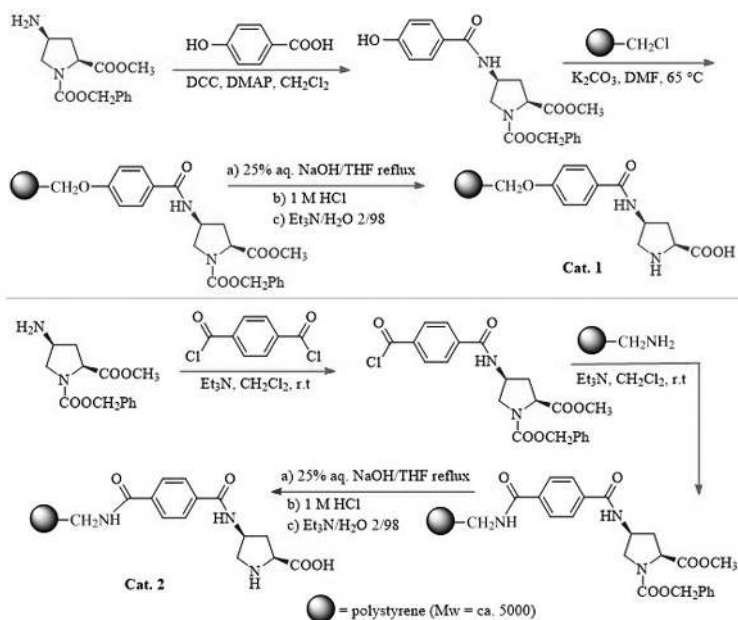
SCHEME 5.147. Synthesis of polystyrene-supported catalysts 1 and 2.
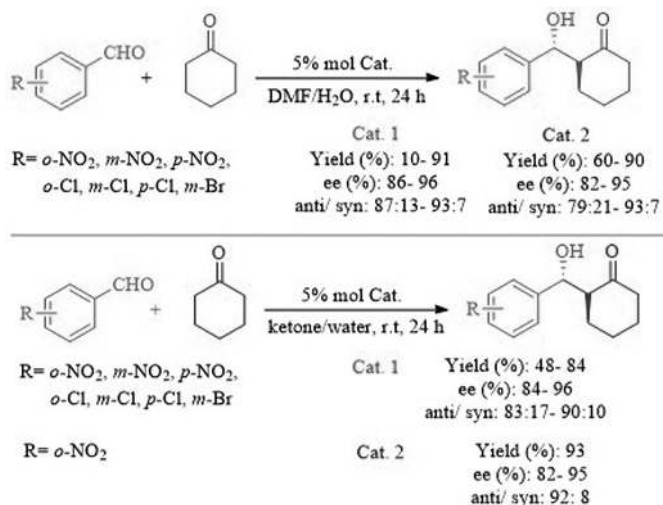
SCHEME 5.148. Asymmetric aldol reaction catalyzed by new recyclable polystyrene-supported L-proline in the presence of water.

were obtained, but the yield of products in solvent H_2O/DMF was more than $H_2O/$ ketone.

Wang and coworkers designed and synthesized two L-proline-derived ligands supported by polystyrene resin (insoluble ligand 1 and soluble ligand 2) (Scheme 5.149). They then used them to react asymmetrically with diethylzinc addition to various aldehydes (Scheme 5.150) [105]. In general, in the presence of this polymer, products with high enantioselectivity were obtained and catalyst recovery was easily performed in several consecutive stages while maintaining efficiency.

Gruttadauria and coworkers designed and synthesized two catalysts of proline and proline amide supported by polystyrene and their catalytic properties in organic reactions were investigated (Scheme 5.151) [106]. The property of the proline catalyst in the aldol reaction between cyclohexanone and benzaldehyde at room temperature and water solvent was investigated and products with high diastereoselectivities and enantiomeric excesses were obtained.

L-proline and L-proline stabilized on mesoporous material were used in asymmetric aldol reaction by Fernández-Mayoralas and coworkers and the best result was found using stabilized L-proline on mesoporous MCM-41, which was performed in a very short time and with excellent efficiency and stereoselectivities, and the results are shown in Scheme 5.152 [107].

Andreae and Davis synthesized various peptides with a proline-supported polystyrene resin as heterogeneous catalysts and investigated their use in the reaction of acetone with 4-nitrobenzaldehyde to produce asymmetric aldol. Among the peptides synthesized with various amino acids, including serine, cytosine, alanine, and
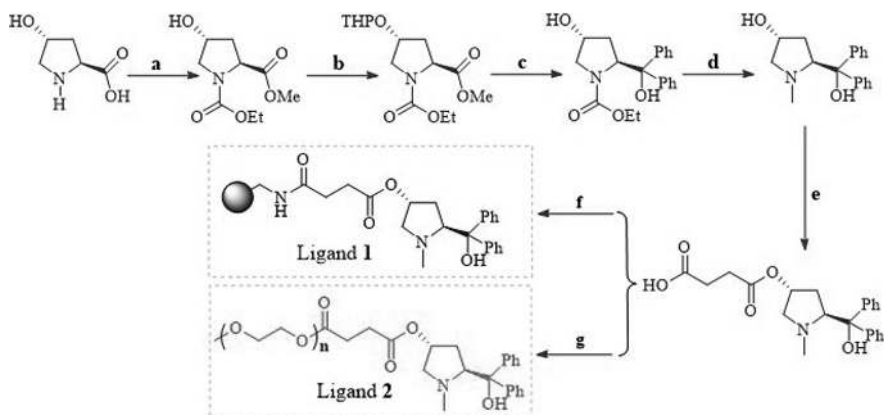
Reagents and condition:
(a) Ethyl chlorformate, K$_2$CO$_3$, methanol, 89% yield.
(b) 3,4-Dihydro-2H-pyran, TsOH, CH$_2$Cl$_2$, 98% yield. (c) (1) PhMgBr, THF; (2) AcOH, THF, H$_2$O, 44 .C, 85% yield.
(d) LiAlH$_4$, THF, 100% yield.
(e) Succinic anhydride, DMAP, CH$_2$Cl$_2$ The mixture was used directly for the next step.
(f) Aminomethylated polystyrene resin, DIC, HOBt, iPr$_2$NEt, DMF/CH$_2$Cl$_2$, rt, 100% yield. (g) MeO-PEG (Mw = 2000), DMAP, DCC, CH$_2$Cl$_2$, rt, 100% conversion.

SCHEME 5.149. Polymer-supported proline-derived ligand 1 and 2 synthesis steps.

R= Ph, 4-MeC$_6$H$_4$, 4-MeOC$_6$H$_4$,
2-ClC$_6$H$_4$, 2,6-Cl$_2$C$_6$H$_3$,
2,3-(MeO)$_2$C$_6$H$_3$,4-ClC$_6$H$_4$,1-Nap,
(E)-PhCH =CH

Ligand 1   Yield (%): 31- 93
               ee (%): 34- 71

Ligand 2   Yield (%): 44- 96
               ee (%): 42- 90
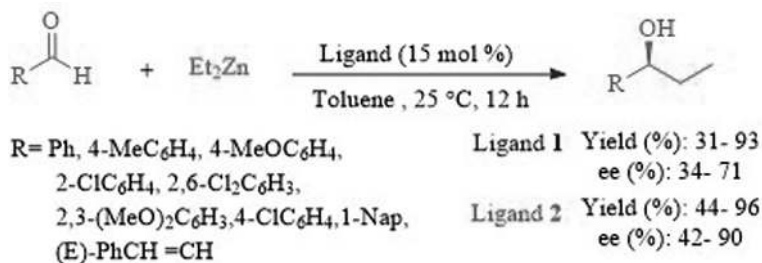
SCHEME 5.150. Supported proline-derived application in asymmetric diethylzinc addition to aldehydes.

tryptophan, the best results were obtained for serine dipeptide, the results of which are shown in Scheme 5.153 [108].

Gruttadauria et al. introduced the production of polystyrene-supported proline via a two-step process (Scheme 5.154): (1) synthesis of hydroxy-L-proline styrene derivative 1 and (2) radical reaction between the polystyrene and 1 followed by deprotection of the proline moiety [109]. Deprotection of the *tert*-butoxycarbonyl group occurred in TFA/CH$_2$Cl$_2$ (20:80), followed by treatment with Et$_3$N/MeOH (2:98). The catalyst was applied in direct asymmetric aldol reactions between several ketones and aryl aldehydes to furnish aldol products in high yields and with excellent stereoselectivities (Scheme 5.155). Optimization studies showed that water or methanol are efficient solvents in direct asymmetric aldol reactions.
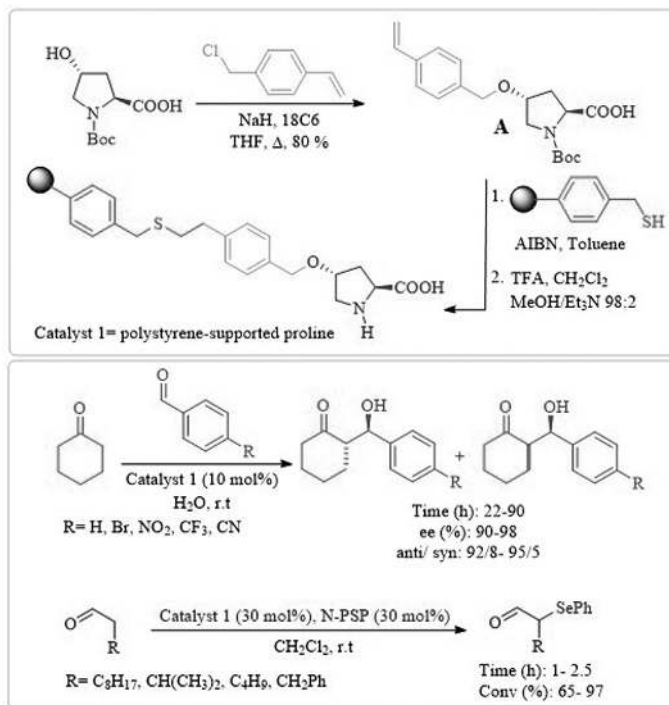
SCHEME 5.151. Polystyrene-supported proline and prolinamide. Versatile heterogeneous organocatalysts both for asymmetric aldol reaction in water and α-selenenylation of aldehydes.
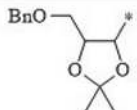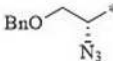
5.10. APPLICATION OF L-PROLINE-BASED IONIC LIQUID AS AN ORGANOCATALYST IN THE ALDOL REACTION
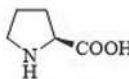
Inani et al. introduced aldol addition of cyclohexanone to various aldehydes, via proline-histidine dipeptide. In their procedure, proline-histidine dipeptide laid the foundation for the production of three new ion-tagged organocatalysts, utilizing the imidazole moiety of histidine for the formation of the quaternary species (Scheme 5.156) [110]. Among the employed organocatalysts for this reaction, organocatalysts 1 was found to be more in preparing some derivatives. The experimental result showed both electron-poor and electron-rich substituents on the aldehydes provide the desired product in 58–99% yields (Scheme 5.157).

Asymmetric aldol reactions of cyclohexanone with various aldehydes are carried out by imidazolium-proline. The product was obtained in high yields and enantioselectivities, along with exceptional diastereoselectivities (Schemes 5.158 and 5.159) [111]. Interestingly, among various counterion screened (e.g., TsO⁻ and Tf₂N⁻), Tf₂N⁻ was the most effective in the H_2O solvent.
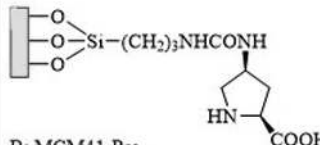
Okafuji group reported the synthesis of thermoresponsive poly(ionic liquid) gels containing proline that were prepared by reaction of IL monomers (P4 and P5),

Aldehyde	Catalyst	Time (min)	Yield (%)	anti/syn	ee (%)
1	A	10	60	>20 : 1	>99
1	B	10	60	>20 : 1	>99
2	A	10	90	>20 : 1	>99
2	B	10	90	>20 : 1	>99
3	A	10	65	2.2:1	75
3	B	30	70	1:1.4	80
4	A	10	60	2.1:1	–
4	B	25	60	1:1.6	–
5	A	10	65	3:1	–
5	B	15	55	1:1.3	–

SCHEME 5.152. Asymmetric aldol reaction using immobilized proline on mesoporous support.

Entry	Catalyst	Yield (%)	ee (%)
1	H-Pro-NH-TG	93	30
2	H-Pro-Ala-NH-TG	78	22
3	H-Pro-Ser-NH-TG	94	63
4	H-Pro-D-Ser-NH-TG	87	68
5	H-Pro-Thr-NH-TG	Quantitative	60
6	H-Pro-D-Thr-NH-TG	87	61
7	H-Pro-Cys-NH-TG	89	51
8	H-Pro-Ser-Phe-NH-TG	22	77
9	H-Pro-Ser-Trp-NH-TG	13	76
10	H-Pro-Ser-Tyr-NH-TG	29	75

H-Pro-Ser-NH-TG = (DMSO: Acetone) (4:1), 16 h, Conversion 70%, ee 59%

SCHEME 5.153. Asymmetric aldol reaction with heterogeneous catalysts.
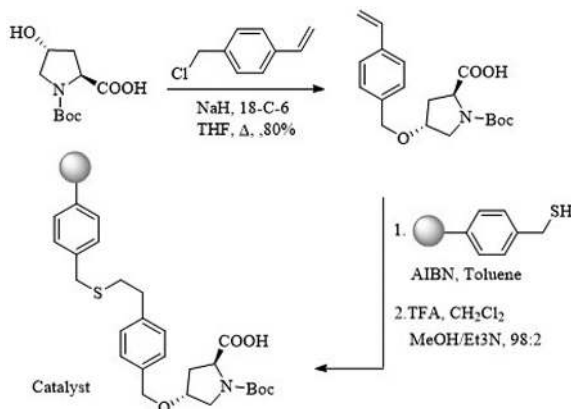
SCHEME 5.154. Synthesis of the polystyrene-supported proline catalyst.

R= C$_6$H$_5$, 4-CH$_3$C$_6$H$_4$, 2-ClC$_6$H$_4$, 3-ClC$_6$H$_4$,4-ClC$_6$H$_4$, 2,3,4,5,6-pentafluorobenzene
4-NO$_2$C$_6$H$_4$, 4-CF$_3$C$_6$H$_4$, 4-CNC$_6$H$_4$, furan, naphthalene,3-NO$_2$C$_6$H$_4$, 4-BrC$_6$H$_4$,

Yield (%): 31- 97 , Conv (%): 33- 99
anti/ syn: 85:15- >99:1 , ee (%): 90- 98

R = 4-NO$_2$C$_6$H$_4$, 4-CNC$_6$H$_4$

Yield (%): 31- 97 , Conv (%): 11- 98
anti/ syn: 50:50-> 95:5 , ee (%): 50- 97

A= cyclopentanone, cycloheptanone, tetrahydro-4H-pyran-4-one, , cyclohexanone,
acetone, butan-2-one, tetrahydro-4H-thiopyran-4-one
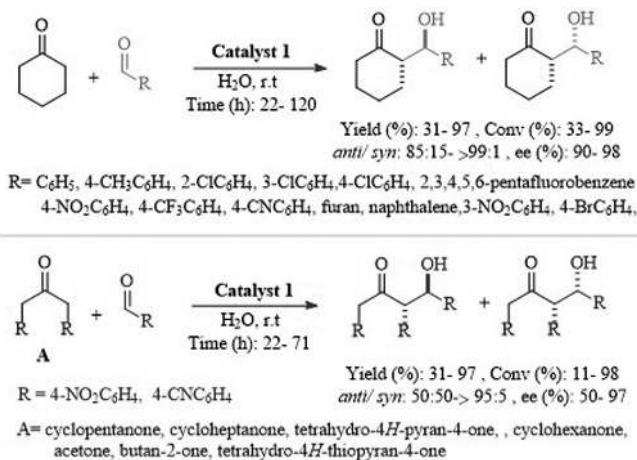
SCHEME 5.155. Direct asymmetric aldol reactions catalyzed by styrene-supported proline in the presence of water.

trans-4-(acryloyloxy)-L-proline hydrochloride, PEG dimethacrylate (cross-linker), and 2-hydroxy-4′-(2-hydroxyethoxy)-2-methylpropiophenone (radical initiator) (Schemes 5.160 and 5.161) [112]. The mixture was mixed with water. The solution was then vortexed and warmed to produce a homogeneous solution and sonicated. Two quartz plates were used to sandwich the solution. Finally, the reaction is irradiated with 365 nm light (2.3 mW/cm^2) for 1 h at room temperature. This ionic liquid polymer gel was applied for an aldol reaction. The authors reported that the yield of the desired product was affected by the water content around the proline unit in the thermoresponsive poly(ionic liquid) gels.
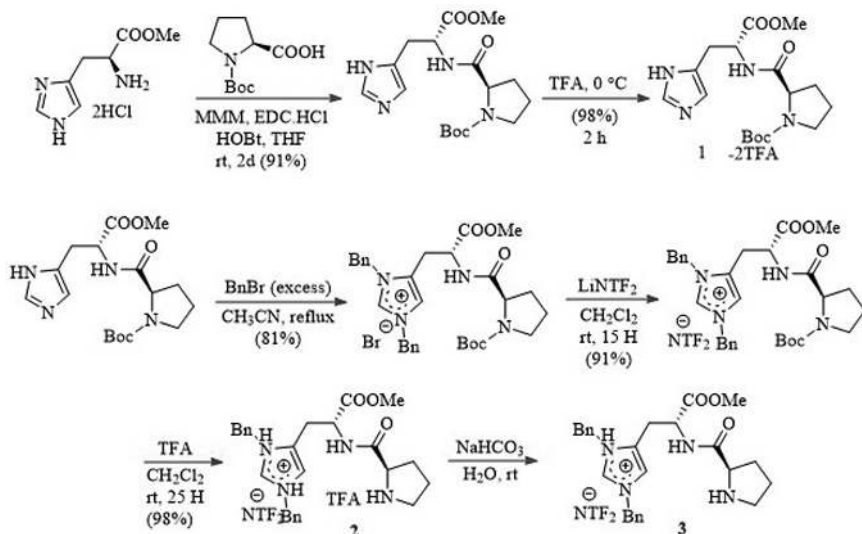
SCHEME 5.156. Synthesis of the proline-histidine dipeptide-derived catalysts.

Ar	Time(h)	Yield(%)	anti/syn	ant ee
4-CNC$_6$H$_4$	5	99	85:15	88
4-CF$_3$C$_6$H$_4$	5	99	86:14	89
4-CF$_3$C$_6$H$_4$	3	99	90:10	94
4-BrC$_6$H$_4$	5	83	89:11	93
4-ClC$_6$H$_4$	7	90	80:20	89
C$_6$F$_5$	2	99	>99:1	98
3-Pyridyl	3	95	93:7	94
2-NO$_2$C$_6$H$_4$	4	99	92:8	97
2-ClC$_6$H$_4$	8	81	93:7	90
3-NO$_2$C$_6$H$_4$	2.5	91	93:7	91
3-ClC$_6$H$_4$	24	98	88:12	86
4-Cl-3-NO$_2$C$_6$H$_3$	2	96	91:9	93
C$_6$H$_5$	18	91	81:19	69
4-MeC$_6$H$_4$	24	85	70:30	60
4-MeOC$_6$H$_4$	36	58	74:26	36
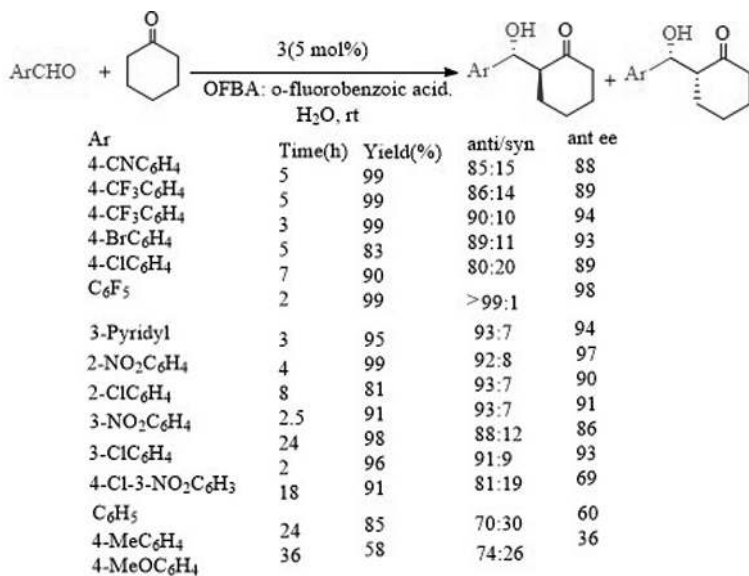
SCHEME 5.157. Asymmetric aldol addition of cyclohexanone to various aldehydes catalyzed by 3.
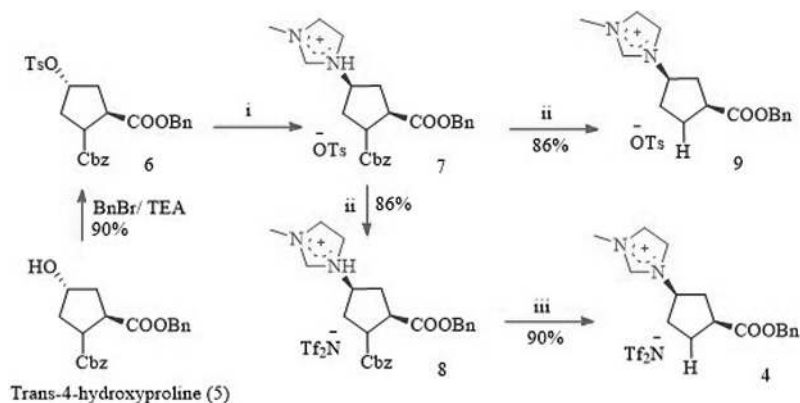
SCHEME 5.158. Synthesis of the *cis*-4-imidazolium-L-proline catalysts 4 and 9.

Ar	Time(h)	Yield(%)	ant:syn	anti ee(%)
2-NO$_2$-C$_6$H$_4$	12	97	99:1	99
4-CN-C$_6$H$_4$	12	95	99:1	95
4-CF$_3$-C$_6$H$_4$	12	72	97:3	96
C$_6$F$_5$	5	95	>99:1	96
3-pyridyl	5	95	98:2	93
4-pyridyl	2.5	99	98:2	90
4-Cl-C$_6$H$_4$	24	76	98:2	95
4-Br-C$_6$H$_4$	36	82	94:6	90
2-Cl-C$_6$H4	24	65	98:2	94
3-Cl-C$_6$H$_4$	24	76	96:4	95
Ph	60	73	93:7	95
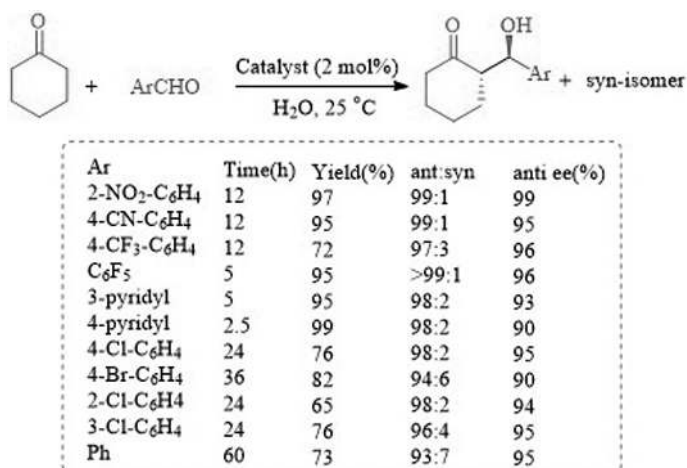
SCHEME 5.159. Asymmetric aldol reactions of cyclohexanone with various aldehydes catalyzed by 4 in the presence of water.

Trombinia and coworkers synthesized a new and efficient catalyst-labeled ion *cis*-(1a–c) with an amide bond between imidazolium and the proline ring (Scheme 5.162) [113]. Catalyst 1a has high efficiency in the reaction between aldehydes and ketones in an aqueous solvent, which leads to the production of a high percentage of the product (Scheme 5.163).

In 2011, Zhang et al. designed a novel asymmetric catalytic system with *N*-substituted pyrrolidine-ionic liquids as chiral additives for asymmetric aldol
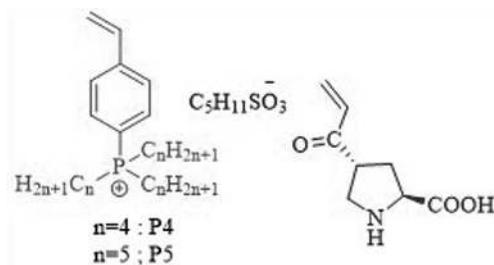
SCHEME 5.160. Structure of IL monomers Pn (n = 4 or 5) (left) and proline monomer (right).
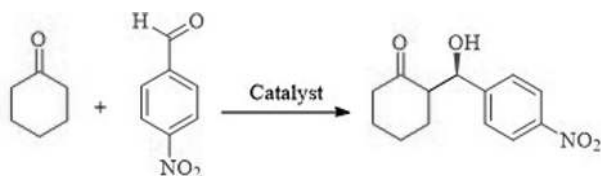
SCHEME 5.161. Asymmetric aldol reactions.
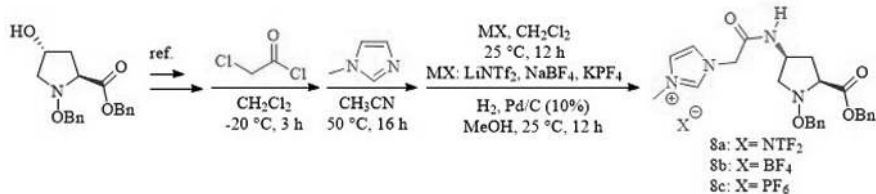
SCHEME 5.162. Synthesis of organocatalysts **1a-c** with ion-tagged.

RCHO: C$_6$F$_5$CHO, 4-MeOC$_6$H$_4$CHO,
n-pentanal, 2-methylpropanal,
4-NO$_2$C$_6$H$_4$CHO, ethyl glyoxalate
Ketone: cyclohexanone, acetone, hydroxyacetone

Yield: 35->99 %
ee: 35->99 %
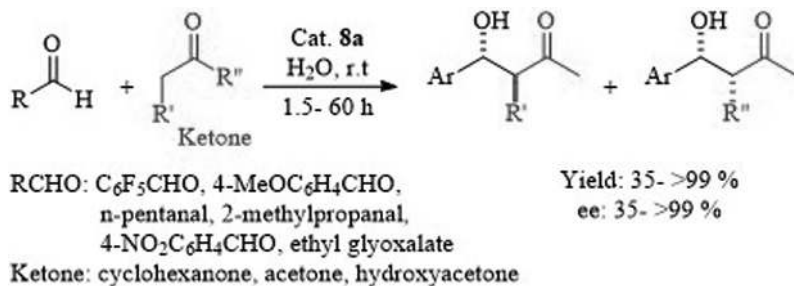
SCHEME 5.163. Asymmetric aldol reaction catalyzed by 1a.
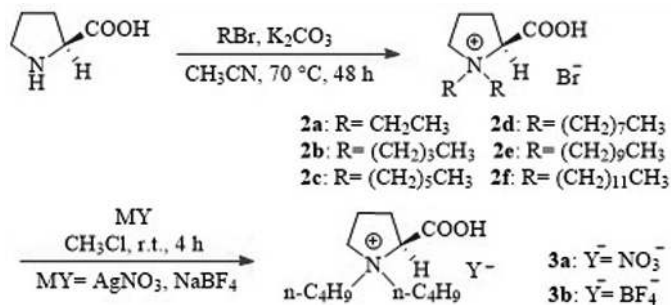
SCHEME 5.164. Synthesis of (L)-proline-based CILs.
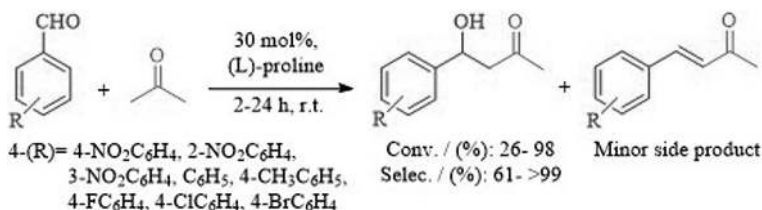
SCHEME 5.165. Aldol reaction of an aromatic aldehyde with acetone by (L)-proline.

reactions. This catalytic system provided high yields (up to 88%), good stereoselectivities (> 99:1), and superior enantiomeric excesses (up to 98%) for *syn*-selective aldol reactions (Schemes 5.164 and 5.165) [114].

5.11. APPLICATION OF METAL COMPLEXES OF L-PROLINE AS A CATALYST IN THE ALDOL REACTION

G/MF@SiO$_2$@ Cu(proline)$_2$ have been employed as catalysts for asymmetric aldol reaction in high yield and excellent enantiomeric excess >90% under solvent-free conditions [115]. The magnetic catalyst was prepared by treating Cu(police)$_2$ with G/MF@Si nanocomposite (Scheme 5.166).

The hybrid ZZnBMMs were reported to be active for asymmetric aldol reaction of cyclohexanone with 4-nitrobenzaldehyde (Scheme 5.167) [116]. The organic–inorganic mesoporous materials (ZZnBMMs) have been prepared by immobilization Zn-grafting into the surface of bimodal mesoporous silicas (BMMs) and followed via coordination of the (2S,2′ S)-N,N′-([2,2′-bipyridine]-3,3′-diyl) bis(pyrrolidine-2-carboxamide) (Z) to the Zn-modified BMMs. The detailed results show that the hybrid ZZnBMMs could recycle and reuse catalysts in petroleum ether and anhydrous methanol (CH$_3$OH). Among these solvents, petroleum ether gave the best result.
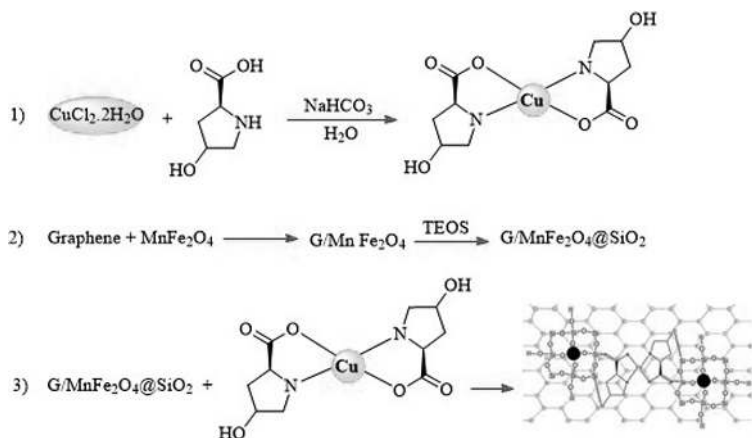
SCHEME 5.166. Stepwise preparation of G/MF@SiO$_2$@ Cu(proline)$_2$ and catalytic studies for the aldol addition.
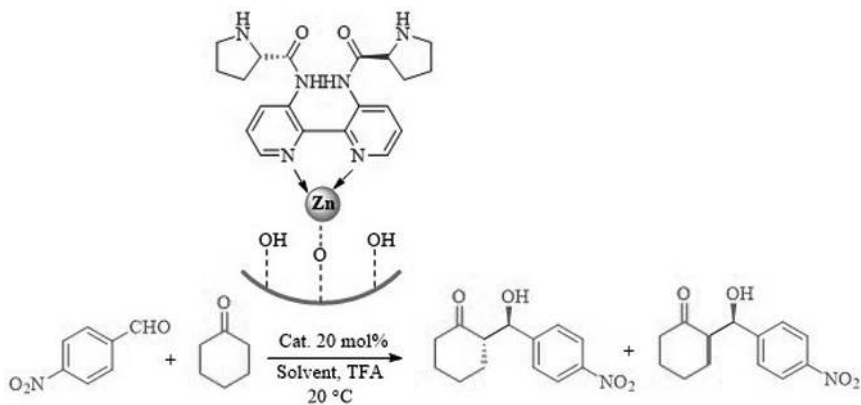
SCHEME 5.167. Application of catalyst (ZZnBMMs) in the direct asymmetric aldol reaction of cyclohexanone with 4-nitrobenzaldehyde.

Chromones are important substituents in many biologically active compounds. These compounds are also key building blocks for the preparation of various important biological heterocycles such as pyrazoline, benzodiazepines, flavonoids, and 1,4-diketone. In 2011, Siddiqui and Musthafa used Zn(L-proline)$_2$ as a catalyst for the synthesis of chromonyl chalcones compounds from the reaction between different heteroaldehydes and ketones (Scheme 5.168) [117].

Carbon–carbon bond synthesis is important in organic chemistry, and one of the reactions to create this bond is a Henry reaction that is performed by mixing nitroalkenes with aldehydes or ketones using a base resulting in the formation of beta-nitro alcohol. Beta-nitro alcohols are important mediators in chemistry because
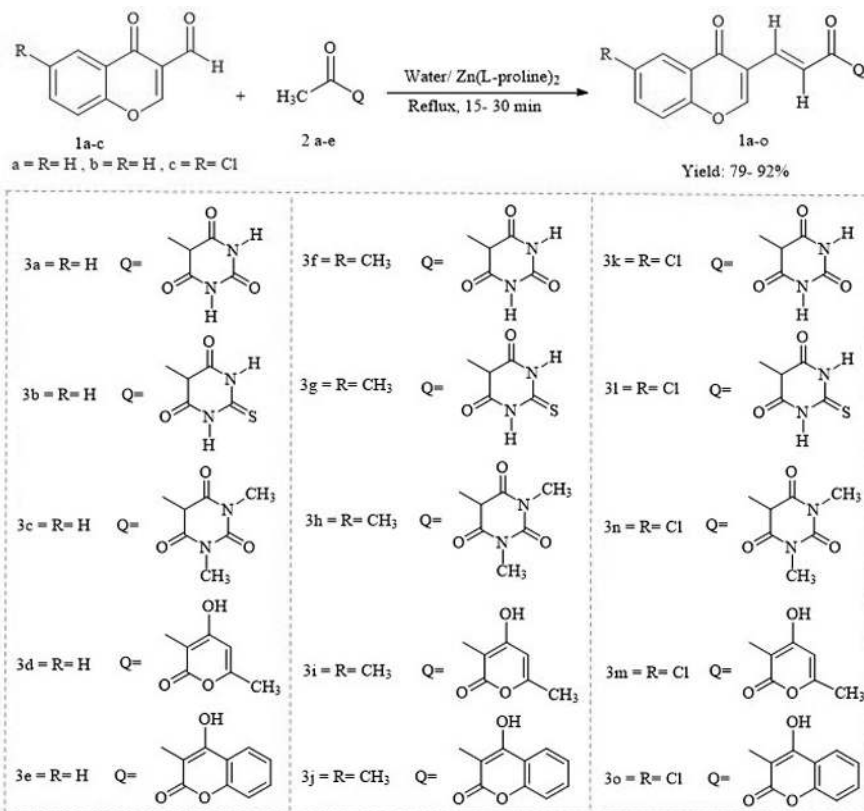
SCHEME 5.168.   Synthesis of chromonyl chalcones by Zn(L-proline)$_2$.

they are converted to alpha-nitro ketones by oxidation, to beta-amino alcohols by reduction, and to nitroalkenes by dehydration. Reddy et al. performed an example of this reaction at room temperature in the presence of Zn(proline)$_2$ complex as a catalyst and water solvent (Scheme 5.169) [118].

5.12. APPLICATION OF L-PROLINE AND L-PROLINE DERIVATIVE-BASED IONIC LIQUID–SUPPORTED MATERIAL AS AN ORGANOCATALYST IN THE ALDOL REACTION

A greener approach was introduced by Kui and Guillen for the preparation of proline-derived dipeptide catalyst 3 by the peptide coupling of proline on a ring-dialkylated histidine salt serving as ionic support, and the catalyst was evaluated in the enantioselective cross-Aldol reaction of substituted benzaldehyde derivatives with acetone in DMSO (Schemes 5.170 and 5.171) [119]. The amino acid containing [NTf$_2$] anion was selected as the ionic tag due to its hydrophobic property. Fully protected dipeptide 2 was produced by treating N-Boc-proline with the C-protected

A= 4-NO$_2$C$_6$H$_4$, 2-NO$_2$C$_6$H$_4$, 4-CNC$_6$H$_4$, 4-CF$_3$C$_6$H$_4$ Time (h): 0.25- 15
2-BrC$_6$H$_4$, C$_6$H$_5$, 2-OMeC$_6$H$_4$, and nicotinaldehyde,   Yield (%): 71- 98
2-naphthaldehyde, furan-2-carbaldehyde
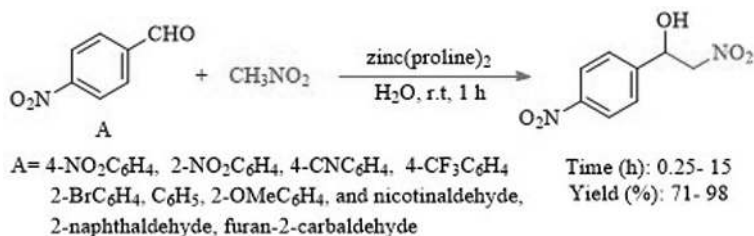
SCHEME 5.169. Direct nitroaldol reaction in aqueous media.
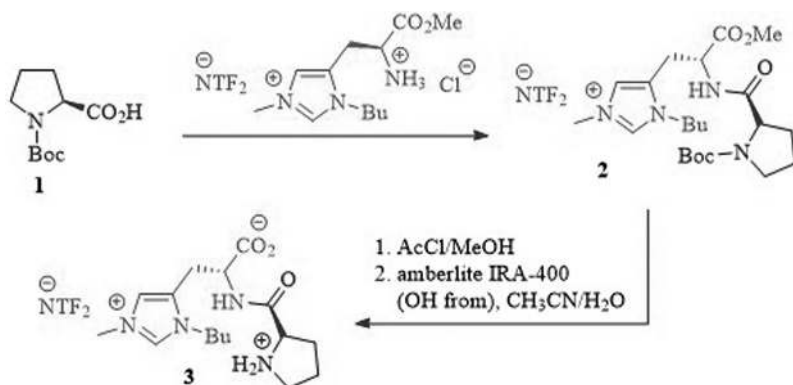
SCHEME 5.170. Production of protected dipeptide 2 and deprotection of dipeptide 3.

R	Time (h)	Conv. %	Ee %
-NO$_2$	9	92	40
-CN	78	92	n.d.
-C(O)CH$_3$	168	72	30
-C(O)OCH$_3$	78	0	-
-CF$_3$	78	100	33
-F	78	0	-
-H	78	0	-
-OMe	78	0	-
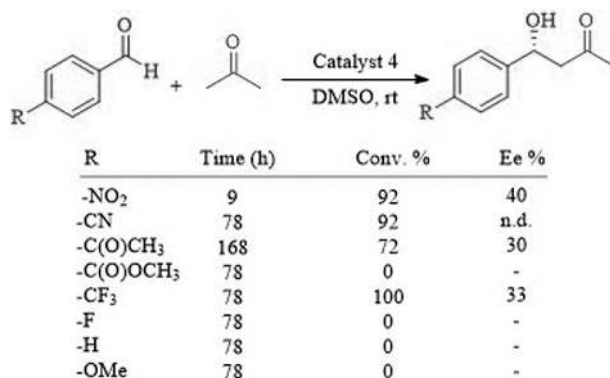
SCHEME 5.171. Aldol reaction catalyzed by dipeptide 3.

immobilized amino acid using HATU as the activation agent. Dipeptide 2 was fully eliminated in three steps to provide the free dipeptide 3 with an 88% yield. Then, the study of the electronic effects of substituents on the benzaldehyde were studied, and experimental results showed the existence of keto group providing the final product in moderate yields (72% conversion in seven days). Nevertheless, the reaction failed using ester groups. Conversely, when the reaction was performed in the presence of

m-CF$_3$ group, due to the inductive effect, the *m*-CF$_3$ group resulted in a relatively fast reaction (3 days), and the positive (donating) mesomeric effect of the fluorine atom prevented any reaction.

In 2016, Yadav and Singh synthesized an (L)-prolinamide imidazolium hexafluorophosphate using *trans*-4-hydroxy-(*S*)-proline. The synthesized ionic fluid was used as an effective organocatalyst for the reaction between ketones and different aldehydes. The Aldol reaction performed by the (L)-prolinamide catalyst produced products in good yield (Scheme 5.172) [120].

Yin and coworkers designed an effective L-proline catalyst by modifying L-proline onto IL-modified MNPs (Scheme 5.173). It is used to promote the aldehydes in direct asymmetric Aldol reaction in water. These NPs exhibited high performance for the reaction between cyclohexanone and 2-nitrobenzaldehyde within 12 h to provide the final product (yield: 92%), diastereoselectivity (dr: 88/12), and enantioselectivity (ee: 85%). The authors reported the existence of an IL linker in the supported L-proline catalyst provided the excellent catalytic activity of the catalyst's direct asymmetric aldol reaction. Moreover, the catalyst can be recycled and used several times without a significant loss of catalytic activity (Scheme 5.174) [121].

Chen et al. presented an example of the aldol reaction in the presence of ionic liquid–supported proline as a catalyst and chiral products with a high enantiomeric excess were obtained (Scheme 5.175) [122]. Also, this catalyst was separated and reused several times.

The asymmetric aldol reaction used proline-modified chiral ionic liquid as an effective organocatalyst between aldehydes and cycloalkanones in water (Scheme 5.176) [123]. Products with high *anti*-diastereoselectivity and enantiomeric excess were obtained and also the catalyst efficiency remained stable after five steps.

Bellis and Kokotos synthesized at the periphery a kind of immobilized poly(propylene imine) dendrimers (five generations) based on proline and applied
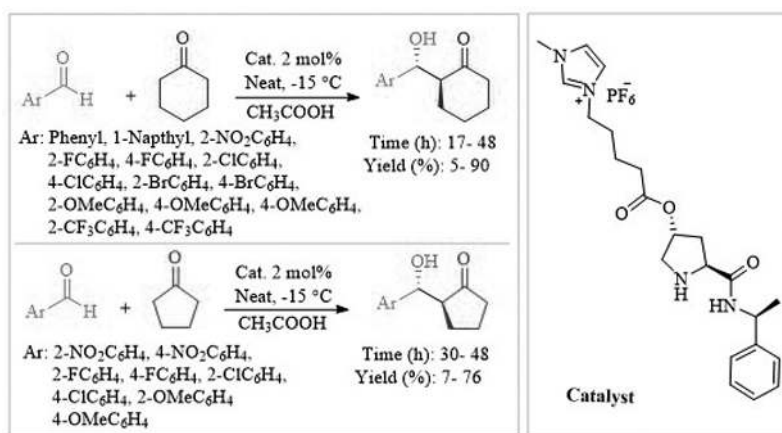
SCHEME 5.172. Aldol reaction between ketones and different aldehydes by prolinamide catalyst.
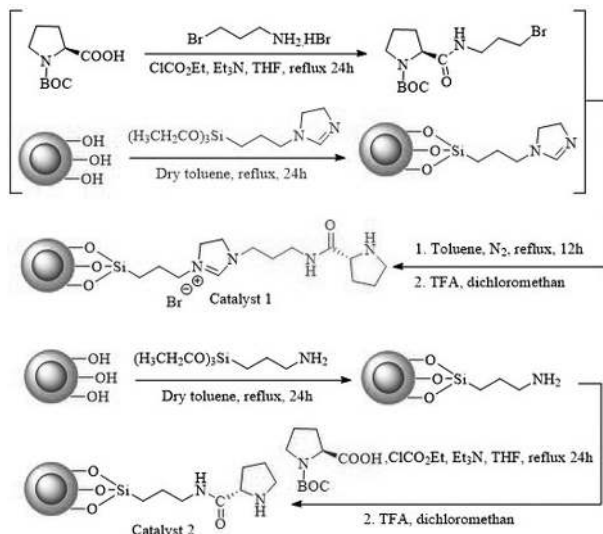
SCHEME 5.173. Synthesis of catalyst 1 and catalyst 2.
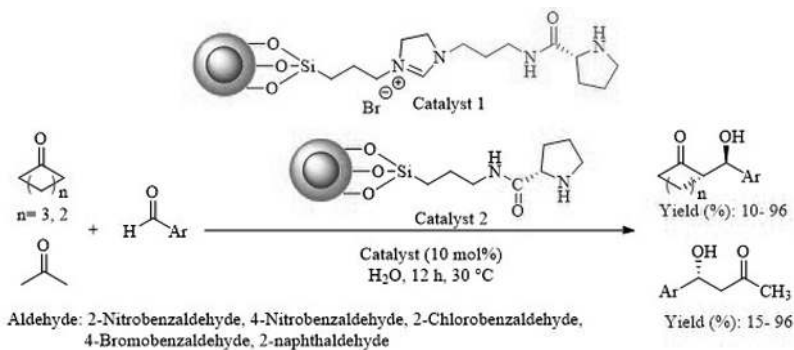
SCHEME 5.174. The aldol reaction is catalyzed by L-proline.

them as catalysts for asymmetric aldol reactions in much less time than similar cases and with good efficiency (Schemes 5.177 and 5.178) [124].

In another study, the performance of chiral ionic liquid containing L-proline as an efficient and recyclable asymmetric organocatalyst for aldol reaction was examined by Zhou and Wang (Scheme 5.179) [125]. The synthesis steps of nanocatalysts are shown in Scheme 5.179. The nanocatalyst showed good functional group tolerance for all the reactions, and the final product was produced in 65–93% yield.

In another important study, Zoltin and coworkers displayed the performance of (S)-proline/poly-(diallyldimethylammonium) hexafluorophosphate for direct asymmetric aldol reaction (Scheme 5.180) [126]. The reaction proceeded well with different benzaldehyde and the desired product was observed in 62–72% (Scheme 5.180).
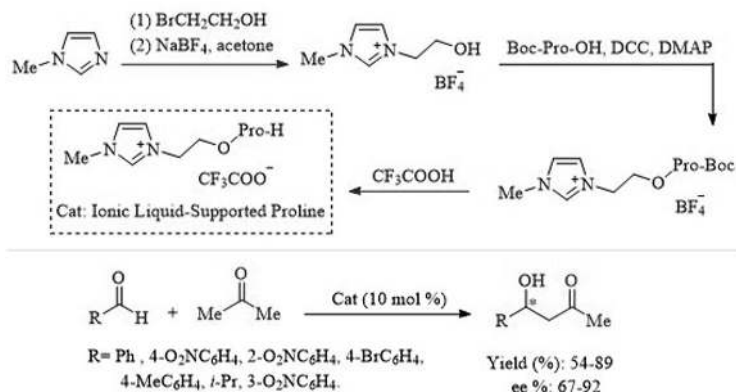
SCHEME 5.175. Ionic liquid-supported proline catalyzed aldol reaction.
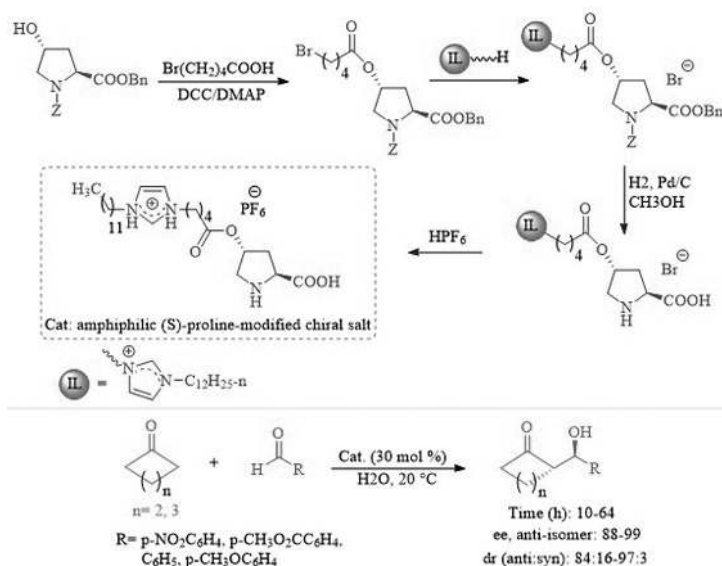
SCHEME 5.176. Production of asymmetric aldol reactions.

5.13. APPLICATION OF L-PROLINE AS AN ORGANOCATALYST IN MICHAEL'S ADDITION

Michael's addition reaction is widely applicable in the preparation of natural products and drugs. In this context, Salunkhe and coworkers described the asymmetric Michael addition of ketones to nitrostyrene in ionic liquid [MOEMIM]OMs using an L-proline catalyst with an enantiomeric excess (Scheme 5.181) [127]. In this reaction, cyclohexanone and nitrostyrene were used as raw materials and the product was synthesized in high yield and with great *syn*-selectivity.

Catalyst A; n= 8 , x= 14
Catalyst B; n= 4 , x= 6
Catalyst C; n= 16 , x=30
Catalyst D; n= 32 , x= 62
Catalyst E; n= 64 , x= 126

Catalyst A=(DAB(AM)₈ −[glt−H[γPro]₈).14HCl
diaminobutane poly(propyleneimine) dendrimers DAB(AM)n (n= 4, 8, 16, 32, 64).
1-hydroxybenzotriazole (HOBt)
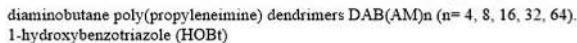
SCHEME 5.177.   Steps of making the dendritic catalyst.

R= 4-NO₂, 4-Br, 2-Cl

Yield (%):   61   70   78
ee (%):   65   67   64

Structure of Dendritic Catalyst

SCHEME 5.178.   Aldol reaction with Catalyst A.
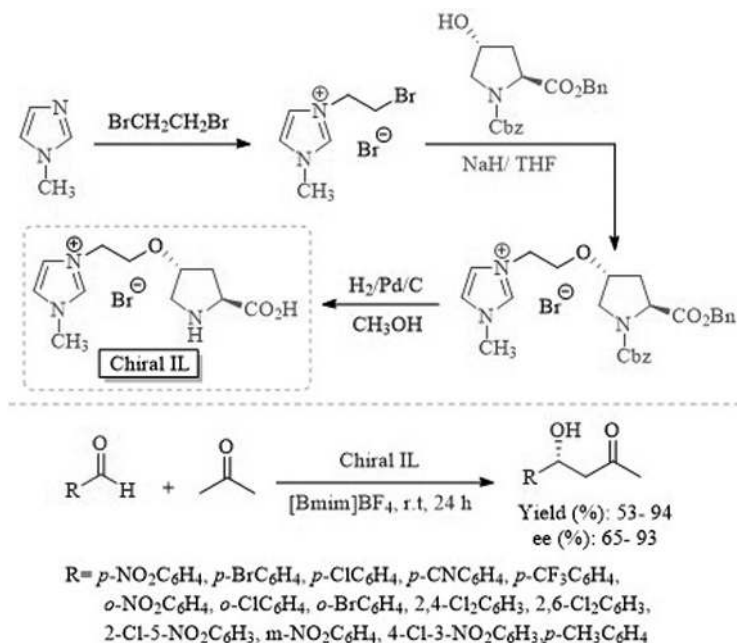
SCHEME 5.179. The performance of chiral ionic liquid containing L-proline for the aldol reaction.

Catalyst	4/5	Yield A [%]	ee A [%]
1a	10:2	55	67
2a	9:1	59	66
3a	15:1	53	69
3b	10:1	55	69

R= m-NO₂, p-NO₂, o-Cl, p-Cl, p-CO₂Me, p-CHO

Yield (%): 58- 98 , ee (%): 62- 72
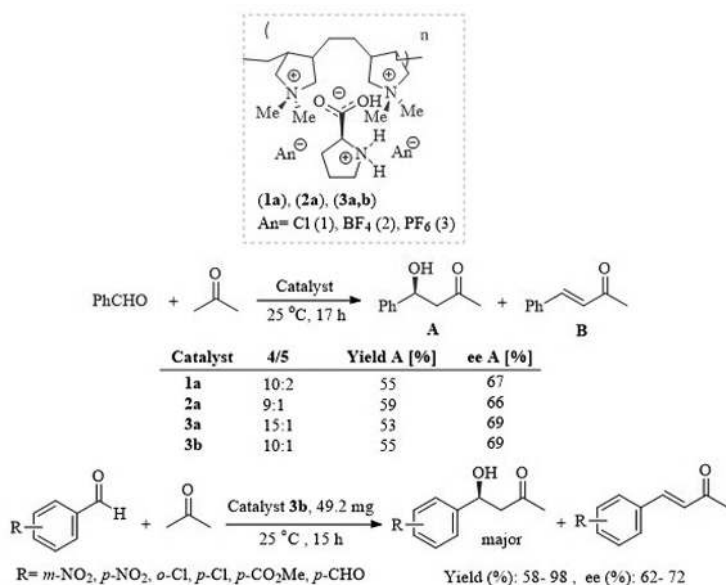
SCHEME 5.180. (*S*)-Proline/polyelectrolyte systems catalyzed direct aldol reaction between acetone and benzaldehyde.
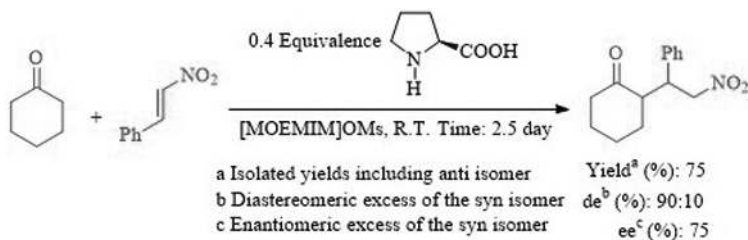
SCHEME 5.181.   Michael's addition of ketones to nitrostyrene catalyzed by ionic liquid-influenced L-proline.

5.14.   APPLICATION OF L-PROLINE DERIVATIVE AS AN ORGANOCATALYST IN MICHAEL'S ADDITION

In 2013, Poelarends and coworkers reported the application of proline-based enzyme-4-oxalocrotonate tautomerase to the asymmetric Michael addition between β-nitrostyrene and the linear aldehydes group (Scheme 5.182) [128]. This reaction was carried out well giving products in high to excellent yields under green conditions.

Anthrone is an atypical nucleophile because its reactive deprotonated form is of tautomeric type, forming a 9-anthranilate ion. This ion can act as a nucleophile, and a diene in Diels–Alder addition with reactive dienophiles. In 2012, Gawronski and coworkers used this combination with 2-cyclohexenone to synthesize *cis*-3-(9-anthryl) cyclohexanol compounds using L-proline as a catalyst (Schemes 5.183 and 5.184) [129].

Pitchumani and coworkers introduced the performance of proline-anchored hydrotalcite clays as an active catalyst for the asymmetric Michael addition. An asymmetric Michael addition was performed between acetone and nitroalkene as well as between nitromethane and α-, β-unsaturated ketones in the presence of catalyst HTLP (both result in the formation of the same product). Also, this chiral catalyst showed better performance than pure L-proline in the reaction of Michael's addition of the enamine and iminium type (Scheme 5.185) [130].

Michael's addition between carbonyl compounds and (*E*)-β-nitrostyrene in the presence of catalyst *N*-toluenesulfonyl-L-proline amide was reported by Berkessel and coworkers. According to the results, the highest velocity and enantioselectivity for ionic liquid bmim[BF$_4$] was obtained at room temperature. Also, the authors reported the activity of the catalyst was strongly dependent on the type and structure of the ionic liquid (Scheme 5.186) [131].

Enders and Chow synthesized 13 L-proline-derived organocatalysts and investigated their catalytic properties for the Michael addition between nitroalkenes and 2,2-dimethyl-1,3-dioxan-5-one (Scheme 5.187) [132]. Based on the results, catalyst M produces products with *syn*-diastereoselectivity and catalyst J produces products with *anti*-diastereoselectivity, which is certain given the proposed absolute transfer and configuration mode.

Oligopeptides are amino acid chains that number less than 15 amino acids and include dipeptides, tripeptides, and tetrapeptides. Peptides are made up of amino acid units that are linked by peptide bonds. In this study, the authors synthesized
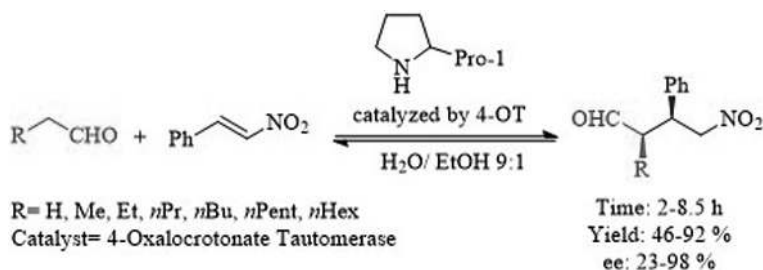
SCHEME 5.182. Proline-based enzyme-4-oxalocrotonate catalyzed Michael's addition.
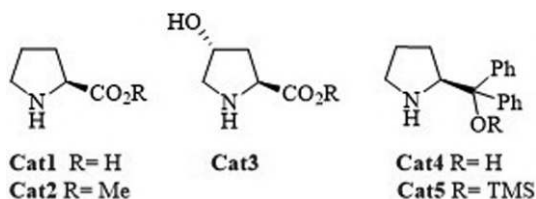
SCHEME 5.183. Catalysts used in the synthesis of *cis*-3-(9-anthryl) cyclohexanol.

Catalyst	Yield of 3 (%)	Ee (%)
Cat1	32	82
Cat2	39	0
Cat3	0	-
Cat4	0	-
Cat5	15	5
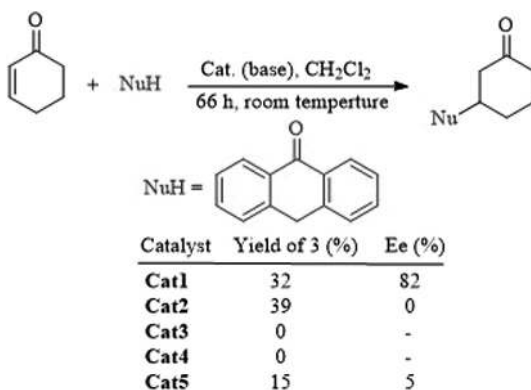
SCHEME 5.184. The reaction between 2-cyclohexenone and antrone by catalysts L-proline.

two chiral peptide catalysts based on 4-*trans*-amino proline and examined their efficiency in carbon–carbon bond formation (Scheme 5.188) [133]. Based on the results, the authors reported the reactivity of two peptide catalysts was higher than L-proline.

Nagata et al. described the application of 3-decyl-β -proline for Michael addition in water as the solvent. The preparation of 3-decyl-β -proline is shown in Schemes 5.189–5.190 [134]. The reaction carries out well to provide the final product in high yields and with excellent diastereoselectivities. The authors reported the presence of a decyl group in the catalyst resulted in an increase in the reaction rate due to hydrophobic interactions.

A	Conv. (%)	ee	% of enantiomers		% of enantiomers		ee	Conv. (%)	D
			E1	E2	E1	E2			
	100	14	57.0	43.0	26.7	73.3	46.6	41.2	
	100	19.4	59.7	40.3	32.2	67.8	35.6	40.5	
	64	8.40	54.2	45.8	27.5	72.5	45.0	21.5	
					46.6	53.4	6.80	50.1	
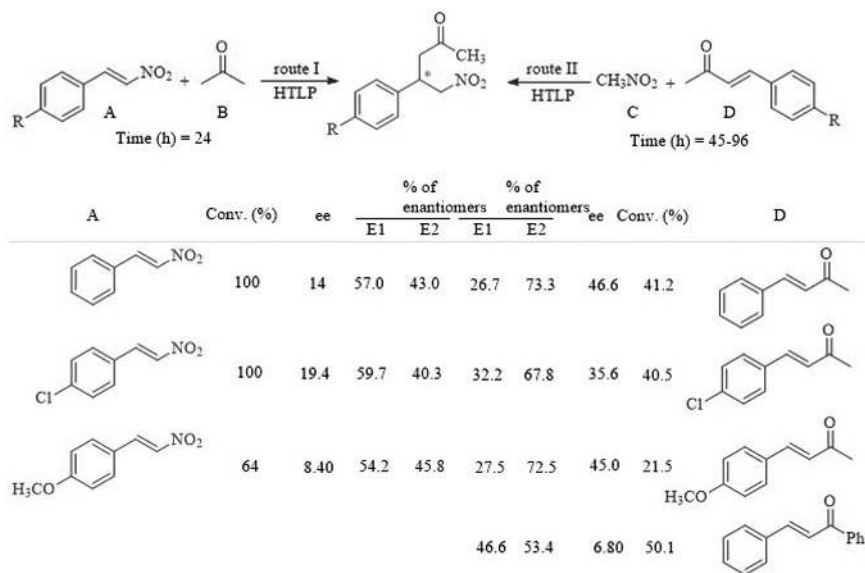
SCHEME 5.185. HTLP catalyzed the synthesis of Michael's adduct.
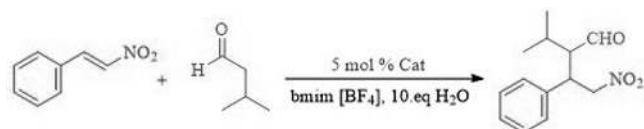
Time (min): 7 , ee (%): 30 (2R,3S)-(+)-2-Isopropyl-4-nitro-3-phenylbutanal
Time (min): 7.5 , ee (%): 36 (2R,3S)-(+)-2-Isopropyl-4-nitro-3-phenylbutanal
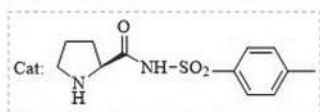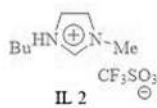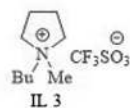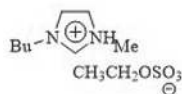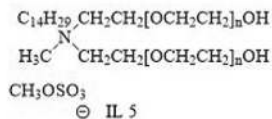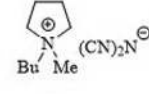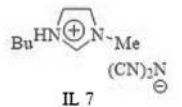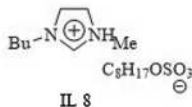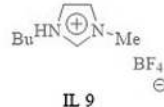
SCHEME 5.186. *N*-Toluensulfonyl-l-proline amide in ionic liquids-catalyzed Michael's addition.
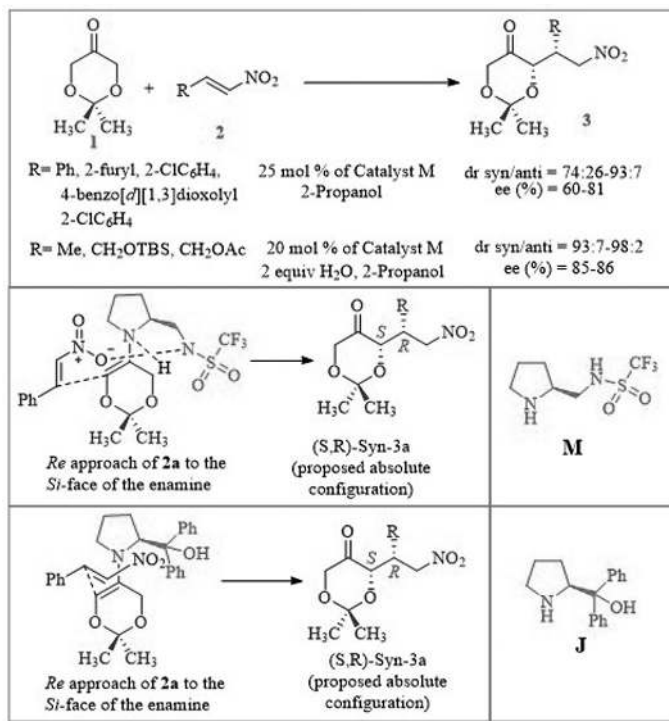
SCHEME 5.187.   Proline-based catalysts promoted asymmetric Michael addition.

5.15.   APPLICATION OF L-PROLINE AND L-PROLINE DERIVATIVE-BASED CHIRAL PHASE-TRANSFER CATALYSTS IN MICHAEL ADDITION

Asymmetric phase-transfer catalysis such as cinchona alkaloids and amino alcohols are powerful tools in many areas of chemistry for efficiently creating chiral functional molecules. Enantioselective Michael addition of various malonate esters to benzalacetophenone was reported under chiral phase-transfer catalysts derived from proline, mandelic acid, and tartaric acid (Schemes 5.191 and 5.192) [135]. Among various asymmetric phase-transfer catalysis examined, mandelic acid was the most effective. Consequently, phase-transfer catalysts with large cyclic rings exhibited more enantioselectivity than small cyclic rings (due to the steric hindrance effect in quaternary nitrogen of mandelic acid more than in quaternary nitrogen of proline and tartaric acid).

Peptide Catalyst (2 mol%)

trans-2,5-Dimethylpiperazine

CHCl$_3$, 5 d, rt

n=1, 2

Peptide Catalyst A	Yield (%): 40- 100 ,	ee (%): 57- 88
Peptide Catalyst B	Yield (%): 41- 100 ,	ee (%): 55- 82

Nitroalkane	CH$_3$NO$_2$	CH$_3$CH$_2$NO$_2$	(CH$_3$)$_2$CHNO$_2$		

Peptide Catalyst A
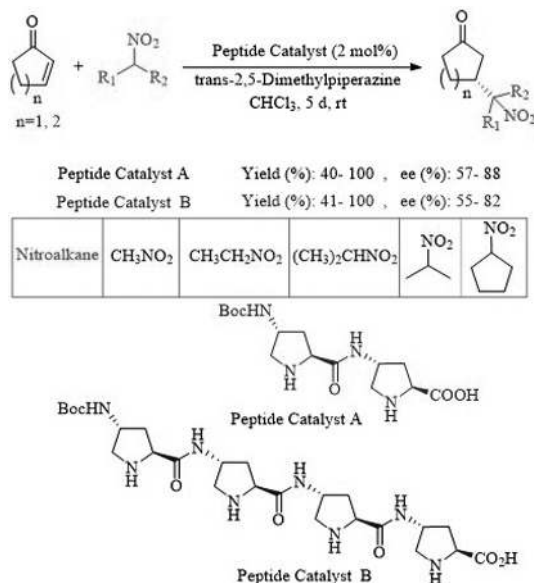
Peptide Catalyst B

SCHEME 5.188. Asymmetric C–C bond formation using 4-*trans*-amino-proline-based di- and tetrapeptides.

decyl-Br, K$_2$CO$_3$

80 °C, 57 h

ICH$_2$CO$_2$Et

TBAB(cat.), KOH

Et$_2$O, rt, 23h

CoCl$_2$, NaBH$_4$

MeOH, rt, 44 h

Lawessons reagent

THF, rt, 3h

1) Raney -Ni, H$_2$

THF

2) Cbz-Cl, K$_2$CO$_3$

THF/ H$_2$O: 3/1

TFA

CH$_2$Cl$_2$, rt, 22 h

H$_2$, Pd/C

MeOH, rt, 24 h
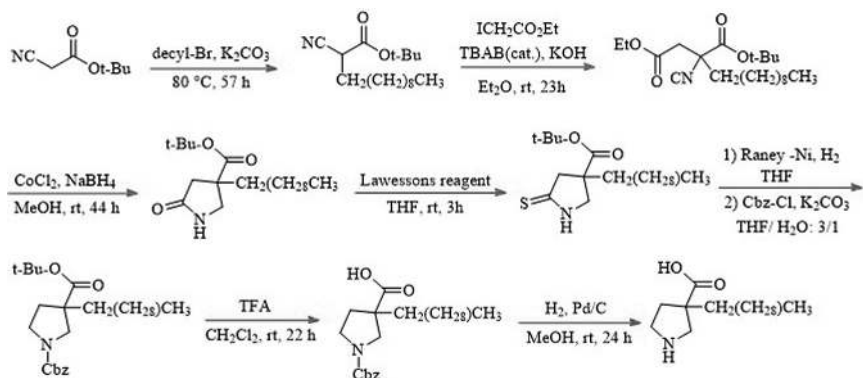
SCHEME 5.189. Synthesis of 3-Decyl-β-proline.

5.16. APPLICATION OF L-PROLINE AND L-PROLINE DERIVATIVE-SUPPORTED MATERIAL AS AN ORGANOCATALYST IN MICHAEL ADDITION

The Michael reaction of cyclohexanone with *trans-β* -nitrostyrene was reported under TOCN/proline catalysis (Scheme 5.193) [136]. In their procedure, TOCNs (2,2,6,6-tetramethylpiperidine 1-oxyl (TEMPO)-oxidized cellulose nanofibers) were generated by adding cellulose nanofibers to deionized water containing TEMPO,
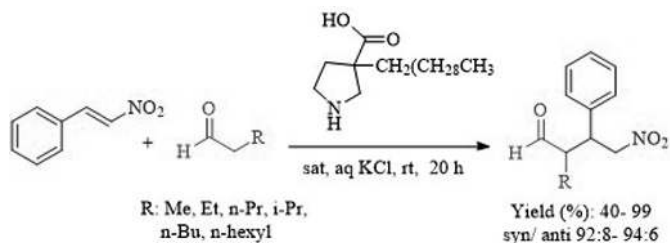
SCHEME 5.190. 3-Decyl-β-proline-catalyzed Michael addition.
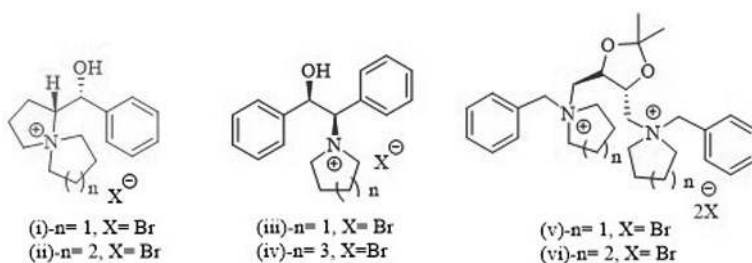
SCHEME 5.191. Chiral cyclic phase-transfer catalysts (i–vi).
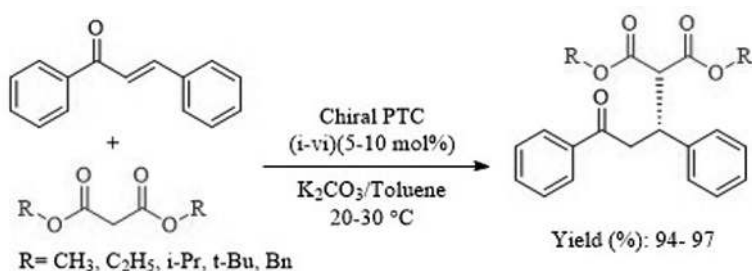
SCHEME 5.192. Chiral PTC prompted Michael's addition.
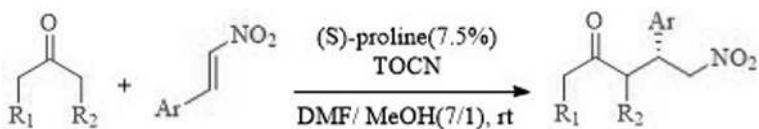
SCHEME 5.193. Nanocellulose and proline in organocatalytic Michael additions.

NaBr and followed by adding hypochlorite (due to TEMPO-mediated oxidation) to the suspension. The resultant reaction mixture was stirred at room temperature, while the suspension was maintained at pH 10 using a pH titrator. The authors found a low yield and poor enantioselectivity were produced in the presence of proline alone. Also, employing TOCNs alone without proline gave only a low yield of the desired product. Thus, (S)-proline/TOCNs was found to be very effective.

Zhao and coworkers designed a kind of poly(ethylene glycol)-supported catalyst based on proline and used for the asymmetric Michael addition of ketones to nitro-styrene at room temperature. Experimental results show that poly(ethylene glycol)-supported catalysts offer higher enantiomeric excesses (up to 86%) than that of nonsupported proline (Scheme 5.194) [137].

5.17. APPLICATION OF METAL COMPLEXES OF L-PROLINE AS A CATALYST IN MICHAEL'S ADDITION

In a very efficient way, Lee et al. synthesized thiophenol of α- and β-enones with thia-Michael addition [138]. In the first method, the reaction between α,β-enones and thiophenol was performed using complex 1 as a catalyst for the Michael addition (Schemes 5.195–5.197). In the second method, cycloenones were used to synthe-size the thiophenol compounds. For the synthesis of complex 1, a combination of 2,6-bis(bromomethyl)pyridine and methyl L-prolinate was used, which reacted each of these compounds separately and finally mixed to synthesize the main compound of complex 1.
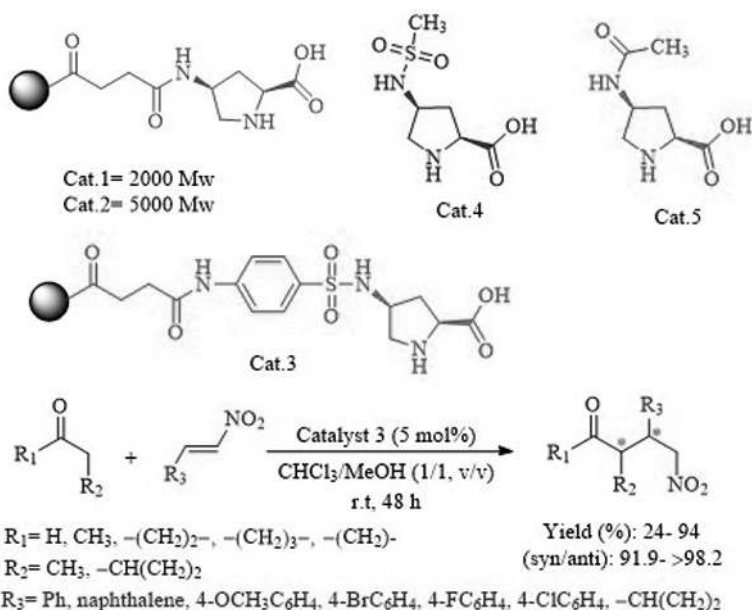
SCHEME 5.194. Poly(ethylene-glycol)-supported catalyst based on proline catalyzed the asymmetric Michael addition.
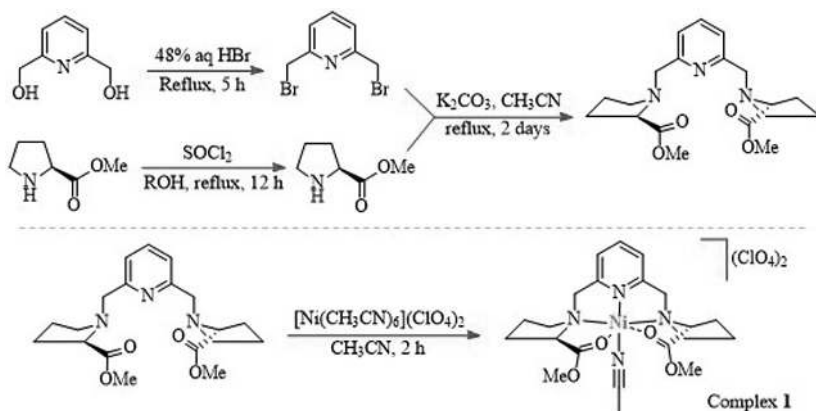
SCHEME 5.195. Synthesis of Complex **1.**

Micheal acceptor:

Micheal donor: 4-CH$_3$OC$_6$H$_5$SH, 4-CH$_3$C$_6$H$_5$SH, C$_6$H$_5$SH, 4-NO$_2$C$_6$H$_5$SH
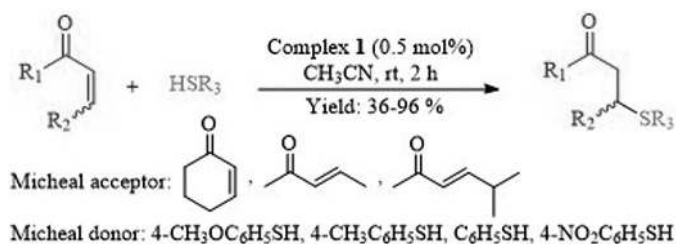
SCHEME 5.196. Synthesis of thiophenol of α,β-enones with thia-Michael addition.

Micheal acceptor:

n= 1   n= 2   n= 3

Micheal donor: 4-CH$_3$OC$_6$H$_5$SH, 3-CH$_3$OC$_6$H$_5$SH, 2-CH$_3$OC$_6$H$_5$SH
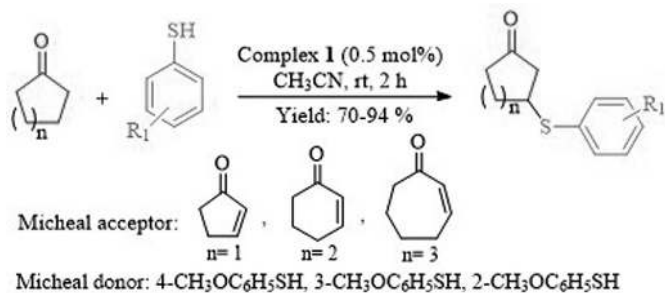
SCHEME 5.197. Synthesis of thiophenol of cycloenones with Thia-Michael addition.

5.18.   APPLICATION OF L-PROLINE AND L-PROLINE DERIVATIVE-BASED IONIC LIQUID AS AN ORGANOCATALYST MICHAEL ADDITION

Michael's addition reaction of *b*-nitrostyrene and *n*-pentanal was reported by L-proline in ionic liquid (Scheme 5.198) [139]. Optimization studies showed that [Bmim][NTf$_2$] ionic liquid was the best medium for this reaction. The advantage of this procedure is the recovery of ionic liquid for five cycles.

In 2017, Chandak and coworkers used the L-proline nitrate ionic liquid as a green and effective catalyst for conjugate addition of thiophenol to the sulfonamide chalcones in thia-Michael reaction to form a C—S bond and produced the β-sulfidocarbonyl compounds (2a–n) (Scheme 5.199) [140].

5.19.   APPLICATION OF L-PROLINE AS AN ORGANOCATALYST IN THE MANNICH REACTION

The Mannich reaction is an organic chemical process resulting in the amino alkylation of an acidic proton placed next to a carbonyl functional group. The Mannich reaction is used in the synthesis of medicinal compounds such as fluoxetine, tramadol, and tolmetin, as well as in the production of detergents and soaps. Barbas and coworkers introduced an asymmetric Mannich reaction between N-PMP protected
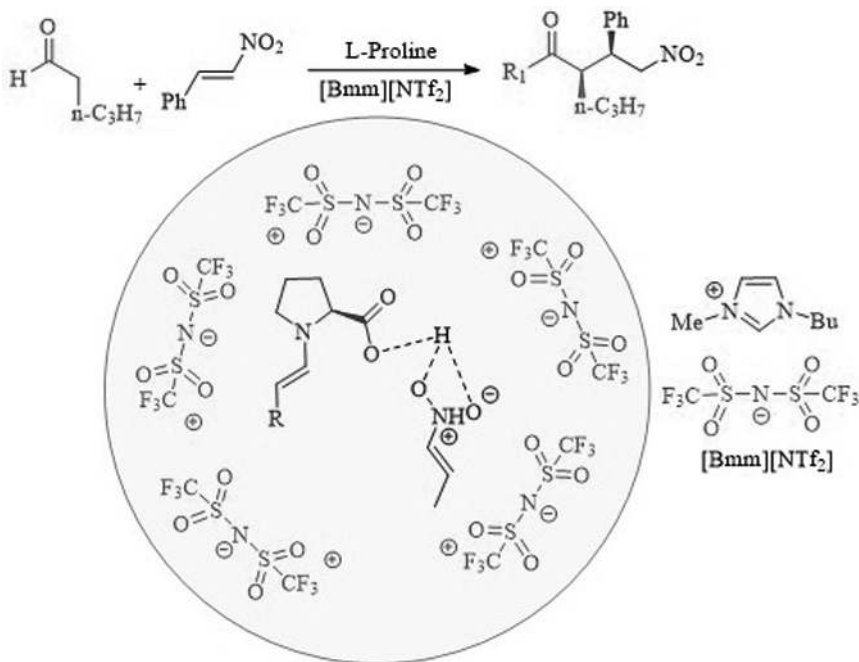
SCHEME 5.198.   Asymmetric Michael reaction.

R: H, CH₃
Ar: 4-OMeC₆H₄, 4-ClC₆H₄, 4-FC₆H₄, 4-Br-C₆H₄,
 4-iPrC₆H₄, 2-ClC₆H₄, 4-MeC₆H₄, C₆H₅
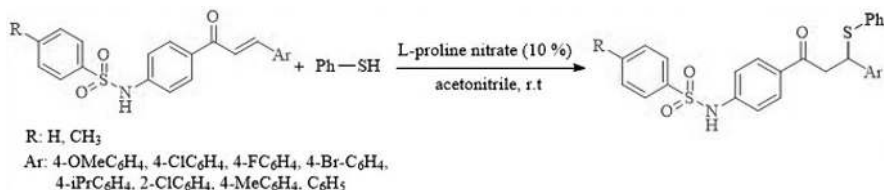
SCHEME 5.199. Synthesis of β-sulfidocarbonyl compounds (2a–n) by thiophenol and sulfonamide chalcones via L-proline nitrate as a catalyst.

and various aldehydes and ketones using L-proline as a catalyst in [bmim][BF₄] ionic liquid (Schemes 5.200 and 5.201) [141]. Also, the system conducted well for different aldehydes and ketones, and *p*-OMe aniline, resulting in the formation of products in excellent yields.

Shun and coworkers presented the performance of amide ionic liquids (AILs)/L-proline for Mannich, and products in good yields and with high stereoselectivities were obtained (Scheme 5.202) [142].

5.20. APPLICATION OF L-PROLINE DERIVATIVE AS AN ORGANOCATALYST IN THE MANNICH REACTION

Active natural and unnatural α-amino acids are important synthetic building blocks for the synthesis of biologically important molecules. In a related example, Wang et al. demonstrated the performance of pyrrolidine-sulfonamide for the Mannich reaction between ketones and α-amino esters to prepare α-amino acids (Scheme 5.203) [143].

Entry	R^1	R^2	Yield (%)	ee (%)
1	H	n-butyl	87	>99
2	H	n-pentyl	96	>99
3	H		95	>99
4	H	i-propyl	90	93
5	Me	Me	77	>99
6c	-(CH2)-	-(CH2)-	99	>99
7	Me	H	80	97

c: 1 mol of L-proline, 1h
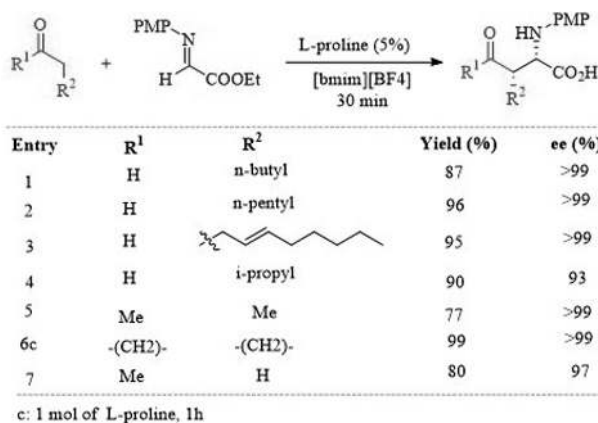
SCHEME 5.200. Direct asymmetric Mannich reaction between N-PMP protected and aldehydes and ketones catalyzed by L-proline in [bmim][BF₄].
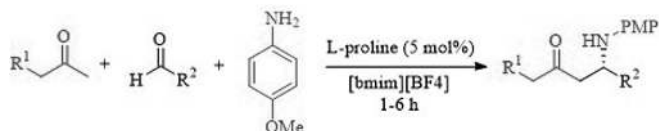
Entry	R¹	R²	Yield (%)	ee (%)
1	H	-Ph-p-NO₂	54	95
2	H	-1-naphthalene	63	82
3	allyl	-Ph-p-NO₂	60	87
4	allyl	-1-naphthalene	52	93
5	H	-i-propyl	80	43
6	H	-CH₂-O-CH₂Ph	98	93

SCHEME 5.201. Mannich reaction catalyzed by L-proline in [bmim][BF₄] ionic liquid.
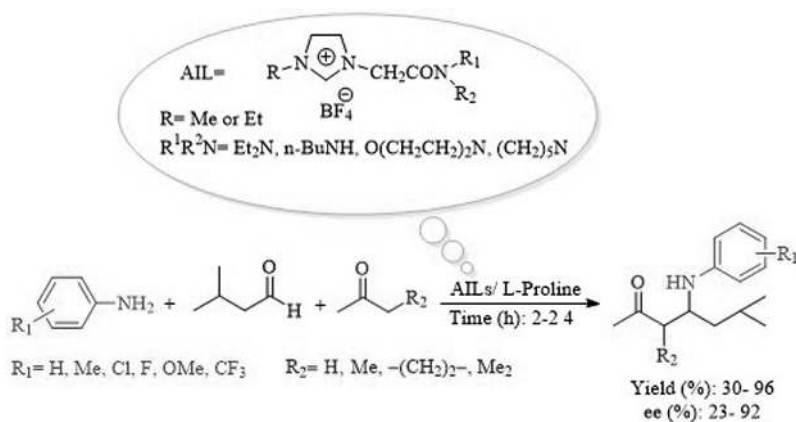
SCHEME 5.202. Mannich reactions prompted by amide ionic liquids (AILs)/L-proline.
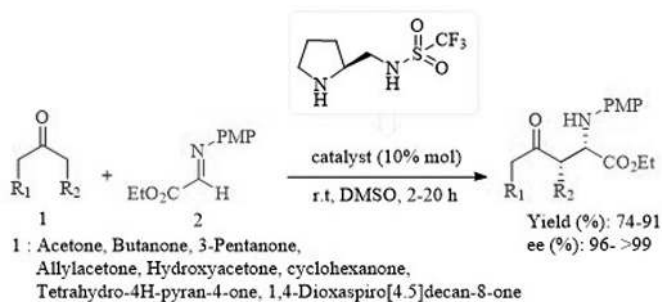
SCHEME 5.203. Mannich reaction between 1 and 2 by catalyst pyrrolidine-sulfonamide.

5.21. APPLICATION OF L-PROLINE AND L-PROLINE DERIVATIVE-SUPPORTED MATERIAL AS AN ORGANOCATALYST IN THE MANNICH REACTION

Safaei-Ghomi and Zahedi have reported a facile and sustainable protocol for the Mannich reaction using Fe_3O_4@L-proline. The catalyst was produced by deploying the amino acid L-proline on the surface of magnetic nanoparticles. This reaction performed well providing the final products in high to excellent yields (Schemes 5.204 and 5.205) [144].

5.22. APPLICATION OF L-PROLINE DERIVATIVE AS AN ORGANOCATALYST IN THE KNOEVENAGEL CONDENSATION

The activity of proline was studied with Knoevenagel concentration between diethyl malonate and various aromatic and aliphatic aldehydes by Shang and coworkers. The reaction was conducted well in ionic liquids [bmim][BF_4] and [emim][BF_4], giving the desired products in 27–100% yield. Moreover, the results showed that ionic liquids were more effective than other organic solvents (Scheme 5.206) [145].
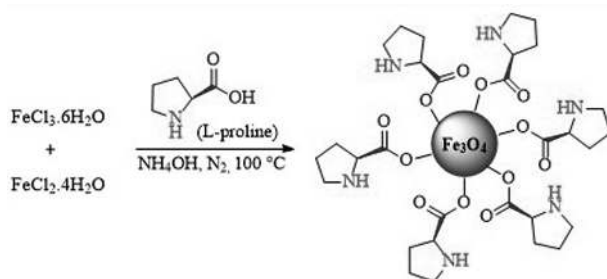
SCHEME 5.204.   Schematic portrait of the preparation of Fe_3O_4@L-proline nanoparticles.

R: H, 2-Cl, 4-Cl, 4-Me, 4-OMe, 2-OMe,
2-Br, 2,3-OMe, 2,5-OMeC₆H₃
R': H, Ph, 4-Cl, 3-Me, 4-Me

Yield (%): 85- 90
Anti/ syn: 97:3- 99:1
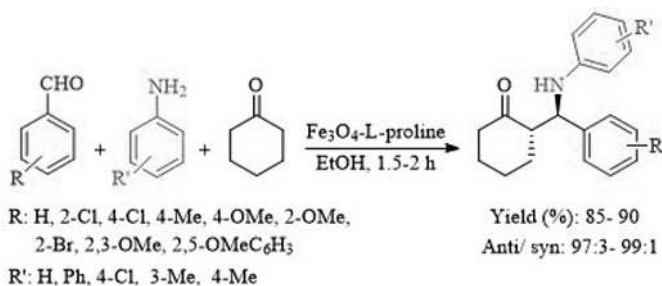
SCHEME 5.205.   Manich reaction by deploying L-proline on the surface of magnetic nanoparticles.

5.23. APPLICATION OF L-PROLINE-SUPPORTED MATERIAL AS AN ORGANOCATALYST IN THE KNOEVENAGEL CONDENSATION

In 2022, Kalantari et al. introduced the performance of proline–Cu complex-based 1,3,5-triazine coated on Fe_3O_4 magnetic nanoparticles as a green and recyclable nanocatalyst for the Knoevenagel condensation through malononitrile as well as different aldehydes in H_2O as a green solvent at room temperature (Scheme 5.207) [146]. This procedure's main advantages over other reported methods are shorter reaction, simpler workup, and eco-friendly.

Poly(*N*-isopropylacrylamide-*co*-L-proline) was reported to be an active catalyst for Claisen–Schmidt and Knoevenagel condensations (Schemes 5.208–5.210) [147]. In this system, poly(*N*-isopropylacrylamide-*co*-L-proline) showed more activity than the corresponding monomer L-proline in Claisen–Schmidt and Knoevenagel condensation reactions. The system is compatible with a range of substrates, offering well to excellent yields. The organocatalyst was separated and reused in the
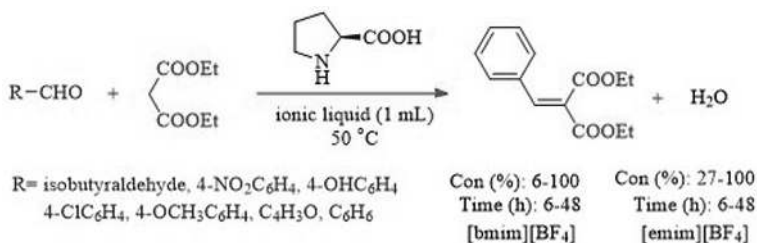
SCHEME 5.206.   Knoevenagel condensation in ionic liquid prompted by proline-catalyzed.
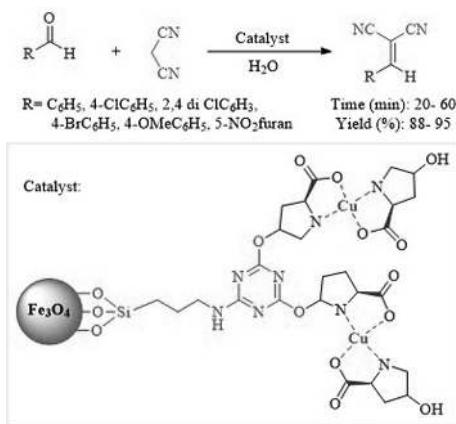
SCHEME 5.207.   The proline-Cu complex-based 1,3,5-triazine coated on Fe_3O_4 MN catalyzed Knoevenagel condensation.
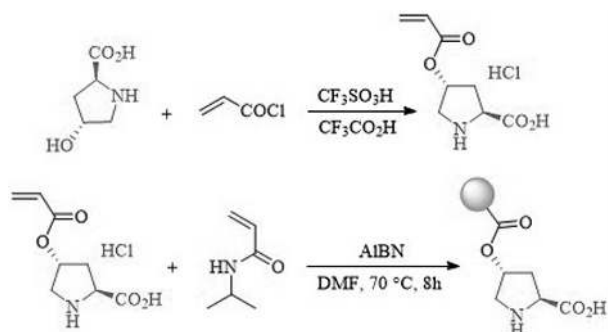
SCHEME 5.208. Preparation of the polymer-supported proline catalyst.
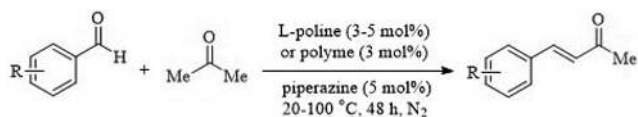
R	Yield (%)	
	L-Proline	Polymer
Ph	70	75
4-Me	40	70
3-Me	53	70
2-Me	47	71
4-MeO	51	61
4-Cl	42	60
3-Cl	48	50
2-Cl	41	42
4-F	44	54
H	71	73

SCHEME 5.209. Catalyst evaluations for the Claisen–Schmidt condensations of aldehydes with acetone.
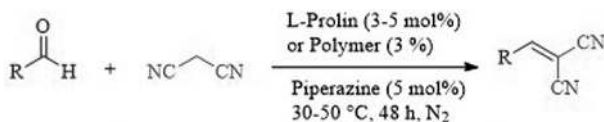
R	Yield (%)	
	L-Proline	Polymer
Ph	48	75
4-MeC$_6$H$_4$	71	70
4-ClC$_6$H$_4$	68	78
2-C$_4$H$_3$S	79	75
2-C$_{10}$H$_7$	60	83
C$_6$H$_{11}$	37	19

SCHEME 5.210. Knoevenagel condensations of aldehydes with malononitrile.

excess acetone and could be easily recycled and reused at least ten times without deactivation.

A simple and comfortable method for multicomponent reactions and the synthesis of different benzylidene malononitrile derivatives using amino acid–efficient silica as a heterogeneous catalyst. In this context, the silica-L-proline designed by Gupta et al. was examined by FT-IR, SEM, TEM, and thermal gravimetric analysis (TGA) analysis. Therefore, this group synthesized benzylidene malononitrile derivatives by SiO_2-L-proline as a catalyst from the reaction between aldehydes with malononitrile in acetonitrile at 80°C (Schemes 5.211 and 5.212) [148].

5.24. APPLICATION OF L-PROLINE AS AN ORGANOCATALYST IN THE BAYLIS–HILLMAN REACTION

The Baylis–Hillman reaction is known to be one of the most important carbon–carbon bond-forming from an aldehyde and an activated alkene. In this context, Gruttadauria et al. presented the Baylis–Hillman reaction in the presence of sodium carbonate and the L-proline catalyst (Scheme 5.213) [149].
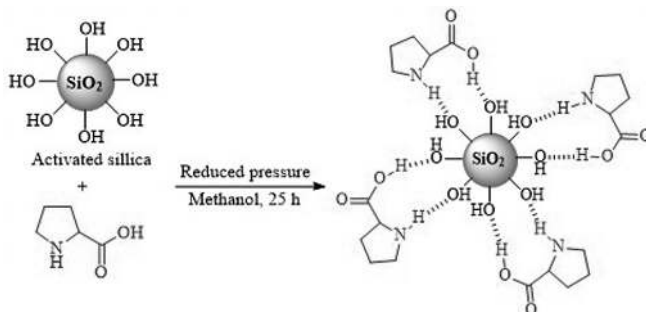
SCHEME 5.211.   Synthesis of SiO_2-L-proline.
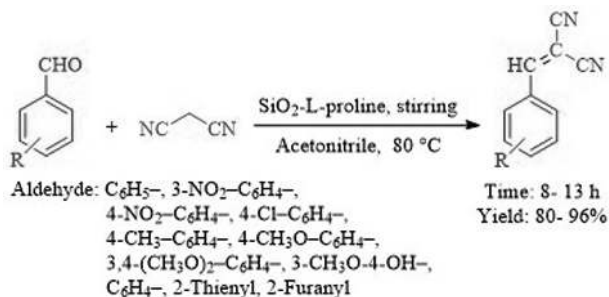
SCHEME 5.212.   The synthesis of benzylidene malononitrile derivatives using SiO_2-L-proline.

Bombonato and coworkers used different amino acids to synthesize amino acids in ionic liquids. In this method, they used ammonium derivatives of glycerol as the cation and the amino acids as the anion (Schemes 5.214 and 5.215) [150]. These AAILs were used to catalyze the Morita–Baylis–Hillman reaction. AAILs made from L-proline and L-histidine were able to catalyze the MBH reaction between methyl vinyl ketone and aromatic aldehydes without the need for a solvent or cocatalyst. However, the AAILs formed from L-valine, L-leucine, and L-tyrosine are not able to perform the MBH reaction without the presence of imidazole as an additive

R^1 = Me, Et

L-proline (10 mol %)
NaHCO$_3$ (25 mol %)
DMF/H$_2$O 9:1, 40 °C

21 example
Time (h): 16– 120
% Conv.[a]: 42– 99
% Isol. yield[b]: 32– 93

R^2 = Ph, 4-Me-C$_6$H$_4$, 4-NO$_2$-C$_6$H$_4$, 4-Cl-C$_6$H$_4$, 4-Br-C$_6$H$_4$, 3-NO$_2$-C$_6$H$_4$, 3-Cl-C$_6$H$_4$, 2-Cl-C$_6$H$_4$, 2-F-C$_6$H$_4$, 2-furyl, 2-CN-C$_6$H$_4$, 2-Cl-C$_6$H$_4$, 3-OMe-C$_6$H$_4$, 2,6-Cl$_2$C$_6$H$_3$, 3-Br-C$_6$H$_4$, 2-Cl-5-NO$_2$C$_6$H$_3$, 4-CN-C$_6$H$_4$, 4-CF$_3$-C$_6$H$_4$

[a] Determined by ^{1}H NMR spectroscopy
[b] After column chromatography
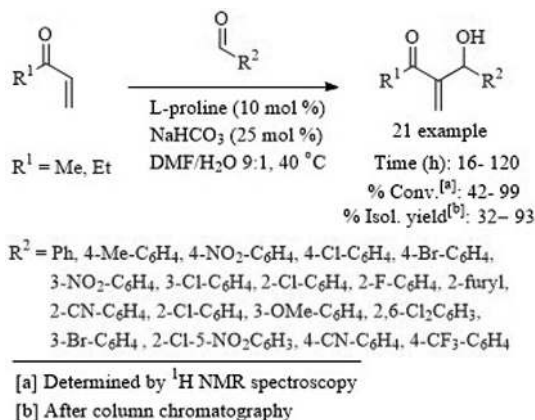
SCHEME 5.213. Baylis–Hillman reaction with L-proline catalyst.

1a-e   n= 1 (1a-d; 2a-d)   2a-e
              n= 2 (1e; 2e)

AA- =

a   b   c
L-valinate   L-leucinate   L-prolinate

d   e
L-histidinate   L-tyrosinate
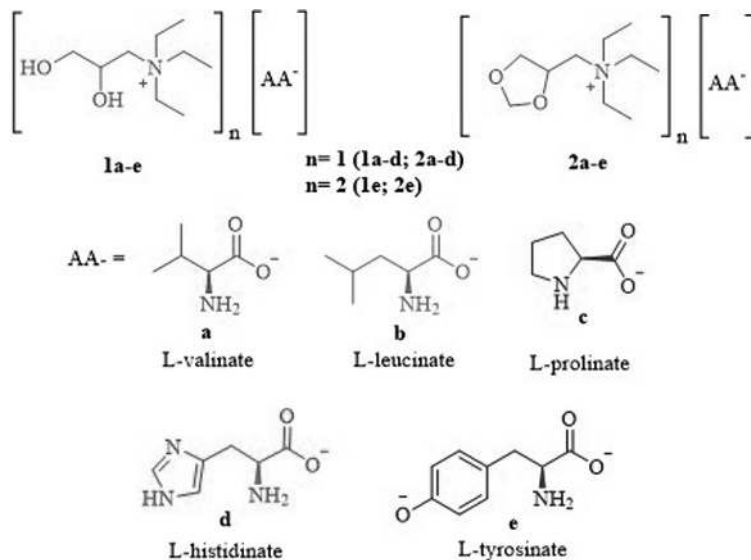
SCHEME 5.214. Structure and formulation of the synthetic AAILs.
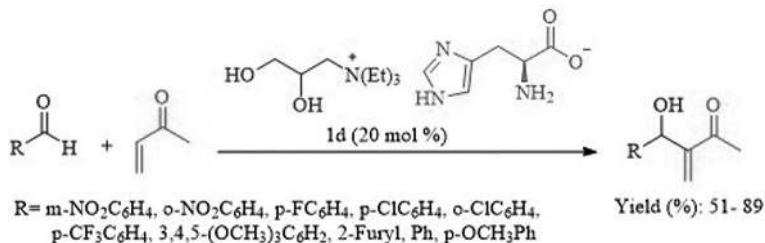
SCHEME 5.215. MBH reaction between methyl vinyl ketone and various aromatic aldehydes catalyzed by AAIL **1d**.

(cocatalyst). Although side reactions occur in the imidazole ring part of the **1d** AAIL, the active part of the catalyst is the first type of amine, which retains its activity after five recoveries and reuses (from 68% to 60%).

5.25. APPLICATION OF L-PROLINE-SUPPORTED MATERIAL AS AN ORGANOCATALYST IN THE BAYLIS–HILLMAN REACTION

In 2011, Kudo and coworkers were able to synthesize indene derivatives through the Morita–Baylis–Hillman reaction in the presence of resin-supported proline as a catalyst (Scheme 5.216) [151].

Gruttadauria and coworkers introduced the performance of polystyrene-supported proline as a catalyst in the Baylis–Hillman reaction. Interestingly, by a change in the solvent from DMF to water, products were obtained in excellent yields even in the absence of any catalyst. Furthermore, the nanocomposite could be recovered and recycled several times without the obvious loss of catalytic activity (Schemes 5.217 and 5.218) [152].
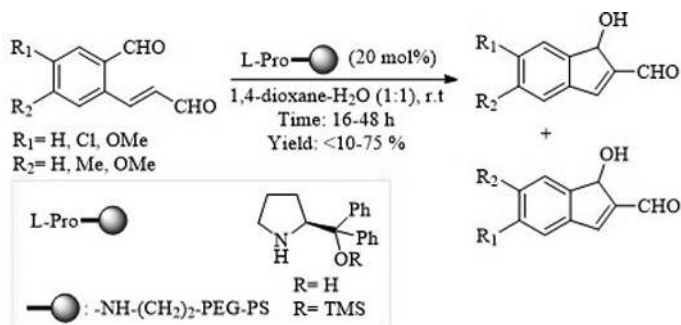
SCHEME 5.216. Intramolecular Morita–Baylis–Hillman reaction catalyzed by resin-supported proline.
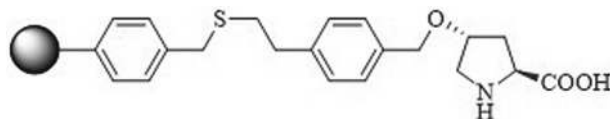
Catalyst: Polystyrene-supported proline

SCHEME 5.217. Structure of styrene-supported proline.

Ar= 4-NO$_2$C$_6$H$_4$, 3-NO$_2$C$_6$H$_4$, 4-CNC$_6$H$_4$, 2-CNC$_6$H$_4$, 4-CF$_3$C$_6$H$_4$, 4-BrC$_6$H$_4$, 3-BrC$_6$H$_4$, 2-ClC$_6$H$_4$, furan 3-ClC$_6$H$_4$, 4-ClC$_6$H$_4$, 2-FC$_6$H$_4$, 2-Cl-5-NO$_2$C$_6$H$_4$, C$_6$H$_5$, 4-MeC$_6$H$_4$, 4-OMeC$_6$H$_4$, naphthalene

Time (h): 20- 120
Yield (%): 17- 95
Conversion (%): 25- 99
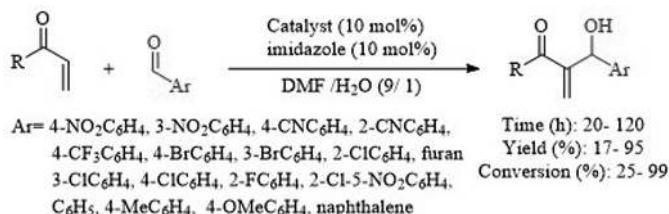
SCHEME 5.218. Baylis–Hillman reaction.

5.26. APPLICATION OF METAL COMPLEXES OF L-PROLINE AND L-PROLINE DERIVATIVE AS A CATALYST IN THE COUPLING REACTION

Coupling reactions such as the Heck, Suzuki, Sonogashira, Stille, and Negishi reactions, as well as decarboxylative, carbonylative, α-arylative, ligand C–S, C–O, C–B, and C–Se couplings, are important reactions in the design and development of novel value-added products and catalyzed by noble and transition metal. In this context, Zhang et al. achieved high efficiencies of biaryl compounds using the Pd(L-proline)$_2$ complex as a catalyst in water solvent and reflux conditions (Schemes 5.219 and 5.220) [153].

In another study, Singh et al. used the amino acid L-proline coated with palladium metals to perform the Heck reaction (Scheme 5.221) [154].

Vinyl sulfides are valuable compounds that are used as intermediates in four- and five-membered cyclic compounds and Michael acceptors. One of the methods for preparing these compounds involved the combination of vinyl bromides with different thiols using L-proline ligand and copper (I) catalyst, which was presented by the Bao group, and the best results were provided by maintaining stereochemistry in the ionic liquid [bmim] BF$_4$ (Scheme 5.222) [155].
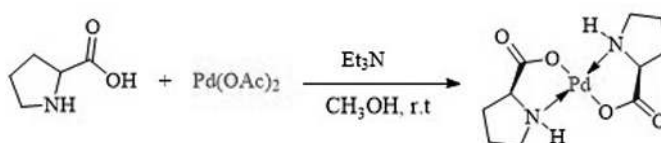
SCHEME 5.219. Production Pd(L-proline)$_2$ complex.

X= I, Br, Cl
R= H, 4-OH, 4-OMe, 4-Me, 4-NO₂, 3-NO₂,
4-COMe, 4-CH₂OH, 4-Cl, 4-CHO, 4-F,
4-COOH, 4-NH₂, 2-CHO, 2-OMe

Time: 2-15 h
Yield: 12-98 %

X= I, Br
R₁= H, F, COMe, OMe,
COMe, CH₂OH, CHO
R₂= OMe, COMe, OH

Time: 4-20 h
Yield: 35-96 %
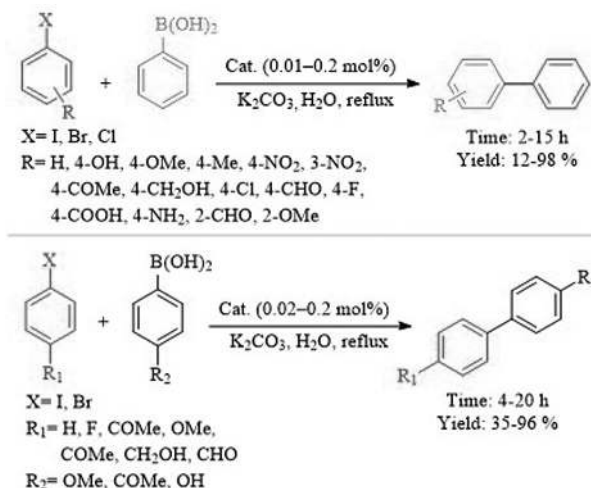
SCHEME 5.220. Pd(L-proline)₂ complex prompted the Suzuki–Miyaura reaction.

R¹= aryl, benzyl
X= Cl, Br, I
R²= COOMe, COOEt, CN, COOn-Bu,
COOt-Bu, n-Hex, Ph
R³= H, Ph
R²–R³= -(CH₂)₄-

Time (min): 10-50
Yield (%): 77-94
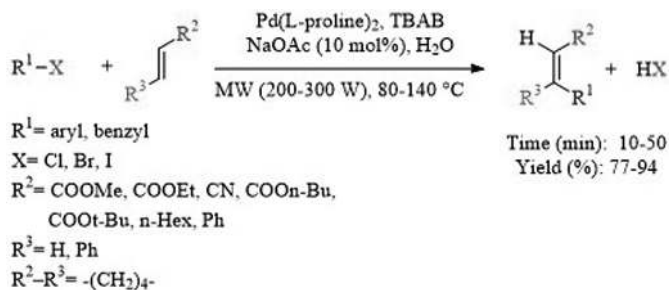
SCHEME 5.221. Pd(L-proline)₂ catalyzed Heck reaction.

R₁= benzene, toluene, P-anisole, chlorobenzene

R₂= benzene, toluene, fluorobenzene, 2-naphthalene,
p-cymene, O-anisole, -CH₂CH₂OH, -CH₂Ph

Time (h): 6- 10
Yield (%): 75- 96
E:Z= 98:2- 86:14
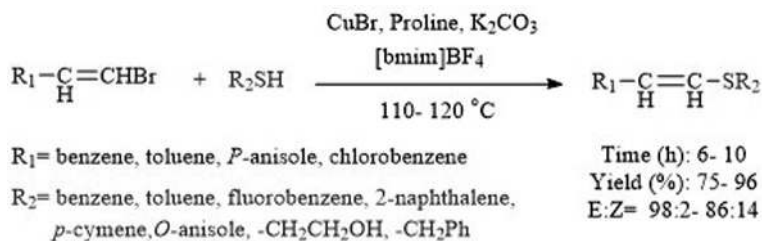
SCHEME 5.222. L-proline and CuBr catalyzed cross-coupling of vinyl bromide with thiols in ionic liquid.

N-vinyl imidazole is a valuable compound that has many applications, including antiparasitic properties in agriculture and medicine, extraction of pigments and polar compounds, as well as in the synthesis of heterocycles. *N*-vinyl imidazoles from the reaction of various imidazoles with vinyl bromides were presented by Bao and coworkers using L-proline ligand and copper (I) as catalysts in ionic liquids (Scheme 5.223) [156]. The advantage of this reaction is the control of spatial chemistry at the double bond site. In other words, this reaction was performed by maintaining configuration at the double bond site.

In another example, Bao and coworkers synthesized vinyl sulfones using the catalyst CuI/l-proline potassium salt and the coupling reaction of sulfonic acid salt with vinyl bromide in ionic liquid [bmim][BF$_4$] under nitrogen atmosphere (Scheme 5.224) [157].

5.27. APPLICATION OF METAL COMPLEXES OF L-PROLINE AND L-PROLINE DERIVATIVE-SUPPORTED MATERIAL AS A CATALYST IN THE COUPLING REACTION

Hajipour and coworkers displayed the synthesis of a palladium-based catalyst supported on proline-functionalized chitosan (CS-proline-Pd (II)) and its use as an efficient nanocatalyst for Suzuki cross-coupling reaction of different aryl halides and phenylboronic acid (Scheme 5.225) [158]. The catalyst was prepared by treating the NH$_2$ functional group chitosan with proline, followed by mixing the solid product with Pd(OAc)$_2$ to give the complex as shown in Scheme 5.288. TEM analysis
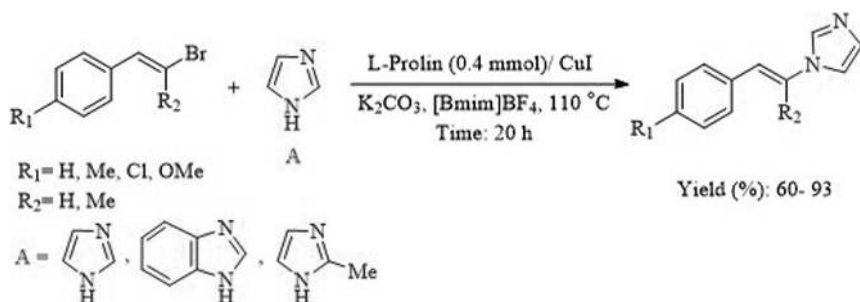
SCHEME 5.223. L-proline and CuI catalyzed the coupling of vinyl bromides with imidazoles in ionic liquids.
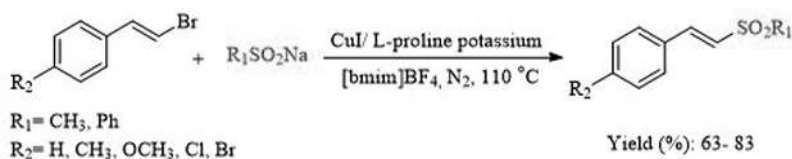
SCHEME 5.224. Production of vinyl sulfones using CuI/L-proline potassium salt.
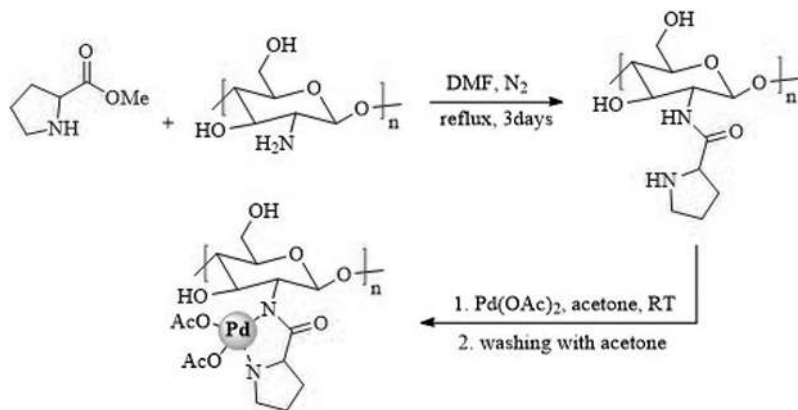
SCHEME 5.225. Production of nanocatalyst.

confirmed that the nanosized particles have been well distributed throughout the polymer matrix and the Pd content of the polymer matrix was found to be 2 wt%, by inductively coupled plasma atomic emission spectroscopy (ICP-AES). Suzuki cross-coupling reaction with aryl halides performed well with a kind of aryl iodides, and bromides bearing both electron-rich and electron-poor substituents (Scheme 5.226).

The performance of MOFs as catalysts and support for metal nanomaterials has received the most attention in recent years. In a related example, Babaei and coworkers prepared multivariate UiO-67-Pd-pro and studied the performance of solid materials as a heterogeneous catalyst for sequential Suzuki coupling/asymmetric aldol reactions with satisfied coupling performance (yields up to 99%) and good enantioselectivities (ee *anti* up to 98%) (Scheme 5.227) [159]. Inductively coupled plasma optical emission spectrometer (ICP-OES) measurements of the supernatant and hot leaching test revealed the heterogeneous nature of the catalyst.

Cheng et al. synthesized chiral proline-decorated bifunctional Pd@NH$_2$-UiO-66, using the "bottle-around-ship" method and coordination and post-synthetic modification (PSM), which led to encapsulated of Pd NPs into the frameworks and decoration of chiral proline to the zirconium nodes, respectively (Figure 5.3) [160]. The N$_2$ adsorption–desorption isotherms were employed to study the porosity of the heterogeneous catalyst, which presented the type-I sorption behavior, indicating the
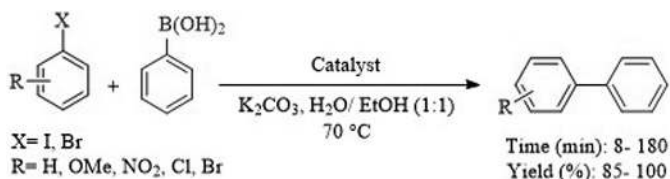
SCHEME 5.226. Suzuki cross-coupling reaction prompted by Cs-proline-Pd (II).
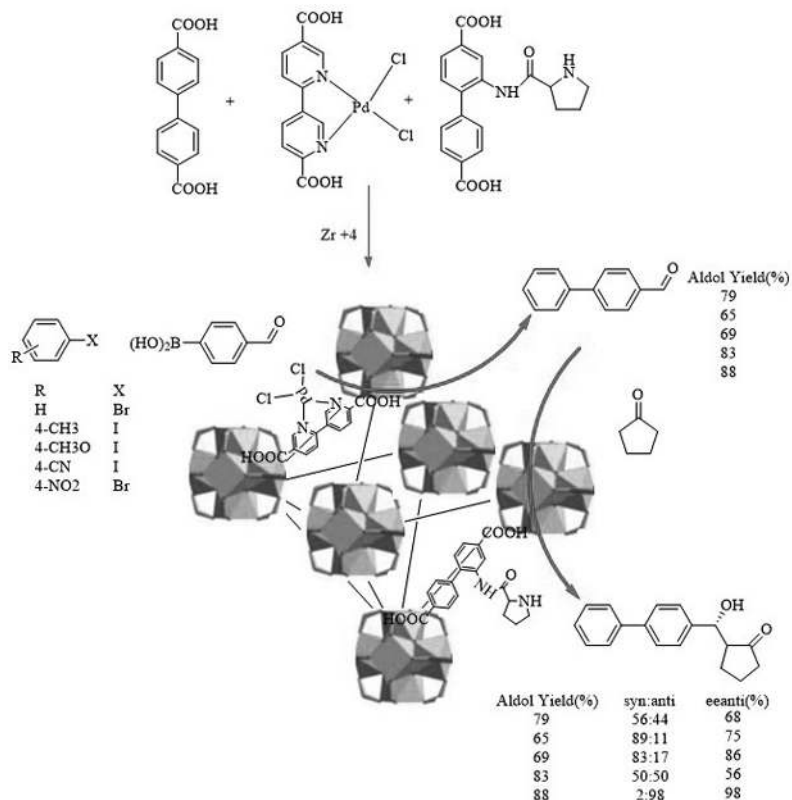
SCHEME 5.227. Production of multivariate UiO-67-Pd-pro and its performance in sequential Suzuki coupling/asymmetric Aldol reactions.

existence of micropores inside the catalysts. Meanwhile, the catalysts with various synthetic methods showed diverse BET surface areas and total pore volumes (Figure 5.4). The BET surface area and the total pore volume in Pd@NH$_2$-UiO66(pro)-1 are 637 m^2/g and 0.38 cm^3/g, respectively, which were lower than those of NH$_2$-UiO-66(pro)-1 (759 m^2/g and 0.53 cm^3/g, respectively) due to the decoration of Pd NPs. The bifunctional catalysts nanoparticles with an average size of 20–50 nm were employed in the sequential Suzuki coupling/asymmetric aldol reactions with excellent coupling performance (yield: 94–99.9%) and good enantioselectivities (ee *anti*: 57–97 %) (Scheme 5.228). Meanwhile, heterogeneous Pd@NH$_2$-UiO-66(pro)-1 was found to be stable and retained its initial catalytic activity even after several runs.

In 2015, Guenin and coworkers synthesized biaryl compounds by a combination of aryl halides with boronic acid derivatives using γ-Fe$_2$O$_3$@Cat-Pro (Pd) catalyst and EtOH/H$_2$O as a solvent at 80°C temperature (Schemes 5.229 and 5.230) [161]. Cat-Pro is produced by a combination of proline and dopamine, followed by immobilization with γ-Fe$_2$O$_3$ to give γ-Fe$_2$O$_3$@Cat-Pro. Solid products were treated with
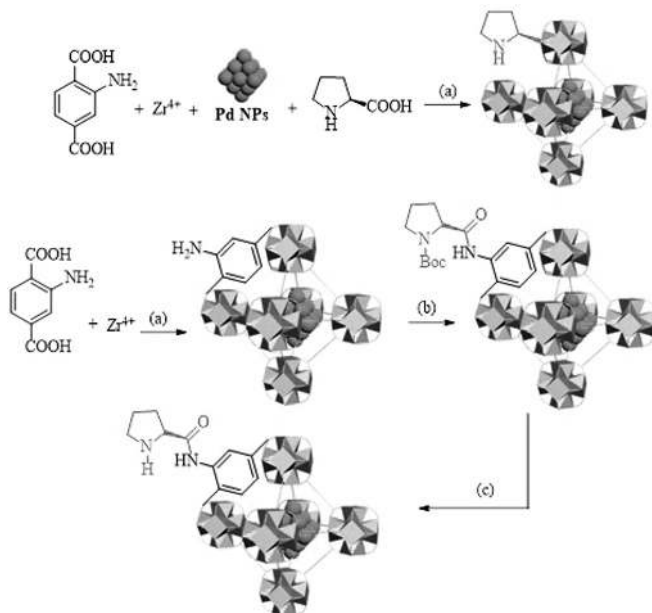
FIGURE 5.3. The production of Pd@NH₂-UiO-66(pro)-1 and Pd@NH₂-UiO-66(pro)-2. (a) Solvothermal method. (b) Amide reaction by PSM microwave method. (c) Thermal removal of the Boc groups. *Source:* Reprinted with permission from Ref. [160]. Copyright 2020, American Chemical Society.
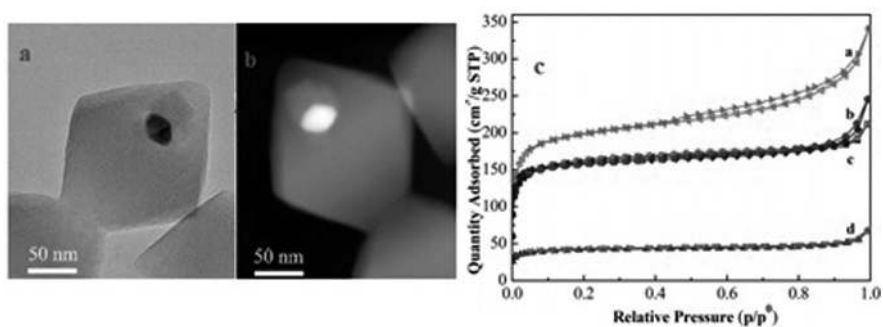
FIGURE 5.4. (a) Transmission electron microscopy (TEM). (b) HAADF-STEM images of Pd@NH₂-UiO-66(pro)-1. (c) N₂ adsorption–desorption isotherms of (a) NH₂-UiO66(pro)-1, (b) Pd@NH₂-UiO-66(pro)-1, (c) NH₂-UiO-66(pro)-2, and (d) Pd@NH₂-UiO-66(pro)-2. *Source:* Reprinted with permission from Ref. [160]. Copyright 2020, American Chemical Society.

R	X	step1 t(min)	step 2 t(days)	RCHO yied(%)	aldol yield(%)	syn/anti	ee anti(%)
4-CH$_3$	I	10	5	>99	82	29:71	57
4-CH$_3$O	Br	10	5	95	59	23:77	63
4-NO$_2$	I	10	5	95	71	2:98	64
4-CN	I	10	5	97	68	64:36	91
2-CN	Br	10	5	94	76	26:74	97

SCHEME 5.228. Sequential Suzuki coupling/asymmetric aldol reactions.

SCHEME 5.229. Production of γ-Fe$_2$O$_3$@Cat-Pro (Pd) catalyst.

SCHEME 5.230. γ-Fe$_2$O$_3$@Cat-Pro (Pd)-catalyzed coupling reaction.

Pd(OAc)$_2$ to produce the desired materials. This system carries out well and the final products were produced in high to excellent yields. Moreover, nanoparticles showed excellent recyclability up to the eight cycles without any leaching of the Pd species.

Chouhan et al. designed the production of Fe$_2$O$_3$@ Pro and employed it along with CuI for the arylation of nitrogen nucleophiles [162]. Moreover, the ligand preparation

process is shown in Scheme 5.231. The application of a catalyst was investigated for the arylation of nitrogen nucleophiles (Scheme 5.232) [162]. Experimental results show that coupling reactions carry out well and the final product is produced in 30–98% yield.

Sonogashira reaction is another carbon–carbon synthesis reaction in organic chemistry that is performed using terminal alkynes and aryl halides or vinyl halides in the presence of palladium or copper catalysts in the play environment. These products have various applications, including in the preparation of drugs, nanomaterials, and organic materials. Wang et al. presented an example of the Sonogashira reaction from end alkynes and aryl iodides and aryl bromides in the presence of proline-Cu(I) catalyst and solvent DMF (Scheme 5.233) [163]. Finally, the relevant catalyst was easily isolated from the reaction mixture and after six reuses, no significant reduction in its catalytic activity was observed.

5.28. APPLICATION OF L-PROLINE AS A CATALYST IN THE OXIDATION REACTION

N-bromosuccinimide (NBS) has been used as an oxidant for the esterification of alcohols. In this context, Shang and coworkers designed a green and active protocol

magnetic nanoparticle-supported proline ligand = MNP-3
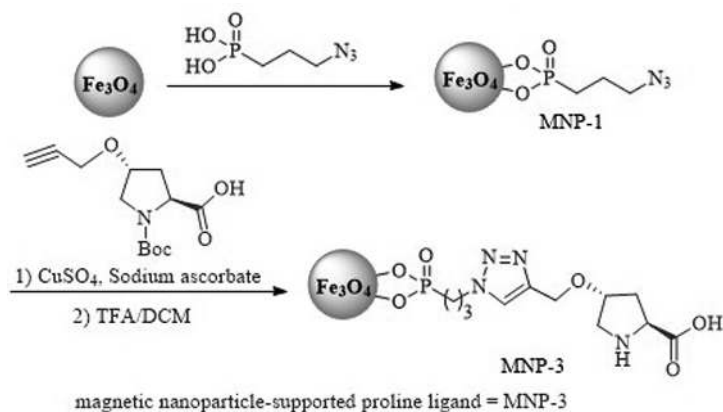
SCHEME 5.231.   Ligand preparation process on magnetic nanoparticles.
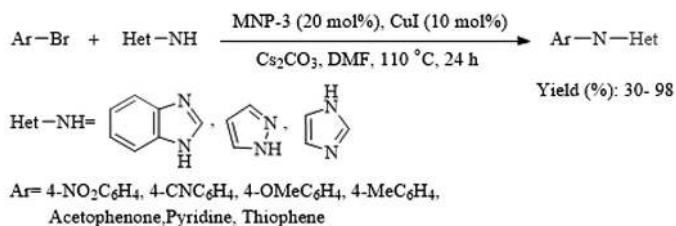
SCHEME 5.232. Fe_2O_3@ Pro- and CuI-catalyzed arylation of nitrogen nucleophiles.

SCHEME 5.233. Silica-anchored proline-copper (I) catalyzed the Sonogashira reaction.

for the dimeric esterification of different primary alcohols. In this system, this method was performed using NBS along with a catalytic amount of L-proline as a catalyst in water at room temperature giving the desired product in 83–97% yields (Scheme 5.234) [164].

Levina and Muzart reported enantioselective allylic oxidation by (S)- or (R)-proline using Cu$_2$O as a catalyst and t-BuOOC(O)Ph or t-BuOOH + RCOOH as oxidants (Scheme 5.235) [165]. The reaction was conducted in acetonitrile, and the final product was produced with low to moderate ee's.

SCHEME 5.234. Esterification of alcohols with L-proline catalyst and NBS as an oxidant.

[Ox] : 70 % Aqueous t-BuOOH or t-BuOOC(O)Ph

Entry	Substrate (Alkenes)	Product	Yield (%)	ee (%) (S)
1		—OCOPh	39	54
2		OCOPh	45	39
3		—OCOPh	27	23
4		OCOPh	32	4

SCHEME 5.235. Allylic oxidation of various alkenes.

5.29. APPLICATION OF L-PROLINE AND L-PROLINE DERIVATIVE-SUPPORTED MATERIAL AS A CATALYST IN THE OXIDATION REACTION

The oxidation reaction is a process that led to a change in oxidation number of molecules, atoms, or ions by gaining or losing an electron. $Prn/Fe_2O_3@SiO_2$ magnetic nanocatalyst was reported following the protocol and then employed as an active catalyst for the preparation of vanillin using isoeugenol and vanillyl alcohol (Schemes 5.236 and 5.237) [166]. This reaction proceeded well in the presence of $Prn/Fe_2O_3@SiO_2$ as the catalyst in CH_3CN.

5.30. APPLICATION OF L-PROLINE AS A CATALYST FOR CYANOSILYLATION

Shen et al. reported the cyanidation reaction of various carbonyl compounds at room temperature and solvent-free conditions using L-proline alkaline salt (Scheme 5.238) [167]. According to the results obtained with 10 mol% of potassium L-proline salt, products in suitable yields were produced. In addition, 4-phenyl-3-buten-2-one was reacted with TMSCN in the presence of alkaline salts different from L-proline and solvent-free conditions at room temperature. The highest yield (91%) was obtained using lithium salt L-proline, which is the result of the effect of the amino part and the carboxylate part of the catalyst.

5.31. APPLICATION OF L-PROLINE AS AN ORGANOCATALYST IN THE SYNTHESIS OF AMIDE

In another important study, Adimurthy and coworkers demonstrated that L-proline could serve as an efficient catalyst for transamidation by reaction between different
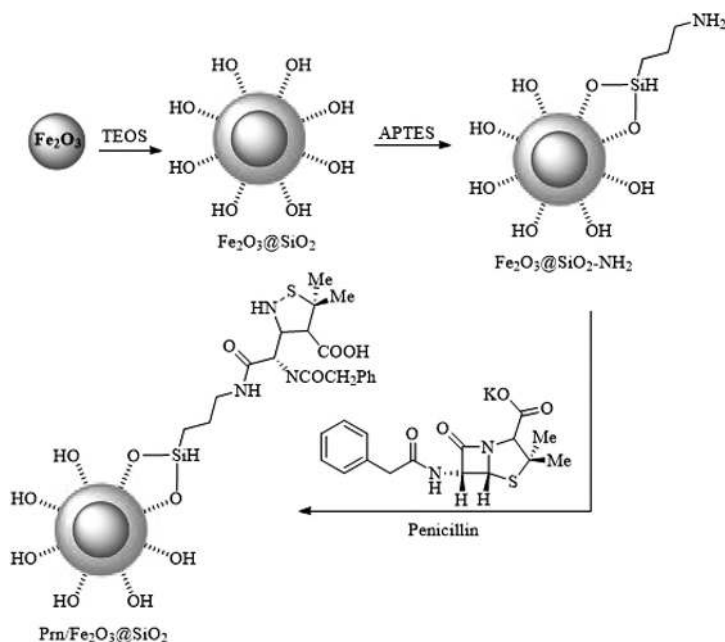
SCHEME 5.236. Preparation of Prn/Fe₂O₃@SiO₂ magnetic nanocatalyst.
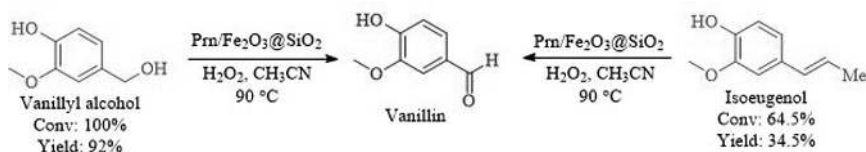
SCHEME 5.237. Schematic depiction of vanillin production from the various reactants.

amines with benzamide (Scheme 5.239) [168]. Under neat conditions, final products were synthesized from different benzamides in 58–92% yields.

5.32. APPLICATION OF L-PROLINE AS AN ORGANOCATALYST IN THE SYNTHESIS OF IMINE

Aldimines are an important and useful group that is used as raw materials for the preparation of various heterocyclic compounds such as aztidinones and thiazolidi-nones. In a related example, Bhusare and coworkers introduced the performance of L-proline for producing aldimine compounds using various aldehydes and 2-amino-thiazole compounds (Scheme 5.240) [169]. This system performed well for different aldehydes and 2-aminothiazole compounds to give a final product in 80–85% yields.

R'= H, CH₃, Et, Benzyl, -(CH₂)₃-,
   -(CH₂)₅-, -C₅H₁₀-, -C₅H₈-
R= H, 2-NO₂C₆H₄, 4-ClC₆H₄, 4-OCH₃C₆H₄,
   ethylbenzene, styrene, C₈H₁₇, 4-NO₂C₆H₄,
   C₆H₅, naphthalene, Benzyl, 4-CH₃C₆H₄,

Yield (%): 64- 99

M= Li, Na, K, Ba   R'= H, OH
                    R= H, Boc

Yield (%): 58- 91
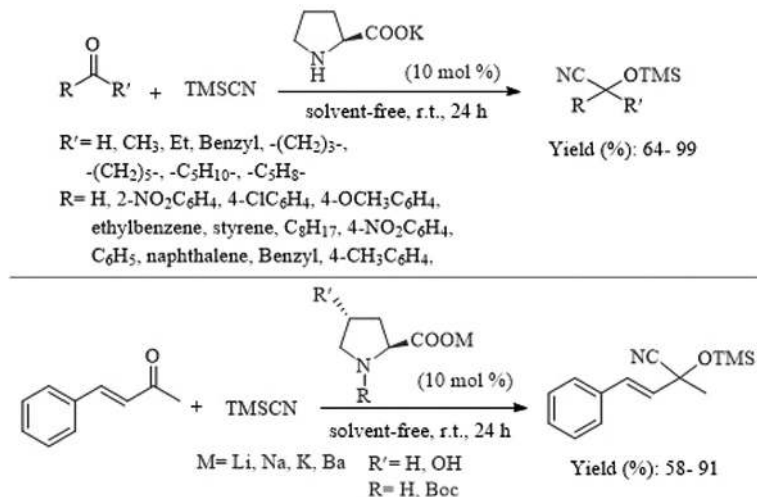
SCHEME 5.238. Alkali salt of L-proline as an efficient and practical catalyst for cyanosilylation.

R₁= H, Ph
amine: benzyl amine, 4-chlorobenzyl amine,
       4-methoxylbenzyl amine, 3-chlorobenzyl amine,
       3-fluorobenzyl amine, aniline, 4-methyl aniline,
       4-chloro aniline, 2-Phenethylamine, morpholine,
       cyclohexanamine, pyridin-2-amine, prop-2-yn-1-amine

Yield (%): 58-92
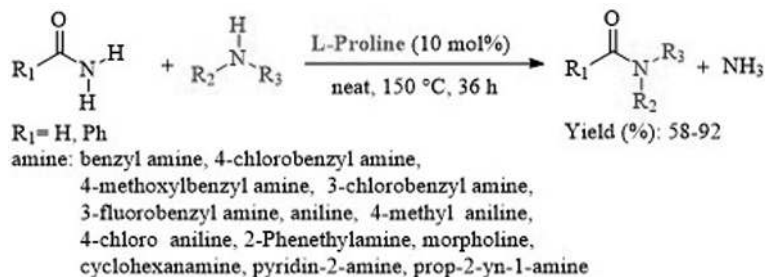
SCHEME 5.239. Transamidation of a variety of amines with benzamide.

R= 3,4,5-Trimethoxy, 2-Hydroxy
   5-Bromo-2-hydroxy, 3-Chloro
R₁= 4-Phenyl, 4-Chlorophenyl,
    4-Naphthalene, 3-Nitrophenyl

Yield (%): 80- 85
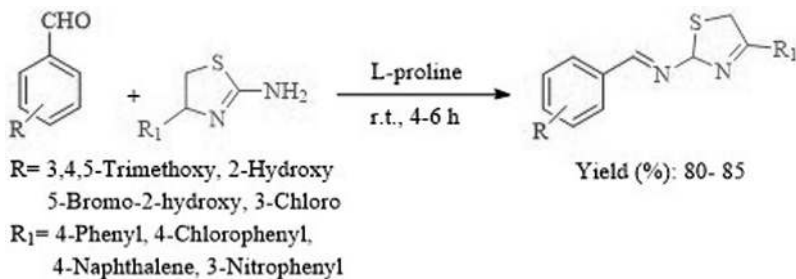
SCHEME 5.240. Synthesis of aldimines.

5.33. APPLICATION OF L-PROLINE-SUPPORTED MATERIAL AS A CATALYST IN THE RING-OPENING REACTION OF EPOXIDES WITH AMINES

The ring-opening reaction of epoxides with amines is one of the most important methods for the synthesis of β-amino alcohols. In another related work, Amini and coworkers described the production of MCM-41 L-proline and used to produce amino alcohols with good efficiency. The process synthesis of nanocatalyst is shown in Scheme 5.241. Nanocatalysts exhibited high activity to offer the final product in 9–100% yields (Scheme 5.242) [170].

5.34. APPLICATION OF L-PROLINE AND L-PROLINE DERIVATIVE-BASED IONIC LIQUID AS A CATALYST IN A-AMINATION REACTION

Ionic liquids are used as solvents in chemical reactions, including Friedel–Crafts and Diels–Alder reactions. In another important study, Zhu and coworkers introduced the performance of L-proline-derived organocatalyst in the α-amination of aldehydes in ionic liquid [bmim] [BF$_4$]. This system performed well for various aldehydes with azodicarboxylates to give the desired product in 92–98% yields with enantiomeric excesses of up to 92% (Scheme 5.243) [171].
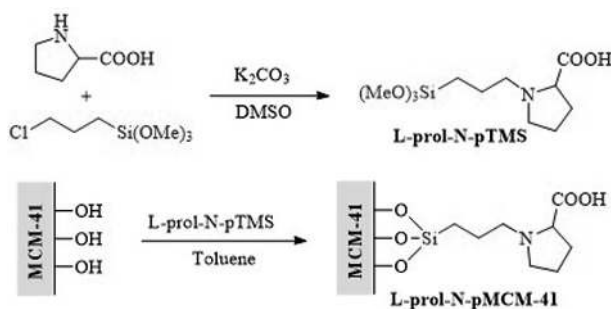
SCHEME 5.241.   Production of MCM-41 nanocatalyst.
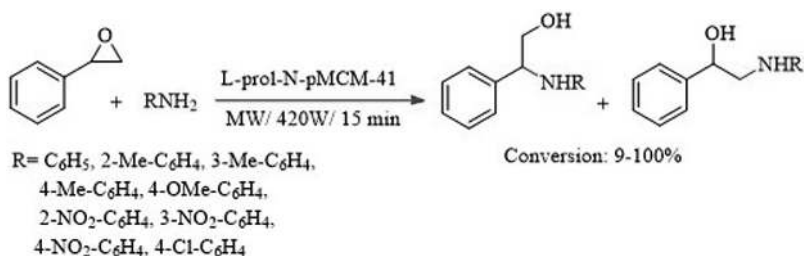
SCHEME 5.242.   Preparation of β-amino alcohols by MCM-41 nanocatalyst.
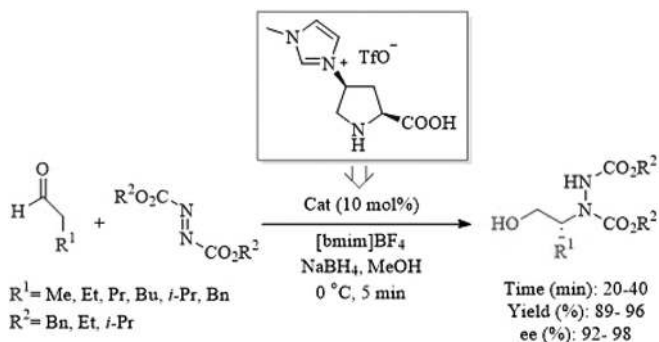
SCHEME 5.243.   Production of asymmetric α-amination of aldehydes.

5.35. CONCLUSION

The significance of organocatalysts has led to great efforts toward sustainable chemistry because of their effectiveness and selectivity. Organocatalysts do assist a number of the core principles of green chemistry by enabling safer syntheses, increased energy efficiency, and atom economy. This chapter primarily focuses on the impressive recent advances in organocatalysis that have been developed using environmentally friendly and sustainable methods. We believe that this critical evaluation will provide the background knowledge required to promote the usage of L-proline as a catalyst.

REFERENCES

1. Neamani, S., Moradi, L. Synthesis of new and highly functionalized 1,4-dihydropyridines and spirooxindole dihydropyridines using L-proline as efficient catalyst. *ChemistrySelect*, 2020, *5*(25), 7439–7446. https://doi.org/10.1002/slct.202002146.

2. Hegde, H., Shetty, N. S. Facile one-pot multicomponent synthesis of 1 H-pyrazolo [3, 4-b] quinolines using L-proline as a catalyst. *Chem. Heterocycl. Compd.*, 2017, *53*(8), 883–886.

3. Yazdani-Elah-Abadi, A., Pour, S. A., Kangani, M., Mohebat, R. L-proline catalyzed domino cyclization for the green synthesis of novel 1,4-Dihydrobenzo[a]Pyrido[2,3-c] Phenazines. *Monatshefte fur Chemie*, 2017, *148*(12), 2135–2142. https://doi.org/10.1007 /s00706-017-2008-7.

4. Dixit, R., Mehta, H., Dixit, B. Synthesis, characterization and antimicrobial studies of new 2-(2-chloroquinolin-3-Yl)-3-(Substituted Phenyl/Pyridinyl)Quinazolin-4(3H)-one derivatives using l-proline as a catalyst. *Med. Chem. Res.*, 2015, *24*(2), 773–786. https:// doi.org/10.1007/s00044-014-1116-8.

5. Srikrishna, D., Tasqeeruddin, S., Kumar Dubey, P. Synthesis of 3-substituted coumarins: An efficient green approach using L-proline as catalyst in triethanolamine medium. *Lett. Org. Chem.*, 2014, *11*(8), 556–563. https://doi.org/10.2174/15701786116 66140512215136.

6. Behbahani, F. K., Alaei, H. S. L-proline-catalysed synthesis of functionalized unsymmetrical Dihydro-1H-Indeno[1,2-b]Pyridines. *J. Chem. Sci.*, 2013, *125*(3), 623–626. https://doi.org/10.1007/s12039-013-0419-5.

7. Hasaninejad, A., Firoozi, S., Mandegani, F. An efficient synthesis of novel Spiro[Benzo[c]Pyrano[3,2-a]Phenazines] via domino multi-component reactions using l-proline as a bifunctional organocatalyst. *Tetrahedron Lett.*, 2013, *54*(22), 2791–2794. https://doi.org/10.1016/j.tetlet.2013.03.073.

8. Roshani, M., Allameh, S., Darkooti, E. An efficient and eco-friendly solvent-free synthesis of β-acetamido ketones using L-proline as a green and reusable catalyst. *Asian J. Chem.*, 2013, *25*(4), 1934–1936. https://doi.org/10.14233/ajchem.2013.13244.

9. Elnagdi, N. M. H., Al-Hokbany, N. S. Organocatalysis in synthesis: L-proline as an enantioselective catalyst in the synthesis of pyrans and thiopyrans. *Molecules*, 2012, *17*(4), 4300–4312.

10. Jain, S., Keshwal, B. S., Rajguru, D. A clean and efficient l-proline-catalyzed synthesis of polysubstituted benzenes in the ionic liquid 1-Butyl-3-methylimidazolium hexafluorophosphate. *J. Serbian Chem. Soc.*, 2012, *77*(10), 1345–1352. https://doi.org/10.2298/JSC111211067J.

11. Khorrami, A. R., Kiani, P., Bazgir, A. L-proline: An efficient catalyst for the synthesis of new spirooxindoles. *Monatshefte für Chemie-Chemical Mon.*, 2011, *142*(3), 287–295.

12. Dabiri, M., Tisseh, Z. N., Nobahar, M., Bazgir, A. Organic reaction in water: A highly efficient and environmentally friendly synthesis of spiro compounds catalyzed by L-proline. *Helv. Chim. Acta*, 2011, *94*(5), 824–830. https://doi.org/10.1002/hlca.201000307.

13. Rajanarendar, E., Reddy, M. N., Raju, S. An efficient one-pot synthesis of isoxazolyl polyhydroquinolines via Hantzsch condensation using L-proline as catalyst. *Indian J. Chem. Sect. B*, 2011, *50B*, 751–755.

14. Mecadon, H., Rohman, M. R., Kharbangar, I., Laloo, B. M., Kharkongor, I., Rajbangshi, M., Myrboh, B. L-proline as an efficient catalyst for the multi-component synthesis of 6-Amino-4-Alkyl/Aryl-3-Methyl-2,4-Dihydropyrano[2,3-c]Pyrazole-5-Carbonitriles in water. *Tetrahedron Lett.*, 2011, *52*(25), 3228–3231. https://doi.org/10.1016/j.tetlet.2011.04.048.

15. Raghuvanshi, D. S., Singh, K. N. An efficient protocol for multicomponent synthesis of spirooxindoles employing L-proline as catalyst at room temperature. *J. Heterocycl. Chem.*, 2010, *47*(6), 1323–1327. https://doi.org/10.1002/jhet.451.

16. Liu, X. H., Fan, J. C., Liu, Y., Shang, Z. C. L-proline as an efficient and reusable promoter for the synthesis of coumarins in ionic liquid. *J. Zhejiang Univ. Sci. B*, 2008, *9*(12), 990–995. https://doi.org/10.1631/jzus.B0820079.

17. Samai, S., Nandi, G. C., Singh, P., Singh, M. S. L-proline: An efficient catalyst for the one-pot synthesis of 2, 4, 5-trisubstituted and 1, 2, 4, 5-tetrasubstituted imidazoles. *Tetrahedron*, 2009, *65*(49), 10155–10161.

18. Shitole, N. V., Shelke, K. F., Sonar, S. S., Sadaphal, S. A., Shingate, B. B., Shingare, M. S. L-Proline as an efficient catalyst for the synthesis of 2,4,5-Triaryl-1H-Imidazoles. *Bull. Korean Chem. Soc.*, 2009, *30*(9), 1963–1966. https://doi.org/10.5012/bkcs.2009.30.9.1963.

19. Karade, N., Budhewar, V., Shinde, S., Jadhav, W. L-proline as an efficient organocatalyst for the synthesis of polyhydroquinoline via multicomponent Hantzsch reaction. *Lett. Org. Chem.*, 2007, *4*(1), 16–19. https://doi.org/10.2174/157017807780037405.

20. Basumatary, G., Mohanta, R., Bez, G. L-proline derived secondary aminothiourea organocatalyst for synthesis of coumarin derived trisubstituted methanes: Rate enhancement by bifunctional catalyst over cooperative catalysis. *Catal. Letters*, 2019, *149*(10), 2776–2786.

21. Titova, Y. A., Gruzdev, D. A., Fedorova, O. V., Alisienok, O. A., Murashkevich, A. N., Krasnov, V. P., Rusinov, G. L., Charushin, V. N. New chiral proline-based catalysts for silicon and zirconium oxides-promoted asymmetric Biginelli reaction. *Chem. Heterocycl. Compd.*, 2018, *54*(4), 417–427. https://doi.org/10.1007/s10593-018-2285-z.

22. Ruß, C., König, B. Low melting mixtures in organic synthesis - an alternative to ionic liquids? *Green Chem.*, 2012, *14*(11), 2969–2982. https://doi.org/10.1039/c2gc36005e.

23. Francisco, M., Van Den Bruinhorst, A., Kroon, M. C. Low-transition-temperature mixtures (LTTMs): A new generation of designer solvents. *Angew. Chemie - Int. Ed.*, 2013, *52*(11), 3074–3085. https://doi.org/10.1002/anie.201207548.

24. Liu, P., Hao, J. W., Mo, L. P., Zhang, Z. H. Recent advances in the application of deep eutectic solvents as sustainable media as well as catalysts in organic reactions. *RSC Adv.*, 2015, *5*(60), 48675–48704. https://doi.org/10.1039/c5ra05746a.

25. Khandelwal, S., Tailor, Y. K., Kumar, M. Deep eutectic solvents (DESs) as eco-friendly and sustainable solvent/catalyst systems in organic transformations. *J. Mol. Liq.*, 2016, *215*, 345–386. https://doi.org/10.1016/j.molliq.2015.12.015.

26. Li, X., Row, K. H. Development of deep eutectic solvents applied in extraction and separation. *J. Sep. Sci.*, 2016, *39*(18), 3505–3520. https://doi.org/10.1002/jssc.201600633.

27. Del Monte, F., Carriazo, D., Serrano, M. C., Gutiérrez, M. C., Ferrer, M. L. Deep eutectic solvents in polymerizations: A greener alternative to conventional syntheses. *ChemSusChem*, 2014, *7*(4), 999–1009. https://doi.org/10.1002/cssc.201300864.

28. Wagle, D. V., Zhao, H., Baker, G. A. Deep eutectic solvents: Sustainable media for nanoscale and functional materials. *Acc. Chem. Res.*, 2014, *47*(8), 2299–2308. https://doi.org/10.1021/ar5000488.

29. Guajardo, N., Müller, C. R., Schrebler, R., Carlesi, C., Dominguez de Maria, P. Deep eutectic solvents for organocatalysis, biotransformations, and multistep organocatalyst/enzyme combinations. *ChemCatChem*, 2016, *8*(6), 1020–1027.

30. Azizi, N., Dezfooli, S., Mahmoudi Hashemi, M. Greener synthesis of spirooxindole in deep eutectic solvent. *J. Mol. Liq.*, 2014, *194*, 62–67. https://doi.org/10.1016/j.molliq.2014.01.009.

31. Ma, C. T., Liu, P., Wu, W., Zhang, Z. H. Low melting oxalic acid/proline mixture as dual solvent/catalyst for efficient synthesis of 13-Aryl-13H-Benzo[g]Benzothiazolo[2,3-b]Buinazoline-5,4-Diones under microwave irradiation. *J. Mol. Liq.*, 2017, *242*, 606–611. https://doi.org/10.1016/j.molliq.2017.07.060.

32. Chandam, D. R., Patravale, A. A., Jadhav, S. D., Deshmukh, M. B. Low melting oxalic acid dihydrate: Proline mixture as dual solvent/catalyst for synthesis of spiro[Indoline-3,9′-Xanthene]trione and dibarbiturate derivatives. *J. Mol. Liq.*, 2017, *240*, 98–105. https://doi.org/10.1016/j.molliq.2017.05.070.

33. Jiang, B. K., Chen, A. Y., Gu, J. F., Fan, J. T., Liu, Y., Wang, P., Li, H. J., Sun, H., Yang, J. H., Wang, X. Y. Corrosion resistance enhancement of magnesium alloy by N-doped graphene quantum dots and polymethyltrimethoxysilane composite coating. *Carbon N. Y.*, 2020, *157*, 537–548. https://doi.org/10.1016/j.carbon.2019.09.013.

34. Zhao, M., Kim, D., Nguyen, V. L., Jiang, J., Sun, L., Lee, Y. H., Yang, H. Coherent thermoelectric power from graphene quantum dots. *Nano Lett.*, 2019, *19*(1), 61–68. https://doi.org/10.1021/acs.nanolett.8b03208.

35. Babaei, P., Safaei-Ghomi, J. L-proline covered N doped graphene quantum dots modified CuO/ZnO hexagonal nanocomposite as a robust retrievable catalyst in synthesis of substituted chiral 2-Amino-4H-chromenes. *Mater. Chem. Phys.*, 2021, *267*, 124668. https://doi.org/10.1016/j.matchemphys.2021.124668.

36. Akhavan, M., Bekhradnia, A. Stereoselective synthesis of spirocyclic pyrrolidines/pyrrolizidines/pyrrolothiazolidines using l-proline functionalized manganese ferrite nanorods as a novel heterogeneous catalyst. *RSC Adv.*, 2021, *11*(24), 14755–14768. https://doi.org/10.1039/d1ra00841b.

37. Safaei-Ghomi, J., Samadi, Z. Synthesis of pyrimidines by Fe3O4@SiO2-L-proline nanoparticles. *Main Gr. Met. Chem.*, 2020, *43*(1), 117–124. https://doi.org/10.1515/mgmc-2020-0014.

38. Fekri, L. Z., Feshalami, M. F. Green, practical and scalable multicomponent reaction for the synthesis of amides and pyridazinones from arenes using L-proline functionalized silicapropyl modified nanomagnetic as a heterogeneous Brønsted catalyst. *Polycycl. Aromat. Compd.*, 2020, 1–21. https://doi.org/10.1080/10406638.2020.1749091.

39. Fekri, L. Z., Nikpassand, M., Khakshoor, S. N. Green, effective and chromatography free synthesis of benzoimidazo[1,2-a]Pyrimidine and tetrahydrobenzo [4,5]Imidazo [1,2-d]Quinazolin-1(2H)-one and their pyrazolyl moiety using Fe3O4@SiO2@L-proline reusable catalyst in aqueous media. *J. Organomet. Chem.*, 2019, *894*, 18–27. https://doi.org/10.1016/j.jorganchem.2019.05.004.

40. Keshavarz, M., Ahmady, A. Z., Vaccaro, L., Kardani, M. Non-covalent supported of L-proline on graphene oxide/Fe3O4 nanocomposite: A novel, highly efficient and superparamagnetically separable catalyst for the synthesis of bis-pyrazole derivatives. *Molecules*, 2018, *23*(2), 330. https://doi.org/10.3390/molecules23020330.

41. Hajipour, A. R., Khorsandi, Z. Application of immobilized proline on CNTs and proline ionic liquid as novel organocatalysts in the synthesis of 2-Amino-4H-Pyran derivatives: A comparative study between their catalytic activities. *ChemistrySelect*, 2017, *2*(28), 8976–8982. https://doi.org/10.1002/slct.201700847.

42. Safaei-Ghomi, J., Masoomi, R., Hamadanian, M., Naseh, S. Magnetic nanoscale core-shell structured Fe3O4@l-Proline: An efficient, reusable and eco-friendly nanocatalyst for diastereoselective synthesis of fulleropyrrolidines. *New J. Chem.*, 2016, *40*(4), 3289–3299. https://doi.org/10.1039/c5nj02960k.

43. Afradi, M., Foroughifar, N., Pasdar, H., Moghanian, H. L-Proline N-sulfonic acid-functionalized magnetic nanoparticles: A novel and magnetically reusable catalyst for one-pot synthesis of 3,4-Dihydropyrimidine-2-(1 H)-thiones under solvent-free conditions. *RSC Adv.*, 2016, *6*(64), 59343–59351. https://doi.org/10.1039/c6ra10558k.

44. Khalafi-Nezhad, A., Nourisefat, M., Panahi, F. L-proline-modified magnetic nanoparticles (LPMNP): A novel magnetically separable organocatalyst. *RSC Adv.*, 2014, *4*(43), 22497–22500. https://doi.org/10.1039/c4ra01121j.

45. Becker, J., Bergander, K., Fröhlich, R., Hoppe, D. Asymmetric total synthesis and X-ray crystal structure of the cytotoxic marine diterpene (+)-vigulariol. *Angew. Chemie Int. Ed.*, 2008, *47*(9), 1654–1657. https://doi.org/10.1002/anie.200704678.

46. Zhi, C., Wang, J., Luo, B., Li, X., Cao, X., Pan, Y., Gu, H. The synthesis of cyclohexenone using L-proline immobilized on a silica gel catalyst by a continuous-flow approach. *RSC Adv.*, 2014, *4*(29), 15036–15039. https://doi.org/10.1039/c4ra01231c.

47. Khalafi-Nezhad, A., Shahidzadeh, E. S., Sarikhani, S., Panahi, F. A new silica-supported organocatalyst based on L-proline: An efficient heterogeneous catalyst for one-pot synthesis of spiroindolones in water. *J. Mol. Catal. A Chem.*, 2013, *379*, 1–8. https://doi.org/10.1016/j.molcata.2013.07.009.

48. Ghorbani-Choghamarani, A., Zamani, P. Supported L-pyrrolidine-2-carboxylic acid-4-hydrogen sulphate on silica gel as an economical and efficient catalyst for the one-pot preparation of ?-acetamido ketones via a four-component condensation reaction. *J. Chem. Sci.*, 2014, *126*(1), 103–109. https://doi.org/10.1007/s12039-013-0538-z.

49. Arya, K., Rajesh, U. C., Rawat, D. S. Proline confined FAU zeolite: Heterogeneous hybrid catalyst for the synthesis of spiroheterocycles via a Mannich type reaction. *Green Chem.*, 2012, *14*(12), 3344–3351. https://doi.org/10.1039/c2gc35822k.

50. Tahmassebi, D., Blevins, J. E., Gerardot, S. S. Zn(L-Proline) ₂ as an efficient and reusable catalyst for the multi-component synthesis of pyran-annulated heterocyclic compounds. *Appl. Organomet. Chem.*, 2019, *33*(4), e4807. https://doi.org/10.1002/aoc.4807.

51. Agarwal, S., Kidwai, M., Poddar, R., Nath, M. A facile and green approach for the one-pot multicomponent synthesis of 2,4,5-Triaryl- and 1,2,4,5-Tetraarylimidazoles by using zinc-proline hybrid material as a catalyst. *ChemistrySelect*, 2017, *2*(32), 10360–10364. https://doi.org/10.1002/slct.201702222.

52. Kaboudin, B., Kazemi, F., Pirouz, M., Khoshkhoo, A. B., Kato, J. Y., Yokomatsu, T. Iron(III) Chloride/l-Proline as an efficient catalyst for the synthesis of 3-substituted 1,2,4-Oxadiazoles from amidoximes and triethyl orthoformate. *Synth.*, 2016, *48*(20), 3597–3602. https://doi.org/10.1055/s-0035-1562431.

53. Maleki, B., Babaee, S., Tayebee, R. Zn(L-Proline)2 as a powerful and reusable organometallic catalyst for the very fast synthesis of 2-Amino-4H-Benzo[g]Chromene derivatives under solvent-free conditions. *Appl. Organomet. Chem.*, 2015, *29*(6), 408–411. https://doi.org/10.1002/aoc.3306.

54. Jia, H. G., Shi, Y. Q., Ma, L. Q., Wang, Y. Z., Zang, Y., Peng, J. J. Asymmetric polymerisation of substituted phenylacetylene using chiral Rh(2,5-Norbornadiene)(L-Proline) catalyst. *Chem. Pap.*, 2015, *69*(5), 756–760. https://doi.org/10.1515/chempap-2015-0075.

55. Siddiqui, Z. N., Farooq, F. Zn(Proline)2: A novel catalyst for the synthesis of dicoumarols. *Catal. Sci. Technol.*, 2011, *1*(5), 810–816. https://doi.org/10.1039/c1cy00110h.

56. Heravi, M. M., Ghods, A., Bakhtiari, K., Derikvand, F. Zn[(L)Proline]2: An efficient catalyst for the synthesis of biologically active pyrano[2,3-d]Pyrimidine derivatives. *Synth. Commun.*, 2010, *40*(13), 1927–1931. https://doi.org/10.1080/00397910903174390.

57. Heravi, M. M., Tehrani, M. H., Bakhtiari, K., Oskooie, H. A. Zn[(l)Proline]: A powerful catalyst for the very fast synthesis of quinoxaline derivatives at room temperature. *Catal. Commun.*, 2007, *8*(9), 1341–1344. https://doi.org/10.1016/j.catcom.2006.11.026.

58. Sivamurugan, V., Kumar, R. S., Palanichamy, M., Murugesan, V. Synthesis of hantzsch 1,4-dihydropyridines under solvent-free condition using Zn[(L)Proline]2 as Lewis acid catalyst. *J. Heterocycl. Chem.*, 2005, *42*(5), 969–974. https://doi.org/10.1002/jhet.5570420534.

59. Tomer, S. O., Soni, H. P. Fe3O4@l-Proline/Pd nanocomposite for one-pot tandem catalytic synthesis of (±)-Warfarin from benzyl alcohol: Synergistic action of organocatalyst and transition metal catalyst. *Catal. Sci. Technol.*, 2019, *9*(22), 6517–6531. https://doi.org/10.1039/c9cy01497g.

60. Davanagere, P. M., Maiti, B. Bifunctional C2-symmetric ionic liquid-supported (S)-proline as a recyclable organocatalyst for Mannich reactions in neat condition. *Results Chem.*, 2021, *3*, 100152. https://doi.org/10.1016/j.rechem.2021.100152.

61. Patil, P. G., Satkar, Y., More, D. H. L-proline based ionic liquid: A highly efficient and homogenous catalyst for synthesis of 5-benzylidene-1,3-Dimethylpyrimidine-2,4,6(1H,3H,5H)-Trione and Pyrano[2,3-d] pyrimidine diones under ultrasonic irradiation. *Synth. Commun.*, 2020, *50*(24), 3804–3819. https://doi.org/10.1080/00397911.2020.1811987.

62. Agrawal, N. R., Bahekar, S. P., Sarode, P. B., Zade, S. S., Chandak, H. S. L-proline nitrate: A recyclable and green catalyst for the synthesis of highly functionalized piperidines. *RSC Adv.*, 2015, *5*(58), 47053–47059. https://doi.org/10.1039/c5ra08022c.

63. Bahekar, S. P., Dahake, N. D., Sarode, P. B., Chandak, H. S. Efficient access to 2,3-dihy-droquinazolin-4(1 H)-ones by environmentally benign L-proline nitrate as recyclable catalyst. *Synlett*, 2015, *26*(18), 2575–2577. https://doi.org/10.1055/s-0035-1560483.

64. Li, J., Lin, S., Dai, J., Su, W. L-proline triflate as an efficient and reusable catalyst for the one-pot synthesis of 2,4,5-trisubstituted imidazoles and 1,2,4,5-tetrasubstituted imidazoles. *J. Chem. Res.*, 2010, *34*(4), 196–199. https://doi.org/10.3184/030823410X1 2698803608765.

65. Obregón-Zúñiga, A., Milán, M., Juaristi, E. Improving the catalytic performance of (S)-proline as organocatalyst in asymmetric aldol reactions in the presence of solvate ionic liquids: Involvement of a supramolecular aggregate. *Org. Lett.*, 2017, *19*(5), 1108–1111. https://doi.org/10.1021/acs.orglett.7b00129.

66. Xu, L., Huang, J., Liu, Y., Wang, Y., Xu, B., Ding, K., Ding, Y., Xu, Q., Yu, L., Fan, Y. Design and application of the recyclable poly(l-Proline-Co-Piperidine) catalyst for the synthesis of mesityl oxide from acetone. *RSC Adv.*, 2015, *5*(52), 42178–42185. https://doi.org/10.1039/c5ra05741h.

67. Zhang, X., Zhao, W., Qu, C., Yang, L., Cui, Y. Efficient asymmetric aldol reaction catalyzed by polyvinylidene chloride-supported ionic liquid/l-proline catalyst system. *Tetrahedron Asymmetry*, 2012, *23*(6–7), 468–473. https://doi.org/10.1016/j.tetasy.2012.03.023.

68. Bhupathi, R. S., Devi, B. R., Dubey, P. K. L-proline as an efficient catalyst for synthesis of N-heterocyclic chalcones as potential antibacterial agents. *Indian J. Chem. - Sect. B Org. Med. Chem.*, 2012, *51*(6), 855–859.

69. Qian, Y., Zheng, X., Wang, X., Xiao, S., Wang, Y. An efficient ionic liquid additive for proline-catalyzed direct asymmetric aldol reactions between cyclic ketones and aromatic aldehydes. *Chem. Lett.*, 2009, *38*(6), 576–577. https://doi.org/10.1246/cl.2009.576.

70. Wang, Z., Yan, J., Zhang, X., Wang, L. Merrifield resin supported ionic liquids/L-pro-line as efficient and recyclable catalyst systems for asymmetric aldol reaction. *Synthesis (Stuttg).*, 2009, *2009*(22), 3744–3750. https://doi.org/10.1055/s-0029-1217013.

71. Reddy, K. R., Chakrapani, L., Ramani, T., Rajasekhar, C. V. L-proline-catalyzed asym-metric direct aldol reaction of heteroaromatic aldehydes and acetone: Improvement of catalytic efficiency in ionic liquid bmim [BF4]. *Synth. Commun.*, 2007, *37*(24), 4301–4307. https://doi.org/10.1080/00397910701575574.

72. Liu, Y. H., Zhang, Y. W., Ding, Y. P., Shen, Z. X., Luo, X. Q. Recycling chiral organo-catalyst (4S)-Phenoxy-(S)-proline for direct asymmetric aldol reaction in ionic liquid (Bmim)PF6. *Chinese J. Chem.*, 2005, *23*(5), 634–636. https://doi.org/10.1002/cjoc.200590634.

73. Kotrusz, P., Kmentová, I., Gotov, B., Toma, Š., Solčániová, E. Proline-catalysed asymmetric aldol reaction in the room temperature ionic liquid [Bmim]PF6. *Chem. Commun.*, 2002, *21*(21), 2510–2511. https://doi.org/10.1039/b206911c.

74. Loh, T. P., Feng, L. C., Yang, H. Y., Yang, J. Y. L-proline in an ionic liquid as an effi-cient and reusable catalyst for direct asymmetric aldol reactions. *Tetrahedron Letters*, 2002, *43*(48), 8741–8743.

75. Xu, G., Zhang, Y., Sun, J., Bai, S., Zhao, H. Synthesis of extended bipyridine-proline chiral catalysts and resulting effects on the asymmetric aldol reactions of bulkier alde-hyde derivatives with cyclohexanone. *ChemistrySelect*, 2020, *5*(35), 10996–11003. https://doi.org/10.1002/slct.202002956.

76. Bhati, M., Kumari, K., Easwar, S. Probing the synergistic catalytic model: A rationally designed urea-tagged proline catalyst for the direct asymmetric aldol reaction. *J. Org. Chem.*, 2018, *83*(15), 8225–8232. https://doi.org/10.1021/acs.joc.8b00962.

77. Yorulmaz, T., Aydogan, F., Yolacan, C. New and effective proline-based catalysts for asymmetric aldol reaction in water. *Synth. Commun.*, 2017, *47*(1), 78–85. https://doi.org /10.1080/00397911.2016.1252988.

78. Li, S., Wu, C., Long, X., Fu, X., Chen, G., Liu, Z. Simple proline derivatives as recoverable catalysts for the large-scale stoichiometric aldol reactions. *Catal. Sci. Technol.*, 2012, *2*(5), 1068–1071. https://doi.org/10.1039/c2cy00549b.

79. Chen, Y. H., Sung, P. H., Sung, K. Synthesis of proline-derived dipeptides and their catalytic enantioselective direct aldol reactions: Catalyst, solvent, additive and temperature effects. *Amino Acids*, 2010, *38*, 839–845.

80. An, Y. J., Zhang, Y. X., Wu, Y., Liu, Z. M., Pi, C., Tao, J. C. Simple amphiphilic isosteviol-proline conjugates as chiral catalysts for the direct asymmetric aldol reaction in the presence of water. *Tetrahedron Asymmetry*, 2010, *21*(6), 688–694. https://doi.org/10 .1016/j.tetasy.2010.04.019.

81. Zamboulis, A., Rahier, N. J., Gehringer, M., Cattoën, X., Niel, G., Bied, C., Moreau, J. J. E., Man, M. W. C. Silica-supported l-proline organocatalysts for asymmetric aldolisation. *Tetrahedron Asymmetry*, 2009, *20*(24), 2880–2885. https://doi.org/10.1016/j .tetasy.2009.11.024.

82. Guo, H. M., Cheng, L., Cun, L. F., Gong, L. Z., Mi, A. Q., Jiang, Y. Z. L-prolinamide-catalyzed direct nitroso aldol reactions of α-branched aldehydes: A distinct regioselectivity from that with L-proline. *Chem. Commun.*, 2006, *4*, 429–431. https://doi.org/10 .1039/b514194j.

83. Cheng, C., Sun, J., Wang, C., Zhang, Y., Wei, S., Jiang, F., Wu, Y. Protonated N′-Benzyl-N′-prolyl proline hydrazide as highly enantioselective catalyst for direct asymmetric aldol reaction. *Chem. Commun.*, 2006, *2*, 215–217. https://doi.org/10.1039/b511992h.

84. Mutiah, M., Rochat, S., Amura, I., Burrows, A. D., Emanuelsson, E. A. C. Immobilisation of L-proline onto mixed-linker zirconium MOFs for heterogeneous catalysis of the aldol reaction. *Chem. Eng. Process. - Process Intensif.*, 2021, *161*, 108315. https://doi .org/10.1016/j.cep.2021.108315.

85. Hu, E., Zhang, X., Xu, L., Li, G. Near-infrared laser–assisted CuS@mSiO2@L-proline catalyzed asymmetric aldol reaction. *Inorg. Chem. Commun.*, 2021, *130*, 108718. https://doi.org/10.1016/j.inoche.2021.108718.

86. Aghahosseini, H., Ramazani, A., Ślepokura, K., Lis, T. The first protection-free synthesis of magnetic bifunctional L-proline as a highly active and versatile artificial enzyme: Synthesis of imidazole derivatives. *J. Colloid Interface Sci.*, 2018, *511*, 222–232. https:// doi.org/10.1016/j.jcis.2017.10.020.

87. Saberikia, I., Safaei, E., Karimi, B., Lee, Y. I. A novel copper complex of proline-based mono(phenol) amine ligand (hlpro) immobilized in SBA-15 as a model catalyst of galactose oxidase. *ChemistrySelect*, 2017, *2*(34), 11164–11171. https://doi.org/10.1002 /slct.201701535.

88. Li, C., Wang, J., Ding, H. Recyclable helical poly(phenyl isocyanide)-supported L-proline catalyst for direct asymmetric aldol reaction in brine. *Catal. Letters*, 2021, *151*(4), 1180–1190. https://doi.org/10.1007/s10562-020-03369-8.

89. Ishihara, K., Obayashi, R., Gotoh, M., Watanabe, Y., Kobayashi, Y., Ishihara, K., Shioiri, T., Matsugi, M. A recyclable and highly stereoselective multi-fluorous proline catalyst for asymmetric aldol reactions. *Tetrahedron Lett.*, 2020, *61*(13), 151657. https:// doi.org/10.1016/j.tetlet.2020.151657.

90. Tang, Y., Wang, Q., Wu, L., Liu, K., Wang, W., Shen, Y., Xue, Y., Dai, S. L-proline functionalized PH-responsive copolymers as supported organocatalysts for asymmetric aldol reaction in water. *React. Funct. Polym.*, 2020, *150*, 104544. https://doi.org/10 .1016/j.reactfunctpolym.2020.104544.

91. Feng, X., Jena, H. S., Leus, K., Wang, G., Ouwehand, J., Van Der Voort, P. L-proline modulated zirconium metal-organic frameworks: Simple chiral catalysts for the aldol addition reaction. *J. Catal.*, 2018, *365*, 36–42. https://doi.org/10.1016/j.jcat.2018.06.013.

92. Ferré, M., Cattoën, X., Wong Chi Man, M., Pleixats, R. Recyclable silica-supported proline sulphonamide organocatalysts for asymmetric direct aldol reaction. *ChemistrySelect*, 2016, *1*(21), 6741–6748. https://doi.org/10.1002/slct.201601859.

93. Guo, G., Wu, Y., Zhao, X., Wang, J., Zhang, L., Cui, Y. Polymerization of L-proline functionalized styrene and its catalytic performance as a supported organocatalyst for direct enantioselective aldol reaction. *Tetrahedron Asymmetry*, 2016, *27*(16), 740–746. https://doi.org/10.1016/j.tetasy.2016.06.014.

94. Li, X., Yang, B., Jia, X., Chen, M., Hu, Z. Temperature-responsive hairy particle-supported proline for direct asymmetric aldol reaction in water. *RSC Adv.*, 2015, *5*(108), 89149–89156. https://doi.org/10.1039/c5ra16393e.

95. Kutzscher, C., Hoffmann, H. C., Krause, S., Stoeck, U., Senkovska, I., Brunner, E., Kaskel, S. Proline functionalization of the mesoporous metal-organic framework DUT-32. *Inorg. Chem.*, 2015, *54*(3), 1003–1009. https://doi.org/10.1021/ic502380q.

96. Li, J., Wang, S., Wang, W. J., Li, B. G. Hyperbranched polyethylene-supported L-proline: A highly selective and recyclable organocatalyst for aldol reactions. *Catal. React. Eng. Div. 2015 - Core Program. Area 2015 AIChE Annu. Meet.*, 2015, *2*(7), 885.

97. Szőllősi, G., Fekete, M., Gurka, A. A., Bartók, M. Reversal of enantioselectivity in aldol reaction: new data on proline/λ-alumina organic-inorganic hybrid catalysts. *Catal. Letters*, 2014, *144*(3), 478–486. https://doi.org/10.1007/s10562-013-1177-1.

98. Lili, L., Xin, Z., Shumin, R., Ying, Y., Xiaoping, D., Jinsen, G., Chunming, X., Jing, H. Catalysis by metal-organic frameworks: proline and gold functionalized MOFs for the aldol and three-component coupling reactions. *RSC Adv.*, 2014, *4*(25), 13093–13107. https://doi.org/10.1039/c4ra01269k.

99. An, Z., Guo, Y., Zhao, L., Li, Z., He, J. L-proline-grafted mesoporous silica with alternating hydrophobic and hydrophilic blocks to promote direct asymmetric aldol and Knoevenagel-Michael cascade reactions. *ACS Catal.*, 2014, *4*(8), 2566–2576. https://doi.org/10.1021/cs500385s.

100. Szollosi, G., Csámpai, A., Somlai, C., Fekete, M., Bartók, M. Unusual enantioselectivities in heterogeneous organocatalyzed reactions: Reversal of direction using proline Di- versus Tri-peptides in the aldol addition. *J. Mol. Catal. A Chem.*, 2014, *382*, 86–92. https://doi.org/10.1016/j.molcata.2013.11.011.

101. Yang, H., Zhang, X., Li, S., Wang, X., Ma, J. The high catalytic activity and reusability of the proline functionalized cage-like mesoporous material SBA-16 for the asymmetric aldol reaction proceeding in methanol-water mixed solvent. *RSC Adv.*, 2014, *4*(18), 9292–9299. https://doi.org/10.1039/c3ra47262k.

102. Wu, X., He, C., Wu, X., Qu, S., Duan, C. An L-proline functionalized metallo-organic triangle as size-selective homogeneous catalyst for asymmetry catalyzing aldol reactions. *Chem. Commun.*, 2011, *47*(29), 8415–8417. https://doi.org/10.1039/c1cc11698c.

103. Zou, J., Zhao, W., Li, R., Zhang, H., Cui, Y. Synthesis of PVC-TEPA-supported proline derivative and its catalytic behavior in the direct asymmetric aldol reaction. *J. Appl. Polym. Sci.*, 2010, *118*(2), 1020–1026. https://doi.org/10.1002/app.29892.

104. Liu, Y. X., Sun, Y. N., Tan, H. H., Tao, J. C. Asymmetric aldol reaction catalyzed by new recyclable polystyrene-supported l-proline in the presence of water. *Catal. Letters*, 2008, *120*(3–4), 281–287. https://doi.org/10.1007/s10562-007-9281-8.

105. Chai, L. T., Wang, Q. R., Tao, F. G. The synthesis of supported proline-derived ligands and their application in asymmetric diethylzinc addition to aldehydes. *J. Mol. Catal. A Chem.*, 2007, *276*(1–2), 137–142. https://doi.org/10.1016/j.molcata.2007.06.022.

106. Giacalone, F., Gruttadauria, M., Marculescu, A. M., Noto, R. Polystyrene-supported proline and prolinamide. Versatile heterogeneous organocatalysts both for asymmetric aldol reaction in water and α-selenenylation of aldehydes. *Tetrahedron Lett.*, 2007, *48*(2), 255–259. https://doi.org/10.1016/j.tetlet.2006.11.040.

107. Calderón, F., Fernández, R., Sánchez, F., Fernández-Mayoralas, A. Asymmetric aldol reaction using immobilized proline on mesoporous support. *Adv. Synth. Catal.*, 2005, *347*(10), 1395–1403. https://doi.org/10.1002/adsc.200505058.

108. Andreae, M. R. M., Davis, A. P. Heterogeneous catalysis of the asymmetric aldol reaction by solid-supported proline-terminated peptides. *Tetrahedron Asymmetry*, 2005, *16*(14), 2487–2492. https://doi.org/10.1016/j.tetasy.2005.06.031.

109. Gruttadauria, M., Giacalone, F., Marculescu, A. M., Lo Meo, P., Riela, S., Noto, R. Hydrophobically directed aldol reactions: Polystyrene-supported l-proline as a recyclable catalyst for direct asymmetric aldol reactions in the presence of water. *European J. Org. Chem.*, 2007, *2007*(28), 4688–4698.

110. Inani, H., Singh, A., Bhati, M., Kumari, K., Kucherenko, A. S., Zlotin, S. G., Easwar, S. Proline-histidine dipeptide: A suitable template for generating ion-tagged organocatalysts for the asymmetric aldol reaction. *Synth.*, 2021, *53*(15), 2702–2712. https://doi.org/10.1055/a-1477-4871.

111. Bhati, M., Upadhyay, S., Easwar, S. Exploring "Through-Bond" proximity between the ion tag and reaction site of an imidazolium-proline catalyst for the direct asymmetric aldol reaction. *European J. Org. Chem.*, 2017, *2017*(13), 1788–1793. https://doi.org/10.1002/ejoc.201700021.

112. Okafuji, A., Kohno, Y., Nakamura, N., Ohno, H. Design of thermoresponsive poly(ionic liquid) gels containing proline units to catalyse aldol reaction in water. *Polymer (Guildf).*, 2018, *134*, 20–23. https://doi.org/10.1016/j.polymer.2017.11.047.

113. Lombardo, M., Easwar, S., Pasi, F., Trombinia, C. The ion tag strategy as a route to highly efficient organocatalysts for the direct asymmetric aldol reaction. *Adv. Synth. Catal.*, 2009, *351*(1–2), 276–282. https://doi.org/10.1002/adsc.200800608.

114. Zhang, L., Zhang, H., Luo, H., Zhou, X., Cheng, G. Novel chiral ionic liquid (CIL) assisted selectivity enhancement to (L)-proline catalyzed asymmetric aldol reactions. *J. Braz. Chem. Soc.*, 2011, *22*(9), 1736–1741. https://doi.org/10.1590/S0103-50532011000900016.

115. Kooti, M., Kooshki, F., Nasiri, E. Preparation and characterization of magnetic graphene nanocomposite containing Cu(Proline) 2 as catalyst for asymmetric aldol reactions. *Res. Chem. Intermed.*, 2019, *45*(5), 2641–2656. https://doi.org/10.1007/s11164-019-03755-x.

116. Zhang, Y., Sun, J., Bai, S., Zhao, H., Wu, X., Panezai, H. Stability of immobilization of bipyridine-proline on Zn-modified bimodal mesoporous silicas and recyclable catalytic performance in asymmetric aldol reaction. *ChemistrySelect*, 2019, *4*(11), 3105–3112. https://doi.org/10.1002/slct.201804000.

117. Siddiqui, Z. N., Musthafa, T. N. M. An efficient and novel synthesis of chromonyl chalcones using recyclable Zn(l-Proline)2 catalyst in water. *Tetrahedron Lett.*, 2011, *52*(31), 4008–4013. https://doi.org/10.1016/j.tetlet.2011.05.118.

118. Reddy, K. R., Rajasekhar, C. V., Krishna, G. G. Zinc-proline complex: An efficient, reusable catalyst for direct nitroaldol reaction in aqueous media. *Synth. Commun.*, 2007, *37*(12), 1971–1976. https://doi.org/10.1080/00397910701354731.

119. Kui, T., Guillen, F. Histidine-based salt as an ionic tag for proline: Application in enantioselective cross aldol reaction in ionic liquids. *Synth. Commun.*, 2020, *50*(10), 1512–1522. https://doi.org/10.1080/00397911.2020.1745241.

120. Yadav, G. D., Singh, S. (L)-prolinamide imidazolium hexafluorophosphate ionic liquid as an efficient reusable organocatalyst for direct asymmetric aldol reaction in solvent-free condition. *RSC Adv.*, 2016, *6*(102), 100459–100466. https://doi.org/10.1039/c6ra23652a.

121. Kong, Y., Tan, R., Zhao, L., Yin, D. L-proline supported on ionic liquid-modified magnetic nanoparticles as a highly efficient and reusable organocatalyst for direct asymmetric aldol reaction in water. *Green Chem.*, 2013, *15*(9), 2422–2433. https://doi.org/10.1039/c3gc40772a.

122. Chen, Z., Li, Y., Xie, H., Hu, C. G., Dong, X. Ionic liquid-supported proline as catalyst in direct asymmetric aldol reaction. *Russ. J. Org. Chem.*, 2008, *44*(12), 1807–1810. https://doi.org/10.1134/S1070428008120154.

123. Siyutkin, D. E., Kucherenko, A. S., Struchkova, M. I., Zlotin, S. G. A Novel (S)-proline-modified task-specific chiral ionic liquid-an amphiphilic recoverable catalyst for direct asymmetric aldol reactions in water. *Tetrahedron Lett.*, 2008, *49*(7), 1212–1216. https://doi.org/10.1016/j.tetlet.2007.12.044.

124. Bellis, E., Kokotos, G. Proline-modified poly(propyleneimine) dendrimers as catalysts for asymmetric aldol reactions. *J. Mol. Catal. A Chem.*, 2005, *241*(1–2), 166–174. https://doi.org/10.1016/j.molcata.2005.05.047.

125. Zhou, L., Wang, L. Chiral ionic liquid containing l-proline unit as a highly efficient and recyclable asymmetric organocatalyst for aldol reaction. *Chem. Lett.*, 2007, *36*(5), 628–629. https://doi.org/10.1246/cl.2007.628.

126. Kucherenko, A. S., Struchkova, M. I., Zlotin, S. G. The (S)-proline/polyelectrolyte system: An efficient, heterogeneous, reusable catalyst for direct asymmetric aldol reactions. *European Journal of Organic Chemistry.* Wiley Online Library 2006, 2000–2004. https://doi.org/10.1002/ejoc.200500888.

127. Rasalkar, M. S., Potdar, M. K., Mohile, S. S., Salunkhe, M. M. An ionic liquid influenced L-proline catalysed asymmetric Michael addition of ketones to nitrostyrene. *J. Mol. Catal. A Chem.*, 2005, *235*(1–2), 267–270. https://doi.org/10.1016/j.molcata.2005.03.024.

128. Miao, Y., Geertsema, E. M., Tepper, P. G., Zandvoort, E., Poelarends, G. J. Promiscuous catalysis of asymmetric michael-type additions of linear aldehydes to β-nitrostyrene by the proline-based enzyme 4-oxalocrotonate tautomerase. *ChemBioChem*, 2013, *14*(2), 191–194. https://doi.org/10.1002/cbic.201200676.

129. Wysocki, J., Kwit, M., Gawronski, J. Absolute configuration determination and convenient asymmetric synthesis of Cis-3-(9-Anthryl)cyclohexanol with proline as a catalyst. *Chirality* 2012, *24*(10), 833–839. https://doi.org/10.1002/chir.22079.

130. Vijaikumar, S., Dhakshinamoorthy, A., Pitchumani, K. L-proline anchored hydrotalcite clays: An efficient catalyst for asymmetric michael addition. *Appl. Catal. A Gen.*, 2008, *340*(1), 25–32. https://doi.org/10.1016/j.apcata.2008.01.030.

131. Mečiarová, M., Hubinská, K., Toma, Š., Koch, B., Berkessel, A. Stereoselective michael addition of carbonyl compounds to (E)-β-Nitrostyrene catalysed by N-Toluensulfonyl-l-proline amide in ionic liquids. *Monatshefte fur Chemie*, 2007, *138*(11), 1181–1186. https://doi.org/10.1007/s00706-007-0732-0.

132. Enders, D., Chow, S. Organocatalytic asymmetric michael addition of 2,2-Dimethyl-1,3-Dioxan-5- one to nitro alkenes employing proline-based catalysts. *Eur. J. Org. Chem.* Wiley Online Library 2006, 4578–4584. https://doi.org/10.1002/ejoc.200600464.

133. Tsogoeva, S. B., Jagtap, S. B., Ardemasova, Z. A. 4-trans-amino-proline based Di- and tetrapeptides as organic catalysts for asymmetric C-C bond formation reactions. *Tetrahedron Asymmetry*, 2006, *17*(6), 989–992. https://doi.org/10.1016/j.tetasy.2006.03.012.

134. Nagata, K., Nakagawa, C., Yokoyama, W., Usui, H., Mochizuki, R., Kanemitsu, T., Miyazaki, M., Itoh, T. Synthesis and catalytic activities of 3-decyl-β-proline for michael reactions in water without an organic solvent. *ACS Omega*, 2021, *6*(30), 19642–19646. https://doi.org/10.1021/acsomega.1c02289.

135. Mahajan, D. P., Godbole, H. M., Singh, G. P., Shenoy, G. G. Enantioselective michael addition of malonic esters to benzalacetophenone by using chiral phase transfer catalysts derived from proline-mandelic acid/tartaric acid. *J. Chem. Sci.*, 2019, *131*(7), 1–9. https://doi.org/10.1007/s12039-019-1642-5.

136. Ranaivoarimanana, N. J., Kanomata, K., Kitaoka, T. Concerted catalysis by nanocellulose and proline in organocatalytic michael additions. *Molecules*, 2019, *24*(7), 1231. https://doi.org/10.3390/molecules24071231.

137. Gu, L., Wu, Y., Zhang, Y., Zhao, G. A new class of efficient poly(ethylene-glycol)-supported catalyst based on proline for the asymmetric michael addition of ketones to nitrostyrenes. *J. Mol. Catal. A Chem.*, 2007, *263*(1–2), 186–194. https://doi.org/10.1016/j.molcata.2006.08.068.

138. Lee, W. Z., Chiang, C. W., Kulkarni, G. M., Kuo, T. S. Highly efficient proline ester-based nickel catalysts for michael addition of thiophenols to α,β-enones. *J. Chinese Chem. Soc.*, 2013, *60*(3), 245–250. https://doi.org/10.1002/jccs.201200386.

139. Omar, E. M., Rahman, M. B. A., Ni, B., Headley, A. D. The role of neutral anions in ionic liquid as solvent media for the reactivity and stereoselectivity towards asymmetric michael addition reaction of N-pentanal with β-nitrostyrene catalyzed by L-proline. *Synth. Commun.*, 2019, *49*(12), 1578–1591. https://doi.org/10.1080/00397911.2019.1604969.

140. Bahekar, S. P., Agrawal, N. R., Sarode, P. B., Agrawal, A. R., Chandak, H. S. L-proline nitrate: An amino acid ionic liquid for green and efficient conjugate addition of thiols to sulfonamide chalcones. *ChemistrySelect*, 2017, *2*(29), 9326–9329. https://doi.org/10.1002/slct.201701891.

141. Chowdari, N. S., Ramachary, D. B., Barbas, C. F. Organocatalysis in ionic liquids: Highly efficient L-proline-catalyzed direct asymmetric Mannich reactions involving ketone and aldehyde nucleophiles. *Synlett*, 2003, *2003*(12), 1906–1909. https://doi.org/10.1055/s-2003-41483.

142. Liu, B., Zhao, D., Xu, D., Xu, Z. Amide ionic liquids (AILs)/L-proline synergistic catalyzed asymmetric mannich reactions. *Chem. Res. Chinese Univ.*, 2007, *23*(2), 163–168. https://doi.org/10.1016/S1005-9040(07)60034-8.

143. Wang, W., Wang, J., Li H. Catalysis of highly stereoselective mannich-type reactions of ketones with Î±-Imino esters by a pyrrolidine-sulfonamide. Synthesis of unnatural α-amino acids. *Tetrahedron Lett.*, 2004, *45*(39), 7243–7246. https://doi.org/10.1016/j.tetlet.2004.08.032.

144. Safaei-Ghomi, J., Zahedi, S. L-proline-functionalized Fe3O4 nanoparticles as a novel magnetic chiral catalyst for the direct asymmetric mannich reaction. *Appl. Organomet. Chem.*, 2015, *29*(8), 566–571. https://doi.org/10.1002/aoc.3333.

145. Wang, Y., Shang, Z., Wu, T., Fan, J., Chen, X. Synthetic and theoretical study on proline-catalyzed Knoevenagel condensation in ionic liquid. *J. Mol. Catal. A Chem.*, 2006, *253*(1–2), 212–221. https://doi.org/10.1016/j.molcata.2006.03.035.

146. Kalantari, F., Rezayati, S., Ramazani, A., Aghahosseini, H., Ślepokura, K., Lis, T. Proline-Cu complex based 1, 3, 5-triazine coated on Fe3O4 magnetic nanoparticles: A nanocatalyst for the Knoevenagel condensation of aldehyde with malononitrile. *ACS Appl. Nano Mater.*, 2022, *5*(2), 1783–1797. https://doi.org/10.1021/acsanm.1c03169.

147. Zhang, H., Han, M., Chen, T., Xu, L., Yu, L. Poly(N-Isopropylacrylamide-Co-l-Proline) -catalyzed Claisen-Schmidt and Knoevenagel condensations: Unexpected enhanced catalytic activity of the polymer catalyst. *RSC Adv.*, 2017, *7*(76), 48214–48221. https://doi.org/10.1039/c7ra09412d.

148. Vaid, R., Gupta, M. Silica-l-Proline: An efficient and recyclable heterogeneous catalyst for the Knoevenagel condensation between aldehydes and malononitrile in liquid phase. *Monatshefte fur Chemie*, 2015, *146*(4), 645–652. https://doi.org/10.1007/s00706-014-1331-5.

149. Gruttadauria, M., Giacalone, F., Lo Meo, P., Marculescu, A. M., Riela, S., Noto, R. First evidence of proline acting as a bifunctional catalyst in the Baylis-Hillman reaction between alkyl vinyl ketones and aryl aldehydes. *European J. Org. Chem.*, 2008, *9*, 1589–1596. https://doi.org/10.1002/ejoc.200701112.

150. Pereira, M. P., Souza Martins, R. De; De Oliveira, M. A. L., Bombonato, F. I. Amino acid ionic liquids as catalysts in a solvent-free Morita-Baylis-Hillman reaction. *RSC Adv.*, 2018, *8*(42), 23903–23913. https://doi.org/10.1039/c8ra02409j.

151. Akagawa, K., Sakamoto, S., Kudo, K. Synthesis of indenes by intramolecular Morita-Baylis-Hillman reaction in aqueous media catalyzed by resin-supported proline. *Synlett*, 2011, *2011*(6), 817–820. https://doi.org/10.1055/s-0030-1259683.

152. Giacalone, F., Gruttadauria, M., Marculescu, A. M., D'Anna, F., Noto, R. Polystyrene-supported proline as recyclable catalyst in the Baylis-Hillman reaction of arylaldehydes and methyl or ethyl vinyl ketone. *Catal. Commun.*, 2008, *9*(6), 1477–1481. https://doi.org/10.1016/j.catcom.2007.12.015.

153. Zhang, G., Luan, Y., Han, X., Wang, Y., Wen, X., Ding, C. Pd(l-Proline)2 complex: An efficient catalyst for Suzuki-Miyaura coupling reaction in neat water. *Appl. Organomet. Chem.*, 2014, *28*(5), 332–336. https://doi.org/10.1002/aoc.3129.

154. Allam, B. K., Singh, K. N. An efficient phosphine-free heck reaction in water using Pd(l-Proline)2 as the catalyst under microwave irradiation. *Synthesis* (Stuttg). 2011, *2011*(7), 1125–1131. https://doi.org/10.1055/s-0030-1258452.

155. Zheng, Y., Du, X., Bao, W. L-proline promoted cross-coupling of vinyl bromide with thiols catalyzed by CuBr in ionic liquid. *Tetrahedron Lett.*, 2006, *47*(7), 1217–1220. https://doi.org/10.1016/j.tetlet.2005.11.164.

156. Wang, Z., Bao, W., Jiang, Y. L-proline promoted Ullmann-type reaction of vinyl bromides with imidazoles in ionic liquidst. *Chem. Commun.*, 2005, *22*, 2849–2851. https://doi.org/10.1039/b501628b.

157. Bao, W., Wang, C. CuI/L-proline potassium salt catalysed synthesis of vinyl sulfones via coupling reaction of vinyl bromides with sulfinic acid salts in ionic liquid. *J. Chem. Res.*, 2006, *2006*(6), 396–397. https://doi.org/10.3184/030823406777946833.

158. Hajipour, A. R., Boostani, E., Mohammadsaleh, F. Proline-functionalized chitosan-palladium(II) complex, a novel nanocatalyst for C-C bond formation in water. *RSC Adv.*, 2015, *5*(31), 24742–24748. https://doi.org/10.1039/c5ra01187f.

159. Cheng, L., Cao, L., Ren, H., Guo, Q., Deng, H., Li, Y. Pd(II)-metalated and l-proline-decorated multivariate UiO-67 as bifunctional catalyst for asymmetric sequential reactions. *Catal. Letters*, 2021, 1–10. https://doi.org/10.1007/s10562-021-03719-0.

160. Cheng, L., Zhao, K., Zhang, Q., Li, Y., Zhai, Q., Chen, J., Lou, Y. Chiral proline-decorated bifunctional Pd@NH2-UiO-66 catalysts for efficient sequential Suzuki coupling/asymmetric aldol reactions. *Inorg. Chem.*, 2020, *59*(12), 7991–8001. https://doi.org/10.1021/acs.inorgchem.0c00065.

161. Nehlig, E., Waggeh, B., Millot, N., Lalatonne, Y., Motte, L., Guénin, E. Immobilized Pd on magnetic nanoparticles bearing proline as a highly efficient and retrievable Suzuki-Miyaura catalyst in aqueous media. *Dalt. Trans.* 2015, *44*(2), 501–505. https://doi.org/10.1039/c4dt02899f.

162. Chouhan, G., Wang, D., Alper, H. Magnetic nanoparticle-supported proline as a recyclable and recoverable ligand for the CuI catalyzed arylation of nitrogen nucleophiles. *Chem. Commun.*, 2007, *45*, 4809–4811. https://doi.org/10.1039/b711298j.

163. Wang, Z., Wang, L., Li, P. Silica-anchored proline-copper(I) as an efficient and recyclable catalyst for the Sonogashira reaction. *Synthesis (Stuttg).*, 2008, *2008*(9), 1367–1372. https://doi.org/10.1055/s-2008-1072562.

164. Liu, X., Wu, J., Shang, Z. Efficient dimeric esterification of alcohols with NBS in water using L-proline as catalyst. *Synth. Commun.*, 2012, *42*(1), 75–83. https://doi.org/10.1080/00397911.2010.521966.

165. Levina, A., Muzart, J. Enantioselective allylic oxidation in the presence of the Cu(I) Cu(II)-proline catalytic system. *Tetrahedron: Asymmetry*, 1995, *6*(1), 147–156. https://doi.org/10.1016/0957-4166(94)00370-Q.

166. Saberi, F., Rodriguez-Padrón, D., Garcia, A., Shaterian, H. R., Luque, R. Unprecedented proline-based heterogeneous organocatalyst for selective production of vanillin. *Catalysts*, 2018, *8*(4), 167. https://doi.org/10.3390/catal8040167.

167. Shen, Z. L., Ji, S. J. Alkali salt of L-proline as an efficient and practical catalyst for the cyanosilylation of a wide variety of carbonyl compounds under solvent-free conditions. *Synth. Commun.*, 2009, *39*(5), 775–791. https://doi.org/10.1080/00397910802431149.

168. Rao, S. N., Mohan, D. C., Adimurthy, S. L-proline: An efficient catalyst for transamidation of carboxamides with amines. *Org. Lett.*, 2013, *15*(7), 1496–1499. https://doi.org/10.1021/ol4002625.

169. Kottawar, S. S., Goswami, S. V., Thorat, P. B., Bhusare, S. R. L-proline as an efficient catalyst for synthesis of aldimines at ambient temperature condition. *E-Journal Chem.*, 2011, *8*(4), 1859–1863. https://doi.org/10.1155/2011/185981.

170. Aghapoor, K., Amini, M. M., Jadidi, K., Darabi, H. R. N-functionalized L-proline anchored MCM-41: A novel organic-inorganic hybrid material for solvent-free aminolysis of styrene oxide under microwave irradiation. *Acta Chim. Slov.*, 2015, *62*(1), 95–102. https://doi.org/10.17344/acsi.2014.755.

171. Ding, X., Jiang, H. L., Zhu, C. J., Cheng, Y. X. Direct asymmetric α-amination of aldehydes with azodicarboxylates in ionic liquids catalyzed by imidazolium ion-tagged proline organocatalyst. *Tetrahedron Lett.*, 2010, *51*(47), 6105–6107. https://doi.org/10.1016/j.tetlet.2010.09.036.

6 The Catalytic Role of L-Serine, L-Asparagine, L-Tryptophan, L-Phenylalanine, and L-Methionine in Organic Reactions

6.1. INTRODUCTION

Significant works reported in the field of supported chiral organic catalysts. But this catalytic system also suffers from poor solubility in conventional solvent systems, high catalyst loading, and catalyst recycling. Immobilization of organocatalysts may provide answers at least partly to the tents. The examples covered in the chapter have explained the significant application of supported and unsupported strategies on asymmetric organocatalysis to improve easy handling and good applicability in several useful examples.

6.2. APPLICATION OF METAL COMPLEXES OF L-SERINE ON THE SUPPORTED MATERIAL AS A CATALYST FOR THE MULTICOMPONENT REACTION

Serine is a nonessential amino acid that plays a vital role in protein synthesis. It comes in two forms: L-serine and D-serine. L-serine is synthesized from glycine or threonine. Proline and its derivatives are covalently supported onto supported material and evaluated as catalysts in organic reactions. In this context, the high reactivity of SBA-15@serine@Pd was exploited by our group for the synthesis of 5-substituted tetrazoles, sulfides, and sulfoxides (Scheme 6.1) [1]. This nanocatalyst was prepared using a combination of L-Serine onto SBA-15 to form a stable complex with Pd ions to form SBA-15@serine@Pd catalyst. Diverse substituents on three of the reactants have been explored to afford good to excellent yields of desired products (Scheme 6.1). This process provides many benefits such as reduced reaction time, recyclable green catalyst, and excellent yields (Scheme 6.2).
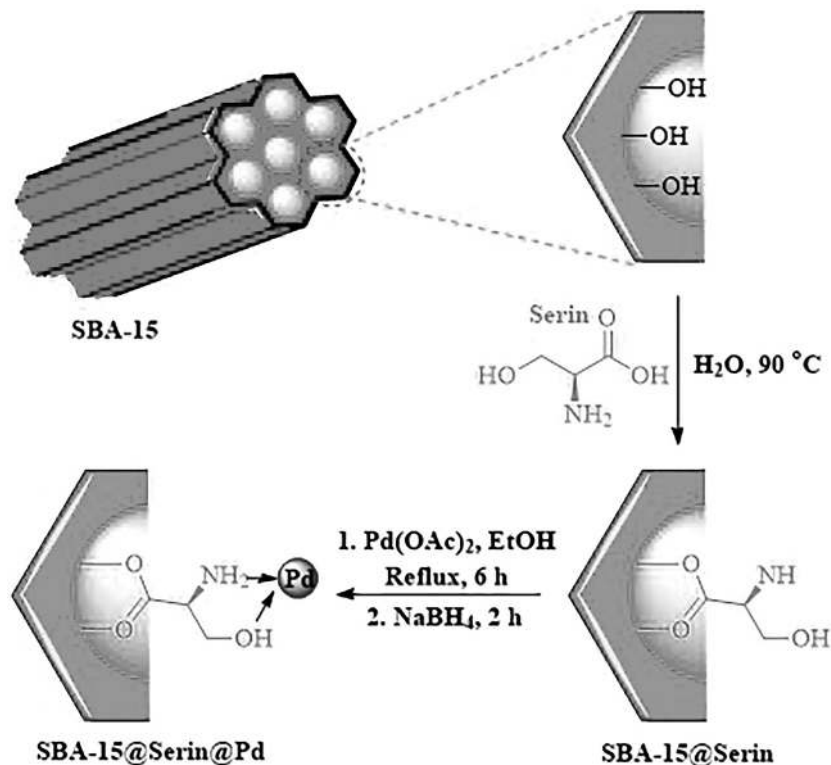
SCHEME 6.1.   Synthesis of SBA-15@serine@Pd catalyst.

MCM-41@serine@Cu(II) is synthesized by incorporation of serine into the mesoporous MCM-41. MCM-41@serine was treated with $Cu(NO_3)_2 \cdot 6H_2O$ and then furnished the MCM-41@serine@Cu(II) (Scheme 6.3). The activity of nanocatalysts was explored for oxidation, coupling, and multicomponent reaction (Scheme 6.4) [2]. Experimental results showed the reaction's scope was broad, and high yields were obtained from desired products.

6.3.   APPLICATION OF METAL COMPLEXES OF L-ASPARAGINE AS A CATALYST FOR CYCLOADDITION REACTION OF CO_2 WITH VARIOUS EPOXIDES

The presence and increase of CO_2 in the atmosphere has created many problems. In recent years, CO_2 has been used to synthesize valuable chemical compounds such as carbonates, carbamates, formamides, benzimidazoles, and urea. In this regard, in 2020, Phatake et al. presented a report on the fixation of atmospheric CO_2 and its conversion to carbonates and formamides using L-serine@ZnO as a catalyst (Scheme 6.5) [3]. The L-serine@ZnO catalyst, like other AAs@ZnO, was prepared
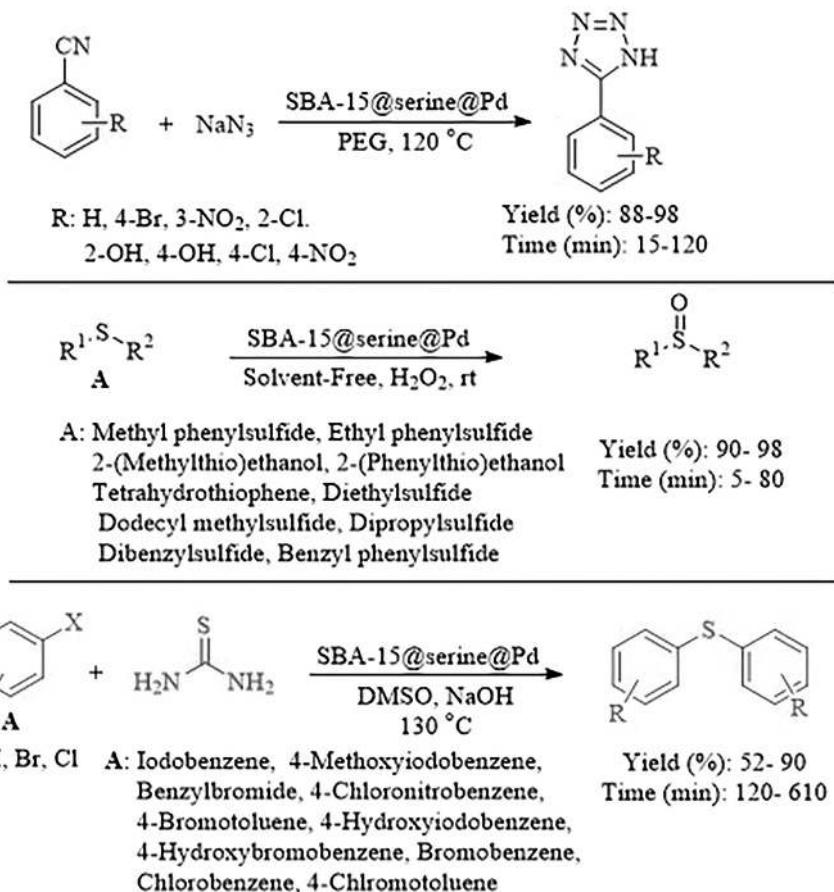
SCHEME 6.2. SBA-15@serine@Pd catalyzed the coupling reaction, oxidation reaction, and synthesis of 5-substituted tetrazoles.
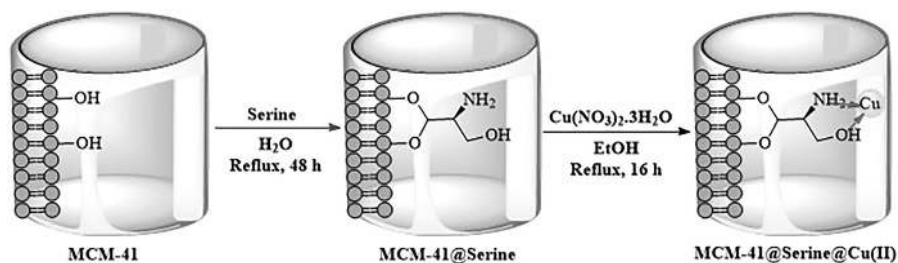
SCHEME 6.3. Synthesis of MCM-41@serine@Cu(II)

X + H_2N—NH_2 $\xrightarrow{\text{MCM-41@Serine@Cu(II)}}$

DMSO, KOH
130 °C

X: I, Br, Cl

A: 2-Methoxyiodobenzene, Iodobenzene,
4-Bromonitrobenzene, Bromobenzene,
4-Chloronitrobenzene, 4-Bromotoluene,
Chlorobenzene, 4-Iodonitrobenzene,
Benzylbromide, 4-Iodotoluene

Yield (%): 32- 67
Time (min): 70- 690

R^1—S—R^2 $\xrightarrow{\text{MCM-41@Serine@Cu(II)}}$ R^1—S(=O)—R^2

A   Solvent-Free, H_2O_2, rt

A: Dipropylsulfide, Diethylsulfide, Dibenzylsulfide,
Benzylphenylsulfide, Tetrahydrothiophene,
Methylphenylsulfide, 2-(Phenylthio)ethanol
Dimethylsulfide, Dodecylmethylsulfide

Yield (%): 89- 97
Time (min): 5- 60

NH$_2$ + H—C(=O)—R $\xrightarrow{\text{MCM-41@Serine@Cu(II)}}$

NH$_2$ EtOH, r.t

R: 4-NO$_2$, 4-OH, 4-F, 4-OMe
4-Br, 4-Me, 4-Cl, 3-NO$_2$, H

Yield (%): 91- 97
Time (min): 30- 75

H—C(=O)—R + OEt ... NOAc $\xrightarrow{\text{MCM-41@Serine@Cu(II)}}$ OEt

EtOH, Reflux

R: H, 4-NO$_2$, 4-OH, 4-F, 4-OMe
4-Br, 4-Me, 4-Cl, 3,4-Di(OMe)

Yield (%): 91- 97
Time (min): 110- 215

SCHEME 6.4. MCM-41@serine@Cu(II) catalyzed the synthesis of sulfides, oxidation of sulfides to sulfoxides, and the synthesis of 2,3-dihydroquinazolin-4(1H)-ones.

via a combination of Zn(OAc)$_2$ and corresponding amino acids. In this study, different epoxides and amines were used to produce cyclic carbonates and amides, respectively.

This group also proposed a mechanism for the formation of cyclocarbonates. According to this mechanism, the oxygen of epoxide is activated by ZnO. Then, CO$_2$ is activated by the amino group of L-serine@ZnO. One of the important features of heterogeneous catalysts is reusability (Scheme 6.6). In both reactions, the catalysts were separated and reused four times without reducing reaction efficiency.
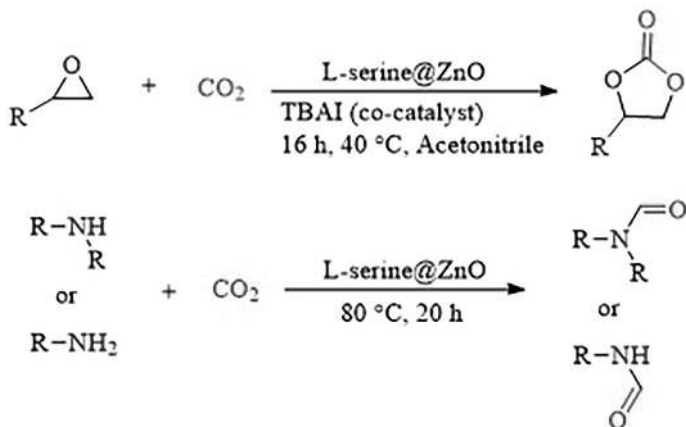
SCHEME 6.5.   .Production of cyclic carbonates and amides

6.4.   CATALYTIC APPLICATION OF METAL COMPLEXES OF L-SERINE DERIVATIVES ON THE SUPPORTED MATERIAL IN THE REDUCTION REACTION

Nitroarenes are the most detected prevalent pollutants in water. Conversion of nitroarene to amino arene is an important reaction in organic synthesis because amino arenes are useful intermediates for the production of organic compounds such as pharmaceutical, natural, and chemical compounds on a bulk scale. In 2018, Costa et al. were able to produce two catalysts using L-serine amino acid and nanoparticle of Au. They used two L-serine derivatives to immobilize montmorillonite followed by coordination with Au nanoparticles (Scheme 6.7) [4].

These catalysts were applied to reduce 4-NP to 4-AP in an aqueous medium in the presence of $NaBH_4$ as a mild reducing agent at room temperature with a conversion of approximately 100%. These catalysts were used for ten times and no significant reduction in their performance was observed after these consequences run.

6.5.   APPLICATION OF L-SERINE DERIVATIVES AS AN ORGANOCATALYST IN MULTICOMPONENT REACTION

In 2011, Yong and coworkers reported the application of siloxy-L-serine to catalyze a three-component asymmetric direct Mannich reaction, via a combination of aromatic aldehydes, ketones, and amines, in hmim[PF_6], with good efficiency and high enantioselectivity (Scheme 6.8) [5]. Siloxy-serine organic catalyst can be recovered up to three times without reducing its enantioselectivity.
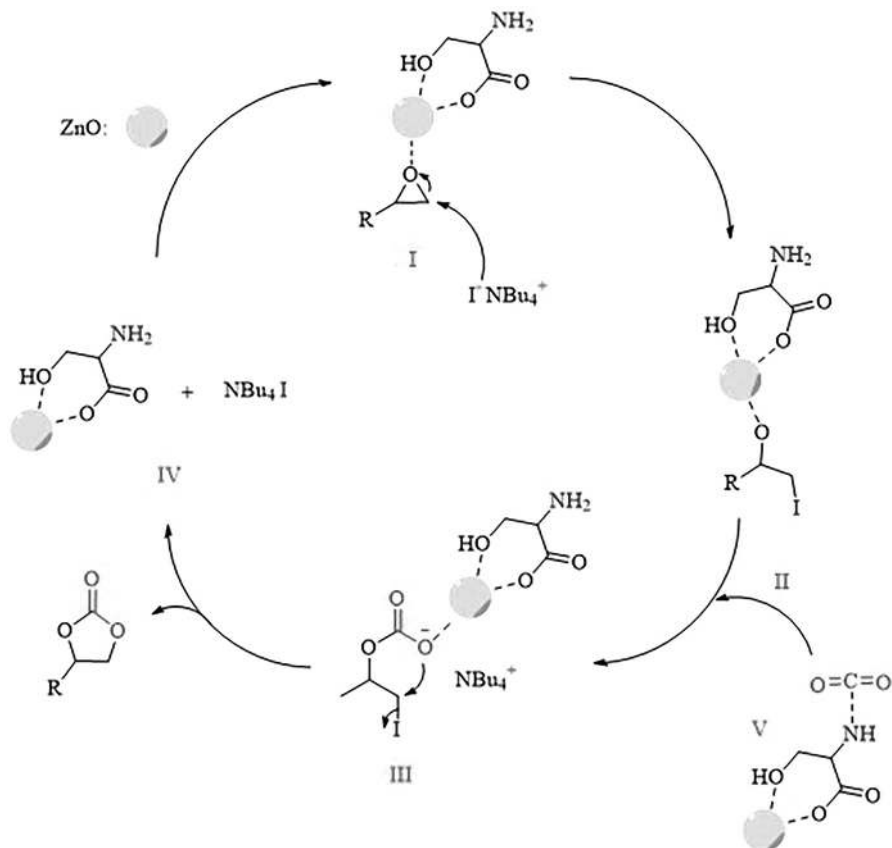
SCHEME 6.6.   The proposed mechanism of cyclic carbonate formation.

6.6.   APPLICATION OF L-SERINE DERIVATIVES FOR ALLYLIC ALKYLATION AND DIETHYL ZINC ADDITION

In 2003, Jones et al. designed a method for synthesizing oxazolines 2, precursors to N–O ligands 3 and N–P ligands 4, potentially incorporating up to three diversity points (R, R0, and R00) (Scheme 6.9). Ligands 3 and 4 were applied to aldehyde alkylation and allylic alkylation (Schemes 6.10 and 6.11) [6].

6.7.   APPLICATION OF L-ASPARAGINE AS AN ORGANOCATALYST FOR THE MULTICOMPONENT REACTION

In recent years, organocatalysis has been recognized as a powerful methodology in organic synthesis for the construction of new materials. The application of solid-supported catalysts would offer the advantage of easy recovery by simple filtration and
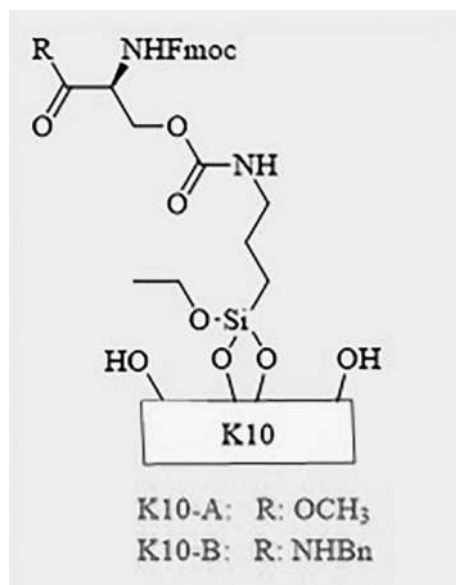
SCHEME 6.7. Scheme of the metal complex of L-serine supported on the montmorillonite.
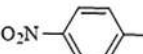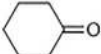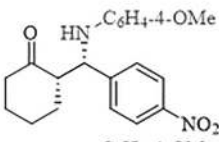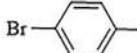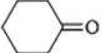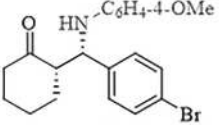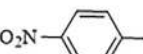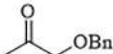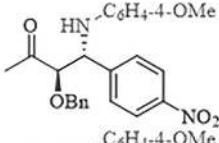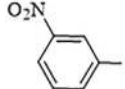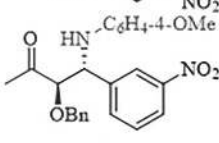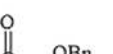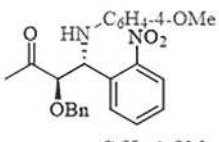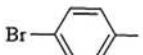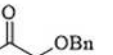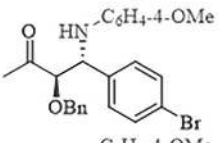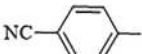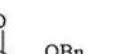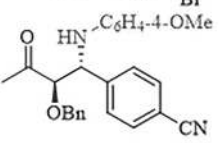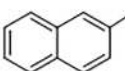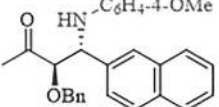
could allow the implementation of continuous flow processes. The catalytic activity and mechanistic pathways are reviewed in this chapter.

2-Aminothiazole and their derivatives constitute an important class of compounds that are employed as a starting material for the synthesis of many compounds such as sulfur drugs, fungicides, biocides, dyes, thyroid inhibitors in the treatment of hyperthyroidism, and chemical reaction accelerators [7]. In this context, Safari et al. demonstrated the synthesis of 2-aminothiazole by a combination of thiourea with methyl carbonyls in the presence of iodine as an oxidant reagent and asparagine as a green organocatalyst. The process is compatible with various aromatic methyl carbonyls containing electron-donating and electron-withdrawing groups at 80°C in DMSO solvent (Scheme 6.12) [8]. The proposed mechanism is shown in Scheme 6.13.

6.8. APPLICATION OF METAL COMPLEXES OF L-ASPARAGINE ON THE SUPPORTED MATERIAL AS A CATALYST FOR THE MULTICOMPONENT REACTION

Safari and coworkers synthesized a heterogeneous catalyst by functionalizing Al_2O_3 nanoparticles with Asp [9]. For this reason, they first grafted the Al_2O_3 nanoparticles with 3-chloropropyltrimethoxysilane (CPTMS) followed by functionalization by asparagine amino acid (Scheme 6.14). The one-pot reaction between different methyl carbonyl and thiourea and iodine was catalyzed by asparagine to produce 2-amino thiazoles (Scheme 6.15). To evaluate the reuse feature, after the reaction
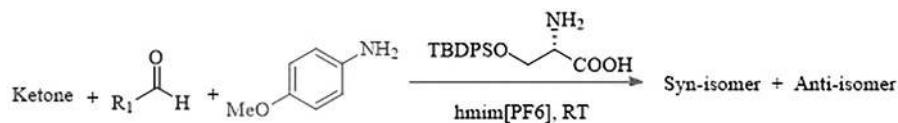
R$_1$	ketone	Product	Yield (%)	syn/anti	Ee (%)
O$_2$N–C$_6$H$_4$–	cyclohexanone	(product)	91	89:11	84
Br–C$_6$H$_4$–	cyclohexanone	(product)	50	75:25	71
O$_2$N–C$_6$H$_4$–	OBn-ketone	(product)	52	18:82	78
O$_2$N (meta)	OBn-ketone	(product)	70	17:83	80
NO$_2$ (ortho)	OBn-ketone	(product)	66	6:94	82
Br–C$_6$H$_4$–	OBn-ketone	(product)	66	30:70	62
NC–C$_6$H$_4$–	OBn-ketone	(product)	64	15:85	91
naphthyl	OBn-ketone	(product)	89	40:60	55

SCHEME 6.8.   Mannich reaction catalyzed by siloxy-L-serine.
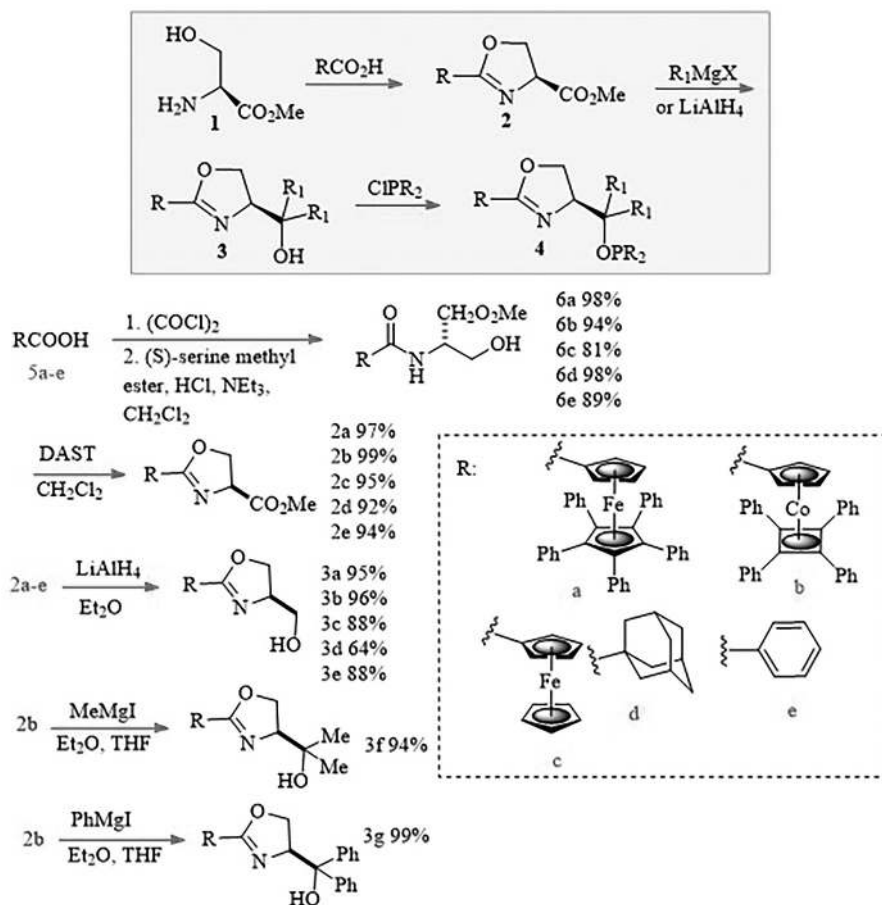
SCHEME 6.9. Synthesis of ligand
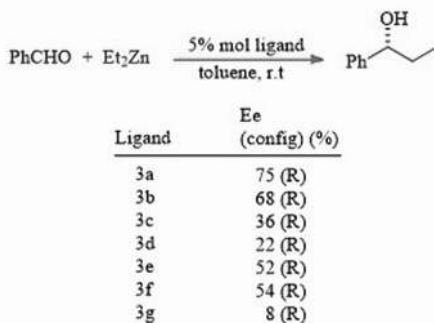
SCHEME 6.10. Catalytic diethyl zinc addition to benzaldehyde.
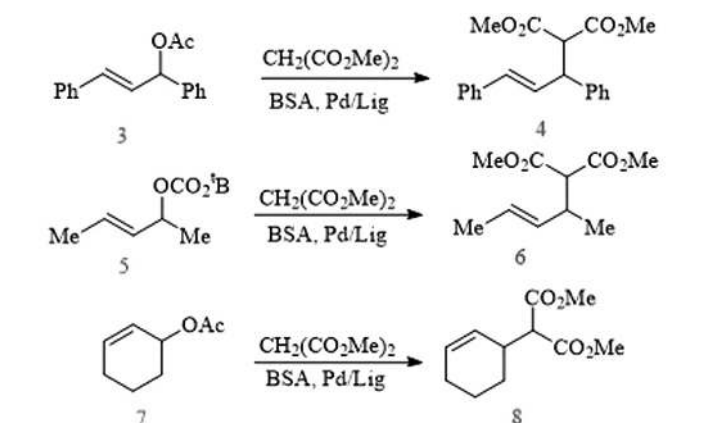
solvent	Ee 4 (config) (%)	Ee 6 (config) (%)	Ee 8 (config) (%)
THF	43 (S)	36 (S)	5 (R)
CH₂Cl₂	24 (R)	6 (S)	25 (R)

Pd-catalysed alylic alkylation of 3, 5, 7 with methylmalonate by ligand 2.

ligand	4a	4b	4c	4d	4e
Ee 4 (config) (%)	80 (S)	52 (S)	90 (S)	67 (S)	90 (S)
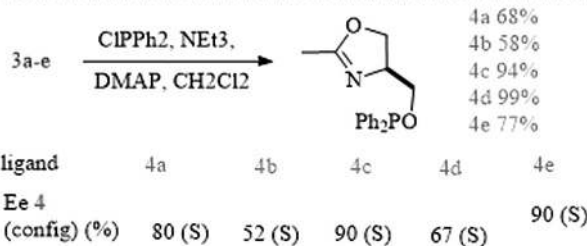
Pd-catalysed alylic alkilation of 3 to 4 by ligans 4a-4e in CH₂Cl₂ as solvent in 20 °C

ligand	4a	4b	4c	4d	4e
Ee 8 (config) (%)	3 (R)	7 (R)	48 (R)	6 (R)	5 (R)

Pd-catalysed alylic alkilation of 7 to 8 by ligans 4a-4e in CH₂Cl₂ as solvent in 20 °C

ligand	4a	4b	4c	4d	4e
Ee 6 (config) (%)	0 (%)	70 (S)	50 (S)	11 (S)	43 (S)

Pd-catalysed alylic alkilation of 5 to 6 by ligans 4a-4e in CH₂Cl₂ as solvent in 20 °C

SCHEME 6.11. Pd-catalyzed allylic alkylation of various compounds by 4a–4e ligands.
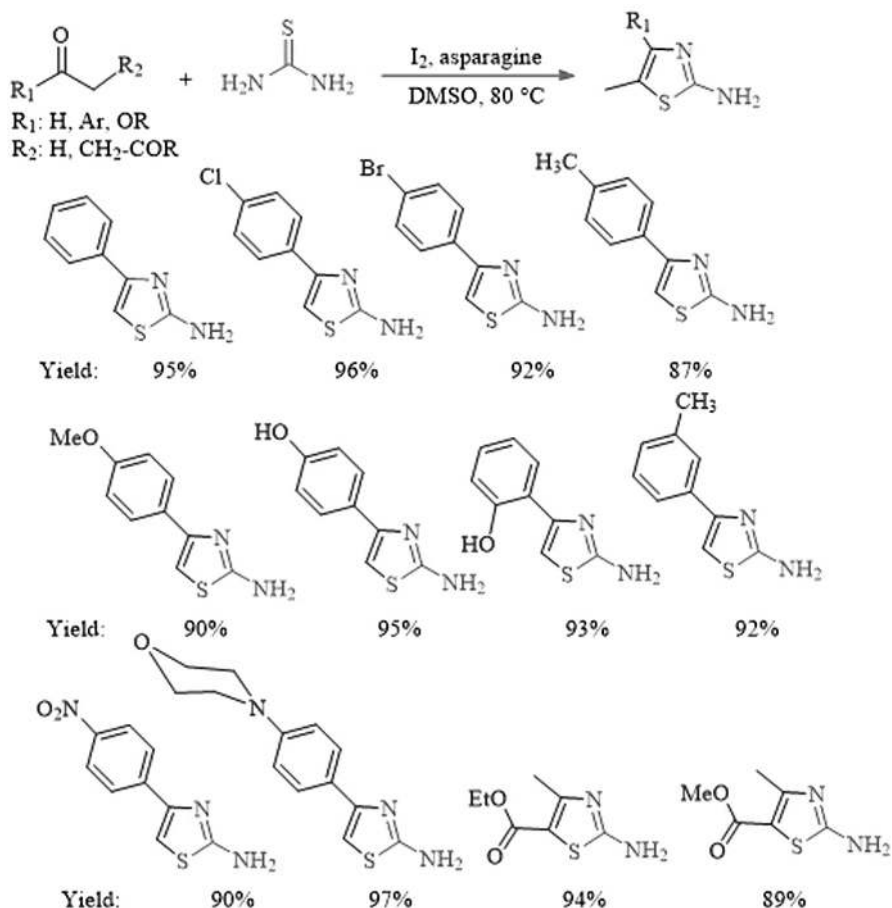
SCHEME 6.12.   The synthesis of 2-aminothiazole using asparagine.

was completed, the catalyst was removed, washed several times with ethyl acetate, and dried at 80°C, and it was concluded that the catalyst could be used five times.

6.9.   APPLICATION OF L-ASPARAGINE-BASED IONIC LIQUID–SUPPORTED MATERIAL AS AN ORGANOCATALYST IN MULTICOMPONENT REACTION

In 2017, Azarifar et al. reported the incorporation of the amino acid ionic liquid tetrabutylammonium asparagine (TBAAsp) on the $Fe_{3-x}Ti_xO_4$ nanoparticles [10]. The nanocatalyst was applied for the synthesis of 1,4-dihydropyrano[2,3-*c*]pyrazoles via a three-component one-pot reaction between different aromatic aldehyde, malono-nitrile, and 3-methyl-2-phenyl-1*H*-2-pyrazol-5(4*H*)-one in solvent-free conditions
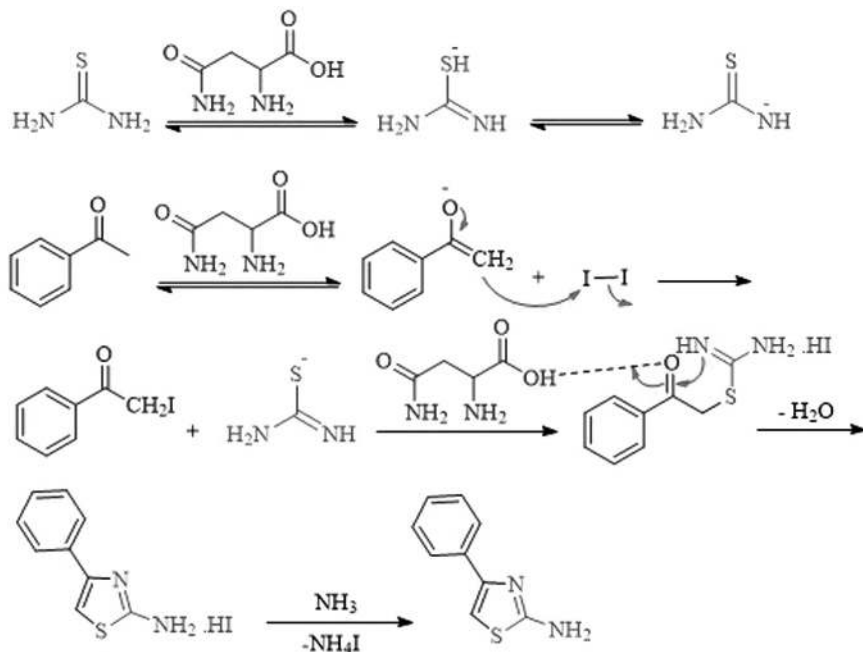
SCHEME 6.13.   A plausible mechanism of the synthesis of 2-amino thiazoles
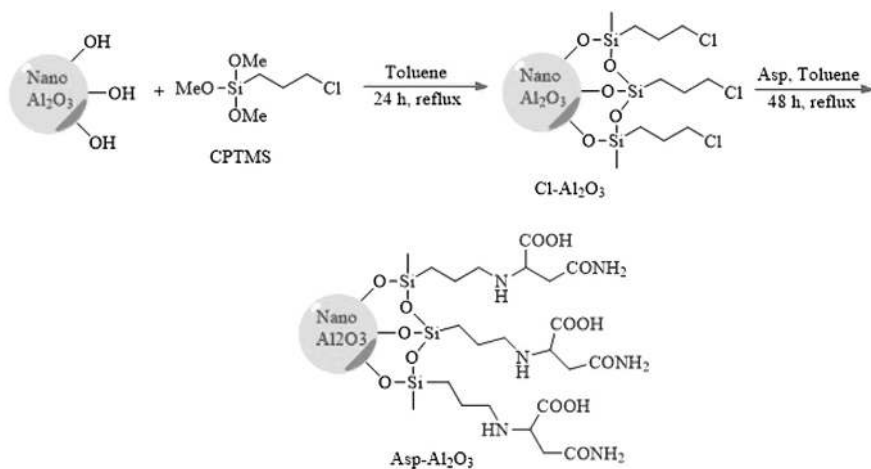
SCHEME 6.14.   Synthetic route of Asp-Al$_2$O$_3$ nanoparticle.
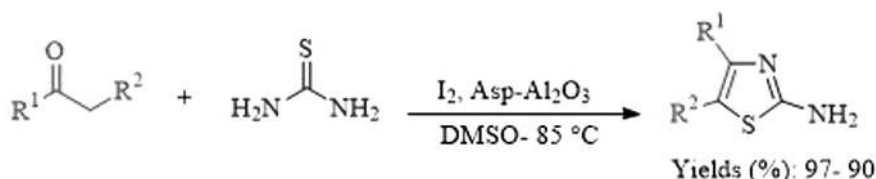
SCHEME 6.15.   Synthesis of 2-amino thiazoles catalyzed by Asp-Al$_2$O$_3$ as a catalyst.

(Scheme 6.16). The catalyst can be recovered and reused several times without significant loss of activity of the catalyst.

6.10.   APPLICATION OF METAL COMPLEXES OF L-TRYPTOPHAN AND L-TRYPTOPHAN DERIVATIVE-SUPPORTED MATERIAL AS A CATALYST IN THE COUPLING REACTION

L-tryptophan is a naturally occurring amino acid found in animal and plant proteins required by all life-forms. Due to its pharmaceutical significance, diverse methods have already been implemented for its production [11]. Although the use of L-proline as a natural amino acid has been intensively employed as a catalyst in organic reactions, the use of other natural amino acids, that is, L-tryptophan as a catalyst, has barely been explored in recent years.

Ar	Product	Yield(%)
C$_6$H$_5$	4a	90
3-O$_2$NC$_6$H$_4$	4b	89
3-ClC$_6$H$_4$	4c	89
3-BrC$_6$H$_4$	4d	88
2,4-Cl$_2$C$_6$H$_3$	4e	89
4-MeOC$_6$H$_4$	4f	88
4-BrC$_6$H$_4$	4g	96
4-MeC$_6$H$_4$	4h	87
3-EtO-4-HOC$_6$H$_3$	4i	86
4-ClC$_6$H$_4$	4j	94
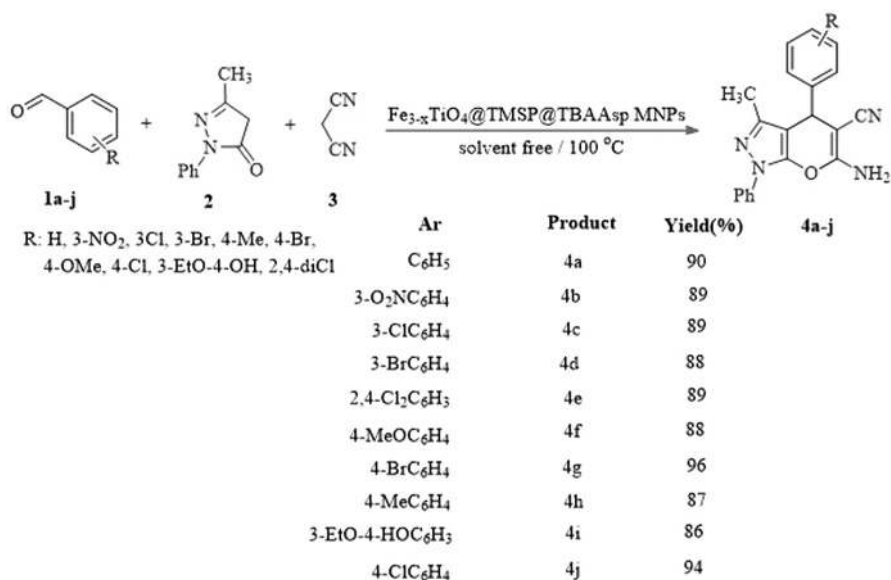
SCHEME 6.16.   Fe$_{3-x}$TiO$_4$@TMSP@TBAAsp MNPs catalyzed a three-component reaction

Haldar groups synthesized gold nanoparticles using modified urea tryptophan and $HAuCl_4$ in water at room temperature. About 200 mg of tryptophan was dissolved in hot water, followed by adding 500 mg of KCNO and stirred at room temperature for 4 h. After cooling to pH = 1, it became acidic, and a white precipitate was obtained, which was dried after filtration and a light pink solid was obtained (Scheme 6.17). After, this catalyst was used in the Suzuki–Mira cross-coupling reaction to form a carbon–carbon bond. The reaction was performed between phenylboronic acid and different aryl halides at 45°C and water solvent in the presence of potassium carbonate as the base, and high-efficiency products were synthesized (Scheme 6.18) [12].

Our laboratory synthesized boehmite@tryptophan-Pd by immobilization of L-tryptophan. Boehmite@ tryptophan was treated with $Pd(OAc)_2$ and then furnished the Boehmite@tryptophan-Pd nanoparticles (Scheme 6.19) [13].

To study the catalytic properties of these nanoparticles, Suzuki, Stille, and Heck cross-coupling reactions were examined (Scheme 6.20). Regarding the recovery and reuse feature, it was found that in the Heck reaction (as a model reaction), the catalytic activities did not change significantly after five times being reused. Also, ICP-OES results showed that the amount of leached palladium in solution for the synthesis of 1,1′-biphenyl, 4-methoxy-1,1′′-biphenyl, and butyl cinnamate were 0.72%, 0.85%, and 1.11%, respectively. Also, hot filtration studies on the Heck reaction showed that only
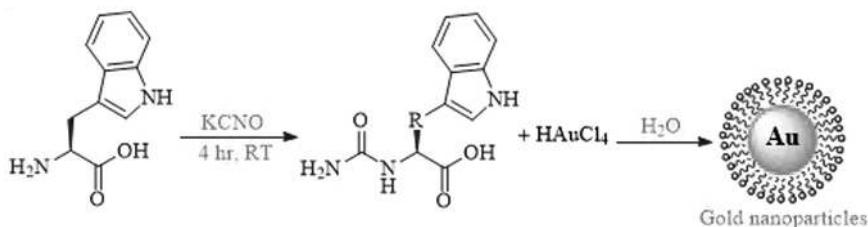
SCHEME 6.17.   Synthesized gold nanoparticles using modified urea tryptophan.
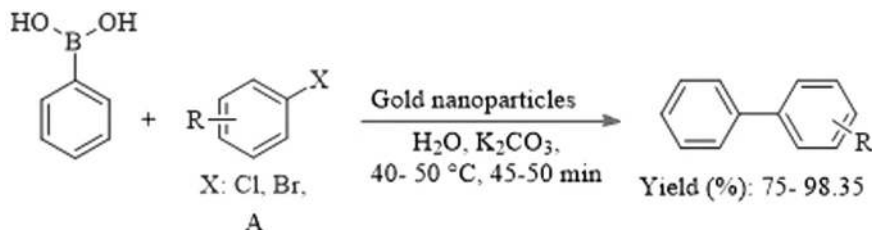
A: 4-bromobenzoic acid, 4-chlorobenzoic acid, 4-chlorobenzene-1,3-diol,
     1-(4-chlorophenyl)ethan-1-one, 2-chlorobenzaldehyde,
     2-chloro-4,6-dimethoxy-1,3,5-triazine, 1-methyl-4-vinylbenzene,
     4-bromo-6-nitro-1,3,5-triazine-2-carbaldehyde,
     6-bromo-1,3,5-triazine-2,4-dicarboxylic acid

SCHEME 6.18.   Suzuki–Miyaura cross-coupling reaction catalyst by gold nanoparticles
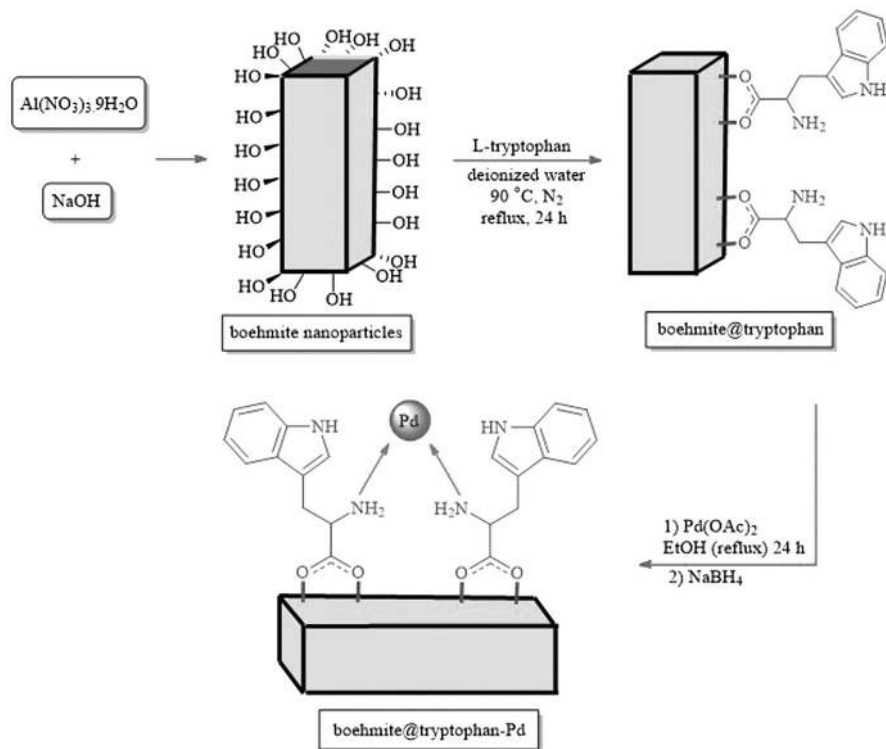
SCHEME 6.19. Synthetic route of boehmite@tryptophan-Pd nanoparticles.

a small amount of the coupling reaction (less than 6%) was performed in the absence of a catalyst in the second half-time of the reaction.

6.11. APPLICATION OF L-TRYPTOPHAN-SUPPORTED MATERIAL AS A CATALYST IN THE OXIDATION REACTION

Our group introduced the synthesis of three nanocatalysts (Fe_3O_4@tryptophan-Cu, Fe_3O_4@tryptophan-Co, and Fe_3O_4@tryptophan-Fe) and the activity of catalysts used for the oxidation of sulfides and thiols [14]. The catalyst was prepared by immobilizing the tryptophan on Fe_3O_4, followed by the addition of metal to afford the final products (Scheme 6.21). Experimental results show the rate of reaction in the presence of Fe_3O_4@tryptophan-Cu was increased significantly. The nanoparticles successfully catalyzed the oxidation of an extensive range of sulfides and thiols to yield the corresponding products in excellent yields (Scheme 6.6). Also, experimental results show reactions were compared under magnetic stirrer conditions and in the presence of ultrasonic irradiation (Scheme 6.22).

In another study, our group reported the use of Ni(II) on Fe_3O_4@tryptophan for the oxidation of sulfides, oxidative coupling of thiols, and synthesis of 5-substituted

R—⟨X⟩ + R—⟨B(OH)₂⟩ $\xrightarrow[\text{EtOH, 70 °C}]{\substack{\text{boehmite@tryptophan-Pd (Cat.)} \\ \text{Na}_2\text{CO}_3}}$ R—⟨Ph-Ph⟩

Ar

X: Cl, Br, I

Ar: Ph, 4-MeC₆H₄, 4-OMeC₆H₄, 2-OMeC₆H₄, 3-OMeC₆H₄, 4-CNC₆H₄,
     3-CF₃C₆H₄, 4-ClC₆H₄, 4-NO₂C₆H₄, 4-NH₂C₆H₄, 4-OHC₆H₄, 4-AcC₆H₄,

Yield (%): 98- 82
Time (min): 30- 230

R—⟨X⟩ + Ph₃SnCl $\xrightarrow[\text{EtOH, 70 °C}]{\substack{\text{boehmite@tryptophan-Pd (Cat.)} \\ \text{Na}_2\text{CO}_3}}$ R—⟨Ph-Ph⟩

Ar

X: Cl, Br, I

Ar: Ph, 4-MeC₆H₄, 4-OMeC₆H₄, 2-OMeC₆H₄, 3-OMeC₆H₄,
     4-CNC₆H₄, 3-CF₃C₆H₄, 4-ClC₆H₄, 4-NO₂C₆H₄,

Yield (%): 77- 96
Time (min): 50- 210

R—⟨X⟩ + ⟨acrylate⟩O–Bu $\xrightarrow[\text{DMSO, 120 °C}]{\substack{\text{boehmite@tryptophan-Pd (Cat.)} \\ \text{K}_2\text{CO}_3}}$ R—⟨cinnamate⟩OBu

Ar

X: Cl, Br, I

Ar: Ph, 4-MeC₆H₄, 4-OMeC₆H₄, 2-OMeC₆H₄, 4-CNC₆H₄,
     4-ClC₆H₄, 4-NO₂C₆H₄, 4-NH₂C₆H₄, 4-OHC₆H₄, 4-AcC₆H₄,

Yield (%): 87- 95
Time (min): 70- 750

SCHEME 6.20.   The application of boehmite@tryptophan-Pd in the coupling reaction.
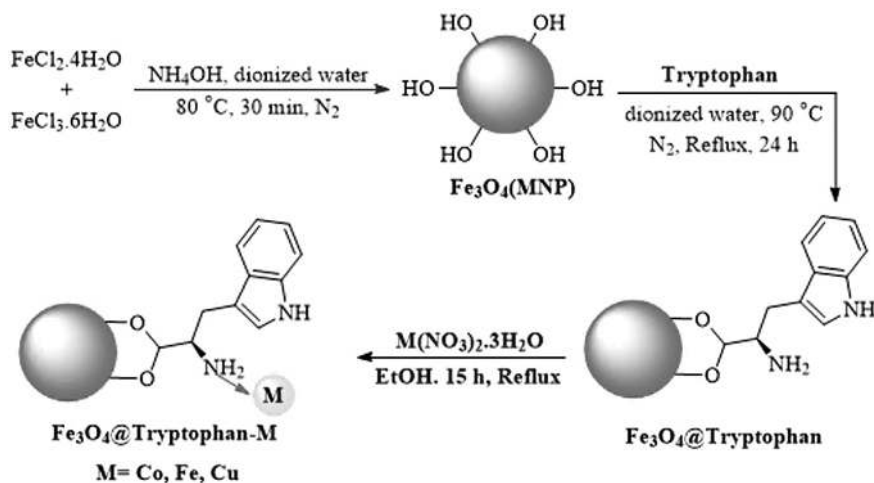
SCHEME 6.21.   Synthetic route of Fe₃O₄@tryptophan-M (M: Cu, Co, and Fe)

$$R_1 \diagdown^S\diagup R_2 \xrightarrow[\text{Solvent-Free, H}_2\text{O}_2\text{, rt}]{\text{Fe}_3\text{O}_4\text{@Tryptophan-M}} R_1\diagdown^{\overset{O}{\underset{\parallel}{S}}}\diagup R_2 + R_1\diagdown^{\overset{O\,O}{\underset{\diagup\diagdown}{S}}}\diagup R_2$$

100%   0%

Substrate	Fe₃O₄@Tryptophan-Cu Time (min)	Yield (%)	Fe₃O₄@Tryptophan-Co Time (min)	Yield (%)	Fe₃O₄@Tryptophan-Fe Time (min)	Yield (%)
Benzylphenylsulfide	60	89	75	86	85	80
Tetrahydrothiophene	15	92	25	90	30	90
3,3'-Thiodipropionic acid	10	90	20	88	25	86
Methylphenylsulfide	45	96	55	95	60	92
Thiodiglycolic acid	10	94	20	89	30	87
Diethylsulfide	55	95	75	93	90	88
Dibenzylsulfide	40	92	65	89	80	85
Ethylphenylsulfide	50	87	70	85	75	86

$$R-SH \xrightarrow[\text{EtOH, H}_2\text{O}_2\text{, rt}]{\text{Fe}_3\text{O}_4\text{@Tryptophan-M}} R_3\diagdown_S\diagup^S\diagdown R_3$$

Substrate	Fe₃O₄@Tryptophan-Cu Time (min)	Yield (%)	Fe₃O₄@TryptophanCo Time (min)	Yield (%)	Fe₃O₄@Tryptophan-Fe Time (min)	Yield (%)
2-Mercaptoethanol	18	83	30	82	30	80
Mercaptosuccinic acid	15	78	35	78	35	75
2-Mercaptobenzoic acid	20	95	25	91	20	92
Benzyl mercaptan	40	82	75	80	235	54
Benzo[d]thiazole-2-thiol	45	86	15	90	45	80
Benzo[d]oxazole-2-thiol	25	91	35	88	50	80
Thiophenol	20	89	30	87	80	72
Methylbenzenethiol	15	96	30	85	80	70

$$HO\diagdown_S\diagup^S\diagdown_{SH} \xrightarrow[\text{EtOH, H}_2\text{O}_2\text{, rt}]{\text{Fe}_3\text{O}_4\text{@Tryptophan-M}} HO\diagdown\diagup^{S-S}\diagup\diagdown OH + O\diagup\diagdown\diagup^{SH}$$

100%   0%
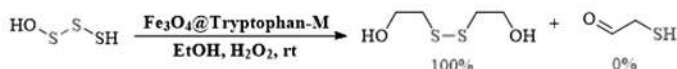
Oxidation sulfides to sulfoxides with Fe₃O₄@Tryptophan-Cu

Substrate	Conventional method Time (min)	Yield (%)	Sonication method Time (min)	Yield (%)
Benzylphenylsulfide	60	89	20	91
Tetrahydrothiophene	15	92	10	95
3,3'-Thiodipropionic acid	10	90	5	95
Methylphenylsulfide	45	96	20	96
Thiodiglycolic acid	10	94	5	96
Diethylsulfide	55	95	25	96
Dibenzylsulfide	40	92	15	94
Ethylphenylsulfide	50	87	20	90

Oxidative coupling of thiols by Fe₃O₄@Tryptophan-Cu under various method

Substrate	Conventional method Time (min)	Yield (%)	Sonication method Time (min)	Yield (%)
2-Mercaptoethanol	18	83	7	85
Mercaptosuccinic acid	15	78	5	80
2-Mercaptobenzoic acid	20	95	5	95
Benzyl mercaptan	40	82	10	90
Benzo[d]thiazole-2-thiol	45	86	5	90
Benzo[d]oxazole-2-thiol	25	91	10	95
Thiophenol	20	89	10	92
Methylbenzenethiol	15	96	96	10

SCHEME 6.22. Oxidation of sulfides to the sulfoxides in the presence of Fe₃O₄@tryptophan-Cu, Fe₃O₄@tryptophan-Co, and Fe₃O₄@tryptophan-Fe.

1*H*-tetrazoles [15]. The magnetic catalyst was prepared by the decoration of Ni as a transition metal on Fe_3O_4 nanoparticles modified with tryptophan (Scheme 6.23). The nanoparticles successfully catalyzed the coupling of thiols and synthesis of 5-substituted 1*H*-tetrazoles with excellent yields. This process provides many benefits such as recyclability and functional group tolerance (Scheme 6.24).

MCM-41@tryptophan-Cd and MCM-41@tryptophan-Hg were employed for the oxidation reaction [16]. The magnetic catalysts were prepared by immobilizing tryptophan, followed by the addition of $Cd(NO_3)_2 \cdot 4H_2O$ or $Hg(NO_3)_2$ that afforded MCM-41@tryptophan-Cd and MCM-41@tryptophan-Hg (Scheme 6.25). To determine the amount of Cd and Hg in MCM-41@tryptophan-M, ICP-OES analysis was performed and they were found to be 0.20 mmol/g and 0.85 mmol/g, respectively. Afterward, the catalyst activity is used to oxidize sulfides to sulfoxides and thiols to disulfides in the presence of H_2O_2 (Scheme 6.26).

6.12. APPLICATION OF METAL COMPLEXES OF L-TRYPTOPHAN AND L-TRYPTOPHAN AMINO ACID AS CATALYSTS FOR CYCLOADDITION REACTION OF CO$_2$ WITH VARIOUS EPOXIDES

Park et al. synthesized Cu(II)-tryptophan MOF catalyst (Scheme 6.27). CuTrp and TBAB were used as catalysts and cocatalysts, respectively, to carry out the cycloaddition reaction of carbon dioxide with various epoxides for the synthesis of cyclic carbonates under solvent-free conditions (Scheme 6.28) [17].

A possible mechanism for the reaction of carbon dioxide cycloaddition with an epoxide in the presence of CuTrp and TBAB was proposed by the mentioned authors (Scheme 6.29).
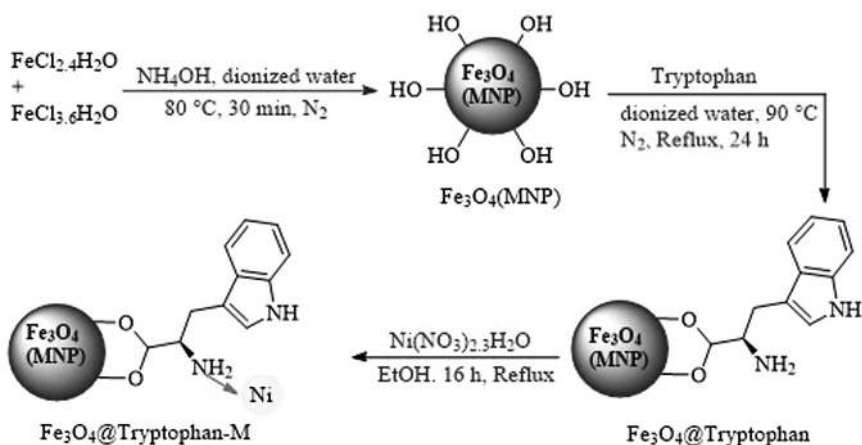
SCHEME 6.23. Synthesis of Fe_3O_4@tryptophan@Ni

$R_1\text{-}S\text{-}R_2 \xrightarrow[\text{Solvent-Free, H}_2\text{O}_2, \text{rt}]{\text{Fe}_3\text{O}_4@\text{Tryptophan-Ni}} R_1\text{-}S(\text{=O})\text{-}R_2$

Substrate	Time (min)	Yield (%)
2-(Phenylthio)ethanol	5	99
Dibenzylsulfide	6	92
2-(Methylthio)ethanol	5	94
Dodecylmethylsulfide	5	80
Allyl sulfide	5	82
3,3'-Thiodipropionic acid	5	94
Dipropylsulfide	5	85
Methylphenylsulfide	20	98
Thiodiglycolic acid	6	98
Ethylphenylsulfide	25	96

$R\text{-SH} \xrightarrow[\text{EtOH, H}_2\text{O}_2, \text{rt}]{\text{Fe}_3\text{O}_4@\text{Tryptophan-Ni}} R\text{-}S\text{-}S\text{-}R$

Substrate	Time (min)	Yield (%)
2-Mercaptoethanol	5	98
Mercaptosuccinic acid	5	99
2-Mercaptobenzoic acid	15	98
2-Mercaptobenzimidazole	60	86
Thiophenol	65	87
Benzyl mercaptan	55	96
Benzo[d]thiazole-2-thiol	50	88
Benzo[d]oxazole-2-thiol	180	85
4-Methylbenzenethiol	60	96
2-Mercaptoacetic acid	10	85

$HO\text{-}S\text{-}S\text{-SH} \xrightarrow[\text{EtOH, H}_2\text{O}_2, \text{rt}]{\text{Fe}_3\text{O}_4@\text{Tryptophan-Ni}}$ HO–S–S–OH (100%) + O=...–SH (0%)

Fe₃O₄@Tryptophan-Ni, EtOH, H₂O₂, rt → 100% + 0%

HO–...–S–... Fe₃O₄@Tryptophan-Ni, EtOH, H₂O₂, rt → HO–...–S(=O)–... (100%) + O–...–S–... (0%)

Ar–CN + NaN₃ $\xrightarrow[\text{PEG-400, 120 °C}]{\text{Fe}_3\text{O}_4@\text{Tryptophan-Ni}}$ tetrazole

Substrate	Time (min)	Yield (%)
Phthalonitrile	5	97
3-Nitrobenzonitrile	480	89
2-Chlorobenzonitrile	327	91
Malononitrile	20	97
4-Nitrobenzonitrile	25	97
Benzonitrile	15	98
Benzyl cyanide	20	88
2-Hydroxybenzonitrile	10	97
3-Chlorobenzonitrile	5	98
Terephthalonitrile	30	91

SCHEME 6.24. Application of Fe₃O₄@tryptophan@Ni for oxidation

To evaluate the recovery and reusability of the CuTrp catalyst, after completion of the reaction, the catalyst was removed from the mixture by centrifugation and then washed with ethanol dried in an oven at 100°C and reused in the next run. This operation was performed three times and no significant change in its activity was observed. XRD and FT-IR studies for the recovered catalyst showed the same properties as the original catalyst, and ICP-OES studies for the recovered catalyst showed that only 40 ppm of copper leached in the reaction media (0.08 % leaching reported).
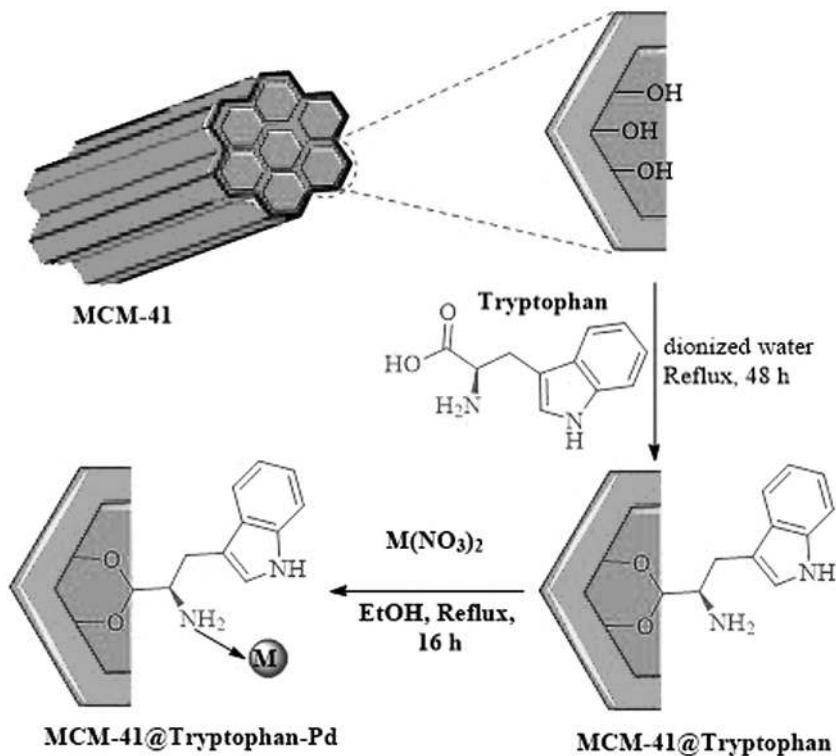
SCHEME 6.25. Synthesis of MCM41@tryptophan-M-41@tryptophan-Hg and recovered MCM-41@tryptophan-Hg.

Substrate	Time (min)		Yield (%)	
	Cd	Hg	Cd	Hg
methyl(phenyl)sulfane	35	30	94	95
2,2'-thiodiacetic acid	2	2	99	99
3,3'-thiodipropionic acid	3	2	98	99
diallylsulfane	2	1	90	93
dibenzylsulfane	7	6	91	94
2-(phenylthio)ethan-1-ol	2	2	95	95
2-(methylthio)ethan-1-ol	2	1	93	94
benzyl(phenyl)sulfane	5	5	91	91
diethylsulfane	5	3	93	95
diphenylsulfane	10	7	89	91

Substrate	Time (min)		Yield (%)	
	Cd	Hg	Cd	Hg
2-mercaptobenzoic acid	5	5	96	96
benzenethiol	1	1	95	95
phenylmethanethiol	2	1	91	92
benzo[d]thiazole-2-thiol	4	4	91	91
1H-benzo[d]imidazole-2-thiol	10	10	94	94
2-mercaptoethan-1-ol	10	5	90	94
4-bromobenzenethiol	25	15	89	91
4-methylbenzenethiol	2	1	93	95
naphthalene-2-thiol	1	1	90	90
2-mercaptosuccinic acid	2	2	98	98

SCHEME 6.26. MCM-41@tryptophan-M for the oxidation reaction.
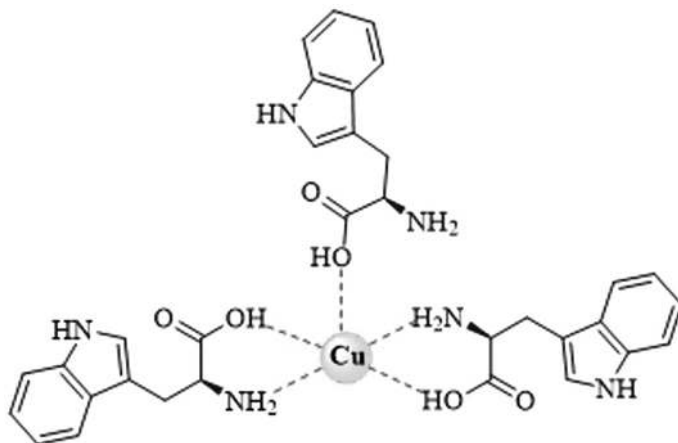
SCHEME 6.27. Structure of Cu(II)-tryptophan MOF catalyst
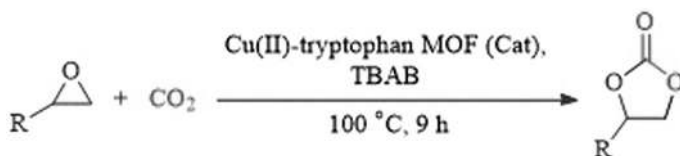
Epoxide	Conversion (%)	Selectivity (%)
Epichlorohydrin	98.6	99.1
Allylglycidyl ether	89.6	97.6
Propylene oxide	96.8	98.6
Styrene oxide	83.6	97.5
Cyclohexene oxide	35.0	96.7

Conditions: CuTrp= 0.83 mol%, TBAB= 0.83 mol%, Epoxide= 25.5mmol, T= 100 °C, t= 9h, P_{CO_2}= 1.2 MPa.

SCHEME 6.28. Cycloaddition reaction of CO_2 with various epoxides using CuTrp and TBAB as catalyst and co-catalyst, respectively.

6.13. APPLICATION OF METAL COMPLEXES OF L-TRYPTOPHAN AND L-TRYPTOPHAN DERIVATIVE-SUPPORTED MATERIAL AS A CATALYST FOR THE REGIOSELECTIVE AMINOLYSIS OF STYRENE OXIDE

Aghapoor et al. synthesized L-tryp≡Ti/MCM-41 using the following steps (Scheme 6.30) [18]. Activated mesoporous MCM-41 (1.5 g) was suspended in THF in an argon atmosphere in a three-necked balloon (in an ice bath for 1 h). By adding 3 ml
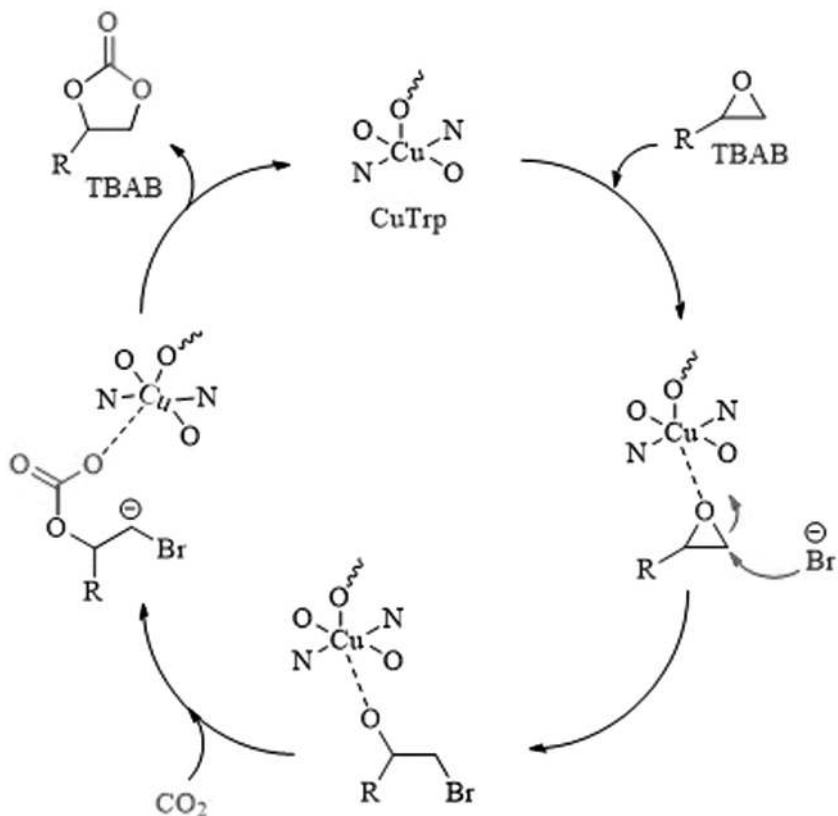
SCHEME 6.29. A possible mechanism for the cycloaddition reaction of CO_2 with epoxides to generate the cyclic carbonate.
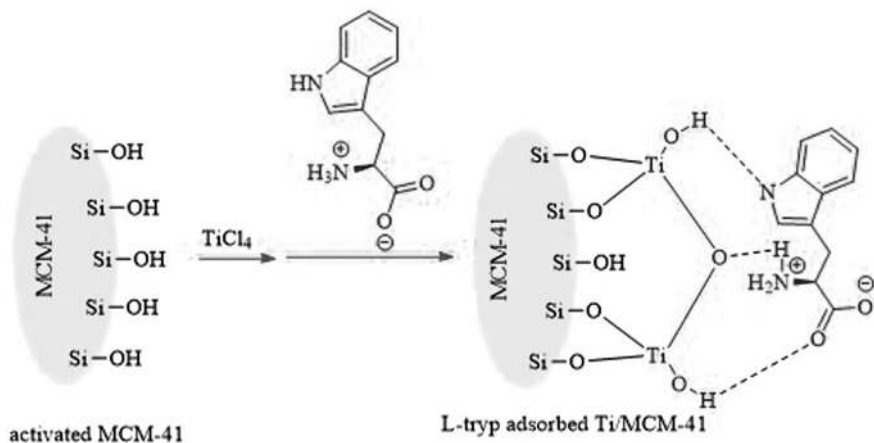
SCHEME 6.30. The two-step method for the preparation of L-tryp≡Ti/MCM-41.

of $TiCl_4$ to the mixture, HCl gas was produced and a yellow suspension was obtained by the release of HCl gas. After removing the ice bath, the mixture was stirred at room temperature for 2 h and subjected to argon barley for 2 h. Finally, a brown suspension was obtained which was washed with ethanol and dried for 8 h at 393 K (0.5 g), Ti/MCM-41 was poured in the deionized water, and 0.4 g of tryptophan was added and stirred at 323 K for 3 h. The suspension was then washed with deionized water and extracted in a Soxhlet extractor to afford Ti/MCM-41. L-tryptophan is then incorporated into SBA-15 to form L-tryp≡Ti/MCM-41.

The authors performed the regioselective aminolysis of styrene oxide in the presence of L-tryptophan adsorbed on Ti/MCM-41 as a catalyst (Scheme 6.31).

6.14. APPLICATION OF METAL COMPLEXES OF L-TRYPTOPHAN AND L-TRYPTOPHAN AMINO ACID AS CATALYSTS FOR EPOXIDATION REACTION

Farzaneh and coworkers synthesized a complex of molybdenum ($[MoO_2(Sal-Tryp) EtOH]$) by $MoO_2(acac)_2$ and (Sal-Tryp) Schiff base ligand (Scheme 6.32) [19]. The catalytic application of $[MoO_2(Sal-Tryp)EtOH]$ was studied for the epoxidation reaction of different alkenes with TBHP (*t*-butyl hydroperoxide) (Scheme 6.33). The study of the catalyst recovery showed that after performing the reaction five times, the conversion of the product decreased by only 4% (from 100% to 96%) without any change in its selectivity.

Jeong et al. designed an amino acid–based copper–tryptophan complex CuTrp MOF that was synthesized by an efficient direct-mixing method under mild conditions. The activity of the catalyst is then used for the synthesis of cyclic carbonates from epoxides and CO_2. The optimal conditions for the cycloaddition reaction were

Amine	Conversion (%)	Product selectivity	
		A	B
aniline	100	98	2
o-toluidine	100	98	2
m-toluidine	100	97	3
p-toluidine	100	99	1
2,4-dimethylaniline	89	76	24
4-bromoaniline	98	98	2
3-chloroaniline	94	98	2
4-chloroaniline	95	98	2
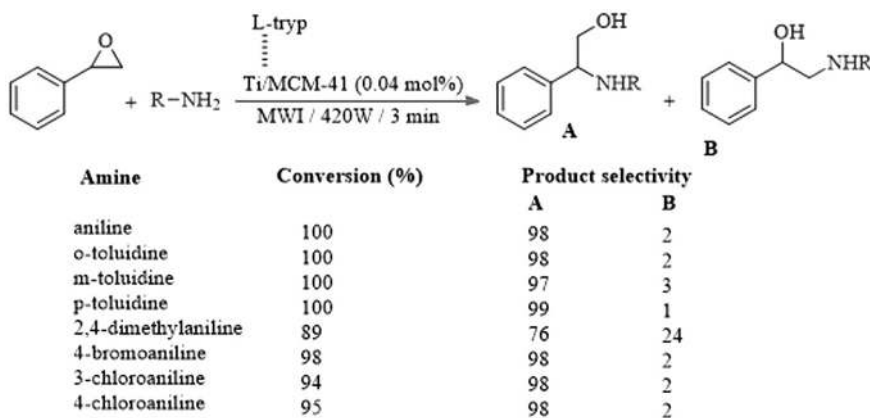
SCHEME 6.31. Aminolysis of styrene oxide with aniline derivatives catalyzed by L-tryp≡Ti/MCM-41.
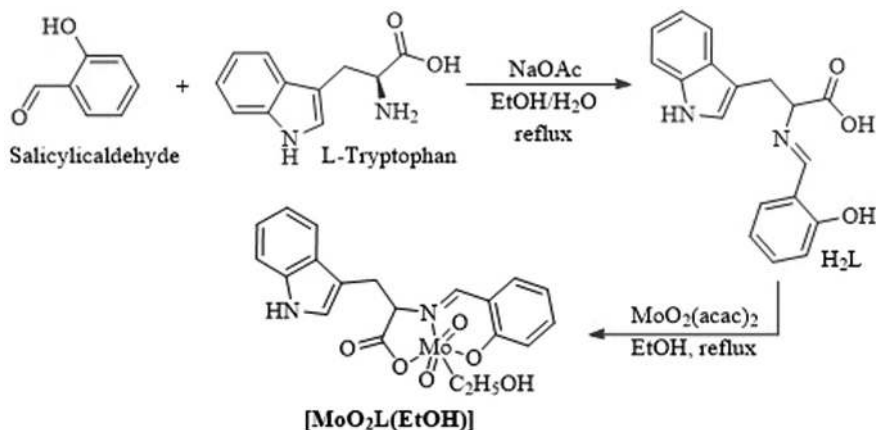
SCHEME 6.32. [MoO$_2$(Sal-Tryp)(EtOH)] complex preparation pathway.

Substrate	Conversion (%)	Selectivity of epoxide (%)
Cyclooctene	100	100
Norbornene	78	100
Cyclohexene	50	64[a]
Styrene	45	70[b]
trans-Stilbene	85	78[c]
α-methylstyrene	72	93[d]

byproduct(s): a) 2-Cyclohexene-1-ol and 2-Cyclohexene-1-one
b) Benzaldehyde and benzoic acid
c) Benzaldehyde and benzoic acid
c) Acetophenone

SCHEME 6.33. [MoO$_2$(Sal-Tryp)EtOH] complex catalyzed epoxidation reaction of various alkenes.

80°C for 9 h and 1.2 MPa of CO$_2$ pressure, which resulted in excellent epichlorohydrin (ECH) conversion and ECHC selectivity [20].

6.15. APPLICATION OF METAL COMPLEXES OF L-PHENYLALANINE AND L-PHENYLALANINE DERIVATIVE AS CATALYSTS IN REDUCTION REACTION

Significant efforts have been made to developing immobilized chiral catalysts with high activity, selectivity, and stability. This study mainly focuses on the

L-phenylalanine-based supported and unsupported organocatalysis. In this sense, Adão and coworkers used a modified L-phenylalanine to form tripodal vanadium complexes [21]. The two tripodal complexes of vanadium were then used as catalysts for reductive coupling of benzaldehyde, and this reaction was carried out under mild aerobic conditions in the presence of zinc metal as a co-reducing agent and ammonium alkyl salts or alkyl pyridinium acetate in ethanol (Scheme 6.34).

Tembeb group used a palladium complex containing the amino acid L-phenylalanine for the hydrogenation of 1-octene to octane and acetophenone to 1-phenyl ethanol in the presence of potassium *tert*-butoxide in methanol. The optimal conditions for these reactions are shown in Schemes 6.35 and 6.36 [22].

6.16. APPLICATION OF L-PHENYLALANINE-BASED IONIC LIQUID AS AN ORGANOCATALYST IN DIELS–ALDER REACTIONS

The Diels–Alder reaction between a diene and dienophile is one of the most important reactions for the formation of a C—C bond. In 2017, Caumul et al. synthesized several *o*-alkyl ester hydrochloride surfactants using two amino acids: phenylalanine and tyrosine (Scheme 6.37) [23].

The effect of synthesized surfactants as catalysts in the Diels–Alder reaction between methyl acrylate and cyclopentadiene was investigated. Phenylalanine ester hydrochloride derivatives showed better catalytic activity than the tyrosine derivatives. Derivatives C10 phenylalanine (Phe 10) and tyrosine (Tyr 10) surfactant provided the highest efficiency and selectivity (Scheme 6.38).

In 2016, Featherston et al. synthesized phenylalanine-derived trifluoromethyl ketones (catalyst A and catalyst B) (Schemes 6.39 and 6.40) [24].

Studies on these catalysts have shown that the catalysts in which the amino functionality of the catalytic residue is replaced with a methyl group, both are more reactive and stable in olefins epoxidation. These derivatives can be used as oxidants that have good stability and reactivity in chemistry (Scheme 6.41).
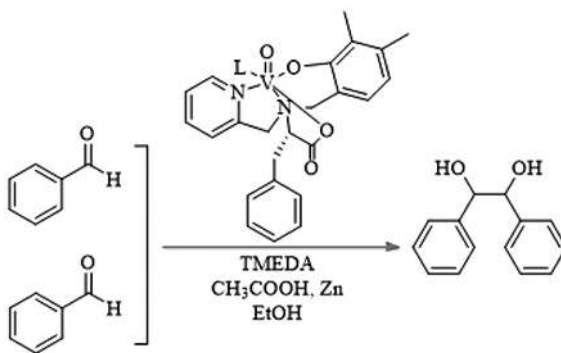
SCHEME 6.34.   L-phenylalanine-derived tripodal vanadium complexes as catalysts for the asymmetric reductive coupling of benzaldehyde
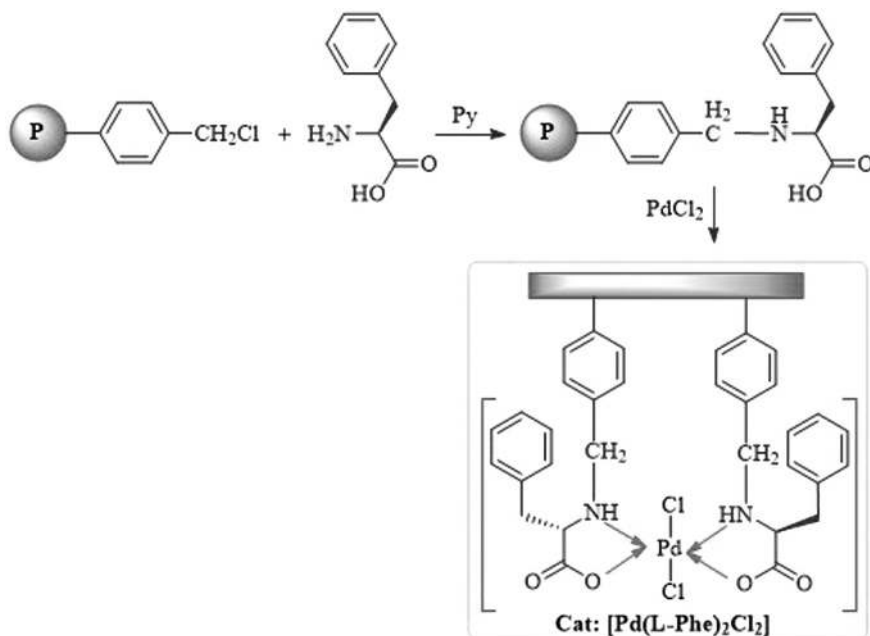
SCHEME 6.35.   Synthesis of poly(S-DVB) supported amino acid Pd(II) complex
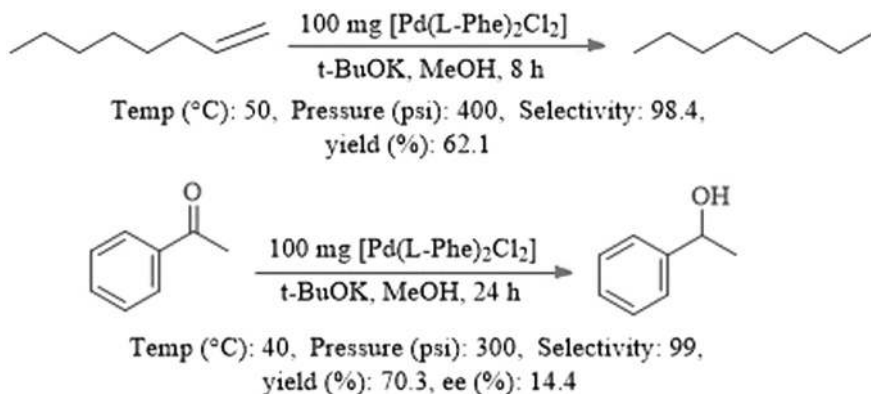
SCHEME 6.36.   Hydrogenation of 1-octene and acetophenone with [Pd(L-Phe)$_2$Cl$_2$]

6.17.   APPLICATION OF METAL COMPLEXES OF L-METHIONINE AND L-METHIONINE DERIVATIVE-SUPPORTED MATERIAL AS A CATALYST IN THE MULTICOMPONENT REACTION

Nowadays, there are widespread interest to the development of new heterogeneous organocatalysts based on L-methionine. This chapter gave examples of applications of supported and unsupported L-methionine in organic reaction. Tacrin derivatives

n   **8**   **10**   **12**   **14**

R= H   Phe 8   Phe 10   Phe 12   Phe 14

R= OH   Tyr 8   Tyr 10   Tyr 12   Tyr 14
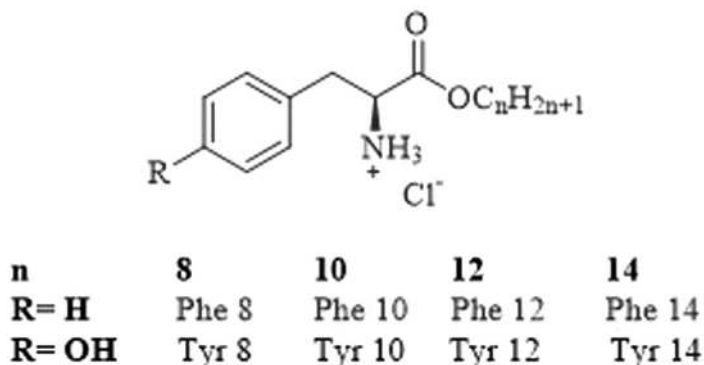
SCHEME 6.37. Structure of L-Phe and L-Tyr ester hydrochloride surfactants.

surfactants.: L-Phenylalanine and L-tyrosine ester hydrochloride

Water, 20 °C, Time (h): 72

Endo   Exo

Surfactant= Phe 8, Phe 10, Phe 12, Phe 14, Tyr 8, Tyr 10, Tyr 12, Tyr 14

Endo: Exo= 75: 25, 80: 20, 81: 19, 89: 11, 86: 14, 80: 20, 85: 15, 85: 15

Yield (%)= 87, 98, 72, 64, 53, 70, 44, 34
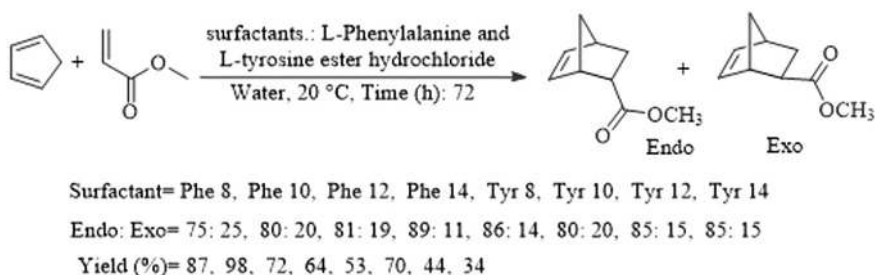
SCHEME 6.38. The Diels–Alder reaction between cyclopentadiene and methyl acrylate was catalyzed by various surfactants (Phe 8–14 and Tyr 8–14) in water.

are bioactive and have biological applications such as anti-inflammatory, hepato-protective, antitumor, anti-allergic, anti-HIV-1, antifungal, antiviral, antimicro-bial, anti-asthmatic, antidiabetic, antinociceptive, antioxidant, and antidepressant. Dehbalaei et al. introduced the preparation of Fe_3O_4@SiO_2@L-methionine@Ni (II)) catalyst (Scheme 6.42) and its use as an efficient nanocatalyst for the synthesis of tacrin derivatives with a combination of various pyrano[2,3-*c*] pyrazoles and cyclo-hexanone or dimedone. Fe_3O_4 MNPs were prepared by the combination of Fe^{+3} and Fe^{2+} ions under an N_2 atmosphere. The solid material decorated with SiO_2 afforded Fe_3O_4/SiO_2 followed by immobilization of L-methionine on the Fe_3O_4/SiO_2. Next, solid material treated with $Ni(NO_3)_2$·$6H_2O$ produced Fe_3O_4@SiO_2@L-methionine@Ni (II)) (Scheme 6.43) [25].

Karimian et al. reported the synthesis of methionine-Fe_3O_4 NPs by mixing the Fe_3O_4 with methionine in deionized water and its use as an efficient nanocatalyst for cycloaddition reaction between nitriles and sodium azide to synthesize 5-substituted 1-*H*-tetrazoles in DMSO at 120°C, and excellent results were obtained for an array of substrates (Schemes 6.44 and 6.45) [26].
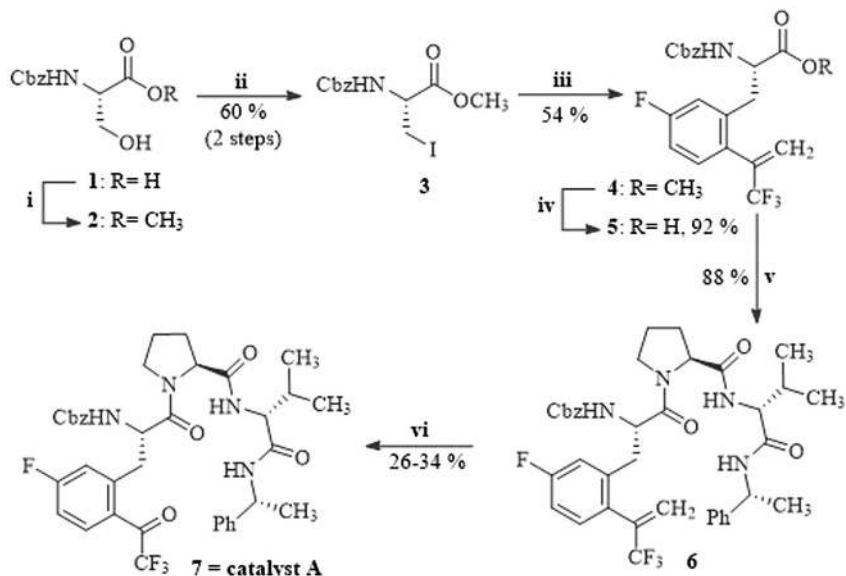
(i) CH₃I, K₂CO₃, DMF, rt; (ii) I₂, imidazole, PPh₃, CH₂Cl₂, 0 °C to rt;
(iii) 6 (1.3 equiv), Zn dust, I₂ (30 mol%), SPhos (10 mol%), Pd₂(dba)₃ (5 mol%), DMF, 55 °C;
(iv) LiOH, H₂O/THF, 0 °C to rt;
(v)H-Pro-D-Val-(R)-a-Mba.HCl ,EDC.HCl, HOBt. H₂O, *i*-Pr₂EtN, CH₂Cl₂, 0 °C to rt;
(vi) O₃, CH₂Cl₂, -78 °C then (CH₃)₂S, -78 °C to rt.
Cbz, carboxybenyzl; Mba, methylbenzylamine; HOBt, hydroxybenzotriazole.
EDC, 1-ethyl-3-(3-dimethylaminopropyl)carbodiimide;

SCHEME 6.39.   Synthesis of trifluoromethyl ketone catalyst A.

In another study, our group reported the synthesis of tetrazoles and polyhydroquin-oline derivatives using magnetically separable and reusable zirconium L-methionine complex immobilized on $ZnFe_2O_4@SiO_2$ nanoparticles (Scheme 6.46) [27]. With the reaction, various substrates could be converted to desired products in excellent yields. The experimental results showed that this catalyst could be reused for at least five times with a mild decrease in its activity in described reactions.

6.18.   APPLICATION OF METAL COMPLEXES OF L-METHIONINE AND L-METHIONINE DERIVATIVE-SUPPORTED MATERIAL AS A CATALYST IN THE COUPLING REACTION

Our laboratory synthesized hercynite@L-methionine-Pd nanoparticles. It is used as a catalyst for Suzuki carbon–carbon cross-coupling reactions between phenylbo-ronic acid and various aryl halides (Schemes 6.47 and 6.48) [28].

4: R= CH$_3$ 3
iii
5: R= H, 78 % from 2

55 % iv

7= catalyst B
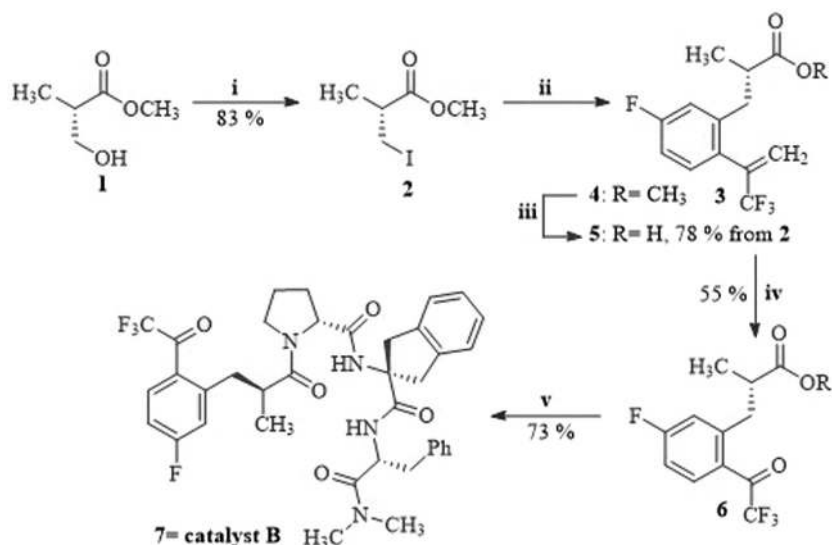
(i) I$_2$, imidazole, PPh$_3$, CH$_2$Cl$_2$, 0 °C to rt;
(ii) 6 (1.0 equiv), Zn dust, I$_2$ (30 mol%), SPhos (10 mol%), Pd$_2$(dba)$_3$ (5 mol%), DMF, 55 °C;
(iii) KOH, H$_2$O/EtOH, 0 °C to rt; (iv) O$_3$, CH$_2$Cl$_2$, -78 °C then (CH$_3$)$_2$S, -78 °C to rt;
(v) H-D-Pro-Aic-D-Phe-N(CH$_3$)$_2$.HCl, HCTU, NMM, CH$_2$Cl$_2$, -10 °C to rt.
HCTU, 2-(6-Chloro-1H-benzotriazole-1-yl)-1,1,3,3-tetramethylaminium hexafluorophosphate;
NMM, N-methylmorpholine.

SCHEME 6.40.   Synthesis of methyl analog (**7 = catalyst B**).

Catalyst A (20 mol%)
K$_2$CO$_3$ (0.6 M), Na$_2$EDTA (4*10^{-4} M),
H$_2$O$_2$ (8.0 equiv), CH$_3$CN (8.0 equiv)

t-amyl alcohol/H$_2$O (1:1), 0→ 4°C, 14h

Catalyst A: 12% conv
No catalyst: <5% conv

Catalyst B (10 mol%)
K$_2$CO$_3$ (0.6 M), Na$_2$EDTA (4*10^{-4} M),
H$_2$O$_2$ (8.0 equiv), CH$_3$CN (8.0 equiv)

t-amyl alcohol/H$_2$O (1:1), 0→ 4°C, 14h

Catalyst B: 99% conv (55:45 er)
No catalyst: <5% conv
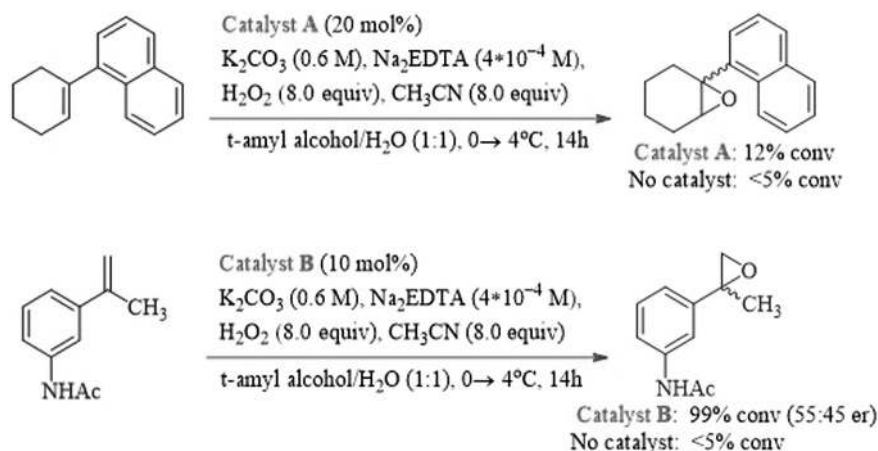
SCHEME 6.41.   Epoxidation reaction by **A** and **B** as oxidizing catalysts.

Fe$_3$O$_4$@SiO$_2$@L-Methionine@Ni

TEOS = Tetraethyl ortosilicate
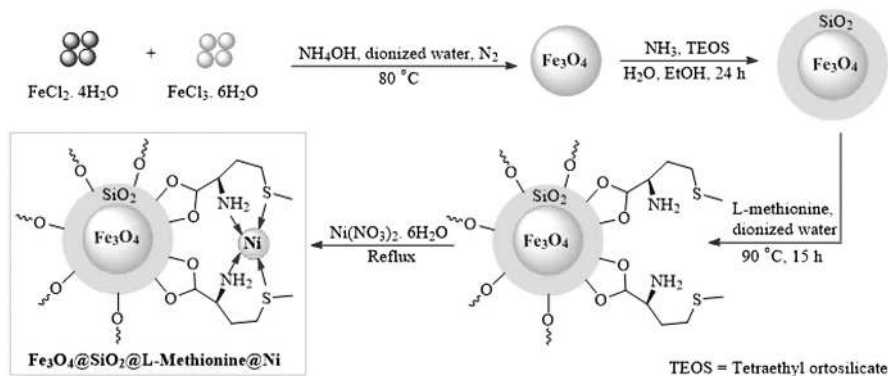
SCHEME 6.42.   Nanocatalyst synthesis Fe$_3$O$_4$@SiO$_2$@L-methionine@Ni
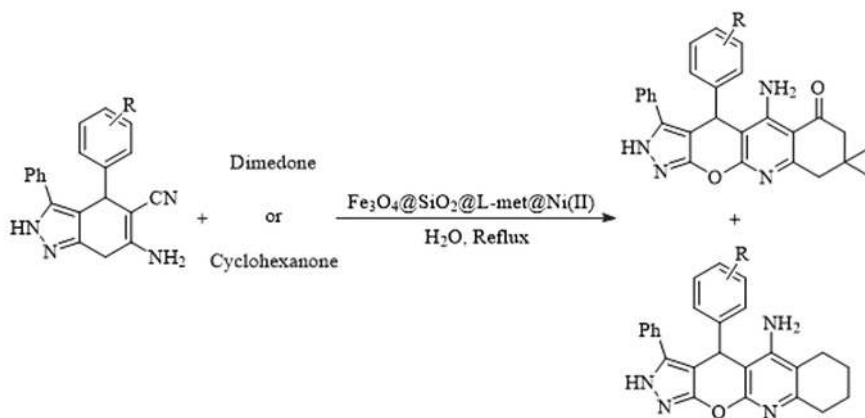
SCHEME 6.43.   Synthesis of tacrin derivatives with pyrano[2,3-*c*] pyrazoles and dimedone or cyclohexanone catalyzed by Fe$_3$O$_4$@SiO$_2$L-met@Ni(II).

Hercynite@L-methionine-Pd NPs were also used for the Heck reaction between butyl acrylate and various aryl halides. This catalyst can be used at least five times without significantly reducing its activity (Scheme 6.49).

Hajipour and Tavangar-Rizi synthesized ImmPd(0)-MNPs catalyst. For the synthesis of this catalyst, they first functionalized the chitosan with methionine and then coated the functionalized chitosan on the Fe$_3$O$_4$ cores, and finally immobilize the Pd(0) on the obtained solid support (Scheme 6.50) [29, 30]. The activity of the catalyst is employed for the coupling reaction (Schemes 6.51 and 6.52). The catalyst was simply recovered using an external magnet from the reaction mixture and recycled eight sequential runs in a Suzuki reaction.

Met-Fe₃O₄ nanoparticles.
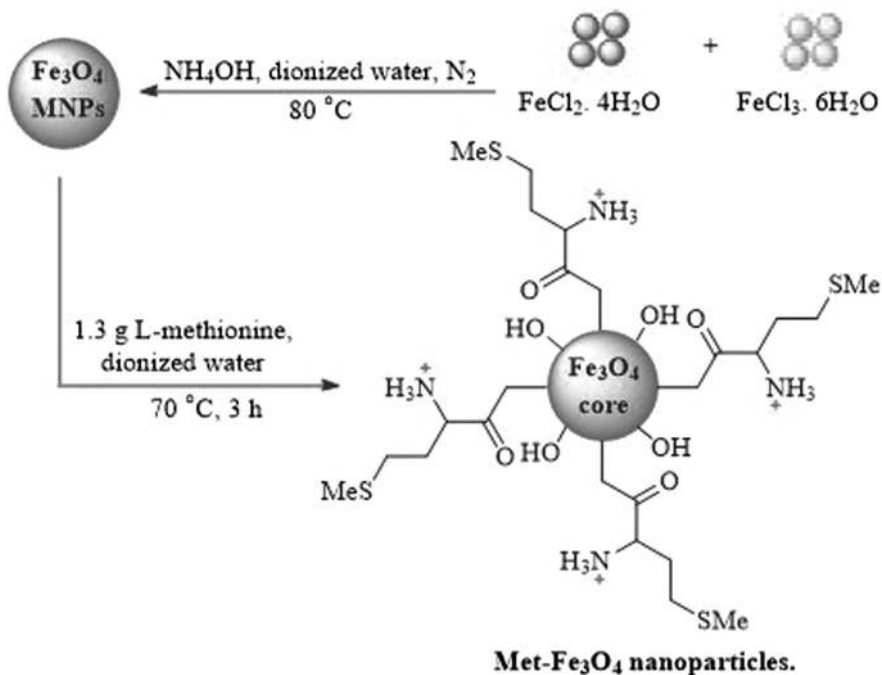
SCHEME 6.44.   Structure of methionine-Fe$_3$O$_4$ NPs
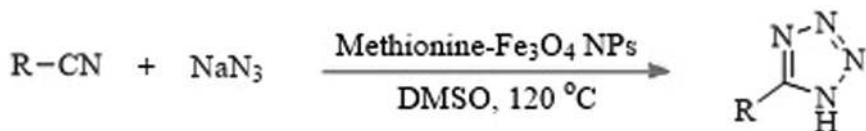
R: Ph, p-BrC$_6$H$_4$, p-ClC$_6$H$_4$, p-O$_2$NC$_6$H$_4$, p-MeC$_6$H$_4$, m-MeC$_6$H$_4$,
p-MeOC$_6$H$_4$, 3,5-(MeO)$_2$C$_6$H$_3$, p-EtOC$_6$H$_4$, p-HOC$_6$H$_4$,
p-Me$_2$NC$_6$H$_4$, Naphthalen-1-yl, 3-Methylbutyl

Yield (%): 100, 98, 100, 100, 95, 90, 90, 85, 90, 85, 80, 90, 85

SCHEME 6.45.   Synthesis of different tetrazoles by various nitriles and sodium azide cata-
lyzed by methionine-Fe$_3$O$_4$ NPs.
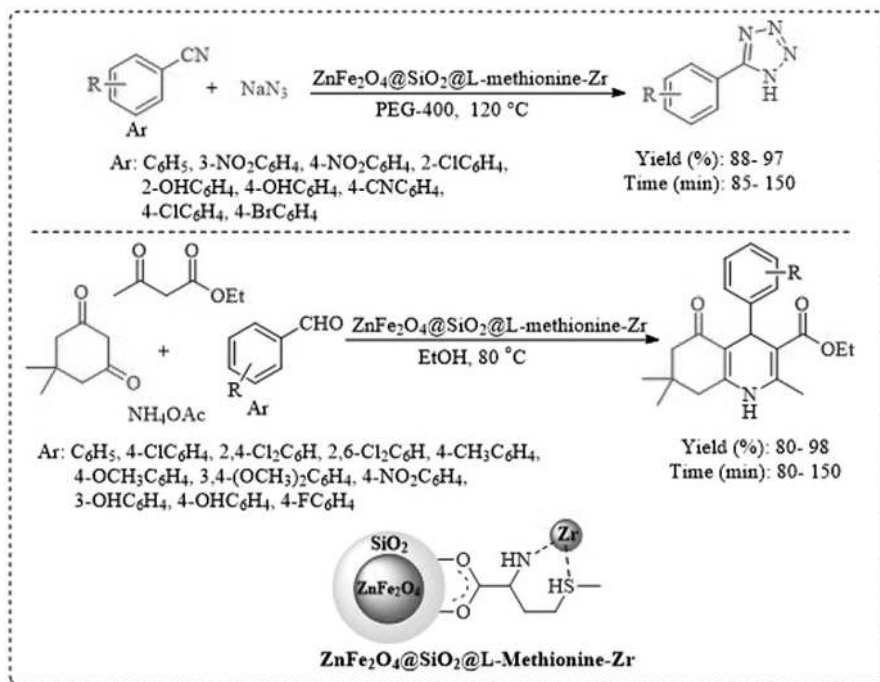
SCHEME 6.46.   Synthesis of tetrazole and polyhydroquinolines derivatives
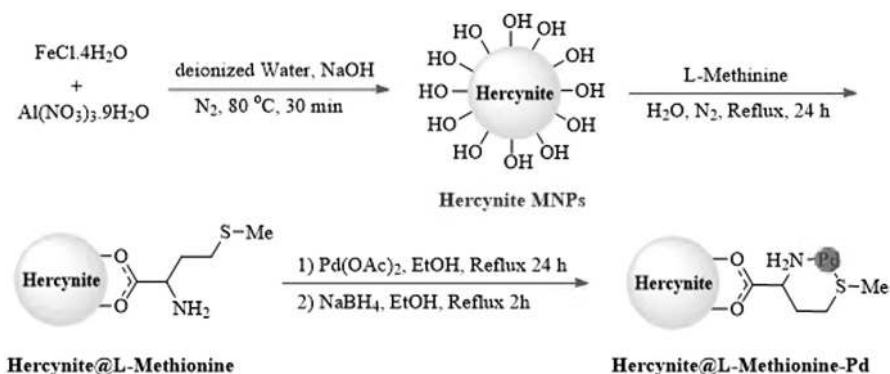
SCHEME 6.47.   Synthetic steps of hercynite@L-methionine-Pd NPs.
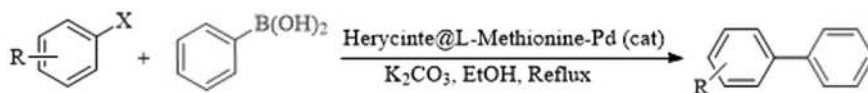
Aryl halide: Ph-I, p-MePh-I, p-OMePh-I, Ph-Br, p-MePh-Br,
            p-CNPh-Br, m-OMePh-Br, m-CF$_3$Ph-Br,
            o-ClPh-Br, p-NO$_2$Ph-Br, Ph-Cl, p-NO$_2$Ph-Cl

Yield (%): 99, 97, 98, 93, 93, 97, 90, 84, 92, 97, 87, 92

SCHEME 6.48.   Hercynite@L-methionine-Pd NPs catalyzed coupling reaction
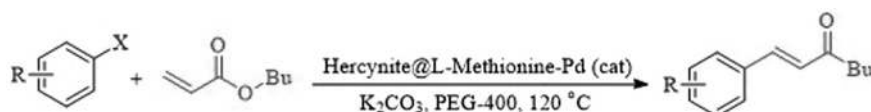
X= Cl, Br, I

Aryl halide: Ph-I, p-MePh-I, p-OMePh-I, o-OMePh-I, Ph-Br,
            p-MePh-Br, p-CNPh-Br, p-ClPh-Br, Ph-Cl,
            p-NO$_2$Ph-Br, p-NO$_2$Ph-Cl, p-CNPh-Cl

Yield (%):98, 96, 93, 91, 96, 89, 96, 91, 97, 93, 95, 93

SCHEME 6.49.   Hercynite@L-methionine-Pd NPs catalyzed coupling reaction.

6.19. APPLICATION OF METAL COMPLEXES OF L-METHIONINE AND L-METHIONINE DERIVATIVE-SUPPORTED MATERIAL AS A CATALYST FOR HYDROALKOXYLATION OF ALKYNES REACTION

Mon et al. reported the preparation of 3D bioMOF of formula {Ca^{II}Cu^{II}6 [(S,S)-methox]$_3$(OH)$_2$(H$_2$O)}·16H$_2$O (1) as a chiral and water-stable catalyst. Its selectivity was examined for the recovery of AuCl$_3$ and AuCl in the presence of other metal cations regularly present in "e-wastes" such as Pd^{2+}, Ni^{2+}, Cu^{2+}, Zn^{2+}, and Al^{3+}. This material exhibits a high selectivity for AuCl$_3$ and AuCl. Achiral and water-stable 3D bioMOF was prepared in several steps by dissolving L-methionine methyl ester hydrochloride in dichloromethane containing trimethylamine and oxalyl chloride to afford a white solid of H$_2$Me$_2$-(S,S)-method [bis[(S)-methionine]oxalyl diamide], followed by the addition of H^{2}Me$_2$-(S,S)-method and methanolic solution of Me$_4$NOH to obtain (Me$_4$N)$_2${Cu$_2$[(S,S)-methox](OH)$_2$}·4H$_2$O [31]. Next, the resulting nanoparticles were dissolved in water, followed by the addition of another aqueous solution containing CaCl$_2$ under stirring to synthesize {Cu$_6$Ca [(S,S)-methox]$_3$(OH)$_2$(H$_2$O)}·16H$_2$O (1). The authors examined the activity of heterogeneous catalysts for the hydroalkoxylation of alkynes under mild conditions in CH$_2$Cl$_2$ (Scheme 6.53).
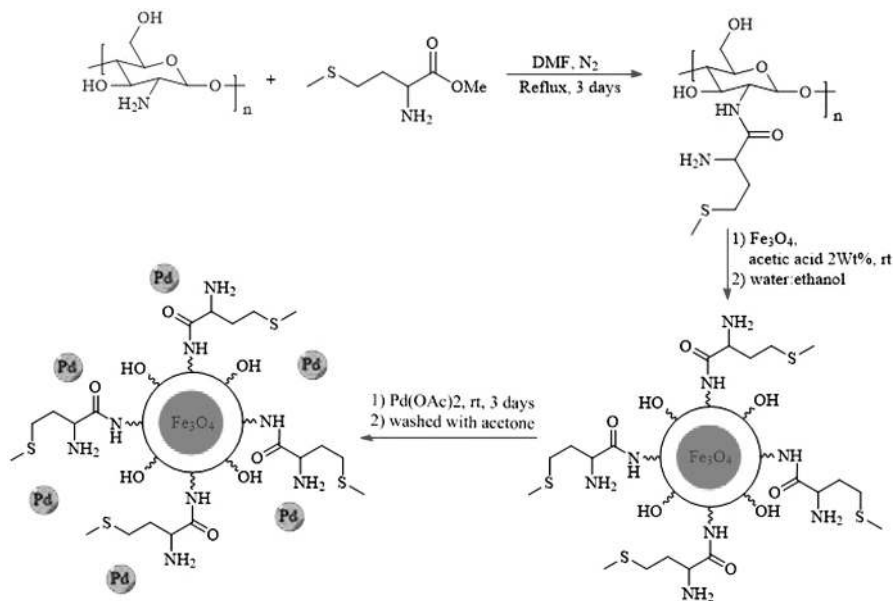
SCHEME 6.50.   Synthetic pathway of ImmPd-MNPs catalyst production.

R: H, 4-OMe, 4-NO$_2$, Formyl,
Acetyl, 4-Me, 4-CN, 4-Cl

Time (h): 0.3- 3.5
Yield(%): 87- 98

Aryl halide: iodobenzene, 1-iodo-4-methoxybenzene,
1-iodo-2-methylbenzene, bromobenzene,
1-(4-bromophenyl)ethan-1-one,
3-bromopyridine, 1-chloro-4-nitrobenzene.

Time (h): 1.5- 6
Yield(%): 84- 94
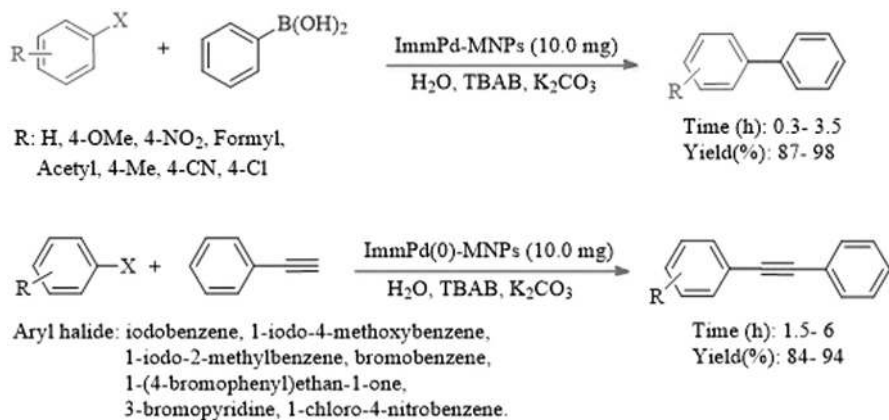
SCHEME 6.51.   Sonogashira reaction of various aryl halides and phenylacetylene and Suzuki reaction between aryl halides and phenylboronic acid in the presence of ImmPd(0)-MNPs as a catalyst.

6.20. APPLICATION OF L-METHIONINE DERIVATIVE AS A CATALYST FOR THE HYDROGENATION REACTION

Kvintovics et al. reported enantioselective hydrogenation of different ketones using a rhodium catalyst containing a methionine sulfoxide ligand and propane-2-ol as the
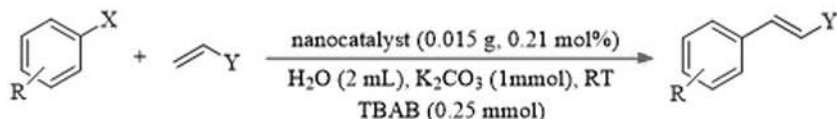
Aryl halides	Y	Yield (%)
4-Me-Ph-I	CO$_2$Me	96
4-Me-Ph-I	CO$_2$Bu	89
4-OMe-Ph-I	CO$_2$Bu	93
4-OMe-Ph-I	Ph	90
Ph-I	CO$_2$Bu	90
4-CN-Ph-I	CO$_2$Bu	86
4-OMe-Ph-Br	CO$_2$Bu	90
4-OMe-Ph-Br	Ph	83
4-CH$_3$CO-Ph-Br	CO$_2$Me	61
Ph-Br	CO$_2$Bu	85
4-Cl-Ph-Br	CO$_2$Me	93
4-NO$_2$-Ph-Cl	Ph	80
Ph-Cl	CO$_2$Bu	73
4-NO$_2$-Ph-Cl	Ph	67

SCHEME 6.52. Heck reaction between different aryl halides and olefins by using ImmPd(0)-MNPs as a catalyst.
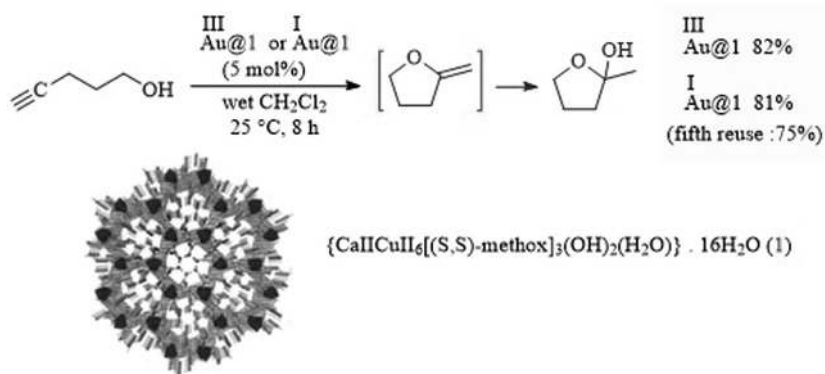
SCHEME 6.53. Hydroalkoxylation of 4-pentyn-1-ol in wet CH$_2$C$_{12}$ catalyzed by Au(III)@1 and Au (I)@1.

hydrogen source. Methionine sulfoxide and acetic anhydride were stirred in equal proportions (1:1) in acetic acid at 10°C for 6 h. The product was crystallized several times in pure ethanol to give white solid AMSO at 70°C (Scheme 6.54) [32]. Also, in this method, the products obtained up to 75% enantiomeric excesses.
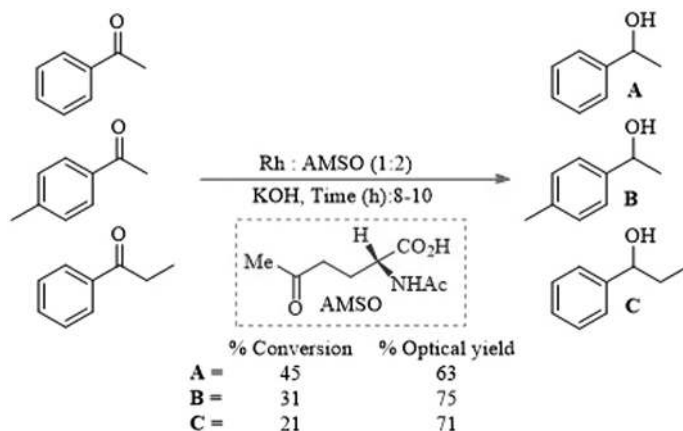
SCHEME 6.54. Hydrogenation of ketones with AMSO: Rh catalyst

6.21. CONCLUSION

This chapter aims to illustrate the significance of amino acids (including L-serine, asparagine, tryptophan, phenylalanine, and methionine) as catalysts in several transformations. In this chapter, we have overviewed the catalytic performance of L-serine, asparagine, tryptophan, phenylalanine, and methionine both as supported (on different solid materials) and unsupported. The most highlighted fact is that these organocatalysts represent an interesting scope for heterogenization. In the chapter, the application of amino acids–based supported and unsupported organocatalysis and various immobilization strategies have been discussed. We believe this chapter highlights the relevance of the amino acids' function in chemistry and materials science.

REFERENCES

1. Tamoradi, T., Ghorbani-Choghamarani, A., Ghadermazi, M. Immobilization of Pd(0) complex on the surface of SBA-15: A reusable catalyst for the synthesis of 5-substituted tetrazoles, sulfides, and sulfoxides. *Polyhedron*, 2019, *157*, 374–380. https://doi.org/10.1016/j.poly.2018.10.013.
2. Tamoradi, T., Ghadermazi, M., Ghorbani-Choghamarani, A. Synthesis of polyhydro-quinoline, 2,3-dihydroquinazolin-4(1H)-one, sulfide and sulfoxide derivatives cata-lyzed by new copper complex supported on MCM-41. *Catal. Letters*, 2018, *148*(3), 857–872. https://doi.org/10.1007/s10562-018-2311-x.
3. Phatake, V. V., Ahire, J. P., Bhanage, B. M. L-Serine@ZnO as an efficient and reusable catalyst for synthesis of cyclic carbonates and formamides in presence of CO2 atmo-sphere. *Mol. Catal.*, 2020, *492*, 111000. https://doi.org/10.1016/j.mcat.2020.111000.
4. Rocha, M., Costa, P., Sousa, C. A. D., Pereira, C., Rodríguez-Borges, J. E., Freire, C. L-serine-functionalized montmorillonite decorated with Au nanoparticles: A new highly efficient catalyst for the reduction of 4-nitrophenol. *J. Catal.*, 2018, *361*, 143–155. https://doi.org/10.1016/j.jcat.2018.02.027.

5. Yong, F. F., Teo, Y. C. Recyclable siloxy serine organocatalyst for the direct asymmetric mannich reactions in ionic liquids. *Synth. Commun.*, 2011, *41*(9), 1293–1300. https://doi .org/10.1080/00397911.2010.481750.

6. Jones, G., Richards, C. J. (S)-serine derived N-O and N-P oxazoline ligands for asymmetric catalysis. *Tetrahedron Asymmetry*, 2004, *15*(4), 653–664. https://doi.org/10.1016 /j.tetasy.2003.11.030.

7. Jakopin, Ž. 2-aminothiazoles in drug discovery: Privileged structures or toxicophores?. *Chem Biol Interact.,* 2020, *330*, 109244.https://doi.org/10.1016/j.cbi.2020.109244.

8. Safari, J., Shokrani, Z., Zarnegar, Z. Asparagine as a green organocatalyst for the synthesis of 2-aminothiazoles. *Polycycl. Aromat. Compd.*, 2020, *40*(4), 1105–1111. https:// doi.org/10.1080/10406638.2018.1528287.

9. Zarnegar, Z., Shokrani, Z., Safari, J. Asparagine functionalized Al2O3 nanoparticle as a superior heterogeneous organocatalyst in the synthesis of 2-amino thiazoles. *J. Mol. Struct.*, 2019, *1185*.

10. Azarifar, D., Badalkhani, O., Abbasi, Y. Amino acid ionic liquid-based titanomagnetite nanoparticles: An efficient and green nanocatalyst for the synthesis of 1, 4-dihydropyrano [2, 3-c] pyrazoles. *Appl. Organomet. Chem.*, 2018, *32*(1), e3949.

11. Aghapoor, K., Mohsenzadeh, F., Darabi, H. R., Sayahi, H., Balavar, Y. L-tryptophan-catalyzed Paal–Knorr pyrrole cyclocondensation: An efficient, clean and recyclable organocatalyst. *Res. Chem. Intermed.*, 2016, *42*, 407–415.

12. Sasmal, S., Debnath, M., Nandi, S. K., Haldar, D. A urea-modified tryptophan based: In situ reducing and stabilizing agent for the fabrication of gold nanoparticles as a suzuki-miyaura cross-coupling catalyst in water. *Nanoscale Adv.*, 2019, *1*(4), 1380–1386. https://doi.org/10.1039/c8na00273h.

13. Ghorbani-Choghamarani, A., Mohammadi, M., Hudson, R. H. E., Tamoradi, T. Boehmite@tryptophan-Pd nanoparticles: A new catalyst for C–C bond formation. *Appl. Organomet. Chem.*, 2019, *33*(8), e4977. https://doi.org/10.1002/aoc.4977.

14. Moeini, N., Ghadermazi, M., Ghorbani-Choghamarani, A. A synthesis of sulfoxides and disulfides under classical and ultrasonic conditions in presence of recoverable inorganic–organic hybrid magnetism nanocatalysts Fe₃O4@Tryptophan-M (M: Cu, Co, and Fe). *Polyhedron*, 2019, *170*, 278–286. https://doi.org/10.1016/j.poly.2019.04.037.

15. Moeini, N., Tamoradi, T., Ghadermazi, M., Ghorbani-Choghamarani, A. Anchoring Ni (II) on Fe3O4@tryptophan: A recyclable, green and extremely efficient magnetic nanocatalyst for one-pot synthesis of 5-substituted 1H-tetrazoles and chemoselective oxidation of sulfides and thiols. *Appl. Organomet. Chem.*, 2018, *32*(9), e4445. https:// doi.org/10.1002/aoc.4445.

16. Molaei, S., Tamoradi, T., Ghadermazi, M., Ghorbani-Choghamarani, A. Highly efficient oxidative coupling of thiols and oxidation of sulfides in the presence of MCM-41@ Tryptophan-Cd and MCM-41@Tryptophan-Hg as novel and recoverable nanocatalysts. *Catal. Letters*, 2018, *148*(7), 1834–1847. https://doi.org/10.1007/s10562-018-2379-3.

17. Jeong, G. S., Kathalikkattil, A. C., Babu, R., Chung, Y. G., Park, D. W. Cycloaddition of CO2 with epoxides by using an amino-acid-based Cu(II)-tryptophan MOF catalyst. *Cuihua Xuebao/Chinese J. Catal.*, 2018, *39*(1), 63–70. https://doi.org/10.1016/S1872 -2067(17)62916-4.

18. Aghapoor, K., Amini, M. M., Jadidi, K., Mohsenzadeh, F., Darabi, H. R., Sayahi, H., Jalali, M. R. Synthesis and stability of L-tryptophan adsorbed on Ti/MCM-41 as a catalyst for the regioselective aminolysis of styrene oxide. *Solid State Sci.*, 2015, *49*, 10–17. https://doi.org/10.1016/j.solidstatesciences.2015.09.008.

19. Asgharpour, Z., Farzaneh, F., Ghiasi, M., Azarkish, M. Synthesis, characterization, density functional theory studies and antibacterial activity of a new schiff base dioxomolybdenum(VI) complex with tryptophan as epoxidation catalyst. *Appl. Organomet. Chem.*, 2017, *31*(11), e3782. https://doi.org/10.1002/aoc.3782.

20. Jeong, G. S., Kathalikkattil, A. C., Babu, R., Chung, Y. G., Park, D. W. Cycloaddition of CO2 with epoxides by using an amino-acid-based Cu (II)–tryptophan MOF catalyst. *Chinese J. Catal.* 2018, *39*(1), 63–70. https://doi.org/10.1016/S1872-2067(17)62916-4.

21. Teixeira, C. M., Adão, P., Carvalho, M. F. N. N., Gomes, C. S. B., Costa Pessoa, J. L-Phenylalanine derived tripodal vanadium complexes as catalysts for the asymmetric reductive coupling of benzaldehyde. *Inorganica Chim. Acta*, 2020, *510*, 119727. https://doi.org/10.1016/j.ica.2020.119727.

22. Valodkar, V. B., Tembe, G. L., Ravindranathan, M., Ram, R., Rama, H. S. Catalytic hydrogenation by recyclable supported Pd(II)-amino acid complex. *React. Kinet. Catal*. *Lett*., 2003, *80*(2), 285–291. https://doi.org/10.1023/B:REAC.0000006137.78049.41.

23. Caumul, P., Koonja, P., Namooya, N., Prayag, A., Joondan, N., Jhaumeer-Laulloo, S. The use of optically active O-alkyl ester hydrochlorides of L-phenylalanine and L-tyrosine as chiral micellar media for the catalysis of diels-alder reactions. *Bull. Chem. Soc. Ethiop.*, 2017, *31*(3), 509–518. https://doi.org/10.4314/bcse.v31i3.15.

24. Featherston, A. L., Miller, S. J. Synthesis and evaluation of phenylalanine-derived tri-fluoromethyl ketones for peptide-based oxidation catalysis. *Bioorganic Med. Chem.*, 2016, *24*(20), 4871–4874. https://doi.org/10.1016/j.bmc.2016.07.012.

25. Dehbalaei, M. G., Foroughifar, N., Khajeh-Amiri, A., Pasdar, H. Ni (II) immobilized on Fe3O4@SiO2@L-methionine: A reusable nanocatalyst and its application in the synthesis of new tetracyclic tacrine derivatives. *Org. Prep. Proced. Int*., 2020, *52*(3), 171–180. https://doi.org/10.1080/00304948.2020.1721958.

26. Karimian, A., Namvar-Mhaboub, M., Abbasi, R. Methionine-coated Fe3O4 nanoparticles: An efficient and reusable nanomagnetic catalyst for the synthesis of 5-substituted 1H-tetrazoles. *Russ. J. Org. Chem.*, 2020, *56*(9), 1646–1653. https://doi.org/10.1134/S1070428020090237.

27. Ghorbani-Choghamarani, A., Aghavandi, H., Talebi, S. M. A novel lanthanum complex of L-histidine immobilized on the surface of ZnFe$_2$O$_4$ Mnps: A novel, green, and efficient heterogeneous magnetic nanocatalyst for the synthesis of tetrazole and tetrahydrobenzo [B] pyran derivatives. Green, and efficient heterogeneous magnetic nanocatalyst for the synthesis of tetrazole and tetrahydrobenzo [B] pyran derivatives. http://dx.doi.org/10.2139/ssrn.4281627.

28. Mohammadi, M., Ghorbani-Choghamarani, A. L-methionine-Pd complex supported on hercynite as a highly efficient and reusable nanocatalyst for C-C cross-coupling reactions. *New J. Chem.*, 2020, *44*(7), 2919–2929. https://doi.org/10.1039/c9nj05325e.

29. Hajipour, A. R., Tavangar-Rizi, Z. Palladium nanoparticles immobilized on magnetic methionine-functionalized chitosan: A versatile catalyst for suzuki and copper-free sonogashira reactions of aryl halides at room temperature in water as only solvent. *Appl. Organomet. Chem.*, 2017, *31*(9), e3638. https://doi.org/10.1002/aoc.3701.

30. Hajipour, A. R., Tavangar-Rizi Z. Methionine-functionalized Chitosan–Pd (0) Complex: A novel magnetically separable catalyst for heck reaction of aryl iodides and aryl bromides at room temperature in water as only solvent. *Appl. Organomet. Chem.*, 2017, *31*(7), e3638.

31. Mon, M., Ferrando-Soria, J., Grancha, T., Fortea-Pérez, F. R., Gascon, J., Leyva-Pérez, A., Armentano, D., Pardo, E. Selective gold recovery and catalysis in a highly flexible methionine-decorated metal-organic framework. *J. Am. Chem. Soc.*, 2016, *138*(25), 7864–7867. https://doi.org/10.1021/jacs.6b04635.

32. Kvintovics, P., James, B. R., Heil, B. Enantioselective transfer hydrogenation of ketones using a rhodium catalyst containing a methionine sulphoxide ligand. *J. Chem. Soc. Chem. Commun*., 1986, *24*, 1810–1811. https://doi.org/10.1039/C39860001810.

7 The Catalytic Role of L-Aspartic Acid, L-Lysine, Glutamate, L-Alanine, and L-Valine in Organic Reactions

7.1. INTRODUCTION

The utilization of inexpensive amino acids as raw materials for producing porous chiral supports for recyclable high-performance asymmetric catalysts for the organic synthesis of optically active compounds is an effective strategy. Herein we provide an overview of very recent advances in the area of asymmetric catalysis with amino acids and their derivatives as effective catalysts or essential components of catalysts.

7.2. APPLICATION OF L-ASPARTIC ACID AND ASPARTIC ACID DERIVATIVE-SUPPORTED MATERIAL AS AN ORGANOCATALYST IN MULTICOMPONENT REACTION

New methodologies have been developed in the last decades in the application of natural and unnatural amino acids from synthetic as well as industrial viewpoints. In the related example, the synthesis of tetrahydroisoquinoline-4-carboxylic acid in acetonitrile via a one-pot three-component reaction between a homophthalic anhydride with ammonium acetate and various aldehydes was accomplished using aspartic acid (Scheme 7.1) [1]. Experimental studies show that aspartic acid provided better diastereoselectivity than previous reported catalysts for this synthetic strategy.

7.3. APPLICATION OF L-ASPARTIC ACID–CONTAINING MATERIAL IN THE MULTICOMPONENT REACTION

In 2022, our group designed and introduced the immobilization of L-aspartic amino acid on the surface of nanomagnetic zirconium ferrite [ZrFe$_2$O$_4$@

AcNH$_4$= anhydride/ammonium acetate
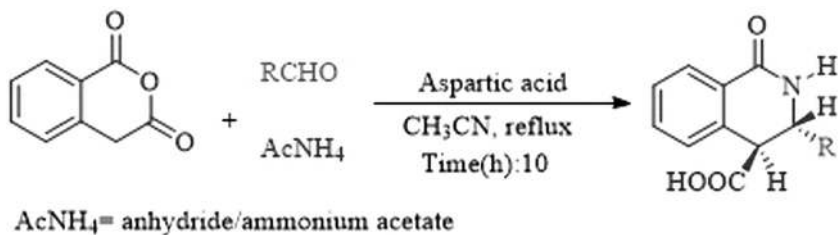
R	Yield (%)
Ph	87
4-Me-C$_6$H$_4$	86
4-F-C$_6$H$_4$	87
4-Cl-C$_6$H$_4$	90
4-Br-C$_6$H$_4$	89
4-OMe-C$_6$H$_4$	83
3,4-(OMe)$_2$-C$_6$H$_3$	91

SCHEME 7.1. Aspartic acid–catalyzed synthesis of *trans*-3-substituted-1-oxo-1,2,3,4-tetrah ydroisoquinoline-4-carboxylic acid.

SiO$_2$-*n*-Pr-ASP-Cu(II)] and it is used as a catalyst for the production of pyrano[2,3-*c*] pyrazoles and 2-amino-3-cyanopyridine derivatives [2]. Under the standard reaction conditions, H$_2$O was used as a solvent for pyrano[2,3-*c*] pyrazole derivatives in good to excellent yield. Also, it was found that desired product was obtained under solvent-free conditions (Scheme 7.2).

[Co$_2$(C$_4$H$_6$NO$_4$)$_2$(Mo$_8$O$_{26}$)(H$_2$O)$_{10}$]·4H$_2$O (AFO), prepared by a combination of Co$_2$Mo$_{10}$ and aspartic acid, was catalytically active in the three-component synthesis of spirochromenes [3]. This multicomponent reaction involving the use of isatin (or acenaphthene quinone), malononitrile (or ethyl cyanoacetate), and different 1,3-diketones (such as dimedone, barbituric acid, or ethyl acetoacetate) or 4-hydroxycoumarin/3-methyl-1*H*-pyrazol-5(4*H*)-one was conducted in aqueous solution and enabled the synthesis of different spirochromenes in high yields and purity (Scheme 7.3). After a simple filtration, the nanocatalyst was easily separated from the reaction mixture; the reaction yield was constant until the three cycles and decreased slightly from catalytic activity.

In 2019, Afradi et al. immobilized aspartic acid on the complicated solid support, which is made of starch, Mn, Fe, Ca, and Fe$_2$O$_4$, (Mn$_{0.25}$Fe$_{0.25}$Ca$_{0.25}$Fe$_2$O$_4$@starch@ aspartic acid) as a green and reusable heterogeneous catalyst (Scheme 7.4) [4]. They used the activity of a catalyst for the synthesis of dihydropyrimidine derivatives through the combination of thiourea/urea, acetylacetone, and various aryl aldehydes under solvent-free conditions (Scheme 7.4). In a model reaction (combination of thiophene-2-carbaldehyde, acetylacetone, and urea under free-solvent conditions), the reusability of the catalyst was studied in six consequence runs; interestingly, it was
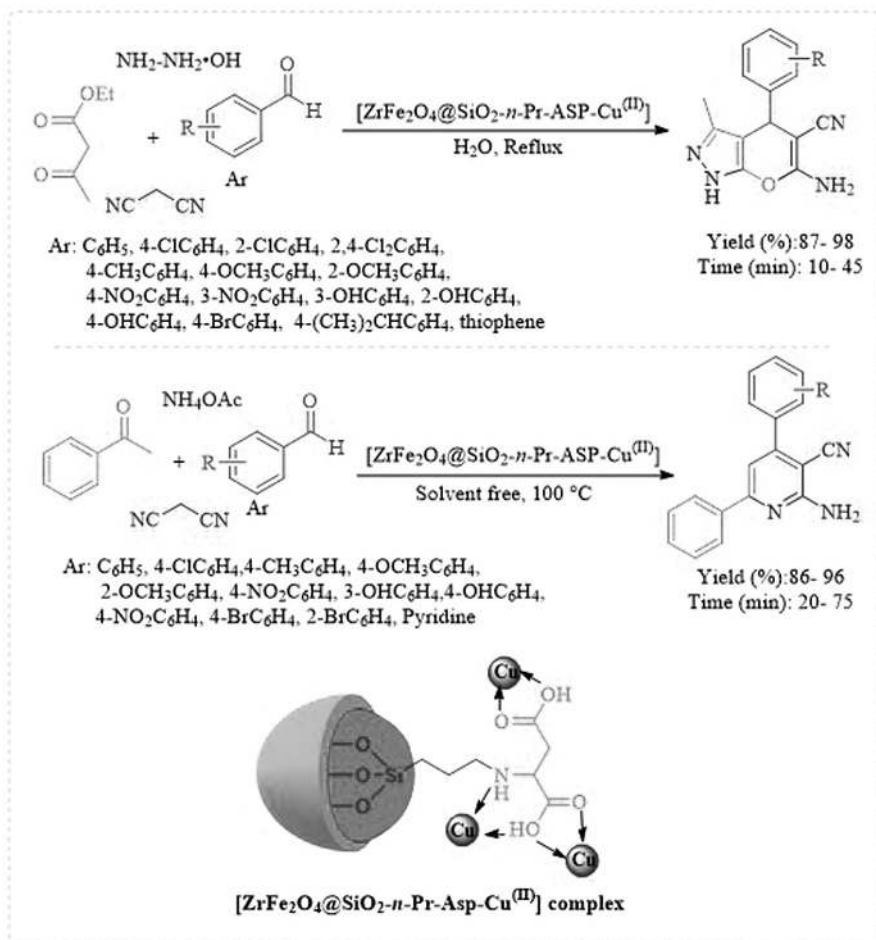
SCHEME 7.2. Synthesis of pyrano[2,3-c]pyrazoles derivatives and 2-amino-3-cyanopyridine.

observed that the reaction efficiency decreased slightly (from 98% to 90% of product yield) (Scheme 7.5).

Nikoofar et al. synthesized an organic–inorganic nanohybrid catalyst [5]. The preparation of the catalyst was achieved by hydroxylation of nano-silica with PEG-400 and in another reaction an ionic liquid was made by a combination of guanine and L-aspartic acid. The products of the mentioned reactions combined to achieve the final catalyst (Scheme 7.6). The authors were able to synthesize tri-carbox-amides through a pseudo-five-component condensation reaction of aromatic alde-hydes, aromatic amines, t-butyl isocyanide, and Meldrum's acid (Scheme 7.7). The authors also studied the performance of the described catalyst for the synthesis of bis(2,3-dihydroquinazolin-4(1H)-one) derivatives using three-component one-pot combination of aldehydes, amines, and isatoic anhydride in the presence of

1a: R_1= H, R_2= H
1b: R_1= Me, R_2= H
1c: R_1= H, R_2= Cl

2a: X= CN
2b: X= COOEt

3a   3b   3c   3d   3e

2a-b
2a: X= CN
2c: X= COOEt
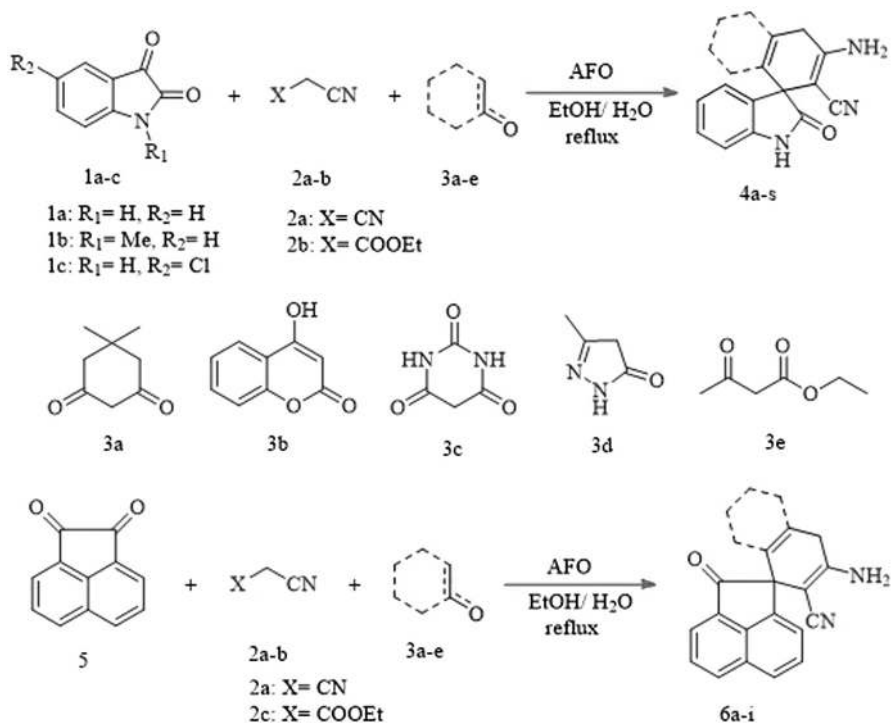
SCHEME 7.3. Synthesis of spirochromenes (**4a–s and 6a–i**) via a three-component reaction catalyzed by AFO.
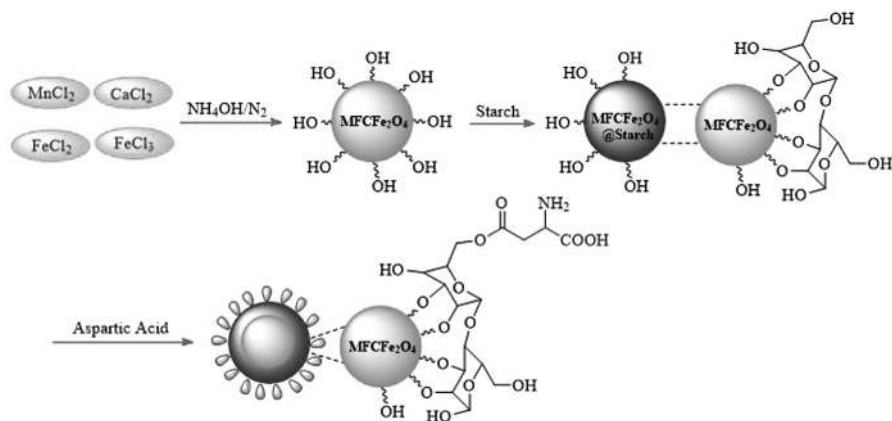
SCHEME 7.4. Preparation of MnFeCaFe$_2$O$_4$@starch@aspartic acid MNPs.
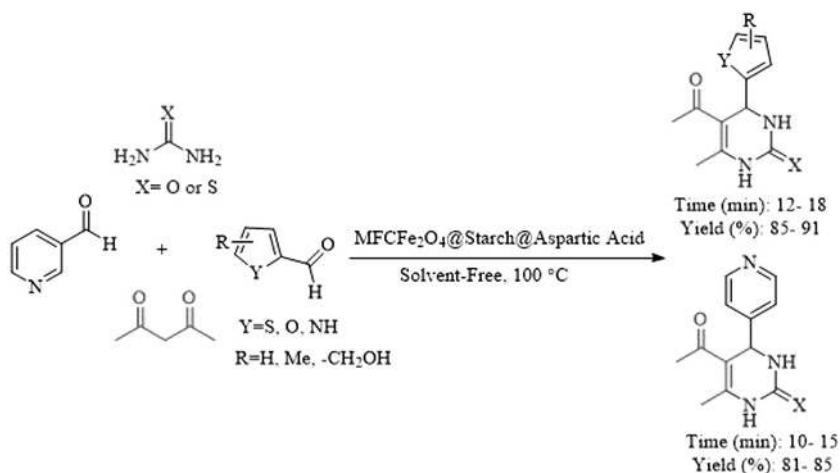
SCHEME 7.5. Synthesis of dihydropyridines catalyzed by MFCFe$_2$O$_4$@starch@aspartic acid.
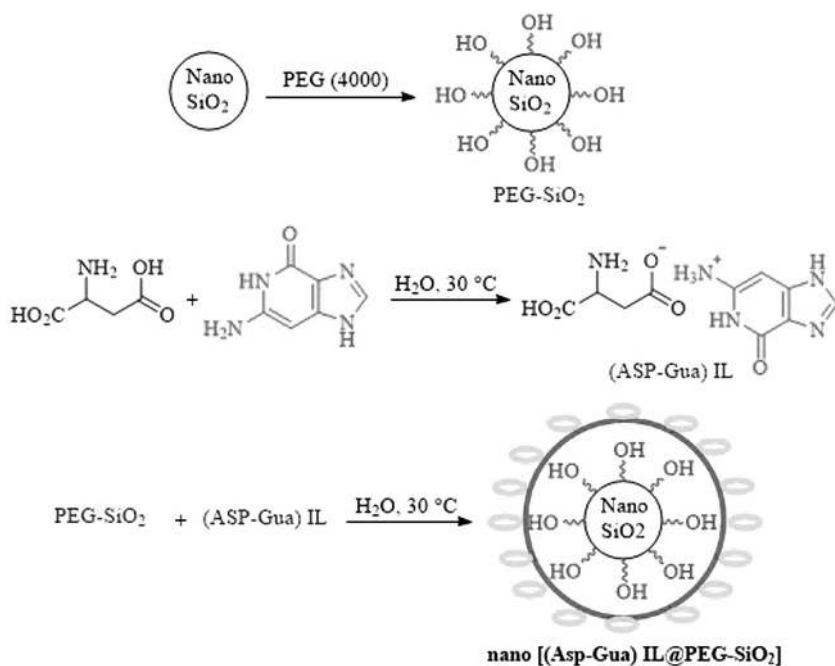
SCHEME 7.6. Synthesis steps of nano[(Asp-Gua)IL@PEG-SiO$_2$].

aspartic acid–guanine ionic liquid on the hydroxylated nano-silica surface (nano [(Asp-Gua) IL@PEG-SiO$_2$]) as a catalyst. The recovery and reuse of the catalyst for compound **7e** were evaluated as a model reaction. For this purpose, after reaction completion, methanol was added to the reaction mixture, the catalyst was separated by a simple filtration, and finally dried and reused in the next run. The results showed that this catalyst can be recovered within three runs without a significant reduction in activity.

7.4. APPLICATION OF L-ASPARTIC ACID AS AN ORGANOCATALYST FOR TRIMETHYLSILYLATION OF ALCOHOL

Our group reported trimethylsilylation of alcohol and phenol derivatives using aspartic acid as an organocatalyst [6] (Scheme 7.8). This protocol offers several

Entry	Ar	Ar$_1$	Product	Yield (%)
1	3-OHC$_6$H$_4$	2-ClC$_6$H$_4$	7a	94
2	2-NO$_2$C$_6$H$_4$	2-OH-3-MeC$_6$H$_4$	7b	95
3	4-MeC$_6$H$_4$	2-naphtyl	7c	94
4	3-OHC$_6$H$_4$	2-pyrolyl	7d	95
5	3-amino-5-methyl-pyrazolyl	3-indolyl	7e	94
6	4-BrC$_6$H$_4$	4-CHOC$_6$H$_4$	7f	90
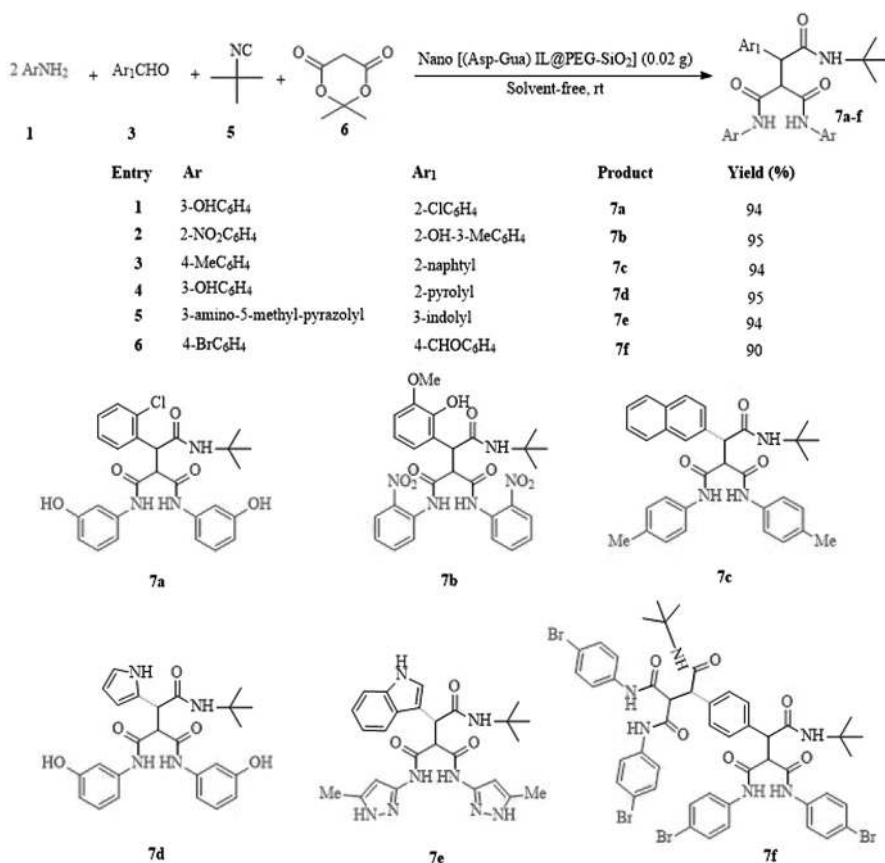
SCHEME 7.7. Synthesis of tricarbxamides catalyzed by nano[(Asp-Gua)]IL@PEG-SiO$_2$.

advantages compared to traditional heating methods, such as easy recovery, high yield, and shorter reaction time.

7.5.   APPLICATION OF SUPPORTED METAL COMPLEXES OF L-ASPARTIC ACID IN THE COUPLING REACTION

Our group has recently designed an efficient protocol for coupling and oxidation reactions using Ni-microsphere and Cu-MOF (Scheme 7.9) [7]. In these materials, copper and nickel metal ions are coordinated under the solvothermal method; then, the morphology of the materials was considered by SEM analysis. The images clearly showed the formation of microspheres was spherical in shape with the octahedral structure for Ni/aspartic acid and rhombic dodecahedral crystals for Cu/aspartic acid coordination polymers. This system was employed for the oxidation of sulfides with various functional groups. Also, these palladium-free coordination polymers exhibit excellent activities in the C—C coupling reaction. It should be noted that only a trace amount of the product was obtained in the absence of the catalyst.

In another study, our research group described the synthesis of a novel metal–organic framework by a combination of peptide (using aspartic acid as a building block) as a linker and cobalt as a metal under the solvothermal method (Scheme 7.10) [8]. The catalytic activity of Co-P-MOFs was examined for the asymmetric sulfoxidative cross-coupling reaction using a combination of different aryl halides, phenylboronic acid, and poly-sulfinylpiperazin (as novel S=O transfer agent) (Scheme 7.11).
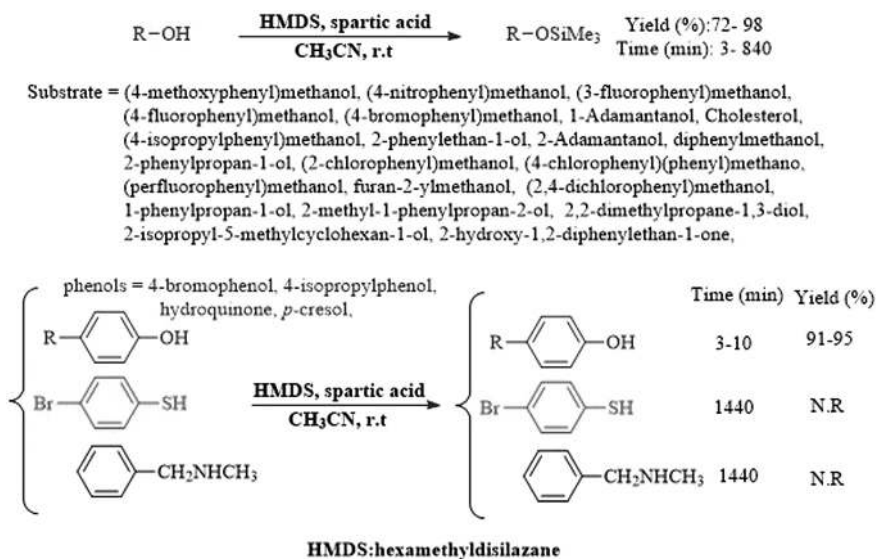
SCHEME 7.8.   Trimethylsilylation of alcohols.

7.6.   APPLICATION OF L-ASPARTIC ACID–BASED IONIC LIQUID IN THE OXIDATION REACTION

In 2012, a new ionic liquid was designed by Karthikeyan et al. via the connection of L-aspartic acid with an imidazolium tag. It is used as a catalyst for the selective oxidation of alcohol to carbonyl compound under solvent-free conditions (Scheme 7.12) [9]. The reaction was performed with a different alcohol including inactive aliphatic alcohols.
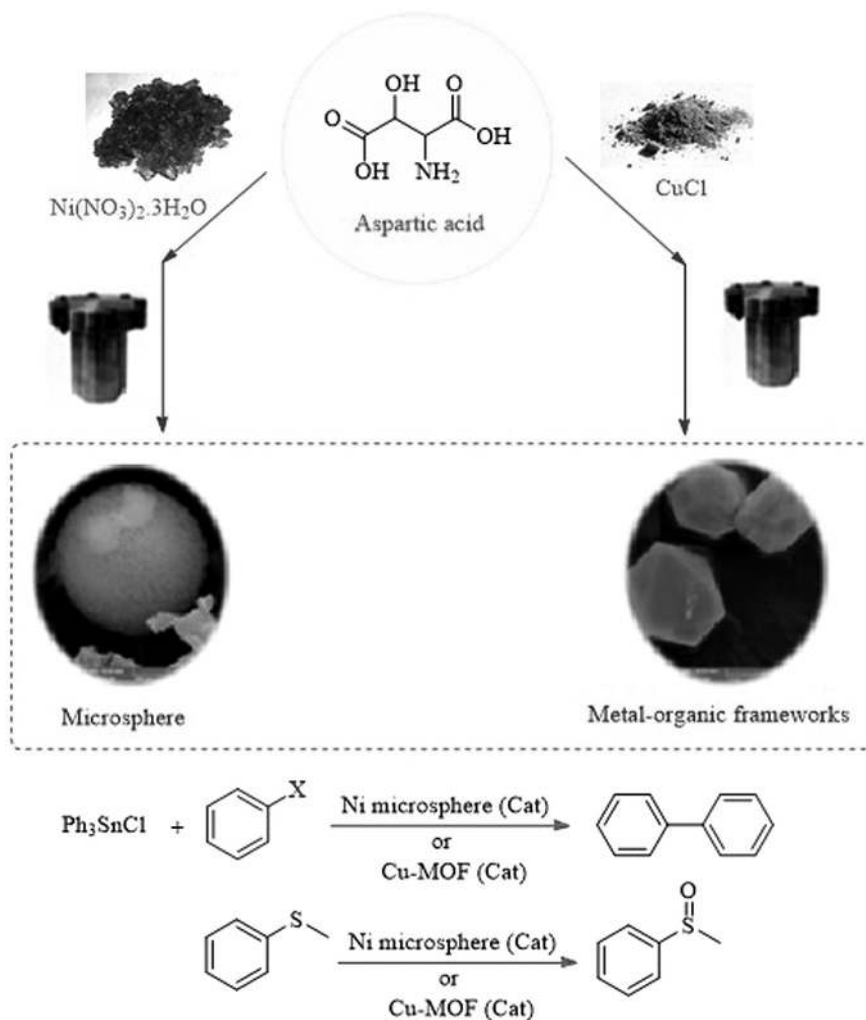
SCHEME 7.9.   Schematic synthesis of Ni microsphere and Cu-MOF and their applications as catalyst. *Source:* Reprinted with permission from Ref. [7]. Copyright 2011, RSC Publishing.
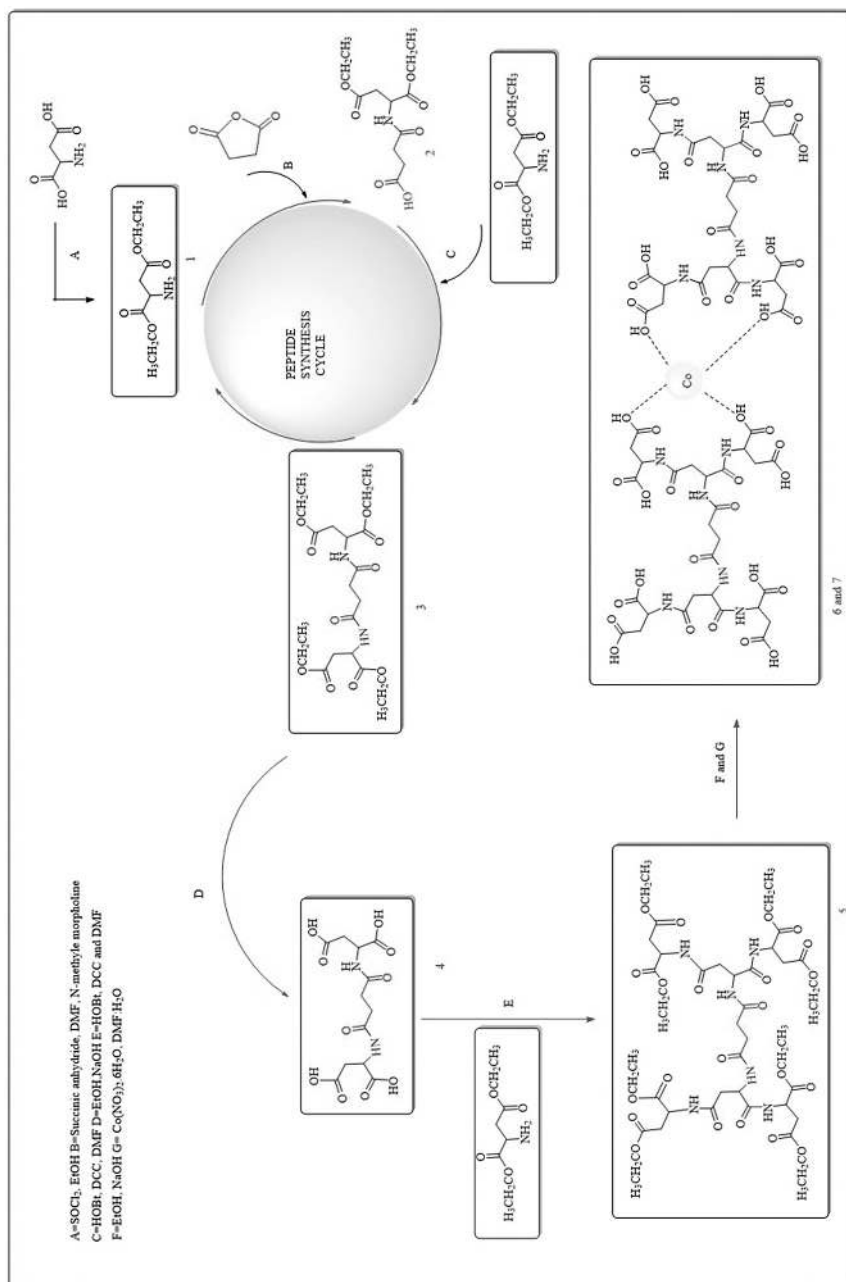
SCHEME 7.10. Schematic synthesis of Cobalt-based peptide metal–organic frameworks (Co-P-MOFs). *Source:* Reprinted with permission from Ref. [8]. Copyright 2020, Elsevier B.V. All rights reserved.
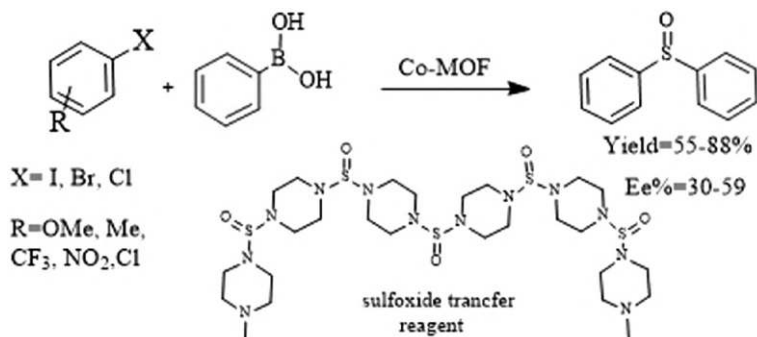
SCHEME 7.11. Asymmetric sulfoxidative cross-coupling reaction. *Source:* Reprinted with permission from Ref. [8]. Copyright 2020, Elsevier B.V. All rights reserved.
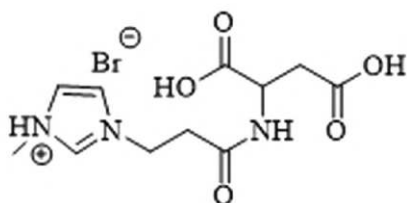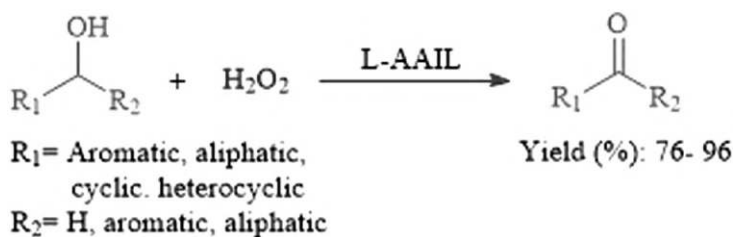
SCHEME 7.12. L-AAIL-catalyzed oxidation of alcohols using hydrogen peroxide at 25°C.

7.7. APPLICATION OF L-ASPARTIC ACID AS A TEMPLATE IN THE SYNTHESIS OF A MESOPOROUS CATALYST IN THE 5-HYDROXYMETHYL-FURFURAL SYNTHESIS

De et al. have reported the synthesis of mesoporous TiO_2 nanoparticle materials using aspartic acid as a template [10]. TiO_2 particles observed under TEM were spherical with dimensions of 10–15 nm (Figure 7.1). The authors studied the performance of TiO_2 nanoparticles for the preparation of 5-hydroxymethylfurfural (5-HMF) from

glucose and fructose catalyzed in aqueous, organic, and DMA-LiCl solvents under microwave-assisted heating (Scheme 7.13).

7.8. APPLICATION OF METAL COMPLEXES OF L-ASPARTIC ACID AS A PHOTOCATALYST

Wang et al. synthesized titanium dioxide@aspartic-β-cyclodexterine@reduced graphene oxide (TiO$_2$@ACD@RGO) composite using a photochemical method (Scheme 7.14) [11]. The photocatalytic degradation behavior of bisphenol A (BPA) was investigated under UV irradiation ($\lambda < 365$ nm) by this nanomaterial. The photocatalytic
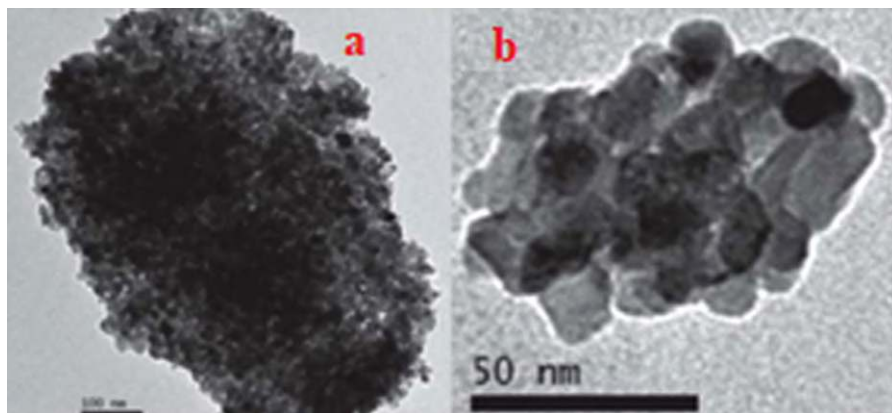
FIGURE 7.1. (a) TEM image of typical TiO$_2$ nanostructure. (b) TEM image of calcined (500°C) TiO$_2$ sample. *Source:* Reprinted with permission from Ref, [10]. Copyright 1991, RSC Publishing.
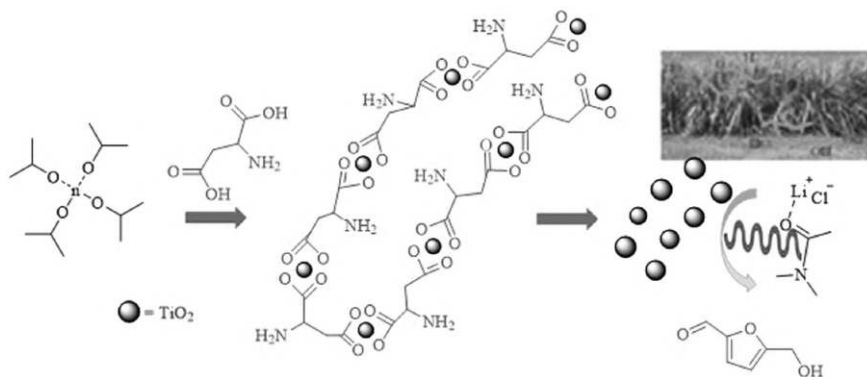
SCHEME 7.13. Catalytic application of mesoporous TiO$_2$ nanospheres for 5-hydroxy-methyl-furfural synthesis.

graphene oxide (GO)

Reduced graphene oxide (RGO)

H_2N-NH_2

H_2O

Graphite

Hummer's

Ultrasonic

100 °C water bath for 24 hours, then wash and dry

Add water and ultrasonicate

Freeze-drying

TiO_2

Xenon lamp for 15 hours

HO OH
RO O

HO OH
OR

COOH

$R = \ -O-CH_2-CHCH_2-NHCHCH_2CH_2COOH$
$\qquad\qquad\qquad OH$
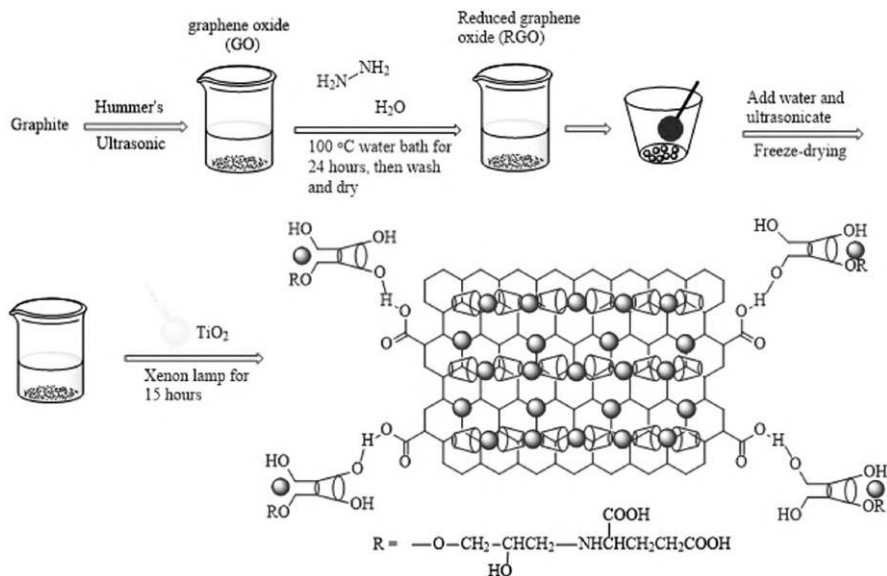
SCHEME 7.14.   Synthetic route of TiO_2@ACD@RGO.

investigations showed that the TiO_2@ACD@RGO possessed high photocatalytic efficiency for the degradation of bisphenol A (BPA), which was better than that of TiO_2 and TiO_2@RGO. It should be noted that aspartic acid-β -cyclodextrin (ACD) acted as an adsorbent of BPA to the catalyst surface. After five times reuse, the photocatalyst showed excellent stability and reusability.

In another research, Wang et al. synthesized aspartic acid-β -cyclodextrin (ACD) using aspartic acid, β-cyclodextrin, and epichlorohydrin. They also prepared a graphene oxide–TiO_2 composite catalyst under the hydrothermal method. The effects of ACD on the photocatalytic degradation of new Coccine (NC) and photocatalytic reduction of Pb^{+2} were investigated in the single pollution system, and the synergistic effects on the simultaneous photocatalytic NC degradation and Pb^{+2} reduction in the presence of ACD were also evaluated. Also, the authors reported the presence of ACD can improve the electron transfer and mass transfer at the GO–TiO_2 interface, which results in enhanced photocatalytic removal of NC and Pb^{+2} in aqueous solutions (Scheme 7.15) [12].

7.9.   APPLICATION OF METAL COMPLEXES OF L-LYSINE-SUPPORTED MATERIAL AS A CATALYST IN THE MULTICOMPONENT REACTION

L-lysine is an essential amino acid investigated for its potential in various fields such as a target for cancer treatment and a catalyst in organic reactions. In 2020, Ashraf et al. designed a high-performance catalyst to prepare 5-substituted 1*H*-tetrazoles using
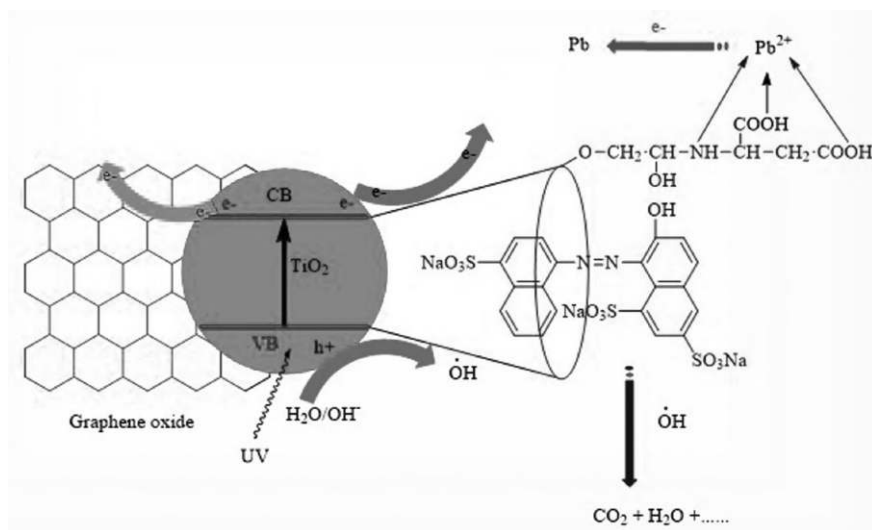
SCHEME 7.15. Photocatalytic mechanism of NC and Pb^{2+} removal by GO-TiO_2 in the presence of ACD.

a supported palladium complex of L-lysine on magnetic nanoparticles (Schemes 7.16 and 7.17) [13]. The Fe_3O_4@L-lysine-Pd compound catalyzed the [3+2] cycloaddition reaction between a variety of aryl cyanides and sodium azide in short reaction times and with high efficiency. The authors claimed that their catalyst was easily separated from the reaction mixture by an external magnet. They studied the recyclability of Fe_3O_4@L-lysine-Pd and exhibited that this magnetic nanocatalyst could be recovered ten times.

7.10. APPLICATION OF L-LYSINE-SUPPORTED MATERIAL AS A CATALYST IN KNOEVENAGEL CONDENSATION REACTION

In 2018, Li et al. synthesized an efficient catalyst by depositing L-lysine on polyacrylonitrile fiber, which facilitates the Knoevenagel reaction aldehydes and different classes of activated carbonyl groups efficiently (Scheme 7.18) [14]. There are two

Time (min): 30- 140
Yield (%): 83- 100
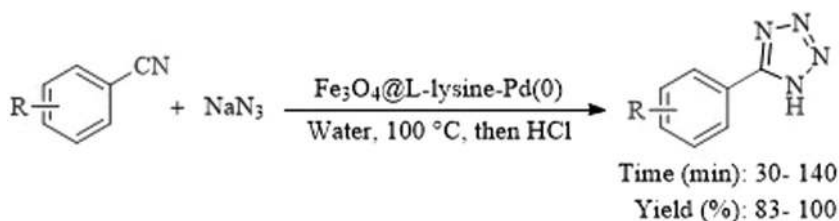
SCHEME 7.16. Synthesis of 5-substituted 1*H*-tetrazoles catalyzed by Fe_3O_4@L-lysine-Pd.
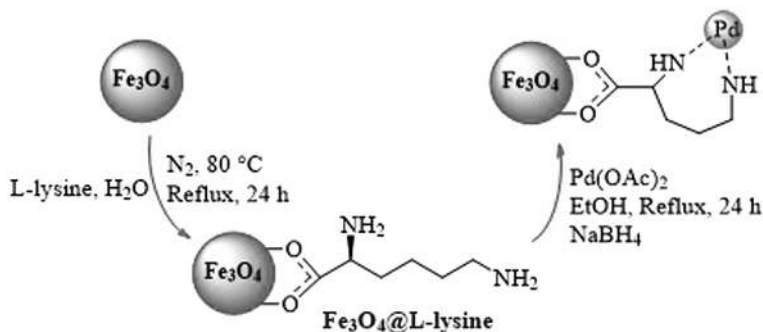
SCHEME 7.17.   Synthesis Fe$_3$O$_4$@L-lysine-Pd catalyst.

R: C$_6$H$_5$, 2-NO$_2$C$_6$H$_4$, 4-NO$_2$C$_6$H$_4$, 2-CF$_3$C$_6$H$_4$,
   2-ClC$_6$H$_4$, 4-ClC$_6$H$_4$, 2-BrC$_6$H$_4$, 4-CH$_3$OC$_6$H$_4$,
   3-CH$_3$OC$_6$H$_4$, 4-CH$_3$OC$_6$H$_4$, C$_4$H$_3$O, C$_4$H$_3$S, C$_6$H$_9$
R$_1$: CN, COCH$_3$
R$_2$: CN, COCH$_3$, CO$_2$Et

Yield: 0–99 %
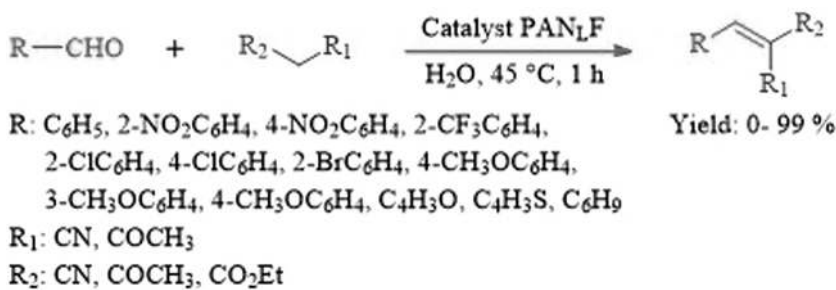
SCHEME 7.18.   Knoevenagel condensation catalyzed by L-lysine-containing catalyst.

available forms of PANLF from the amino acid lysine as a catalyst. The possible mechanism of the immobilization process is described in Scheme 7.19.

7.11. APPLICATION OF L-LYSINE AS AN ORGANOCATALYST IN A CONDENSATION REACTION

L-lysine is an inexpensive and cost-effective amino acid that can be easily removed from the reaction mixture due to its solubility in water. Therefore, the use of L-lysine as a catalyst facilitates the isolation and recovery of the catalyst from the reaction mixture. In 2010, Shang et al. studied the catalytic behavior of L-lysine in the condensation reaction of substituted aromatic aldehydes with different types of 1,3-dicarbonyl compounds (Scheme 7.20) [15].

7.12. APPLICATION OF METAL COMPLEXES OF L-LYSINE-SUPPORTED MATERIAL AS A CATALYST IN THE COUPLING REACTION

In 2020, Ashraf et al. successfully produced an efficient catalyst through the immobilization of Pd-L-lysine on the surface of magnetic nanoparticles. The catalytic
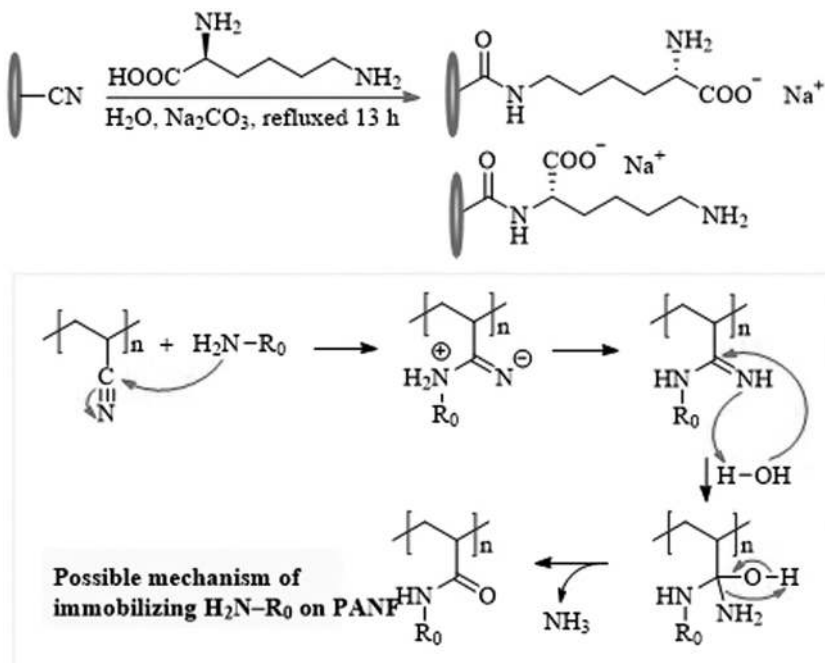
SCHEME 7.19. Proposed scheme for PANLF synthesis.

capability of this catalyst was examined by the authors for the synthesis of biphenyl via a cross-coupling reaction of phenylboronic acid and a wide range of aryl halides (Scheme 7.21) [16].

7.13. APPLICATION OF SUPPORTED L-LYSINE ON THE CARBON NANOTUBE FOR THE ASYMMETRIC ELECTROREDUCTION OF AROMATIC KETONES

Lu and coworkers prepared a variety of functionalized multiwalled nanotubes with different amino acids. These supported amino acids on the carbon nanotubes were used as cathodes for the asymmetric electroreduction of 2,2,2-trifluoro acetophenone in n-amyl alcohol (1:1)-TEAI (0.1 M) (Schemes 7.22 and 23). The catalytic activity of L-lysine-MWCNTs after six reuses, the yield and ee did not change significantly and remained at 64% and 29%, respectively[17].

7.14. APPLICATION OF L-GLUTAMATE-SUPPORTED MATERIAL AS A CATALYST IN THE MULTICOMPONENT REACTION

The application of amino acids is particularly exciting as they are the building blocks of enzymes which promote asymmetric reactions in nature. In 2015, Zhang and

R= 4-NO$_2$C$_6$H$_4$, 4-CNC$_6$H$_4$, 4-BrC$_6$H$_4$, 4-ClC$_6$H$_4$, 3-NO$_2$C$_6$H$_4$,
   4-MeC$_6$H$_4$, 4-MeOC$_6$H$_4$, 3-BrC$_6$H$_4$, C$_6$H$_5$, 2-NO$_2$C$_6$H$_4$

L-lysine: H$_2$N
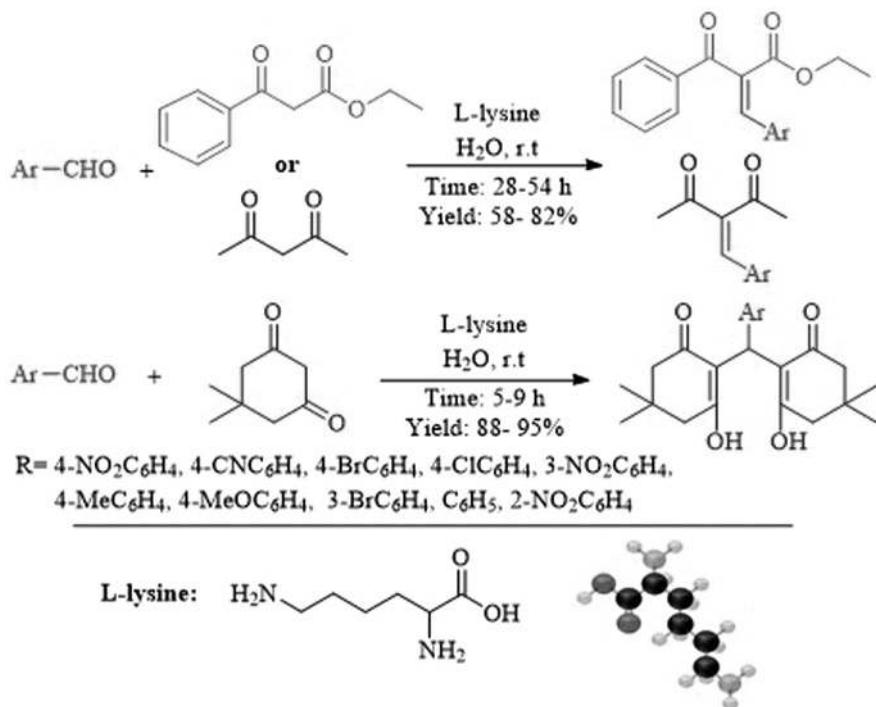
SCHEME 7.20.   The reaction between aldehydes with methylene acid and dimedone.

X= I, Br, Cl
R= 4-H, 4-CH$_3$, 4-OCH$_3$, 4-OH, 4-NO$_2$, 2-CH$_3$-4-NO$_2$,
   4-NH$_2$, 4-Cl, 3-NO$_2$, 2-NO$_2$, 4-CN, 3-CH$_3$, 3-OCH$_3$,
   2-OCH$_3$, 4-CHO, 3-CHO-4-OH, 4-Ph, 3-CHO, 2-NH$_2$,
   3-I-4-OH-5-CHO

Time (min): 15- 220
Yield (%): 49- 99
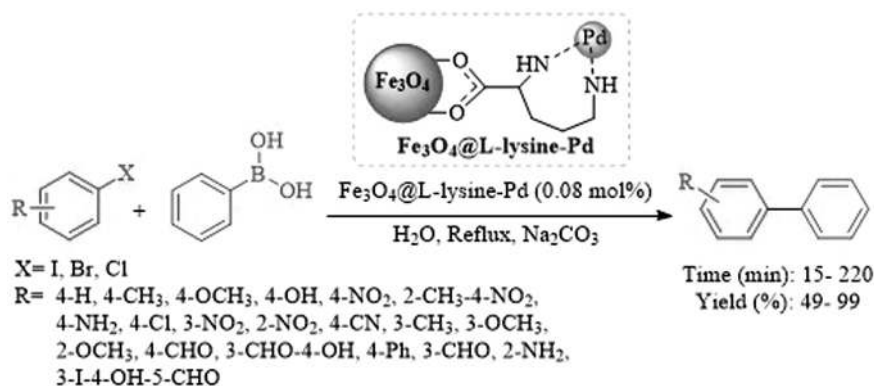
SCHEME 7.21.   C—C cross-coupling reaction catalyzed by Fe$_3$O$_4$@L-lysine-Pd.
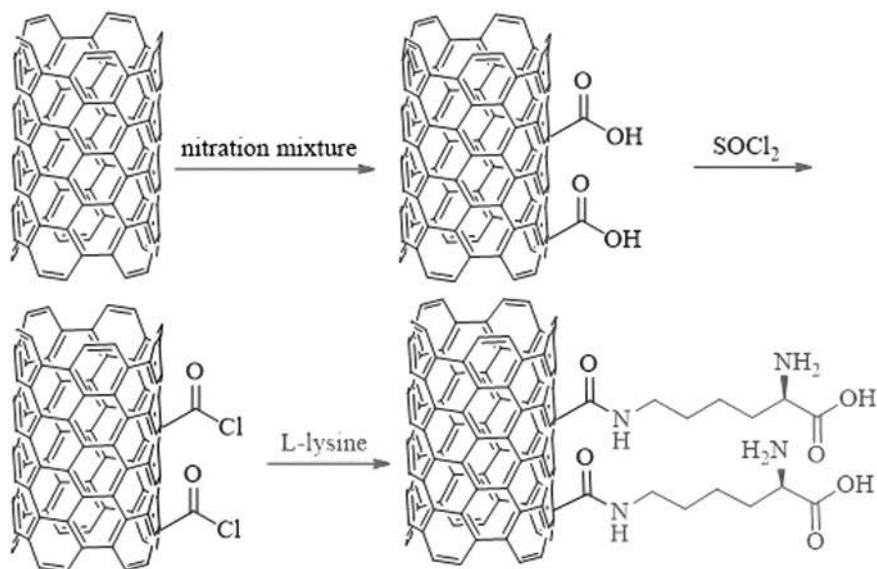
SCHEME 7.22. Synthetic route of L-lysine-MWCNTs.

Cathode	Yield (%)	ee (%)
L-lysine-MWCNTs	64	30 (R)
L-argenine-MWCNTs	61	43 (R)
D-argenine-MWCNTs	60	44 (S)
L-methionine-MWCNTs	31	0
L-glutamic acid-MWCNTs	22	0
L-isoleucine-MWCNTs	26	0
D-phenylalanine-MWCNTs	28	0

SCHEME 7.23. Enantioselective electroreduction of 2,2,2-trifluoro acetophenone by different cathodes.

coworkers reported $NiFe_2O_4$ as the nanomagnetic support that has been applied for the immobilization of copper complex of L-glutamate to obtain an efficient heterogeneous nanocatalyst (Scheme 7.24) [18]. As shown in Scheme, the catalyst is prepared in a three-step process. Initially, $NiFe_2O_4$ NPs were produced by a combination of $FeCl_3$ and $NiCl_2$. Then, L-glutamic acid and Cu $(OAc)_2$ were added to the surface of $NiFe_2O_4$ NPs.

Subsequently, the authors studied the catalytic properties of $NiFe_2O_4$-glutamate-Cu to provide a variety of 1,4-disubstituted-1,2,3-triazole derivatives through the combination of sodium azide, inactive terminal alkynes, and epoxides or benzyl chloride or aryl boronic acid at room temperature in water in moderate to excellent yields.
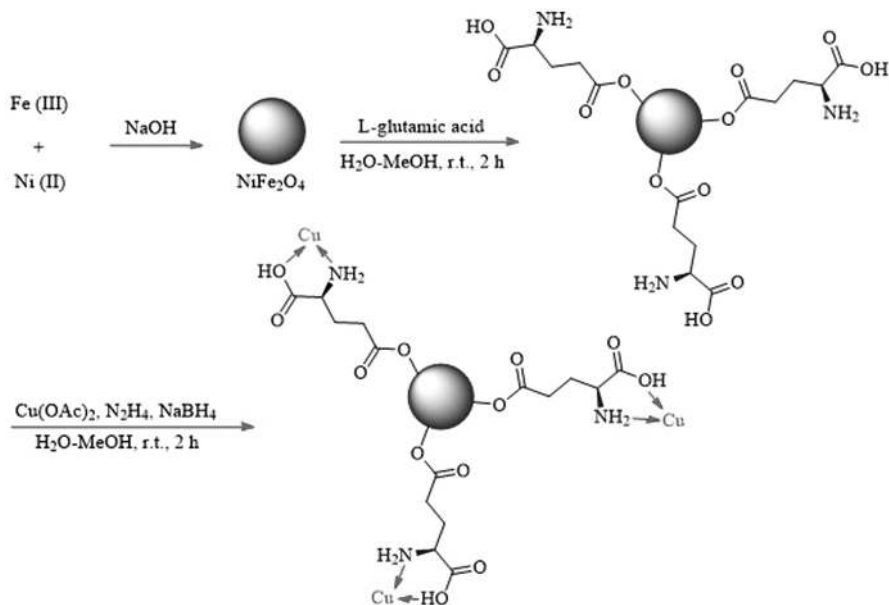
SCHEME 7.24. Synthesis of NiFe$_2$O$_4$-glutamate-Cu.

This method is supported by outstanding advantages, including an aqueous reaction medium, suitable reaction conditions, high efficiency, and easy separation of the catalyst (Scheme 7.25).

7.15. APPLICATION OF METAL COMPLEXES OF L-GLUTAMATE AS A CATALYST FOR THE SYNTHESIS OF CYCLIC CARBONATES

One of the most important ways to protect our surrounding environment is the conversion of industrially produced greenhouse gases, such as CO_2, into valuable chemicals. In one of the known procedures, carbon dioxide is used for the synthesizing of cyclic compounds and urethanes. In 2016, Park and coworkers synthesized propylene carbonate (PC) and 4-methyl-2-oxazolidinone (4-MeO$_x$) using an organic metal framework made from the L-glutamate and zinc sulfate (Scheme 7.26) [19].

7.16. APPLICATION OF METAL COMPLEXES OF L-GLUTAMATE-SUPPORTED MATERIAL AS A CATALYST IN THE OXIDATION REACTION

Selective oxidation of alcohols is an important transformation in the synthesis of compounds that are widely employed in industry, medicine, and photographic materials. The important point in the oxidation of alcohol into the aldehyde group is heat and distillation. The selected temperatures should be the suitable temperature for the

R= C$_6$H$_5$, 4-Cl-C$_6$H$_4$, 3-F-C$_6$H$_4$, C$_3$H$_6$, 3-Me-C$_6$H$_4$, 4-Br-C$_6$H$_4$, C$_4$H$_3$S,
   C$_{12}$H$_9$, C$_8$H$_9$, 4-Me-C$_6$H$_4$, 4-OMe-C$_6$H$_4$, C$_5$H$_{10}$, 4-F-C$_6$H$_4$, C$_5$H$_4$N

R$_1$= C$_6$H$_5$, 4-Cl-C$_6$H$_4$, 4-F-C$_6$H$_4$, 4-Br-C$_6$H$_4$, 4-OMe-C$_6$H$_4$, C$_6$H$_5$OCH$_2$,
   4-OMe-C$_6$H$_3$OCH$_2$, 2-Me-C$_6$H$_3$OCH$_2$, C$_4$H$_9$OCH$_2$, C$_3$H$_6$OCH$_2$, C$_3$H$_6$, CH$_2$Cl

R$_2$= H

R$_3$= C$_6$H$_5$, 4-Br-C$_6$H$_4$, 4-Me-C$_6$H$_4$

R4= C$_6$H$_5$, 3-F-C$_6$H$_4$, 4-Cl-C$_6$H$_4$
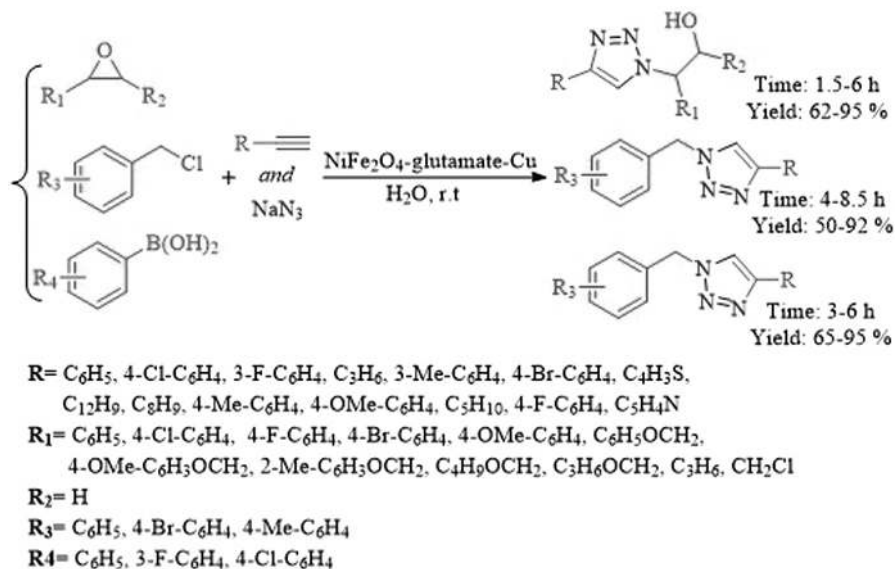
SCHEME 7.25.   Synthesis of 1,2,3-triazoles catalyzed by NiFe$_2$O$_4$-glutamate-Cu.
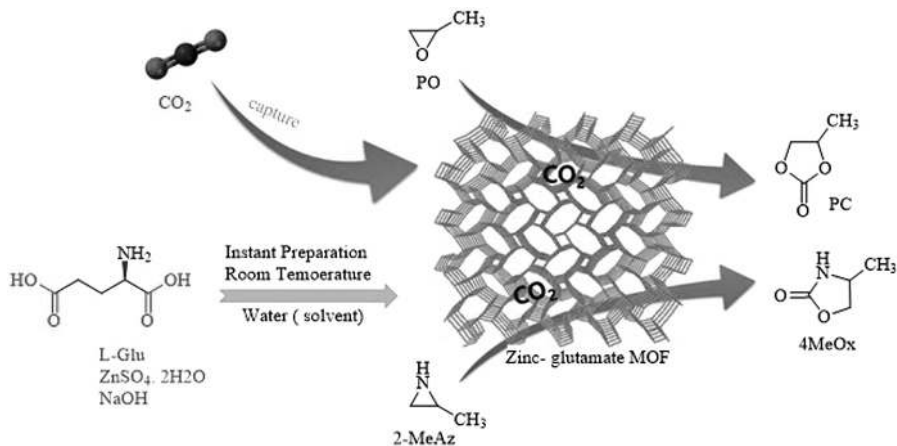
SCHEME 7.26.   Preparation of zinc-glutamate-MOF, which catalyzed the forming of pro-pylene carbonate (PC), and 4-methyl-2-oxazolidinone (4-MeO$_x$)

alcohol groups and the aldehyde compound. In 2013, Yang and coworkers designed a heterogeneous catalyst through the immobilization of Pd(II)-L-glutamate complex on carbon materials such as XC-72 and graphite (Scheme 7.27) that was used for the selective oxidation of primary alcohols to the aldehydes (Scheme 7.28) [20]. The synthesized catalyst shows a good performance in the oxidation of primary alcohols.

7.17. APPLICATION OF METAL COMPLEXES OF L-ALANINE AS A CATALYST IN THE MULTICOMPONENT REACTION

An easy and effective method for the preparation of 1,8-dioxodecahydroacridine derivatives is the three-component reaction of aryl ammonium or ammonium acetate with dimedone and various aldehydes. In 2019, Alam et al. reported synthesizing these compounds in the presence of a catalytic amount of cobalt/L-alanine metal complex in ethanol (Scheme 7.29) [21]. This protocol offers several advantages,
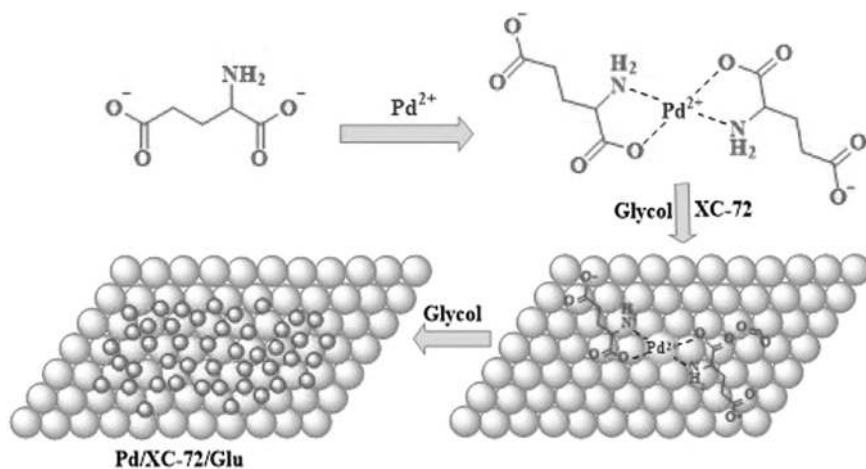
SCHEME 7.27.   Synthesis of Pd/XC-72/Glu.
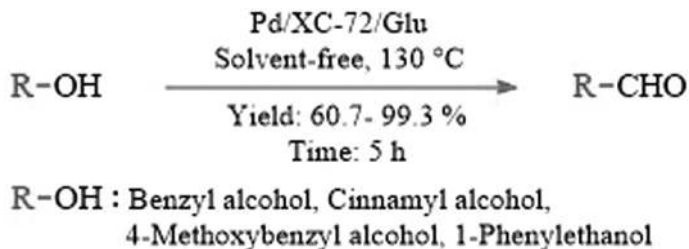
SCHEME 7.28.   Oxidation of alcohols catalyzed by Pd/XC-72/Glu.
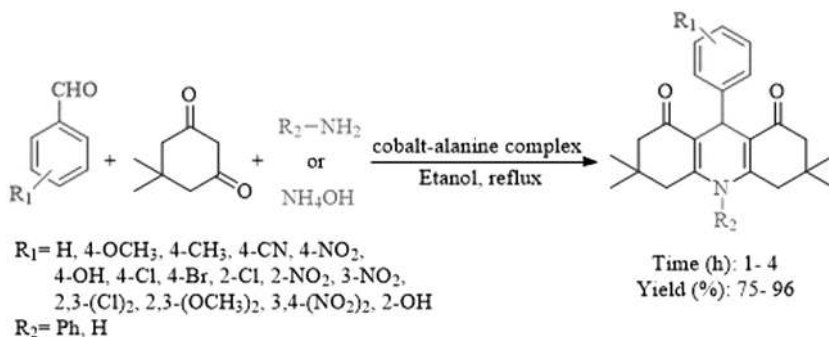
SCHEME 7.29. Cobalt/L-alanine complex catalyzed synthesis of 1,8-dioxodecahydro-acridines.

including mild reaction conditions, inexpensive high-performance catalysts, short reaction times, and excellent product yields.

7.18. APPLICATION OF L-ALANINE-SUPPORTED MATERIAL AS A CATALYST IN THE MULTICOMPONENT REACTION

In 2017, Safaei-Ghomi et al. designed an efficient catalyst by attaching L-phenyl alanine on Fe_3O_4 nanoparticles that can be easily separated from the reaction media by an external field. The performance of synthesized heterogeneous was studied by authors in a one-put multicomponent reaction to synthesize chromene compounds (Scheme 7.30) [22]. In this work, a coprecipitation method was used to synthesize Fe_3O_4 magnetic nanoparticles, then the magnetic nanoparticles were modified using tetraethyl orthosilicate and L-phenylalanine, and finally, the nano-Fe_3O_4@SiO_2/L-phenylalanine nanocatalyst was obtained (Scheme 7.31).

Ultrasound is a fast way to perform a wide variety of organic reactions. In 2018, Safaei-Ghomi et al. reported an ultrasound methodology with the aim of L-alanine-containing magnetic nanoparticles as versatile catalysts for the combination of different aldehydes, dimedone, and 4-hydroxy coumarin to synthesize chromone compounds (Scheme 7.32) [23]. In Scheme 7.33, the mechanism of chromone synthesis using aldehyde, dimedone, and 4-hydroxy coumarin is given.

7.19. APPLICATION OF L-ALANINE-SUPPORTED MATERIAL AS A CATALYST IN KNOEVENAGEL CONDENSATION REACTION

L-alanine was found to be an effective catalyst for asymmetric organic reactions, several reactions have been developed. The application of natural and modified amino acids as chiral catalysts and ligands for synthesis is the subject of this section. In 2017, the Selvaraj group designed an efficient catalyst for Knoevenagel condensation using immobilized L-alanine on MCM-41 (Scheme 7.34) [24]. Knoevenagel

R= 4-Cl-C$_6$H$_4$, 4-Br-C$_6$H$_4$, 2-Cl-C$_6$H$_4$, C$_6$H$_5$, 4-NO$_2$-C$_6$H$_4$,
4-Me-C$_6$H$_4$, 4-OMe-C$_6$H$_4$, 3-NO$_2$-C$_6$H$_4$, 2-NO$_2$-C$_6$H$_4$

Yield (%): 65- 92
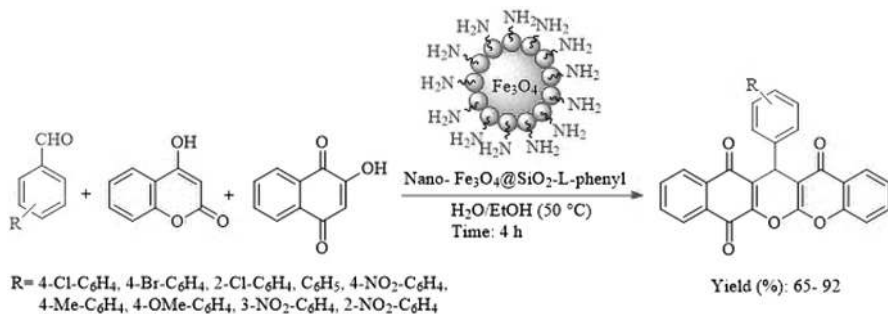
SCHEME 7.30.   Synthesis of chromene compounds by nano-Fe$_3$O$_4$@SiO$_2$/L-phenyl alanine.
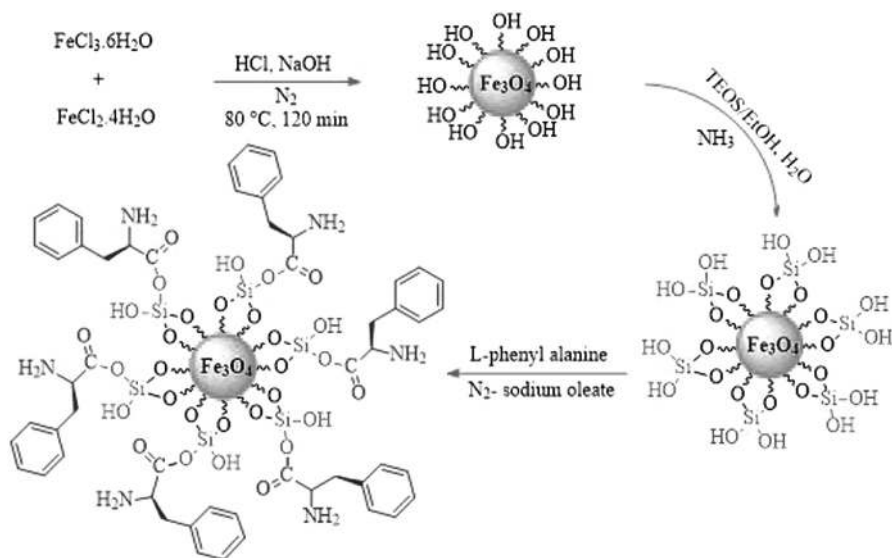
SCHEME 7.31.   Synthesis nano-Fe$_3$O$_4$@SiO$_2$/L-phenyl alanine.

R= Me, OMe, Cl, Br, NO$_2$

Yield: 74- 96%
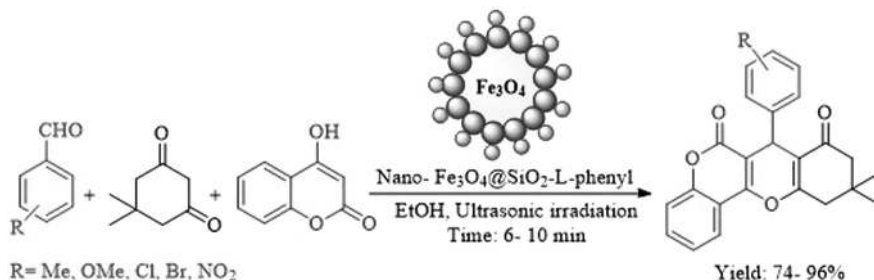
SCHEME 7.32.   Nano-Fe$_3$O$_4$@SiO$_2$-L-phenyl catalyzed the synthesis of chromenes under ultrasound conditions.
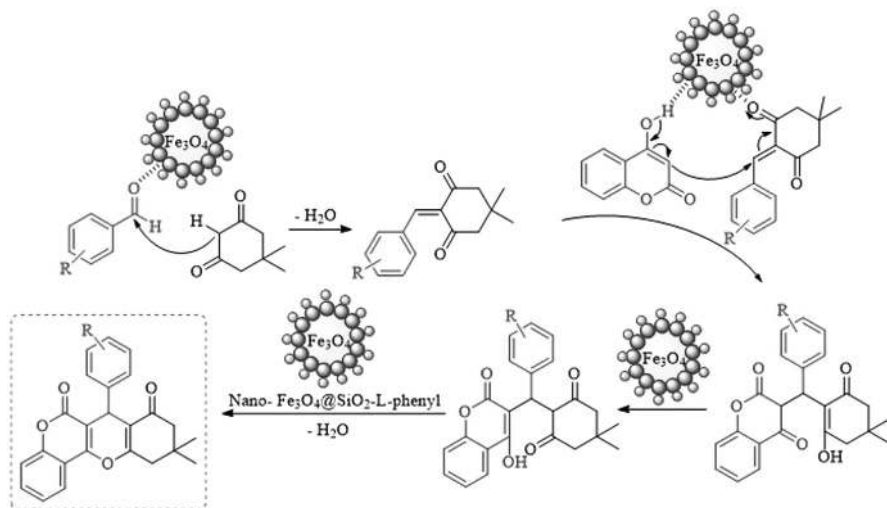
SCHEME 7.33. Proposed mechanism of chromenes synthesis by Nano-Fe$_3$O$_4$@ SiO$_2$/L-phenyl.

condensation was performed by the reaction of furfural with acetylacetone in the presence of 16 Alanine-MCM-41 as a catalyst in the absence of any solvent (neat conditions) in a short reaction time.

7.20. APPLICATION OF METAL COMPLEXES OF L-ALANINE AS A CATALYST IN THE REDUCTION REACTION

Fe$_3$O$_4$/β-alanine-acrylamide-Ni nanocomposite as a new magnetic catalyst was successfully prepared and used as a new heterogeneous magnetic catalyst for the reduction of several nitroaromatic under mild reaction conditions (Scheme 7.35 and 7.36) [25].

7.21. APPLICATION OF METAL COMPLEXES OF L-ALANINE-SUPPORTED MATERIAL AS A CATALYST FOR CYCLOADDITION REACTION OF CO$_2$ WITH VARIOUS EPOXIDES

Mallakpour et al. synthesized the supported Cu-L-alanine complex on graphene oxide through several convenient sequences. To prepare this catalyst, they first examined the coordination of various amino acids with copper. Then they connected the Cu–AAs complex on the surface of graphene oxide (Schemes 7.37 and 7.38) [26]. Go–Cu–AAs were used by the authors as heterogeneous catalysts for the epoxidation of norbornene using H$_2$O$_2$ as an oxidant (Scheme 7.39). Recovery and reusability

furural

+

acetylacetone

16Alanine-MCM-41

100 °C, 30 min, solvent-less

Conversion: 92.4%
Selectivity: 100%
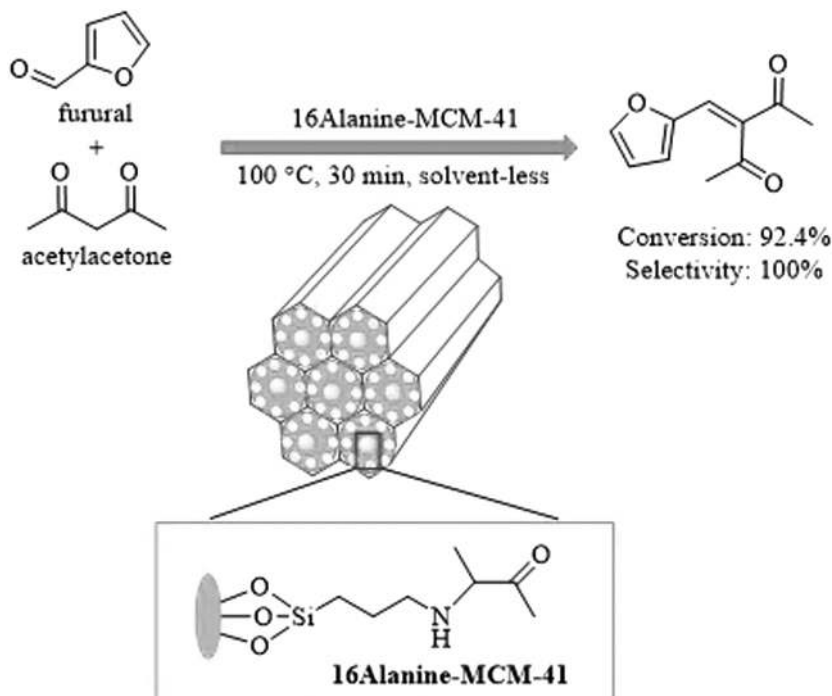
16Alanine-MCM-41

SCHEME 7.34. Preparation of 3-(2-furyl methylene)-2,4-pentane dione in the presence of 16 alanine-MCM-41.

NO_2

Fe$_3$O$_4$/Ala-AA-Ni catalyst

H_2O, r.t

NH_2

R= 4-H, 4-NH$_2$, 3-NH$_2$,
2-CH$_3$, 4-Cl, 4-Br, 3-OH,

Time: 5- 15 min
Yield: 90- 98 %
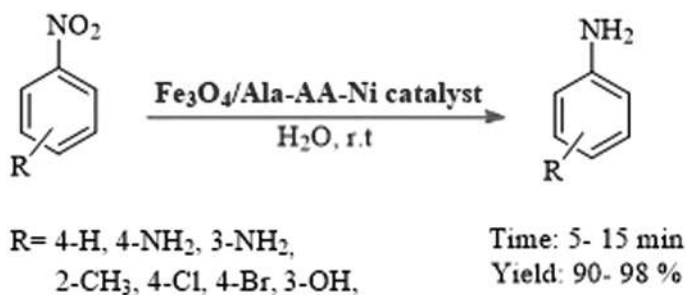
SCHEME 7.35. Fe$_3$O$_4$/β-alanine-acrylamide-Ni nanocomposite as a new magnetic catalyst for the reduction of nitroaromatic compounds.
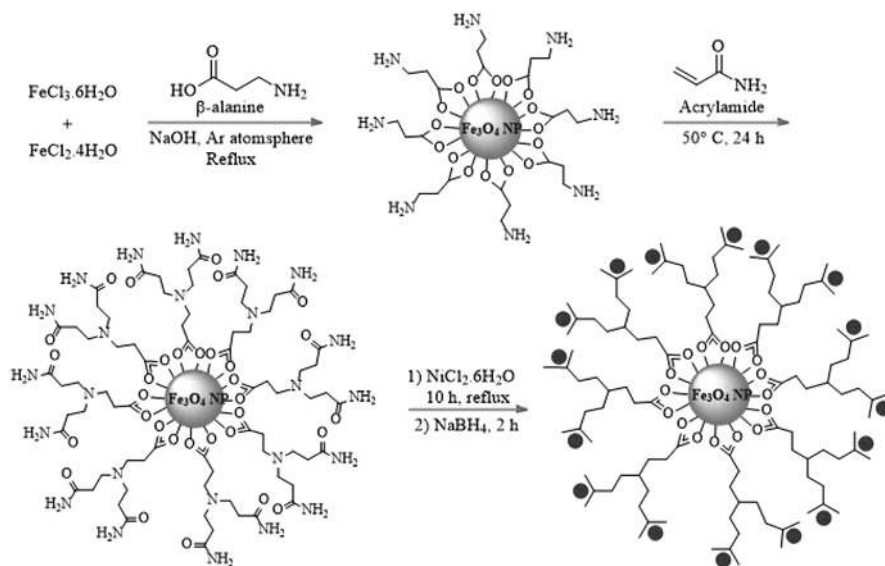
SCHEME 7.36. Synthesis method of Fe$_3$O$_4$/β-alanine-acrylamide-Ni nanocomposite.
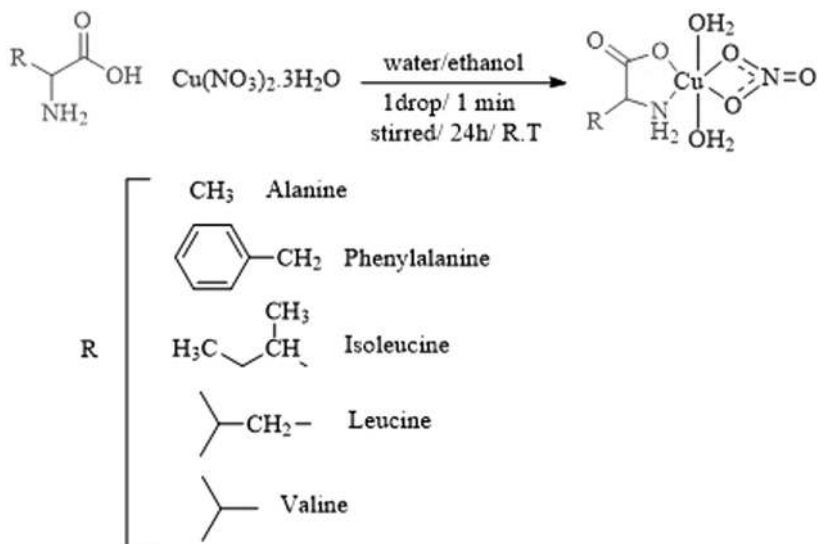
SCHEME 7.37. Synthetic route for the copper (II) complexes with different amino acids.
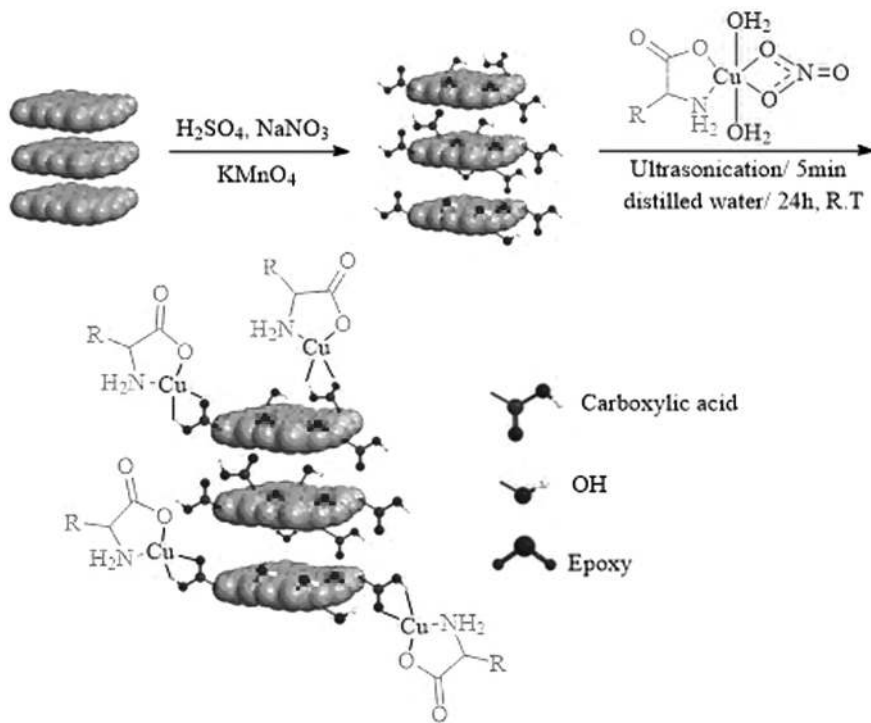
SCHEME 7.38.   Synthetic route for GO and modified graphene oxide.

Catalyst	Conversion (%)	Product Selectivity (%)	Yield (%)
Phe	Nil	Nil	Nil
$H_3PW_{12}O_{40}$	96.7	90.0	87.0
$[PheH]H_2PW_{12}O_{40}$	97.9	97.4	95.4
$[PheH]_2HPW_{12}O_{40}$	97.5	92.0	89.7
$[PheH]_3PW_{12}O_{40}$	96.3	91.8	88.4
$[AlaH]H_2PW_{12}O_{40}$	97.8	94.7	92.7
$[GlyH]H_2PW_{12}O_{40}$	97.7	92.9	90.8

SCHEME 7.39.   Epoxidation of norbornene catalyzed by various catalysts (conditions: cata-lyst 60 mg, substrate 10 mmol, 30% H_2O_2 [20 mmol], acetonitrile [12 ml], reflux conditions, 12 h).

of GO-Cu-phenylalanine were investigated by the authors, after each run, the solid catalyst was separated from the reaction mixture by centrifugation, then washed with acetonitrile, and finally dried and employed in the next run. This operation was repeated three times, and the amount of leached copper from the catalyst was determined by AAS which was found to be 0.8 mg. This amount of leaching is the main factor in reducing catalyst activity.

7.22. APPLICATION OF METAL COMPLEXES OF L-ALANINE-SUPPORTED MATERIAL AS A CATALYST FOR THE OXIDATION REACTION

Han et al. reported the preparation of a series of amino acid–based composite catalysts. They used phenylalanine, alanine, and glycine as the amino acid to synthesize these nanocomposites (Scheme 7.40) [27]. The performance of $(MH)xH_3$-$xPW_{12}O_{40}$ (M= Phe, Ala, and Gly) was used as a heterogeneous catalyst for the selective oxidation of benzyl alcohol to benzaldehyde using hydrogen peroxide as an oxidant. Among these catalysts, $[PheH]H_2PW_{12}O_{40}$ was found to be a reusable catalyst, and after six times recovery and reuse, its activity was slightly reduced.

7.23. APPLICATION OF L-VALINE AS AN ORGANOCATALYST IN THE MULTICOMPONENT REACTION

L-valine is an important useful chiral amino acid, which can be applied to catalyze asymmetric reactions.

Singh et al. reported the application of L-valine as an organocatalyst for the synthesis of 4H-pyran compounds that have anticancer, antitumor, anti-HIV, etc. properties (Scheme 7.41) [28]. This reaction proceeded well giving the desired products in 45–80% yields.

Catalyst	Conversion (%)	Product Selectivity (%)	Yield (%)
Phe	Nil	Nil	Nil
$H_3PW_{12}O_{40}$	96.7	90.0	87.0
$[PheH]H_2PW_{12}O_{40}$	97.9	97.4	95.4
$[PheH]_2HPW_{12}O_{40}$	97.5	92.0	89.7
$[PheH]_3PW_{12}O_{40}$	96.3	91.8	88.4
$[AlaH]H_2PW_{12}O_{40}$	97.8	94.7	92.7
$[GlyH]H_2PW_{12}O_{40}$	97.7	92.9	90.8

SCHEME 7.40. $(MH)_xH_{3-x}PW_{12}O_{40}$ (M = Phe, Ala, and Gly) catalyzed the oxidation of benzyl alcohol to benzaldehyde.

R$_1$= 3-NO$_2$-C$_6$H$_4$, C$_6$H$_5$, 4-F-C$_6$H$_4$, 4-Br-C$_6$H$_4$,
    4-CH$_3$-C$_6$H$_4$, 4-OCH$_3$-C$_6$H$_4$, 4-OH-C$_6$H$_4$, 2-Furyl
R$_2$= CH$_3$, OCH$_3$, OC$_2$H$_5$

Time (min): 45- 80
Yield (%): 78- 94
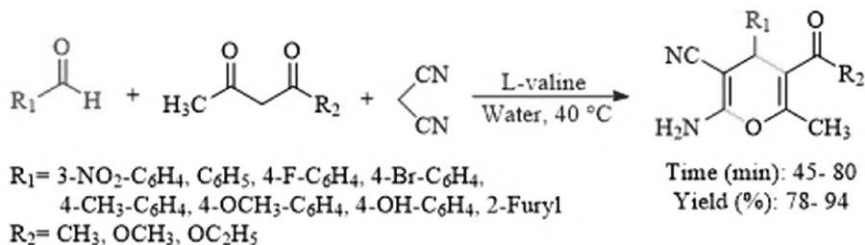
SCHEME 7.41.   L-valine catalyzed the synthesis of 2-amino-3-cyano-4H-pyrans.

7.24.   APPLICATION OF L-VALINE AS A CATALYST IN THE COUPLING REACTION

One of the conventional procedures is the O-arylation of aryl compounds with phenol in the presence of effective catalysts. Anilkumar et al. were able to easily perform an O-arylation from the reaction between phenols and electron-deficient aryl iodides using a catalytic mixture of cobalt acetate and L-valine (Scheme 7.42) [29]. The authors reported that when the reaction was carried out in the absence of L-valine, the product yield was very low.

7.25.   APPLICATION OF L-VALINE DERIVATIVE AS A CATALYST FOR ASYMMETRIC HYDROSILYLATION OF *N*-ALKYL AND *N*-ARYL-PROTECTED KETIMINES

Reduction of enantioselective prochiral imines or enamines by trichlorosilane (HSiCl$_3$) using amino acids as an organocatalyst is recognized as a strategy for the preparation of chiral amines. In this context, Sun and coworkers introduced a new series of amino acids–based organocatalysts for the production of chiral amines using trichlorosilane. Among the applied catalysts, catalyst **3c** was a high-performance catalyst for the amine reduction reaction and the production of high-yield products (Schemes 7.43 and 7.44) [30].

R^1= H, 2-Me; X= I   Y= C, N

Yield (%): 17- 95
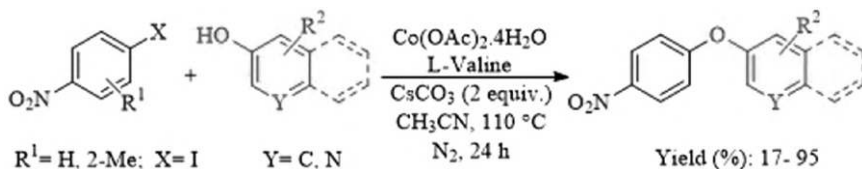
SCHEME 7.42.   Cobalt acetate and L-valine catalyzed O-arylation of aryl compounds with phenol
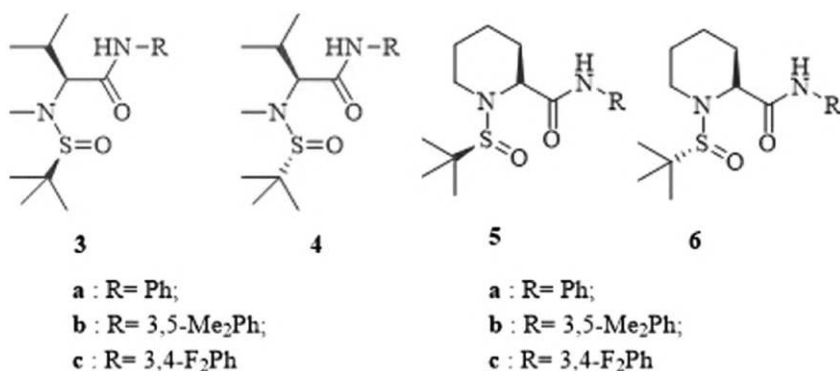
SCHEME 7.43. Derived catalysts 3–6 from L-valine and L-pipecolinic acid.

One of the usual procedures for the synthesis of diaryl methylamines is the reaction between *N*-tosylarylimines and arylboroxines. In 2004, Tomioka's group synthesized several types of chiral phosphane ligands **1–7** using L-valine and amino phosphonates (Scheme 7.45). Among them rhodium (I) complex of compound **7** has been selected as an efficient catalyst for the synthesis of diaryl methylamine compounds (Scheme 7.46) [31].

7.26. CONCLUSION

Green chemistry is an approach that strives to achieve reducing or eliminating the use of harmful substances. Catalysis is known as "green chemistry" or "sustainable technology" to reduce the environmental impact of chemical processes. A succinct account will summarize some of the research and developments in the field. This chapter tries to bring many outstanding types of research together and shows the vitality of organocatalysis through several aspects. In this chapter, we have considered several organic reactions, which has been catalyzed by some amino acid, including L-aspartic acid, L-lysine, glutamate, L-alanine, and L-valine. The results show these amino acids could act as a very effective catalyst in different organic functional group transformations either as immobilized on solid supports or as bare amino acids.

$$\text{HSiCl}_3$$

$$\underset{R^1 \quad R^2}{\overset{N\text{-}Bn}{\big\|}} \quad \xrightarrow[\substack{\text{Toluene, } -40\ ^\circ\text{C, 48 h} \\ \text{Yield (\%): 20-95} \\ \text{ee (\%): 57-94}}]{\substack{20 \text{ mol\% 3c}}} \quad \underset{R^1 \quad R^2}{\overset{HN\text{-}Bn}{\big|}}$$

R^1 = C_6H_5, 4-ClC_6H_4, 4-MeC_6H_4, 4-BrC_6H_4, 2-ClC_6H_4,
naphthalene, 4-$CF_3C_6H_4$, 4-FC_6H_4, 4-$NO_2C_6H_4$,
3-ClC_6H_4, 3-BrC_6H_4, 4-$OMeC_6H_4$, 2-ClC_6H_4,
2-methoxynaphthalene

R^2 = Me, Et

$$\underset{R^1 \quad R^2}{\overset{N\text{-}Alkyl}{\big\|}} \quad \xrightarrow[\substack{\text{Toluene, } -40\ ^\circ\text{C, 48 h} \\ \text{Yield (\%):55-99} \\ \text{ee (\%): 71-95}}]{\substack{20 \text{ mol\% 3c, HSiCl}_3}} \quad \underset{R^1 \quad R^2}{\overset{HN\text{-}Alkyl}{\big|}}$$

R^1 = C_6H_5, 4-ClC_6H_4, 4-MeC_6H_4, 4-BrC_6H_4, 2-ClC_6H_4,
naphthalene, 4-$CF_3C_6H_4$, 4-FC_6H_4, 4-$NO_2C_6H_4$,
3-ClC_6H_4, 3-BrC_6H_4, 4-$OMeC_6H_4$, 2-ClC_6H_4,
2-methoxynaphthalene

R^2 = Me, Et
Alkyl = isobutane, prop-1-ene

$$\underset{R^1 \quad R^2}{\overset{N\text{-}Aryl}{\big\|}} \quad \xrightarrow[\substack{\text{DCM, } -20\ ^\circ\text{C, 48 h} \\ \text{Yield (\%): 43-98} \\ \text{ee (\%: 92-98}}]{\substack{20 \text{ mol\% 3c, HSiCl}_3}} \quad \underset{R^1 \quad R^2}{\overset{HN\text{-}Aryl}{\big|}}$$

R^1 = C_6H_5, 4-ClC_6H_4, 4-MeC_6H_4, 4-$OMeC_6H_4$,
4-$NO_2C_6H_4$, naphthalene, 4-FC_6H_4

R^2 = Me, Et, n-Pr
Aryl= C_6H_5, 4-$NO_2C_6H_4$, 4-$OMeC_6H_4$, 4-ClC_6H_4,
2-$OMeC_6H_4$

SCHEME 7.44. Asymmetric reduction of imines or enamines by trichlorosilane (HSiCl$_3$) in the presence of **3c** catalyst.

1 : $R^1 = H$
2 : $R^1 = PhCH_2$

3 : (S)-BINAP

4 : $R^2 = 2,4,6\text{-}Me_3C_6H_2CH_2$, $R^3 = \beta\text{-}H$
5 : $R^2 = 2,4,6\text{-}Me_3C_6H_2CH_2$, $R^3 = \alpha\text{-}H$
6 : $R^2 = H$, $R^3 = \beta\text{-}H$
7 : $R^2 = H$, $R^3 = \alpha\text{-}H$
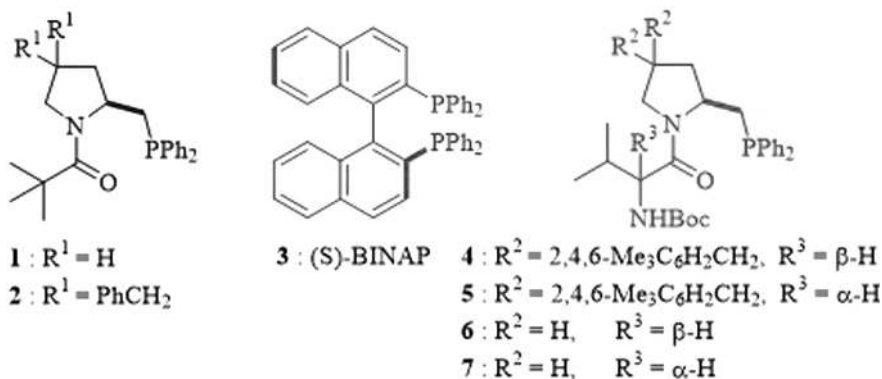
SCHEME 7.45. Synthesis of chiral phosphane ligands **1-7** by L-valine and amino phosphonates.

$Ar^1 = 4\text{-}MeC_6H_4$, $3\text{-}MeC_6H_4$, $2\text{-}MeC_6H_4$, $2\text{-}TMSC_6H_4$, Ph, 1-Naphthyl
$Ar^2 = 4\text{-}PhC_6H_4$, $4\text{-}MeOC_6H_4$, $4\text{-}ClC_6H_4$, $3\text{-}MeOC_6H_4$, $3\text{-}ClC_6H_4$
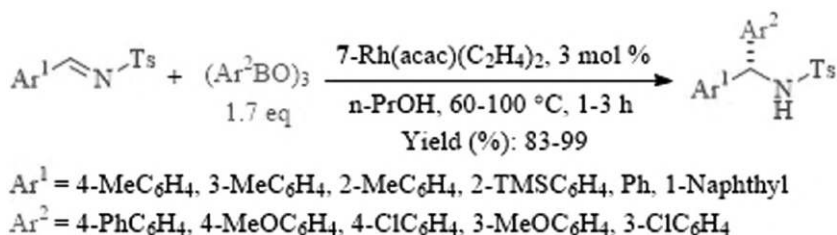
SCHEME 7.46. Synthesis of diaryl methylamines by rhodium (I)-**7** as a catalyst.

REFERENCES

1. Ghorbani-Choghamarani, A., Hajjami, M., Norouzi, M., Abbasityula, Y., Eigner, V., Dušek, M. Diastereoselective and one-pot synthesis of trans-isoquinolonic acids via three-component condensation of homophthalic anhydride, aldehydes, and ammonium acetate catalyzed by aspartic acid. *Tetrahedron*, 2013, *69*(32), 6541–6544. https://doi.org/10.1016/j.tet.2013.06.010.
2. Mohammadi, M., Ghorbani-Choghamarani, A., Hussain–Khil, N. l–aspartic acid chelan–Cu (II) complex coted on ZrFe$_2$O$_4$ MNPs catalyzed one–pot annulation and cooperative geminal-vinylogous anomeric–based oxidation reactions. *J. Phys. Chem. Solids.*, 2023, *177*, 111300. https://doi.org/10.1016/j.jpcs.2023.111300.
3. Heravi, M. M., Momeni, T., Mirzaei, M., Zadsirjan, V., Tahmasebi, M. An amino acid@ isopolyoxometalate nanoparticles catalyst containing aspartic acid and octamolybdate for the synthesis of functionalized spirochromenes. *Inorg. Nano-Metal Chem.*, 2021, *51*(6), 896–909. https://doi.org/10.1080/24701556.2020.1813172.
4. Afradi, N., Foroughifar, N., Pasdar, H., Qomi, M. Aspartic-acid-loaded starch-functionalized Mn–Fe–Ca ferrite magnetic nanoparticles as novel green heterogeneous nanomagnetic catalyst for solvent-free synthesis of dihydropyrimidine derivatives as potent antibacterial agents. *Res. Chem. Intermed.*, 2019, *45*(5), 3251–3271. https://doi.org/10.1007/s11164-019-03791-7.

5. Nikoofar, K., Shahriyari, F. Novel bio-based core-shell organic-inorganic nanohybrid from embedding aspartic acid-guanine ionic liquid on the hydroxylated nano silica surface (Nano [(Asp-Gua) IL@PEG-SiO2]): A versatile nanostructure for the synthesis of Bis(2,3-Dihydroquinazolin-4(1H. *Polyhedron*, 2020, *179*, 114361. https://doi.org/10.1016/j.poly.2020.114361.

6. Ghorbani-Choghamarani, A., Norouzi, M. Protection of hydroxyl groups as a trimethylsilyl ether by 1, 1, 1, 3, 3, 3-hexamethyldisilazane promoted by aspartic acid as an efficient organocatalyst. *Cuihua Xuebao/Chinese J. Catal.*, 2011, *32*(4), 595–598. https://doi.org/10.1016/s1872-2067(10)60210-0.

7. Ghorbani-Choghamarani, A., Bastan, H., Kakakhani, Z., Taherinia, Z. Preparation of Ni-microsphere and Cu-MOF using aspartic acid as coordinating ligand and study of their catalytic properties in stille and sulfoxidation reactions. *RSC Adv.*, 2021, *11*(25), 14905–14914. https://doi.org/10.1039/d1ra00734c.

8. Ghorbani-Choghamarani, A., Taherinia, Z. Chiral cobalt-peptide metal-organic framework (Co-P-MOF): As an efficient and reusable heterogeneous catalyst for the asymmetric sulfoxidative cross-coupling reaction using poly sulfinylpiperazine. *Synth. Met.*, 2020, *263*(November 2019). https://doi.org/10.1016/j.synthmet.2020.116362.

9. Karthikeyan, P., Arunrao, A. S., Narayan, M. P., Kumar, S. S., Kumar, S. S., Bhagat, P. R. Selective oxidation of alcohol to carbonyl compound catalyzed by L-aspartic acid coupled imidazolium based ionic liquid. *J. Mol. Liq.*, 2012, *173*, 180–183. https://doi.org/10.1016/j.molliq.2012.06.018.

10. De, S., Dutta, S., Patra, A. K., Bhaumik, A., Saha, B. Self-assembly of mesoporous TiO2 nanospheres via aspartic acid templating pathway and its catalytic application for 5-hydroxymethyl-furfural synthesis. *J. Mater. Chem.*, 2011, *21*(43), 17505–17510. https://doi.org/10.1039/c1jm13229f.

11. Wang, G., Dai, J., Luo, Q., Deng, N. Photocatalytic degradation of bisphenol A by TiO2@aspartic acid-β-cyclodextrin@reduced graphene oxide. *Sep. Purif. Technol.*, 2021, *254*, 117574. https://doi.org/10.1016/j.seppur.2020.117574.

12. Wang, G., Fan, W., Li, Q., Deng, N. Enhanced photocatalytic new Coccine degradation and Pb(II) reduction over graphene oxide-TiO2 composite in the presence of aspartic acid-B-cyclodextrin. *Chemosphere*, 2019, *216*, 707–714. https://doi.org/10.1016/j.chemosphere.2018.10.199.

13. Ashraf, M. A., Liu, Z., Li, C., Zhang, D. Fe₃O₄@ L-lysine-Pd (0) organic–inorganic hybrid: As a novel heterogeneous magnetic nanocatalyst for chemo and homoselective [2+ 3] cycloaddition synthesis of 5-substituted 1H-tetrazoles. *Appl. Organomet. Chem.*, 2021, *35*(3), e6133.

14. Li, P., Liu, Y., Ma, N., Zhang, W. L-lysine functionalized polyacrylonitrile fiber: A green and efficient catalyst for Knoevenagel condensation in water. *Catal. Letters*, 2018, *148*(3), 813–823. https://doi.org/10.1007/s10562-017-2287-y.

15. Zhang, Y., Sun, C., Liang, J., Shang, Z. Catalysis by L-lysine: A green method for the condensation of aromatic aldehydes with acidic methylene compounds in water at room temperature. *Chinese J. Chem.*, 2010, *28*(11), 2255–2259. https://doi.org/10.1002/cjoc.201090373.

16. Ashraf, M. A., Liu, Z., Zhang, D., Alimoradi, A. L-lysine-Pd complex supported on Fe3O4 MNPs: A novel recoverable magnetic nanocatalyst for Suzuki C-C cross-coupling reaction. *Appl. Organomet. Chem.*, 2020, *34*(8), e5668. https://doi.org/10.1002/aoc.5668.

17. Yue, Y.-N., Meng, W.-J., Liu, L., Hu, Q.-L., Wang, H., Lu J.-X. Amino acid-functionalized multi-walled carbon nanotubes: A metal-free chiral catalyst for the asymmetric electroreduction of aromatic ketones. *Electrochim. Acta*, 2018, *260*, 606–613.

18. Lu, J., Ma, E.-Q., Liu, Y.-H., Li, Y.-M., Mo, L.-P., Zhang, Z.-H. One-pot three-component synthesis of 1,2,3-triazoles using magnetic $NiFe_2O_4$–glutamate–cu as an efficient heterogeneous catalyst in water. *RSC Adv.*, 2015, *5*(73), 59167–59185. https://doi.org/10.1039/c5ra09517d.

19. Kathalikkattil, A. C., Roshan, R., Tharun, J., Babu, R., Jeong, G. S., Kim, D. W., Cho, S. J., Park, D. W. A sustainable protocol for the facile synthesis of zinc-glutamate MOF: An efficient catalyst for room temperature CO_2 Fixation reactions under wet conditions. *Chem. Commun.*, 2016, *52*(2), 280–283. https://doi.org/10.1039/c5cc07781h.

20. Wang, F., Yang, L., Tang, Q., Guo, Y., Hao, G. Synthesis of Pd/XC-72 catalysts by a facile glutamate-mediated method for solvent-free selective oxidation of DL-Sec-Phenethylalcohol. *Catal. Sci. Technol.*, 2013, *3*(5), 1246–1252. https://doi.org/10.1039/c3cy20803f.

21. Mujahid Alam, M., Mubarak, A. T., Assiri, M. A., Merajuddin Ahmed, S., Fouda, A. M. A facile and efficient synthesis of 1,8-dioxodecahydroacridines derivatives catalyzed by cobalt-alanine metal complex under aqueous ethanol media. *BMC Chem.*, 2019, *13*(3), 1–10. https://doi.org/10.1186/s13065-019-0545-3.

22. Safaei-Ghomi, J., Eshteghal, F., Shahbazi-Alavi, H. L-phenyl alanine-attached Fe_3O_4@ SiO_2 nanoparticles as an efficient catalyst for the synthesis of chromenes. *J. Iran. Chem. Soc.*, 2018, *15*, 661–669. https://doi.org/10.1007/s13738-017-1266-y.

23. Safaei-Ghomi, J., Eshteghal, F., Shahbazi-Alavi, H. Sonochemical synthesis of chromenes catalyzed by L-phenyl alanine-attached nano-Fe_3O_4@SiO_2. *Green Chem. Lett. Rev.*, 2018, *11*(3), 345–351. https://doi.org/10.1080/17518253.2018.1502819.

24. Appaturi, J. N., Selvaraj, M., Abdul Hamid, S. B., Bin Johan, M. R. Synthesis of 3-(2-Furylmethylene)-2,4-pentanedione using DL-alanine functionalized MCM-41 catalyst via Knoevenagel condensation reaction. *Microporous Mesoporous Mater.*, 2018, *260*, 260–269. https://doi.org/10.1016/j.micromeso.2017.03.031.

25. Zamani, F., Kianpour, S. Fast and efficient reduction of nitro aromatic compounds over Fe 3O4/β-Alanine-Acrylamide-Ni nanocomposite as a new magnetic catalyst. *Catal. Commun.*, 2014, *45*, 1–6. https://doi.org/10.1016/j.catcom.2013.10.027.

26. Mallakpour, S., Abdolmaleki, A., Karshenas, A. Graphene oxide supported copper coordinated amino acids as novel heterogeneous catalysts for epoxidation of norbornene. *Catal. Commun.*, 2017, *92*, 109–113. https://doi.org/10.1016/j.catcom.2017.01.017.

27. Han, X., Kuang, Y., Xiong, C., Tang, X., Chen, Q., Hung, C. Te; Liu, L. L., Liu, S. Bin. Heterogeneous amino acid-based tungstophosphoric acids as efficient and recyclable catalysts for selective oxidation of benzyl alcohol. *Korean J. Chem. Eng.*, 2017, *34*(7), 1914–1923. https://doi.org/10.1007/s11814-017-0097-y.

28. Tiwari, J., Singh, S., Saquib, M., Tufail, F., Sharma, A. K., Singh, S., Singh, J. Organocatalytic mediated green approach: A versatile new L-valine promoted synthesis of diverse and densely functionalized 2-amino-3-cyano-4H-pyrans. *Synth. Commun.*, 2018, *48*(2), 188–196. https://doi.org/10.1080/00397911.2017.1393087.

29. Ujwaldev, S. M., Saranya, S., Harry, N. A., Anilkumar, G. Novel cobalt-valine catalyzed O-arylation of phenols with electron deficient aryl iodides. *Monatsh. Chem.*, 2019, *150*, 339–346. https://doi.org/10.1007/s00706-018-2324-6.

30. Wang, C., Wu, X., Zhou, L., Sun, J. L-Valine derived chiral N-sulfinamides as effective organocatalysts for the asymmetric hydrosilylation of N-alkyl and N-aryl protected ketimines. *Org. Biomol. Chem.*, 2015, *13*(2), 577–582. https://doi.org/10.1039/C4OB01257G.

31. Kuriyama, M., Soeta, T., Hao, X., Chen, Q., & Tomioka, K. N-Boc-L-valine-connected amidomonophosphane rhodium (I) catalyst for asymmetric arylation of N-tosylarylimines with arylboroxines. *J. Am. Chem. Soc.*, 2004, *126*(26), 8128–8129. https://doi.org/10.1021/ja0475398.

8 The Catalytic Role of L-Histidine and L-Threonine in Organic Reactions

8.1. INTRODUCTION

L-histidine and L-threonine are essential amino acids that play vital biological roles inside the body; they have now become even more critical owing to their application as catalysts in asymmetric synthesis. The development of novel chiral catalysts based on amino acids is the most important aspect of this area of green chemistry. Herein we provide an overview of very recent advances in the area of asymmetric catalysis using L-histidine and L-threonine.

8.2. APPLICATION OF L-HISTIDINE AS AN ORGANOCATALYST IN THE MULTICOMPONENT REACTION

L-histidine (L-His) is a natural amino acid featuring an aromatic imidazole unit; it is mainly employed as a catalyst in organic reactions. The versatility of histidine coordination with transition metal bindings makes it an ideal platform for metal binding.

Pyranopyrazoles are special heterocyclic compounds with antitumor, antifungal, hypertensive, anticancer, and antimicrobial activity. Various methods were reported for the synthesis of pyranopyrazoles. In 2017, Khatri et al. reported a new procedure for the synthesis of pyrano[2,3,c]pyrazoles via a combination of hydrazines, ethylacetoacetate, malenonitrile, and aromatic aldehydes in the presence of L-histidine as a natural catalyst in water (Scheme 8.1) [1].

8.3. APPLICATION OF METAL COMPLEXES OF L- HISTIDINE DERIVATIVES IN THE MULTICOMPONENT REACTION

L-histidine is used as a building block to design peptides. Recently, research projects in our group have developed the synthesis of histidine peptide nanofibers through a self-assembly method and applied them as templates for the coordination of metallic ions (e.g., Zn, Cu) (Scheme 8.2).

R₁= H, Ph

R₂= 4-Cl, 2-Cl, 3-NO₂, H

Time (h): 1.5- 2.5
Yield (%): 70- 97
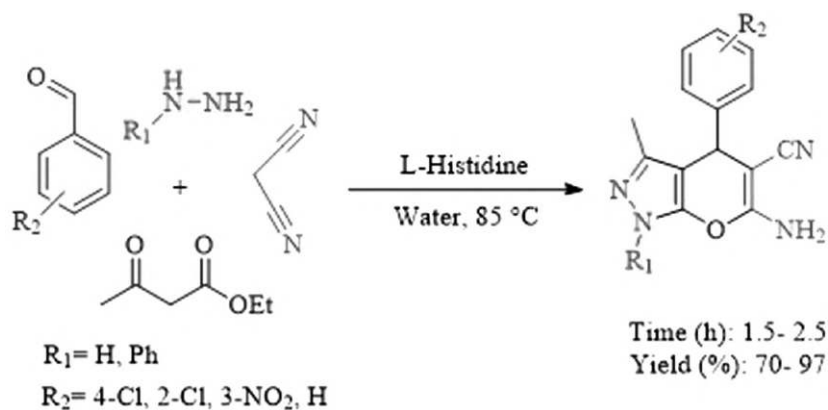
SCHEME 8.1.   Synthesis of pyrano [2,3-*c*] pyrazoles catalyzed by L-histidine.

M= Cu, ZnO
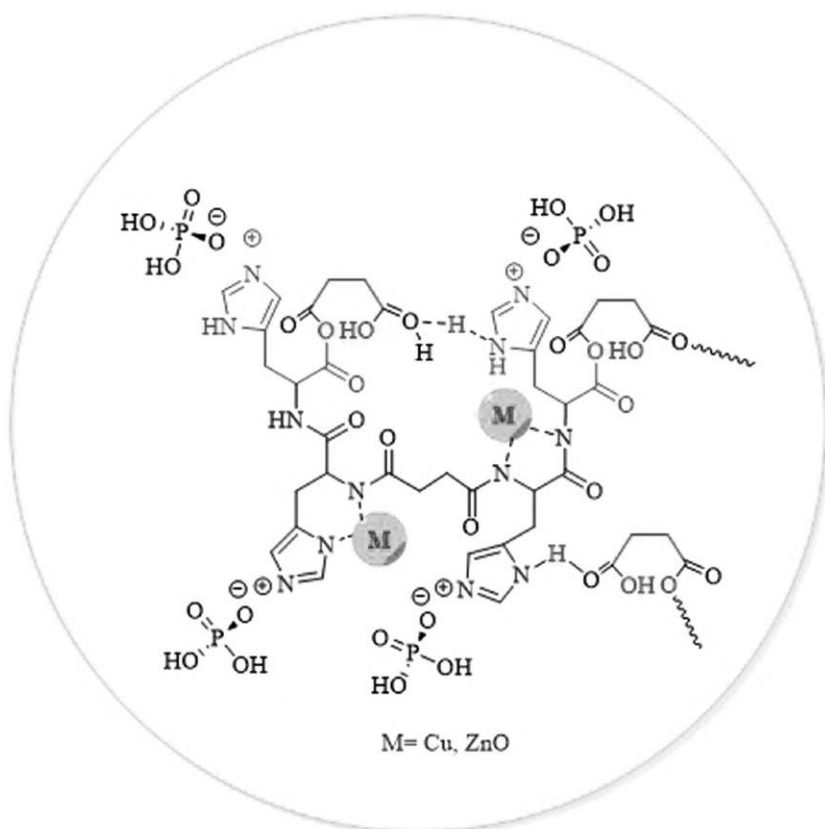
SCHEME 8.2.   Peptide nanofiber decorated with Cu and ZnO

We employed these peptide nanofibers as catalysts for a wide range of reactions, including cross-coupling and multicomponent domino reactions [2, 3]. An extensive review by our group in 2020 focusing exclusively on the catalytic application of nanofibers is based on natural materials in an organic reaction, which are briefly shown in Schemes 8.3–8.7 [4].

8.4. APPLICATION OF METAL COMPLEXES OF L-HISTIDINE-SUPPORTED MATERIAL AS A CATALYST FOR THE MULTICOMPONENT REACTION

The catalytic activity of Cu-MCM-41, mcm-41-Cu, and MCM-41@histidine@Cu was investigated to synthesize 5-substituted 1H-tetrazole derivatives [5]. In this study, immobilization of copper on the mesoporous MCM-41 materials was examined via

X= -NH$_2$, CH$_2$NH-
R= Cl, Br, NO$_2$, H, OMe

ZnONP-PNF (Cat)
DMSO, KOH, 130 °C
Time: 8-15 h

Yield (%): 47-88
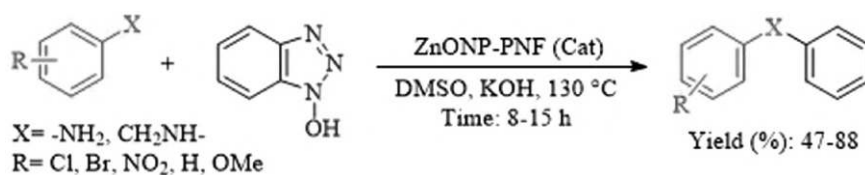
SCHEME 8.3. Application peptide nanofiber decorated with ZnO as a catalyst in N-arylation of amine.

X= F, Br, NO$_2$, OH

ZnO NP-PNF (Cat)
PEG, 100 °C
Time: 10-20 h

Yield (%): 55-95
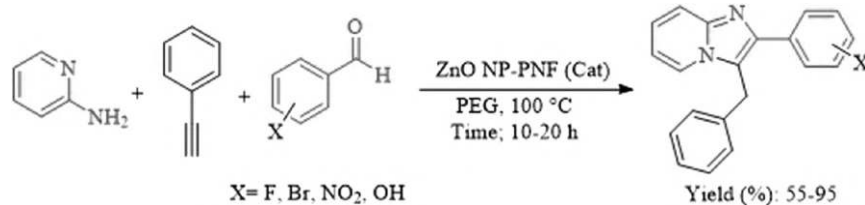
SCHEME 8.4. Application peptide nanofiber decorated with ZnO as a catalyst in the multicomponent reaction.

+ R–NH$_2$ +

R= Ph-, PhCH$_2$-, r-OMePhCH$_2$-, r-EtPh-,
r-(CH$_3$)$_2$CHPh-, C$_4$H$_9$-, Cyclo-C$_3$H$_5$-,
Cyclo-C$_6$H$_{11}$-, Cyclo-C$_8$H$_{15}$-

ZnO NP-PNF (Cat)
PEG, 100 °C
Time: 7-15 h

Yield (%): 55-90
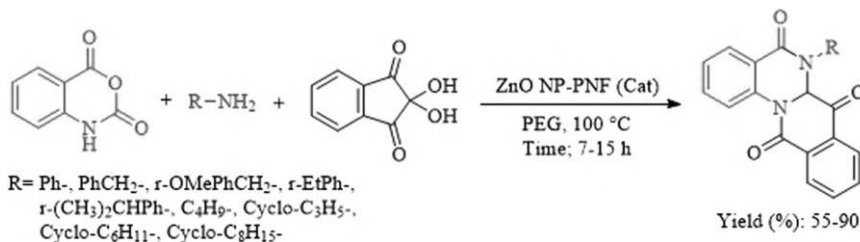
SCHEME 8.5. Application peptide nanofiber decorated with ZnO as a catalyst for the synthesis of tetracyclic quinazolinones.
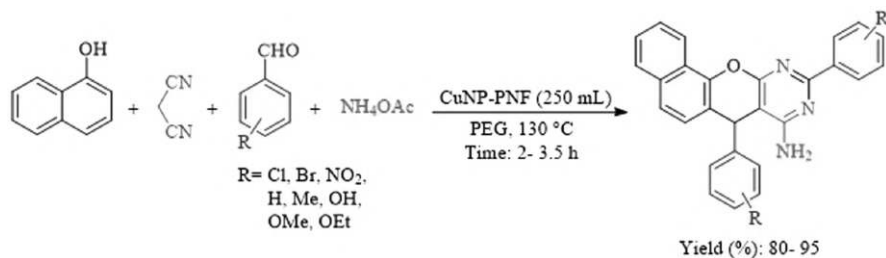
SCHEME 8.6. Application peptide nanofiber decorated with Cu for the synthesis of 7, 10-diaryl-7*H*-benzo[7,8] chromeno[2,3-*d*] pyrimidine-8-amines.
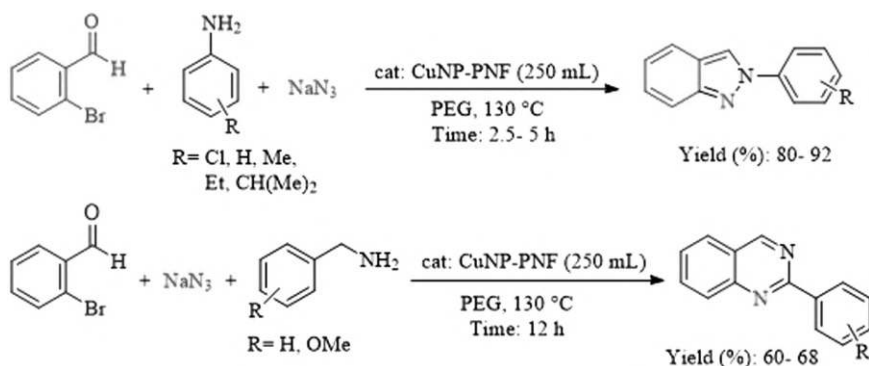
SCHEME 8.7. Application peptide nanofiber decorated with Cu for the synthesis of the preparation of 2*H*-indazoles and quinazolines.

two methods: without the ligand (MCM-41@Cu) and with ligand (MCM-41@histidine@Cu). The activity of the nanocatalysts was explored for the synthesis of 5-substituted 1*H*-tetrazoles derivatives using various aldehydes and sodium azide (Scheme 8.8). The experimental result showed Cu-functionalized MCM-41 sample prepared with the direct co-condensation method (Cu-MCM-41) demonstrated better catalytic activity than Cu-functionalized mesoporous MCM-41 materials prepared with post-synthesis grafting methods (MCM-41-Cu).

An environmental method for the synthesis of tetrazole derivatives using $Fe_3O_4@SiO_2@L-His@Cu$ (II) as catalysts in PEG has been reported [6]. The catalysts were prepared via immobilization histidine and copper on the $Fe_3O_4@SiO_2$. The reasonable conversions in the case of various organic nitriles further demonstrate the versatility of the reaction (Schemes 8.9 and 8.10). The catalyst did not undergo metal leaching and could be easily recovered and reused many times.

The synthesis of Cu(II)/L-His@Fe_3O_4 nanomaterials and their catalytic properties for the synthesis of 2,3-dihydroquinazolin-4(1*H*)-ones, polyhydroquinolines, and 2-amino-6-(arylthio)pyridine-3,5-dicarbonitriles have been reported (Schemes 8.11–8.14) [7]. Good yields were obtained with various aldehydes as shown in the
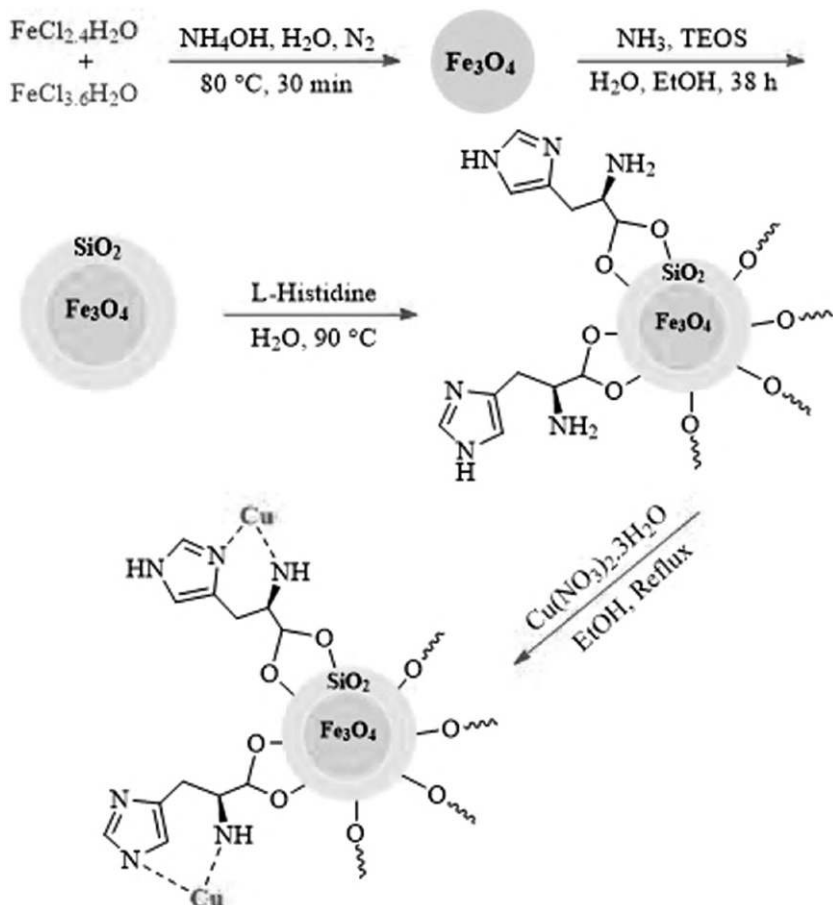
SCHEME 8.8. Application of Cu-MCM-41, mcm-41-Cu, MCM-41@histidine@Cu for the synthesis of 5-substituted 1*H*-tetrazoles derivatives.

Scheme. Moreover, it could be recycled up to six times without any noteworthy loss of conversion or selectivity.

8.5.   APPLICATION OF L-HISTIDINE-BASED IONIC LIQUID IN THE MULTICOMPONENT REACTION

Fe_3O_4@propylsilane@histidine[HSO_4^-] magnetic nanoparticles were synthesized by Mousavifar et al. (Scheme 8.15) [8]. They characterized the structure of this magnetic nanocatalyst with FT-IR, XRD, SEM, and TEM techniques.

To consider the performance of Fe_3O_4@propylsilane@histidine [HSO_4^-], the synthesis of xanthene derivatives was studied in the presence of this catalyst (Scheme 8.16).
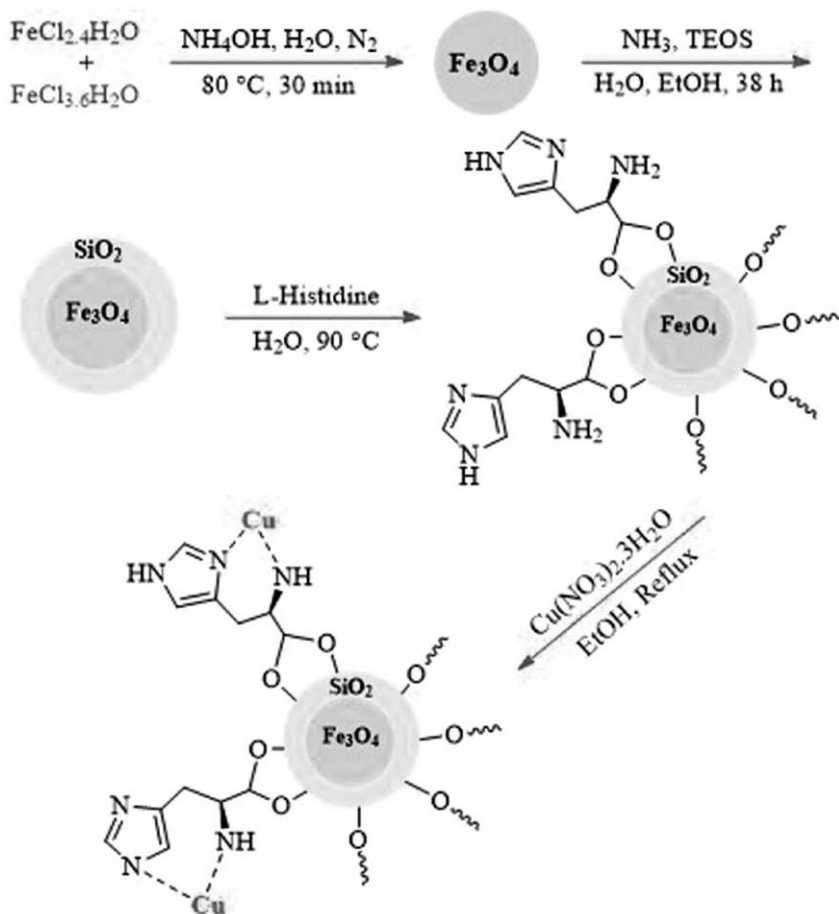
SCHEME 8.9.   Synthesis of Cu(II) immobilized on Fe$_3$O$_4$@SiO$_2$@L-histidine.

R= Cl, Br,OMe, OH, NO$_2$,
CN, Acetyl, Isopropyl

Time (h): 1- 24
Yield (%): 70- 98
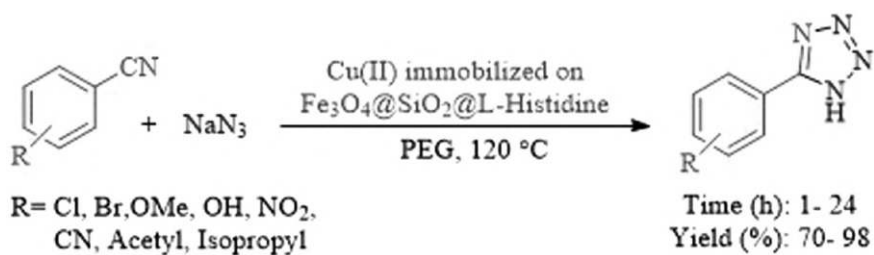
SCHEME 8.10.   Fe$_3$O$_4$@SiO$_2$@L-His@Cu(II) catalyzed the synthesis of 5-substutiuted 1H-tetrazoles.
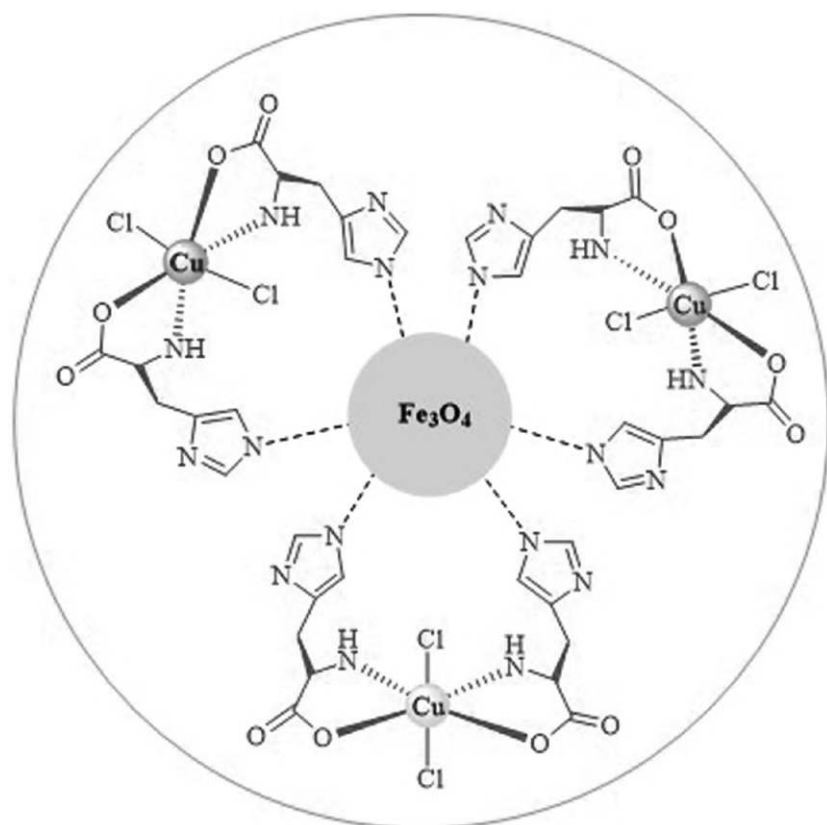
SCHEME 8.11.   Structure of Cu(II)/L-His@Fe$_3$O$_4$.

Aldehyde: 4-chlorobenzaldehyde, 4-methylbenzaldehyde, 4-bromobenzaldehyde, 4-methoxybenzaldehyde, 3,4-dimethoxybenzaldehyde, benzaldehyde, 4-ethoxybenzaldehyde, 4-fluorobenzaldehyde, 3-bromobenzaldehyde, terephthalaldehyde, phthalaldehyde, 4-hydroxybenzaldehyde, 2-hydroxybenzaldehyde, 2-nitrobenzaldehyde, 3-nitrobenzaldehyde, butyraldehyde, isobutyraldehyde

Time (min): 10- 100
Yield (%): 84- 98

SCHEME 8.12.   Cu(II)/L-His@Fe$_3$O$_4$ catalyzed the synthesis of 2,3-dihydroquinazolin-4(1H)-one derivatives.

Aldehyde: 4-chlorobenzaldehyde, 4-methylbenzaldehyde,
4-bromobenzaldehyde, 4-methoxybenzaldehyde,
3,4-dimethoxybenzaldehyde, benzaldehyde,
4-ethoxybenzaldehyde, 4-fluorobenzaldehyde,
3-bromobenzaldehyde, 4-hydroxybenzaldehyde,
3-hydroxybenzaldehyde, isobutyraldehyde,
3-nitrobenzaldehyde, butyraldehyde

Time (min): 90- 150
Yield (%): 90- 98
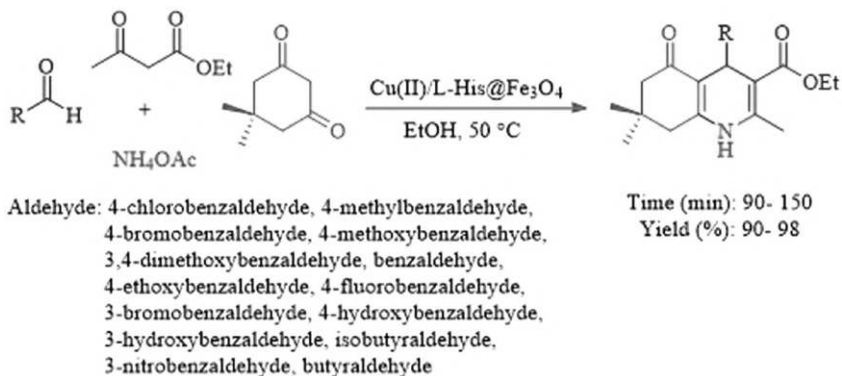
SCHEME 8.13. Cu(II)/L-His@Fe$_3$O catalyzed the synthesis of polyhydroquinoline derivatives.

Yield (%): 86- 94

Aldehyde: 4-chlorobenzaldehyde, 4-methylbenzaldehyde,
4-bromobenzaldehyde, 4-methoxybenzaldehyde,
4-bromobenzaldehyde, benzaldehyde,
4-chlorobenzaldehyde, 4-bromobenzaldehyde,
4-fluorobenzaldehyde, 4-hydroxybenzaldehyde,
4-methylbenzaldehyde, 3,4-dimethoxybenzaldehyde,
4-nitrobenzaldehyde, 4-methoxybenzaldehyde

Thiophenol: 4-methylbenzenethiol, 4-bromobenzenethiol, benzenethiol

SCHEME 8.14. Synthesis of 2-amino-3,5-dicarbonitrile-6-thio-pyridines catalyzed by Cu(II)/L-His@Fe$_3$O$_4$

The authors recycled this catalyst in four consequence runs without any decrease in its efficiency. At the end of the reaction, the catalyst was separated by a magnet, washed with ethanol, and dried at 100°C. Also, this research group studied the catalytic activity of these magnetic nanoparticles in the synthesis of various spiroindolines under ultrasound irradiation conditions. Fe$_3$O$_4$@propylsilane@histidine[HSO$_{4-}$] showed very efficient catalytic activity for the synthesis of these heterocyclic compounds through a combination of acetylenedicarboxylate, istatin derivatives, and 6-amino-1,3-dimethyluracil under ultrasound and reflux conditions (Scheme 8.17) [9].

The proposed catalytic mechanism exhibited by authors suggested that the catalyst activates the carbonyl group of isatin to do Knoevenagel condensation with 6-amino-1,3-dimethyluracil (Scheme 8.18).
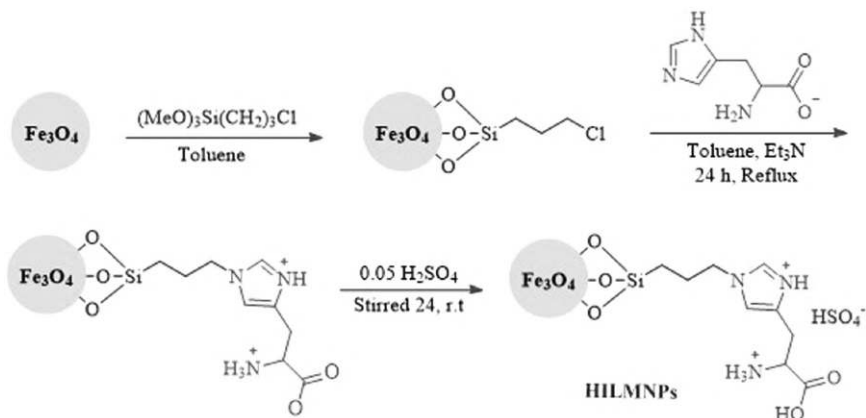
SCHEME 8.15.   Synthesis of Fe_3O_4@propylsilane@histidine [HSO_4^-] magnetic nanocatalysts.

Magnetic ionic liquid NPs have also been used in the synthesis of tetracyclic quinazoline via an A3 coupling multicomponent reaction of isatoic anhydride, amine, and ninhydrin in PEG and the desired products were obtained in good to excellent yields (Scheme 8.19) [10].

The magnetic catalyst was prepared in several steps by sonicating Fe_3O_4 magnetic nanoparticles with (3-chloropropyl)trimethoxysilane (CPTMS) in toluene for 24 h Subsequently, Fe_3O_4/SiO_2-propyl-Cl was added to the solution of Pip-His, followed by mechanical mixing of the solid product with chlorosulfonic acid in dry CH_2Cl_2 at room temperature and then the mixture was filtered and washed with CH_2Cl_2 and dried at room temperature to afford the title compound (Scheme 8.20).

8.6. APPLICATION OF L-HISTIDINE DERIVATIVE AS AN ORGANOCATALYST FOR ASYMMETRIC ALDOL REACTIONS

Small peptides have been used in enantioselective conjugate additions [11], asymmetric acylation [12], enantioselective phosphorylation [13], Strecker synthesis [14], Baylis–Hillman reactions [15], and enantioselective aldol [16]. In 2012, Tsogoeva and Wei used (*S*)-histidine-based dipeptide catalyst to form C—C bonds in direct asymmetric aldol condensation (Scheme 8.21) [17].

8.7. APPLICATION OF L-HISTIDINE-SUPPORTED MATERIAL IN MANICH REACTION

In 2020, Zirak et al. synthesized L-His@Fe_3O_4 MNPs via a one-pot combination of L-histidine, Fe^{3+}, and Fe^{2+} ions in an alkaline solution. Then, they reacted —NH_2 group of supported L-histidine on the magnetic nanoparticles with 2-pyridine
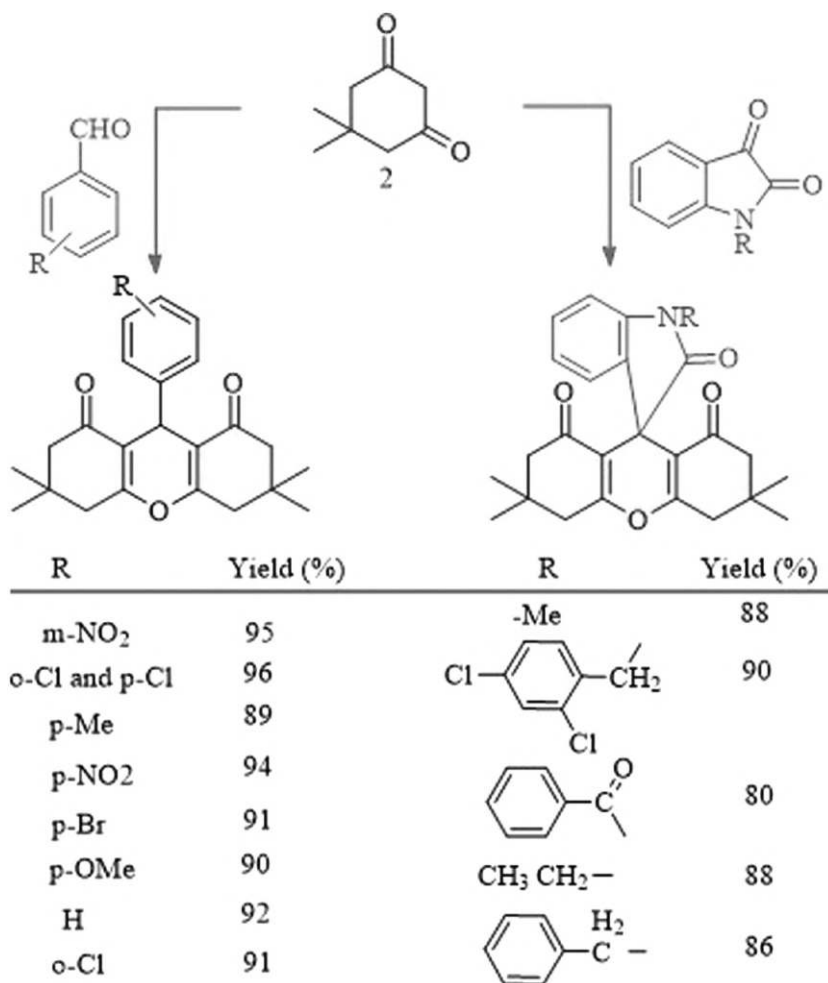
SCHEME 8.16. Synthesis of xanthene derivatives catalyzed by Fe$_3$O$_4$@propylsilane@histidine [HSO$_4^-$]

R	Yield (%)	R	Yield (%)
		-Me	88
m-NO$_2$	95		
o-Cl and p-Cl	96	Cl—⟨⟩—CH$_2$	90
p-Me	89	(Cl)	
p-NO2	94		
		⟨⟩—C⟨	80
p-Br	91		
p-OMe	90	CH$_3$ CH$_2$—	88
H	92		
o-Cl	91	⟨⟩—C⟨H$_2$ —	86

carbaldehyde through a reductive amination process in the presence of NaBH$_4$ to produce PMHis@Fe$_3$O$_4$ (Scheme 8.22) [18].

After the synthesis of PMHis@Fe$_3$O$_4$, the diastereoselectivity effect of the catalyst on the Manich reaction was studied. Manich reaction performed via the combination of cyclohexanone, aniline, and benzaldehyde catalyzed by PMHis@Fe$_3$O$_4$ under solvent-free conditions. When the water was used as a solvent, Manich and Aldol reactions occurred. The yield of the Manich product was 63% in 84/16 *anti/syn* ratio and the aldol reaction was a subside reaction. In ethanol, as a solvent, the product of the aldol reaction was increased (Scheme 8.23).
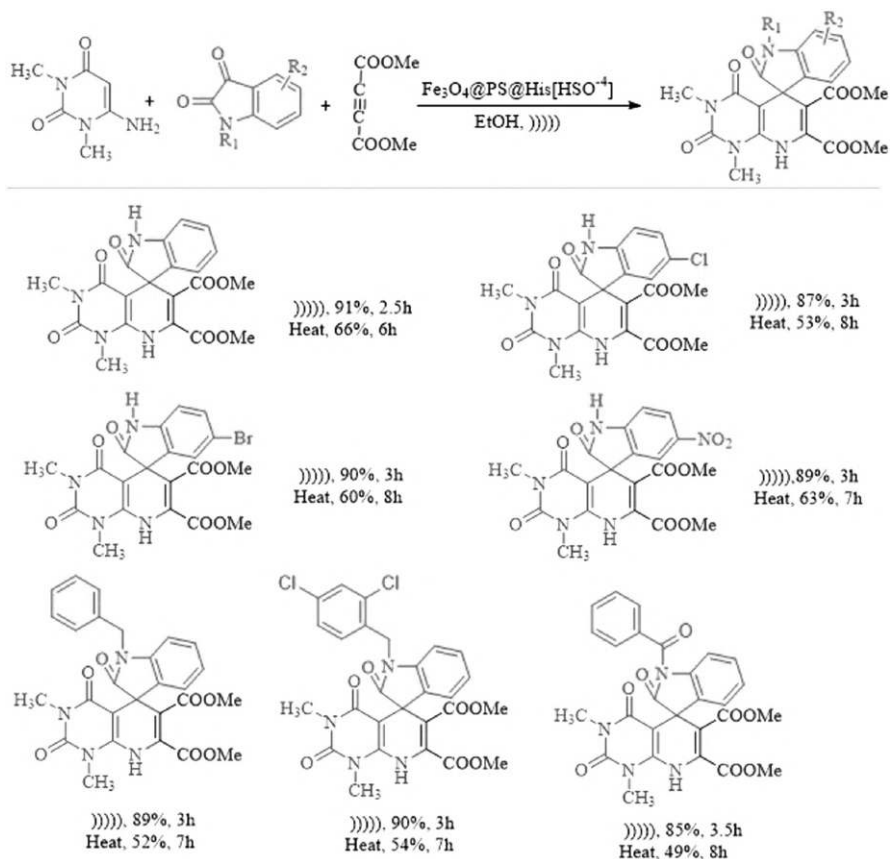
SCHEME 8.17. Synthesis of spiro[indoline-3,5′-pyrido[2,3-*d*]pyrimidine] catalyzed by Fe$_3$O$_4$@propylsilane@histidine[HSO$_4^-$]

8.8.   APPLICATION OF METAL COMPLEX OF L-HISTIDINE DERIVATIVES IN THE COUPLING REACTION

L-histidine-functionalized chitosan-Cu(II) (Cu(II)-His@CS) nanocatalyst has been synthesized by Hajipour et al. in 2017 [19]. The schematic pathway for the preparation of this nanomaterial is shown in Scheme 8.24.

The catalytic properties of this material were examined for the synthesis of diaryl sulfides and aryl benzene thioethers. This reaction was performed in water as solvent and K$_2$CO$_3$ as a base at 100°C. The catalyst can be used six times without significantly decreasing activity (Scheme 8.25) [19].

Our laboratory reported the preparation of Fe$_3$O$_4$@SiO$_2$@His@Ni(II), as illustrated in Scheme 8.26 [20].

The catalytic efficiency of described magnetic nanoparticles was examined in the synthesis of sulfides via the reaction of aryl/alkyl halides with S8 as a sulfur-transfer
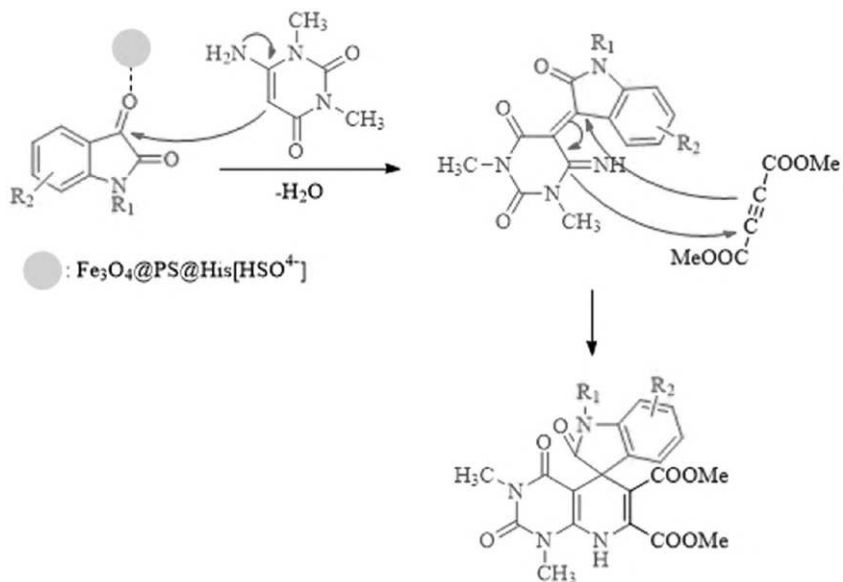
SCHEME 8.18. The proposed catalytic mechanism for the one-pot synthesis of spiro[indoline-3,5′-pyrido[2,3-*d*]pyrimidine].
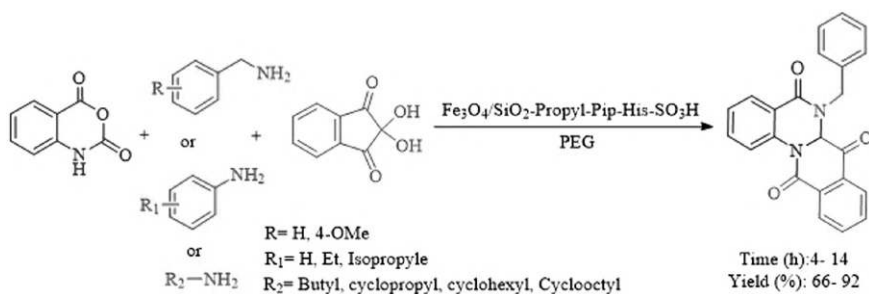
SCHEME 8.19. Magnetic ionic liquid catalyzed one-pot synthesis of tetracyclic quinazoline in PEG at 80°C

reagent (Scheme 8.27). Different bases and solvents were screened, which in KOH and DMSO had the best performance. The favorable temperature for this purpose was 100°C. This catalyst can recycle for five consequence runs without decreases in its efficiency.

In 2016, Farzaneh et al. synthesized an immobilized Schiff-base complex of Cu(I) [21]. In this, a layer of silica was coated on the surface of Fe_3O_4 nanoparticles, and then modified with (3-aminopropyl) triethoxysilane (APTMS); subsequently,
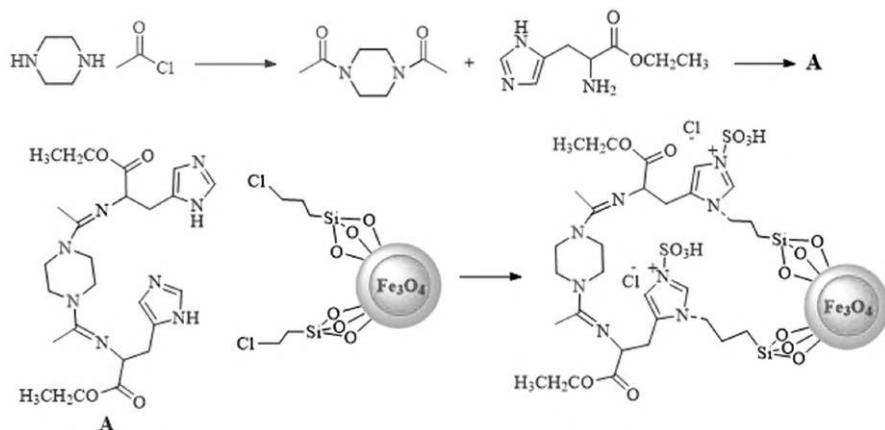
SCHEME 8.20. Schematic synthesis of nano-Fe$_3$O$_4$-supported ionic liquid.

X= NO$_2$, Br, Cl

Yield (%): 57- 96
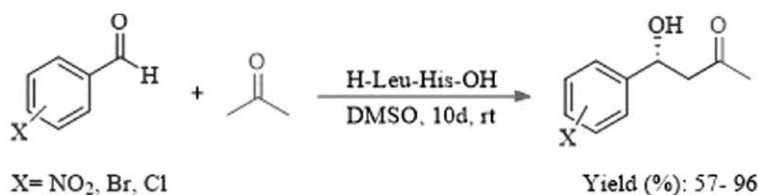
SCHEME 8.21. Direct asymmetric aldol reaction catalyzed by H-Leu-His-OH dipeptide as a catalyst.
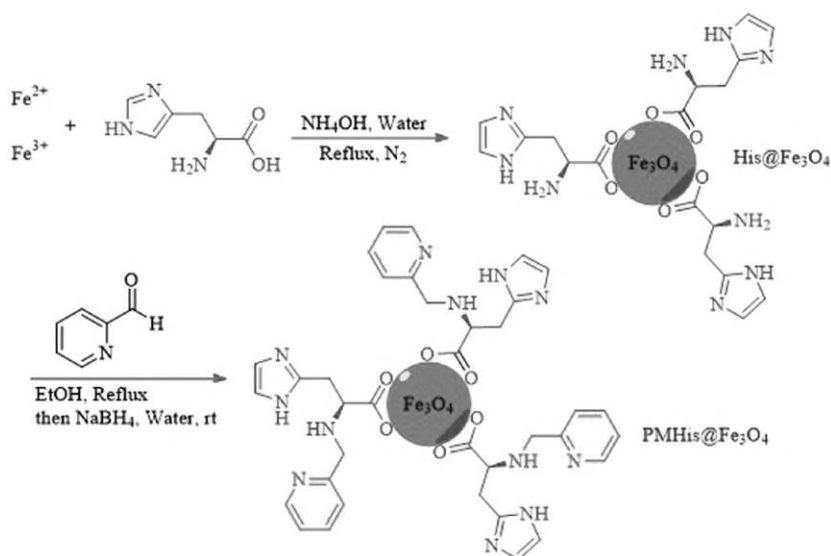
SCHEME 8.22. Preparation steps of PMHis@Fe$_3$O$_4$
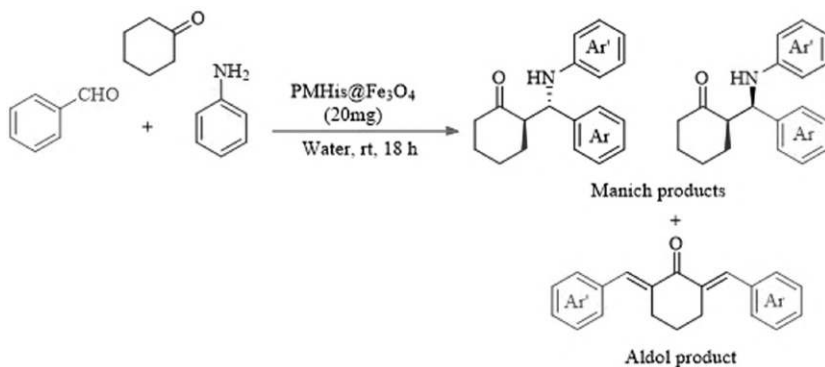
SCHEME 8.23. PMHis@Fe$_3$O$_4$ catalyzed the Manich reaction.
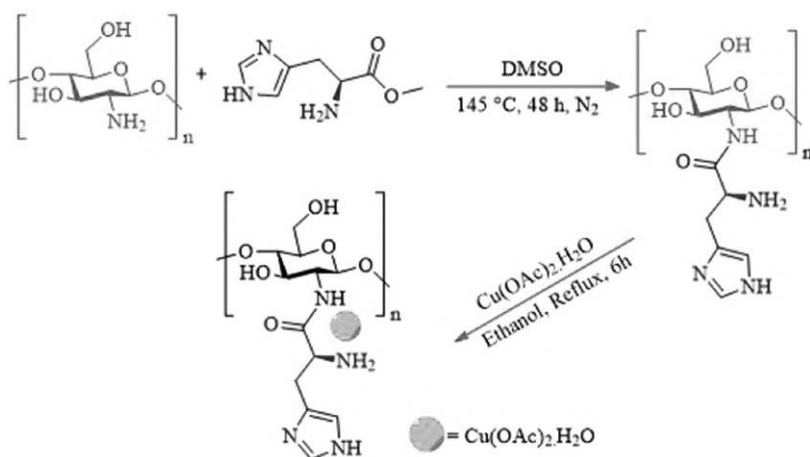
SCHEME 8.24. Synthesis of L-histidine-functionalized chitosan–Cu(II) complex.

Fe$_3$O$_4$@SiO$_2$-nPrNH$_2$ reacted with the corresponding Schiff-base from a combination of L-histidine and glutaraldehyde (Scheme 8.28). The obtained nanoparticles were mixed with CuI to synthesis a fine al catalyst (Fe$_3$O$_4$@SiO$_2$-NH$_2$-Glu-His-Cu).

The catalytic properties of Fe$_3$O$_4$@SiO$_2$-NH$_2$-Glu-His-Cu were studied for the oxidative homocoupling of terminal alkynes (Scheme 8.29), based on reusability studies; the catalyst was recyclable up to the 5 consequence cycles.

8.9. APPLICATION OF METAL COMPLEX OF L-HISTIDINE DERIVATIVES IN THE OXIDATION REACTION

Nikkhoo et al. synthesize oxide–peroxide W(VI)-histidine-MgAl-layered double hydroxide composite (Scheme 8.30) [22]. For the characterization of the catalyst,

X= Br, Cl
R= H, 3-CH₃, 4-OMe, 4-NO₂,
    4-MeCO, 2-CHO, 2-NO₂, 4-NO₂

Time (h): 10- 12
Yield (%): 62- 86

X= I, Br, Cl
R= H, 4-Me, 4-OMe, 4-NO₂,
    4-MeCO, 2-CHO, 2-NO₂, 4-NO₂

Time (h): 24- 26
Yield (%): 61- 96
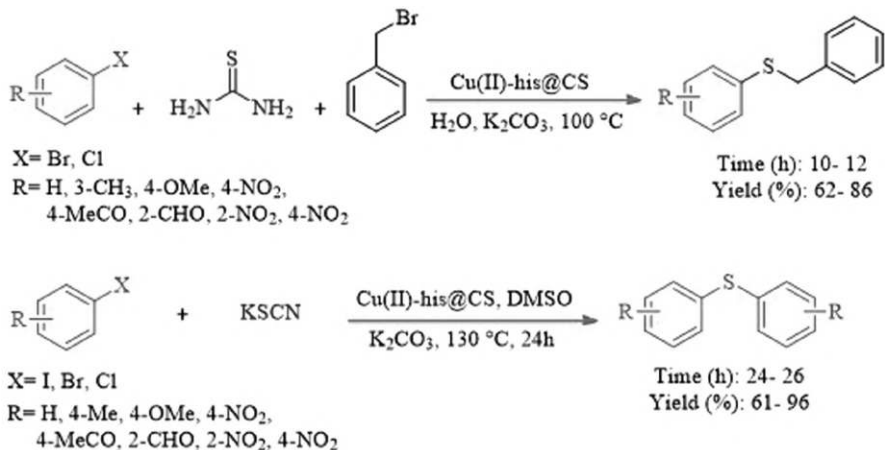
SCHEME 8.25. Histidine-functionalized chitosan–Cu(II) catalyzed C—S coupling reactions.
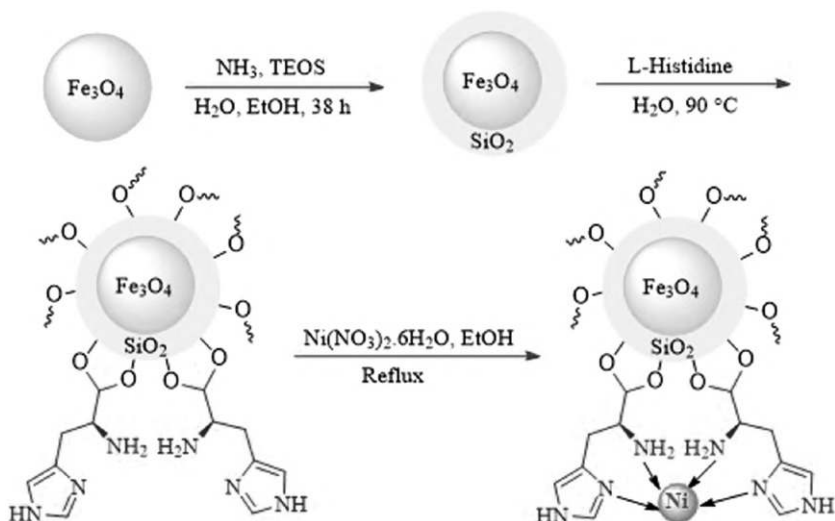
SCHEME 8.26. Synthetic route for the preparation of Fe₃O₄-magnetic-nanoparticles-supported L-histidine-Ni(II) [Fe₃O₄@SiO₂@His@Ni(II)]

they used XRD, IR, EDX, SEM, and TEM techniques. The efficiency of this catalyst was studied by selective oxidation of sulfides. In this catalyst, MgAl-layered double hydroxide is a host, and oxide W(VI)-histidine complex is a guest. Oxidation of sulfide to sulfoxide with H_2O_2 in the presence of a catalyst has been shown in Scheme 8.30. To study reusability, authors separated the catalyst from reaction media by
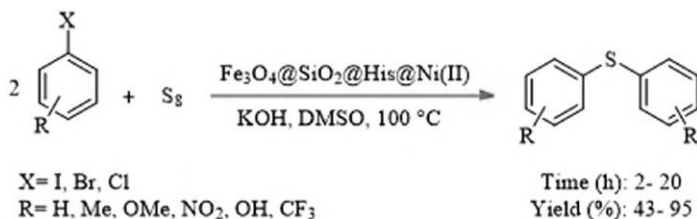
SCHEME 8.27. Synthesis of sulfides via reaction of aryl or alkyl halides with S_8 catalyzed by Fe_3O_4@SiO_2@His@Ni(II).
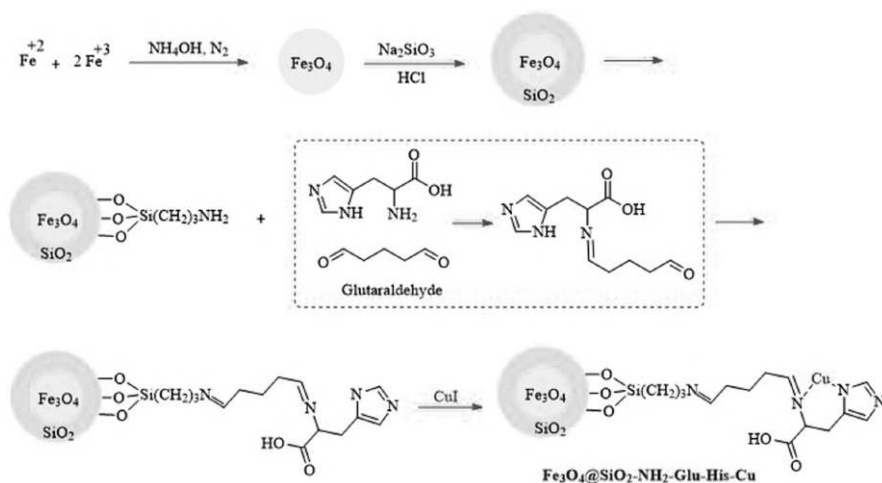
SCHEME 8.28. Preparation steps of Fe_3O_4@SiO_2@APTMS@Glu-His@Cu complex magnetic nanoparticles

filtration and washed it with ethanol and acetone and then dried and used in the next run. This operation could occur five times without decreases in catalyst selectivity.

8.10. APPLICATION OF L-HISTIDINE AS AN ORGANOCATALYST FOR THE SYNTHESIS OF CYCLIC CARBONATES

Qi et al. studied a catalyst system from epoxides and CO_2 under metal-free and halide-free conditions. In their study, the effect of the base was examined and the experimental result showed that 1,8-diazabicyclo[5.4.0]-undec-7-ene (DBU) is the most effective [23]. The best amino acid for this system was found to be L-histidine. Under these conditions, different epoxides were examined. The results are summarized in (Scheme 8.31). A possible mechanism for the cycloaddition of CO_2 and epoxide by the L-histidine/DBU system is introduced in Scheme 8.32.
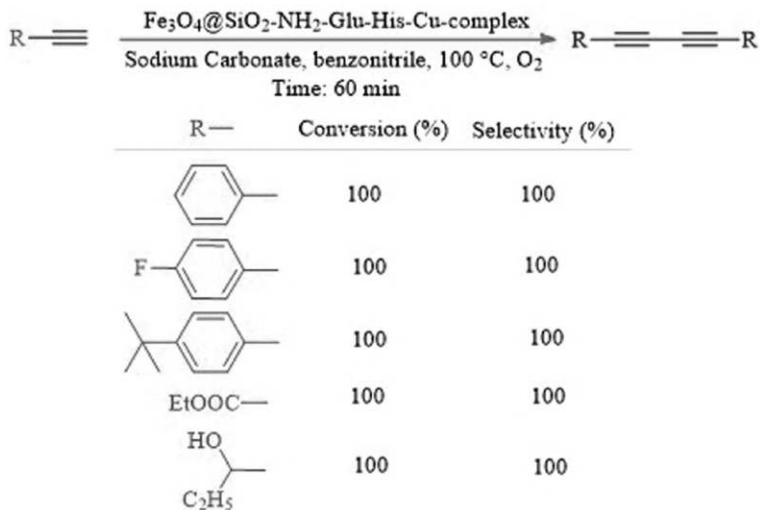
SCHEME 8.29. Synthesis of dialkynes catalyzed by Fe_3O_4@SiO_2-NH_2-Glu-His-Cu.
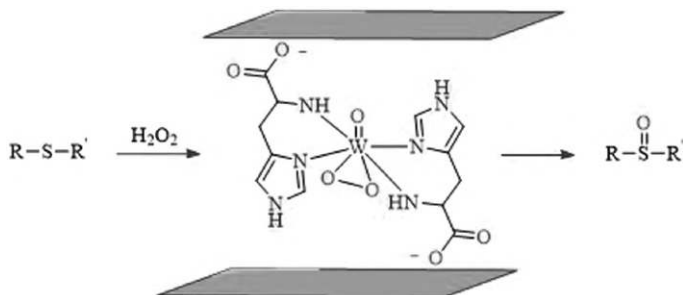
SCHEME 8.30. Synthetic route for oxido-peroxide W(VI)-histidine–MgAl-layered double hydroxide composite

8.11.   APPLICATION OF METAL COMPLEXES OF L-HISTIDINE-SUPPORTED MATERIAL FOR EPOXIDATION CATALYST OF ALLYL ALCOHOLS

In 2021, Geravand et al. introduced an immobilization of [VO(His)$_2$]complex on UiO-66-NH$_2$ for epoxidation of some allyl alcohols with 94% conversion, 100% selectivity, and TOF of 1,093 h^{-1}. [VO(His)$_2$] complex was synthesized via decoration of histidine (His) with VOSO$_4$ (Scheme 8.33) [24]. The prepared [VO(His)$_2$] complex@UiO-66-NH$_2$ was characterized using FTIR, XRD, NMR, MS, EDX, TGA, BET, and XPS techniques.

Pd-His/SiO$_2$ was synthesized by incipient wetness impregnation (the metal precursor is dissolved in an organic solution to immobilization catalyst support), and their catalytic applications were explored for selective hydrogenation of acetylene.
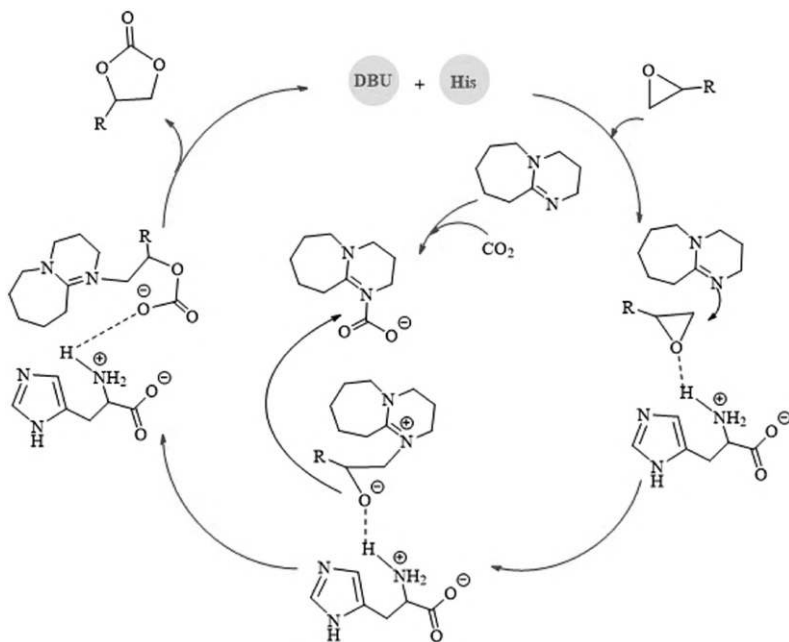
SCHEME 8.31. L-histidine/DBU catalyzed cycloaddition of CO_2 and epoxide
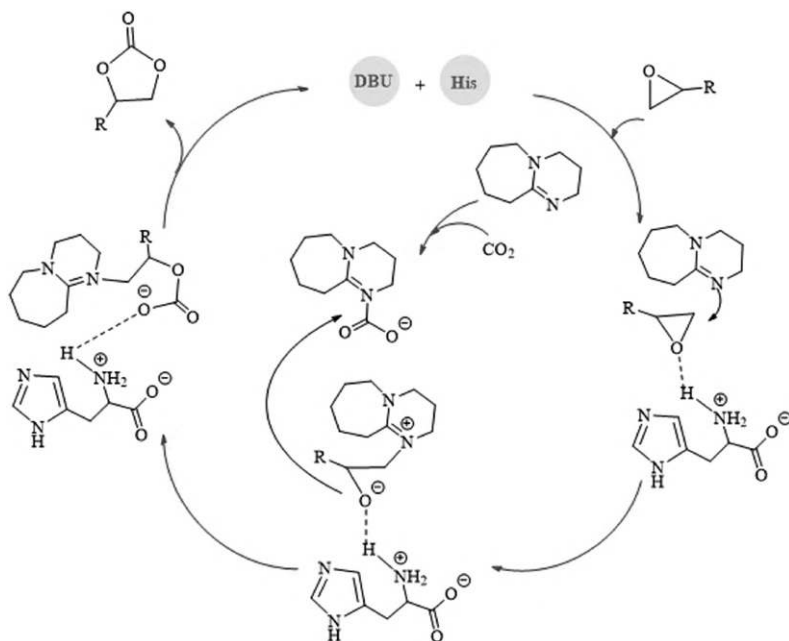
SCHEME 8.32. The proposed mechanism for the L-histidine/DBU-catalyzed reaction.
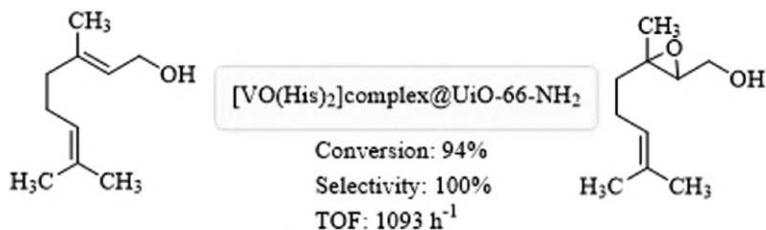
SCHEME 8.33.   [VO(His)$_2$]complex@UiO-66-NH$_2$ epoxidation catalyst of allyl alcohols

Catalyst	Conversion(%)	Epoxide(%)	Alcohol(%)	Ketone(%)	Diol(%)
-	21	64	4	2	30
SG-His-OMe-Cu(II)	12	84	3	2	11
SG-His-OMe-Cu(II)-H-His-OMe	20	91	1	5	3
SG-(Cys-OMe)$_2$-Cu(II)	26	91	2	3	4
SG-(Cys-OMe)$_2$-Cu(II)-H-(Cys-OMe)$_2$	33	88	4	1	7
SG-His-OMe-Cu(II)-(H-Cys-OMe)$_2$	8	88	2	4	6
SG-(Cys-OMe)$_2$-Cu(II)-H-His-OMe	33	86	3	2	9
SG-His-OMe;(Cys-OMe)$_2$-Cu(II)	20	87	4	4	5
SG-His-OMe;(Cys-OMe)$_2$-Cu(II)-H-His-OMe;(H-Cys-OMe)$_2$	21	86	3	2	9

SCHEME 8.34.   The conversion and selectivity results of the oxidation of cyclohexene after 3 h.

Experimental results showed hydrogenation of acetylene in the presence of Pd-His/SiO$_2$ carry out with high yields (100%) while the ethylene selectivity reaches 81.5%. A 50-h test at 160°C confirms the good stability of Pd-His/SiO$_2$ [25].

Varga et al. described the immobilization of C-protected Cu(II)-amino acid (methyl esters of L-histidine and L-cystine) uniform and mixed ligand complexes with two different amino acid esters on the chloropropylated silica gel as the support [26]. The experimental result of the immobilized catalysts in the oxidation of cyclohexene with peracetic acid in acetone is shown in Scheme 8.34.

8.12.   APPLICATION OF L-THREONINE DERIVATIVES AS ORGANOCATALYSTS IN THE ALDOL REACTION

L-threonine is an important amino acid that can be added to food, medicine, or feed, it is also employed as a homogeneous and heterogeneous catalyst in organic reactions.

In 2012, Wu et al. described the application of O-benzoyl-L-threonine as an organocatalyst in the aldol condensation of different ketones with a variety of aldehydes (Scheme 8.35) [27]. These reactions were performed in aqueous solvent at room temperature and the products yielded high enantiopurity.

R = p-NO₂-C₆H₄, o-NO₂-C₆H₄,
m-NO₂-C₆H₄, C₆H₄, p-CF₃-C₆H₄,
p-CN-C₆H₄, p-F-C₆H₄, p-Cl-C₆H₄,
o-Cl-C₆H₄, m-Cl-C₆H₄, 2,6-Cl-C₆H₄,
p-Br-C₆H₄, o-Br-C₆H₄, m-Br-C₆H₄,
p-MeO-C₆H₄, m-MeO-C₆H₄, 2-furaldehyde
p-Me-C₆H₄, 1-naphthyl, 2-naphthyl, pyridinthyl, 2-thiophenaldehyde

Yield (%): 60- 98
dr (anti/syn): 99:1
ee (anti/syn): 98/70

R = p-NO₂-C₆H₄, o-NO₂-C₆H₄,
m-NO₂-C₆H₄, C₆H₄, p-CF₃-C₆H₄,
p-Cl-C₆H₄, o-Cl-C₆H₄, p-Br-C₆H₄,
m-MeO-C₆H₄, p-Me-C₆H₄, 1-naphthyl,

Yield (%): 65- 98
dr (anti/syn): 85:15
ee (anti/syn): 99/96

R = p-NO₂-C₆H₄, o-NO₂-C₆H₄,
m-NO₂-C₆H₄, C₆H₄, p-CF₃-C₆H₄,
p-CN-C₆H₄, p-F-C₆H₄, p-Cl-C₆H₄

Yield (%): 54-92
dr (anti/syn): 97:3
ee (anti/syn): 98/99

SCHEME 8.35. Aldol reaction of ketones with different aldehydes catalyzed by O-benzoyl-L-threonine.

8.13. APPLICATION OF L-THREONINE DERIVATIVE-SUPPORTED MATERIAL AS A CATALYST IN THE ALDOL REACTION

In 2014, Pericàs and coworkers introduced multiple types of organocatalysts containing connected threonine structures to polystyrene (Schemes 8.36 and 8.37) [28]. Among the catalysts introduced, catalyst 6a is efficient and was effective for the aldol reaction that produces high-efficiency of products (Scheme 8.3).

8.14. APPLICATION OF L-THREONINE-BASED IONIC LIQUID AS AN ORGANOCATALYST IN THE ALDOL REACTION

Zlotin and coworkers used L-threonine to create an efficient and recyclable ionic liquid as an organocatalyst (Scheme 8.38). This ionic liquid is employed for the aldol reaction of aromatic aldehydes and a wide variety of ketones, which produce products in high yield in short reaction times (Scheme 8.39) [29].
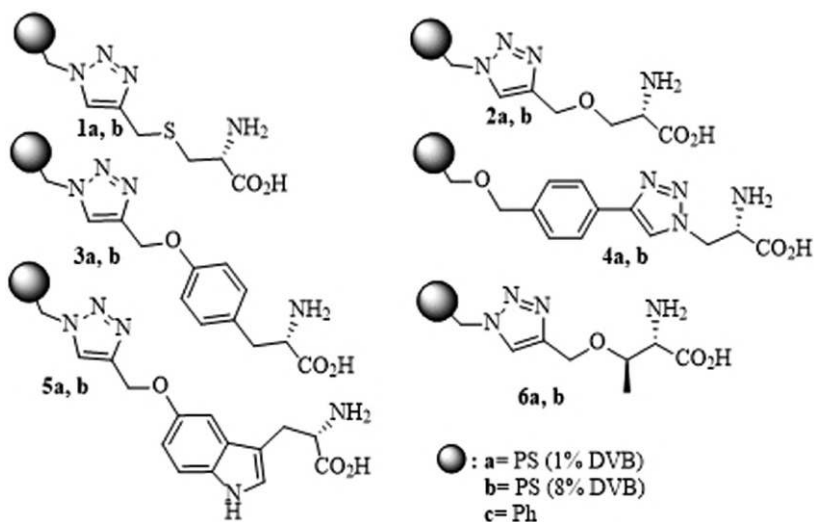
SCHEME 8.36.　Threonine amino acid–derived catalysts
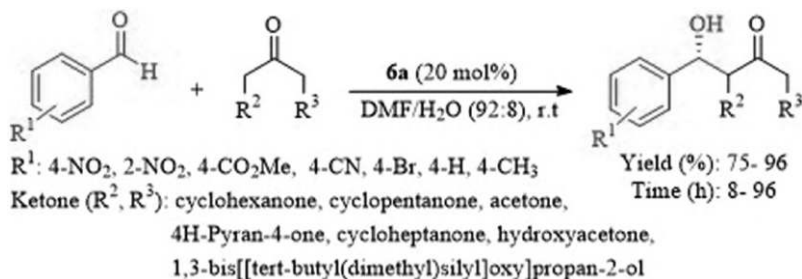
SCHEME 8.37.　Asymmetric aldol reaction by catalyst **6a**
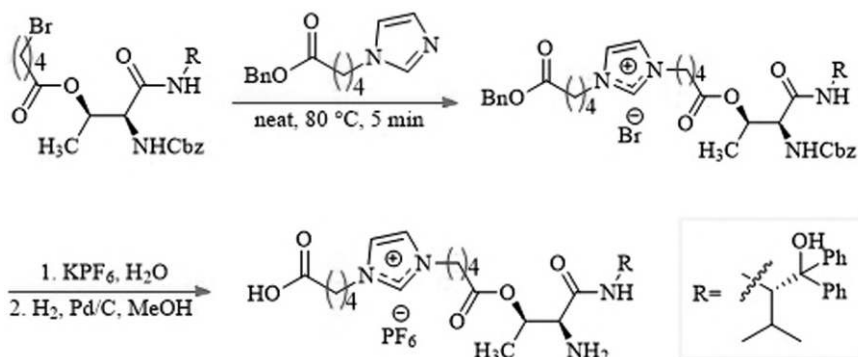
SCHEME 8.38.   Preparation of catalyst L-threonine-based ionic liquid
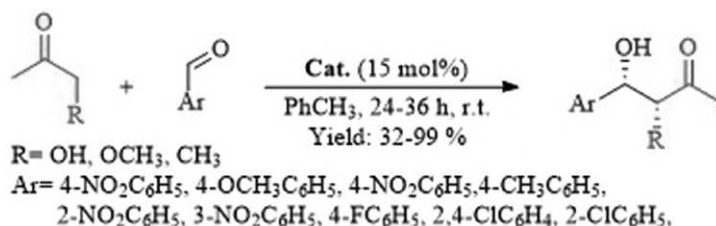
SCHEME 8.39.   Aldol reaction catalyzed by L-threonine-based ionic liquid.

It has recently been found that some organocatalysts are made from amino acids with hydroxyl groups; these organocatalysts have been considered in asymmetric aldol condensation to form syn corresponding products. With this aim, Zlotin and coworkers developed an organocatalyst containing an alcohol group that readily catalyzed the aldol condensation reaction to synthesize syn products (Scheme 8.40) [30].

8.15.   APPLICATION OF L-THREONINE DERIVATIVES AS A CATALYST FOR THE SYNTHESIS OF A-TERTIARY NH₂-AMINES

Primary amines are among the most valuable constituents for the preparation of pharmaceutical amines and natural compounds. In 2020, Hoveyda and coworkers reported a convenient pathway for the synthesis of homoallilic NH$_2$-amines via the reaction between silyl ketamine and allyl-B(pin) by a threonine-based and boron-containing catalyst, which synthesized the desired products at low temperatures in short time (Scheme 8.41) [31].

R¹: H, OH

R²: OH, OMe, Me

Ar: 4-NO₂C₆H₄, 2-NO₂C₆H₄, 2-ClC₆H₄,
4-FC₆H₄, 4-MeO₂CC₆H₄, 4-OHCC₆H₄,
4-MeOC₆H₄, 3-PhOC₆H₄, 2-Naphthyl, 2-Thienyl

Syn-9a-o (3R, 4S)   *anti*-9a-o (3S, 4S)

Yield (%): 40- 99
dr (syn/anti): 97/3
ee (syn) %: 87- 99
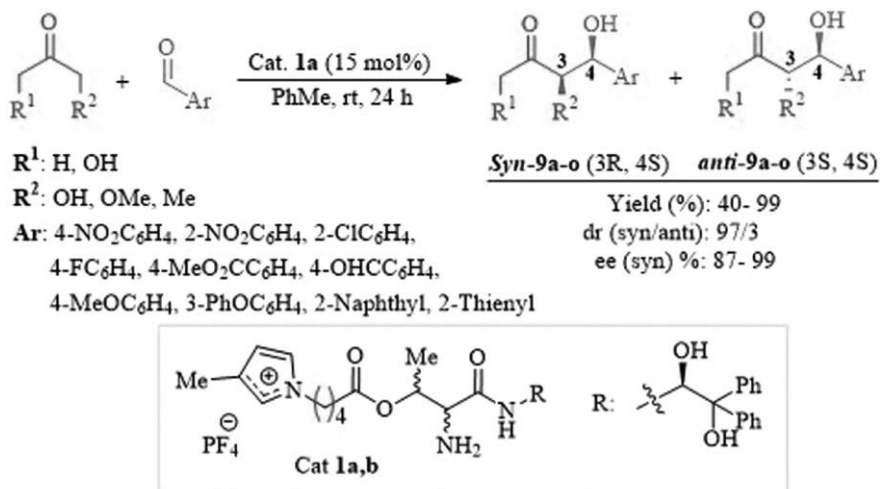
SCHEME 8.40.   Aldol reaction to synthesize syn products

Ar: *o*FC₆H₄, *o*ClC₆H₄, *o*MeOC₆H₄, *o*MeC₆H₄,
*m*ClC₆H₄, *m*F₃CC₆H₄, *p*FC₆H₄, *p*ClC₆H₄,
*p*BrC₆H₄, *p*F₃CC₆H₄, *p*MeOC₆H₄, *p*Me₂NC₆H₄

Conv. [%]: >98
α:γ : 74:26- >98:2
Yield (pureα)[%]: 50- 90
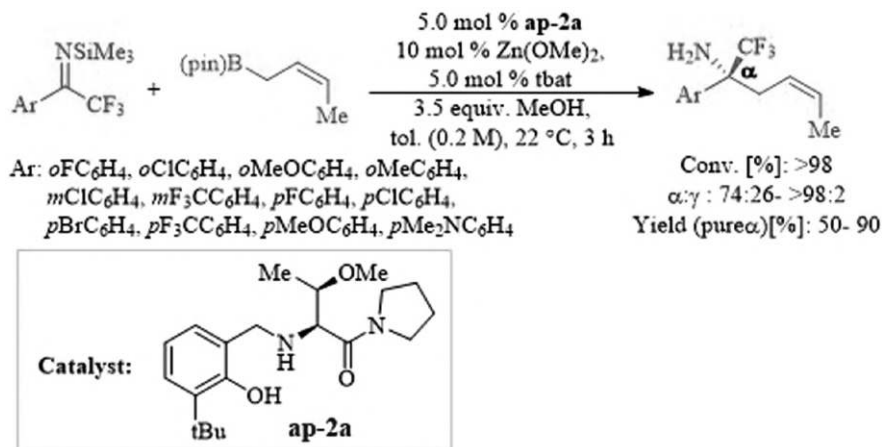
SCHEME 8.41.   Synthesis of α-tertiary NH₂-amines by treatment of threonine-based catalyst

8.16.   CATALYTIC APPLICATION OF SUPPORTED L-THREONINE IN COUPLING REACTION

Mesostructured cellular foam (MCF) silica is a very interesting new mesoporous *silica* material, which has attracted great interest because of its unique porous structures such as large pore size in the range of 150–500 Å [32], which is larger than that of common mesoporous materials like SBA and MCM, continuous three-dimensional (3D) pore system, and allow favorable conditions for incorporating active sites

to produce modified MCF silica as catalysts [33]. In this sense, our group designed the decoration of palladium nanocatalyst on magnetic mesocellular silica foams functionalized with L-threonine (MMCF@Thr-Pd)(Scheme 8.42) [34].

The structure of this mesoporous material was characterized by FT-IR, XRD, BET, SEM, EDS, VSM, TGA, and ICP-OES [34]. The catalyst activity was examined for Stille, Suzuki, and Heck coupling reactions. The experimental result showed the reaction proceed in reasonable yields, using a variety of aryl halides (Scheme 8.43).

Fe_3O_4@SiO_2@threonine-Pd^0 are effective for Heck cross-coupling reaction. The nanoscale catalyst was prepared by modification of L-threonine to the surface of Fe_3O_4@silica, followed by the addition of $PdCl_2$ and its reduction into Pd NPs with $NaBH_4$ (Scheme 8.44) [35]. In the presence of a catalyst, the coupling reaction with a variety of aryl halides proceeded in water as the solvent at 80°C with good to excellent conversions (Scheme 8.45) (85–96).

8.17. CONCLUSION

Amino acids play vital roles in health, either in their native form or chemically modified. The recovery of a catalyst is important from both the economic and the environmental points of view. Due to the vast importance of amino acids, there is an escalating need for the immobilization of amino acids due to their being used in a wide variety of applications. This chapter highlighted the potential utility of L-histidine and L-threonine as organocatalysts and catalysts in organic reactions. Also, this chapter provides guidance and procedures used for the immobilization of L-histidine and L-threonine on various inorganic materials to achieve advantages like more economy, higher stability, and several recycling in different reactions to make greener the industrial processes.
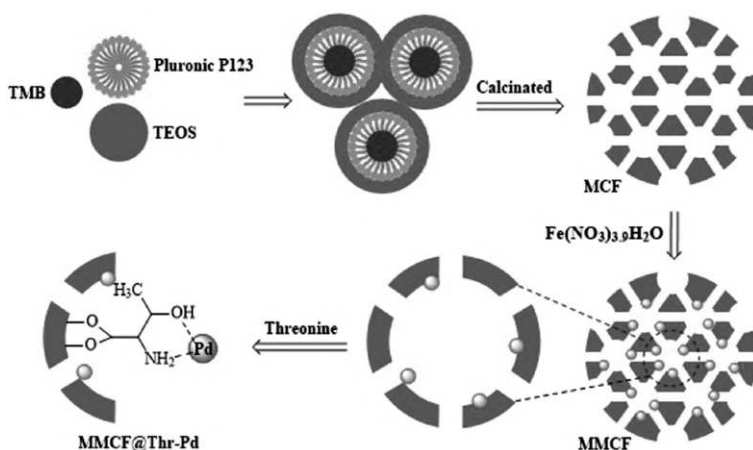
SCHEME 8.42. The synthesis of MMCF@Thr-Pd
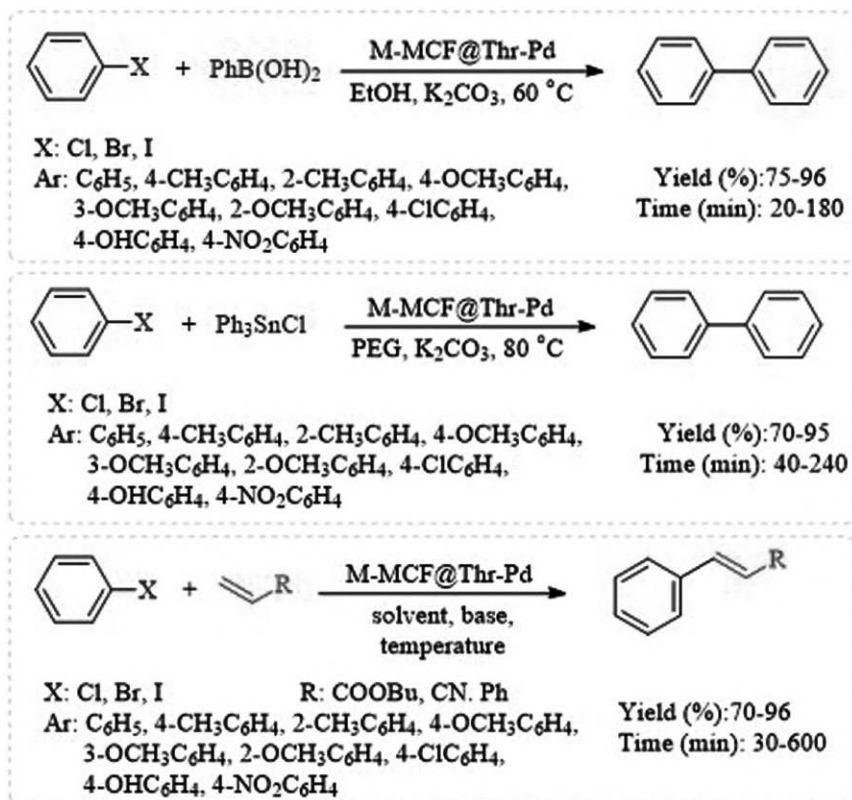
SCHEME 8.43. MMCF@Thr-Pd catalyzed Suzuki, Style, and Heck reactions.
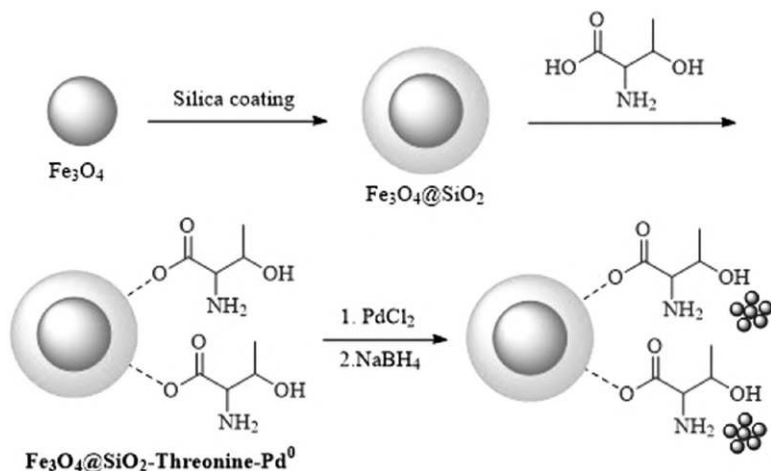
SCHEME 8.44. Schematic synthesis of FST-Pd0 MNPs

X= I, Br
Y= H, Me, Et, MeO, Formyl
R= Me, Et, Butyl

Yield (%): 40- 96
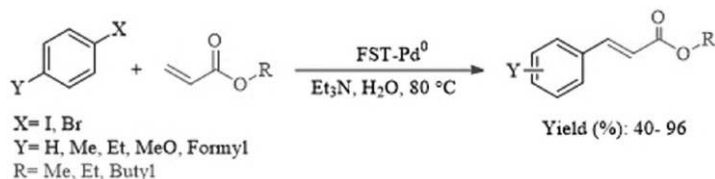
SCHEME 8.45. Fe_3O_4@SiO_2@threonine-Pd^0 catalyzed Heck cross-coupling reaction

Acronym	Abbreviation
AAS	Atomic absorption spectroscopy
AAs	Amino acids
AcCl	Acetyl chloride
ACD	Aspartic-β-cyclodexterine
Ac_2O	Acetic anhydride
AcOH	Acetic acid
AFO	Aspartate-functionalized γ-octamoolybdate
AGHD	Alanine glycine histidine aspartic acid
AIBN	Azobisisobutyronitrile
AILs	Amide ionic liquids
Ala	Alanine
Al-MCM-41	Aluminum-Mobil Composition of Matter No. 41
AMP	Adenosine monophosphate
AmpSCMNPs	Aminopropyltrimethoxysilane-coated magnetite nanoparticles
AMSO	N-acetyl-(S)-methionine (R,S)-sulfoxide
a.t.	Ambient temperature
BET	Brunauer–Emmett–Teller
β-CD	β-Cyclodextrin
BH_3.THF	Borane tetrahydrofuran
BINAP	2,2′-Bis(diphenylphosphino)-1,1′-binaphthyl
Bmim	Butyl methyl imidazolium
[bmim] [BF_4]	1-Butyl-3-methylimidazolium tetrafluoroborate
(bmim) PF_6	1-Butyl-3-methylimidazolium hexafluorophosphate
Bmpy	Butyl methyl pyrolidinium
Bn	Benzyl
BOC	*tert*-Butoxy carbonyl
Boc_2O	Di-*tert*-butyl dicarbonate
BPA	Bisphenol A
CbzCl	Benzyl chloroformate
CH_2Cl_2	dichloromethane
$CHCl_3$	Chloroform
Chiral IL	Chiral ionic liquid
$Cl(CH_2)_2Cl$	1,2-Dichloroethane

Acronym	Abbreviation
$C_{14}mim$	1-Tetradecyl-3-methylimidazolium
$Co(NO_3)_2.6H_2O$	Cobalt (II) nitrate hexahydrate
Conv.	Conversion
CP Mas solid state NMR	Cross-polarization/magic angle spinning nuclear magnetic resonance
CPTMS	3-Chloropropyltrimetoxysilane
CS	Chitosan supported
Cs_2CO_3	Cesium carbonate
Cu	Copper
$Cu(OTf)_2$	Copper (II) trifluoromethanesulfonate
Cys	L-cysteine
DAA	Diacetone alcohol
DABCO	1,4-Diazabicyclo[2.2.2]octane
DBU	1,8-Diazabicyclo(5.4.0)undec-7-ene
DCC	*N,N'*-Dicyclohexylcarbodiimide
DCM	Dichloromethane
DEA	Diethylamine
DEOA	Diethanolamine
DFT	Density functional theory
DIPEA	*N,N*-diisopropylethylamine
DMAP	4-Dimethylaminopyridine
Dmba	Dimethyl benzene amine
DME	Dimethyl ether
DMF	Dimethylformamide
DMP	Dimethyl phosphate
DMSO	Dimethyl sulfoxide
DVB	Divinylbenzene
EDS	Energy dispersive spectroscopy
Ee	Enantiomeric excess
[emim][BF$_4$]	1-Ethyl-3-methylimidazolium tetrafluoroborate
[EMIm] [CF$_3$COO]	1-Ethyl-3-methylimidazolium trifluoroacetate
Emim	Ethyl methyl imidazolium
Equiv.	Equivalent
Et_3N	Triethylamine
Et_2O	Diethyl ether
EtOH	Ethanol
Et_2Zn	Diethylzinc
Fmoc	Fluorenylmethyloxycarbonyl chloride
FTIR	Fourier transform infrared spectroscopy
Glu	Glutamate
GO	Graphene oxide
HAAD	Histidine alanine
HAFD	Histidine alanine phenylalanine aspartic acid

(*Continued*)

Acronym	Abbreviation
HATU	Hexafluorophosphate azabenzotriazole tetramethyl uronium
HAuCl$_4$	Hydrogen tetrachloroaurate (III) hydrate
HAVD	Histidine alanine valine aspartic acid
H-bond	Hydrogen bond
HBTU	Hexafluorophosphate benzotriazole tetramethyl uronium
HCl	Hydrogen chloride
HCOOH	Formic acid
HHBS	Hank's buffer with Hepes
His	Histidine
HILMNPs	Histidine ionic liquid/magnetite nanoparticles
HiQuin	*N*-hexylisoquinilium
Hmim	1-Hexyl-3-methyl-imidazolium
HNO$_3$	Nitric acid
HOAc	Acetic acid
HOBt	1-Hydroxybenzotriazole
HSiCl$_3$	Trichlorosilane
H$_2$SO$_4$	Sulfuric acid
IP	Isophorone
i-Pr	Isopropyl
i-PrOH	Isopropyl alcohol
K10	Montmorillanite
K$_2$CO$_3$	Potassium carbonate
KMnO$_4$	Potassium permanganate
KOH	Potassium hydroxide
KPF$_6$	Potassium hexafluorophosphate
LCMNP	l-Cysteine-functionalized magnetic nanoparticles
LDH	Layered double hydroxide
LiNTf$_2$	Lithium bis(trifluoromethanesulfonyl)imide
LPMNP	L-proline-modified magnetic nanoparticles
L-Pro-L-Phe	L-proline-L-phenylanaline
MBH	Morita–Baylis–Hillman
MBHA	*p*-Methylbenzhydrylamine
MBH Reaction	Morita–Baylis–Hillman reaction
MC	Methylcellulose
m-CPBA	*meta*-Chloroperoxybenzoic acid
MeCN	Acetonitrile
MEOA	Monoethanolamine
MeOH	Methanol
4-MeOx	4-Methyl-2-oxazolidinone
MimBr	3-Allyl-1-vinyl-1*H*-imidazol-3-ium bromide
m-Nitro	*meta*-Nitro
MNPs	Magnetic nanoparticles

(*Continued*)

Acronym	Abbreviation
MO	Methyl orange
MO	Mesityl oxide
[MOEMIM]Oms	1-Methoxyethyl-3-methylimidazolium methanesulfonate
MOF	Metal–organic framework
MOP	Hydrochloric acid
Mor$_{1,8}$	N-octyl-N-methylmorpholinium
MPAA	Mono-N-protected amino acids
MTBD	7-Methyl-1,5,7-triazabicyclo(4.4.0)dec-5-ene
MW	Microwave
MWCNTs	Multiwalled carbon nanotubes
NaBF$_4$	Sodium tetrafluoroborate
NaBH$_4$	Sodium borohydride
Na$_2$CO$_3$	Sodium carbonate
NaH	Sodium hydride
NaHCO$_3$	Sodium bicarbonate
NaN$_3$	Sodium azide
NaOH	Sodium hydroxide
NaOMe	Sodium methoxide
nbd	Nitrobenzoxadiazole
N-Boc	Nitrogen-*tert*-butyloxycarbonyl
NBS	N-Bromosuccinimide
NEt$_3$	Triethylamine
NH$_4$HCO$_3$	Ammonium bicarbonate
NH$_4$OAc	Ammonium acetate
NH$_4$OH	Ammonium hydroxide
NH$_4$PF$_6$	Ammonium hexafluorophosphate
NH$_2$SCN	Thiocyanate
Ni	Nickel
NIPAM	N-isopropyl acrylamide
NMM	4-Methylmorpholine
NP	Nanoparticle
N-PMP	Nitrogen-p-methoxyphenyl
N-PSP	N-(phenylseleno)-phthalimide
OAPAI	Optically active poly(amide imide)
OAPIL	Optically active poly ionic liquid
o-Cl	*ortho*-chloride
Omim	Octa-methyl imidazolium
ORR	Oxygen reduction reaction
OTAC	N,N,N-trimethyloctadecan-1-aminium chloride
OTf	Oxygen-trifluoromethanesulfonate
PalHis	N-(2-1H-imidazol-5-yl)ethyl)palmitamide

(*Continued*)

Acronym	Abbreviation
PC	Propylene carbonate
Pd	Palladium
PDBP	PVC-DTA-supported Boc-proline
PDP	Polyvinyl chloride-diethylenetriamine
Pd(PPh$_3$)$_4$	Tetrakis(triphenylphosphine)palladium(0)
PEBP	PVC-TETA-supported Boc-proline
PEG	Polyethylene glycole
PEMFCs	Polymer electrolyte membrane fuel cells
PEP	Polyvinyl chloride-tetraethylenepentamine
PGHD	Proline glycine histidine aspartic acid
PGMe	Phenyl glycine methyl ester
PhCO$_2$H	Benzoic acid
PhMe	Toluene
PILs	Poly-ionic liquids
PL	Photoluminescence
PMHis	*N*-(2-pyridylmethyl)-L-histidine
PMOs	Periodic mesoporous organosilicas
Pmpi	Propyl methyl piperidinium
PNBA	*p*-Nitrobenzoic acid
p-Nitro	*para*-Nitro
Pro	Proline
PS	Phosphorus (V) sulfide
PS	Polysilane
PS-SalGlu-Co	Polymer-bound glutamic acid salicylaldehyde Schiff-base complex
Pt	Platinum
PTBP	PVC-TEPA-supported Boc-proline
PTP	Polyvinyl chloride-triethylenetetramine
PTSA	*p*-Toluenesulfonic acid
PVC-DTA	Polyvinyl chloride-diethylenetriamine
PVC-TEPA	Polyvinyl chloride-tetraethylenepentamine
PVC-TETA	Polyvinyl chloride-triethylenetetramine
PVDC	Polyvinylidene chloride
PVPA	Poly(vinylphosphonic acid)
Py	Pyridine
PyBOP	Benzotriazol-1 yloxytripyrrolidinophosphonium hexafluorophosphate
RB	Rhodamin B
RGO	Reduced graphene oxide
Rt	Room temperature
Sal-Tryp	Salicylaldehyde
SBA-15	Santa Barbara Amorphous-15
SBA-16	Santa Barbara Amorphous-16
SDS	Sodium dodecyl sulfate

(*Continued*)

Acronym	Abbreviation
SiO$_2$	Silicon dioxide
SiO$_2$-AA-L-Glu-Pt	Silica-supported alginic acid-L-glutamic acid-Pt complex
SiO$_2$-ST-Glu-Fe	Silica-supported starch-L-glutamic acid–Fe complex
SLPCs	Solid supported liquid phase catalysts
SOCl$_2$	Thionyl chloride
TBAAsp	Tetrabutylamonium asparginate
TBAB	Tetrabutylammonium bromide
TBD	Triazabicyclodecene
TBDMS	*tert*-Butyldimethylsilyl
TBHP	*tert*-Butyl hydroperoxide
TBT	Tributyltin
t-BuOK	Potassium *tert*-butoxide
t-BuOMe	Methyl *tert*-butyl ether
TEA	Triethylamine
TEAI	Tetraethylammonium iodide
TEM	Transmission electron microscopy
TEOA	Triethanolamine
TEOS	Tetraethyl orthosilicate
TFA	Trifluoroacetic acid
TGA	Thermogravimetric analysis
THF	Tetrahydrofuran
TMCH	Trimethylcyclohexanone
TMEDA	Tetramethylethylenediamine
TMS	Tetramethylsilane
TMSCN	Trimethylsilyl cyanide
TMSP	Trimethylsilylpropanoic acid
TPB	Tetraphenyl butadiene
TPP	Thiamine pyrophosphate
TsOH	*p*-Toluenesulfonic acid
UV-vis	Ultraviolet-visible
VO(acac)$_2$	Vanadyl acetylacetonate
VO@MCM-41-Cys	Oxo-vanadium immobilized on L-cysteine-modified Mobil Composition of Matter No. *41*
XO	Xylenol orange
XPS	X-ray photoelectron spectroscopy
XRD	X-ray powder diffraction

REFERENCES

1. Khatri, T. T., Khursheed, A., Kumar, P. Water mediated synthesis of pyrano[2, 3-c] pyrazoles using L-histidine as an effective catalyst. In *AIP Conference Proceedings*; AIP Publishing LLC., 2017; Vol. 1860, p 20060. https://doi.org/10.1063/1.4990359.

2. Taherinia, Z., Ghorbani-Choghamarani, A., Hajjami, M. Peptide nanofiber templated zinc oxide nanostructures as non-precious metal catalyzed N-arylation of amines, one-pot synthesis of imidazoheterocycles and fused quinazolines. *Catal. Letters.*, 2019, *149*(1), 151–168. https://doi.org/10.1007/s10562-018-2580-4.

3. Ghorbani-Choghamarani, A., Taherinia, Z., Heidarnezhad, Z., & Moradi, Z. Application of nanofibers based on natural materials as a catalyst in organic reactions. *J. Ind. Eng. Chem.*, 2021, *94*, 1–61. https://doi.org/10.1016/j.jiec.2020.10.028.

4. Taherinia, Z., Ghorbani-Choghamarani, A., Hajjami, M. Decorated peptide nanofibers with Cu nanoparticles: An efficient catalyst for the multicomponent synthesis of chromeno [2, 3-d] Pyrimidin-8-Amines, Quinazolines and 2H- indazoles. *ChemistrySelect*, 2019, *4*(9), 2753–2760. https://doi.org/10.1002/slct.201803412.

5. Ghadermazi, M., Molaei, S., & Khorami, S. Synthesis, characterization and catalytic activity of copper deposited on MCM-41 in the synthesis of 5-substituted 1H-tetrazoles. *J. Porous Mater.*, 2023, *30*(3), 949–963. https://doi.org/10.1007/s10934-022-01398-9.

6. Azadi, G., Ghorbani-Choghamarani, A., Shiri, L. Copper(II) immobilized on Fe3O4@SiO2@l-histidine: A reusable nanocatalyst and its application in the synthesis of substituted 1H-tetrazoles. *Transit. Met. Chem.*, 2017, *42*(2), 131–136. https://doi.org/10.1007/s11243-016-0115-7.

7. Norouzi, M., Ghorbani-Choghamarani, A., Nikoorazm, M. Heterogeneous Cu(II)/l-His@Fe$_3$O$_4$ nanocatalyst: A novel, efficient and magnetically-recoverable catalyst for organic transformations in green solvents. *RSC Adv.*, 2016, *6*(95), 92387–92401. https://doi.org/10.1039/c6ra19776k.

8. Mousavifar, S. M., Kefayati, H., Shariati, S. Fe$_3$O$_4$@Propylsilane@Histidine[HSO4-] magnetic nanocatalysts: Synthesis, characterization and catalytic application for highly efficient synthesis of xanthene derivatives. *Appl. Organomet. Chem.*, 2018, *32*(4), e4242. https://doi.org/10.1002/aoc.4242.

9. Mousavifar, S. M., Kefayati, H., Shariati, S. Ultrasound-assisted synthesis of novel spiro[Indoline-3,5′-Pyrido[2,3-d]Pyrimidine] derivatives using Fe3O4@Propylsilane@Histidine[HSO4−] as an effective magnetic nanocatalyst. *J. Heterocycl. Chem.*, 2020, *57*(1), 157–162. https://doi.org/10.1002/jhet.3758.

10. Ghorbani-Choghamarani, A., Taherinia, Z., Nikoorazm, M. Ionic liquid supported on magnetic nanoparticles as a novel reusable nanocatalyst for the efficient synthesis of tetracyclic quinazoline compounds. *Res. Chem. Intermed.*, 2018, *44*(11), 6591–6604. https://doi.org/10.1007/s11164-018-3510-1.

11. Nielsen, M., Zhuang, W., Jørgensen, K. A. Asymmetric conjugate addition of azide to α,β-unsaturated nitro compounds catalyzed by cinchona alkaloids. *Tetrahedron*, 2007, *63*(26), 5849–5854. https://doi.org/10.1016/j.tet.2007.02.047.

12. Lewandowski, B., Wennemers, H. Asymmetric catalysis with short-chain peptides. *Curr. Opin. Chem. Biol.*, 2014, *22*(1), 40–46. https://doi.org/10.1016/j.cbpa.2014.09.011.

13. Sculimbrene, B. R., Morgan, A. J., Miller, S. J. Enantiodivergence in small-molecule catalysis of asymmetric phosphorylation: Concise total syntheses of the enantiomeric D-Myo-Inositol-1-Phosphate and D-Myo-Inositol-3-Phosphate. *J. Am. Chem. Soc.*, 2002, *124*(39), 11653–11656. https://doi.org/10.1021/ja027402m.

14. Iyer, M. S., Gigstad, K. M., Namdev, N. D., Lipton, M. Asymmetric catalysis of the Strecker amino acid synthesis by a cyclic dipeptide. *Amino Acids*, 1996, *11*(3–4), 259–268. https://doi.org/10.1007/BF00807935.

15. Debnath, M., Sasmal, S., Podder, D., Haldar, D. Pentapeptide nanoreactor as a platform for halogenations, Diels-Alder reaction, and Morita-Baylis-Hillman reaction. *ACS Omega*, 2019, *4*(9), 13872–13878. https://doi.org/10.1021/acsomega.9b01393.

16. Tang, Z., Yang, Z. H., Cun, L. F., Gong, L. Z., Mi, A. Q., Jiang, Y. Z. Small peptides catalyze highly enantioselective direct aldol reactions of aldehydes with hydroxyacetone: Unprecedented regiocontrol in aqueous media. *Org. Lett.*, 2004, *6*(13), 2285–2287. https://doi.org/10.1021/ol049141m.

17. Tsogoeva, S. B., Wei, S. (S)-histidine-based dipeptides as organic catalysts for direct asymmetric aldol reactions. *Tetrahedron Asymmetry*, 2005, *16*(11), 1947–1951. https://doi.org/10.1016/j.tetasy.2005.04.027.

18. Zirak, M., Bahrami, Z., Büyükgüngör, O., Eftekhari-Sis, B. N-(2-Pyridylmethyl)-L-histidine functionalized Fe3O4 magnetic nanoparticles as an efficient catalyst for synthesis of β-amino ketones. *Sci. Iran.*, 2020, *27*(3 C), 1207–1215. https://doi.org/10.24200/SCI.2020.54123.3607.

19. Hajipour, A. R., Hosseini, S. M., Jajarmi, S. Histidine-functionalized chitosan-Cu(II) complex: A novel and green heterogeneous nanocatalyst for two and three component C-S coupling reactions. *New J. Chem.*, 2017, *41*(15), 7447–7452. https://doi.org/10.1039/c7nj00595d.

20. Azadi, G., Taherinia, Z., Naghipour, A., Ghorbani-Choghamarani, A. Synthesis of sulfides via reaction of Aryl/Alkyl halides with S8 as a sulfur-transfer reagent catalyzed by Fe3O4-magnetic-nanoparticles-supported L-histidine-Ni(II). *J. Sulfur Chem.*, 2017, *38*(3), 303–313. https://doi.org/10.1080/17415993.2017.1287265.

21. Farzaneh, F., Rashtizadeh, E. A new Cu Schiff base complex with histidine and glutaraldehyde immobilized on modified iron oxide nanoparticles as a recyclable catalyst for the oxidative homocoupling of terminal alkynes. *J. Iran. Chem. Soc.*, 2016, *13*(6), 1145–1154. https://doi.org/10.1007/s13738-016-0829-7.

22. Nikkhoo, M., Amini, M., Morteza, S., Farnia, F., Bayrami, A., Bagherzadeh, M., Gautam, S., Chae, K. H. Oxido-Peroxido W(VI)-Histidine–MgAl-Layered double hydroxide composite as an efficient catalyst in sulfide oxidation. *Appl. Organomet. Chem.*, 2018, *32*(6), e4358. https://doi.org/10.1002/aoc.4358.

23. Qi, Y., Cheng, W., Xu, F., Chen, S., Zhang, S. Amino acids/superbases as eco-friendly catalyst system for the synthesis of cyclic carbonates under metal-free and halide-free conditions. *Synth Commun.*, 2018, *48*(8), 876–886. https://doi.org/10.1080/00397911.2017.1339802.

24. Geravand, E., Farzaneh, F., Ghiasi, M. Synthesis and DFT study of binding models of histidine in [VO (His) $_2$] complex and immobilization on UiO-66-NH$_2$ as epoxidation catalyst of allyl alcohols. *J. Mol. Struct.*, 2022, *1253*, 132248. https://doi.org/10.1016/j.molstruc.2021.132248.

25. Wu, Q., Shen, C., Liu, C. J. Amino acid (histidine) modified Pd/SiO$_2$ catalyst with high activity for selective hydrogenation of acetylene. *Appl. Surf. Sci.,* 2023, *607*, 154976. https://doi.org/10.1016/j.apsusc.2022.154976.

26. Varga, G., Timár, Z., Schemhl, H., Csendes, Z., Bajnóczi, É. G., Carlson, S., Pálinkó, I. Bioinspired covalently grafted Cu (II)–C protected amino acid complexes: Selective catalysts in the epoxidation of cyclohexene. *React. Kinet. Mech. Catal.*, 2015, *115*, 33–43. https://doi.org/10.1007/s11144-014-0796-x.

27. Wu, C., Long, X., Li, S., Fu, X. Simple and inexpensive threonine-based organocatalysts as highly active and recoverable catalysts for large-scale asymmetric direct stoichiometric aldol reactions on water. *Tetrahedron Asymmetry*, 2012, *23*(5), 315–328. https://doi.org/10.1016/j.tetasy.2012.02.023.

28. Henseler, A. H., Ayats, C., Pericàs, M. A. An enantioselective recyclable polystyrene-supported threonine-derived organocatalyst for aldol reactions. *Adv. Synth. Catal.*, 2014, *356*(8), 1795–1802. https://doi.org/10.1002/adsc.201400033.

29. Gerasimchuk, V. V., Romanov, R. R., Woo, G. H. T., Dmitriev, I. A., Kucherenko, A. S., Zlotin, S. G. Novel L-threonine-based ionic liquid supported organocatalyst for asymmetric syn-aldol reactions: Activity and recyclability design. *Arkivoc*, 2017, *2017*(3), 241–249. https://doi.org/10.24820/ark.5550190.p010.149.

30. Larionova, N. A., Kucherenko, A. S., Siyutkin, D. E., Zlotin, S. G. (S)-Threonine/α ,α-(S)-diphenylvalinol-derived chiral ionic liquid: An immobilized organocatalyst for asymmetric syn-aldol reactions. *Tetrahedron*, 2011, *67*(10), 1948–1954. https://doi.org /10.1016/j.tet.2011.01.017.

31. Fager, D. C., Morrison, R. J., Hoveyda, A. H. Regio- and enantioselective synthesis of trifluoromethyl-substituted homoallylic α-tertiary NH2-amines by reactions facilitated by a threonine-based boron-containing catalyst. *Angew. Chemie - Int. Ed.*, 2020, *59*(28), 11448–11455. https://doi.org/10.1002/anie.202001184.

32. Beck, J. S., Vartuli, J. C., Roth, W. J., Leonowicz, M. E., Kresge, C. T., Schmitt, K. D., Schlenker, J. A new family of mesoporous molecular sieves prepared with liquid crystal templates. *J. Am. Oil Chem. Soc.*, 1992, *114*, 10834–10843. https://doi.org/10.1021/ja00053a020.

33. Hermida, L., Agustian, J., Abdullah, A. Z., Mohamed, A. R. Review of large-pore mesostructured cellular foam (MCF) silica and its applications. *Open Chem.*, 2019, *17*(1), 1000–1016. https://doi.org/10.1515/chem-2019-0107.

34. Shirvandi, Z., Rostami, A., & Ghorbani-Choghamarani, A. Magnetic mesocellular foams with nickel complexes: As efficient and reusable nanocatalysts for the synthesis of symmetrical and asymmetrical diaryl chalcogenides. *Nanoscale Adv.*, 2022, *4*(9), 2208–2222. https://doi.org/10.1039/d1na00822f.

35. Sarvi, I., Gholizadeh, M., Izadyar, M. Threonine stabilizer-controlled well-dispersed small palladium nanoparticles on modified magnetic nanocatalyst for heck cross-coupling process in water. *Appl. Organomet. Chem.*, 2019, *33*(3), e4645. https://doi.org/10 .1002/aoc.4645.

Index